Department of Pure and Applied Chemistry

EXPERIMENTAL AND COMPUTATIONAL STUDIES ON THE ROLE OF SINGLE ELECTRON TRANSFER IN SELECTED ORGANIC REACTIONS
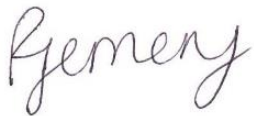
by

KATIE J. EMERY

A thesis submitted to the Department of Pure and Applied Chemistry, University of Strathclyde, in part fulfilment of the regulations for the degree of Doctor of Philosophy in Chemistry.

2017

Declaration of ownership

This thesis is the result of the author's original research. It has been composed by the author and has not been previously submitted for examination which has led to the award of a degree.

The copyright of this thesis belongs to the author under the terms of the United Kingdom Copyright Acts as qualified by University of Strathclyde Regulation 3.50. Due acknowledgement must always be made of the use of any material contained in, or derived from, this thesis.

Signed: *Gemeny*   Date: 17th April 2017

Acknowledgements

I would like to thank both Professor John Murphy, for his teaching and guidance both in and out of the laboratory, and Dr Tell Tuttle, for his support and help with regards to the computational work, as well as the members of both the Murphy group and the Tuttle group, for making my PhD so enjoyable. Further thanks to Dr Alan Kennedy and the National X-ray service for the X-ray analysis data, and a thanks to the EPSRC National Mass Spectrometry Service Centre in Swansea for the high resolution mass spectrometry results. Additional thanks go to Craig Irving for help with ^{1}H-NMR analysis, Pat Keating for mass spectrometry assistance, and all the other members of staff at University of Strathclyde. I would also like to thank the EPSRC and the University of Strathclyde for funding.

A huge thanks go to my fantastic mum, Rachel Emery, who has always supported me in every aspect of my life and I am so lucky to have such a patient and understanding mum and a fantastic role model. Of course, I have to thank the rest of my family just for being their nutty selves; Becky Boo, Rowley, Sammy Jo, Jess and our Rohan Bear. Finally, I thank Tom Burns for always being there for me throughout my PhD and for his constant belief in me.

Publications

1. J. P. Barham, G. Coulthard, **K. J. Emery**, E. Doni, F. Cumine, G. Nocera, M. P. John, L. E. A. Berlouis, T. McGuire, T. Tuttle, J. A. Murphy, *J. Am. Chem. Soc.*, 2016, **138**, 7402-7410. "KO^{t}Bu: a privileged reagent for electron transfer reactions?"
    (Chapter 5)

2. **K. J. Emery**, T. Tuttle, A. R. Kennedy, J. A. Murphy, *Tetrahedron*, 2016, **72**, 7875-7887. "C-C bond-forming reactions of ground-state aryl halides under reductive activation." *(Chapter 6)*

3. **K. J. Emery**, J. A. Murphy, T. Tuttle, *Org. Biomol. Chem.*, 2017, **15**, 920-927. "Effect of solvent on radical cyclisation pathways: S$_{RN}$1 *vs.* aryl-aryl bond forming mechanisms."
    (Chapter 6)

4. **K. J. Emery**, J. A. Murphy, T. Tuttle, *Manuscript in preparation*. "Mechanistic understanding of alkoxide-induced halogenation of alkanes."
    (Chapter 5)

5. **K. J. Emery**, J. A. Murphy, T. Tuttle, *Manuscript in preparation*. "Design and synthesis of a *N,N'*-dipropyldiketopiperazine additive: Evidence of single electron transfer from its enolate anion."
    (Chapter 4)

Abbreviations

%mol	mole percentage
$\Delta G^{\ddagger}$	Gibbs free energy for the transition state
ΔG_{rxn}	Gibbs free energy for the relative energies
μW	microwave
Ac	acetate
AE	all-electron
AIBN	azobisisobutyronitrile
APCI	atmospheric pressure chemical ionisation
BDE	bond dissociation energy
BHAS	base-promoted homolytic aromatic substitution
br	broad
b.p.	boiling point
bpydc	2,2'-bipyridine-5,5'-dicarboxylate
cald.	calculated
CGF	contracted Gaussian functional
CI	chemical ionisation
CV	cyclic voltammetry
d	doublet
dec.	decomposed
DFT	density functional theory

DIPEA	diisopropylethylamine
DKP	*N,N'*-dipropyldiketopiperazine
DMEDA	*N,N'*-dimethylethylenediamine
DMF	dimethylformamide
DMSO	dimethyl sulfoxide
2,4-DNPH	2,4-dinitrophenylhydrazine
ECP	effective core potential
EI	electron ionisation
EPR	electron paramagnetic resonance
ESI	electrospray ionisation
Et	ethyl
eq.	equivalents
g	grams
GCMS	gas chromatography mass spectrometry
GGA	generalised gradient approximation
GTO	Gaussian-type orbitals
h	hours
Ĥ	Hamiltonian operator
HF	Hartree-Fock
Hz	hertz
HMBC	heteronuclear multiple bond correlation
HOMO	highest occupied molecular orbital
HRMS	high resolution mass spectrometry

HSQC	heteronuclear single quantum correlation
hv	light irradiation
ICP-AES	inductively coupled plasma atomic emission spectrometry
ICP-MS	inductively coupled plasma mass spectrometry
^{i}Pr	isopropyl
IR	infrared
J	coupling constant
kcal/mol	kilocalories per mole
KHMDS	potassium bis(trimethylsilyl)amide
KS	Kohn-Sham
LCAO	linear combination of atomic orbitals
LCMS	liquid chromatography-mass spectrometry
LD	local density
LDA	lithium diisopropylamide
LiHMDS	lithium bis(trimethylsilyl)amide
lit.	literature value
LOD	limit of detection
LS	local spin
LUMO	lowest unoccupied molecular orbital
m	multiplet
*m*CPBA	*meta*-chloroperoxybenzoic acid
Me	methyl
mL	millilitres

mmol	millimoles
mg	milligrams
min	minutes
mol%	molar percentage
MHz	megahertz
MOF	metal organic framework
m.p.	melting point
M	molarity
NHC	*N*-heterocyclic carbene
nm	nanometres
NMR	nuclear magnetic resonance
NSI	nanospray ionisation
^{n}Bu	*n*-butyl
O/N	overnight
pp	pages
ppb	parts per billion
ppm	parts per million
q	quartet
RDS	rate determining step
RT	room temperature
Rf	retention time
s	singlet
SCE	saturated calomel electrode

(S)ET	(single) electron transfer
SPE	single point energy
S$_{RN}$1	radical nucleophilic substitution
STO	Slater-type orbitals
sx	sextet
t	triplet
TBAB	tetrabutylammonium bromide
TBAF	tetrabutylammonium fluoride
^{t}Bu	*tertiary*-butyl
TD-DFT	time-dependent density function theory
TEMPO	2,2,6,6-tetramethylpiperidine 1-oxyl
THF	tetrahydrofuran
TMEDA	*N,N'*-tetramethylethylenediamine
TMS	trimethylsilyl
UV-vis	ultraviolet-visible spectroscopy

Table of contents

Abstract

The transition metal-free reaction conditions that couple haloarenes to benzene using a combination of KO^{t}Bu and an organic additive is proposed to be initiated by a single electron transfer (SET) into the haloarene. It was initially believed that KO^{t}Bu was the electron donor, however mounting experimental evidence suggests that electron donors are formed *in situ*. Within this thesis, both of these potential initiation pathways are investigated.

Experimental evidence is presented to support the proposal that the electron-rich enolate anion **6** (formed by deprotonation of the additive *N,N'*-dipropylketopiperazine **5**) acts as an electron donor (Scheme 1). When the additive **7** was used in the transition metal-free reactions, the cyclised product **10** was isolated, which arose by SET from the enolate anion **8**.

Computational analysis has shown that when DMF is used as the additive in these transition metal-free reaction conditions, the electron donors, **13** or **14**, can form from the dimerisation of the carbamoyl anion of DMF. This work lead towards the development of new additives for these transition metal-free reaction conditions.

Computational analysis and experimental evidence is presented that puts into question the previously proposed mechanism that KO^{t}Bu can donate a single electron to CBr$_4$ in the bromination of adamantane (Scheme 2). It is proposed that alkoxides, like **16**, form hypobromite intermediates when reacted with CBr$_4$ **15** (rather than undergoing SET) and these hypohalites have been shown to successfully achieve this transformation.

These transition metal-free reaction conditions have been used to achieve S$_{RN}$1 reactions to couple aryl halides with enolate anions (Scheme 3). A thorough study of the reaction mechanism and possible selectivity of reaction pathways, between S$_{RN}$1 and aryl-aryl bond formations, was performed. The conclusion is that neither

photoactivation nor transition metal-induced activation is needed, and solvent is shown to influence the product selectivity.
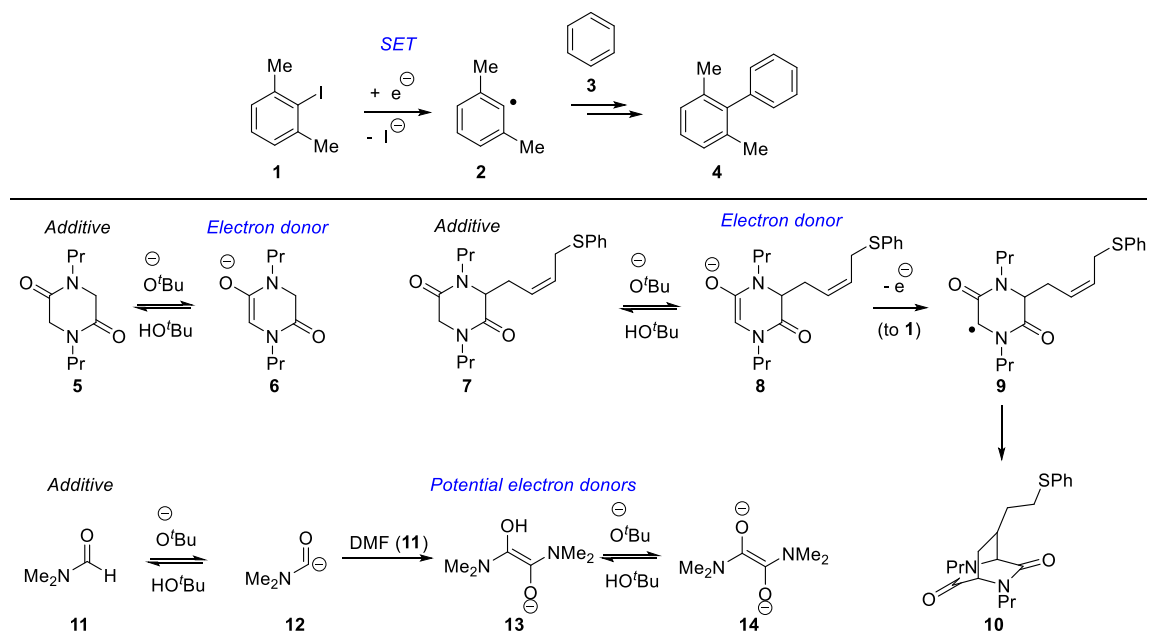
Scheme 1 The proposal of the formation electron donors from *N,N'*-dipropylketopiperazine **5** and DMF **11** that can donate a single electron to haloarenes, such as **1**, in the transition metal-free coupling reactions.
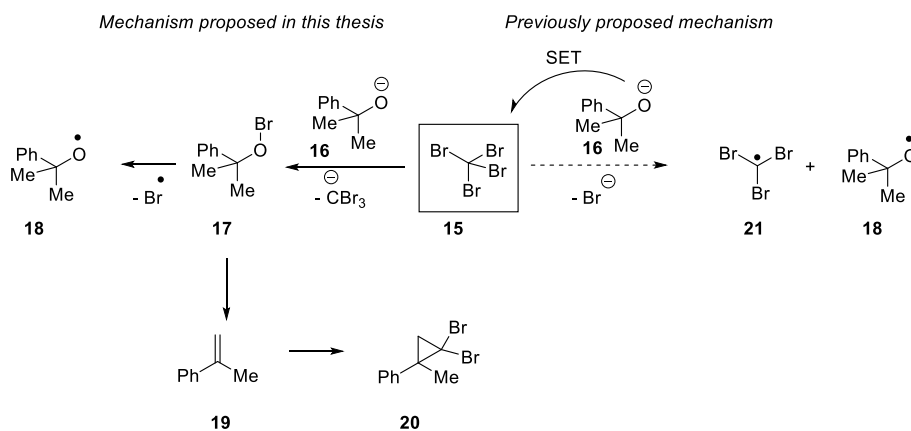
Scheme 2 The formation of radical species from the reaction of alkoxides, like **16**, with tetrabromomethane occurs through the formation of hypobromites like **17**, as opposed to SET from alkoxide **16**, as previously proposed.
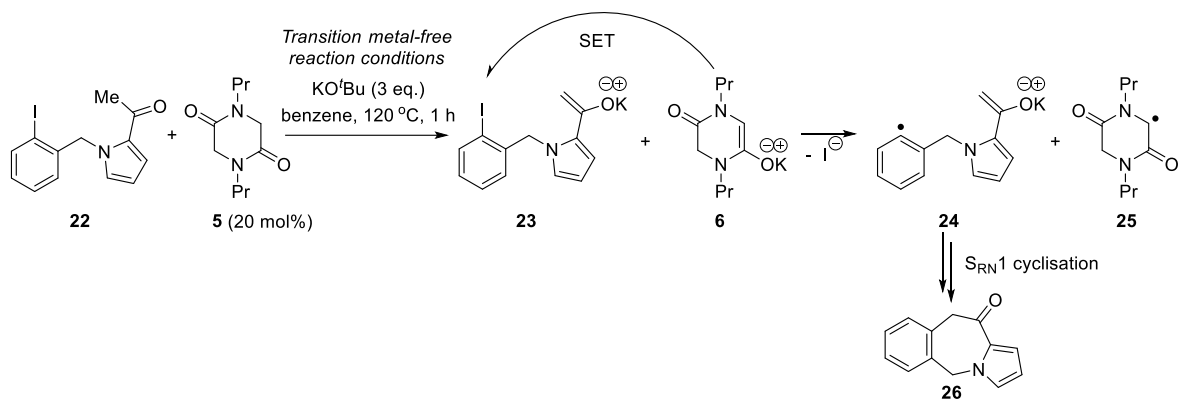
Scheme 3 Transition metal-free reaction conditions used to activate haloarenes to form aryl radicals in S$_{RN}$1 cyclisation of substrate **22** and analogues.

1.

Literature review

In the approach towards greener chemical syntheses, chemists are driven towards finding alternative reaction conditions to achieve the conventional palladium cross-coupling reactions. Efforts are made to use more abundant transition metals, such as nickel, copper and iron,[1-2] to replace palladium or other heavy metals. Recent discoveries have shown that transition metal-free reaction conditions can be employed to achieve aryl-aryl bond formations or Heck-type couplings of aryl halides to either unactivated arenes or alkenes respectively. Due to the predominance of biaryl motifs in pharmaceutical molecules and biologically active compounds, it is desirable to focus on aryl-aryl bond formations. This chapter provides an introduction to the discovery and development of the transition metal-free approach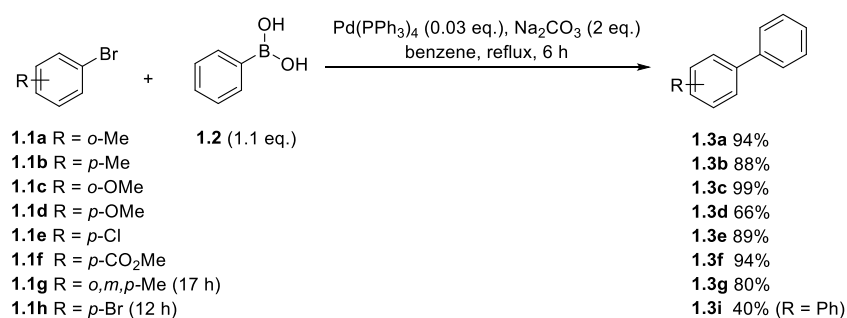es to aryl-aryl bond formations, which are otherwise commonly achieved using expensive transition metals, such as gold or palladium. Section 1.1 briefly describes the more conventional reaction conditions to achieve aryl-aryl bond formations, which involve transition metals, in particular palladium. Section 1.2 summarises the early work performed in the area of transition metal-free aryl-aryl bond formations, such as 1) through benzyne intermediates, 2) using the base-promoted homolytic aromatic substitution (BHAS) mechanism and 3) light irradiation (*hv*). Section 1.3 describes the small progression that has been made into using these transition metal-free reaction conditions to achieve alternative bond formations, such as coupling aryl halides to alkenes. Section 1.4 describes the recent debate within the literature as to the nature of the electron donor in the initiation step in the BHAS pathway. These reviews have instigated experimental and computational studies reported in this thesis.

1.1 Aryl-aryl bond formations using transition metals

There is a large and diverse appearance of biaryl motifs in commercial applications, such as pharmaceutical drugs, herbicides and within the materials science domain. The first reported successful symmetrical biaryl synthesis was published by Ullmann at the start of the last century, who observed the coupling between two identical aryl halides *via* a copper-mediated aryl-aryl bond formation.[3] Over the last century, the use of transition metals as catalysts for biaryl synthesis has expanded; catalytic

amounts of nickel[4-5] successfully couple aryl halides to form biaryl structures using zinc dust as a reductant in the system, but the most popular transition metal used for these transformations is palladium, which efficiently performs cross-coupling reactions between an aryl halide and an organometallic reagent. The organometallic reagents employed range from aryl-magnesium bromides[6] or aryl-zinc halides[7-8] as the nucleophile, to aryl-tin[9] or aryl-boron[10] reagents. The latter organometallic reagent for the palladium-catalysed cross-coupling reactions, used in the Suzuki reaction,[10] is nowadays applied as a general synthetic tool for all organic chemists (Scheme 1.1). The importance of these palladium-catalysed cross-coupling reactions was even recognised with the Nobel prize in chemistry in 2010, which was awarded to Heck, Negishi and Suzuki for their contributions to this field.[11]

1.1a R = *o*-Me   **1.2** (1.1 eq.)   **1.3a** 94%
1.1b R = *p*-Me   **1.3b** 88%
1.1c R = *o*-OMe   **1.3c** 99%
1.1d R = *p*-OMe   **1.3d** 66%
1.1e R = *p*-Cl   **1.3e** 89%
1.1f R = *p*-CO$_2$Me   **1.3f** 94%
1.1g R = *o,m,p*-Me (17 h)   **1.3g** 80%
1.1h R = *p*-Br (12 h)   **1.3i** 40% (R = Ph)

Scheme 1.1 The reaction of aryl bromides **1.1a-h** with phenylboronic acid **1.2** in a Suzuki reaction.

An alternative approach to the formation of these biaryl motifs is the application of C-H activation reactions. Heavy transition metals, such as ruthenium,[12-14] rhodium,[15-17] iridium[18] and palladium,[19-21] are capable of coupling one activated aryl substrate, such as an aryl halide or arylboronate, through C-H activation with a non-activated aromatic substrate (Scheme 1.2).

A)

1.4a R^1 = H; R^2 = Me (2 eq.)
1.4b R^1 = H; R^2 = ^{i}Pr (2 eq.)
1.4c R^1 = H; R^2 = ^{t}Bu (2 eq.)
1.4d R^1 = p-OMe; R^2 = ^{t}Bu (2 eq.)
1.4e R^1 = p-F; R^2 = ^{t}Bu (2 eq.) (2 h)
1.4f R^1 = o-CF$_3$; R^2 = Me (2 eq.)

1.5 (1 eq.)

1.6a R^1 = H; R^2 = Me; R^3 = Ph; 60%
1.6b R^1 = H; R^2 = ^{i}Pr; R^3 = Ph; 76%
1.6c R^1 = H; R^2 = ^{t}Bu; R^3 = H; 95%
1.6d R^1 = p-OMe; R^2 = ^{t}Bu; R^3 = H; 78%
1.6e R^1 = p-F; R^2 = ^{t}Bu; R^3 = H; 88%
1.6f R^1 = o-CF$_3$; R^2 = Me; R^3 = Ph; 90%

B)

1.7a R = o-Me
1.7b R = p-Me
1.7c R = o-OMe
1.7d R = p-OMe
1.7j R = 3,5-dimethyl
1.7k R = H

1.8 (40 eq.)

1.3a 43%
1.3b 56%
1.3c 32%
1.3d 66%
1.3j 51%
1.3k 72%
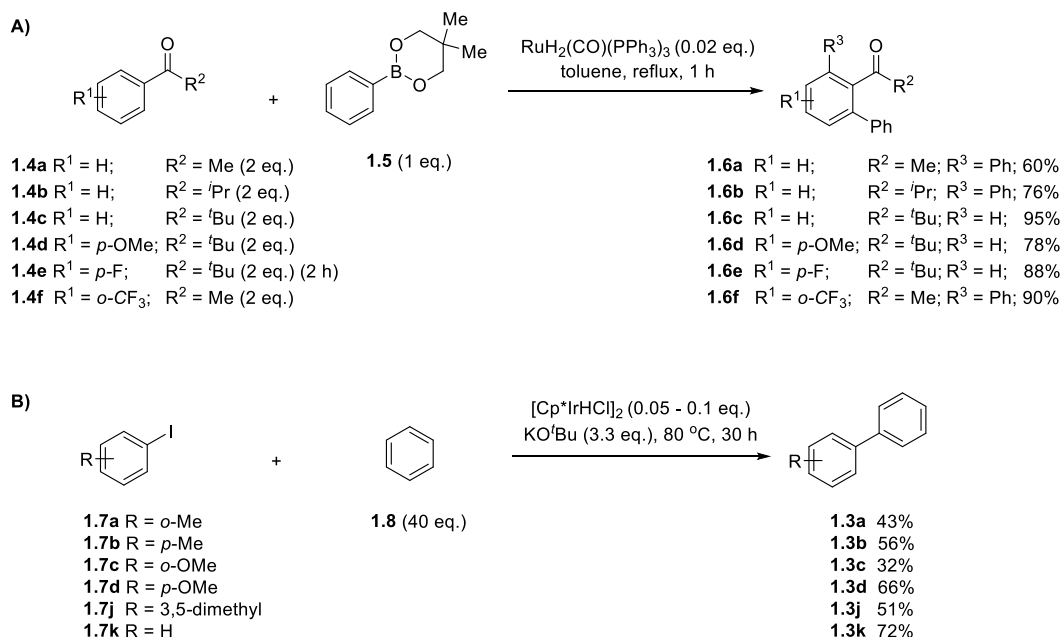
Scheme 1.2 Examples of aryl-aryl bond formations through C-H activation: **A)** Ruthenium-catalysed cross-coupling of phenylboronate **1.5** with unactivated aryl ketones **1.4a-f**.[14] **B)** Iridium-catalysed cross-coupling of iodoarenes **1.7a-d,j-k** with unactivated benzene **1.8**.[18]

In the drive towards greener chemistry, researchers have focused efforts on attempting to eliminate heavy transition metals from synthesis, with the aim of using more sustainable and non-toxic reagents. The current methods to synthesise these scaffolds using heavy transition metal-mediated coupling reactions are very efficient, well known and well studied, and can provide stereo- and regioselectivity. However, these methods have their drawbacks, one drawback is that the metals used are very expensive. Hence, alternatives have been investigated to achieve the aryl-aryl bond formations using cheaper and abundant metals such as nickel[22] and copper.[23] Recent success was reported that used inexpensive first row transition metals, such as iron and cobalt, in combination with NaO^{t}Bu, to achieve a range of reactions, such as hydroboration, hydrosilylation, hydrovinylation, hydrogenation and [2+2] alkene cycloaddition.[2] The second drawback is that the purification of these metals from final products, such as drug-like molecules, can be a laborious and costly process. Trace metal impurities within the final compounds can be hazardous to the consumers' health and thus there is a drive towards the elimination of transition metals from biaryl synthesis.

In 2003, Leadbeater *et al.* reported the first supposed transition metal-free Suzuki-type coupling reaction of various aryl halides with electron-poor or electron-neutral arylboronic acids in water under microwave (μW) conditions. In the initial investigations they were using palladium acetate as the catalyst and tetrabutylammonium bromide (TBAB) as an additive.[24] Whilst investigating the role of TBAB in the Suzuki coupling of 4-bromoacetophenone **1.1l** to phenylboronic acid **1.2** they observed that, under appropriate conditions, high yields of 1-([biphenyl]-4-yl)ethan-1-one **1.3l** were achieved in the absence of palladium (Scheme 1.3).[25]
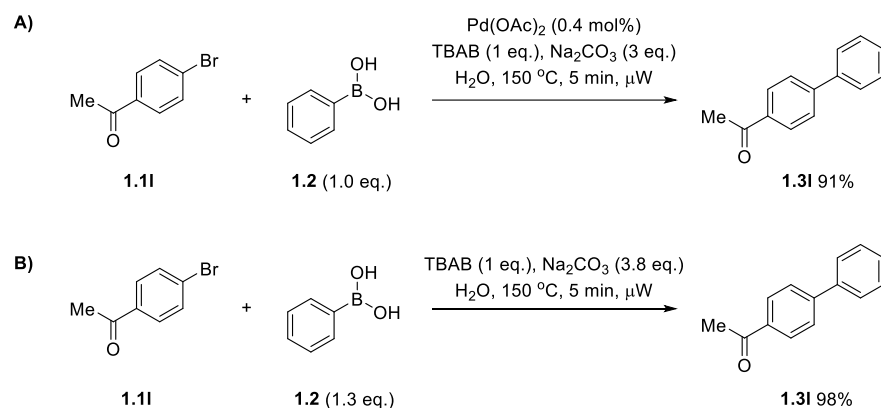
Scheme 1.3 Leadbeater *et al.*[24-25] reported a supposed transition metal-free Suzuki reaction.

Within another publication, Leadbeater *et al.* reported the measures they had taken to assess the absence of transition metals in this coupling.[26] The measures taken involved using new glassware and apparatus, as well as new reagents provided by different suppliers. With all these precautions, they achieved reproducible yields of coupling for all reactions performed. Finally, the crude mixture of the reaction, both the organic and the aqueous phases, was analysed by inductively coupled plasma atomic emission spectrometry (ICP-AES) to determine the content of palladium and other metals. No palladium content was found within the limit of detection (LOD) of the instrument (LOD quoted at < 0.1 ppm), and other metals that are known to activate aryl halides were found in very low quantities: nickel, platinum and copper were present at levels of < 0.5 ppm, and ruthenium was present at levels of < 1.0 ppm. This method was therefore reported as the first transition metal-free Suzuki reaction. These publications, however, received a lot of scrutiny because they
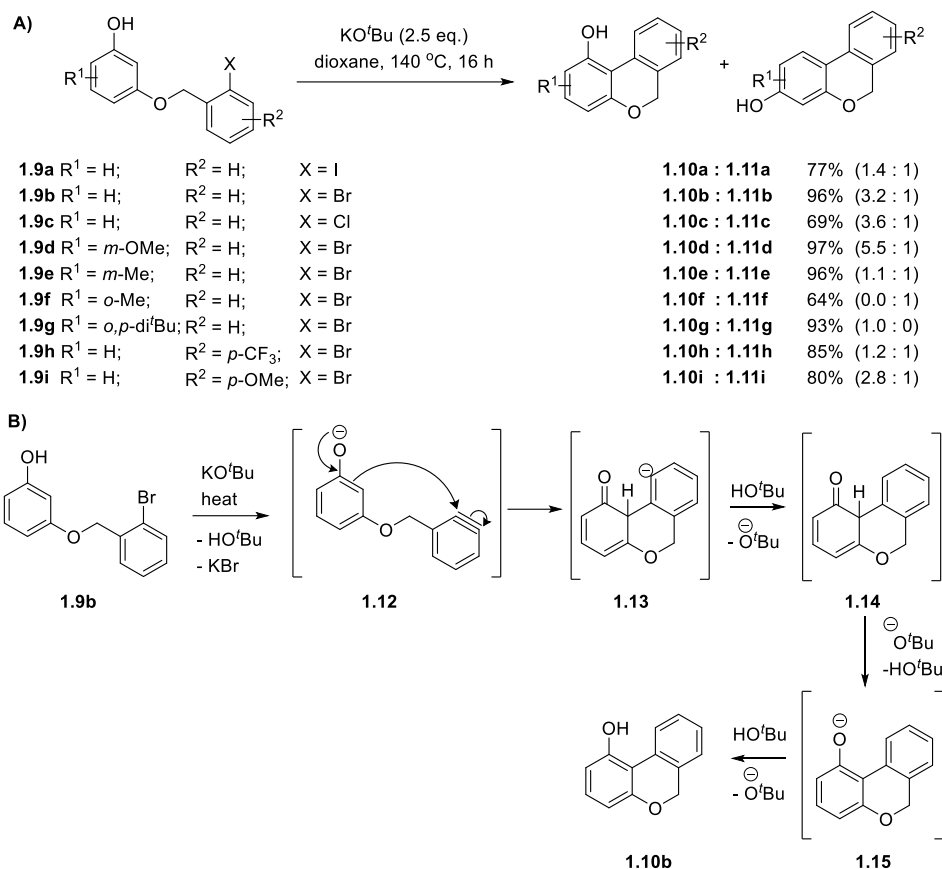
boasted the first transition metal-free biaryl synthesis, and in 2005, Leadbeater *et al.* chose to reassess the paper after publications by de Vries *et al.* stated that Heck reactions could be performed with ligand-free palladium in low amounts (0.01 mol%).[27] Upon revisiting the paper, Leadbeater *et al.* reported that the commercially supplied Na_2CO_3 contained trace palladium contaminants (< 50 ppb), that they suggested was capable of promoting the coupling.[28]

1.2 Transition metal-free aryl-aryl bond formations

With the increasing cost of transition metal catalysts, and the requirement for costly separation and recovery of heavy metals from waste-streams, the attractions of the transition metal-free couplings are clear. There are three types of transition metal-free aryl-aryl bond formations that can take place with aryl halides under basic conditions: 1) nucleophilic aromatic substitution, 2) benzyne coupling reactions and, more recently, 3) the base-promoted homolytic aromatic substitution (BHAS) reaction. In reactions like the latter, where electron transfer is involved, light irradiation can also be used to achieve these aryl-aryl bond formations.

1.2.1 Benzyne pathway

In 2008, Daugulis *et al.* reported a transition metal-free intramolecular aryl-aryl bond formation of 3-(2-halobenzyloxy)phenols **1.9a-i** (Scheme 1.4).[29] In the presence of KO*t*Bu, intramolecular aryl-aryl bond formation of 3-(2-halobenzyloxy)phenols **1.9a-i** was observed to afford regioisomeric coupled products. The regioisomers **1.10b** and **1.11b** were identified as products arising from the reaction of **1.9b**. The proposed mechanism involves the formation of the benzyne intermediate **1.12**, from the reaction of **1.9b** and a strong base, such as KO*t*Bu (the benzyne intermediate was confirmed by deuteration studies). The phenol undergoes cyclisation onto the benzyne in the *ortho* position to yield **1.15**, and ultimately **1.10b** upon protonation (alternatively, cyclisation may occur in the *para* position to form **1.11b**). This approach to use benzyne intermediates for the formation of aryl-aryl bonds has also been applied intermolecularly by Daugulis *et al.* to couple heterocycles to aryl halides,[30] and anilines to aryl halides, at the *ortho* position to the nitrogen.[31]
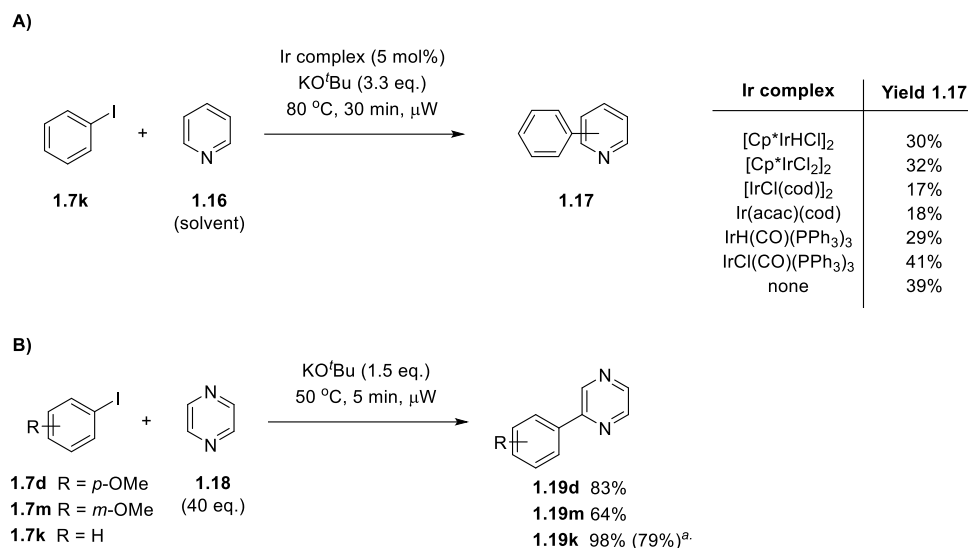
Scheme 1.4A) Daugulis reported intramolecular cyclisation **B)** and proposed a benzyne pathway.[29]

1.2.2 Base-promoted homolytic aromatic substitution pathway

1.2.2.1 Intermolecular couplings

The first reported transition metal-free aryl-aryl bond formation between haloarenes and unactivated aromatic coupling partners was reported in 2008 by Itami *et al.*[32] During the optimisation of an iridium-catalysed cross-coupling reaction between iodobenzene **1.7k** and pyridine **1.16**, in the presence of KO^{t}Bu, they reported that phenylpyridine **1.17** was still formed as a mixture of isomers (2-phenylpyridine, 3-phenylpyridine and 4-phenylpyridine), even when the iridium catalyst was omitted (Scheme 1.5A). To further investigate the reaction conditions and the substrate scope, Itami *et al.* coupled various iodoarenes **1.7** to pyrazine **1.18** with moderate to

high yields (64 - 98%) (Scheme 1.5B). The reaction was carried out under thermal conditions (120 °C, 13 h) instead of microwave irradiation, giving a higher yield of **1.19k** (79%).
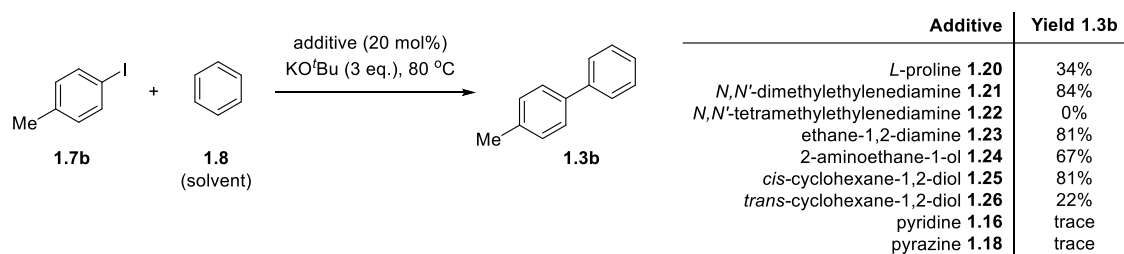
A)

Ir complex	Yield 1.17
[Cp*IrHCl]₂	30%
[Cp*IrCl₂]₂	32%
[IrCl(cod)]₂	17%
Ir(acac)(cod)	18%
IrH(CO)(PPh₃)₃	29%
IrCl(CO)(PPh₃)₃	41%
none	39%

B)

a. Reaction performed under thermal conditions at 120 °C for 13 h (no µW irradiation)

Scheme 1.5A) Itami *et al.*[32] reported the first transition metal-free coupling of iodobenzene with pyridine in the presence of KO*t*Bu alone. **B)** Itami *et al.*[32] coupled pyrazine with haloarenes in the absence of transition metals.

Due to Leadbeater's research,[28] which showed that even 50 ppb of palladium present in Na₂CO₃ was capable of catalysing the Suzuki reaction, Itami *et al.*[32] took precautions and did numerous experiments to ensure that their reactions were indeed transition metal-free. The mechanism proposed involves the generation of an aryl radical from the iodoarene because when radical scavengers, such as galvinoxyl, TEMPO and acrylonitrile, were added to the reaction, only trace yields of product (< 1%) were observed, thus indicating that the mechanism involves radical intermediates. It should be noted at this point that the addition of new additives, such as TEMPO, to the reaction mixture may also divert the reactions towards other mechanisms that are not present in their absence. Therefore, caution should be made when deducing concrete conclusions from the addition of new additives, such as radical scavengers, into the reaction mixture.

This research reported by Itami *et al.* initiated a large effort to identify alternative conditions to achieve transition metal-free aryl-aryl bond formations, and to

investigate the mechanism involved. In 2010, several research groups reported similar reactions to that reported by Itami *et al.*, however they observed transition metal-free coupling between haloarenes and benzene, in the presence of KO*t*Bu and an organic additive. Kwong and Lei *et al.*[33] showed that, in the presence of KO*t*Bu and several simple organic molecules as additives, 4-iodotoluene **1.7b** can couple to benzene *via* radical intermediates, in the absence of transition metals (Scheme 1.6). The correct precautions were taken to ensure that the reaction was not promoted by trace metal catalysts in the reaction mixture.

Additive	Yield 1.3b
L-proline **1.20**	34%
N,N'-dimethylethylenediamine **1.21**	84%
N,N'-tetramethylethylenediamine **1.22**	0%
ethane-1,2-diamine **1.23**	81%
2-aminoethane-1-ol **1.24**	67%
cis-cyclohexane-1,2-diol **1.25**	81%
trans-cyclohexane-1,2-diol **1.26**	22%
pyridine **1.16**	trace
pyrazine **1.18**	trace

additive (20 mol%)
KO*t*Bu (3 eq.), 80 °C

1.7b   **1.8** (solvent)   **1.3b**

Scheme 1.6 Kwong and Lei *et al.* reported aryl-aryl bond formation promoted by KO*t*Bu and various organic additives.[33]

During the optimisation of the reaction conditions, the most efficient additive identified was *N,N'*-dimethylethylenediamine (DMEDA) **1.21**. They suggested that DMEDA, and the other additives, were acting as "organocatalysts". However, they never reported recovery of DMEDA, nor did they demonstrate catalysis, and therefore it is more appropriate to describe the role of the DMEDA as an organic reagent used in sub-stoichiometric quantities. Interestingly, under these reaction conditions, pyridine **1.16** and pyrazine **1.18** were not effective at promoting coupling in this reaction. These results compare to those of Itami *et al.* who used pyridine and pyrazine to achieve these couplings, albeit the additives in the case of Itami *et al.* were used in much larger quantities (as the solvent). Kwong and Lei *et al.*[33] also performed various experiments to gain more of an understanding about the mechanism involved in this transformation. They repeated the coupling of 4-iodotoluene **1.7b** with benzene to analyse the product distribution of **1.3b** throughout the reaction, and they found that the coupling proceeds with an induction period. It was determined that the only base successful for this transformation was KO*t*Bu, and both the butoxide anion and the potassium counter-ion were vital for efficient

yields, because other bases generated low yields or no product [LiHMDS (10%), NaH (0%), KOH (0%), Na$_2$CO$_3$ (0%), KOAc (0%), LiO^{t}Bu (0%) and NaO^{t}Bu (0%)]. To support the requirement for the potassium cation, 18-crown-6 ether was added to the reaction mixture, which led to a much lower yield of product **1.3b** (15%). However, alternative explanations for the role of the 18-crown-6 ether in the reaction were not considered.

Kwong and Lei *et al.*[33] suggested that radical intermediates were mechanistically involved because radical trapping reactions, using TEMPO and 1,1-diphenylethylene, shut down the aryl-aryl bond formation, which agreed with the results reported by Itami *et al.*[32] They reported further studies that suggested the involvement of aryl radical anionic intermediates, such as **1.28** (Scheme 1.7). Under the optimised reaction conditions, only iodobenzene **1.7k** underwent coupling with benzene, whereas bromobenzene **1.1k** and chlorobenzene **1.27k** did not. In contrast, when 1-halo-4-iodobenzenes **1.7n,h,e** were reacted under the same reaction conditions, the terphenyl product **1.3i** was formed in high yields (68 – 74%), regardless of the halogen present (Scheme 1.7). It is proposed that the coupling reaction proceeds through the formation of an aryl radical from the haloarene, and this aryl radical couples to benzene to form the aryl-aryl bond (this will be discussed in more detail later, Scheme 1.11). The aryl radical is formed from iodobenzene **1.7k**, however chlorobenzene **1.27k** is not activated under these reaction conditions. Therefore, the observation that 1-chloro-4-iodobenzene **1.7e** efficiently coupled to benzene to give the terphenyl product **1.3i** suggests the involvement of a radical anionic intermediate **1.28** in the reaction pathway. The radical anionic intermediate **1.28e** undergoes the loss of a chloride anion, to form a second aryl radical that couples to benzene to form the observed product **1.3i**.
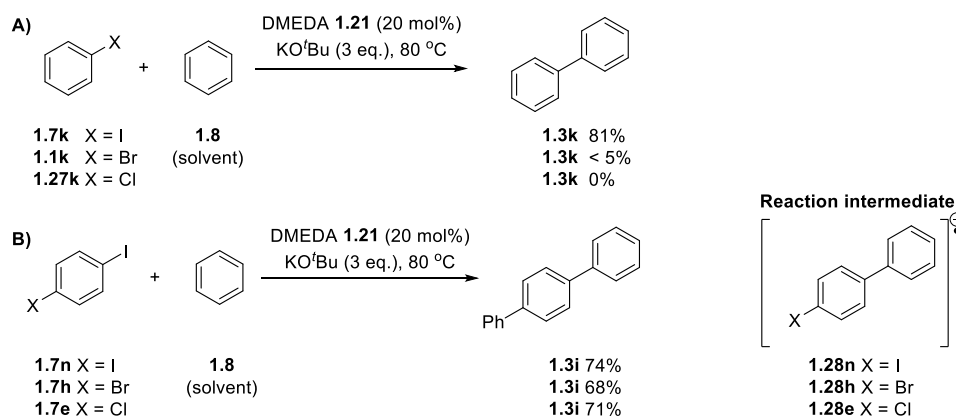
Scheme 1.7 A comparison of the reactivity of different halobenzenes and halo-4-iodobenzenes in the coupling reactions.[33]

Almost simultaneously, two research groups, Shi *et al.*[34] and Shirakawa and Hayashi *et al.*[35] described the coupling of haloarenes with benzene using 1,10-phenanthroline **1.29** as the additive. Shi *et al.*[34] reported the coupling of various iodoarenes **1.7** (and bromoarenes) with benzene **1.8**, using a combination of KO*t*Bu and 1,10-phenanthroline **1.29** (Scheme 1.8). Extensive control experiments were performed to confirm whether transition metals were involved in this coupling, including ICP-AES and inductively coupled plasma mass spectrometry (ICP-MS) analysis, which determined that metal species capable of performing C-H arylation were present in very low quantities (Pd, Fe, Cu: 10 ppb – 10 ppm). Studies were performed to increase the amount of metal by 10 – 1000 fold, and since the rate and yields remained unaffected, and sometimes decreased, it was concluded that aryl-aryl bond formations occurred in the absence of transition metal catalysts. Shi *et al.* suggested that the KO*t*Bu initiates the formation of an aryl radical from the haloarene molecule, and they proposed that the formation of the radical species is facilitated by 1,10-phenanthroline **1.29**. They proceeded to propose that an additional role of 1,10-phenanthroline **1.29** is that it forms the complex **1.30**, *via* π-stacking and π-ion interactions with both the potassium cation and benzene, and in doing so it activates benzene towards the C-H arylation (Figure 1.1). However, no evidence for this proposal was produced.
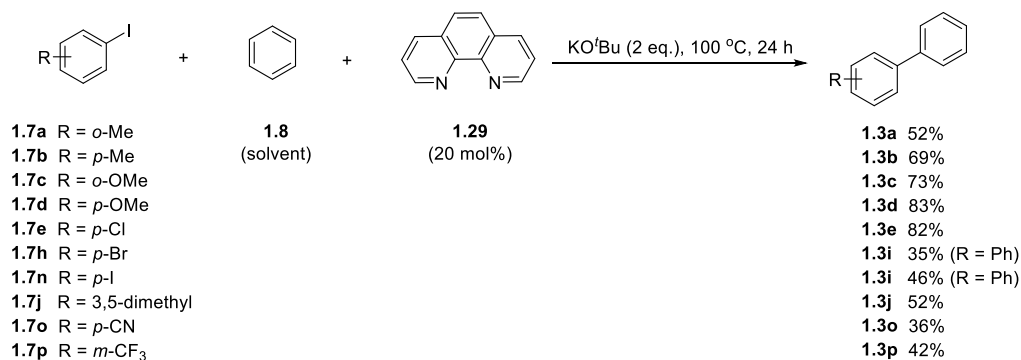
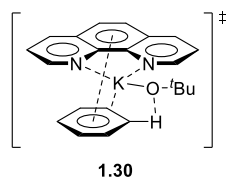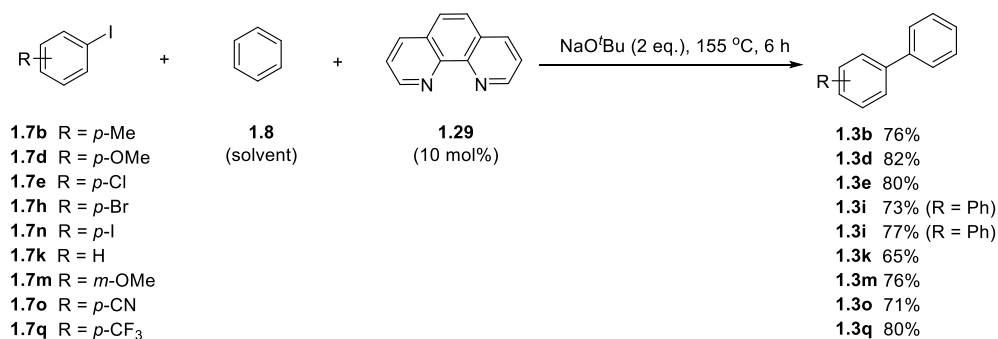**Scheme 1.8** Shi *et al.*[34] reported C-H arylation using KO*t*Bu and 1,10-phenanthroline **1.29**.

1.7a R = *o*-Me	**1.3a** 52%
1.7b R = *p*-Me	**1.3b** 69%
1.7c R = *o*-OMe	**1.3c** 73%
1.7d R = *p*-OMe	**1.3d** 83%
1.7e R = *p*-Cl	**1.3e** 82%
1.7h R = *p*-Br	**1.3i** 35% (R = Ph)
1.7n R = *p*-I	**1.3i** 46% (R = Ph)
1.7j R = 3,5-dimethyl	**1.3j** 52%
1.7o R = *p*-CN	**1.3o** 36%
1.7p R = *m*-CF$_3$	**1.3p** 42%

1.30

Figure 1.1 Shi *et al.*[34] proposed that the complex **1.30** forms by chelation of 1,10-phenanthroline **1.29** with the KO*t*Bu, to activate the C-H in benzene towards coupling.

Shirakawa and Hayashi *et al.*[35] also used 1,10-phenanthroline **1.29**, and its derivatives, as the additive in the coupling between iodoarenes and benzene. However, they reported the reaction was just as efficient when they used NaO*t*Bu, as opposed to KO*t*Bu, and therefore they used the sodium base throughout their publication (Scheme 1.9). However, the reaction temperatures they used are much higher (155 °C) than when KO*t*Bu was used by both Shi *et al.*[34] (100 °C) and Kwong and Lei *et al.* (80 °C).[33]

1.7b R = *p*-Me	**1.3b** 76%
1.7d R = *p*-OMe	**1.3d** 82%
1.7e R = *p*-Cl	**1.3e** 80%
1.7h R = *p*-Br	**1.3i** 73% (R = Ph)
1.7n R = *p*-I	**1.3i** 77% (R = Ph)
1.7k R = H	**1.3k** 65%
1.7m R = *m*-OMe	**1.3m** 76%
1.7o R = *p*-CN	**1.3o** 71%
1.7q R = *p*-CF$_3$	**1.3q** 80%

Scheme 1.9 Shirakawa and Hayashi *et al.* reported C-H activation promoted by NaO*t*Bu and 1,10-phenanthroline **1.29**.

Interestingly, when Shirakawa and Hayashi *et al.*[35] used KO*t*Bu they found the reaction proceeded at a faster rate. However they report lower product yields due to a side-reaction, which is the attack of a molecule of *tert*-butoxide onto a benzyne intermediate (Scheme 1.10). This is similar to the work reported by Daugulis *et al.*[29-31] and it highlights that caution should be taken when reporting the reaction of KO*t*Bu with haloarenes that are capable of forming benzyne intermediates, because it suggests that the benzyne formation competes with the proposed radical pathway involved in the aryl-aryl bond formation.

a. 18% conversion of 1.1b
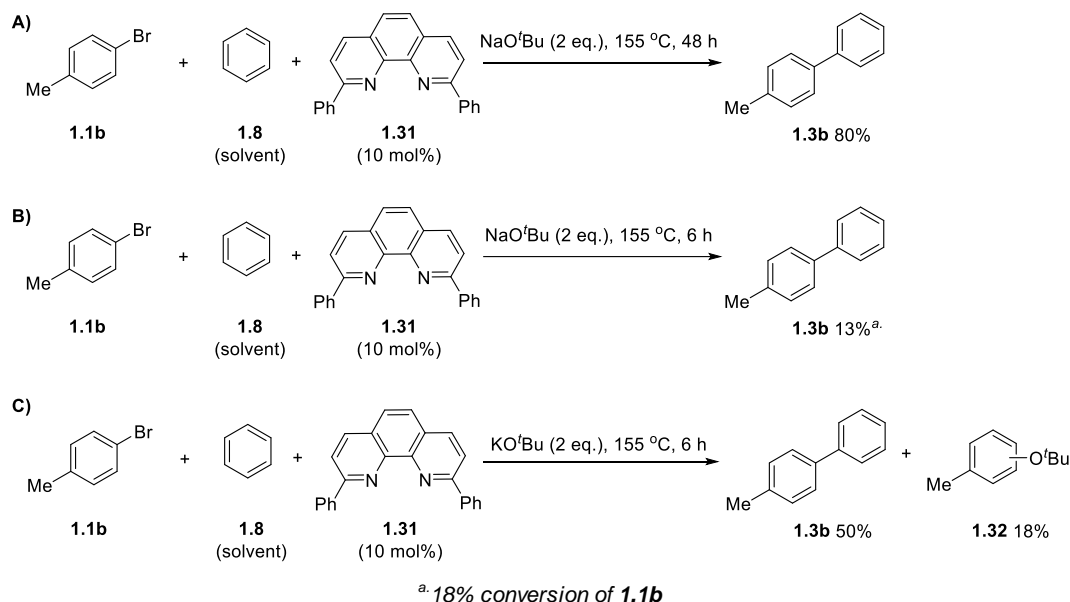
Scheme 1.10 Comparison of the effect of the counter-ion of the butoxide base.[35]

Despite this result, Shirakawa and Hayashi *et al.* reported that the reaction proceeded through a radical mechanism that involves a radical initiation step, whereby a single electron is donated to the 4-iodotoluene **1.7b** to form an aryl radical intermediate. They proposed an aryl radical intermediate because they observed complete regioselectivity in the products; the benzene added at the site where the halogen was in the starting haloarene. They further demonstrated that an aryl radical is formed in the reaction by performing the reaction of 4-iodotoluene **1.7b**, with 1,10-phenanthroline **1.29** and NaO*t*Bu, in d[8]-THF, which yielded 4-deuterotoluene (79%). This results from the aryl radical abstracting a deuterium atom from the solvent. (Interestingly 2% yield of the 4-deuteroiodotoluene was achieved in a background

reaction in the absence of base). They proposed that the aryl radical arises from SET from the butoxide anion, and they reported literature precedent for SET from alkoxides.[36-37] 1,10-Phenanthroline **1.29** was proposed to complex to the sodium cation of NaO*t*Bu, and this complex containing the butoxide anion was proposed to be the electron donor in this reaction.

The currently accepted mechanism for these transition metal-free couplings was proposed by Studer and Curran[38] a year later, and it is named the base-promoted homolytic aromatic substitution (BHAS) mechanism (Scheme 1.11). The BHAS mechanism involves a single electron being donated into the aryl halide, such as **1.7b**, to form the radical anion **1.33**. The formation of a radical anion **1.33** is supported within the literature by the studies reported by Kwong and Lei *et al*.[33] (discussed previously in Scheme 1.7). The radical anion **1.33** will undergo cleavage of the C-I bond to lose the iodide anion, and form the aryl radical **1.34**. The aryl radical **1.34** undergoes homolytic attack on benzene to generate the phenylcyclohexadienyl radical **1.35**, which undergoes deprotonation by the base, commonly KO*t*Bu, to form the biphenyl radical anion **1.36**. This intermediate **1.36** is a powerful reducing agent, which propagates the BHAS mechanism by donating an electron to the starting substrate, the aryl halide **1.7b**, to yield the observed product **1.3b** and a new aryl radical **1.34**. Although Studer and Curran proposed that the formation of the aryl radical might occur *via* electron transfer to the haloarene, they did not further elaborate on this initiation step. It should be noted that the formation of **1.34** from **1.7b** is proposed to proceed through the transient radical anion **1.33**. However, depending on the driving force for the single electron transfer in the initiation step, the SET and C-I bond cleavage may occur through a concerted mechanism instead.[39] Itami *et al*., Kwong and Lei *et al*., Shi *et al*. and Shirakawa and Hayashi *et al*. have suggested that the electron donor may be KO*t*Bu, however more recently, new evidence has been reported that suggests KO*t*Bu is not the electron donor, but rather an electron donor is formed *in situ*[40-45] in the basic reaction mixture (a more detailed discussion of this initiation is reported in Section 1.4.2).
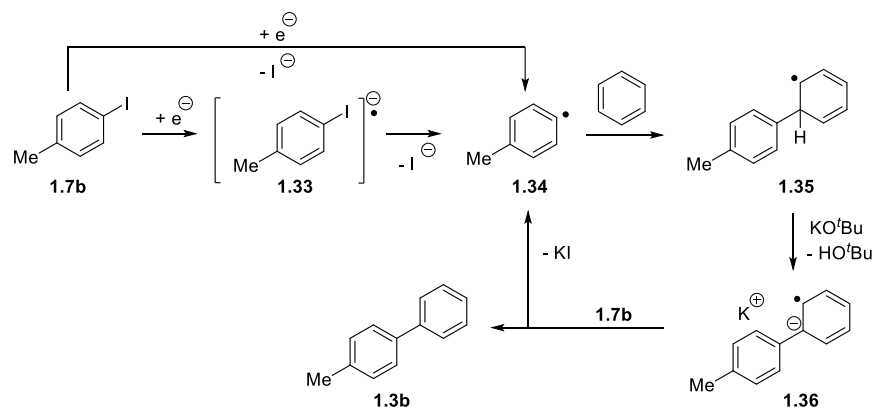
Scheme 1.11 The BHAS mechanism to achieve coupling of aryl halides, such as 4-iodotoluene **1.7b**, with benzene as reported by Studer and Curran.[38]

Since these initial reports, there has been an explosion of interest in this field of transition metal-free aryl-aryl bond formations through the BHAS mechanism. In particular, there have been numerous reports of many different additives that are capable of promoting these coupling reactions. The common feature of many of the additives reported is the presence of heteroatoms, which are capable of binding to or chelating to the metal cation of the butoxide base (either KO*t*Bu or NaO*t*Bu). This was observed by Jiang *et al.*[46] who proposed that a bidentate chelation to the potassium ion on KO*t*Bu is important to achieve the cross-coupling reaction. To find a new additive for these reactions that would perform the reaction at lower temperatures, they investigated several *N*-oxide or *N*-amino functionalised pyridines and related "ligands" for the reaction (Scheme 1.12). All succeeded in promoting aryl-aryl bond formation between aryl halides and benzene with low to high yields (34 – 88%). The most efficient ligand was quinoline-1-amino-2-carboxylate **1.40**, which was capable of promoting coupling with aryl bromides when the reaction temperature was increased to 120 °C [4-bromotoluene yielded **1.3b** (81%)]. The decreased reactivity of 4-bromotoluene, compared to 4-iodotoluene, is understandable based upon the BHAS mechanism proposed; the initiation step requires breakage of the C-X bond, and C-I bonds are weaker and hence easier to break, than C-Br bonds. Thus 4-bromotoluene requires higher temperatures for the reaction to occur. Jiang *et al.* proposed that strong interactions between the

potassium cation and the chelating additive (or ligand) can aid in the formation of the aryl radical in the initiation of the BHAS mechanism.

"Ligand"	Yield 1.3b
1.37	34%
1.38	47%
1.39	64%
1.40	88%
1.41	60%
1.20	67%
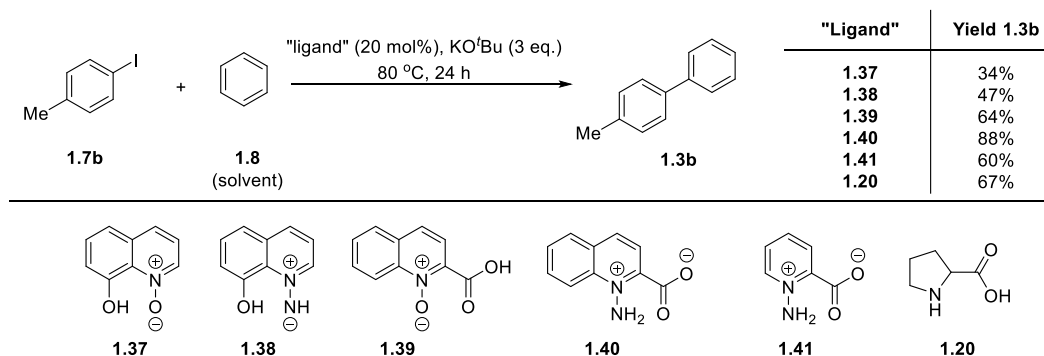
Scheme 1.12 Jiang *et al.* reported aryl-aryl bond formation using designed chelating "ligands" **1.37-1.41** and **1.20**.[46]
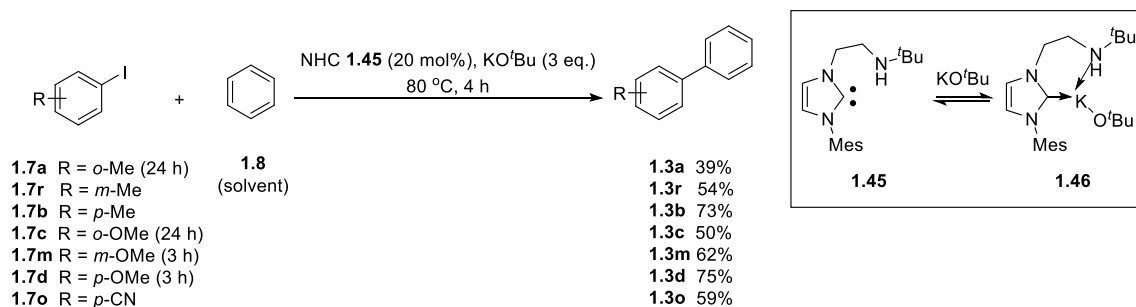
In an attempt to identify a heterogeneous system for these transition metal-free direct arylation between aryl halides and benzene, Jiang and Li *et al.*[47] assembled 2,2'-bipyridine-5,5'-dicarboxylate (bpydc), **1.42**, within an aluminium metal-organic framework (MOF) (Scheme 1.13A). The system worked well for iodoarenes, but also worked for bromoarenes if they were reacted at elevated temperatures (120 °C) with prolonged reaction times (60 h). Additionally, the system could be used to couple haloarenes to alternative unactivated arenes, **1.43a-b**, instead of benzene, with the expected regioselectivity observed for this radical addition (Scheme 1.13B).[48-49]
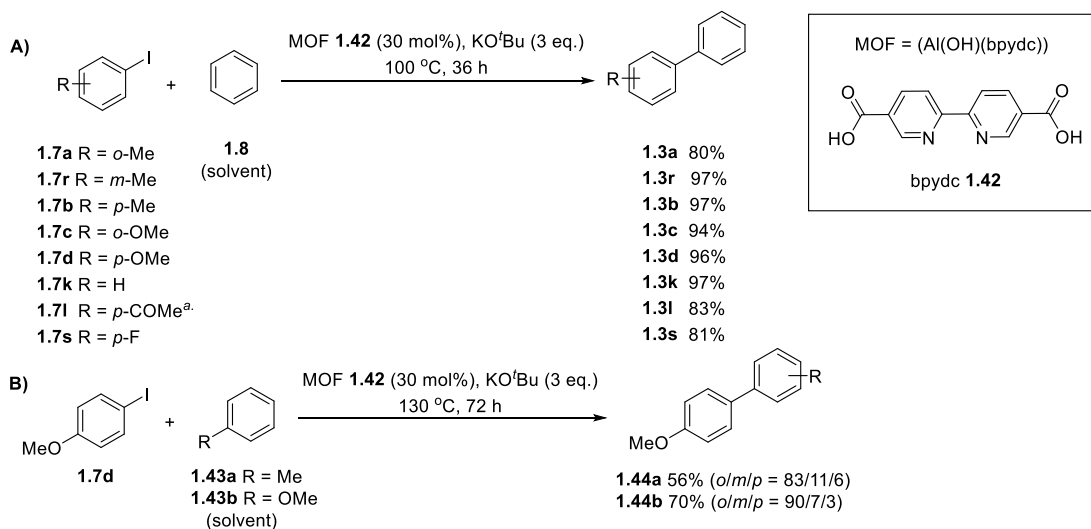
Scheme 1.13 Jiang and Li *et al.*[47] constructed an aluminium MOF containing bpydc **1.42** to achieve transition metal-free aryl-aryl bond formation.

Chen *et al.*[50] used *N*-heterocyclic carbene (NHC), **1.45**, as the organic additive, in combination with KO*t*Bu, to couple iodoarenes with benzene **1.8** (and pyridine **1.16**), in the absence of transition metals (Scheme 1.14). They proposed that the coupling is initiated by the formation of a KO*t*Bu-amino-NHC adduct **1.46**, which donates a single electron to the iodoarenes to form the aryl radical involved in the coupling. They reported electron paramagnetic resonance (EPR) studies to confirm that the reaction proceeds *via* radical intermediates, however they did not identify the radical species observed. They assumed that this radical species was the radical cation of the KO*t*Bu-amino-NHC adduct **1.46**, although efforts to identify the exact nature of the radical should be made. An NMR study identified that the role of the NHC **1.45** was acting as a "catalyst" because it was observed after the reaction. To my knowledge this is the first reported reaction of this nature where the additive was observed after the reaction was complete. However, no attempt was made to recover the NHC **1.45** and possibly what they observed at the end of the reaction was residual unreacted NHC **1.45** and, as such, the additive would not act catalytically. They also coupled 4-iodotoluene **1.7b** to pyridine **1.16** in the presence of the NHC "catalyst" **1.45** (80%, *o*/*m*/*p* : 2.5/1.9/1), which can be compared to the work of Itami *et al.* who performed the same coupling reaction but they did it without an additive, albeit using a stronger base, KO*t*Bu, and microwave irradiation.

1.7a R = *o*-Me (24 h)
1.7r R = *m*-Me
1.7b R = *p*-Me
1.7c R = *o*-OMe (24 h)
1.7m R = *m*-OMe (3 h)
1.7d R = *p*-OMe (3 h)
1.7o R = *p*-CN

1.8 (solvent)

1.3a 39%
1.3r 54%
1.3b 73%
1.3c 50%
1.3m 62%
1.3d 75%
1.3o 59%

Scheme 1.14 Chen *et al.*[50] reported that NHC **1.45**, in the presence of KO*t*Bu achieves coupling of haloarenes with benzene.

Throughout the literature many additives have been reported that, when used in combination with alkoxide bases (mainly KO*t*Bu), are capable of promoting transition metal-free cross-coupling upon thermal activation. Zeng *et al.*[51] synthesised a macrocycle **1.47** (Scheme 1.15) made up from five pyridone molecules, which they

proposed is capable of binding to the potassium cation to form a macrocycle-KO^{t}Bu complex. The mechanism proposed involves a SET from the macrocycle-KO^{t}Bu to the haloarene to initiate the BHAS mechanism. Many groups have tried the reaction with alternative bases during the optimisation investigations and discovered that KO^{t}Bu is often the most successful, whilst NaO^{t}Bu often gives a lower yields or lower rate of formation of products. It is believed that the KO^{t}Bu is more electron-rich at the alkoxide moiety due to the highly ionic bond to the potassium counter-ion, and therefore some authors propose that the *tert*-butoxide is a better electron donor when potassium is the counterion. It was proposed that removal of the potassium counterion, using the macrocycle **1.47**, would make the *tert*-butoxide anion more basic and hence more electron-rich for SET. Interestingly, this contradicts previous reports in the literature by Kwong and Lei *et al*.,[33] whereby the addition of 18-crown-6 ether to the KO^{t}Bu reactions resulted in lower yields of product. However, it must be stated that the addition of the macrocycle **1.47** or 18-crown-6 ether could play alternative roles in the reaction than has been proposed.
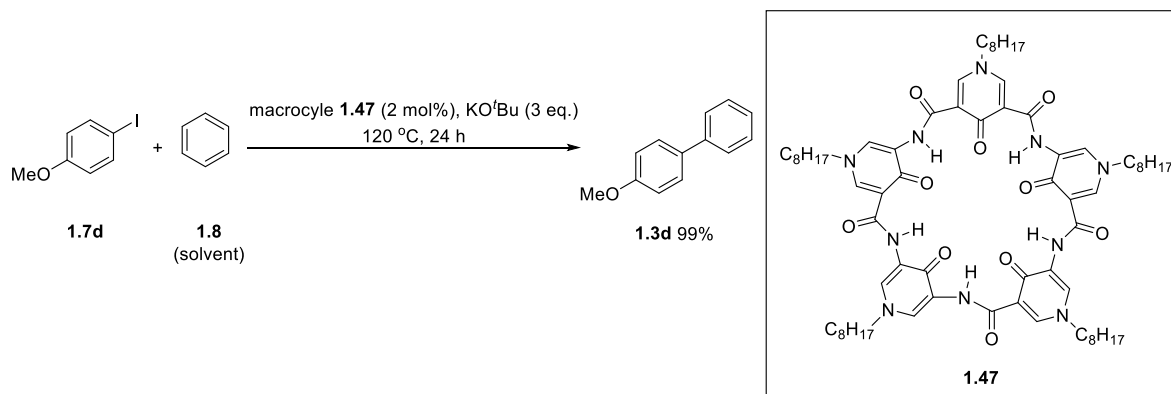
Scheme 1.15 The macrocycle **1.47** used by Zeng *et al*.[51] to promote transition metal-free biaryl synthesis.

The initial reports of transition metal-free aryl activations employed simple organic molecules, such as DMEDA **1.21** and 1,10-phenanthroline **1.29**, that are commercially available and cheap. The additives used by Jiang *et al*., Jiang and Li *et al*., Chen *et al*. and Zeng *et al*. are more complex molecules than those initially reported to the point where Jiang and Li *et al*. required pre-assembly of the additive,
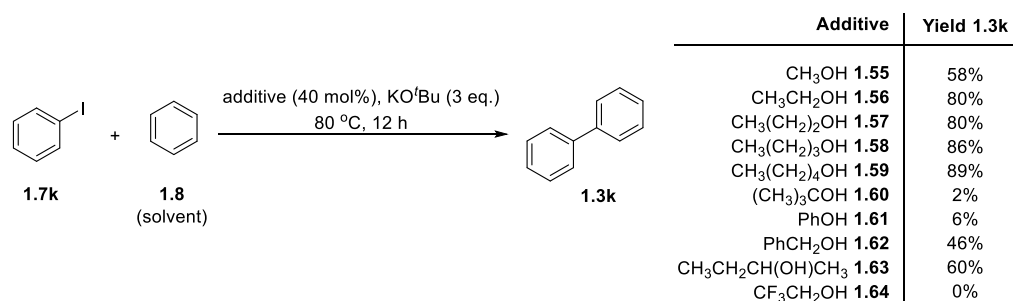
bpydc **1.42**, in a MOF prior to the aryl-aryl bond formation reaction (discussed previously Scheme 1.13).

More recently, Tanimoro *et al.*[52] and Liu *et al.*[53] have returned to investigating the ability of simple organic molecules to achieve this BHAS mechanism in the presence of KO*t*Bu. Tanimoro *et al.*[52] demonstrated that amino acids and their derivatives were often efficient additives for the coupling of 4-iodoanisole **1.7d** with benzene *via* the BHAS mechanism (Scheme 1.16). In particular, *L*-proline **1.20** and sarcosine **1.48** gave high yields of the coupled product **1.3d** (87% and 80% respectively). This observation can be compared to other reports within the literature that use *L*-proline **1.20** and KO*t*Bu to achieve the coupling between 4-iodotoluene and benzene (discussed previously Scheme 1.6 and 1.12); Kwong and Lei *et al.*[33] and Jiang *et al.*[46] achieved formation of 4-methylbiphenyl at 80 °C in 34% and 67% respectively. The method Tanimoro *et al.* reported was applicable to a gram scale coupling of 4-iodopentylbenzene and benzene to yield 1-pentyl-4-phenylbenzene (76%), a building block in materials chemistry for liquid crystals. The mechanism they propose is initiated by an electron donation from a complex of KO*t*Bu and *L*-proline **1.20**. It must be noted, however, that, in the absence of any additive, the coupling of 4-iodoanisole **1.7d** with benzene still yielded **1.3d** (35%). This result suggests that at these high temperatures (150 °C) the iodoarenes undergo an additional pathway to form these products; however they did not propose any explanation. Relating these results to those previously reported by Shirakawa and Hayashi *et al.* (performed at 155 °C, Scheme 1.10B) highlights the need to question whether the haloarene, such as **1.7d**, involved in the coupling could, in the presence of KO*t*Bu, form benzyne intermediates, which can couple to benzene to form the observed product.[35,44]
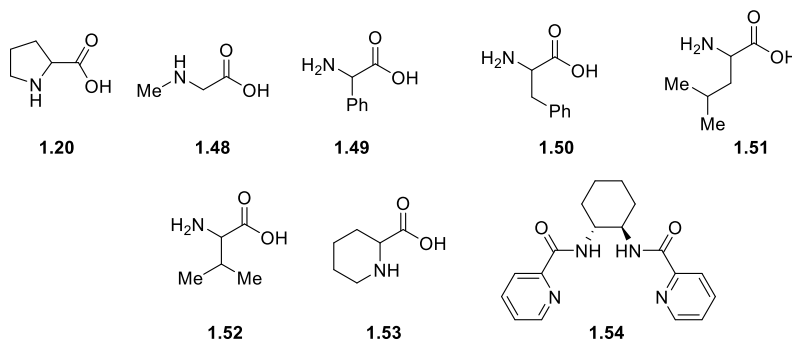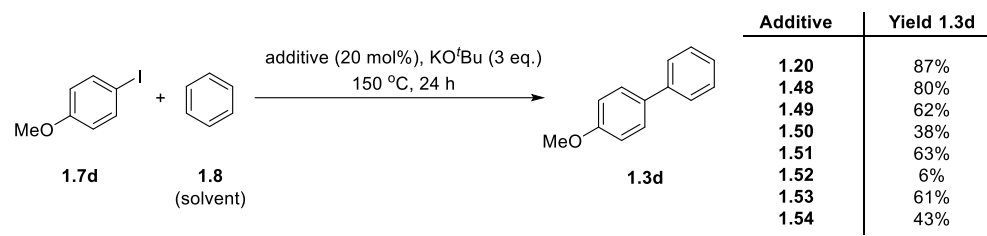
Scheme 1.16 Tanimoro *et al.* reported coupling 4-iodoanisole with benzene in the presence of amino acids and their derivatives.

Liu *et al.*[53] investigated the efficiency of simple alcohols at promoting the transition metal-free coupling of iodoarenes and benzene in the presence of KO^{t}Bu. Various alcohols were successful at promoting this reaction to produce biaryl products in moderate to high yields depending on the structure of the alcohol employed (Scheme 1.17). So far within the literature the proposed initiation step when 1,10-phenanthroline **1.29** or bidentate heteroaromatic compounds are employed as additives in the BHAS reactions, is that these additives act as "ligands" to bind to the metal cation of the base and form a complex, which is capable of donating electrons. However, Liu *et al.* used alcohols incapable of chelation and thus the initiation process may proceed *via* a mechanism different to that which many have postulated, or the mechanism may be different depending on the additives used. Instead, they postulated that the combination of the alcohols and KO^{t}Bu generated *in situ* alkoxide bases that promote the generation of the aryl radical and hence initiate the BHAS mechanism. The structure of the alcohol, and hence the alkoxide base, was believed to be influential in the initiation of the reaction, *i.e.* the SET step.

Additive	Yield 1.3k
CH$_3$OH **1.55**	58%
CH$_3$CH$_2$OH **1.56**	80%
CH$_3$(CH$_2$)$_2$OH **1.57**	80%
CH$_3$(CH$_2$)$_3$OH **1.58**	86%
CH$_3$(CH$_2$)$_4$OH **1.59**	89%
(CH$_3$)$_3$COH **1.60**	2%
PhOH **1.61**	6%
PhCH$_2$OH **1.62**	46%
CH$_3$CH$_2$CH(OH)CH$_3$ **1.63**	60%
CF$_3$CH$_2$OH **1.64**	0%

Scheme 1.17 Liu *et al.*[53] showed that simple alcohols are successful at promoting biaryl synthesis.

Within the reports described thus far in this chapter, very few examples achieved efficient coupling of bromoarenes to benzene unless high temperatures were employed. In 2014, Kwong *et al.*[54] reported that a combination of KO*t*Bu and 2-pyridyl carbinol **1.65** is capable of promoting the coupling of bromoarenes to benzene even occur at room temperature (RT), albeit with lower yields and after prolonged reaction time (Scheme 1.18).
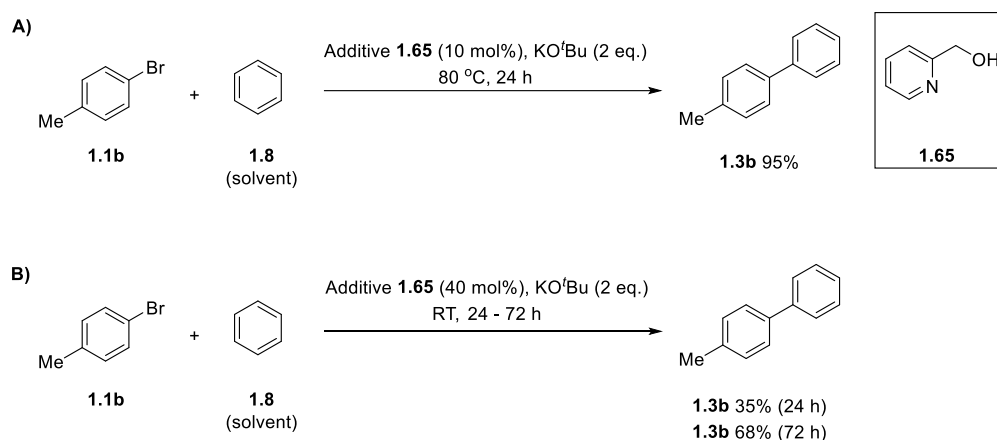
Scheme 1.18 Kwong *et al.*[54] showed that 2-pyridyl carbinol **1.65** efficiently couples bromoarenes with benzene under transition metal-free reaction conditions.

Finally, some of these reactions have also been reported to occur in alternative solvents to benzene, such as DMF, whereby the solvent is no longer acting as the coupling partner. Gryko *et al.*[55] reported the coupling of iodoarenes with *N*-methylpyrrole **1.66** in the presence of LiO*t*Bu and DMF as the solvent, without the need for any additional additives (Scheme 1.19). Interestingly they found that the reaction did not occur if DMF was not present as the solvent, and when the reaction

was performed in neat *N*-methylpyrrole **1.66** no product was formed, suggesting that DMF was crucial for the reaction (this will be elaborated on in Section 1.3 and 4.4).


1.7d R = *p*-OMe	**1.67d** 52%
1.7o R = *p*-CN	**1.67o** 90%
1.7t R = *m*-CN	**1.67t** 70%
1.7u R = *o*-CN	**1.67u** 55%
1.7v R = *p*-NO$_2$	**1.67v** 92%
1.7w R = *m*-NO$_2$	**1.67w** 83%
1.7x R = *o*-NO$_2$	**1.67x** 61%
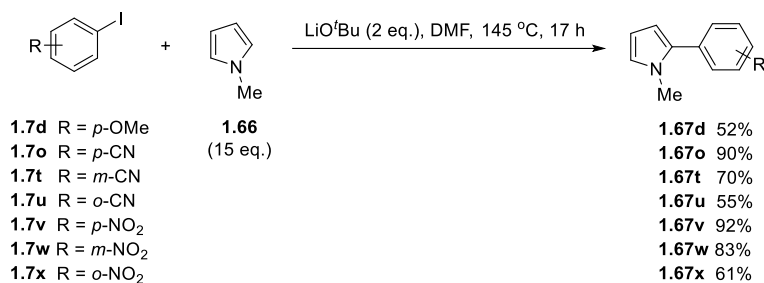
Scheme 1.19 Gryko *et al.*[55] reported coupling between iodoarenes and *N*-methylpyrrole **1.66** in DMF.

1.2.2.2 Intramolecular cyclisations

The majority of publications within this field of chemistry have focused on intermolecular aryl-aryl bond formations but a few intramolecular reactions have also been reported. Fused aryl ring moieties are common substructures within drug-like molecules and natural products, and are currently synthesised by transition metal-mediated processes within industry, so a transition metal-free option is desirable, especially within pharmaceutical industries.

As already mentioned, Shi *et al.*[34] reported an intermolecular coupling reaction between a broad scope of haloarenes and unactivated benzene using KO*t*Bu and sub-stoichiometric quantities of 1,10-phenanthroline **1.29** under thermal reaction conditions. Within the same publication, they reported an intramolecular cyclisation of **1.68** under similar reaction conditions (Scheme 1.20A). Due to the applications of fused ring systems within commercial products, Shi *et al.*[56] further investigated these intramolecular cyclisations. In 2011, they published an intramolecular BHAS synthesis of 6*H*-benzo[*c*]chromene **1.69** using 1,10-phenanthroline derivatives, of which neocuproine **1.71** was the most efficient (Scheme 1.20B). Shi *et al.*[56] reported that the reaction was performed in various solvents, and they found that changing the solvent affected the product distribution; the BHAS cyclised product **1.69** was the major product in benzene or toluene, but by-products such as the reduced substrate **1.72** or the benzene-coupled product **1.73** also formed within the reaction. They also explored other substrates that contained alternative heteroatoms in the tether

between the haloarene moiety and the unactivated arene moiety. They found that the cyclisation was possible if the linker contained a tertiary amine, a thioether or if it was simply a carbon chain.
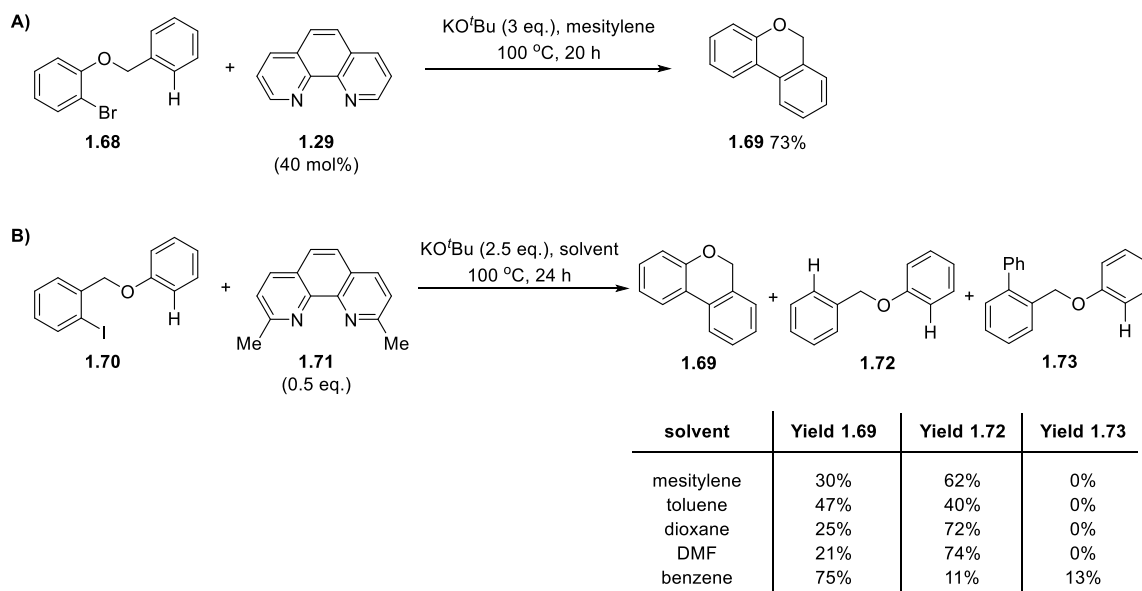
Scheme 1.20 The intramolecular reaction of **1.68** and **1.70**, promoted by KO*t*Bu and either 1,10-phenanthroline **1.29** or neocuproine **1.71**.

Charette *et al.*[57] reported the intramolecular cyclisation of similar tethered species to those reported by Shi *et al.*[56], however they used pyridine as the solvent and microwave conditions (µW) to achieve the BHAS cyclisation of the bromine-containing substrates **1.68**, **1.74** and **1.75**, in the presence of 1,10-phenanthroline **1.29** and KO*t*Bu (Scheme 1.21A). They observed that 1,10-phenanthroline **1.29** was not required in the cyclisation of the iodine-containing substrates **1.78**, **1.79** and **1.80** (Scheme 1.21B). A comparison of the reaction conditions reported in this work, for the cyclisation of the iodine-containing substrates, to those reported by Itami *et al.*,[32] shows that they are both common in that no external additives were required if the reaction was performed in pyridine as the solvent. Itami *et al.* coupled iodobenzene to pyridine using KO*t*Bu alone, however his conclusion at the time was that both KO*t*Bu and an additive, pyridine in this case, form a complex *in situ*, which is capable of promoting the radical chain reaction. As such, a possible explanation for the cyclisation in the absence of 1,10-phenanthroline **1.29**, is that pyridine is capable of

performing a similar role to 1,10-phenanthroline **1.29** in the initiation of the BHAS radical chain pathway.
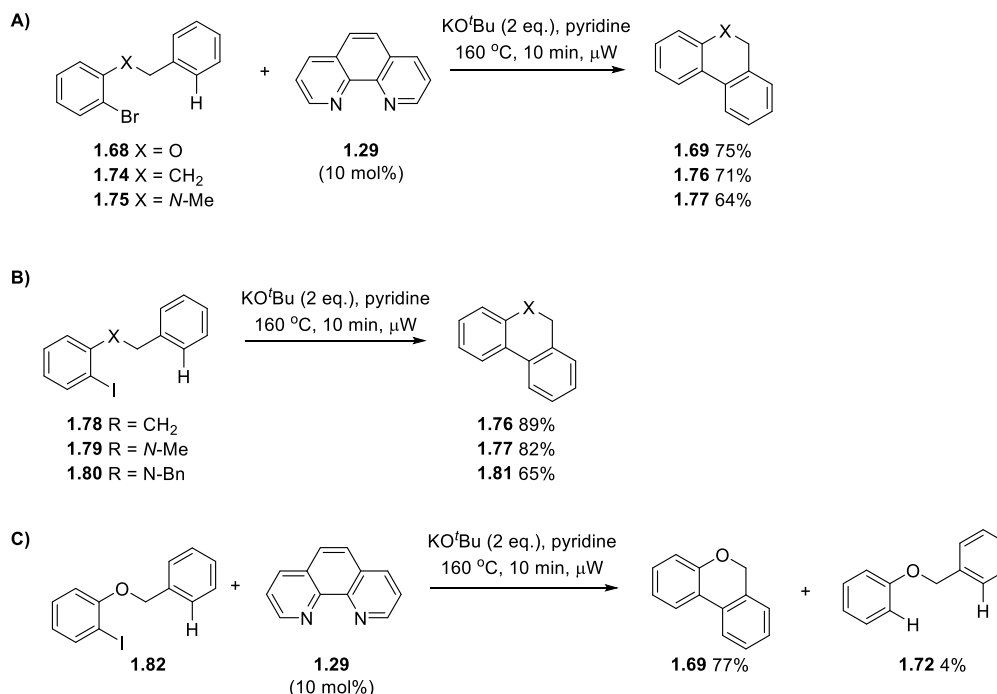
Scheme 1.21 Charette *et al.*[57] reported intramolecular cyclisation through aryl-aryl bond formation.

The yield of the major product **1.69** obtained under these conditions (Scheme 1.21A) was similar to that reported by Shi *et al.*[56] (Scheme 1.20A). However, for the iodine analogue **1.70** *vs.* **1.82** the two groups reported different yields of by-products, which provides a contrast between the two methods (Scheme 1.20B and 1.21). Charette *et al.* reported only a minor yield (4%) of the reduced product **1.72** and any possible products that may arise from the coupling of the aryl radical and the solvent were not reported.

The unsaturated analogue to product **1.77** resembles a phenanthridine core, which is a relevant pharmaceutical structure found in natural products.[58-59] Kwong *et al.*[60] demonstrated that these structures could be synthesised using the transition metal-free approach by subjecting substrates **1.83a-d** to KO*t*Bu and 1,2-ethanediol **1.84** as the additive (Scheme 1.22). They reported that using the 1,2-ethanediol **1.84** as the additive in the reaction was applicable to chloroarenes, unlike the 1,10-

phenanthroline **1.29** (7%) or DMEDA **1.21** (0%) which were only applicable to initiate the reaction of iodo- or bromoarene analogues.

1.83a R = H
1.83b R = *o*-OMe
1.83c R = *m*-CN
1.83d R = *m*-Ph

1.84
(10 mol%)

KO*t*Bu (2 eq.), toluene, 120 °C, 18 h

1.85a 98%
1.85b 94%
1.85c 88%
1.85d 90%
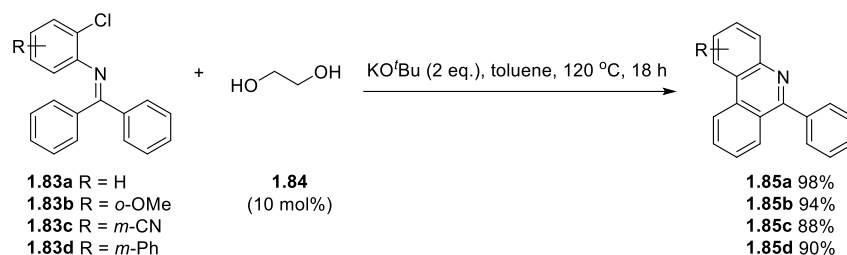
Scheme 1.22 Kwong *et al.*[60] reported the formation of phenanthridine-core molecules **1.85** using KO*t*Bu and 1,2-ethanediol **1.84**.

In reactions that require a C-X bond cleavage, C-Cl bonds are harder to react compared to C-Br and C-I, because the C-Cl bond has the highest bond dissociation energy (BDE). Kwong *et al.*[60] suggested that the mechanism involves complexation between the potassium cation of KO*t*Bu and 1,2-ethanediol **1.84**, and in the presence of this complex, a single electron is transferred into the haloarene moiety in substrates **1.83a-d** to initiate the radical BHAS cycle. It was proposed that good complexation between the 1,2-ethanediol and the potassium cation is crucial for the initiation step of the reaction to occur, because diols that contained a longer carbon chain between the terminal alcohols, such as 1,3-propanediol and 1,4-butanediol generated low yields of cyclised product **1.85a** (48% and 34% respectively) in the optimisation studies, supposedly due to weaker complexation of the potassium cation. This work presented by Kwong *et al.*[60] is comparable to previous work by Kwong and Lei *et al.*[33] who reported using DMEDA **1.21** and diols, such as *cis*-1,2-cyclohexanediol **1.25**, for intermolecular coupling of haloarenes with benzene. However, this work by Kwong *et al.*[60] describes efficient activation of C-Cl bonds, which has not been reported previously. Another interesting result from this paper is that during the optimisation steps performed by Kwong *et al.*,[60] they attempted using *tert*-butanol to see the effect of using a simple alcohol at promoting these couplings. A low yield of cyclised product **1.85a** (26%) was achieved; however, this result demonstrates that the proposed mechanism, which involves chelation of the potassium cation, may not be the mode of initiation because alcohols, such as *tert*-

butanol, are not capable of chelating with KO*t*Bu, and therefore an alternative mechanism is likely for the initiation step. In agreement with this result, Liu *et al.*[53] more recently reported that simple alcohols can perform the BHAS reaction. When they employed *tert*-butanol, only trace yields (2%) of product were isolated, however other simple alcohols such as butanol gave high yields of coupled product. This suggests that chelation is not required for the initiation step of the BHAS mechanism and further work is required to shed light on the initiation step of this mechanism.

The phenanthridinone motif **1.87** is another relevant building block in pharmaceutical chemistry due to the biological activity of the moiety. In 2012, Kumar *et al.*[61] reported the successful synthesis of phenanthridinones **1.87** and 7-membered lactams **1.90** *via* C-H arylation of the amides **1.86** or **1.89** respectively, using KO*t*Bu and 1,10-phenanthroline **1.29** under thermal conditions (Scheme 1.23A and 1.23C). It must be noted that they also employed azobisisobutyronitrile (AIBN) **1.88** to achieve these transformations, and in that case the product yield was improved and all the starting material was consumed to form product **1.87** (96%) (Scheme 1.23B).
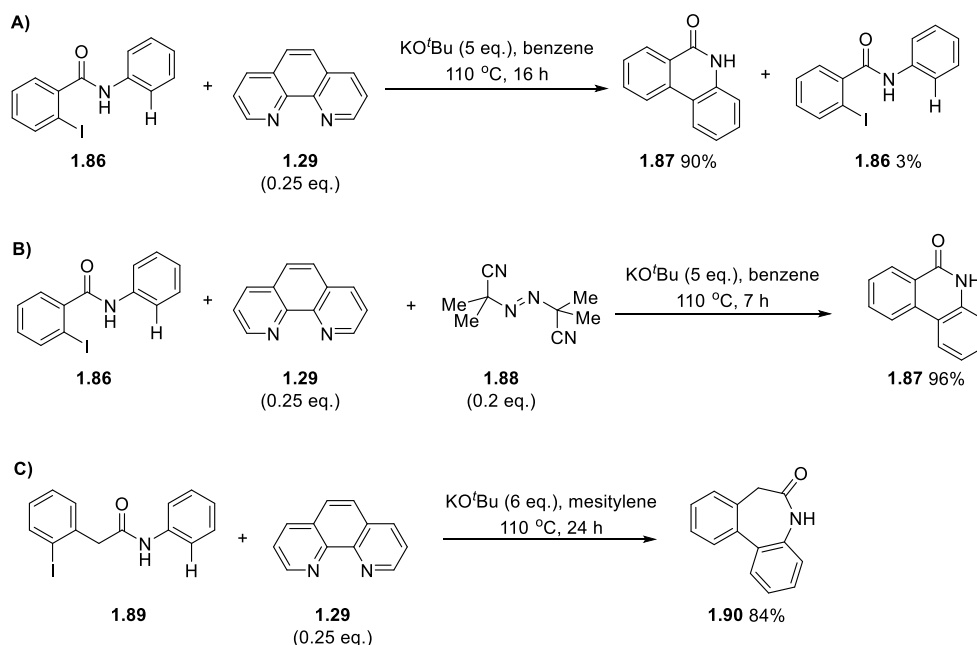
Scheme 1.23 Cyclisation of substrates **1.86** and **1.89** to form **A)-B)** phenanthridone **1.87** and **C)** 7-membered lactams **1.90** as reported by Kumar *et al.*[61]

It was suggested that the ligand 1,10-phenanthroline **1.29** or AIBN **1.88** were not crucial in the reaction, as the KO*t*Bu alone produced cyclised product **1.87** (35%, and 60% recovered starting material **1.86**) in an overnight reaction. It was therefore proposed that the KO*t*Bu was responsible for generating the aryl radical, and the role of 1,10-phenanthroline **1.29** was to make the SET more efficient. Protection of the nitrogen in the amide tether with a methyl group lowered the yield of cyclisation to form the *N*-methyl analogue of **1.87** (28%). This agrees with the work of Charette *et al.*[57] who also reported a low yield of the *N*-methyl analogue of **1.87** (43%) when cyclising the *N*-methyl protected analogue of **1.86** under their reaction conditions [1,10-phenanthroline **1.29** (10 mol%), KO*t*Bu, pyridine, 160 °C, 10 min, μW]. The reaction mechanism Kumar *et al.*[61] proposed, based on the results presented in their paper, proceeds by an initial deprotonation of the amide nitrogen, followed by a SET from KO*t*Bu to the haloarene moiety of the substrates **1.86** or **1.89**, to form their respective aryl radicals by cleavage of the C-I bond. In comparison with this work, Charette *et al.*[57] reported that the cyclisation of a similar substrate, containing a tertiary amine tether instead of the amide tether, was achieved in high yields (64% - 82%) (previously discussed in Scheme 1.21). This suggests that under their conditions they did not require the deprotonation of the nitrogen in the tether to achieve successful synthesis of phenanthridine-type core structures, unlike Kumar *et al.*[61]

In contrast to this last statement, a paper published by Bisai *et al.*[62] also reported that the cyclisation of substrates **1.91** and **1.92**, which both contain a tertiary amide tether, was efficient under their reaction conditions (Scheme 1.24). They used this protocol to synthesise pyrrolo- and dihydrophenanthridine core structures, which are structures found in several alkaloids in nature.

		KO*t*Bu (3 eq.), mesitylene, 100 °C, 5 - 7 h	
1.91a *n* = 1, X = I	**1.29**		**1.93** 56%
1.91b *n* = 1, X = Br	(0.4 eq.)		**1.93** 60%
1.92a *n* = 2, X = I			**1.94** 56%
1.92b *n* = 2, X = Br			**1.94** 61%
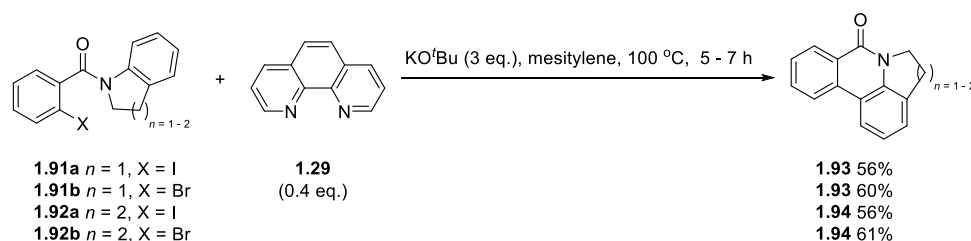
Scheme 1.24 Bisai *et al.*[62] reported cyclisation of substrates **1.91 – 1.92** to form products **1.93-1.94**.

An interesting application of these intramolecular transition metal-free cyclisations was reported by Masters and Bräse.[63] They reacted two substrates, **1.95** and **1.98**, that contained an acetal tether between a haloarene moiety and an unactivated arene, in contrast to the amide linkers previously reported by Kumar *et al*.[61] and Bisai *et al*.[62] After the cyclisation, the acetal group was hydrolysed to afford the diphenol products **1.97** and **1.100** (Scheme 1.25).
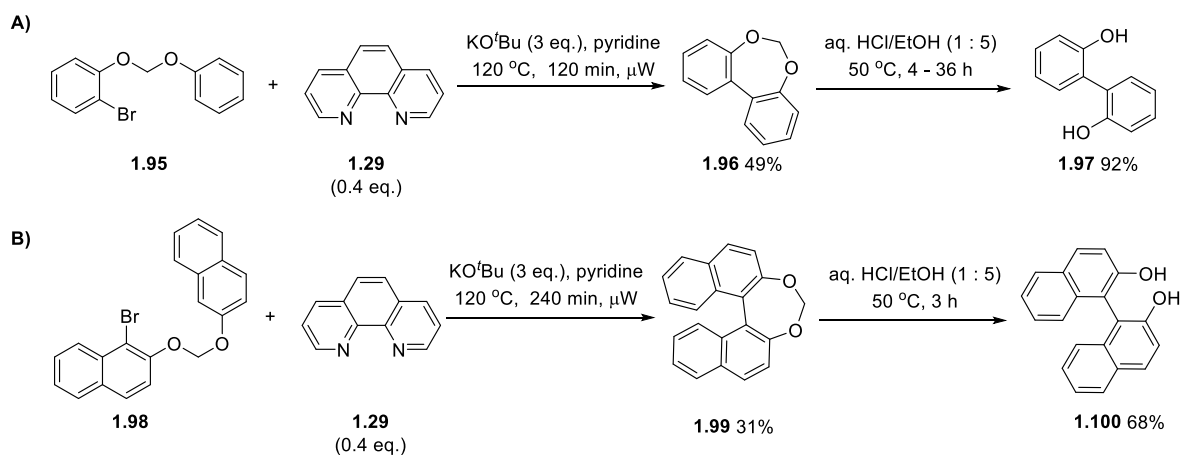
Scheme 1.25 Masters and Bräse[63] used acetal linkers in the synthesis of *ortho,ortho*-diphenols **1.97** and **1.100**.

The transition metal-free reactions described so far have been proposed to proceed *via* the BHAS pathway,[38] which is a mechanism that is now generally accepted within the research community; however the initiation step of this mechanism has been under some debate over the last few years. Many papers reported within this section propose that both the additive and base are vital for the BHAS reaction. They propose that the organic additives chelate to the KO^{t}Bu, and either this complex, or KO^{t}Bu alone, can donate an electron to haloarenes to initiate the BHAS mechanism. However, there are some inconsistencies within the literature that do not support this reaction pathway, such as the success of simple mono-alcohols at promoting these reactions, even though they cannot chelate to the potassium counterion of the *tert*-butoxide base. Additionally, some reactions proceed even without an additive under some reaction conditions (commonly when pyridine is the solvent), whilst others require an additive to get any reaction at all. Recent reports by Murphy *et al*.[42,44]

have proposed an alternative mode of initiation in these reaction conditions (discussed in Section 1.4.2).

1.2.3 Light irradiation

The transition metal-free reaction conditions have been studied in great detail recently because the reaction conditions could potentially be developed in order to identify alternative reaction conditions that are efficient enough to compete with the well-known palladium-catalysed cross-coupling reactions. In addition to the transition metal-free reaction conditions recently discovered, which use high temperatures and benzene as the common solvent for the reactions, light irradiation can be used to activate haloarenes towards coupling with an unactivated arene, to form biaryl structures in the absence of transition metals.

Rossi *et al.*[64] recently described the photoinduced coupling of iodoarenes **1.7** with benzene in the presence of KO^{t}Bu at room temperature using light irradiation (HPI-T 400 W lightbulbs), without the need for any organic additives (Scheme 1.26). The mechanism proceeds *via* the BHAS mechanism described by Studer and Curran (previously discussed in Section 1.2.2, Scheme 1.11).[38] The initiation step is a photo-induced SET to the haloarene, which leads to the cleavage of the C-I and the formation of the aryl radical, however Rossi *et al.* did not indicate what species or complex is capable of performing this initiation step.

1.7a R = *o*-Me	**1.8**	**1.3a** 61%
1.7r R = *m*-Me	(solvent)	**1.3r** 83%
1.7b R = *p*-Me		**1.3b** 91%
1.7c R = *o*-OMe		**1.3c** 84%
1.7d R = *p*-OMe		**1.3d** 97%
1.7i R = *p*-Ph		**1.3i** 74%
1.7k R = H		**1.3k** 90%
1.7o R = *p*-CN		**1.3o** 85%
1.7q R = *p*-CF$_3$		**1.3q** 61%
1.7y R = *p*-NH$_2$		**1.3y** 44%
1.7z R = *p*-CO$_2$^{t}Bu		**1.3z** 67%
1.7aa R = *p*-CONH$_2$		**1.3aa** 76%
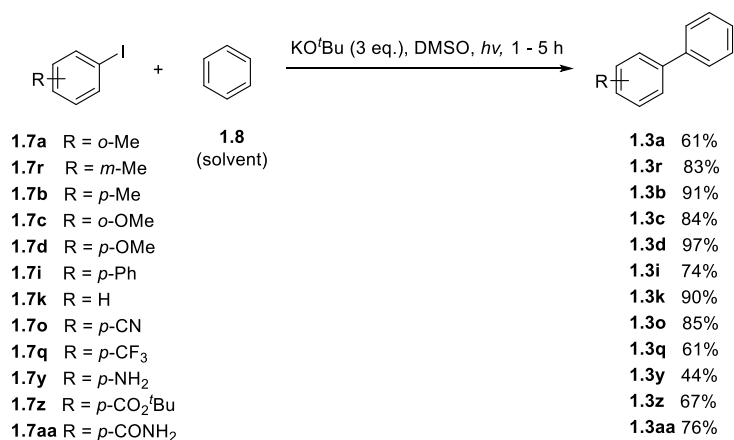
Scheme 1.26 Rossi *et al.*[64] reported photoinduced "C-H activation" to couple aryl halide with benzene.

A paper reported by Zheng and Guo *et al.*[65] use light irradiation (λ = 254 nm) to achieve the coupling of haloarenes with benzene at room temperature, using *N,N'*-tetramethylethylenediamine (TMEDA) **1.22** as an additive (Scheme 1.27). When compared with the initial publication by Kwong and Lei *et al.*,[33] they reported that TMEDA **1.22** was unsuccessful for these transformations under thermal reaction conditions (80 °C) (previously shown in Scheme 1.6). This highlights the ability of light irradiation to access these reactions under milder conditions.
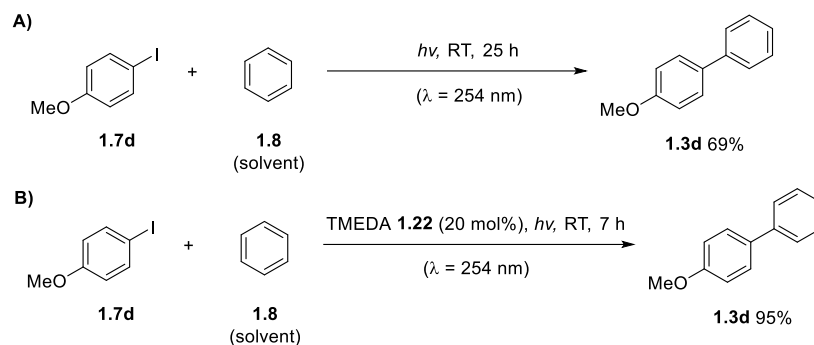
Scheme 1.27 Zheng *et al.*[65] reported light irradiation in the presence of TMEDA **1.22** successfully yielded coupled product under mild reaction conditions.

1.3 Transition metal-free alternative bond formations

There are many examples in the literature of various additives that, in the presence of a strong base like KO*t*Bu, are capable of performing transition metal-free biaryl synthesis through a BHAS mechanism. However, within this field of research, little is reported on the successful applications of these conditions to achieve alternative transformations, away from aryl-aryl bond formations.

Itami *et al.*[32,66] reported on two different occasions the coupling between aryl halides and either alkenes or alkanes (Scheme 1.28); in 2008, Itami *et al.*[32] successfully coupled iodostyrene **1.101** and pyrazine **1.18** to generate product **1.102** in low yields (33%), and in 2009,[66] they reported successful coupling between pyrazine **1.18** and cyclohexane **1.103** in the presence of iodobenzene **1.7k**.
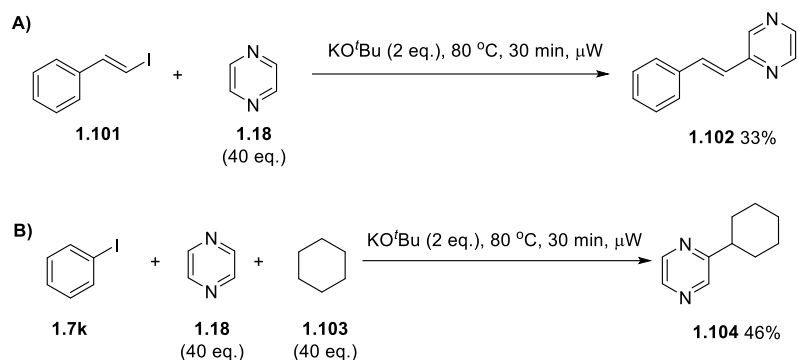
Scheme 1.28 Itami *et al*.[32,66] reported the coupling of **A)** iodostyrene **1.101** with pyrazine **1.18**, and **B)** pyrazine **1.18** with cyclohexane **1.103** in the presence of iodobenzene **1.7k**.

Several groups have also investigated the coupling of haloarenes to alkenes, which shows similar reactivity to the Mizoroki-Heck reaction. Shi *et al*.[67] demonstrated that haloarenes could couple to substituted styrenes **1.106a-g**, in the presence of KO*t*Bu and bathophenanthroline **1.105** (Scheme 1.29A). The bathophenanthroline additive **1.105** was vital for the reaction to proceed and a broad substrate scope demonstrated that the synthesis tolerated various substituents on the haloarenes, however, aliphatic alkenes were not tolerated as reaction partners. They also reported an intramolecular example of this reaction (Scheme 1.29B).
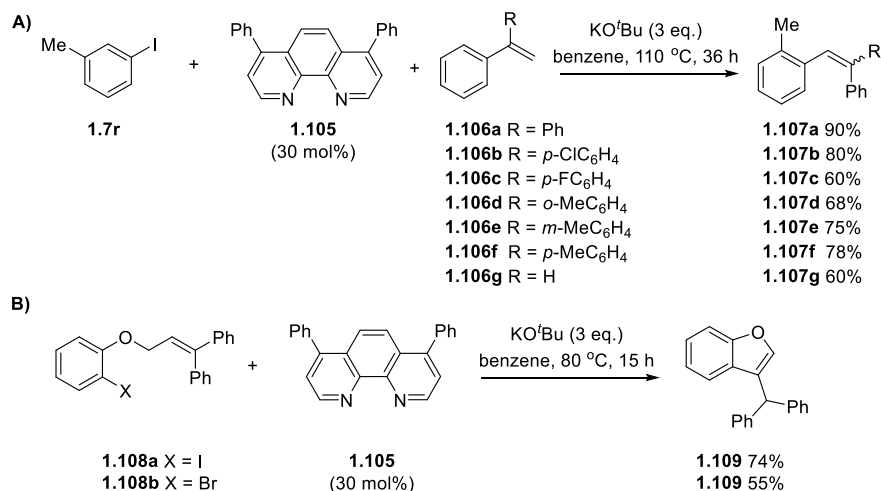
Scheme 1.29 Shi *et al*.[67] reported coupling between haloarene and substituted styrene either **A)** intermolecularly or **B)** intramolecularly.

Similar results were published by Rueping *et al*.[68] who performed the intramolecular Heck-type reactions in the formation of various analogues of benzofuran **1.109**. The

reaction proceeded by SET to the haloarene, followed by loss of the iodide anion and the resulting aryl radical underwent 5-*exo*-cyclisation onto the alkene moiety to eventually afford the product **1.109** in moderate yield (63%). Compared to the reaction conditions of Shi *et al.*, Rueping *et al.* used much higher temperatures, 160 °C, for 2 hours and 1,10-phenanthroline **1.29** as the additive; however, they expanded the scope of aryl substituents that can be present on the alkene moiety. Additionally, other intermolecular examples of coupling of haloarene to styrene were reported by Murphy *et al.*[41] who used *N,N'*-dipropyldiketopiperazine (DKP) **1.110** as the additive to achieve the coupling (Scheme 1.30).
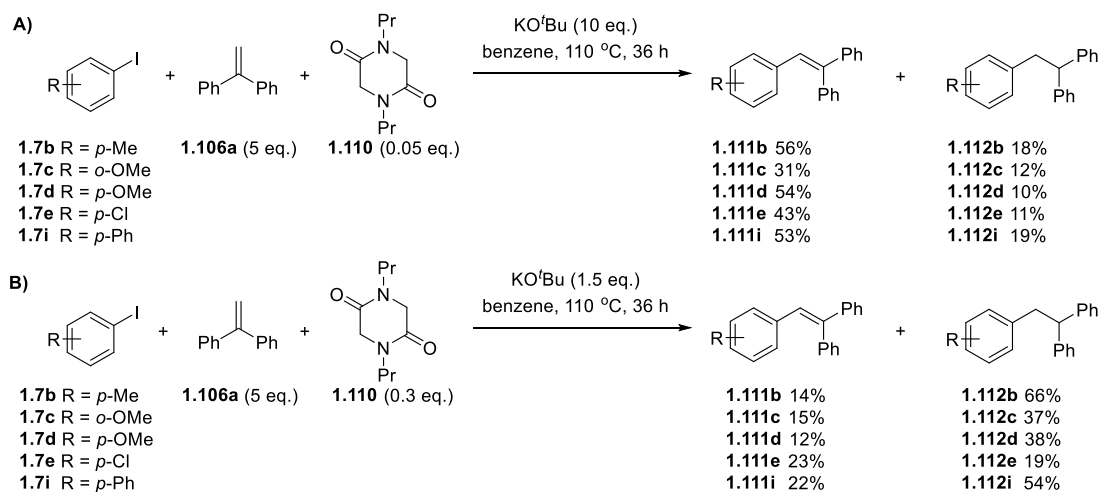
Scheme 1.30 Murphy *et al.* reported Mizoroki-Heck-type coupling using a DKP additive **1.110** with KO*t*Bu.

A photoactivated initiation of the Mizoroki-Heck-type coupling of haloarenes with styrene was later reported by Rossi *et al.*[69] (Scheme 1.31A). They reported that the reaction could also be performed in the absence of solvent when 18-crown-6 ether was used to aid solubility of the KO*t*Bu (Scheme 1.31B).
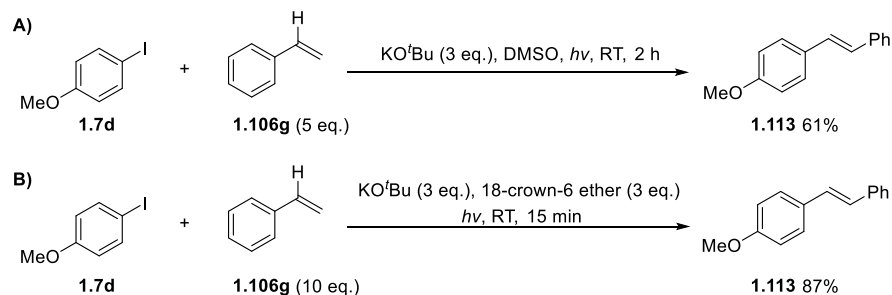
Scheme 1.31 Rossi *et al.*[69] reported light irradiation procedure to achieve transition metal-free Mizoroki-Heck coupling of haloarenes to styrene **1.106g**.

Lei *et al.*[70] showed that alkoxycarbonylation of 4-iodotoluene **1.7b** was possible under a pressure of carbon monoxide, using KO*t*Bu and 1,10-phenanthroline **1.29**, to form *tert*-butyl 4-methylbenzoate **1.114** (Scheme 1.32A). The mechanism proposed (Scheme 1.32B) involves an initiation step, which is a SET into the C-I σ* of **1.7b**, to form the aryl radical **1.34**. The aryl radical then attacks a molecule of carbon monoxide to form an acyl radical intermediate **1.115**, which is attacked by a *tert*-butoxide anion to form the electron-rich radical anionic intermediate **1.116**. This intermediate can propagate the chain mechanism by donating an electron to a new molecule of 4-iodotoluene **1.7b**, to form *tert*-butyl 4-methylbenzoate **1.114** as the product, and a new aryl radical intermediate **1.34**.
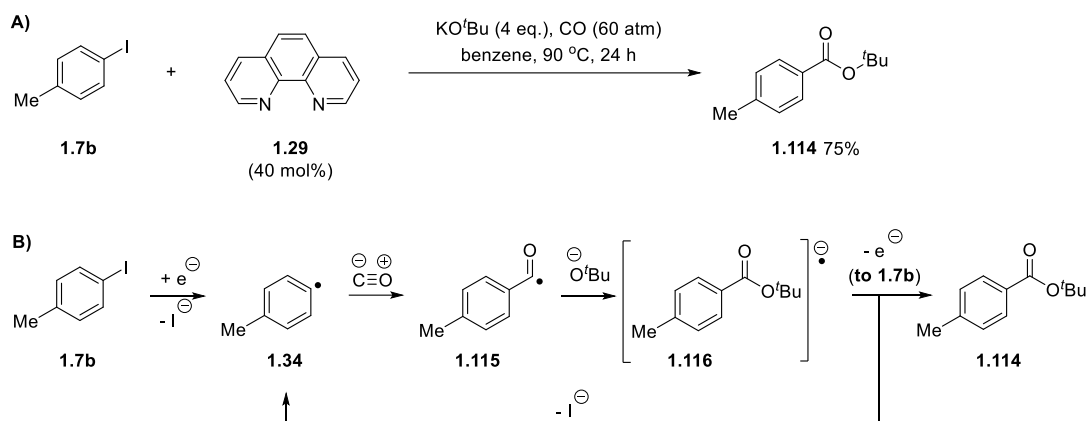
Scheme 1.32 Lei *et al.*[70] reported the first transition metal-free alkoxycarbonylation.

It was shown that the position of the substituents on the haloarene had little effect on the yield. The solvent, however, did affect the yields because a by-product formed, which occurred through aryl-aryl bond formation when the aryl radical **1.34** reacts with benzene instead of carbon monoxide. The competitive arylation reaction was avoided when benzotrifluoride was employed as the solvent.

A light-initiated example of a transition metal-free aminocarbonylation of aryl halides was reported by Ryu *et al.*[71] (Scheme 1.33), which is similar to that reported by Lei *et al.* (previously discussed in Scheme 1.32). However Ryu *et al.* used light irradiation to achieve the initiation step of the mechanism, instead of the combination of 1,10-phenanthroline **1.29** and KO*t*Bu. They reported that the aryl radical formed

in the mechanism could couple to primary and secondary amines to achieve aminocarbonylation (Scheme 1.33).

	HNR^{1}R^2	Yield 1.118
	morpholine **1.117a**	**1.118a** 81%
	piperidine **1.117b**	**1.118b** 74%
	diethylamine **1.117c**	**1.118c** 72%
	^{n}butylamine **1.117d**	**1.118d** 68%
	^{t}butylamine **1.117e**	**1.118e** 82%
	aniline **1.117f**	**1.118f** 38%
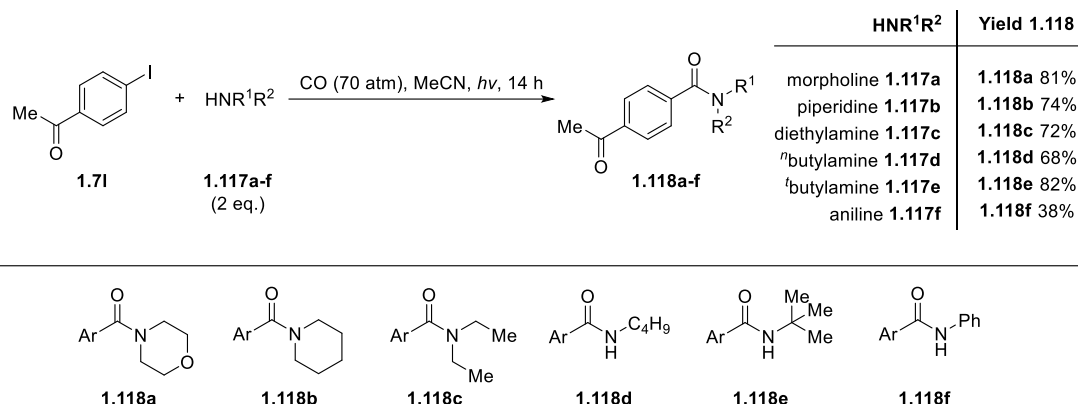
Scheme 1.33 Ryu *et al.*[71] achieved aminocarbonylation of haloarenes using light irradiation.

The ability to generate alternative bonds between a haloarene and other substrates using transition metal-free procedures is highly desirable. One transition metal-free approach to activate haloarenes towards coupling, is to react the haloarene in the presence of a strong base, such as KNH$_2$, to convert the haloarene into an aryne intermediate that can couple with nucleophiles.[72] However, the formation of arynes can lead to an equal product distribution of regioisomers, whereby the nucleophile can attack at either carbon on the aryne with equal probability. However, Kim and Bunnett[72-73] observed that when 5-iodo-*pseudo*-cumene **1.7bb** reacted with KNH$_2$ and liquid ammonia, the reaction preferentially yielded 5-amino-*pseudo*-cumene **1.119**. 6-Iodo-*pseudo*-cumene **1.7cc** formed 6-amino-*pseudo*-cumene **1.120** as the major product) (Scheme 1.34).
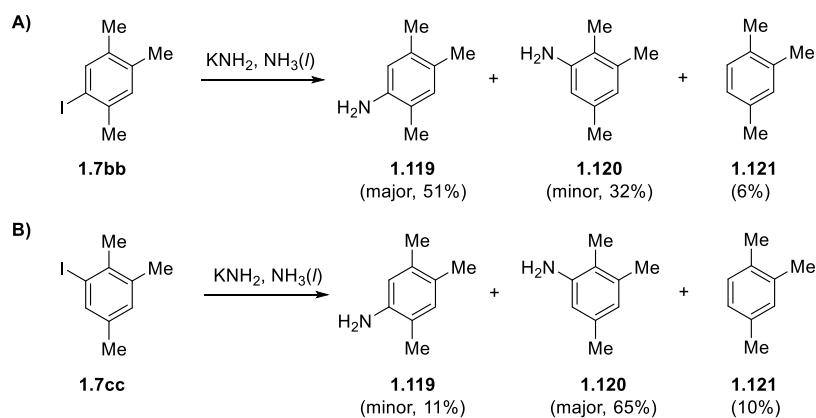
Scheme 1.34 The unusual product distribution achieved when iodo-*pseudo*-cumene **1.7bb-cc** reacted with KNH$_2$ in liquid ammonia observed by Kim and Bunnett.[73]

They proposed that aryne intermediates are formed in the reaction, agreeing with the previous reports on these substrates. However, the product distribution observed was unusual because it did not give the expected 1:1 ratio of products that is indicative that a benzyne intermediate is formed in the reaction. Therefore they proposed that an additional radical mechanism occurs as the major pathway. They proposed that an electron transfer step occurs to the iodoarene, which forms an aryl radical that couples to the NH_2 anion in a radical nucleophilic substitution reaction ($S_{RN}1$). They went on to propose that the SET step occurs due to solvated electrons in the ammonia, and indeed, when potassium metal was added to the reaction, the 5-iodo-*pseudo*-cumene **1.7bb** yielded only two products: 5-amino-*pseudo*-cumene **1.119** (50%) and *pseudo*-cumene **1.121** (40%) formed, and no 6-amino-*pseudo*-cumene **1.120** was observed.[72]

This is one of the first reported examples of transition metal-free $S_{RN}1$ reactions of haloarenes and a nucleophile, to my knowledge. Over the following years, several authors reported other nucleophiles that could couple to aryl radicals, which formed from haloarenes, either by reacting with solvated electrons or by photoactivation. The nucleophiles reported were: an enolate anion of acetone,[74] enolate anions of pinacolone and other ketones,[75-77] carbanions of hydrocarbons, such as 1,3-pentadiene and fluorene and indene,[76] thiophenoxide,[78] potassium diethyl phosphite,[79] potassium diphenylphosphide[80] and cyanomethyl anion.[81]

Interestingly, when Scamehorn and Bunnett[75] and Scamehorn *et al.*[82] performed the coupling of halobenzenes to several enolate anions, the reaction proceeded in DMSO at room temperature in the dark (Scheme 1.35A). Therefore a new initiation step was proposed for these dark reactions, as opposed to the light irradiation previously discussed. It was proposed that the enolate anion, such as **1.124**, is capable of donating an electron to the haloarene in the initiation step of the radical chain mechanism (Scheme 1.35B). The authors reported that the reaction was stimulated by light and inhibited by radical scavengers, but also the benzyne mechanism was observed as a possible competing reaction (this competition will be shown in chapter 6). A radical chain mechanism was proposed that involves a SET step, from the enolate anion **1.124** to iodobenzene **1.7k**, to give the aryl radical **1.126**

upon loss of KI. The aryl radical **1.126** undergoes a S$_{RN}$1 step, coupling onto an enolate anion **1.124** to form the radical anion **1.127**. SET from this radical anion, to a new molecule of iodobenzene **1.7k** yields the coupled product **1.123** and a new aryl radical **1.126**, in a radical chain mechanism. It should be noted that the aryl radical **1.126** could directly couple to the α–carbonyl radical **1.125** to form the final product in a linear reaction pathway.

Ketone 1.122a-f	Yield 1.123a-f
acetone **1.122a**	50%
pinacolone **1.122b**	60%
cyclohexanone **1.122c**	75%[a.]
2-butanone **1.122d**	70%[b.]
3-pentanone **1.122e**	70%
phenylacetone **1.122f**	< 1%
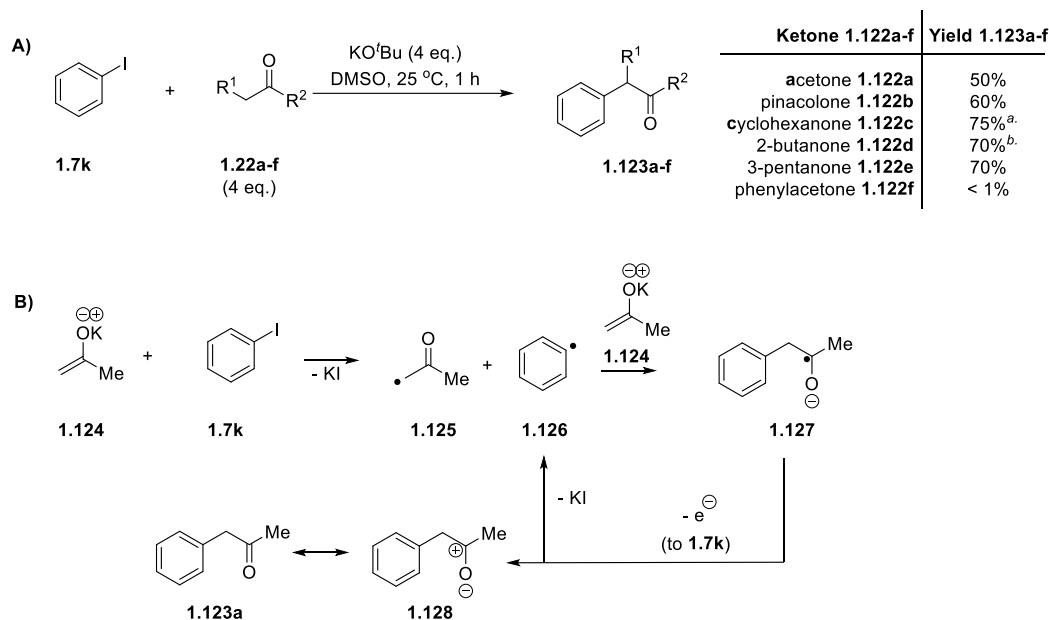
[a.]*25% benzene also observed.* [b.]*Isomers of 3-phenyl and 1-phenyl ratio 2.8 : 1 were observed.*

Scheme 1.35A) Dark reactions to couple enolate anions of several ketones with haloarenes.[75,82] **B)** Proposed S$_{RN}$1 mechanism in the dark in DMSO.

More recently, similar reactions have been reported in the literature by Taillefer *et al.*[83] whereby α-arylation of propiophenone **1.129** with various haloarenes, such as **1.7k**, was achieved in the presence of KO*t*Bu (5 eq.) in DMF at 60 °C (Scheme 1.36). It was found that the reaction also proceeded using DMF as 5 equivalents, albeit with lower yields of product. Interestingly, when they did the reaction in DMSO it was found to be an unsuitable solvent for the reaction, giving a trace yield of coupled product. This contrasts with the work reported by Scamehorn and Bunnett (previously shown in Scheme 1.35). Comparing propiophenone **1.129** in this reaction, with phenylacetone **1.122f** reported by Scamehorn *et al.*, shows that they have similar structures and reactivity in DMSO, since phenylacetone **1.122f** was not

reactive in DMSO, under the conditions Scamehorn *et al*. used. Taillefer *et al*. proposed that the reaction proceeds through the $S_{RN}1$ mechanism; however, they proposed that the electron donor is the carbamoyl anion **1.131**, formed by deprotonation of DMF, and not the enolate anion of **1.129**. Therefore the mechanism proposed contrasts with the initiation pathway proposed by Scamehorn and Bunnett.[84]

1.7k **1.129** KO^{t}Bu (5 eq.), DMF, 60 °C, 13 h **1.130** 99% (85%)[a.] **1.131**
(2 eq.)

[a.] *Yield obtained when DMF (5 eq.) was used.*
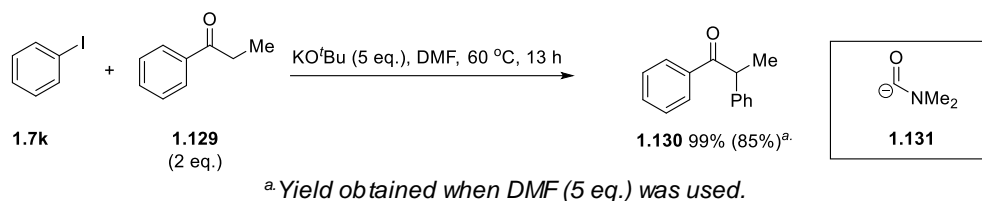
Scheme 1.36 Taillefer *et al*.[83] reported the coupling of propiophenone with iodobenzene in DMF.

Rossi *et al*.[85] reported an analogous intramolecular α-arylation reaction using light irradiation and KO^{t}Bu (Scheme 1.37). The substrates used in the study (**1.132, 1.134** and **1.136a-c**) consisted of a haloarene moiety tethered to an enolisable aryl ketone. Light irradiation of these substrates predominantly led to α-arylation cyclisation, however aryl-aryl bond formation was competing as an alternative mechanism, and for some substrates this pathway was seen to dominate (Scheme 1.37C). Successful intramolecular α-arylation or aryl-aryl bond formation of most substrates, such as **1.136a-c**, was achieved in liquid ammonia using light irradiation. However, light irradiation of substrate **1.134** yielded the α-arylation product **1.135** in low yields (38%) (Scheme 1.37B), and an alternative procedure to achieve more efficient cyclisation of substrate **1.134**; a combination of pinacolone, KO^{t}Bu and FeCl$_2$ gave high yields of **1.135** (84%) (Scheme 1.37D). Interestingly, Scamehorn and Bunnett[75] showed that the pinacolone **1.122b** could be used to couple to haloarenes without the need of iron salts, and therefore, it would be interesting to investigate the product yields in the absence of FeCl$_2$ with just pinacolone as an additive.
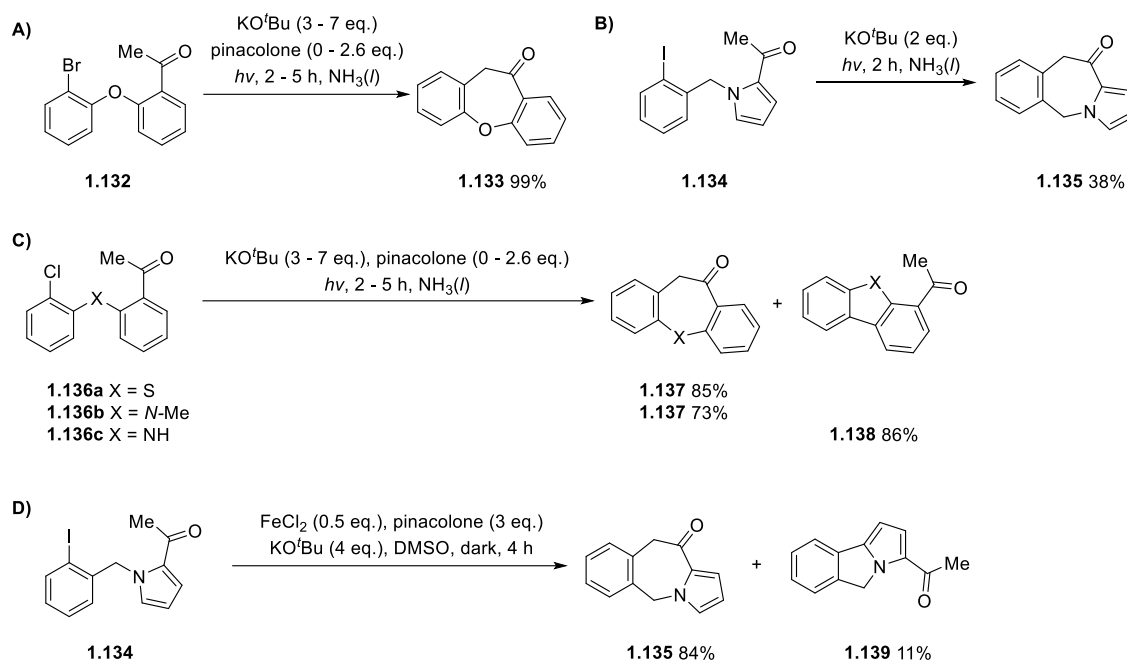
Scheme 1.37A) Rossi *et al.*[85] used light irradiation to achieved intramolecular cyclisations of substrate **1.132**, **B)** of substrate **1.134** and **C)** substrates **1.136a-c**. **D)** Substrate **1.134** underwent intramolecular α-arylation or aryl-aryl bond formation from using FeCl₂ and pinacolone.

The experiments reported in this section show a variety of alternative bond formations that can be achieved through transition metal-free synthesis, which expand the reaction scope away from just aryl-aryl bond formation. By expanding the reaction scope of these transition metal-free reactions, it could drive synthesis away from the conventional methods commonly employed today that use transition metals, and towards greener alternatives. Within the literature, it was shown that the light-initiated coupling of aryl halides and enolate anions could be performed in the dark. This raises the question as to whether other light-initiated reactions that proceed *via* the $S_{RN}1$ mechanism could be successfully performed using KO^{t}Bu and an additive, to further expand the scope of the transition metal-free reactions. The reports by Scamehorn *et al.*[75,82] and Taillefer *et al.*[83] that propose either enolate anions or carbamoyl anions are possibly electron donors to haloarenes, raises the question as to what other species could be initiating these transition metal-free BHAS or $S_{RN}1$ reactions.

Although the field of transition metal-free reaction synthesis is expanding and being developed, there is a long way to go before it is capable of competing with, or replacing, the traditional palladium-catalysed cross-coupling reactions. The future challenges in the transition metal-free reaction conditions are to address the limited reaction scope that is reported, as well as to understand and develop systems that will efficiently react chlorobenzenes in these reactions. Finally, it is important to develop conditions to achieve regioselective transition metal-free coupling reactions. Currently the transition metal-free reactions occur with a limited regioselectivity on the coupling partner, which is no issue if the aryl radical couples to benzene; however when other reaction partners are employed there is little control of the regioisomeric products formed.

1.4 The initiation step of the base-promoted homolytic aromatic substitution mechanism

1.4.1 KO*t*Bu acting as the electron donor?

Ashby *et al.*[36-37] proposed that alkoxides, such as KO*t*Bu, can act as electron donors because they observed an EPR-active species in the reaction of metal alkoxides (KO*t*Bu and LiO*t*Bu) with triphenylmethyl bromide **1.140** (or chloride) in THF. The radical species was identified as the triphenylmethyl radical **1.141** when the EPR spectrum was compared with that of a reference spectrum. They proposed that the radical **1.141** forms when a single electron is donated from KO*t*Bu to triphenylmethyl bromide **1.140**, followed by the loss of a bromide anion (Scheme 1.38A). The major product reported was (*tert*-butoxymethanetriyl)tribenzene **1.142**, and [{4-(*tert*-butoxy)cyclohexa-2,5-dien-1-ylidene}methylene]dibenzene **1.143** formed as a minor product.
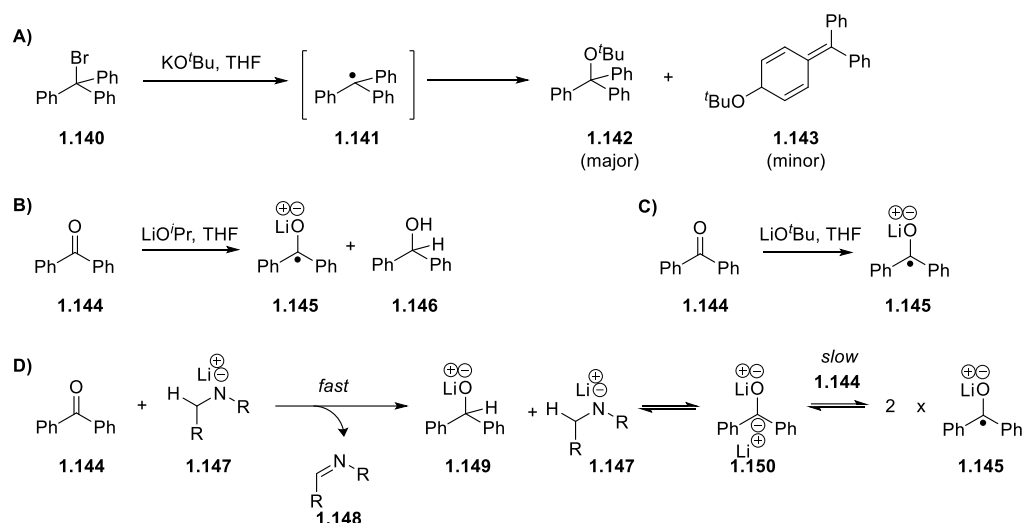
Scheme 1.38A) Ashby *et al.*[36] reported the formation of an EPR active species, triphenylmethyl radical **1.141**, when KO*t*Bu reacts with triphenylmethyl bromide **1.140 B)-C)** and they reported alkoxides were capable of reducing benzophenone.[37] **D)** Proposed mechanism to form ketyl radical from benzophenone.[86]

Another substrate that is reported to be a probe for SET from alkoxides, such as LiO*t*Bu, is benzophenone **1.144**. Ashby *et al.*[37] reported that when benzophenone **1.144** reacts with lithium alkoxides (LiO*n*Bu, LiO*t*Bu), the lithium benzophenone ketyl radical **1.145** forms, and they characterised the formation of the ketyl radical by comparing an EPR spectrum with a reference sample (Scheme 1.38B). When alkoxides LiO*n*Bu and LiO*i*Pr were used, the product benzhydrol **1.146** (the reduced form of benzophenone **1.144**) was observed, in addition to the benzophenone ketyl radical **1.145** (Scheme 1.38B). The proposed mechanism is that the alkoxide donates an electron to the benzophenone **1.144** to form the benzophenone ketyl radical **1.145**. This radical could abstract a hydrogen atom to form the benzhydrol product **1.146**. Interestingly, when Al(O*i*Pr)₃ was used as the alkoxide in the reaction, only the reduction of the benzophenone to form benzhydrol **1.146** was observed. They proposed that this is because the Al(O*i*Pr)₃ is a worse electron donor than LiO*i*Pr. However, it should be noted that these alkoxide bases, LiO*n*Bu and LiO*i*Pr, can form the lithium benzhydrol intermediate *via* hydride transfer by the Meerwein-Ponndorf-Verley reduction. In fact, Newcomb *et al.*[86] warned against proposing that SET to benzophenone **1.144** was occurring based only on the observation of lithium

benzophenone ketyl radicals formed in the reaction.[86] They were discussing the proposed SET mechanism from lithium dialkylamides to benzophenone **1.144** to form the lithium benzophenone ketyl radicals **1.145** and they proposed that the lithium benzophenone ketyl radicals **1.145** did not form through SET but could form *via* secondary processes (Scheme 1.38D).[86] They showed that the lithium dialkylamides **1.147** perform a Meerwein-Ponndorf-Verley reduction of benzophenone **1.144** to give product **1.149**. A second deprotonation of the lithium benzhydrol intermediate **1.149** generates low amounts of the dianion **1.150**, and it is proposed that this species **1.150** acts as the electron donor to benzophenone, instead of the lithium dialkylamides **1.147** previously proposed (Scheme 1.38D). In relation to this method, comparison of the reduction of benzophenone **1.144** obtained using either LiO^{n}Bu or LiO^{t}Bu show that when LiO^{t}Bu was used, no formation of benzhydrol was observed (Scheme 1.38C), unlike the reaction of LiO^{n}Bu (Scheme 1.38B), but the lithium benzophenone ketyl radical **1.145** was observed by EPR to form in 3% yield relative to the ketone. This suggests that the β–hydride reduction by the alkoxide base is required for the formation of benzhydrol **1.146**, and within the paper they propose that the presence of the lithium benzophenone ketyl radical **1.145** is evidence that LiO^{t}Bu performs SET to benzophenone. However, based on the warning by Newcomb *et al.*, in reactions whereby alkoxides are proposed to perform SET to the substrates, care should be taken to identify if an electron donor could be an alternative species formed through secondary processes, proposed by Newcomb *et al.*

A recent paper by Wilden *et al.*[87] claimed to contain experimental evidence to support the hypothesis that KO^{t}Bu is indeed an electron donor. They realised that the additives, such as 1,10-phenanthroline **1.29**, were not essential in these transition metal-free reactions, but they did make the reactions proceed more efficiently and at a higher rate (Scheme 1.39A). These observations agree with others within the literature who observed that the coupled products could be formed in the absence of additives, albeit in much lower yield.[52,62] Wilden *et al.* found that if they increased the reaction time to 6 h, efficient yields of the coupled product **1.3b** could be achieved without an additive, such as **1.29** (66%). It must be noted that

although a broad range of haloarenes successfully coupled to benzene in the presence of KO*t*Bu and the absence of any additive, all the substrates tested contained protons *ortho* to the halogen, therefore not ruling out a benzyne mechanism. Wilden *et al.*[87] claimed that metal alkoxides **1.151**, such as KO*t*Bu, exist in equilibrium with their charge-separated ion pair **1.152**, which is essentially the "dissociated" anion (Scheme 1.39B). The choice of metal counterion of the alkoxide, or the addition of additives to the reaction mixture, are proposed to alter this equilibrium to drive the reaction towards the charge-separated ion pair **1.152**. They reported that the species **1.152** is in equilibrium with species **1.153**, whereby the alkoxide exists as an alkoxyl radical, with its electron loosely bound to it, however no evidence for the existence of this species was presented. They proposed that the loosely bound electron in species **1.153** at high temperatures can be donated to an aryl halide in the BHAS mechanism, to ultimately form an alkoxyl radical, like *tert*-butoxyl radical **1.154**. The *tert*-butoxyl radical **1.154** can react by two pathways; 1) the first pathway is hydrogen atom abstraction to form *tert*-butanol, and 2) the second possibility is β-scission to form acetone **1.122a** with the loss of the methyl radical. Wilden *et al.* provide experimental data that they claim is evidence for the formation of these alkoxyl radicals and their β–scission.

	Additive	Yield 1.3b
	None	38%
	1,10-phenanthroline **1.29**	65%
	DMEDA **1.21**	67%
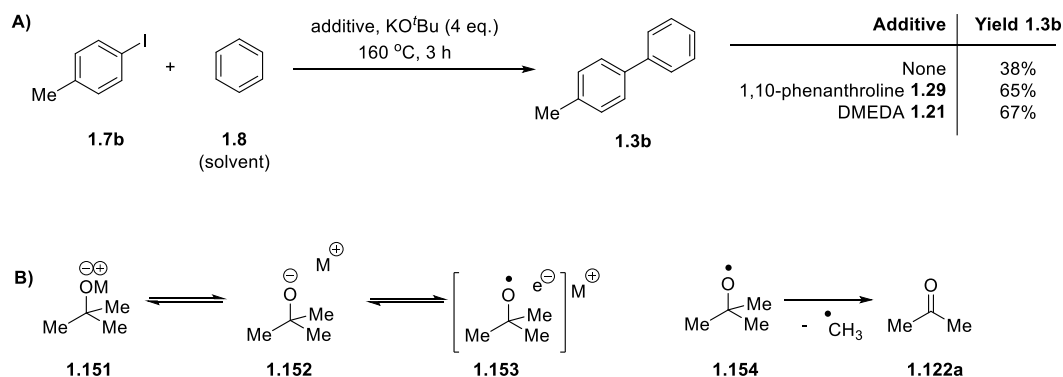
Scheme 1.39 Wilden *et al.* reported transition metal-free reactions could occur in the absence of the additives, such as 1,10-phenanthroline **1.29**, by the proposed SET from alkoxides, MO*t*Bu (M = K, Na or Li).

The proposal that the additives drive the equilibrium towards the charge-separated species **1.152** is in agreement with the previous mechanisms postulated in the literature, whereby it was proposed that only the complex of KO*t*Bu and the additive

is capable of donating the electron to initiate the BHAS pathway. However, in contrast to this proposal, Liu *et al.*[53] reported that simple alcohols that are not capable of chelating to KO*t*Bu, were capable of promoting the transition metal-free aryl-aryl bond formations.

Jutand and Lei *et al.*[88] have recently used EPR analysis and cyclic voltammetry (CV) to gain more insight into the interactions involved between 1,10-phenanthroline **1.29** and KO*t*Bu in these transition metal-free reaction conditions. The mechanism they propose still involves the formation of a complex between KO*t*Bu and 1,10-phenanthroline **1.29**, however they propose that the KO*t*Bu first donates its electron to the 1,10-phenanthroline **1.29** through an inner-sphere electron transfer, and not directly to the haloarene as previously proposed. This SET forms the radical anion of 1,10-phenanthroline, which they propose is the electron donor that initiates the BHAS pathway by donating an electron to the haloarene.

Although several mechanisms are proposed for this SET step, there is very little reported evidence to support them. Several research groups have turned to using computational chemistry to analyse the SET step for these reactions. Tuttle and Murphy *et al.*[44] used computational methods, density functional theory (DFT), to determine the thermodynamics for the electron transfer from the KO*t*Bu complex to iodobenzene, in benzene as the solvent. Alarmingly, the free energy change for this SET was calculated to be impossibly high, ΔG_{rxn} = 59.5 kcal/mol. Taillefer *et al.*[83] also calculated the energy profile for the electron transfer from a free molecule of KO*t*Bu (without chelation to any additive) to a molecule of iodobenzene in DMF (without additives because the reaction successfully occurred without additives) and found that the proposed initiation step was energetically unfavourable (ΔG_{rxn} = 50.5 kcal/mol). Patil recently investigated the reaction pathway in more detail using DFT.[89] He computationally investigated the energy profiles for three proposed mechanisms of SET from KO*t*Bu to initiate the transition metal-free BHAS pathways: (1) SET from KO*t*Bu directly to iodobenzene in benzene, ΔG_{rxn} = 114.5 kcal/mol; (2) a SET from the 1,10-phenanthroline-KO*t*Bu complex to iodobenzene in benzene, ΔG_{rxn} = 109.6 kcal/mol; (3) the consecutive SET pathway: the first SET is from KO*t*Bu to 1,10-phenanthroline, ΔG_{rxn} = 42.0 kcal/mol, followed by SET from the radical anion

of 1,10-phenanthroline to iodobenzene, ΔG_{rxn} = 61.2 kcal/mol. All of these barriers calculated suggest that KO^{t}Bu is not capable of donating an electron to haloarenes under the reported reaction conditions, and therefore an alternative mechanism must be occurring for the initiation step of the transition metal-free reaction conditions.

Throughout the literature of the transition metal-free reaction conditions, KO^{t}Bu is often crucial for the reaction to occur, but in some cases other bases work well, such as KHMDS or NaO^{t}Bu, can be employed if harsher reaction conditions are used.[35,50] It is also reported that the organic additive is vital for the reaction, unless the solvent is pyridine, or very high temperatures (> 150 °C) are used. Various researchers have all proposed similar reaction pathways for these aryl-aryl bond formations (Section 1.2.2). Shirakawa and Hayashi *et al.*[35] report that a complex forms between MO^{t}Bu (M = K, Na or Li) and 1,10-phenanthroline **1.29**, and the complex donates a single electron to the haloarene to form an aryl radical, which reacts with benzene as described in the BHAS chain mechanism. Shi *et al.*[34] believed that a bidentate complex forms between the 1,10-phenanthroline **1.29** and MO^{t}Bu (M = K, Na or Li), and this complex is capable of interacting with benzene through π-stacking and π-ion interactions to activate the C-H of the unactivated benzene towards coupling with the aryl radical. Other researchers believe that the BHAS mechanism is initiated by a SET step to the haloarene, and many propose that the electron donor is the KO^{t}Bu, which is supported by the work reported by Ashby *et al.*[36-37]. However, in the reactions reported by Ashby *et al.*[36-37] the alkoxide base used is LiO^{t}Bu and the reaction conditions are very different to the transition metal-free reactions, and therefore this does not necessarily provide evidence for SET from KO^{t}Bu under transition metal-free reaction conditions. In some recent papers, the reactions are performed in the presence of alternative bases; Chen *et al.*[50] performed the coupling of a 1-naphthyl iodide with benzene using the NHC additive **1.45** (previously shown in Scheme 1.14) and achieved comparable yields when KHMDS (45%) was used instead of KO^{t}Bu (41%). Kappe *et al.*[90] replicated the conditions of Shi *et al.*[35] and showed that it was possible to form biaryl structures in the presence of 1,10-phenanthroline **1.29** using LiHMDS as the base, with higher yields than when KO^{t}Bu was used. They noted that the reaction using LiHMDS yielded cleaner products,

albeit the reaction had to be monitored to deduce the duration for completion of the reaction, which is longer than when KO^{t}Bu is used. All these inconsistencies suggest an alternative mechanism could be occurring, and recently Murphy *et al*.[40,42,44] proposed that the combination of a strong base with an organic additive forms an electron donor *in situ*, and this is the species responsible for the initiation of the BHAS pathway (Section 1.4.2).

1.4.2 Organic molecules as precursors for electron donors

There are many examples of organic molecules that can form electron donors. Examples of this are reducing sugars, such as glucose **1.155**, which is believed to be the electron donor that reduces Ag(I) and Cu(II) in the Tollens' and Benedict's test respectively. The ability of various simple molecules, such as aldehydes and α-hydroxy ketones, to reduce Ag(I) in the Tollens' test will be discussed within the results of this thesis in Chapter 7. Recently, glucose **1.155** has also been applied to the transition metal-free coupling of haloarenes to benzene; however only 8% coupled product was achieved when the reaction was performed in benzene (Scheme 1.40).[91]
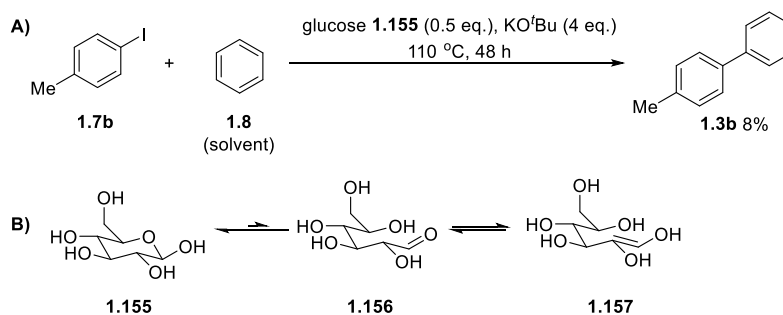
Scheme 1.40 Kumar e*t al*.[91] attempted to use glucose **1.155** to achieve transition metal-free aryl-aryl bond formation.

The Murphy group has been involved in the development of "super-electron-donors", which are defined as organic molecules that are capable of reducing iodobenzene (E^0 = - 2.2 V *vs*. SCE).[43] This was achieved by assessing the reducing ability of tetrathiafulvalene (TTF) **1.158** (E^0 = 0.3 V *vs*. SCE)[92] and tetrakis(dimethylamino)ethene (TDAE) **1.159** (E^0 = - 0.78 V *vs*. SCE)[93] (Scheme 1.41A). On analysis of the reducing ability of various TTF-based structures and

TDAE **1.159**, it was determined that to design a good reducing agent, firstly the extent of aromatisation driving force is important, and secondly, the presence of heteroatoms make better electron donors. In particular it was found that the replacing sulfur atoms with nitrogen atoms improved the strength of the electron donor. The four nitrogen atoms in TDAE **1.159** donate electron density into the double-bond making it more electron-rich, hence more able to donate electrons. The four nitrogen atoms also stabilise the radical that forms after electron donation, thus making loss of an electron possible. Design of a stronger electron donor was performed by Murphy *et al.*[94] and in 2005 they reported the formation of the first organic "super-electron-donor" **1.160** (Scheme 1.41A). Formation of these "super-electron-donors" is performed by deprotonation. For example, deprotonation of **1.161** forms the carbene **1.162**, which intramolecularly attacks the iminium on the tethered imidazolium salt (Scheme 1.41C). Further deprotonation of **1.163** forms the electron donor **1.160**. These reported "super-electron-donors" bear resemblances to the NHC molecule **1.45** used by Chen *et al.*[50] to initiate the coupling of haloarenes to benzene, under transition metal-free reaction conditions (Scheme 1.41B).
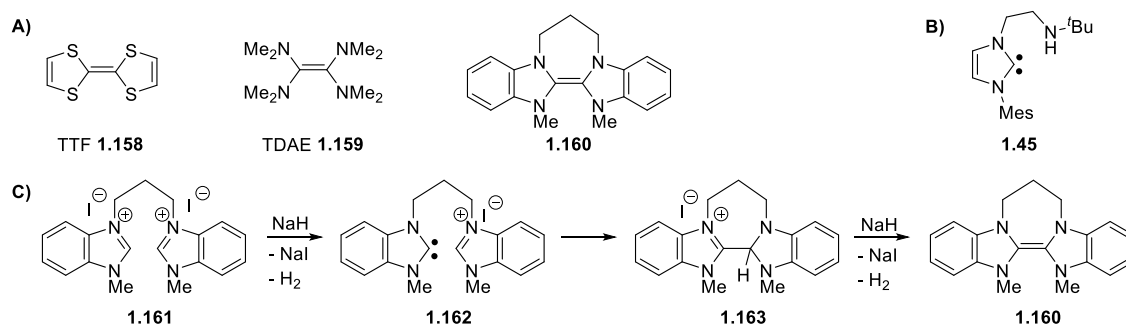
Scheme 1.41A) The evolution of organic electron donors into "super-electron-donors." **B)** The NHC additive **1.45** used by Chen *et al.* to initiate the coupling of haloarenes to benzene. **C)** The formation of the electron donor **1.160** from salt **1.161**.

The proposal that organic molecules form electron donors *in situ* has already been discussed briefly in Section 1.3. Scamehorn and Bunnett[75] proposed that the potassium enolate anions of several ketones donated electrons to the haloarenes to initiate $S_{RN}1$ reactions. The concept that organic molecules can act as electron donors could be applied to these transition metal-free reaction conditions. Murphy *et al.*[42,44] proposed that the numerous simple organic molecules that have been

reported to be successful in promoting the BHAS mechanism in the presence of a strong base, such as KO*t*Bu, form organic electron donors *in situ* (Scheme 1.42). Over the last few years they have reported evidence of the formation of electron donors from various organic additives that are used to achieve transition metal-free coupling of haloarenes to benzene. The most common additive used for the transition metal-free coupling reactions is 1,10-phenanthroline **1.29** (Scheme 1.42A). They proposed that in the reaction mixture the 1,10-phenanthroline **1.29** complexes with KO*t*Bu, in agreement with the other researchers within this field of chemistry. However, they proposed that complexation of KO*t*Bu and 1,10-phenanthroline **1.29** aided the deprotonation of 1,10-phenanthroline **1.29** by KO*t*Bu, to form **1.165**. This anionic intermediate attacks another molecule of 1,10-phenanthroline **1.29** to form a dimeric species **1.166**, which is deprotonated a second time by KO*t*Bu to form **1.167**. It is the formation of this species **1.167** *in situ* that is believed to be the crucial step to initiate the transition metal-free coupling reactions, because Murphy *et al.*[44] proposed that this species **1.167** is an electron-donor. To support their proposal they went so far as to isolate the oxidised form **1.164**[44] of the organic electron donor **1.167** formed in the reaction mixture (Scheme 1.42A). They propose that pyridine acts similarly to 1,10-phenanthroline **1.29** to form similar electron donors, such as **1.172** (Scheme 1.42B).
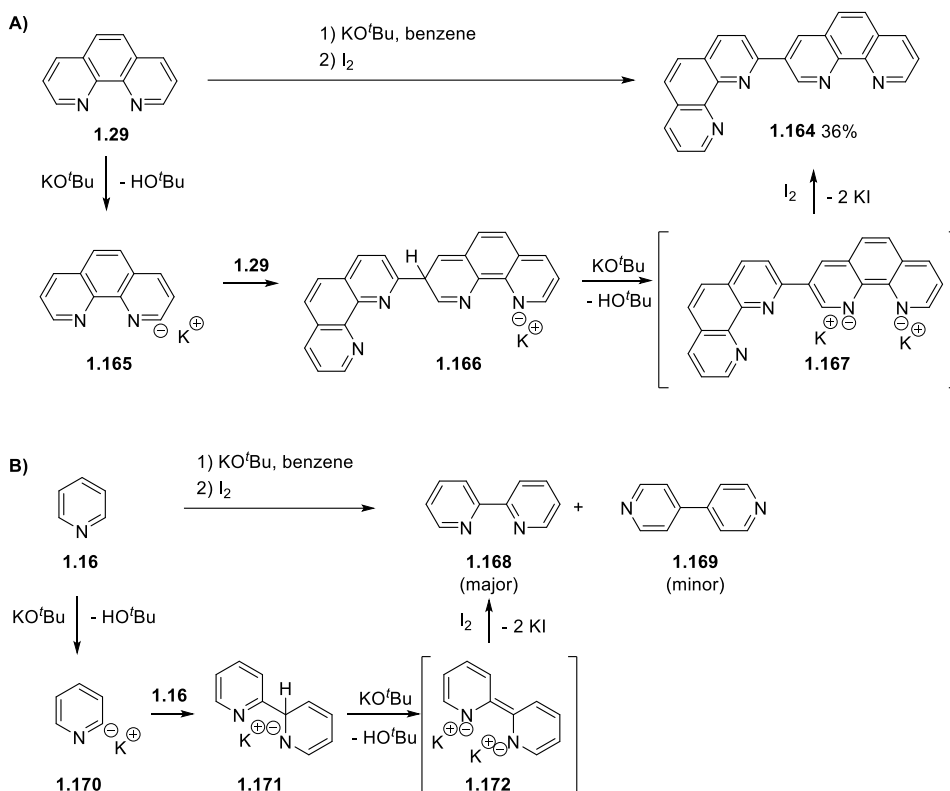
Scheme 1.42 The formation of electron donors *in situ* from 1,10-phenanthroline **1.29** and pyridine **1.16**.[44]

Since their initial paper within this field, Murphy *et al*. have proposed possible electron donors formed from other additives within these transition metal-free reactions, such as 2-pyridyl carbinol **1.65** and DMF **1.175** (Scheme 1.43A and B).[40,43] Based on their current insights made into these potential electron donors, Murphy *et al*.[39] have also published their views on the possible electron donors formed from other additives that are successful at coupling haloarenes with benzene under these reaction conditions, such as 1,2-diamines like DMEDA **1.21** and diols such as *cis*-1,2-cyclohexane-1,2-diol **1.25** (Scheme 1.43C and D respectively). Work is continuing with the Murphy lab (and will be discussed in parts in this thesis) as to these possible electron donors formed *in situ* from the action of KO*t*Bu on simple, cheap and bench-stable organic additives.
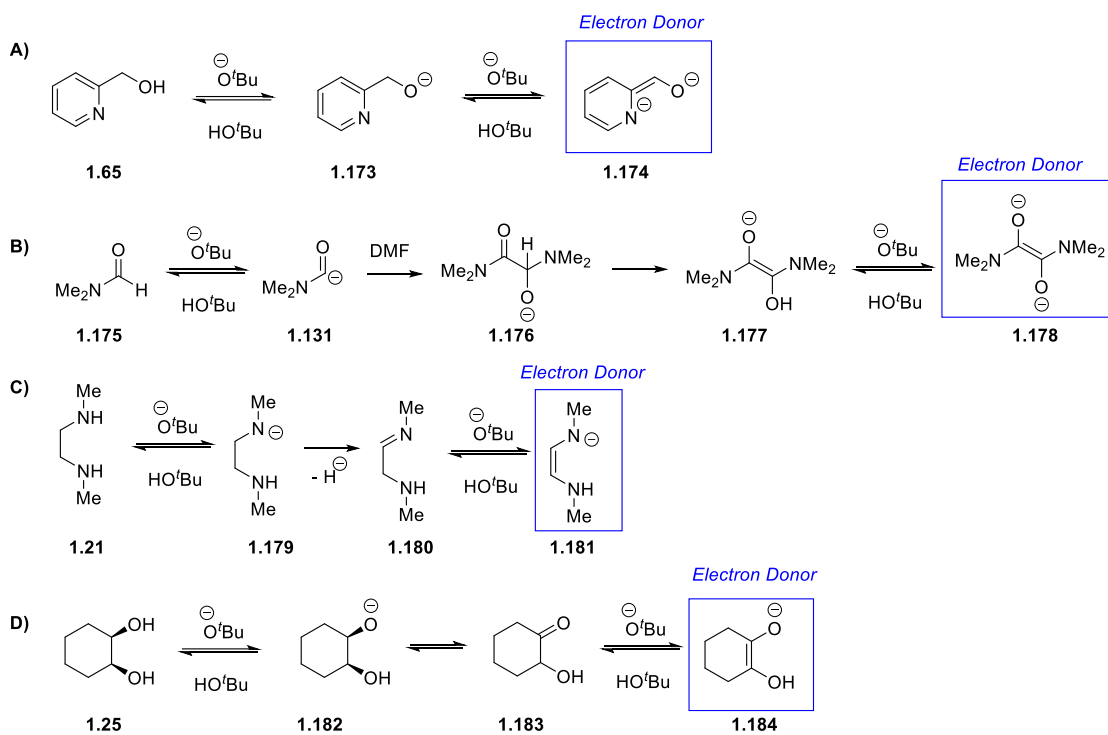
Scheme 1.43 The formation of electron donors *in situ* from 2-pyridyl carbinols **1.65**[40] and DMF **1.175**,[43] and proposed electron donors formed from DMEDA **1.21** and *cis*-cyclohexane-1,2-diol **1.25**.[44]

2.

Introduction

2.1 Motivation for the thesis and aims

Upon starting my PhD, Professor John A. Murphy and his group were interested in the recently reported transition metal-free reaction conditions that were most commonly used to achieve aryl-aryl bond formations between a haloarene and benzene, which was used as the solvent (described in Chapter 1). The work discussed within this thesis is a continuation of the efforts that the Murphy group make to this field of radical chemistry. The research was focussed on two objectives. The first was to identify the electron donor species responsible for the single electron transfer step in the initiation of these coupling reactions (described in Chapter 4). Due to the benefits associated with transition metal-free reaction conditions, it was considered desirable that these transition metal-free reaction conditions could be used for alternative transformations as well. Therefore, the second objective was to expand the scope of these reaction conditions in order to move away from solely aryl-aryl bond formations, and to find possible applications of these transition metal-free reaction conditions at achieving $S_{RN}1$ reactions (as described in Chapter 6). In order to achieve these aims, organic experimental work was performed, in addition to computational analysis, implementing quantum mechanics to investigate reaction pathways.

2.2 Layout of the thesis

The thesis begins by providing a brief description of density functional theory (DFT) and the computational methods that will be used within the thesis to give support and deeper understanding to the conclusions drawn from experimental results (Chapter 3).

The main results are reported in four chapters. Chapter 4 investigates the possible electron donors formed from both the *N,N'*-dipropyldiketopiperazine (DKP) additive and DMF using both experimental and computational techniques. Chapter 5 describes the initial attempts made to find evidence as to whether the butoxide anion is capable of donating an electron, either to iodoarenes or to tetrahalomethanes under various reaction conditions; the evidence reported suggests that KO^{t}Bu is not

an electron donor to either substrate. Chapter 6 explores the possibility of using these transition metal-free reaction conditions to achieve S$_{RN}$1 cyclisation of substrates, using computational and experimental techniques to understand the reaction mechanisms, and the observed role of solvent in the product formation. Finally, Chapter 7 is used to investigate whether glucose could act as an additive in the transition metal-free reaction conditions, similar to the proposal and report of Kumar *et al.*,[91] and effort was made to gain mechanistic understanding of the Tollens' reaction, and the possible electron donors that form from the many possible classes of substrates that can be used to reduce ammoniacal silver nitrate.

Chapter 8 is used to summarise the key conclusions of this thesis and propose possible work for the future. Chapter 9 gives complete characterisation and information on the experimental work performed within this thesis.

3.

Computational theory

Quantum mechanics is a sub-section of computational chemistry that is applied to systems on the atomic level, with the aim to determine the exact wavefunction of a particular system. If the wavefunction is known for any system, then the physical properties, including the energy of the system, can be deduced on the application of a specific operator to the wavefunction, such as the Hamiltonian operator ($\hat{H}$). One approach to extracting the energy of a system in quantum mechanics is to solve the *N*-electron wavefunction, such as the Hartree-Fock (HF) approximation. However, an alternative approach is to determine the electron density of a system, because physical properties of the system are dependent on the electron density.[95] This method is known as density functional theory (DFT).[96-98]

3.1 Density functional theory

The electron density ($\rho(\vec{r})$) is the probability of finding any one of the *N* electrons with any spin function within the volume $d\vec{r}_1$, where all *N*-1 electrons are represented by Ψ (Equation 3.1). This is achieved by determining the probability of finding one electron within volume $d\vec{r}_1$ and then multiplying this by *N* because all electrons are indistinguishable.

$$\rho(\vec{r}) = N \int \dots \int |\Psi(\vec{x}_1, \vec{x}_2, \dots, \vec{x}_N)|^2 ds_1 \, \vec{x}_1, \vec{x}_2, \dots, \vec{x}_N.$$

<div align="right">Equation 3.1</div>

The electron density has several important properties: (1) it is a function of only three spatial variables; (2) at infinite distance from the nucleus the electron density should go to zero, $\rho(\vec{r} \rightarrow \infty) = 0$; (3) if $\rho(\vec{r})$ is integrated over all space, this gives the total number of electrons, $\int \rho(\vec{r}) d\vec{r}_1 = N$; and (4) unlike the wavefunction, the electron density can be physically measured, for example, by X-ray diffraction. Additionally, the $\rho(\vec{r})$ reaches a maxima at the position of the nuclei (R_A) and hence R_A can be determined from electron density, and this density at R_A contains information about the nuclear charge (Z_A). Hence, electron density provides information of R_A, Z_A and *N*, which is all the information required to approximate the Hamiltonian operator for any particular system.

3.1.1 Hohenberg-Kohn theorem

The Hohenberg-Kohn theory describes how electron density could be used to determine the Hamiltonian operator, and hence it can be used to extract the physical properties of the particular system.[95] Each molecular system is uniquely described by three factors that are required to study the system; the number of electrons (N), the position of the nuclei (R_A) and the charges of the nuclei (Z_A). The electron density $\rho(\vec{r})$ contains all this information and can be shown to directly relate to the Hamiltonian operator, and hence the ground state energies (E_0) (Equation 3.2).

$$\rho(\vec{r}) \Rightarrow \{N, Z_A, R_A\} \Rightarrow \hat{H} \Rightarrow \Psi_0 \Rightarrow E_0 \qquad \text{Equation 3.2}$$

The ground state energy (E_0) and its energy components are all functionals of the ground state electron density (Equation 3.3). The E_{Ne} component is system dependent, i.e., it depends on the R_A, Z_A and N, and thus can be described using the electron density and an external potential (Equation 3.4). The last two terms, $T[\rho_0]$ and $E_{ee}[\rho_0]$, are independent of the system variables, and together they form the Hohenberg-Kohn functional, F_{HK} (Equation 3.5). This equation suggests that the ground state energy can be determined if the F_{HK} functional was known. The F_{HK} functional contains the functional for both the kinetic energy ($T[\rho]$) and the interelectronic repulsion ($E_{ee}[\rho]$), however these functionals are not known and hence the ground state energy cannot be determined (Equation 3.5 – 3.7). The $E_{ee}[\rho]$ functional can be further broken down because this functional consists of the Coulomb interaction potential ($J[\rho]$) which can be calculated, and the non-classical contribution to the electron-electron interaction ($E_{ncl}[\rho]$) such as self-interactions and the exchange and correlation of the electrons (Equation 3.7). The major challenge of DFT is finding expressions for the unknown functionals, $T[\rho]$ and $E_{ncl}[\rho]$.

$$E_0[\rho_0] = E_{Ne}[\rho_0] + T[\rho_0] + E_{ee}[\rho_0] \qquad \text{Equation 3.3}$$

$$E_0[\rho_0] = \int \rho_0(\vec{r}) V_{Ne} d\vec{r} + T[\rho_0] + E_{ee}[\rho_0] \qquad \text{Equation 3.4}$$

$$E_0[\rho_0] = \int \rho_0(\vec{r}) V_{Ne} d\vec{r} + F_{HK}[\rho_0] \qquad \text{Equation 3.5}$$

$$F_{HK}[\rho] = T[\rho] + E_{ee}[\rho] = \langle \Psi_0 | \hat{T} + \hat{V}_{ee} | \Psi_0 \rangle \qquad \text{Equation 3.6}$$

58

$$E_{ee}[\rho] = \frac{1}{2} \int \int \frac{\rho(\vec{r}_1)\rho(\vec{r}_2)}{r_{12}} d\vec{r}_1 d\vec{r}_2 + E_{ncl}[\rho] = J[\rho] + E_{ncl}[\rho] \qquad \text{Equation 3.7}$$

The second Hohenberg-Kohn principle involves using the variational principle to determine the ground state density (Equation 3.8). This states that when the $F_{HK}[\tilde{\rho}]$ functional is applied to a reasonable trial density, $\tilde{\rho}(\vec{r})$, the energy calculated will be either greater than or equal to, the ground state energy. It will only be equal to the ground state energy if the trial density matches the exact density, i.e. $\tilde{\rho}(\vec{r}) \equiv \tilde{\rho}_0(\vec{r})$.

$$E_0 \leq E[\tilde{\rho}] = F_{HK}[\tilde{\rho}] + E_{Ne}[\tilde{\rho}] \qquad \text{Equation 3.8}$$

This theory proves that density can be used as a replacement to the wavefunction when solving the Schrödinger equation. In order to practically apply this theory however, an approximation of the functional must be developed.

3.2 Functionals

3.2.1 Kohn-Sham approach

The Hohenberg-Kohn theory introduced the $F_{HK}[\rho]$ functional that contains contributions from the kinetic energy (T), the coulombic interaction potential (J) and the non-classical electron-electron interactions (E_{ncl}). The Kohn-Sham approach builds upon the Hohenberg-Kohn theory and has provided a practical implementation of the electron density within DFT methods, by finding an accurate way to describe the kinetic energy functional (T). In the Kohn-Sham approach, the Slater determinant Θ_s is constructed (Equation 3.9), which gives the wavefunction for the reference orbital-based system of non-interacting electrons, which move within an effective potential Vs, and is described by the Hamiltonian ($\hat{H}_s$) (Equation 3.10). The ground state wavefunction is therefore represented by the Slater determinant (Θ_s), that is made up of Kohn-Sham spin orbitals (φ), where the $\hat{f}^{KS}$ is the one-electron Kohn-Sham (KS) operator (Equation 3.11 – 3.12).

$$\Theta_s = \frac{1}{\sqrt{N!}} \begin{vmatrix} \varphi_1(\vec{x}_1) & \varphi_2(\vec{x}_1) & \cdots & \varphi_N(\vec{x}_1) \\ \varphi_1(\vec{x}_2) & \varphi_2(\vec{x}_2) & \cdots & \varphi_N(\vec{x}_2) \\ \vdots & \vdots & \ddots & \vdots \\ \varphi_1(\vec{x}_N) & \varphi_2(\vec{x}_N) & \cdots & \varphi(\vec{x}_N) \end{vmatrix} \approx \Psi_0$$

Equation 3.9

$$\widehat{H}_s = -\frac{1}{2} \sum_i^N \nabla_i^2 + \sum_i^N V_s(\vec{r}_i).$$

Equation 3.10

$$\hat{f}^{KS} \varphi_i = \varepsilon_i \varphi_i, \quad i = 1, 2, \dots, N.$$

Equation 3.11

$$\hat{f}^{KS} = -\frac{1}{2} \nabla_i^2 + V_S(\vec{r})$$

Equation 3.12

The Hamiltonian ($\widehat{H}_s$) is a sum of the one electron KS operators, $\hat{f}^{KS}$. The kinetic energy of the system is thus determined by using the fictitious system of non-interacting electrons that is given an effective potential (V_s) to match the resulting density with that of the actual system (Equation 3.13). The kinetic energy of the non-interacting system is determined (Equation 3.14) and a functional ($F[\rho]$) was introduced (Equation 3.15 – 3.16). This equation essentially sums up all the unknown parameters within the system and combines them into the E_{XC}, which is defined as the exchange-correlation energy, which includes the residual kinetic energy that was not accounted for by the non-interacting system, as well as the non-classical interactions such as the electron-electron correlation and exchange and the correction for the self-interaction of the electrons.

$$\rho_s(\vec{r}) = \sum_i^N \sum_s |\varphi_i(\vec{r}, s)|^2 = \rho_0(\vec{r})$$

Equation 3.13

$$T_s = -\frac{1}{2} \sum_i^N \langle \varphi_i | \nabla^2 | \varphi_i \rangle$$

Equation 3.14

$$F[\rho(\vec{r})] = T_s[\rho(\vec{r})] + J[\rho(\vec{r})] + E_{XC}[\rho(\vec{r})]$$

Equation 3.15

$$E_{XC}[\rho(\vec{r})] \equiv (T[\rho] - T_s[\rho]) + (E_{ee}[\rho] - J[\rho]) = T_C[\rho] + E_{ncl}[\rho]$$

Equation 3.16

So, for the interacting real system the energy can be expressed (Equation 3.17).

$$E[\rho(\vec{r})] = T_s[\rho] + J[\rho] + E_{XC}[\rho] + E_{Ne}[\rho]$$

Equation 3.17

$$E[\rho(\vec{r})] = T_s[\rho] + \frac{1}{2} \int \int \frac{\rho(\vec{r}_1)\rho(\vec{r}_2)}{r_{12}} d\vec{r}_1 d\vec{r}_2 + E_{XC}[\rho] + \int V_{Ne}\rho(\vec{r})d\vec{r}$$

$$E[\rho(\vec{r})] = -\frac{1}{2} \sum_i^N \langle \varphi_i | \nabla^2 | \varphi_i \rangle + \frac{1}{2} \sum_i^N \sum_j^N \int \int |\varphi_i(\vec{r}_1)|^2 \frac{1}{r_{12}} |\varphi_j(\vec{r}_2)|^2$$

$$d\vec{r}_1 d\vec{r}_2 + E_{XC}[\rho(\vec{r})] + \sum_i^N \int \sum_A^M \frac{Z_A}{r_{1A}} |\varphi_i(\vec{r}_1)|^2 d\vec{r}_1$$

Hence, the Kohn-Sham approach focuses on determining the unknown E_{XC} functional and many methods have been designed to approximate this functional.

3.2.2 The exchange-correlation functional

The quality of DFT depends on the accuracy of the approximated exchange-correlation functional (E_{XC}). This is achieved by finding the best functional to describe the system. Hartree-Fock is a wave function based method, meaning that the exact wavefunction is, in principle, known, and hence improvements involve systematically progressing towards the exact form. However, DFT is not a wavefunction based method, and therefore the major drawback is that, when trying to improve the method, the form of the exact functional is completely unknown. In DFT, to find an improved method, it is largely trial and error. The E_{XC} functional is an approximation, and the quality of this approximation depends on each system and on how well the kinetic energy, exchange energy and electron correlation are described for that system.

3.2.2 Local density approximations

The early model systems used to approximate exchange correlation functionals were based upon the uniform (or homogeneous) electron gas model. It states that the interacting electrons are evenly distributed within a uniform, positively charged background, so that a constant value for the electron density is uniformly distributed throughout the model. Although this is not a realistic model of a molecular system, which usually contains rapidly varying densities, this model is used because the form of the exchange and correlation functionals are accurately known (Equation 3.18).

$\varepsilon_{XC}(\rho(\vec{r}))$ is the exchange-correlation energy per particle of a uniform electron gas of density $\rho(\vec{r})$, i.e., the energy density per particle density. The energy per particle is weighted by the probability $\rho(\vec{r})$ that there is an electron at this position. This is the definition of the local density (LD) approximation. $\varepsilon_{XC}(\rho(\vec{r}))$ is the sum of the energies for the exchange, $\varepsilon_X(\rho(\vec{r}))$, and correlation, $\varepsilon_C(\rho(\vec{r}))$, parts (Equation 3.19 – 3.20).

$$E_{XC}^{LD}[\rho] = \int \rho(\vec{r})\, \varepsilon_{XC}(\rho(\vec{r}))\mathrm{d}\vec{r} \qquad \text{Equation 3.18}$$

$$E_{XC}[\rho] = \varepsilon_X(\rho(\vec{r})) + \varepsilon_C(\rho(\vec{r})) \qquad \text{Equation 3.19}$$

$$\varepsilon_X = -\frac{3}{4}\sqrt[3]{\frac{3\rho(\vec{r})}{\pi}}\, \varepsilon_C(\rho(\vec{r})) \qquad \text{Equation 3.20}$$

The LD approximation can be written as the unrestricted version, where the functional is divided into two functionals for the different spin densities, which are $\rho_\alpha(\vec{r}) + \rho_\beta(\vec{r})$ (Equation 3.21). This allows greater accuracy for open-shell systems whereby the spin densities are different due to differences in the population of electron spins α and β. This unrestricted form of the LD approximation is called the local spin-density (LS) approximation.

$$E_{XC}^{LS}[\rho_\alpha,\rho_\beta] = \int \rho(\vec{r})\, \varepsilon_{XC}\left(\rho_\alpha(\vec{r}),\rho_\beta(\vec{r})\right)\mathrm{d}\vec{r} \qquad \text{Equation 3.21}$$

The spin densities at any position are expressed by the normalised spin polarisation parameter (ξ) (Equation 3.22) where $\rho_\alpha(\vec{r}) \neq \rho_\beta(\vec{r})$. ξ ranges from 0 (where the spins are matched equally) to 1 when it is fully spin polarised (where all electrons are one specific spin) (Equation 3.22). This means that for an open-shell system at the coordinate $\vec{r}$, there are both α and β spin densities to be used in the LS approximation. Therefore, the spin densities, $\rho_\alpha(\vec{r})$ and $\rho_\beta(\vec{r})$, are associated with the exchange correlation energies, $E_{XC}(\vec{r})$, of the homogeneous electron gas (Equation 3.21). This is done at each point in space and integrated over the density. Since the LS approximation assumes that the electron spin density is homogenous

at each coordinate throughout the system, the exchange correlation potentials depend only on local spin densities.

$$\xi = \frac{\rho_\alpha(\vec{r}) - \rho_\beta(\vec{r})}{\rho(\vec{r})}$$

Equation 3.22

This approximation is far from what is observed within real molecular systems however, surprisingly, it can deliver superior results, relative to Hartree-Fock. However, due to the low accuracy of the energetic details, improvements are required.

3.2.3 The generalised gradient approximation

One improvement is to incorporate a gradient of the charge density, $\nabla\rho(\vec{r})$, at each point $\vec{r}$, in addition to the information about the density $\rho(\vec{r})$. This means that the non-homogeneity of the electron density in a true molecular system is incorporated. This inclusion of a gradient forms the generalised gradient approximation (GGA) (Equation 3.23 – 3.24). This means that the function, f, (Equation 3.23) depends on both the densities ($\rho(\vec{r})$) and density gradients ($\nabla\rho(\vec{r})$). To solve the E_{XC}^{GGA}, it is split into the individual E_X^{GGA} and E_C^{GGA} contributions and each is approximated individually. The E_X^{GGA} (Equation 3.24) contains the functional F, that is the reduced density gradient for the spin (σ), and s_σ that is the local inhomogeneity parameter (Equation 3.25).

$$E_{XC}^{GGA}\left[\rho_\alpha,\rho_\beta\right] = \int f\left(\rho_\alpha,\rho_\beta,\nabla\rho_\alpha,\nabla\rho_\beta\right)d\vec{r}$$

Equation 3.23

$$E_X^{GGA} = E_X^{LDA} - \sum_\sigma \int F(s_\sigma)\,\rho_\sigma^{4/3}(\vec{r})\,d\vec{r}$$

Equation 3.24

$$s_\sigma(\vec{r}) = \frac{|\nabla\rho_\sigma(\vec{r})|}{\rho_\sigma^{4/3}(\vec{r})}\,(\vec{r})\,d\vec{r}$$

Equation 3.25

The inhomogeneity parameter ($s_\sigma(\vec{r})$) assumes large values for large gradients $\nabla\rho_\sigma$, and also for regions with small densities, because of the denominator $\rho_\sigma^{4/3}(\vec{r})$. From this equation, it is also deduced that small values of s_σ are achieved in regions of high electron density or small gradients of density, such as in the regions of bonding

interactions. This is one of the main differences of GGA compared to LD approximations whereby s_σ equals zero over all of the space.

The GGA has led to the development of several functionals, F, such as the Becke exchange functional (B). This is the most commonly used GGA exchange functional and it is used in combination with several gradient-corrected correlation functionals. The most popular correlation functional today was derived by Lee, Yang and Parr (LYP). The LYP correlation functional is not based on the uniform electron gas but is derived from an expression for the correlation energy of the helium atom.

3.2.4 Hybrid functionals

The aim of DFT development is to get the most accurate exchange-correlation energy, and one way to perform this is to use hybrid functionals, to combine (with different weightings) the approximate DFT exchange functional with the exact HF exchange functional, which is calculated from the Slater determinant, with a correlation functional (Equation 3.26). *X* is optimised for these hybrid functionals to find the most appropriate value. Within this thesis the M06-2X functional is used, which is a generally applicable functional for various systems, however it is suited for main group thermochemistry or for the kinetics of such systems.[99] The M06 suite contains a series of hybrid functionals, some that contain HF exchange at various weightings, and meta-GGA functionals.

$$E_{XC}^{hybrid} = \frac{X}{100} E_X^{HF} + \left(1 - \frac{X}{100}\right) E_X^{DFT} + E_C^{DFT}$$

Equation 3.26

3.3 Basis sets

In order to accurately determine the energy of the system, an accurate wavefunction must be constructed. In computational chemistry a basis set is used to describe the molecular orbitals by using a combination of functions. The two main types of basis functions used are Gaussian-type orbitals (GTO) and Slater-type orbitals (STO). Cartesian GTO, of the form in Equation 3.27, construct the set of basis functions that are used in wave function-based methods such as HF. N is the normalisation factor,

α is the orbital component that determines how diffuse (small α) or compact (large α) the functional is, and *l*, *m*, and *n* sum up to determine the nature of the orbitals, whether s, p, d. etc. The STO basis functions differ from GTO functions because they contain spherical and angular parts to the function, and the orbitals take on an appearance of hydrogen atomic orbitals (Equation 3.28). Where, *n* is the principle quantum number, ξ is the orbital exponent and Y$_{lm}$ are the spherical harmonics that describe the angular part of the function.

$$\eta^{\mathrm{GTO}} = N\, x^l\, y^m\, z^n\, e^{-\alpha r^2}$$ Equation 3.27

$$\eta^{\mathrm{STO}} = N\, r^{n-1}\, e^{-\xi r}\, Y_{lm}(\Theta,\phi)$$ Equation 3.28

The STO basis function has a large dependence on r, which means that the orbitals exhibit a cusp as $r \to 0$, which mimics the behavior of hydrogen atomic orbitals, as well as giving the exponential decay observed at tail regions of the orbitals ($r \to \infty$). Although STO basis sets are the more accurate way to describe the orbitals, the computational cost means that GTO basis sets are often used instead. As a method to achieve a similar accuracy as that which is achieved with STO basis sets, contracted GTO basis sets are used.[100] These basis sets consist of several primitive Gaussian functions that are linearly combined to give one contracted Gaussian function (CGF) (Equation 3.29). $d_{a\tau}$ is the contraction coefficient which can be chosen to get the CGF to resemble the STO function as closely as possible. A is the number of functions in the contraction.

$$\eta_\tau^{\mathrm{CGF}} = \sum_a^A d_{a\tau}\, \eta_a^{\mathrm{GTO}}$$ Equation 3.29

The CGF generates an approximation of the STO, but at lower computational cost. This strategy yields the STO-nG basis sets, where n is the number of primitive Gaussian functions contracted to form the CGF.

There are several categories of basis sets, from the simplest and least accurate minimal basis sets, to double or triple-zeta basis sets, however increasing the number of functions, although it increases the accuracy, does come at a higher

computational cost. Minimal basis sets are the least accurate, this expansion of the molecular orbitals uses one basis function for each atomic orbital, both core and valence. This basis function may be a contracted function of primitive Gaussian functions to form a single CGF set, e.g. STO-nG basis sets. The accuracy of the calculations is improved by using double-zeta basis sets, whereby two functions are used to describe each atomic orbital. However, this larger basis set is only required on the valence orbitals, since these are the electron wavefunctions that undergo the most changes during chemical processes. Therefore, a reasonable accuracy can still be achieved if the valence orbitals are treated with a double-zeta basis sets, whilst the inert core orbitals are treated with a minimal basis set. This basis set, where the valence and core electrons are treated differently is called a split-valence type set, such as the 6-31G Gaussian basis set. It is clear to see how these schemes can be extended to triple-zeta and quadruple-zeta, etc, to achieve more accurate results. For example, the 6-311G is a triplet-zeta, split-valence basis set that describes Gaussian-type orbitals. The 6 in the basis set means that 6 primitive Gaussian functions generate a single contracted Gaussian function, and this single CGF is applied to each of the core orbitals of the molecule. The -311 in this basis set, means that three basis functions are used to describe the valence orbitals. Of these three basis functions, the 3, is a CGF consisting of three primitive Gaussian functions, whilst the 1's are all a single primitive Gaussian function

Additionally, polarisation functions (d,p), can also be added to the basis set. These functions are of higher angular momentum than is required for the atom, to give the orbital more flexibility. The d is added for polarisation of the non-hydrogen atoms, and the p is for polarisation of the hydrogen atoms. The addition of these functions distort the atomic orbitals form their original symmetry into more realistic molecular orbitals. Diffuse functions can also be added to basis sets to extend the CGFs further from the nucleus. These are useful when modelling species such as anions. These are also important for larger elements, such as d-block, where the orbitals are further from the nucleus. These functions are denoted with a '+', for diffuse functions on the non-hydrogen atoms, or '++' where the latter is for both hydrogen and non-hydrogen atoms.

Systems that contain heavy elements ($Z > 36$), should be modelled with additional functions.[97] Heavy elements contain a larger number of electrons, which are mostly located within the core of the atom. Therefore, an effective core potential, or pseudo potential, should be incorporated into the calculation to accurately model the chemically "inert" core electrons. An effective core potential (ECP) replaces the core basis functions (of the core electrons) with functions that represent a combined nuclear-electron core and the interactions with the valence electrons. A main reason to incorporate these ECPs is because of the relativistic effect of heavy atoms. Electrons at the core of heavy elements can reach velocities close to the speed of light, because the increase in the nuclear charge leads to a contraction of the innermost core orbitals. Due to this increase in contraction of the orbital, the speed of the electrons is increased. Therefore, the usual non-relativistic Hamiltonian does not account for the relativistic effects and as such many chemical properties do not accurately represent the true value. There are two models of the ECPs that vary by the number of electrons that are included in the core. A "large-core" ECP includes all the electrons as core electrons, except for the valence electrons, whereas "small-core" ECPs include less electrons in the core. "Small core" ECPs view the electrons in the valence shell (principal quantum number, $n = x$) and the electrons of the sub-valence shell ($n = x\text{-}1$) as the "valence electrons" and all others as the core electrons. The benefit of a small-core ECP is that in heavy elements the polarisation of the sub-valence shell can be significant and thus it can be worth the additional computational cost to include them as "valence" electrons in the calculation.

As has been demonstrated basis sets can be tailored to any system that is to be studied. The accuracy of the calculations depends on the system used and whether additional functions were included, if needed. Once the appropriate functional and basis set has been selected for the molecular system to be modelled, then the required properties of that system can be determined using a software package such as Gaussian. However, to assure that an efficient basis set is being used, which obtains accurate results with a minimal computational cost, it can be beneficial to compare basis sets to ensure the correct functions are present.

3.4 Computational methods

3.4.1 Single electron transfer

To model an electron transfer step computationally, the Marcus-Hush theory[101] should be employed. The Franck-Condon principle states that the electronic transitions occur instantaneously and are followed by the structural relaxation of the molecule. Therefore, the electron transfer can be visualised using two energetic parabolas (Figure 3.1). The intersection of the two parabolas is where electron transfer can occur, and thus the energy for electron transfer is the activation energy, $\Delta G^{\ddagger}$ (Equation 3.30). Upon the transfer of the electron significant structural change and solvent reorganisation is required to account for the changes of the electronic environment. The energy of the reorganisation is labelled as λ.
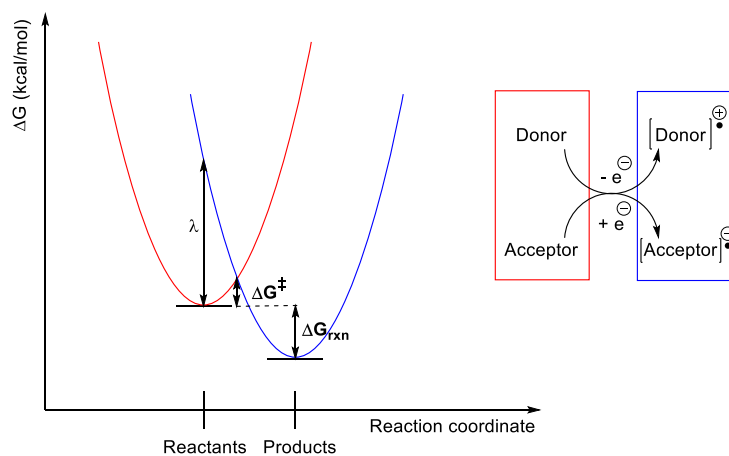
Figure 3.1 A representation of the thermodynamics of the electron transfer step.

$$\Delta G^{\ddagger} = \frac{1}{4}\frac{(\lambda + \Delta G_{rxn})^2}{\lambda}$$

Equation 3.30

The reorganisation energy (λ) is determined computationally by splitting the reorganisational energy into its internal and external components, and because studies showed that the external reorganisation effect is minimal, only the internal reorganisation energy is used (Equation 3.31). The reorganisational energy (λ) is calculated computationally by optimising the geometries' of both the acceptor and donor species, before and after the electron transfer.

$$\lambda = \frac{\lambda_i(D) + \lambda_i(A)}{2}$$

Equation 3.31

To calculate the energetic profile for SET it is commonly performed using Nelson's four-point method, employing Marcus theory.[101,102] The electron donor and the electron acceptor species are optimised individually, both before and after SET. When the optimised geometry was obtained for the electron donor species, before SET, then a single point energy (SPE) calculation is performed using a different charge and multiplicity of the system to reciprocate that of the electron donor species after SET. This is repeated for all the optimised geometries (both of the electron acceptor and donor).

A more modern method to model the SET was recently reported.[45] Instead of optimising the donor and acceptor molecules individually, the new method optimised the donor and acceptor species as a complex, both before and after SET. A SPE calculation is performed using a different charge and multiplicity of the system to reciprocate that of the complex after SET. This is repeated for the optimised geometries of the complex after SET, using the charge and multiplicity of the system to reciprocate that of the complex before SET.

4.

Electron donors from simple organic molecules

4.1 Introduction

Over the past couple of years, the Murphy group has investigated the roles of various organic additives in the transition metal-free coupling reactions of haloarenes with benzene. Expanding on their efforts to identify the electron donor species in these BHAS reaction pathways within this chapter, attempts were made to identify the electron donor formed *in situ* from the action of KO^{t}Bu and *N,N'-*dipropyldiketopiperazine (DKP). In this chapter, evidence is provided that other simple organic molecules can form electron-rich species in the presence of KO^{t}Bu, and can donate to haloarenes in the transition metal-free reaction conditions.

4.2 Computational methods

The calculations were run using the M06-2X functional[103-104] with the 6-311++G(d,p) basis set[105-109] on all atoms, except for the iodine. Iodine was modelled with the MWB46 relativistic pseudo potential and associated basis set.[110] All calculations were carried out using the C-PCM implicit solvent model.[111-112] All calculations were performed in Gaussian09.[113]

4.3 Design of a new *N,N'*-dipropyldiketopiperazine additive

There has been a lot of interest in the transition metal-free coupling of a haloarene with benzene, through the reported BHAS mechanism (that was introduced in Section 1.2.2, Scheme 1.11).[38] The initiation step is a SET to the haloarene to form the aryl radical **4.2**,[44] and this aryl radical attacks a molecule of benzene to form **4.3**.[38] This radical **4.3** undergoes a deprotonation to yield the radical anion **4.4**, which is electron-rich and thus will donate an electron to the starting material **4.1** to form the product **4.5** and propagate the radical chain.[38] Although it is accepted that the initiation step is a SET process, the species responsible for this electron donation to **4.1** has been debated. Recent findings point to the formation of an organic electron donor formed by the reaction between KO^{t}Bu and an organic additive.[40,42,44] Within the Murphy lab, one of the most successful additives is the DKP additive **4.6** which was shown to be very good at promoting both the transition metal-free aryl-aryl bond formation and S$_{RN}$1 bond formation (described in Chapter 6).[42,114] It has been

proposed that the DKP additive **4.6**, in the presence of KO*t*Bu, forms an electron-rich enolate anion **4.7**, which is capable of donating a single electron to the haloarene **4.1** in the initiation step of the BHAS reaction pathway (Scheme 4.1A).[42] The aim of this project was to find evidence that the enolate anion of DKP **4.7** donates an electron to the haloarene, such as **4.1**, under the transition metal-free reaction conditions. The enolate anion of DKP **4.7** contains an electron-rich double-bond which bears three heteroatom substituents that donate electron density into it. A SET from the enolate anion moiety of **4.7** will form the captodatively stabilised radical **4.8** (Scheme 4.1B).
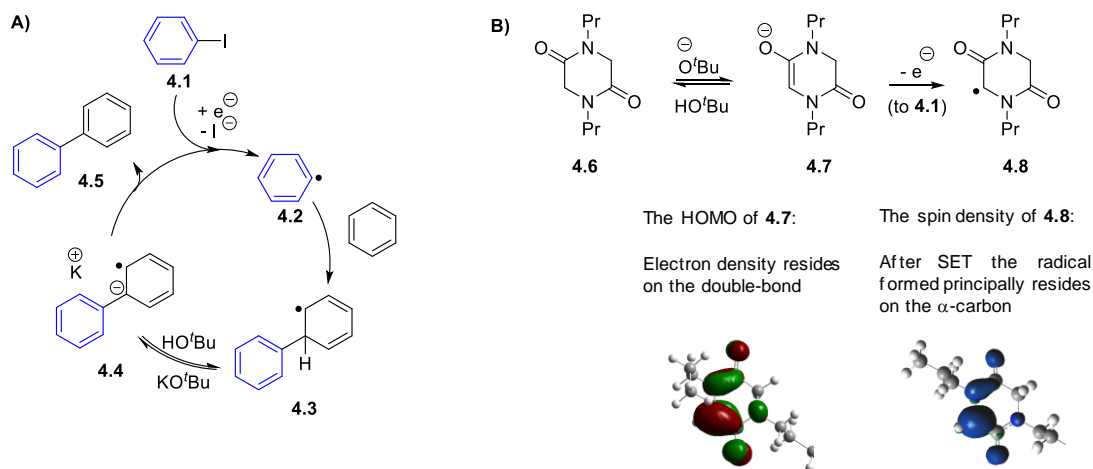
Scheme 4.1A) The BHAS mechanism.[38] **B)** The proposed electron donor **4.7** formed *in situ* from DKP **4.6**.

According to the literature the radical **4.8** can be intramolecularly trapped by the design of an appropriate tether on the DKP scaffold.[115] Jahn *et al.* synthesised many diketopiperazines that contained various "tethers" attached to the DKP scaffold, using a different method to that used in this chapter (Scheme 4.2). They synthesised a DKP molecule **4.9** that contained an alkene tether attached to the DKP core structure. In the presence of base, **4.9** is converted into its enolate anion, and this enolate anion is oxidised and subsequently coupled to TEMPO to form **4.11**. Bond thermolysis of the alkoxyamine **4.11** generates the captodatively stabilised radical **4.14** and a molecule of TEMPO **4.10**.[115] Upon the formation of **4.14**, the radical can cyclise onto the alkene to form the radical **4.15**, which affords **4.12** from radical

combination with TEMPO **4.10**. Based upon this literature precedent, a DKP analogue was designed that would be used as an additive in the transition metal-free reaction conditions, to find evidence that the DKP additive is responsible for initiating the BHAS reaction pathway by performing SET to haloarenes, such as **4.1**.
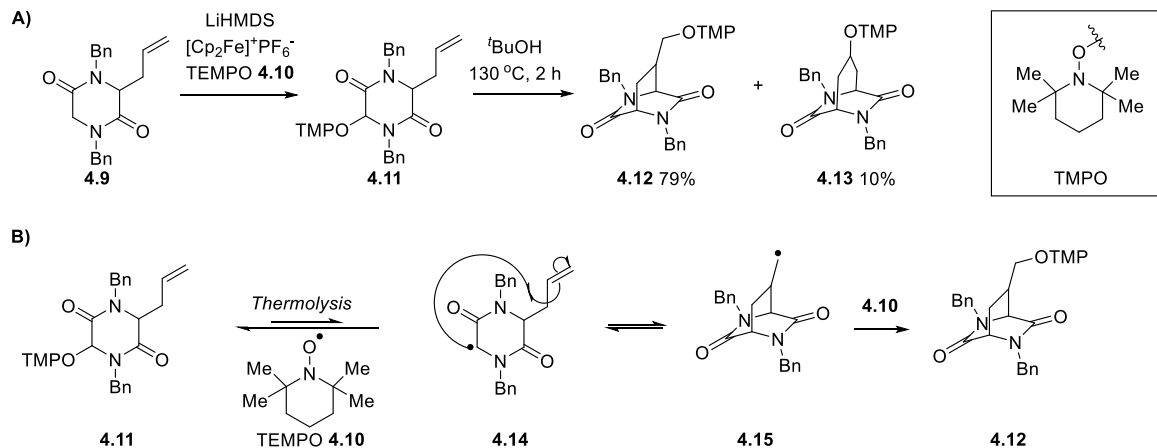
Scheme 4.2 Literature synthesis of bridged diketopiperazines using radical cyclisation and the proposed mechanism.[115]

The additive designed for the study was **4.19**, which contains a tether attached to the α-carbon on the DKP core that contains both a *cis*-alkene and a SPh moiety (Scheme 4.3). This additive **4.19** has two radical probes to indicate that the captodatively stabilised radical was formed in the reaction: (1) In the presence of KO*t*Bu, the DKP additive **4.19** will exist as its enolate anion; either the kinetic **4.20** or the thermodynamic enolate anion **4.21** will form from **4.19** in the presence of KO*t*Bu. If the kinetic enolate anion **4.20** donates an electron, the stabilised radical **4.22** will form; however, a similar species **4.26** can also form by SET from the thermodynamic enolate anion **4.21**. The radical **4.22** will cyclise onto the *cis*-alkene moiety in the tether to form the intermediate radical **4.23**, and alternatively the radical **4.26** will cyclise to produce **4.27**. In both cases, if the radical cyclisation is reversible, the principal product of SET from the DKP additive **4.19** may be the corresponding alkene *trans*-stereoisomer. (2) Cyclisation of the radical **4.22** onto the *cis*-alkene may lead to a C-S bond cleavage of radical **4.23** to eliminate a thiyl (SPh) radical **4.25** and form the cyclised product **4.24**.[116] The loss of the thiyl radical, SPh, would be evidence for the cyclisation of the captodatively stabilised radical, and hence

evidence for SET from the enolate anion of DKP. The thiyl group, SPh, was chosen because it is a good radical leaving group and the SPh radical, or products derived from it, can easily be isolated, e.g. as diphenyl disulfide. Thiyl radicals can also add to alkenes in a reversible addition/elimination.[117-118] Isolation of any of these products will be indicative that SET has occurred from the enolate anion moiety of DKP additive **4.19**.
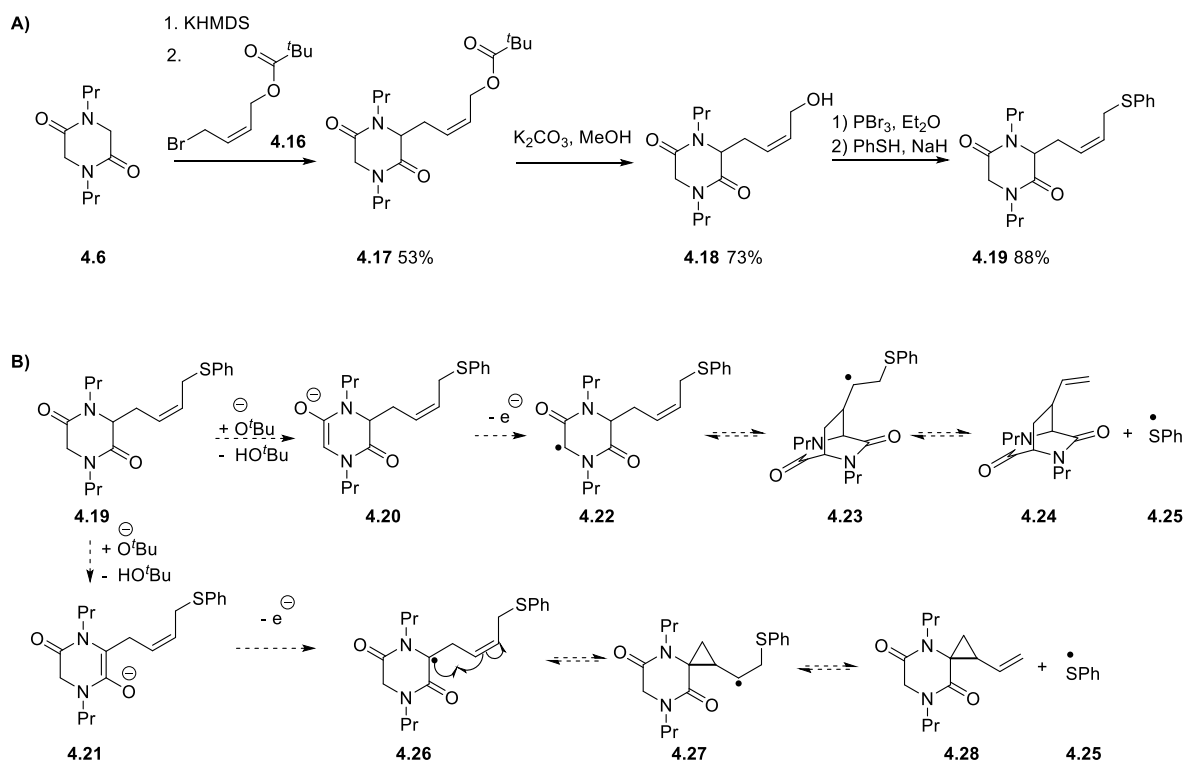
Scheme 4.3 A) Formation of the additive **4.19** from **4.6**. **B)** The mechanism of cyclisation of either **4.22** or **4.26**, both of which form through SET from an enolate anion of DKP additive **4.19**.

The initial investigations were to determine whether the enolate anion of the additive, either **4.20** or **4.21**, was capable of donating an electron, and, if so, whether the radical formed would cyclise onto the *cis*-alkene within the tether. The substrate chosen as the electron acceptor in this initial study was 1,2-diiodoethane **4.29**, which is a good electron acceptor substrate (reduction potential 0.115 V *vs.* SCE).[119-121] The additive **4.19** was reacted with KO*t*Bu and 1,2-diiodoethane **4.29**, in benzene as

a solvent under the reaction conditions most commonly used for the transition metal-free reaction conditions (Table 4.1).

Table 4.1 Reduction of 1,2-diiodoethane **4.29** using stoichiometric amounts of additive **4.19**, in the presence of KO^{t}Bu.
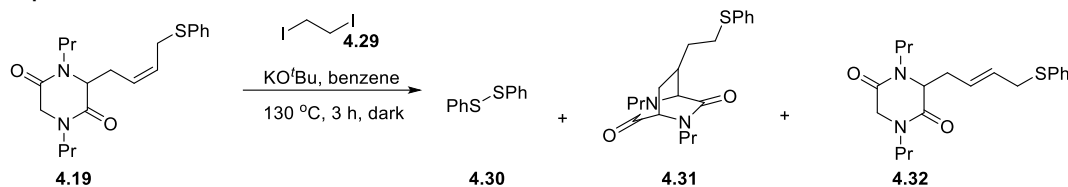
Entry	**4.29** (eq.)	**KO^{t}Bu** (eq.)	**4.30** (%)	**4.31** (%)	**4.32** (%)
1	1	2	18[a.]	-	< 27[a.b.]
2	3	2	17[c.]	-	13[a.]
3	2	1.4	14[c.]	-	28[a.]
4	0	2	2[c.]	11[b.]	-

[a.] Isolated yield. [b.] Could not be isolated pure. [c.] Yield calculated using 1,3,5-trimethoxybenzene as the internal standard in ^{1}H-NMR of the crude mixture.

Using 1,2-diiodoethane **4.29** as the electron acceptor, in the presence of KO^{t}Bu the additive **4.19** yielded diphenyl disulfide **4.30** as well as product **4.32**, which is the *trans*-isomer of the starting DKP additive **4.19**, which was identified from the *J* values of the alkene protons in the ^{1}H-NMR (for the substrate **4.19**: J_{cis} = 10.8 Hz; for the product **4.32**: J_{trans} = 15.2 Hz) (Table 4.1, entries 1 - 3). Interestingly, in the absence of 1,2-diiodoethane **4.29**, diphenyl disulfide **4.30** was still observed, albeit in very low yields (2%), as well as product **4.31** (Table 4.1, entry 4). The diphenyl disulfide **4.30** can only be formed through a radical C-S cleavage to eliminate a thiyl radical **4.25** from the tether of the additive **4.19** (Scheme 4.4).[122] The formation of these products **4.30 – 4.32** are proposed to occur by SET from either of these enolate anions. That will lead to the formation of a captodatively stabilised radical, such as **4.22** or **4.26** respectively. Both of these radicals can cyclise onto the *cis*-alkene in the tether, and thus the radical intermediates **4.23** or **4.27** will be formed. These two intermediates may eliminate the thiyl radical **4.25** to form either **4.24** or **4.28** as potential products. The thiyl radical **4.25** can dimerise to form diphenyl disulfide **4.30**. The rates for the addition and elimination of thiyl radicals to alkene moieties have been widely studied, and an equilibrium is often established.[123] For example, the rate constant for the

addition of *tert*-butylthiyl radical onto 1-octene was reported at 1.9 x 10^6 M^{-1} s^{-1}, and the reverse fragmentation was 3.5 x 10^5 s^{-1}, and the addition of the thiyl radical **4.25** onto methyl methacrylate was reported at 3.2 x 10^6 M^{-1} s^{-1}, with the equilibrium constant of 7.8 favouring the addition step.[123] It is proposed that upon reversible C-S bond cleavage the eliminated thiyl radical **4.25** will attack the alkene of **4.24** or **4.28** to regenerate the intermediate radicals **4.23** or **4.27**. These radicals undergo a C-C bond cleavage to generate the most stable radical species **4.33**, which contains the captodatively stabilised radical in addition to principally the *trans*-isomer of the double-bond in the tether. The radical **4.33** will form the *trans*-isomer product **4.32** upon quenching of the stable radical through a hydrogen atom abstraction. Another possibility is that the radicals **4.23** or **4.27** could undergo hydrogen atom abstraction to form their analogues, for example **4.31** from the radical **4.23** (Table 4.1). It must be noted that the intermediates **4.23** and **4.27** could form **4.33** directly, without eliminating **4.25** if the cyclisation pathway was reversible.
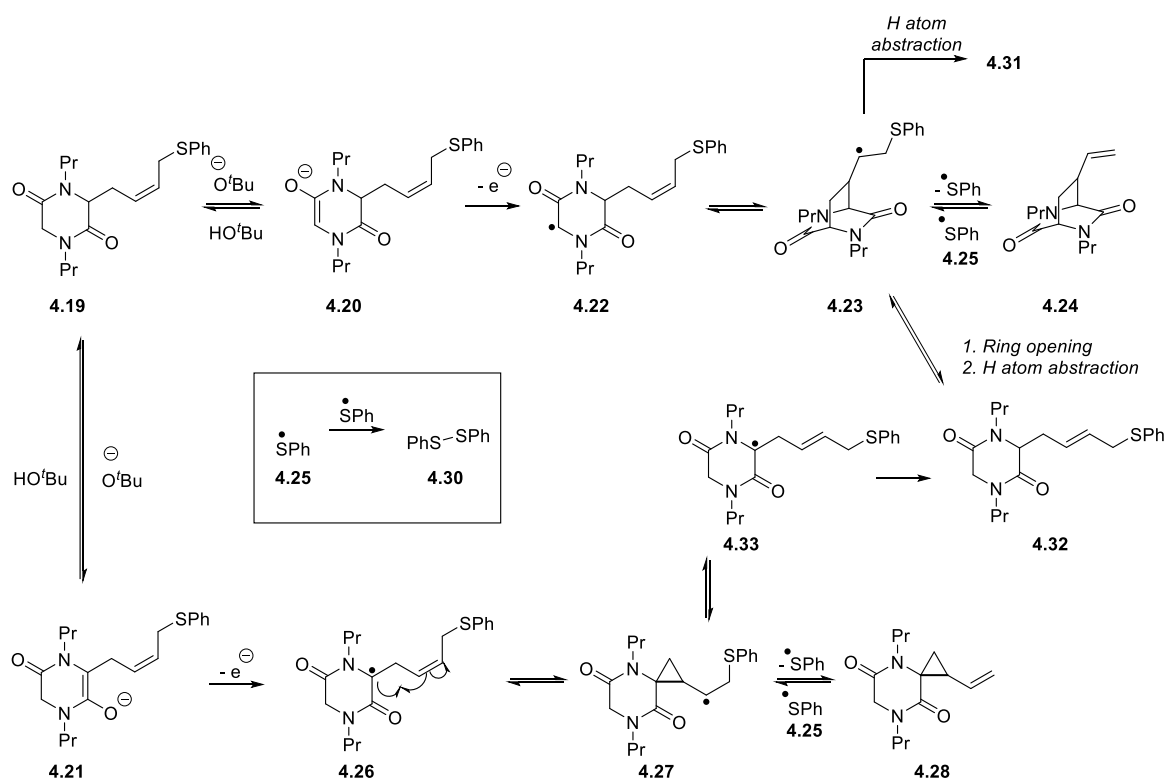
Scheme 4.4 Proposed mechanism in the formation of products **4.30 – 4.32**.

As mentioned above, when the reaction was performed without the 1,2-diiodoethane **4.29** (Table 4.1, entry 4) the additive **4.19**, in the presence of KO^{t}Bu, formed both diphenyl disulfide **4.30** and product **4.31**. This suggests that, in the absence of any external electron acceptors, the additive **4.19** is capable of forming the captodatively stabilised radical **4.22** (or **4.26**). Computational analysis of the HOMO and LUMO of the enolate anion **4.20** suggests that it could act as an electron donor, from the corresponding enolate anionic moiety, as well as an electron acceptor, at the allylic sulfide moiety (Scheme 4.5). If an electron is donated into the allylic sulfide moiety, an intermediate such as **4.34** will be formed.[122] This species will undergo a loss of the thiyl radical to form intermediates such as **4.35** (Scheme 4.5), which may react further to form unidentified products. The low yields of product formed in the absence of an external electron acceptor, such as 1,2-diiodoethane, suggest that, as expected, this intermolecular SET to **4.20** is more difficult than SET to 1,2-diiodoethane.
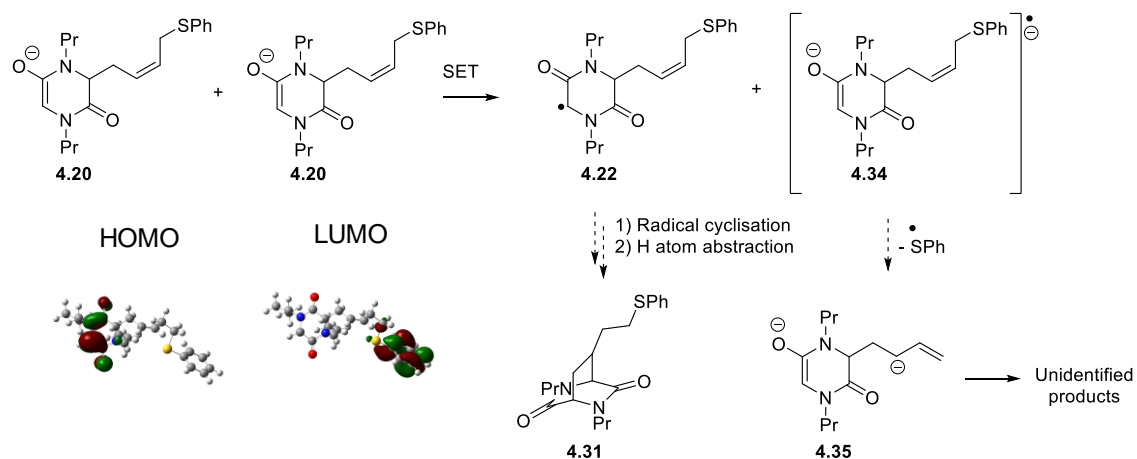
Scheme 4.5 Proposed mechanism for intermolecular SET between two enolate anions of the DKP additive **4.20** that occurs in the absence of external electron acceptor.

The energy profile for the SET from a molecule of **4.20** to another molecule of itself, or to the neutral additive **4.19**, was modelled and the results show that the barriers for the SET were very high; SET to **4.20** $\Delta G^{\ddagger}$ = 74.9 kcal/mol and ΔG_{rxn} = 62.2 kcal/mol, and SET to **4.19** $\Delta G^{\ddagger}$ = 50.1 kcal/mol and ΔG_{rxn} = 45.5 kcal/mol. These results suggest that this SET is not possible. However, more recently, Tuttle *et al.*[45] described a new method to describe SET within these reactions that they claim

results in more accurate values. When the reaction was modelled for SET from **4.20** to another molecule of itself using the new method, lower barriers were calculated, however they were still unachievable, $\Delta G^{\ddagger} = 49.0$ kcal/mol and $\Delta G_{rxn} = 49.0$ kcal/mol. Unfortunately, the SET calculation from **4.20** to **4.19** could not be modelled, but from the trends observed it is expected that this SET would be more favourable in these reactions. However, due to the inability to calculate this SET, additional experiments were performed to deduce whether the radical **4.22** is formed and can cyclise to form the intermediate **4.23**; 1) the ionic cyclisation pathway was computationally modelled and 2) an intermolecular system, analogous to the additive **4.19**, was studied.

An alternative mechanism to form **4.31** involves an ionic pathway rather than the radical pathway, and so computational analysis of the two possibilities was performed (Scheme 4.6). *In silico*, the cyclisation of **4.20** formed **4.24** in a concerted mechanism involving C-S bond cleavage *via* the intermediate **4.36**. Therefore, under these reaction conditions the intermediate **4.36** would not be stable, and hence this ionic cyclisation mechanism would not lead to the isolated product **4.31**. However, the cyclisation *via* the radical pathway shows that the intermediate **4.23** will be the most stable species in the reaction pathway. The equilibrium for the thiyl radical elimination from **4.23** was computationally modelled and the C-S fragmentation to form **4.24** and **4.25** was calculated to be endergonic: $\Delta G^{\ddagger} = 6.6$ kcal/mol and $\Delta G_{rxn} = 1.9$ kcal/mol. This agrees with previously reported rates of elimination of thiyl radicals from alkenes, as was previously discussed.[123] Hence, based on the computational analysis the radical cyclisation will lead to the formation of **4.31**, unlike the ionic pathway, which supports the proposal that the mechanistic pathway involved in the formation of **4.31** is the radical cyclisation of **4.22**.
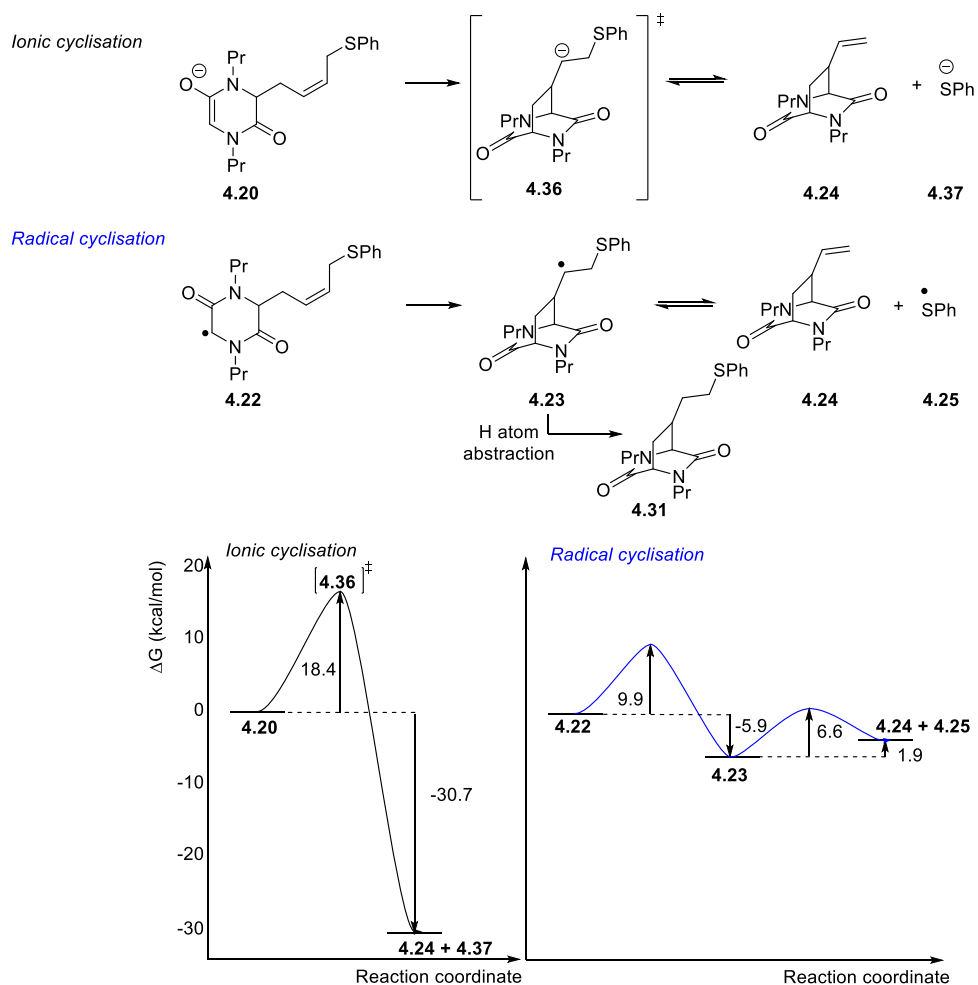
Scheme 4.6 Ionic (black line) *vs.* radical cyclisation (blue line) and cleavage of the C-S bond in benzene.

The ionic cyclisation of the enolate anion onto the allylic thioether within **4.20** was suggested to be possible from the computational studies to form **4.24** and a thiyl anion **4.37** (Scheme 4.6). To experimentally probe the possibility of the ionic attack of an enolate anion onto an allylic thioethers, the substrate **4.41**, which is analogous to the tether on the additive **4.19**, was synthesised and reacted under several reaction conditions to find evidence as to whether diphenyl disulfide is formed (Table 4.2). When the substrate **4.41** was reacted in the presence of KO^{t}Bu, no diphenyl disulfide **4.30** was observed in the crude reaction mixture (Table 4.2, entry 1). When either the DKP additive **4.6** (Table 4.2, entry 2) or pinacolone **4.42** (Table 4.2, entry 3) were used in the presence of KO^{t}Bu, low yields of diphenyl disulfide **4.30** were

formed (6% and 4% respectively). In the presence of 1,2-diiodoethane, the substrate **4.41** yielded **4.30** (19%).

Table 4.2 The synthesis of allylic thioether **4.41** and its reactions with KO^{t}Bu, in the presence of various additives.
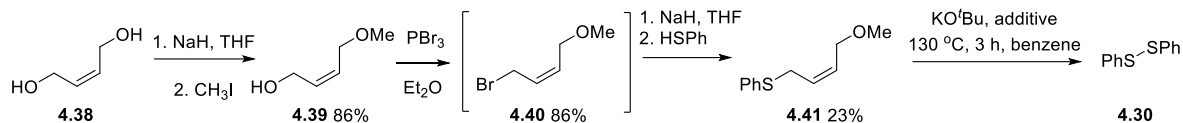
Entry	Additive (eq.)	KO^{t}Bu (eq.)	**4.30**[a.] (%)
1	--	1	0[b.]
2	DKP **4.6** (1)	2	6[b.]
3	pinacolone **4.42** (1)	2	4[b.]
4	1,2-diiodoethane **4.29** (1)	0	19

[a.] *Yield calculated using 1,3,5-trimethoxybenzene as the internal standard in ^{1}H-NMR of the crude mixture.* [b.] *Other products were identified as components in the reaction mixture but they could not be identified.*

Diphenyl disulfide **4.30** was not observed when substrate **4.41** was reacted in the presence of KO^{t}Bu alone, without any additives (Table 4.2, entry 1); however when the additives DKP **4.6** and pinacolone **4.42** were added to the reaction mixture (Table 4.2, entry 2 and 3 respectively), low yields of diphenyl disulfide **4.30** were observed in both reactions. Both DKP **4.6** and pinacolone **4.42** are capable of forming their respective enolate anions, and pinacolone **4.42** has previously been reported to be capable of donating an electron to haloarenes to initiate S$_{RN}$1 reactions in DMSO.[75] It is therefore possible that the diphenyl disulfide **4.30** in these two reactions forms from SET to the substrate **4.41**. However, future work should be performed to confirm this. When substrate **4.41** was exposed to the reaction conditions in the presence of 1,2-diiodoethane **4.29**, a larger amount of diphenyl disulfide **4.30** (19%) was formed than when the reaction was performed with other additives in this study. This result suggests that under these reaction conditions, 1,2-diiodoethane **4.29** in the presence of **4.41** leads to the formation of the product diphenyl disulfide **4.30**. This suggests that the previous reactions performed using additive **4.19** in the presence of 1,2-diiodoethane **4.29**, and the products arising from it, are not evidence for SET from the enolate anion of additive **4.20**. However, in the absence of 1,2-diiodoethane **4.29**, the DKP additive **4.19** formed product **4.31** through the proposed

mechanism that involves a SET from the enolate anion of additive **4.20**. Therefore, it was of great interest to apply the additive **4.19** to the transition metal-free reaction conditions used in the coupling of iodoarenes to benzene. The iodo-*m*-xylene **4.43** substrate was used to assess whether an electron donor is formed from the DKP additive, because in the transition metal-free coupling reactions the substrate **4.43** is activated towards coupling exclusively through a SET initiation step (Table 4.3).[42]

Table 4.3 Aryl-aryl bond formation between iodo-*m*-xylene **4.43** and benzene using various additives.[a.]

Entry	Additive (eq.)	4.43 (%)	4.44 (%)	4.45 (%)	4.5 (%)	4.30 (%)	4.31 (%)
1	--	98	--	--	--	--	--
2	**4.6** (0.2)	16	6	3	26	--	--
3	**4.19** (0.2)	53	4	10	13	28 (27)[b.]	20 (14)[b.]

[a.] *Yield calculated using 1,3,5-trimethoxybenzene as the internal standard in ¹H-NMR of the crude mixture (isolated yield).* [b.] *Yield calculated using the DKP additive* **4.19** *as the limiting reagent.*

Three reactions were performed, under inert atmosphere, for a direct comparison to determine how efficiently the additive **4.19** can promote the coupling between the iodo-*m*-xylene **4.43** and benzene. The first reaction exposed iodo-*m*-xylene **4.43** to KO*t*Bu in the absence of any organic additive (Table 4.3, entry 1) and after 3 h at 130 °C, 98% of the starting material **4.43** remained unreacted. Next, the iodo-*m*-xylene **4.43** was treated with KO*t*Bu and sub-stoichiometric amounts of additive **4.6** under the same reaction conditions. This reaction gave much higher conversion of the iodo-*m*-xylene **4.43** (only 16% remaining), and the rest of the products formed were **4.44** (6%), xylene **4.45** (3%) and biphenyl **4.5** (26%) (Table 4.3, entry 2). The

81

ratio of yields of **4.44** to **4.5** (approximately 1 : 4) was characteristic of previous experiments performed in these transition metal-free reaction conditions.[40,42-44] The final reaction was to expose **4.43** to KO*t*Bu and sub-stoichiometric amounts of additive **4.19** (Table 4.3, entry 3). Using **4.19** as the additive, the compounds obtained were: unreacted starting material **4.43** (53%), in addition to products **4.44** (4%), **4.45** (10%), **4.5** (13%), **4.30** (28%) and **4.31** (20%).

To couple iodo-*m*-xylene **4.43** with benzene, through the BHAS reaction pathway, an additive, either **4.6** or **4.19**, is required in the reaction because the reaction of **4.43** with KO*t*Bu and no additive returned only starting material (Table 4.3, entry 1). Iodo-*m*-xylene **4.43** in the presence of KO*t*Bu and either **4.6** or **4.19** (Table 4.3, entries 2 – 3) formed products **4.44**, **4.45** and **4.5**, which are known products for the reaction of iodo-*m*-xylene **4.43** *via* the BHAS pathway, thus providing evidence that the additive **4.19** is capable of promoting the transition metal-free aryl-aryl bond formation, similarly to DKP **4.6**. (Scheme 4.7).[42] SET to **4.43** leads to cleavage of the C-I bond and the formation of the aryl radical **4.46** and loss of an iodide anion. The aryl radical **4.46** can react in two ways: 1) it attacks a molecule of benzene to ultimately form product **4.44** through the BHAS pathway (previously shown in Scheme 4.1A). 2) The aryl radical **4.46** abstracts a hydrogen atom from a molecule of benzene to form xylene **4.45** and the aryl radical **4.2**. The aryl radical **4.2** will undergo the BHAS mechanism and ultimately lead to biphenyl product **4.5** (previously described in Scheme 4.1A). The formation of the product **4.31** suggests that the captodatively stabilised radical **4.22** forms in the reaction conditions. The formation of the radical **4.22** occurs through a SET from the enolate anion of the additive **4.20**, which provides evidence that the enolate anion is capable of donating a single electron to iodo-*m*-xylene **4.43** to initiate the transition metal-free aryl-aryl bond formation. Comparison of the reactions performed using the two possible additives, **4.6** and **4.19**, suggests they both react through similar reaction pathways. This is supported with the computational analysis; SET from the enolate anion **4.7** (Scheme 4.7) to iodo-*m*-xylene **4.43** is possible under the reaction conditions, $\Delta G^{\ddagger}$ = 23.0 kcal/mol and ΔG_{rxn} = 10.3 kcal/mol, and SET from the enolate anion **4.20** to iodo-*m*-xylene **4.43** has the energy profile, $\Delta G^{\ddagger}$ = 25.0 kcal/mol and ΔG_{rxn} = 13.3

kcal/mol. Both these energy profiles for SET are accessible at 130 °C, however the enolate anion of the DKP additive **4.7** has a more favourable overall energy profile for SET, which suggests that the conversion of **4.43** into products would be more efficient using the DKP additive **4.6** rather than additive **4.19**, which was seen experimentally.
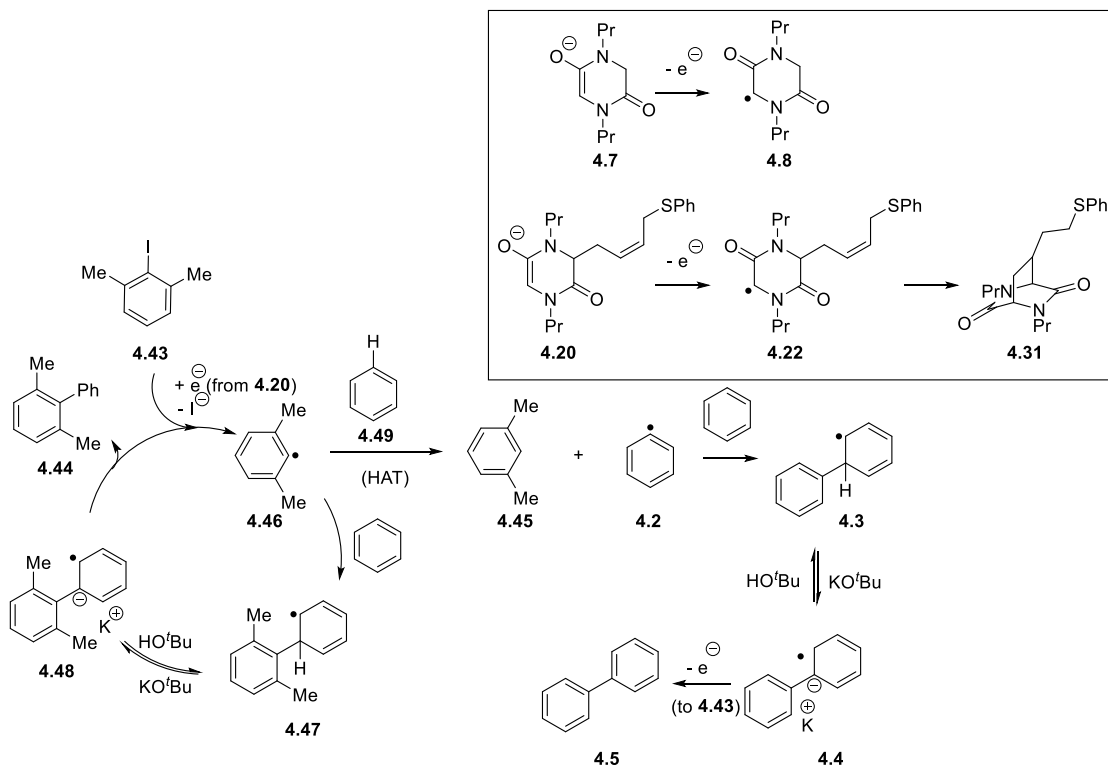
Scheme 4.7 A modification of the BHAS pathway for the reaction of substrate iodo-*m*-xylene **4.43**.[42]

This section has provided evidence that the additive **4.19** behaves analogously to **4.6** in these reaction conditions, and that the enolate anion of additive **4.19** will donate an electron to haloarenes under these transition metal-free reaction conditions. Therefore, it can be assumed that the role of the additive **4.6** in these transition metal-free reaction conditions, is to form the enolate anion *in situ* and this enolate anion **4.7** is the electron donor species that initiates the BHAS mechanism (Scheme 4.7). This supports the growing body of evidence relating to the role of organic electron donors in these reactions

4.4 The role of DMF in the transition metal-free coupling reactions

Taillefer *et al.*[83] reported the arylation of enolisable aryl ketones, such as propiophenone **4.50**, with iodobenzene **4.1** in DMF as the solvent (Scheme 4.8A). They proposed that the reaction proceeds by the deprotonation of DMF **4.52** to form the carbamoyl anion **4.53**, which acts as the electron donor to iodoarenes, such as iodobenzene **4.1**, to produce the aryl radical **4.2** in the initiation step of the S$_{RN}$1 pathway (Scheme 4.8B). The aryl radical **4.2** attacks the enolate anion of propiophenone **4.56**, to form the radical anionic species **4.57**, which can donate an electron to the haloarene **4.1** to propagate the radical chain mechanism and form the product **4.51**.
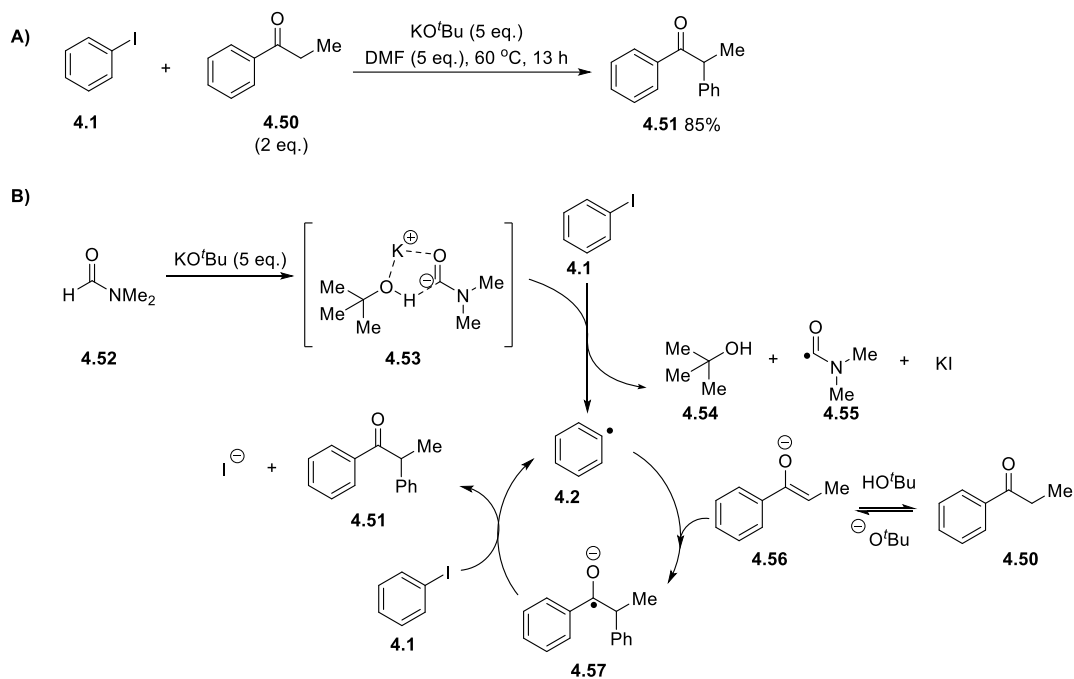
Scheme 4.8A) Taillefer *et al.*[83] reported the coupling of propiophenone **4.50** with iodobenzene using DMF **4.52** and KO*t*Bu. **B)** The proposed S$_{RN}$1 mechanism for the formation of product **4.51**.

They reported their computational studies of the reaction pathway, and the rate determining step was determined to be the SET from the carbamoyl anion **4.53** to iodobenzene **4.1**, ΔE = 15.9 kcal/mol (Scheme 4.9). However, on analysis of their reported results, the "energy barrier" that they reported was actually the relative

energy differences between the starting materials (**4.53** and **4.1**) and the products after SET (**4.60** and **4.2**), and the transition state energy profile therefore needed to be computed to provide a more accurate description for the energy profile of the SET step. Therefore, computational analysis for this SET step was performed using Marcus-Hush theory (Scheme 4.9, Method A).[101-102] The result was compared to the energy profile calculated using the method Taillefer *et al.*[83] had used (Scheme 4.9, Method B: comparison of relative energies of the starting materials and the products).
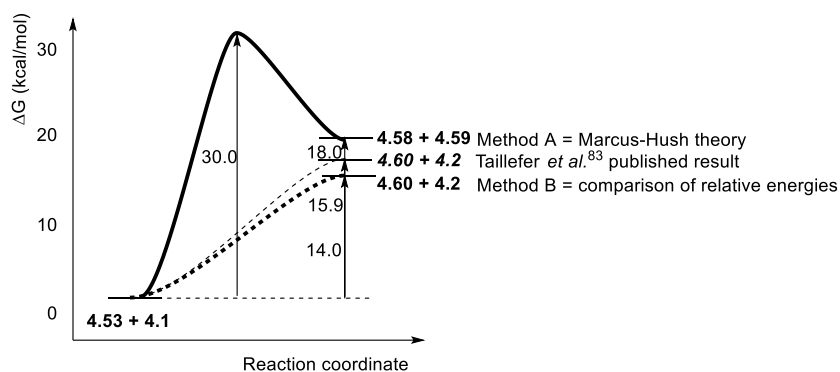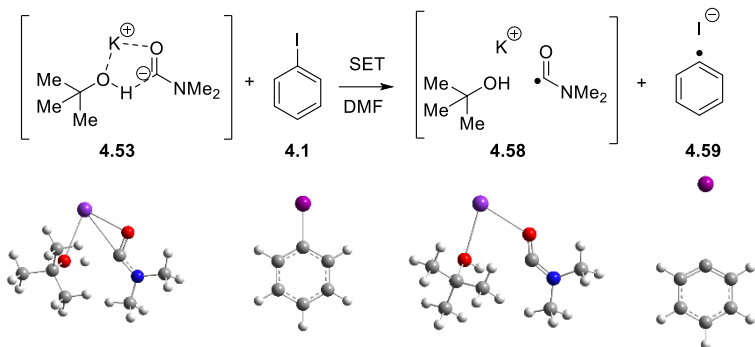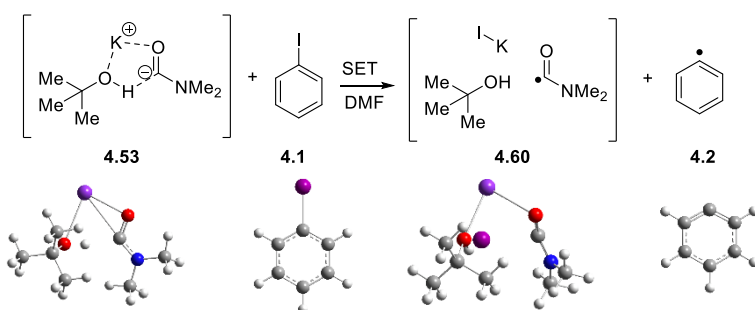
Scheme 4.9 The computationally determined energy profile for SET from the carbamoyl anion of DMF **4.53** to iodobenzene **4.1** using either Marcus-Hush theory (Method A) or comparing relative energies of the reaction starting materials and products (Method B).

The energetic barrier for SET from the carbamoyl anion **4.53** to iodobenzene **4.1** using Marcus-Hush theory (Method A) was $\Delta G^{\ddagger}$ = 30.0 kcal/mol, and the relative energy was ΔG_{rxn} = 18.0 kcal/mol, which can be compared to the relative energy ΔG_{rxn} = 14.0 kcal/mol, calculated using the method Taillefer *et al.*[83] reported (Method B). There are several comments that should be made regarding these results. Firstly, a direct comparison between the results obtained using the method Taillefer *et al.*[83] used (Method B), and the results Taillefer *et al.*[83] published (ΔE = 15.9 kcal/mol), shows a difference in the results. This is because the computational method used by Taillefer *et al.* (M06-2X/6-311+G(d,p) level of theory and the PCM solvent model) is at a different level of theory than used in this study. In this study the M06-2X/6-311++G(d,p) level of theory and the C-PCM implicit solvent model was chosen because the studies involve negatively charged species, so additional diffuse functions should be included in the calculation to increase the accuracy of the results. The second comment is that the method Taillefer *et al.*[83] used to computationally describe the SET step (Method B) only involved calculating the relative energy between the starting material before SET, and the compounds after SET, and no barrier for SET was calculated, unlike the Marcus-Hush method (Method A) used within this work. Importantly, when the barrier for the SET from the carbamoyl anion **4.53** to iodobenzene **4.1** was modelled, the results suggest that the SET step would not be accessible at 60 °C, which is the temperature at which the reactions were performed and therefore disagrees with the mechanism Taillefer *et al.*[83] proposed. Finally, the two methods produced different relative energies (Method A: ΔG_{rxn} = 18.0 kcal/mol and Method B: ΔG_{rxn} = 14.0 kcal/mol). The reason for this is that the structures modelled to represent the species after SET are different depending on the method used; Method A gives products **4.58** and **4.59**, whereas Method B forms products **4.60** and **4.2**, and therefore there is some small variation in the values of the relative energies calculated, depending on the method that is used.

Since the computational results suggest that the carbamoyl anion **4.53** could not donate an electron to iodobenzene **4.1** at the reaction temperatures used, it was proposed that in the presence of KO*t*Bu, the DMF anion would form an electron

donor *in situ*, possibly through the dimerisation of DMF. There is precedent for this proposal; Nudelman and García Liñares[124] discovered that lithium carbamoyl species undergo dimerisation. They provided experimental evidence that lithium carbamoyl molecules will form dimeric species by reacting either with another molecule of lithium carbamoyl, or with a neutral analogue. Therefore, computational studies were performed to probe the mechanism in more detail. Within the Murphy lab, the transition metal-free reaction conditions are performed in benzene as a solvent, and iodo-*m*-xylene **4.43** is used as the substrate because it is indicative of SET.

The initial studies were to return to the carbamoyl anion of DMF and model the initial deprotonation and SET to iodo-*m*-xylene **4.43**, this time using benzene as a solvent (Scheme 4.10).[45] The overall energetic barrier calculated for both the deprotonation of DMF **4.52** and the SET from carbamoyl anion **4.61** to iodo-*m*-xylene **4.43** was calculated to be endergonic, $\Delta G^{\ddagger}$ = 32.2 kcal/mol and ΔG_{rxn} = 22.0 kcal/mol. This energetic barrier is accessible at 130 °C to form the aryl radical **4.46** and thus initiate the radical mechanism (Scheme 4.8).
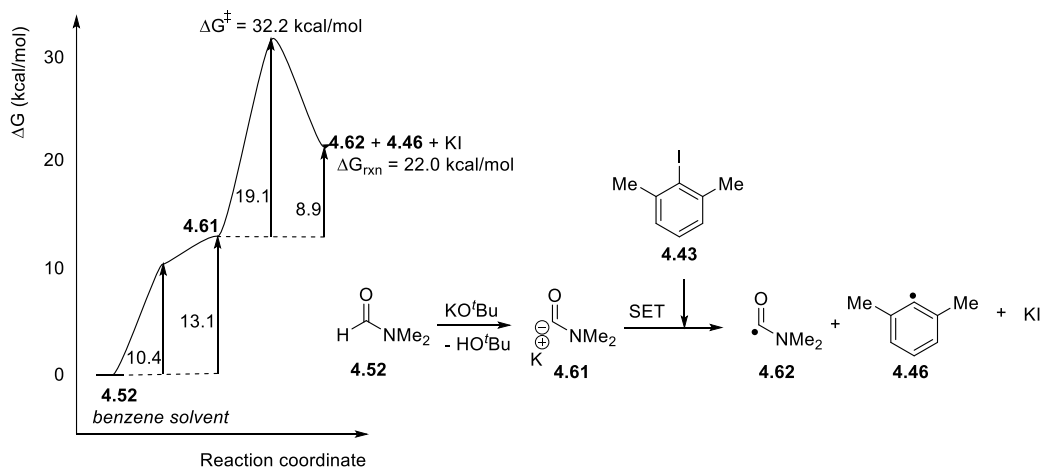
Scheme 4.10 Deprotonation of DMF and SET to iodo-*m*-xylene in benzene solvent.

It was proposed that if the carbamoyl anion **4.61** forms, then it could dimerise with another molecule of DMF to form **4.63** (Scheme 4.11). The species **4.63** could undergo several pathways: (1) a second deprotonation would form two possible

electron donors, either the *cis* isomer **4.64** or in the *trans* isomer **4.66** (Scheme 4.11). (2) Alternatively, the intermediate **4.63** could tautomerise to produce the enolate anion **4.68**, which could undergo a second deprotonation to form the dianion **4.64**. (3) Finally the intermediate **4.63** acts as an electron donor to iodo-*m*-xylene **4.43**.
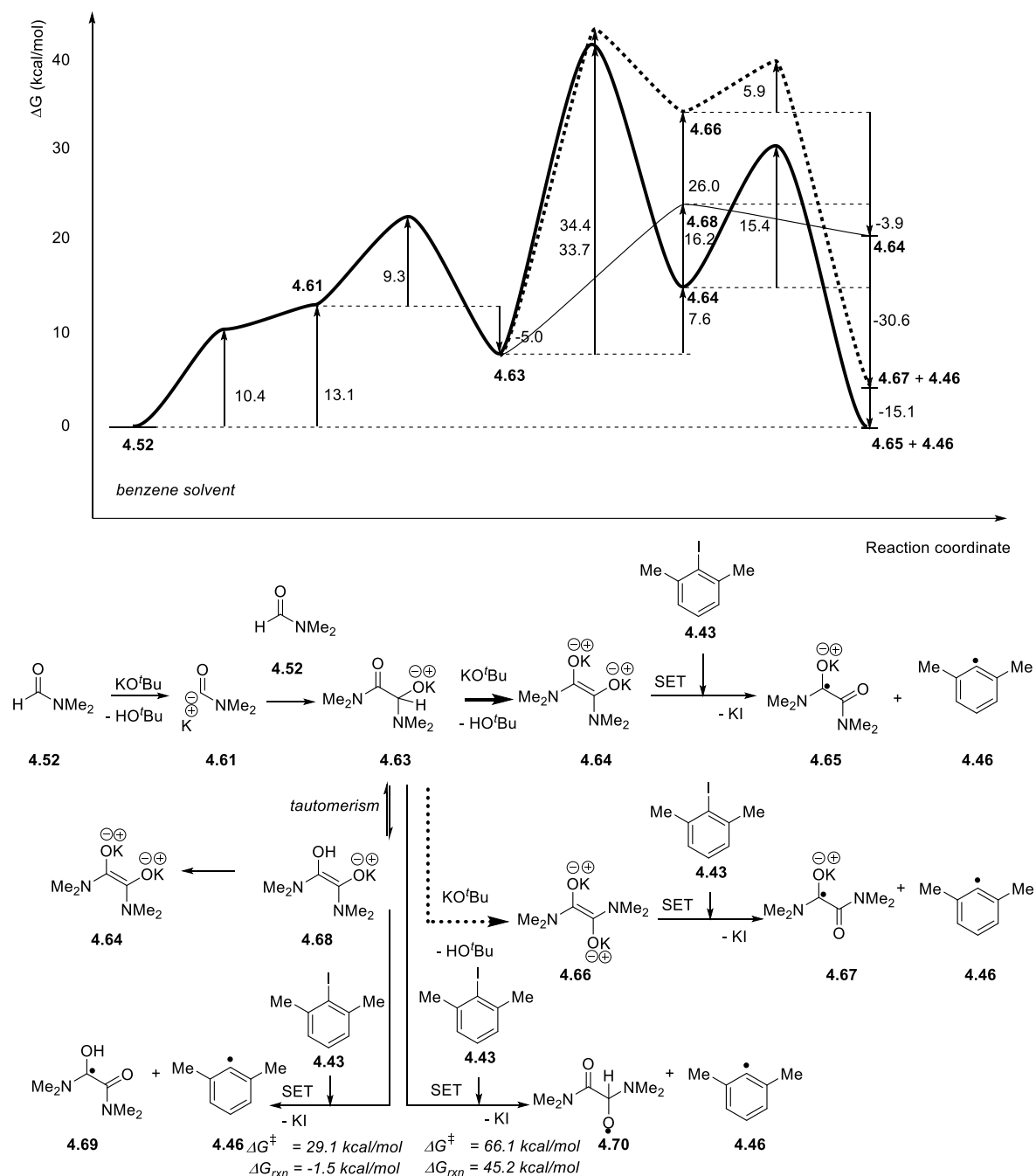
Scheme 4.11 The energy profile for the formation of DMF dimers and SET to iodo-*m*-xylene **4.43**.

The energetic profile for the formation of the two dimeric electron donor species, **4.64** (*cis*) and **4.66** (*trans*), and their subsequent SET to iodo-*m*-xylene **4.43** were calculated. The energetic barrier for the SET from either the *cis* **4.64** or the *trans* **4.66** dimers, $\Delta G^{\ddagger}$ = 15.4 kcal/mol and $\Delta G^{\ddagger}$ = 5.9 kcal/mol respectively, were more favourable than the reaction with the carbamoyl anion **4.61** in benzene, $\Delta G^{\ddagger}$ = 19.1 kcal/mol (Scheme 4.10), suggesting that if these dimers formed then the SET is more favourable from the dimer species than the carbamoyl anion **4.61**. However, the formation of the dimers **4.64** and **4.66** had a higher energetic barrier ($\Delta G^{\ddagger}_{total\text{-}cis}$ = 41.8 kcal/mol and $\Delta G^{\ddagger}_{total\text{-}trans}$ = 42.5 kcal/mol) than the formation of the carbamoyl anion **4.61** ($\Delta G^{\ddagger}_{total}$ = 32.2 kcal/mol). The formation of the dimer **4.64** was calculated *via* intermediate **4.63**, however, according to the observations reported by Nudelman and García Liñares,[124] **4.64** could form directly from the dimerization of two molecules of the carbamoyl anion **4.61**. Unfortunately, the attempts to computationally model this dimerisation were unsuccessful. At this point it must be stated that the reaction was modelled in benzene; however the reaction actually occurs with a low quantity of DMF present, which could change the local dielectric constant of the system and therefore lower the energies. The single electron transfers from both **4.63** and **4.68** were also calculated, however the energy profile for SET from these species (including the formation of **4.68** from **4.63**) are higher than the formation and subsequent SET from **4.64** and **4.66**. Deprotonation of **4.68** would form the dianionic species **4.64** and so this energy profile was modelled. The relative energies were first modelled and it showed that the formation of **4.64** through tautomerisation of **4.63**, followed by subsequent deprotonation, was less energetically favourable than direct deprotonation of **4.63**. Therefore, no further computational analysis was performed regarding this pathway. The analysis of these results suggest that if species analogous to **4.64**, **4.66** and **4.68** could be encouraged to form *in situ*, by overcoming this barrier of formation, then these species would be very good at initiating the transition metal-free coupling reactions of aryl halides to benzene.

In the Murphy lab, Graeme Coulthard and Giuseppe Nocera synthesised two additives, **4.71** and **4.72**, to be used in the transition metal-free coupling reactions and they used them to achieve aryl-aryl bond formation with iodo-*m*-xylene **4.43** and benzene (Table 4.4). The additive **4.71** is analogous to two tethered DMF molecules, whilst the additive **4.72** was designed to be a conformationally restricted analogue of **4.71**. It is proposed that if the reaction occurs through a deprotonation followed by a dimerisation of DMF **4.52** to form the dimer species **4.63**, or the doubly deprotonated species, **4.64**, then the additives **4.71** and **4.72** should improve the yields of the coupling reaction because they will cyclise more easily, and the dimerization will favour the *cis* configuration. The results obtained from the coupling reactions show that **4.72** is the better additive, as was predicted due to added conformational constraint, and this provides an alternative proposal for the electron donor that is formed in this reaction, compared to the carbamoyl anion of DMF proposed by Taillefer *et al.*[43]

Table 4.4 Comparing the effect of DMF and diformamides **4.71** and **4.72**.
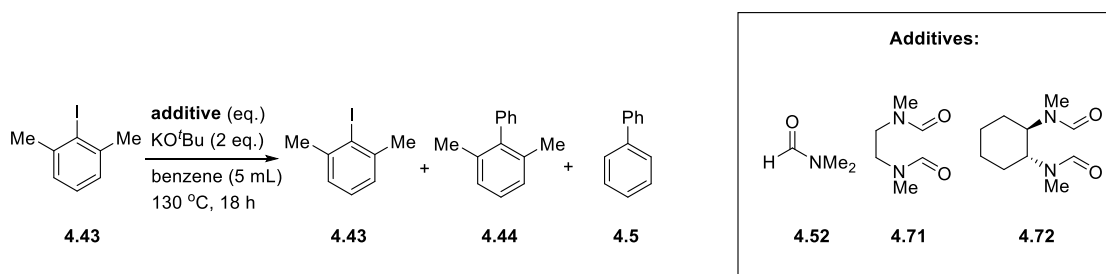
Entry	Additive (eq.)	4.44 (%)[a.]	4.5 (%)[a]
1	--	0.1	0.4
2	**4.52** (0.2)	0.1	0.5
3	**4.52** (1.3)	0.6	2.0
4	**4.71** (0.1)	1.3	6.7
5	**4.72** (0.1)	3.3	12.8

[a.] *Yields calculated using 1,3,5-trimethoxybenzene as the internal standard in ^{1}H-NMR of the crude mixture. Work performed by Graeme Coulthard and Giuseppe Nocera.*

4.5 Future work

If more time was given to continue this research, the top priority would be to return to the design of the DKP additive. It is important to design an analogous DKP additive that would not be capable of accepting an electron. An approach to achieving this goal would be to perform a computational screening of various radical leaving groups to replace thiophenyl ether moiety, to identify a possible replacement for the tether. Additionally, a new additive could be designed that is incapable of undergoing the proposed ionic cyclisation.

5.

Investigating alkoxides as single electron donors

5.1 Introduction

In the literature review (Chapter 1) and in the previous chapter (Chapter 4), experimental evidence was described to support the proposal of the formation of single electron donors *in situ* in these transition metal-free reaction conditions. [40,42,44] However, within the literature, it was proposed that KO^{t}Bu itself is capable of donating an electron to certain substrates, such as benzophenone and triphenylmethyl bromide.[36-37,40,42,44,87-88] This chapter describes the efforts made to investigate the role of KO^{t}Bu as a single electron donor, under various reaction conditions, such as the coupling of a haloarene with benzene, or in the halogenation of alkanes using CBr$_4$.

5.2 Computational methods

The calculations were run using the M06-2X functional[103-104] with the 6-311++G(d,p) basis set[105-109] on all atoms except bromine and iodine. Bromine was modelled with the MWB28 relativistic pseudo potential and associated basis set.[110] All calculations were carried out using the C-PCM implicit solvent model.[111,112] All calculations were performed in Gaussian09.[113]

5.3 Attempts to detect the β-scission products of alkoxyl radicals

The transition metal-free reaction conditions for coupling haloarenes to arenes are most commonly performed using KO^{t}Bu **5.1** in combination with sub-stoichiometric amounts of an organic additive, such as 1,10-phenanthroline **5.2**. As previously discussed, it was proposed that 1,10-phenanthroline **5.2** chelates to the potassium cation of the KO^{t}Bu to form complex **5.3** (Scheme 5.1A). This chelation was suggested to activate the butoxide anion **5.4** towards donating a single electron to the haloarene to form the alkoxyl radical **5.5** (Scheme 5.1B) in the initiation step of the BHAS mechanism (as was described in Section 1.2.2, Scheme 1.11 and Section 4.3, Scheme 4.7). The alkoxyl radical **5.5** can undergo β-scission to form acetone **5.6** and a methyl radical or it can abstract a hydrogen atom to form the *tert*-butanol **5.7**.[125] The initial experiments planned were to determine whether the β-scission product **5.6** was formed within these transition metal-free reactions. To detect the β-

scission product formed, upon completion of the reaction, 2,4-dinitrophenylhydrazine (2,4-DNPH) **5.11** was added (Table 5.1).
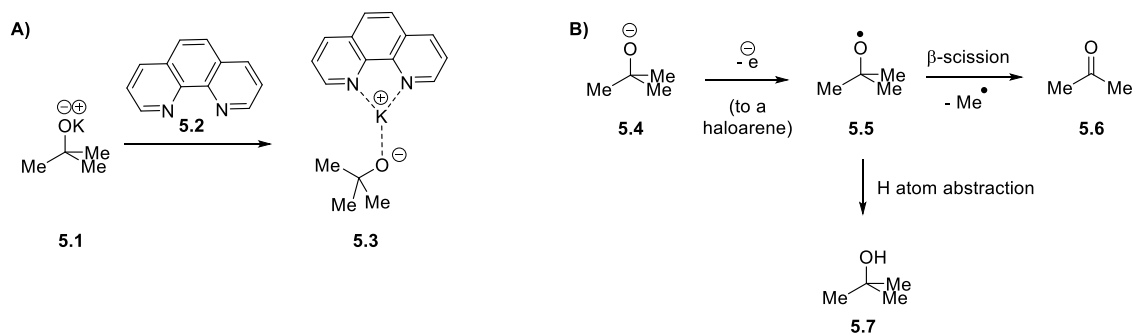
Scheme 5.1A) The proposed activation of *tert*-butoxide anion towards SET, and **B)** the expected β-scission product formation from *tert*-butoxyl radicals **5.5**.

Table 5.1 Aryl-aryl bond formation between 4-iodotoluene **5.8** and benzene, in the presence of KO^{t}Bu at 160 °C.
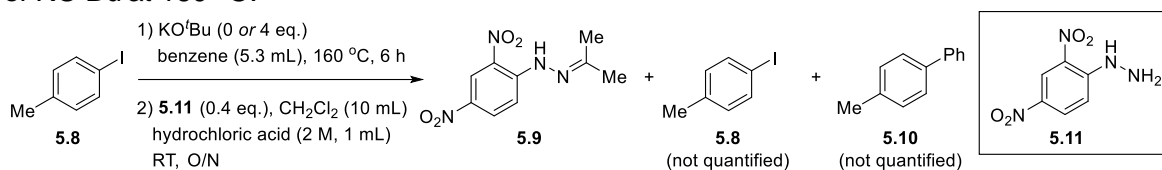
Entry	KO^{t}Bu (eq.)	Yield 5.9 (µmol)
1[a.]	4	0.87
2[a.]	0	0.43

[a.] *All equipment was oven-dried to remove adventitious acetone. The adduct **5.9** was identified using ^{1}H-NMR (a reference sample of **5.9** was overlaid onto the crude mixture to identify if **5.9** was present in the crude mixture).*

The reaction conditions employed were those initially reported by Wilden *et al.*,[87] (KO^{t}Bu, 160 °C, 6 h, using benzene as the solvent) who coupled 4-iodotoluene **5.8** to benzene to form 4-methylbiphenyl **5.10** in the absence of any additives.[87] When 4-iodotoluene **5.8** was subjected to these reaction conditions, followed by the addition of 2,4-dinitrophenylhydrazine (2,4-DNPH) **5.11**, the adduct **5.9** was observed, which suggested that acetone was formed in the reaction (Table 5.1, entry 1). However, when the reaction was performed in the absence of KO^{t}Bu, the adduct **5.9** was also observed (Table 5.1, entry 2). This suggested that adventitious acetone was present in the reaction to form adduct **5.9**. Therefore, many precautions were taken to remove the adventitious acetone; new solvents were used, all equipment

was oven-dried or flame-dried, the reaction was performed in the glove box (Scheme 5.2). Unfortunately, even with all these precautions, adventitious acetone was still trapped in the reaction mixture. Therefore, the formation of acetone as a β-scission product from an alkoxyl radical could not be determined, and hence this method to determine whether SET occurs from KO*t*Bu is not appropriate. It was proposed that a new alkoxide, potassium 2-phenylpropan-2-olate **5.12**, be synthesised and used as the base instead of KO*t*Bu in this study.
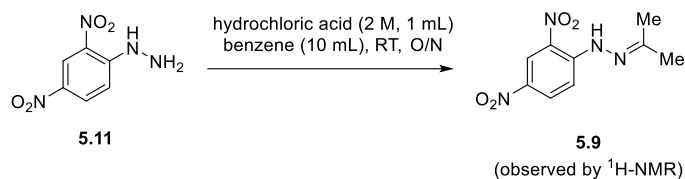
Scheme 5.2 Reaction of 2,4-DNPH **5.11** in anhydrous benzene in the glovebox, with extra precautions taken to remove adventitious acetone.

The potassium 2-phenylpropan-2-olate **5.12** was chosen because if SET occurs from this alkoxide then the alkoxyl radical **5.13** will form (Scheme 5.3). The radical **5.13** can undergo β-scission to form acetophenone **5.14**, which will be easily identifiable and isolatable if it is formed in the reaction conditions.[87,126-128] The potassium 2-phenylpropan-2-olate **5.12** was synthesised by reacting 2-phenylpropanol **5.15** with potassium hydride in anhydrous solvent, and upon formation of the alkoxide **5.12**, it was subjected to the reaction conditions similar to those reported by Wilden *et al.*[87] (160 °C, 3 h, using benzene as the solvent) (Table 5.2).
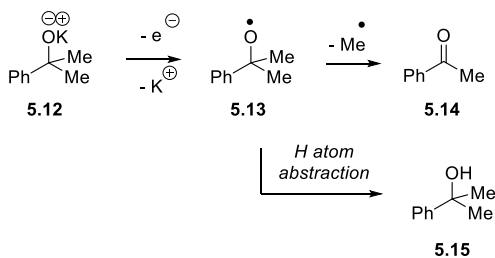
Scheme 5.3 The potassium 2-phenylpropan-2-olate **5.12** and the predicted alkoxyl intermediate **5.13** that would form if SET occurs from the alkoxide. The predicted products **5.14** and **5.15** of fragmentation of **5.13**.

Table 5.2 Aryl-aryl bond formation between 4-iodotoluene **5.8** and benzene in the presence of 1,10-phenanthroline **5.2** and potassium 2-phenylpropan-2-olate **5.12** at 160 °C.
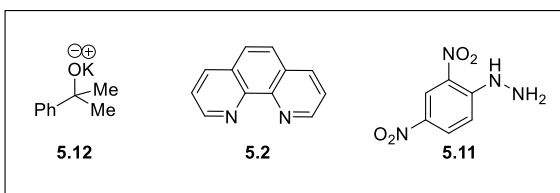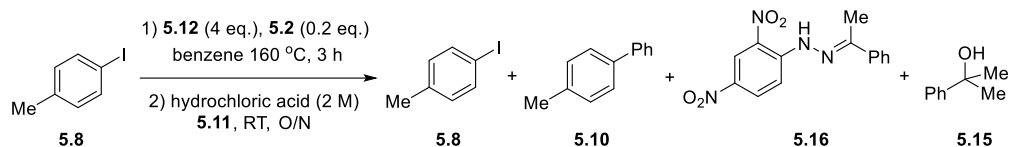
Entry	5.8 (mmol)	Benzene (mL)	Yield 5.8 (%)	Yield 5.10 (%)	Yield 5.16 (%)	Yield 5.15 (%)
1	1	10	39	16	trace[a.]	77
2	0.5	5	43	25	trace[a.]	70

[a.] trace = the product is observed through comparison with a reference ^{1}H-NMR of the product, however yields cannot be quantified accurately (< 1%).

The coupling reactions between 4-iodotoluene **5.8** and benzene under the transition metal-free reaction conditions were performed on 1.0 mmol and 0.5 mmol scale (Table 5.2, entry 1 and 2 respectively). In both reactions, both the coupled product, 4-methylbiphenyl **5.10**, and the adduct **5.16** were observed. The formation of 4-methylbiphenyl **5.10** occurs through the BHAS reaction pathway (described previously in Chapter 1 and 4). The adduct **5.16** is the product of a condensation reaction between acetophenone **5.14** and 2,4-DNPH **5.11**, so therefore the formation of the adduct **5.16** means that acetophenone **5.14** is present in the reaction mixture. There are two possible sources of the acetophenone **5.14**: 1) the potassium 2-phenylpropan-2-olate **5.12** donates an electron to 4-iodotoluene **5.8** and the resulting alkoxyl radical **5.13** fragments to form acetophenone **5.14** (as previously shown in Scheme 5.3), or 2) the acetophenone **5.14** is an impurity from the commercially available starting material. Both these possibilities must be addressed before drawing conclusions on the mechanism occurring. It is important to note here that within these reactions the acetone adduct **5.9** was seen. The product **5.9** may have formed from adventitious acetone in the reaction mixture, as has been

previously described, however there is another possible source of acetone in this reaction. Within the literature there are reports that alkoxides, analogous to **5.12**, have been shown to undergo heterolytic fragmentation to eliminate a phenyl anion.[129-130] Unfortunately, based on the previously studies, it was shown that the adduct **5.9** is formed by a background reaction, and therefore the yields of possible heterolytic fragmentation from **5.12** could not be quantified accurately.

First, the commercially available 2-phenylpropanol **5.15** was analysed for trace amounts of acetophenone **5.14** by reacting it with 2,4-DNPH **5.11** (Scheme 5.4A). In the presence of acid, the adduct **5.16** was observed as a product in trace amounts (< 1%) suggesting that the commercially available starting material contains trace amounts of acetophenone **5.14** (Scheme 5.4A). Therefore, the commercially available 2-phenylpropanol **5.15** was purified before being used to make a pure sample of potassium 2-phenylpropan-2-olate **5.12***. Unfortunately, when this pure sample of potassium 2-phenylpropan-2-olate **5.12*** was tested with 2,4-DNPH **5.11** the adduct **5.16** was still observed (Scheme 5.4B). As a result, this study was inconclusive because it showed that acetophenone is present in trace amounts in the potassium 2-phenylpropan-2-olate **5.12** and therefore the source of acetophenone in the reaction mixture cannot be determined.
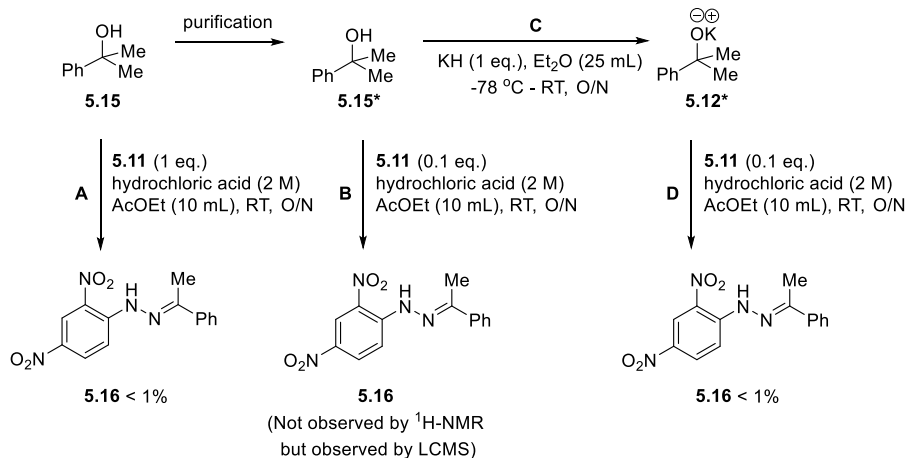
Scheme 5.4 Analysis of trace amounts of acetophenone in the starting materials (* = purified material).

Within the literature, KO*t*Bu **5.1** is the most common base used for these transition metal-free aryl-aryl bond formations, however NaO*t*Bu has sometimes been used for the transformations, albeit at higher reaction temperatures. Throughout this study it was interesting to observe that the potassium 2-phenylpropan-2-olate **5.12** was less efficient than KO*t*Bu at promoting the transition metal-free coupling of 4-iodotoluene **5.8** and benzene (Table 5.3). The cation remains the same, however changing a methyl substituent on the alkoxide base to a phenyl has lowered the reactivity of the alkoxide towards promoting the arylation of 4-iodotoluene **5.8**.

Table 5.3 The reaction of potassium 2-phenylpropan-2-olate **5.12** or KO*t*Bu to couple 4-iodotoluene **5.8** with benzene under transition metal-free reaction conditions.
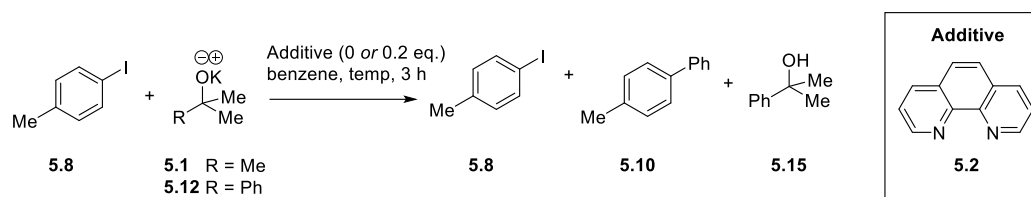
Entry	Additive (eq.)	Base (eq.)	Solvent (mL)	Temp. (°C)	Time (h)	5.8 (%)	5.10 (%)	5.15 (%)
1	**5.2** (0.2)	**5.12** (2)	benzene (5)	130	3	19[a.]	74[a.]	93[a.]
2	**5.2** (0.2)	**5.1** (2)	benzene (5)	130	3	0	95[a.]	--
Lit[42]	-	**5.1** (2)	benzene (5)	130	3	-	4	--
3	**5.2** (0.2)	**5.12** (4)	benzene (5)	160	3	0	76	73
4	-	**5.12** (4)	benzene (5)	160	3	93[a.]	4[a.]	80
Lit[87]	-	**5.1** (4)	benzene (5)	160	3	-	38	-

[a.] *Yield calculated using 1,3,5-trimethoxybenzene as the internal standard in* ^{1}*H-NMR of the crude mixture.*

The first reaction conditions used to couple 4-iodotoluene **5.8** to benzene in the absence of transition metals were reported by Murphy *et al.*[42] [1,10-phenanthroline **5.2** (0.2 eq.), 130 °C, 3 h, using benzene as the solvent, in the presence of KO*t*Bu]. Under the reaction conditions, 4-iodotoluene **5.8** was converted to the coupled product **5.10** (74%) when the alkoxide **5.12** was used as the base in the reaction (Table 5.3, entry 1). However, when KO*t*Bu **5.1** was used, the conversion of the starting material was higher, all starting material was reacted and **5.10** was formed in very high yields (95%) (Table 5.3, entry 2). When the reaction temperature was increased to 160 °C, similar to the reaction conditions reported by Wilden *et al.*,[87] the

coupling product 4-methylbiphenyl **5.10** was formed in high yields (76%) (Table 5.3, entry 3). When the reaction was performed in the absence of 1,10-phenanthroline **5.2**, only trace amounts of 4-methylbiphenyl **5.10** were observed and the starting material 4-iodotoluene **5.8** was recovered in high yields (93%) (Table 5.3, entry 4). This demonstrates that the alkoxide base chosen for these couplings influences the efficiency of the reaction. Murphy *et al.*[44] showed that 1,10-phenanthroline **5.2** forms an electron donor *in situ* by an initial deprotonation, followed by subsequent coupling of 1,10-phenanthroline **5.2** to another molecule of itself. If this is the mode for the initiation of the radical chain process, it would be expected that alkoxide **5.12** would be a weaker base for the initial deprotonation, due to the presence of the electron-withdrawing phenyl adjacent to the alkoxyl moiety, and hence would lead to less activity as an electron donor and give lower yields of conversion.

The conclusions to be drawn from this short study are that, at 130 °C, the presence of a phenyl group at α-C to the alkoxide moiety, instead of a methyl group, leads to a decrease in the yields of coupled product. More recently, Murphy *et al.*[43] demonstrated that at the high temperatures of 160 °C using KO*t*Bu and no additive, 4-iodotoluene **5.8** reacts to form 4-methylbiphenyl **5.10**, as well as the regioisomeric products **5.18** and **5.19** (Scheme 5.5). The formation of **5.18** and **5.19** in this reaction suggests that, at 160 °C, KO*t*Bu reacts with 4-iodotoluene **5.8** to form the benzyne intermediate **5.17**, which is attacked by the *tert*-butoxide anion to form the two regioisomeric products. In contrast, when potassium 2-phenylpropan-2-olate **5.12** was reacted under the same conditions (Table 5.3, entry 4) the major compound in the crude mixture was the recovered starting material and no alkoxide adducts, analogous to **5.18** and **5.19**, were observed. This demonstrates that potassium 2-phenylpropan-2-olate **5.12** is a weaker base than KO*t*Bu and is not capable of efficiently forming benzyne intermediate **5.17** from 4-iodotoluene **5.8** under the reaction conditions employed at 160 °C. However, because benzyne intermediates have been formed from 4-iodotoluene **5.8** by KO*t*Bu at 160 °C, iodo-*m*-xylene **5.20** was used in a coupling reaction, with potassium 2-phenylpropan-2-olate **5.12** and 1,10-phenanthroline **5.2**, to confirm that the reaction was proceeding through a SET mechanism and not benzyne intermediates (Scheme 5.6).[43]
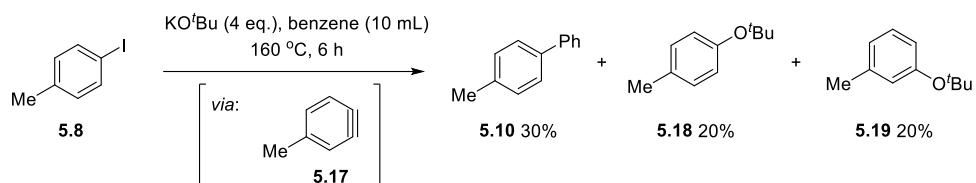
Scheme 5.5 The formation of the regioisomeric products **5.18** and **5.19**, which provides evidence of a benzyne intermediate **5.17** in the reaction of KO*t*Bu with 4-iodotoluene **5.8** at 160 °C.[43]
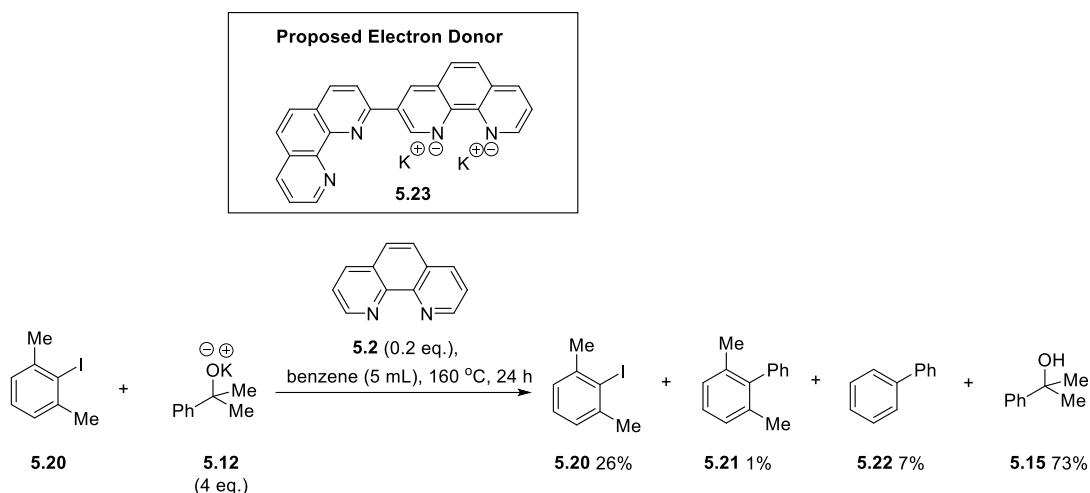
Scheme 5.6 The reaction of alkoxide **5.12** with iodo-*m*-xylene **5.20** in combination with 1,10-phenanthroline **5.2**.

When iodo-*m*-xylene **5.20** was reacted with a combination of 1,10-phenanthroline **5.2** and potassium 2-phenylpropan-2-olate **5.12** in benzene at 160 °C, two products formed containing new aryl-aryl bonds, 2,6-dimethylbiphenyl **5.21** (1%) and biphenyl **5.22** (27%). The formation of 2,6-dimethylbiphenyl **5.21** and biphenyl **5.22** occurs through the BHAS mechanism (as previously shown Section 4.3, Scheme 4.7). From the previous work reported by Murphy *et al.*[44] it is proposed that the electron donor is the dimeric species of 1,10-phenanthroline **5.23**, that is formed *in situ* in these reactions by the action of a strong base on 1,10-phenanthroline **5.2**.

Due to the inconclusive evidence obtained using potassium 2-phenylpropan-2-olate **5.12** thus far, it was proposed that an appropriate alkoxide base could be designed to act as a radical probe. If SET occurred from potassium 1,1a,2,3-tetrahydro-7bH-cyclopropa[a]naphthalen-7b-olate **5.26**, then the resulting alkoxyl radical **5.27** would undergo C-C bond cleavage to open the cyclopropane ring and form either **5.28** or

5.29 following hydrogen atom transfer (Scheme 5.7). Unfortunately, the formation of the alkoxide base, potassium 1,1a,2,3-tetrahydro-7bH-cyclopropa[a]naphthalen-7b-olate **5.26**, as a stable species was unsuccessful. Upon exposing 1,1a,2,3-tetrahydro-7bH-cyclopropa[a]naphthalen-7b-ol **5.25** to potassium hydride, potassium 2-methyl-3,4-dihydronaphthalen-1-olate **5.30** was formed, which was confirmed by performing a work-up procedure on **5.30** to give 2-methyl-3,4-dihydronaphthalen-1(2H)-one **5.29** (100%). Research in the literature has shown that cyclopropanols can convert to the ketone by acid or base induced ring opening of the cyclopropane.[131] This work supports the findings that this ring-opening is a rapid process.
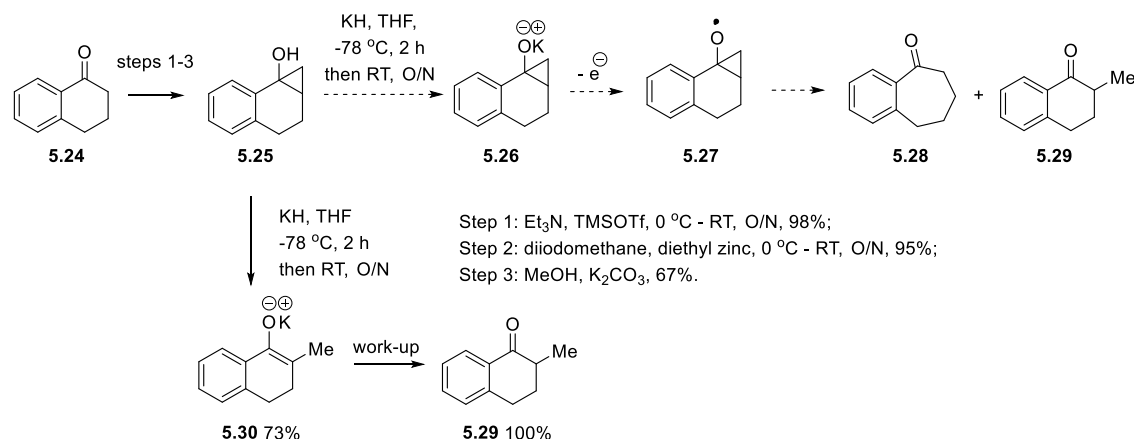
Scheme 5.7 Attempted synthesis of alkoxide **5.26** and the expected products that would form from fragmentation of alkoxyl radical **5.27** if it forms by SET from **5.26**.

5.4 Can alkoxides donate an electron to tetrahalomethanes?

So far within this chapter, despite numerous efforts, no experimental evidence has been found to either support or disprove the theory that KO^{t}Bu can act as a single electron donor. In a final attempt to identify whether SET can occur from KO^{t}Bu, tetrahalomethanes were used as an alternative electron acceptor molecule to the haloarenes that have been used thus far in this chapter. Within the literature, Schreiner and Fokin *et al.*[132] used sodium hydroxide and tetrahalomethanes, in the presence of a phase transfer catalyst, to halogenate adamantane through a radical chain mechanism (Scheme 5.8). They proposed that SET occurs from hydroxide anion to CBr$_4$ to form a bromide anion and tribromomethyl radical **5.34** (Scheme

5.8A). This radical **5.34** undergoes a chain reaction (Scheme 5.8B); **5.34** abstracts a hydrogen atom from a hydrocarbon **5.36** to form the alkyl radical **5.38** and bromoform **5.37**. The alkyl radical **5.38** abstracts a bromine atom from CBr_4, forming the alkyl bromide **5.39** and regenerating the CBr_3 radical **5.34**. The oxidation potential of KO^tBu in DMF (0.10 V *vs.* SCE) is not too different from the reduction potential of CBr_4 in DMF (-0.31 V *vs.* SCE)[133] and it was therefore proposed that KO^tBu might reduce CBr_4 through a similar mechanism.
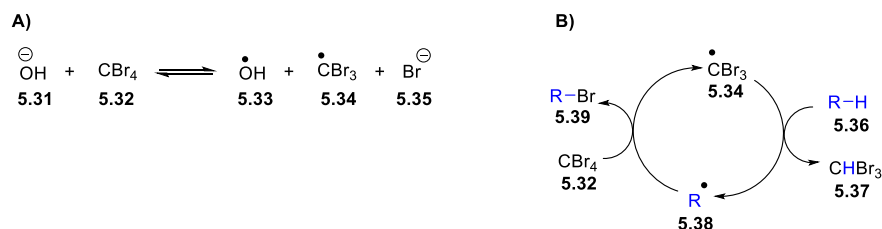
Scheme 5.8 Schreiner *et al.*[132] proposed a radical chain mechanism for the halogenation of adamantane using hydroxide and tetrahalomethanes.

5.4.1 Reactions of alkoxides and CBr_4 at high temperatures

The initial studies in this investigation were to use potassium 2-phenylpropan-2-olate **5.12** and react it in the presence of CBr_4 under the transition metal-free coupling reaction conditions [potassium 2-phenylpropan-2-olate **5.12** (4.0 eq.), CBr_4 (0.5 mmol), benzene and high temperatures of 160 °C for 6 h] (Table 5.4).[87]

Table 5.4 The reaction of the alkoxide potassium 2-phenylpropan-2-olate **5.12** in benzene at 160 °C.
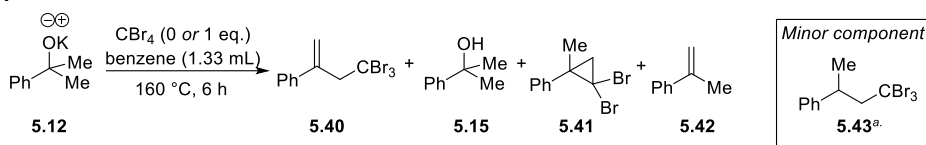
Entry	CBr_4 (eq.)	**5.40** (%)	**5.15** (%)	**5.41** (%)	**5.42** (%)
1	1	18	0	3	46
2[b.]	0	0	76	0	< 0.5

*The yields were calculated using 1,3,5-trimethoxybenzene as the internal standard in ¹H-NMR of the crude mixture. [a.] The compound **5.43** was tentatively proposed based on ¹H-NMR spectra. [b.] Performed in the dark.*

The reaction of the potassium 2-phenylpropan-2-olate **5.12** with CBr_4 in benzene under these reaction conditions gave several products (Table 5.4, entry 1); (4,4,4-

tribromobut-1-en-2-yl)benzene **5.40** (18%), (2,2-dibromo-1-methylcyclopropyl)benzene **5.41** (3%) and methylstyrene **5.42** (46%). In a blank reaction (i.e. in the absence of CBr₄), 2-phenylpropanol **5.15** (76%) was formed along with trace amounts of methylstyrene **5.42** as the only products of the reaction (Table 5.4, entry 2). The formation of methylstyrene **5.42** is proposed to occur *via* a hypobromite intermediate **5.44** (Scheme 5.9A). Potassium 2-phenylpropan-2-olate **5.12** nucleophilically attacks a molecule of CBr₄ to form *tert*-butyl hypobromite **5.44** and eliminate a CBr₃ anion. The *tert*-butyl hypobromite **5.44** can then undergo an elimination to form methylstyrene **5.42**. The CBr₃ anion will undergo decomposition (α-elimination of bromide) and lead to the formation of a CBr₂ carbene **5.45** (Scheme 5.9A); the formation of (2,2-dibromo-1-methylcyclopropyl)benzene **5.41** occurs by CBr₂ carbene **5.45** attack onto methylstyrene **5.42**. To support this mechanism, KO*t*Bu **5.1** was used instead of potassium 2-phenylpropan-2-olate **5.12** as the base for the reaction, and it was exposed to either CBr₄ or HCBr₃ in the presence of methylstyrene **5.42** under the same reaction conditions (Scheme 5.9B - C respectively). The products from the reaction of KO*t*Bu **5.1** with methylstyrene **5.42** and CBr₄ were (4,4,4-tribromobut-1-en-2-yl)benzene **5.40** and (2,2-dibromo-1-methylcyclopropyl)benzene **5.41**. When the additive was changed to HCBr₃, the major product of the reaction was the predicted (2,2-dibromo-1-methylcyclopropyl)benzene **5.41**.
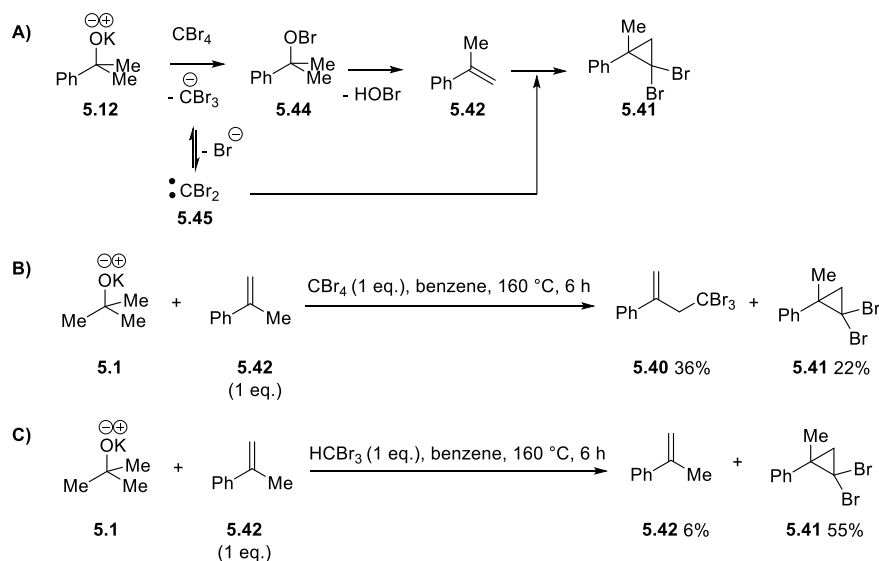
Scheme 5.9A) Proposed mechanism in the formation of products **5.41** and **5.42** and **B) - C)** experimental proof of concept.

The product (4,4,4-tribromobut-1-en-2-yl)benzene **5.40** formed only when CBr_4 was the additive, and not $HCBr_3$. The proposed mechanism in the formation of **5.40** involves CBr_3 radicals, which could react with methylstyrene **5.42** through either a radical addition onto the alkene moiety, or a hydrogen atom abstraction at the allylic position (Scheme 5.10). The radical addition of a CBr_3 radical onto methylstyrene **5.42** would form the radical **5.46**. Radical **5.46** could abstract a bromine atom from CBr_4 to form the brominated intermediate **5.47**, which upon loss of HBr would give (4,4,4-tribromobut-1-en-2-yl)benzene **5.40**. Alternatively, the radical **5.46** could abstract a hydrogen atom to form **5.43**. The second possibility is a CBr_3 radical abstracts a hydrogen atom from methylstyrene **5.42** to form the stabilised allylic radical **5.48**, which could react with another molecule of CBr_4 to yield the allylic bromide **5.49**. The addition of either a CBr_3 radical or CBr_3 anion onto the alkene moiety would ultimately yield product **5.40** upon the elimination of either a bromine radical or a bromide anion.
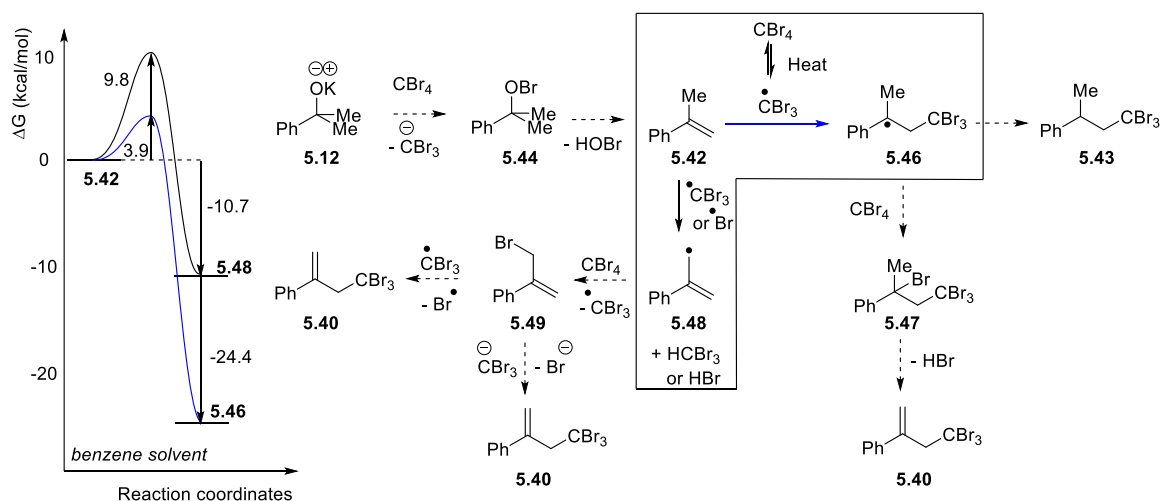
Scheme 5.10 Computational analysis of the two proposed mechanisms to form **5.40**.

Computational analysis was used to differentiate the possible reaction pathways in the formation of (4,4,4-tribromobut-1-en-2-yl)benzene **5.40**. The calculated energy difference between CBr_3 radical attack onto the alkene **5.42** ($\Delta G^{\ddagger} = 3.9$ kcal/mol and $\Delta G_{rxn} = -24.4$ kcal/mol) *vs*. hydrogen atom abstraction pathway ($\Delta G^{\ddagger} = 9.8$ kcal/mol and $\Delta G_{rxn} = -10.7$ kcal/mol) suggests that the pathway is more likely to occur *via*

CBr_3 radical attack to give intermediate **5.46** (Scheme 5.10). Further analysis of the impurities present in the formation of **5.40** shows evidence that the intermediate **5.46** is formed, since the saturated analogue **5.43** was proposed, by ^{1}H-NMR analysis, to be present as an impurity (previously shown in Table 5.4).

Within the literature it was suggested that, at high reaction temperatures (160 °C), CBr_4 may decompose into Br radicals and CBr_3 radicals.[134] To test this hypothesis, CBr_4 was reacted with adamantane **5.50** under these reaction conditions (Scheme 5.11A). When adamantane **5.50** was reacted with CBr_4 at 160 °C, bromination of adamantane occurred to form **5.51** (41%), **5.52** (6%) and **5.53** (8%). The bromination of adamantane occurs from hydrogen atom abstraction (Scheme 5.11B), which can occur either at the bridgehead, C-1, or at C-2 to yield the two isomers **5.51** and **5.52** respectively (Scheme 5.11B shows only the major isomer, resulting from a hydrogen atom abstraction from C-1).[135-136] The high yields of brominated adamantane in the absence of any alkoxide base suggests that the initiation of the bromination pathway at 160 °C is a C-Br bond homolysis of CBr_4 (and not requiring SET from alkoxide). The resulting CBr_3 radical **5.34** abstracts a hydrogen atom from adamantane **5.50** to form adamantyl radical **5.54** (Scheme 5.11B). This radical **5.54** abstracts a bromine from CBr_4 to propagate the chain mechanism, and form product **5.51** (or **5.52** depending on the site of the hydrogen atom abstraction). With the knowledge that CBr_4 is decomposed to radical intermediates at high temperatures, these reaction conditions (160 °C) are not viable for testing the ability of alkoxides as single electron donors to CBr_4.
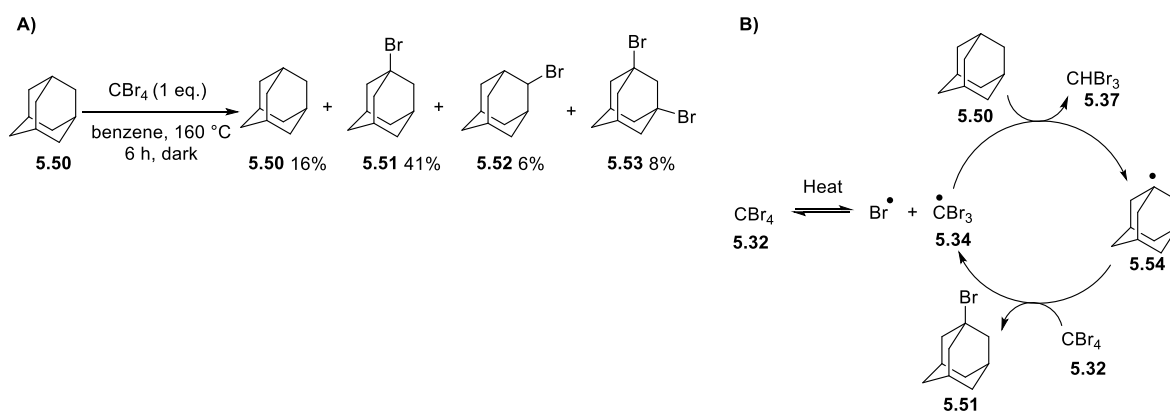
Scheme 5.11A) The reaction of CBr_4 and adamantane **5.50** at 160 °C. **B)** A proposed mechanism in the bromination of adamantane **5.50** at 160 °C.

5.4.2 Alkoxides and CBr₄ at 40 °C

Since CBr_4 underwent C-Br bond homolysis at high temperatures, the reaction was repeated using conditions similar to those used by Schreiner *et al.*[132] (40 °C in dichloromethane for 90 h). To ensure that CBr_4 did not decompose to its radical species under these new reaction conditions, CBr_4 was reacted with adamantane **5.50** in the absence of any alkoxide (Scheme 5.12).[137] After 90 h at 40 °C the only compound observed in the ^{1}H-NMR and ^{13}C{^{1}H}-NMR of the reaction mixture was the unreacted adamantane **5.50**, which meant that CBr_4 was stable under these reaction conditions, and therefore low temperature studies could be used to probe the role of alkoxides in the halogenation of adamantane.

5.50   CBr₄ (1 eq.), CH₂Cl₂ (3.13 mL), 40 °C, 90 h, dark   **5.50** 93%
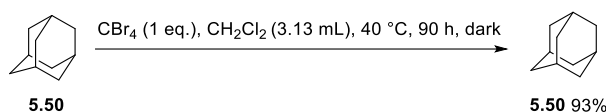
Scheme 5.12 Reaction of adamantane **5.50** and CBr₄ at 40 °C.

Murphy *et al.*[43] reported that when KO*t*Bu was reacted with CBr_4 and adamantane **5.50**, at 40 °C in dichloromethane, bromination of adamantane **5.50** was observed, and the conclusion drawn was that KO*t*Bu is capable of donating an electron to CBr_4 to yield the CBr_3 radicals.[43] Therefore, it was proposed that potassium 2-phenylpropan-2-olate **5.12** would also be capable of brominating adamantane **5.50** under these reaction conditions (Table 5.5).

Table 5.5 Reaction of potassium 2-phenylpropan-2-olate **5.12** in dichloromethane at 40 °C.[a]
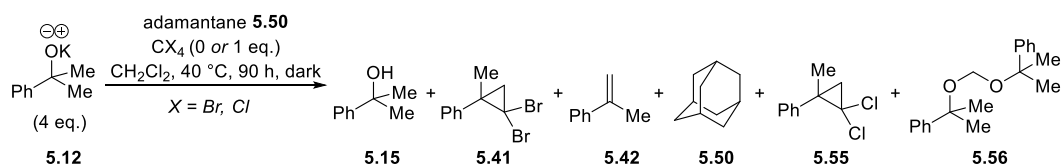
Entry	Additive (eq.)	5.15 (%)[c]	5.41 (%)	5.42 (%)	5.50 (%)	5.55 (%)	5.56 (%)[c]
1[b]	CBr₄ (1)	66	33	18	91	17	0
2	none	39	0	1	84	0	52 (26%) [d]
3	CCl₄ (1)	67	0	3	76	50	3

[a] Yields calculated using 1,3,5-trimethoxybenzene as the internal standard in ^{1}H-NMR of the crude mixture. [b] Not performed in the dark. [c] Yields based on potassium 2-phenylpropan-2-olate **5.12**. [d] Isolated yields.

When potassium 2-phenylpropan-2-olate **5.12** was exposed to CBr$_4$ in dichloromethane, at 40 °C, no bromination of adamantane was observed (Table 5.5, entry 1). The products 2-phenylpropanol **5.15**, (2,2-dibromo-1-methylcyclopropyl)benzene **5.41**, methylstyrene **5.42** and (2,2-dichloro-1-methylcyclopropyl)benzene **5.55** were observed, as well as unreacted adamantane **5.50** (Table 5.5, entry 1). A blank reaction performed in the absence of CBr$_4$ resulted in the formation of a new product, bis((2-phenylpropan-2-yl)oxy)methane **5.56** (Table 5.5, entry 2, see discussion below).[138] To avoid the complexity of having compounds bearing different halogens within the reaction mixture, the reaction was repeated using CCl$_4$ as the reagent, instead of CBr$_4$, in dichloromethane (Table 5.5, entry 3) which yielded (2,2-dichloro-1-methylcyclopropyl)benzene **5.55** as a major product.

Analogous to (2,2-dibromo-1-methylcyclopropyl)benzene **5.41**, the formation of (2,2-dichloro-1-methylcyclopropyl)benzene **5.55** means that CCl$_2$ carbenes **5.61** are formed under the reaction conditions (Scheme 5.13). The CCl$_2$ carbene **5.61** forms when potassium 2-phenylpropan-2-olate **5.12** acts as a base and deprotonates dichloromethane, CH$_2$Cl$_2$. The resulting CHCl$_2$ anion **5.57** undergoes halogen exchange with CBr$_4$ to form bromodichloromethane **5.58**. A second deprotonation would lead to the bromodichloromethyl anion **5.60** and decomposition of this anion would give the CCl$_2$ carbene **5.61**.
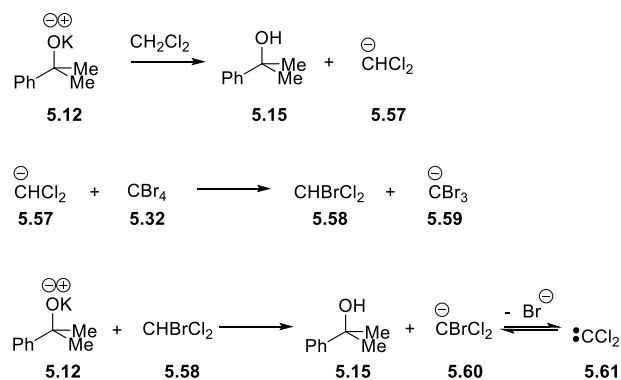
Scheme 5.13 Proposed mechanism to form carbene **5.61**.

The formation of bis((2-phenylpropan-2-yl)oxy)methane **5.56** was observed in the blank reaction (without CBr$_4$) and a proposed mechanism for its formation involved the nucleophilic displacement of chloride from dichloromethane by two molecules of

potassium 2-phenylpropan-2-olate **5.12** (Scheme 5.14A). As a proof of concept, following literature precedent,[139-140] benzyl alcohol **5.63** was reacted in the presence of KO^{t}Bu and dichloromethane, and the product **5.64** was formed (Scheme 5.14B). Next, the formation of **5.56** was proven to be successful when potassium 2-phenylpropan-2-olate **5.12** was heated to 40 °C in dichloromethane (Scheme 5.14C). The fact that **5.56** is only observed in the absence of CBr$_4$ suggests that the reaction of potassium 2-phenylpropan-2-olate **5.12** with dichloromethane is slower than the reaction with CBr$_4$.
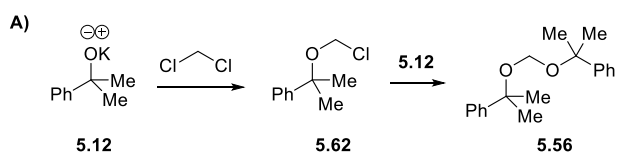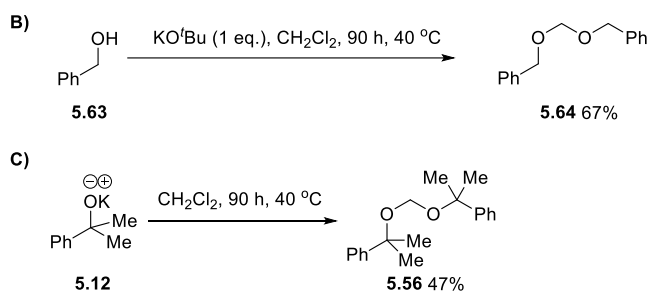
Scheme 5.14 Proposed mechanism and proof of concept to form **5.56**.

Next, the reaction was repeated with KO^{t}Bu as the base instead of potassium 2-phenylpropan-2-olate **5.12** (Scheme 5.15A). Interestingly, when KO^{t}Bu was used, the bromination of adamantane **5.50** was observed unlike when the reaction is performed using potassium 2-phenylpropan-2-olate **5.12**.[43] This suggests that either the two alkoxide bases do not react with CBr$_4$ through the same mechanisms, or the methylstyrene **5.42** formed in the reaction from potassium 2-phenylpropan-2-olate **5.12** shuts down the radical chain pathway (precedent for this is that 1,1-diphenylethylene is a radical trap that is known to shut down radical pathways).[33] To probe the possibility that methylstyrene **5.42** may shut down the radical pathway, the reaction of KO^{t}Bu with CBr$_4$ and adamantane **5.50** was repeated in the presence of methylstyrene **5.42** (Scheme 5.15B). The addition of methylstyrene **5.42** stopped the

bromination of adamantane, which suggests that it can shut down the radical mechanism, maybe by acting as a source of hydrogen atoms for the CBr$_3$ radical in preference to adamantane **5.50**. Indeed, computational analysis shows that hydrogen atom abstraction by the CBr$_3$ radical from methylstyrene **5.42** ($\Delta G^{\ddagger}$ = 10.7 kcal/mol and ΔG_{rxn} = -7.7 kcal/mol) is thermodynamically more favourable than from adamantane **5.50** ($\Delta G^{\ddagger}$ = 13.9 kcal/mol and ΔG_{rxn} = 1.1 kcal/mol) (Scheme 5.15C). Hence, methylstyrene **5.42** is acting as a radical sink in the reaction mixture, thus preventing the formation of the adamantyl radical **5.54**, and hence the bromination of adamantane.
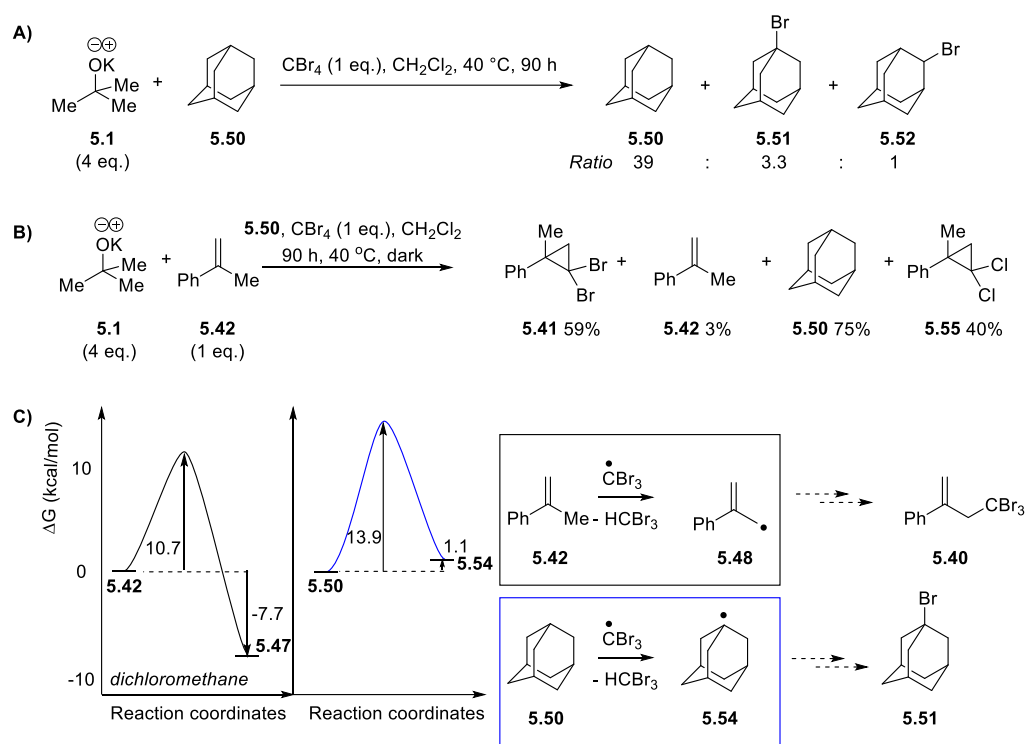
Scheme 5.15A) Reaction of KO*t*Bu with CBr$_4$ and adamantane. **B)** Using methylstyrene **5.42** to block the bromination of adamantane. **C)** Computational analysis of hydrogen atom abstraction by CBr$_3$ radical from methylstyrene **5.42** *vs.* adamantane **5.50**.

With the knowledge that methylstyrene **5.42** is capable of preventing bromination of adamantane, the mechanism of product formation from potassium 2-phenylpropan-2-olate **5.12** was revisited and applied to KO*t*Bu. In Section 5.4.1, it was proposed that potassium 2-phenylpropan-2-olate **5.12** reacts with CBr$_4$ to form a hypobromite intermediate, which then formally eliminates hypobromous acid to form

methylstyrene **5.42** at high temperatures (160 °C) (Section 5.4.1, Scheme 5.9). However, methylstyrene **5.42** was formed from potassium 2-phenylpropan-2-olate **5.12** at the lower temperatures (40 °C) used within this section, which suggests hypobromite intermediates are also formed in these lower temperature reactions. If KO^{t}Bu reacted with CBr$_4$ by the same mechanism as potassium 2-phenylpropan-2-olate **5.12**, the elimination of hypobromous acid from *tert*-butyl hypobromite would form isobutylene. Under the reaction conditions, if isobutylene (b.p. -6.9 °C) did form from the elimination of *tert*-butyl hypobromite it may not be present in solution to efficiently trap the radicals formed in the reaction mixture, due to its volatility, and therefore halogenation of adamantane **5.50** can occur. Therefore the reason KO^{t}Bu leads to the formation of bromoadamantane but potassium 2-phenylpropan-2-olate **5.12** does not, could be because the alkene formed in the reaction from KO^{t}Bu does not efficiently trap the radical intermediates, unlike the alkene from potassium 2-phenylpropan-2-olate **5.12**. This would explain the difference in the bromination of adamantane between the alkoxides; however so far in this discussion the mode of generation of the radical intermediates at 40 °C remains unknown.

Due to the proposed involvement of hypobromite intermediates, there are two possible mechanisms for the generation of radical intermediates in the bromination pathway of adamantane **5.50** from CBr$_4$. The first possibility is SET from the alkoxide to a molecule of CBr$_4$ to give a bromide anion and CBr$_3$ radicals as described previously. However a second possibility is that the hypobromite intermediate formed in the reaction undergoes O-Br bond homolysis to generate a bromine radical and an alkoxyl radical, which will abstract a hydrogen atom from adamantane to initiate the bromination chain mechanism. There is precedent within the literature for the bromination of alkanes by hypobromites; Wirth *et al.*[141] used *tert*-butyl hypobromites to achieve the bromination of alkanes, and they also proposed that the mechanism proceeded *via* thermolysis of *tert*-butyl hypobromites. The propagation step in the mechanism for this bromination of alkanes could proceed analogously to the report of Schreiner *et al.*[132] whereby the adamantyl radical abstracts a bromine from CBr$_4$, to generate a CBr$_3$ radical as the radical chain carrier, or alternatively, the hypobromite itself could act as radical chain carrier, as proposed by Wirth *et al.*[141]

110

So far within this study, the experimental evidence cannot distinguish between the two proposed radical pathways. In an attempt to deduce the ability of alkoxides to donate a single electron, computational modelling was implemented to calculate the energy profile for the SET from both KO^{t}Bu and potassium 2-phenylpropan-2-ola te **5.12** to CBr$_4$ in dichloromethane (Figure 5.1). The energy barriers for SET from either KO^{t}Bu or potassium 2-phenylpropan-2-olate **5.12** to a molecule of CBr$_4$ were calculated to be $\Delta G^{\ddagger}$ = 35.4 kcal/mol and 36.1 kcal/mol respectively (SET from KO^{t}Bu to CCl$_4$ in dichloromethane: $\Delta G^{\ddagger}$ = 38.8 kcal/mol and ΔG_{rxn} = 16.0 kcal/mol), and these barriers are not accessible for a reaction performed at 40 ^{o}C. When the reaction was performed in CCl$_4$ a similar energy profile was obtained for the SET from either of the two alkoxides to a molecule of CCl$_4$ (Figure 5.1B). The energy barriers calculated were $\Delta G^{\ddagger}$ = 42.5 kcal/mol and 44.5 kcal/mol for SET to CCl$_4$ from KO^{t}Bu and potassium 2-phenylpropan-2-olate **5.12** respectively. From these computationally derived energy profiles for the SET step, it suggests that the initiation for this halogenation of adamantane **5.50** is not *via* SET from the alkoxide, and therefore the only possible mechanism in the formation of the radical intermediates is through homolysis of the hypohalite intermediate.[45]
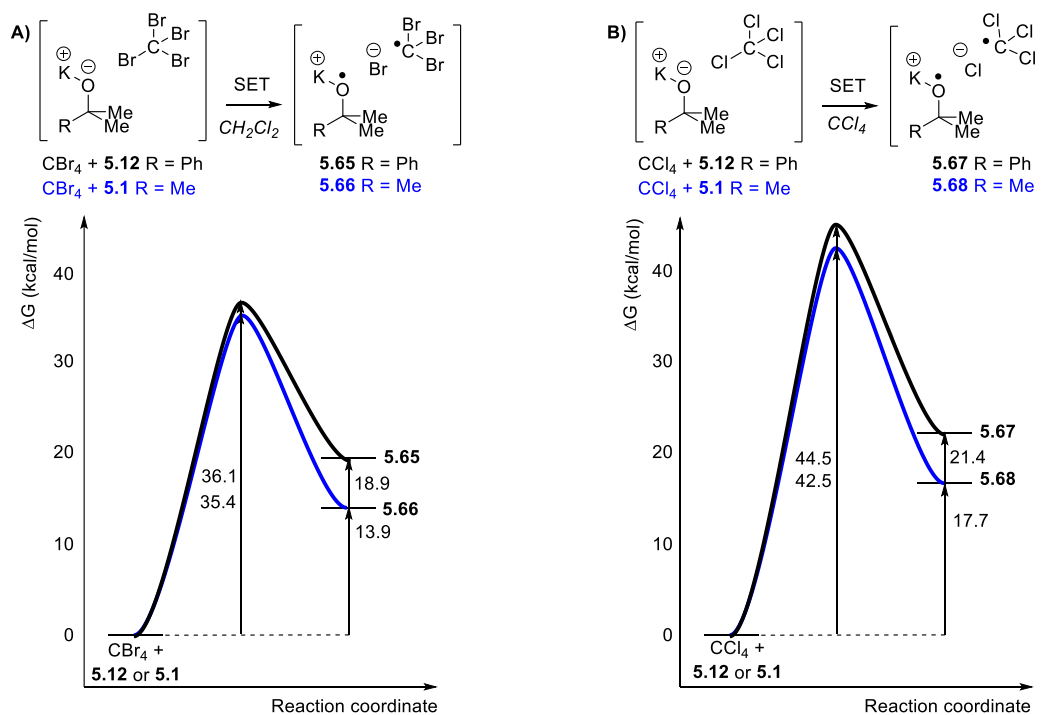
Figure 5.1 Energetic profile for SET from potassium 2-phenylpropan-2-olate **5.12** (black line) or KO^{t}Bu **5.1** (blue line) to **A)** CBr$_4$ in dichloromethane (left) and **B)** CCl$_4$ in CCl$_4$ (right).

Previously in this chapter, potassium 2-phenylpropan-2-olate **5.12** was reacted with CCl₄ as the additive, instead of CBr₄, in an attempt to achieve chlorination of adamantane, however this was unsuccessful in dichloromethane. From the analysis with CBr₄, it is proposed that the chlorination of adamantane **5.50** was inhibited by the formation of methylstyrene **5.42**, which traps radical species formed in the reaction. Therefore, it was proposed that if KO*t*Bu was used as the alkoxide in the reaction with CCl₄ then chlorination of adamantane should occur. Since CCl₄ can be used as a solvent, the reaction was performed in CCl₄ instead of dichloromethane, and 1-chloroadamantane **5.69** (5%) was observed (Scheme 5.16A). To provide a direct comparison between the two alkoxides, potassium 2-phenylpropan-2-olate **5.12** was also reacted in the presence of adamantane **5.50**, with CCl₄ as both the solvent and the additive (Scheme 5.16B). Interestingly, the reaction also yielded 1-chloroadamantane **5.69** (4%), as well as 2-phenylpropanol **5.15**, methylstyrene **5.42**, unreacted adamantane **5.50** and (2,2-dichloro-1-methylcyclopropyl)benzene **5.55**. The chlorination of adamantane was unexpected because it was proposed that the methylstyrene **5.42** formed in the reaction mixture would trap the radical intermediates like it did with CBr₄ and CCl₄ in dichloromethane. One explanation for this chlorination in CCl₄, but not dichloromethane, is that the chain mechanism for the halogenation of adamantane is more efficient in CCl₄ because there is more CCl₄ present to propagate the chain mechanism. Another explanation may be that there is a lower concentration of methylstyrene **5.42** formed in the reaction in CCl₄ compared to dichloromethane, which means there may not be enough methylstyrene **5.42** in CCl₄ to shut down the radical chlorination pathway.
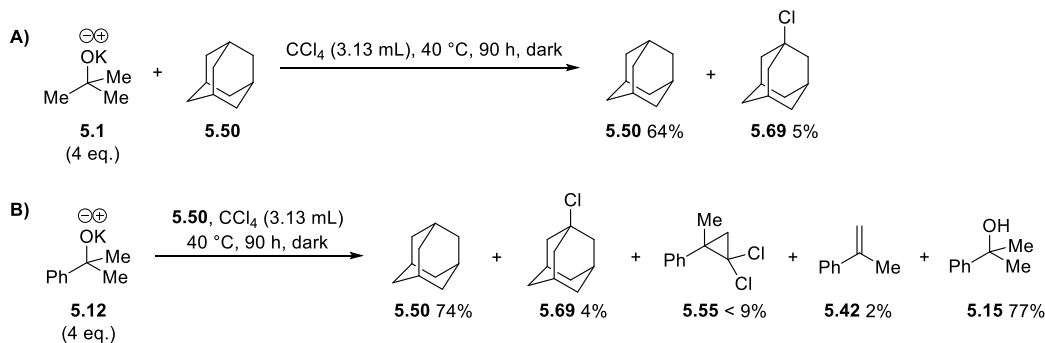
Scheme 5.16 The reaction of the alkoxides with adamantane and CCl₄ as the additive and solvent.

Potassium 2-phenylpropan-2-olate **5.12** was exposed to these reaction conditions with tetrahalomethanes and adamantane in an attempt to find evidence for SET from KO^{t}Bu, such as the formation of acetophenone from β-scission of the alkoxyl radical. However, throughout this study it has been determined that potassium 2-phenylpropan-2-olate **5.12** is capable of forming hypohalite intermediates that eliminate hypohalous acid to form methylstyrene **5.42** and its derivatives. The use of the alkoxide as a probe in this reaction has thus far provided useful information, but it would be interesting to see what would occur if elimination to form alkenes, like isobutylene or methylstyrene **5.42**, were not possible. Therefore, to simplify the reaction a new alkoxide, potassium triphenylmethanolate **5.70**, was synthesised and subjected to the reaction conditions with CBr$_4$ and adamantane **5.50** (Table 5.6). Potassium triphenylmethanolate **5.70** was designed because the three phenyl groups will prevent elimination of hypobromous acid from the hypobromite intermediate.

Table 5.6 The reaction of the potassium triphenylmethanolate **5.70** in dichloromethane at 40 °C.
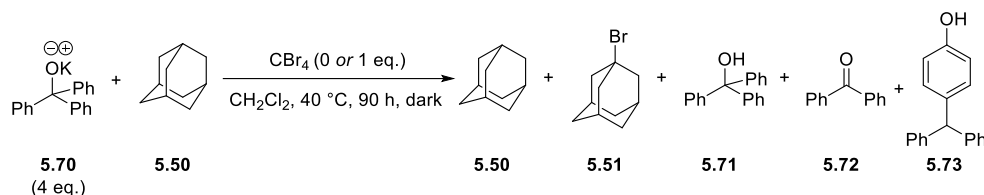
Entry	**Additive** (eq.)	**5.50** (%)	**5.51** (%)	**5.71**[a.] (%)	**5.72** (%)	**5.73** (%)
1	CBr$_4$ (1)	49	7	88	5 (4%)[b.]	12 (7%)[b.]
2	none	87	0	81	1	0

[a.] *Yields based on potassium triphenylmethanolate* **5.70**. [b.] *Isolated yields.*

When potassium triphenylmethanolate **5.70** was exposed to the reaction conditions in the presence of CBr$_4$, several products were observed: 1-bromoadamantane **5.51**, triphenylmethanol **5.71** and unreacted adamantane **5.50**, as well as two new products, benzophenone **5.72** and 4-benzhydrylphenol **5.73** (Table 5.6, entry 1). When the CBr$_4$ was not present in the reaction mixture similar products were formed, except that no 1-bromoadamantane **5.51** or 4-benzhydrylphenol **5.73** were observed (Table 5.6, entry 2). Interestingly, benzophenone **5.72** was formed both with and

113

without the CBr$_4$, however further analysis of the starting material showed trace amounts of **5.72** present in the commercially supplied triphenylmethanol **5.71**. Background formation of benzophenone **5.72** in trace amounts from heterolytic fragmentation of similar tertiary alkoxides is precedented.[129-130]

The important difference between the reaction in the presence of CBr$_4$ and in its absence (Table 5.6, entry 1 and 2 respectively) is the formation of 4-benzhydrylphenol **5.73**. It is proposed that 4-benzhydrylphenol **5.73** can form through the hypobromite **5.74** (Scheme 5.17A). The alkoxide **5.70** reacts with CBr$_4$ to generate the hypobromite **5.74**. This hypobromite can react by three pathways (1) the OBr anion may leave through an E1 elimination to form the stabilised-cation **5.75** and (2) the O-Br bond may fragment ionically upon migration of a phenyl moiety, to form **5.77**, or (3) the O-Br bond undergoes homolysis to form alkoxyl and bromine radicals, for which there is literature precedent.[141] If pathway (1) is followed, the carbocation **5.75** is attacked by another molecule of alkoxide **5.70**, and due to steric effects, the alkoxide will attack at the *para* position of one of the benzene rings, in doing so, the species **5.76** is formed, which ultimately gives **5.73**. Pathway (2) and (3) ultimately lead to the formation of benzophenone **5.72**; pathway (2) involves the formation of intermediate **5.77**, which reacts with water to form **5.78**, and ultimately benzophenone **5.72**. Pathway (3) involves formation of the alkoxyl radical **5.79**, which could form *via* O-Br homolysis of **5.74**, or alternatively by SET from alkoxide **5.70** to a molecule of CBr$_4$. This alkoxyl radical was initially believed to undergo β-scission to form benzophenone **5.72**, however alternatively the radical **5.79** could undergo a neophyl-like rearrangement to form radical **5.80** (Scheme 5.17B).[142] The product **5.82** forms when the radical **5.81** abstracts a bromine atom from either CBr$_4$ (or the hypobromite **5.74**), and **5.82** in turn undergoes a rearrangement to form benzophenone **5.72**. Previous fragmentations of related alkoxyl radicals have been studied.[143-147] The enhanced formation of **5.72** in the presence of CBr$_4$ is proposed to occur through either β-scission of the alkoxyl radical **5.79**, (Scheme 5.17B), or the ionic mechanism (Scheme 5.17A), although this cannot be said for certain.
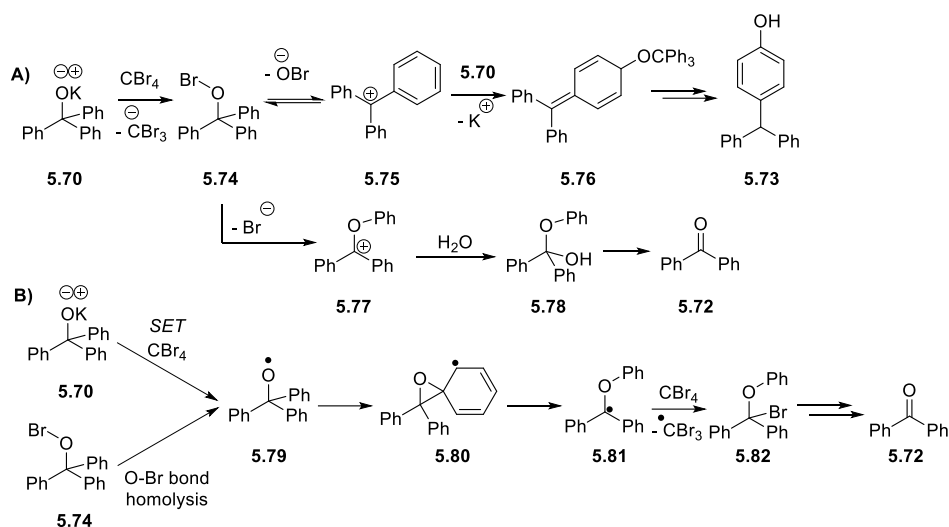
Scheme 5.17 Proposed reaction pathways for the formation of **5.72** and **5.73**, from **5.70**.

Thus far it has been proposed that adamantane **5.50** is halogenated through one of two possible pathways: (1) an alkoxide reacts with the tetrahalomethanes to form a hypobromite (or hypochlorite) intermediate, which could either undergo an elimination of hypobromous (or hypochlorous) acid to form the respective alkene, or O-Br (or O-Cl) bond homolysis to form the corresponding alkoxyl radical and a bromine (or chlorine) radical. (2) SET from the alkoxide to the tetrahalomethanes would form the radical anion of CBr4 (or CCl4) which fragments to give bromide anion and CBr3 radicals that initiate the radical chain mechanism to halogenate adamantane **5.50**. It was vital to determine which of these two pathways was occurring to identify what mechanism was responsible for the halogenation of adamantane **5.50** and whether KO*t*Bu is able to donate a single electron in these reactions.

5.4.3 The halogenation of adamantane with hypohalites

In the previous section, the computational results reported suggest that it is not possible to halogenate adamantane *via* SET from an alkoxide. Therefore it is proposed that the KO*t*Bu forms the *tert*-butyl hypohalites, which undergoes decomposition to form radical species that initiate the halogenation of adamantane **5.50**. However, there is no concrete evidence that the halogenation of adamantane **5.50** occurs through the formation of a hypochlorite intermediate. To determine if this

pathway is occurring, *tert*-butyl hypochlorite **5.83** was prepared (Scheme 5.18) and immediately subjected to the reaction conditions (Table 5.7). The *tert*-butyl hypochlorite **5.83** chlorinated adamantane in both dichloromethane and CCl₄ as the solvents, to give 1-chloroadamantane **5.69** (25% and 11% respectively) and 1,3-dichloroadamantane **5.84** (16% and 26% respectively) (Table 5.7, entry 1 and 2). When the reaction was performed in dichloromethane, a third product was formed as the minor product, 2-chloroadamantane **5.85** (13%). Next, KO*t*Bu **5.1** was reacted with CCl₄ in an analogous reaction to compare the yields of products (Table 5.7, entry 3). To compare the efficiency of KO*t*Bu *vs. tert*-butyl hypochlorite **5.83** at the chlorination of adamantane **5.50**, KO*t*Bu **5.1** was reacted with adamantane **5.50** in CCl₄ and only low yields of 1-chloroadamantane **5.69** (5%) were formed and recovery of unreacted adamantane **5.50** (64%) was achieved.
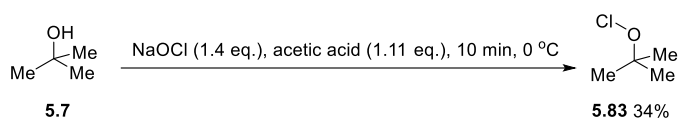
Scheme 5.18 The formation of *tert*-butyl hypochlorite **5.83**.

Table 5.7 The reaction of either *tert*-butyl hypochlorite **5.83** or KO*t*Bu **5.1** in dichloromethane or CCl₄ at 40 °C.
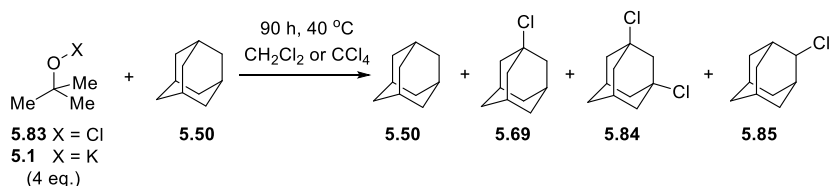
Entry	5.50 (mmol)	Substrate (eq.)	Solvent (mL)	5.50 (%)	5.69 (%)	5.84 (%)	5.85 (%)
1	(0.5)	**5.83** (4)	CH₂Cl₂ (3.13)	10	25	16	13
2[a.]	(0.5)	**5.83** (4)	CCl₄ (3.13)	2	11	26	0
3	(0.5)	**5.1** (4)	CCl₄ (3.13)	64	5	0	0

[a.] *Other products of chlorination of adamantane may have formed but they could not be identified.*

The halogenation of adamantane **5.50** was observed in significantly higher yields from the *tert*-butyl hypochlorite **5.83** compared to the combination of KO*t*Bu and CCl₄, which suggests that the chlorination of adamantane by KO*t*Bu may occur, at least

partially, through a hypochlorite intermediate. The formation of the 1,3-dichloroadamantane **5.84** occurs through a second chlorination of 1-chloroadamantane **5.69**. A comparison of the yields of products **5.69** and **5.84** in dichloromethane and CCl₄ show that the chlorination mechanism is more efficient in CCl₄ because more of the di-chlorinated product **5.84** observed, as well as a higher conversion of adamantane **5.50**. Comparison of the yields of products achieved when *tert*-butyl hypochlorite **5.83** was used (Table 5.7, entry 1-2) instead of KO^{t}Bu (Table 5.7, entry 3) suggest that the *tert*-butyl hypochlorite **5.83** is more efficient at the chlorination of adamantane **5.50**. It is proposed that, because the alkoxides give lower yields of halogenation than the direct use of the hypohalites, then the rate determining step is likely to be the formation of the hypohalite. The combination of the experimental results presented here and the computational results (previously discussed in Figure 5.1) all suggest that the halogenation of the adamantane **5.50** occurs by hypohalite formation, and not *via* SET from the alkoxide as previously proposed. It must be noted that within the literature there are reports of the halogenation of alkanes using sodium hypohalites or alkyl hypohalites.[141,148]

Finally, the *tert*-butyl hypobromite **5.86** was synthesised and subjected to similar reaction conditions (Scheme 5.19). When a sub-stoichiometric amount of *tert*-butyl hypobromite **5.86** was used, bromination of adamantane was observed to yield 1-bromoadamantane **5.51** (16%) and 2-bromoadamantane **5.52** (4%). However when an excess of KO^{t}Bu **5.1** was reacted with adamantane **5.50** in the presence of CBr₄, the major product was the unreacted adamantane **5.50** (84%), with 1-bromoadamantane **5.51** as the minor product (4%). This demonstrates that even using substoichiometric amounts of the *tert*-butyl hypobromite **5.86** (0.4 eq.), higher yields of brominated adamantane, **5.51** and **5.52**, are achieved compared to when KO^{t}Bu and CBr₄ were used.

A)

5.7
(4 eq.)

5.86
(0.4 eq.)

5.50 70%   **5.51** 16%   **5.52** 4%   **5.53** < 1%

(Yields based on adamantane 5.50 as the limiting reagent)

B)

5.1
(4 eq.)

5.50

5.50 84%   **5.51** 4%
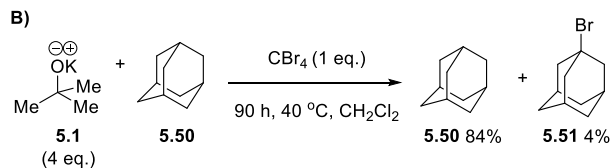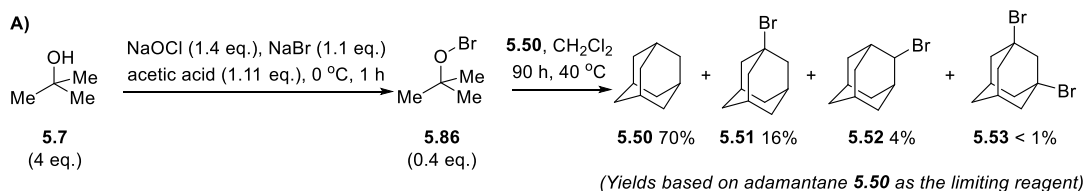
Scheme 5.19 The mechanism for halogenation of adamantane **5.50**.

This study has led to a revision of earlier thoughts on the mechanism for the halogenation of adamantane **5.50**, by using a combination of KO^{t}Bu and CBr$_4$. It is now proposed that the mechanism does not occur through SET as was previously believed, but it actually proceeds through hypobromite intermediates (Scheme 5.20) (only the bromination is described here; however it is proposed that the chlorination occurs through an analogous mechanism). The alkoxide in the reaction mixture, such as **5.12**, forms a hypobromite in the presence of CBr$_4$. The hypobromite **5.44** can undergo two pathways. The first option is an elimination reaction to form methylstyrene **5.42**, which reacts with carbenes formed in the reaction to afford final product **5.41**. The second pathway is the O-Br bond homolysis of the hypobromite **5.44**. This forms the alkoxyl radical **5.13** and a bromine radical. These radical intermediates perform a hydrogen atom abstraction from adamantane **5.50** to form adamantyl radical **5.54** (alternatively the hydrogen atom abstraction may occur at the C-2 position to ultimately give the 2-Br isomer). The radical **5.54** will abstract a bromine from a hypobromite molecule **5.44**, or CBr$_4$, to form **5.51** and a CBr$_3$ radical, or alkoxyl radical **5.13**. The CBr$_3$ radical, or alkoxyl radical **5.13**, will propagate the chain pathway by hydrogen atom abstraction from adamantane **5.50** thus creating a radical chain mechanism.
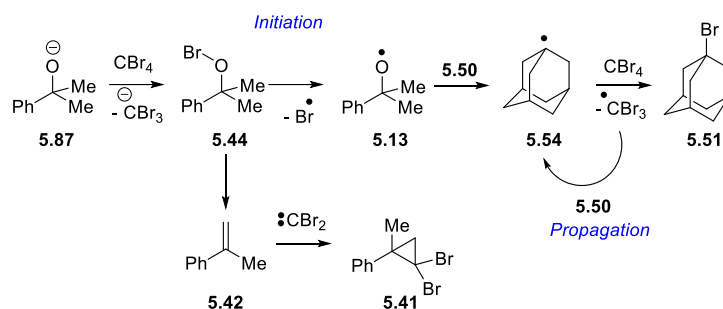
Scheme 5.20 The modified mechanism for halogenation of adamantane.

This section has provided evidence that hypohalites can form in the reactions, through the isolation of methylstyrene, and its related molecules. It has also provided proof that hypohalites are capable of halogenating adamantane, which is supported by previous work reported in the literature by Wirth *et al.*[141] Finally, computational analysis suggests that SET from KO^{t}Bu to CBr$_4$ is not accessible at temperatures, such as 40 °C, used throughout the latter parts of this study, but rather that hypohalites formed could undergo fragmentation to radical intermediates. If KO^{t}Bu is not capable of donating an electron to CBr$_4$, which has a much less negative reduction potential than iodobenzene (-0.31 V in DMF *vs.* SCE and -2.2 V *vs.* SCE respectively), it is therefore not likely that KO^{t}Bu is able to donate an electron to haloarenes to initiate the transition metal-free BHAS mechanism.

5.5 Future work

The mechanism for the formation of hypohalites, by the reaction of alkoxides with CBr$_4$, and subsequent bromination of adamantane was reported in this chapter. This mechanism is different to the mechanism Schreiner *et al.* reported for the halogenation of adamantane using the combination of sodium hydroxide and CBr$_4$. They proposed SET occurs from the hydroxide anion to CBr$_4$, and they rule out a hypobromite intermediate because they reported that hypobromous acid did not achieve the halogenation. However, it would still be interesting to readdress this reaction, using sodium hydroxide, to further investigate the hypobromite formation as a possibility.

Within this section, it has been proposed that KO^{t}Bu may not be a single electron donor, as was previously believed. In this chapter, the role of KO^{t}Bu was addressed for both its involvement in the transition metal-free reaction conditions and in the halogenation of adamantane. Evidence is mounting that supports the proposal that the role of KO^{t}Bu in these reactions is the formation of electron donors or radical precursors *in situ*, and not to perform SET. To continue this work, it would be interesting to address the proposal that KO^{t}Bu is capable of donating an electron to both benzophenone and tritylbromide, as Ashby *et al.*[36-37] proposed (previously described in detail in Section 1.4.1) and this is ongoing in our research group.

6.

Expanding the scope of transition metal-free coupling reactions

6.1 Introduction

For transition metal-free coupling chemistry to advance and progress to compete with palladium-catalysed cross-coupling reactions, more complex substrates need to be studied, including those where different types of coupling reactions are in competition. The possibility of $S_{RN}1$ coupling of aryl halides to an anionic nucleophile has previously been introduced in the coupling of aryl halides to enolate anions.[75,82-83] Rossi has been a pioneer of much of the recent development of the $S_{RN}1$ reaction.[85,149-151] One of his recent studies generated aryl radicals from haloarenes either (i) under transition metal-free photoactivation conditions, or (ii) without photoactivation but in the presence of iron (II) salts and pinacolone.[149-151] The aryl radical formed could undergo either $S_{RN}1$ cyclisation or BHAS coupling, which meant that the substrates used in his study were ideal candidates for probing alternative reaction pathways that can be accessed through transition metal-free reaction conditions.

This chapter focusses on a series of competing reactions, based on examples from the literature by Rossi *et al*.[85], for a selection of substrates that are carried out under thermal reaction conditions using the DKP additive and KO^{t}Bu, to generate the enolate anion of DKP as the electron donor in these reaction conditions. Computational chemistry has been applied to the study to gain deeper mechanistic insight into the reactions.

6.2 Computational methods

The calculations were run using the M06-2X functional[103-104] with the 6-311++G(d,p) basis set[105-109] on all atoms, except for the iodine. Iodine was modelled with the MWB46 relativistic pseudo potential and associated basis set.[110] All calculations were carried out using the C-PCM implicit solvent model.[111-112] All calculations were performed in Gaussian09.[113]

6.3 Transition metal-free ground state access to S$_{RN}$1 pathways

Within this thesis it has been shown that the enolate anion, **6.5**, of the *N,N'*-dipropyldiketopiperazine (DKP) **6.2** (Table 6.1) donates an electron to aryl halides, such as iodo-*m*-xylene, in the initiation step of the BHAS mechanism (previously discussed in Chapter 4, Section 4.3). Therefore, DKP **6.2** was used as an additive, in the presence of KO*t*Bu, in an attempt to achieve S$_{RN}$1 cyclisations of substrate **6.1**. Most reactions reported in the literature that proceed *via* the BHAS mechanism are performed using benzene as the solvent, since benzene is the coupling partner in these reactions. In the few examples where aryl radicals couple to enolate anions *via* the S$_{RN}$1 pathway the solvents used are DMSO, liquid ammonia or DMF.[149,152] Given that the polarity of the medium is expected to play an important role in facilitating electron transfer reactions, the reaction outcomes in both benzene and DMSO were investigated and the results are compared throughout this study. The initial studies exposed substrate **6.1** to these transition metal-free reaction conditions (Table 6.1).

Table 6.1 Thermally activated electron transfer reaction of substrates **6.1**.
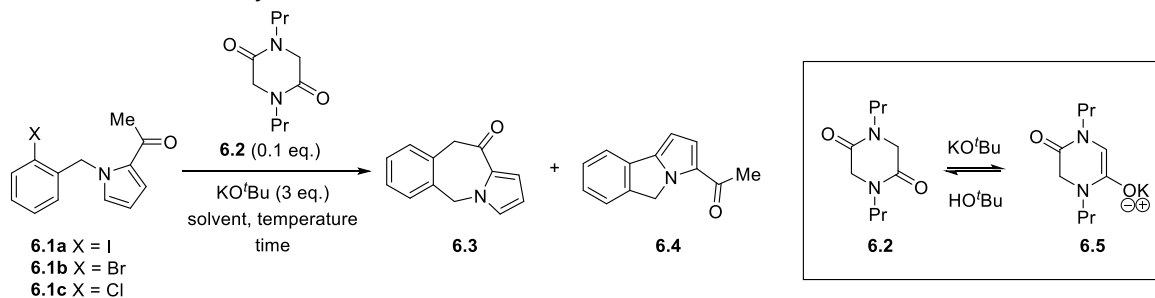
Entry	Substrate	Time (h)	Temperature (ºC)	Solvent (mL)	6.3 (%)	6.4 (%)
1	**6.1a**	1	120	benzene (5)	55	7
2	**6.1a**	1	120	DMSO (2)	79	10
3	**6.1b**	1	120	DMSO (2)	25	0
4[a.b.]	**6.1b**	16	160	benzene (5)	30	0
5	**6.1c**	1	120	DMSO (2)	20	0
6	**6.1c**	16	160	benzene (2)	24	0

[a.]*At 120 ºC, only starting material was observed in the crude mixture.* [b.]*KO*t*Bu used in 5 equivalents.*

These initial investigations were performed using substrate **6.1** and several conclusions can be drawn. When **6.1a** (X = I) was stirred at 120 °C for 1 h in the presence of KO^{t}Bu and DKP **6.2**, and in either anhydrous benzene or anhydrous DMSO, two products were isolated. The major product in both solvents was 5H-benzo[e]-pyrrolo[1,2-a]azepin-11(10H)-one **6.3**, which was isolated in moderate yields in benzene (55%) and high yields in DMSO (79%), and the minor product isolated was 3-acetyl-5H-pyrrolo[2,1-a]isoindole **6.4**, which was isolated in low yields in both benzene and DMSO (7% and 10% yields respectively) (Table 6.1, entries 1 and 2). Comparison of the product yields with those reported in the literature shows that these transition metal-free conditions used in this study are capable of competing with both the light irradiation procedure and a procedure that used iron(II) salts for the transformation.[85] [Within the literature light irradiation of **6.1a** in the presence of KO^{t}Bu afforded **6.3** (38%) in low yields, but using FeCl$_2$ catalyst and pinacolone in the presence of KO^{t}Bu, higher yields of **6.3** were achieved (84%).[85] The reaction of **6.1a** with FeCl$_2$ also formed the minor product **6.4** in low yields (11%)]. The effect of the halogen on these reactions was investigated in the two solvents. It is demonstrated that changing the halogen largely affects the reactivity of the substrate, and hence the yields of products. When the reaction was performed in benzene, the bromo substrate **6.1b** required harsher reaction conditions to achieve product formation (Table 6.1, entry 4). Finally, the reaction of **6.1a-c** appears to have a strong solvent dependence; in DMSO, yields of the cyclised products from **6.1a** were higher than in benzene, and the reaction of **6.1b-c** could be performed at a 120 °C in DMSO, rather than 160 °C in benzene (Table 6.1, entries 3-6). It has been reported that the dimsyl anion could act as an electron donor in transition metal-free reaction conditions,[153] and hence this may contribute to the higher yields observed in DMSO. If the activation of **6.1a-c** occurs through a SET initiation step, then the possibility that the dimsyl anion is contributing to the formation of products should be considered.

The cyclisation of substrate **6.1a-c** to form **6.3** in the presence of a strong base, KO^{t}Bu, under the ground-state conditions could occur through several pathways (Scheme 6.1):

1. The benzyne formation pathway.[29] KO^{t}Bu would deprotonate substrate **6.6**, at the proton *ortho* to the iodine, to eliminate HI and form a benzyne intermediate **6.7**. Cyclisation of the enolate anion onto the benzyne would form **6.3** upon protonation during work-up.

2. Intermolecular SET to the haloaryl moiety of **6.6** would yield the aryl radical **6.8** upon loss of the iodide anion (initiation). The aryl radical would cyclise onto the enolate anion *via* an S$_{RN}$1 mechanism to yield **6.3** upon the loss of an electron (propagation).[85]

3. Another possibility is intramolecular SET from the enolate anion to the haloaryl moiety, which will form intermediate **6.9**. Radical recombination would lead to the product **6.3**.
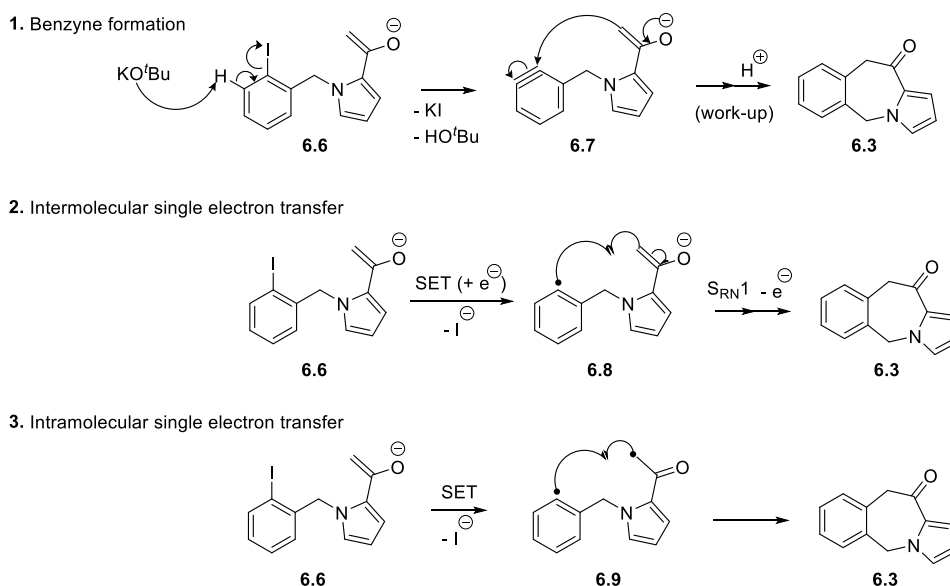
Scheme 6.1 Possible initiation pathways for the enolate anion **6.6** (from deprotonation of substrate **6.1a**).

Using computational analysis, the reaction pathways could be modelled to provide an estimation of the feasibility of each possibility. However, in order to begin studying the systems, it was important to identify what reactive species will form in the reaction mixture from both the substrate **6.1a** and the DKP additive **6.2**, in the presence of KO^{t}Bu. KO^{t}Bu is known to exist as a cubic tetramer **6.15**, which has been observed in the solid state using X-ray crystallography.[154-155] The initial attempts to model the

deprotonation of substrate **6.1a** with the cubic tetramer of KO^{t}Bu **6.15** was computationally expensive, therefore the substrate **6.1a** was truncated to 2-acetyl-1-methylpyrrole **6.10**. Furthermore, an appropriate approximation of the KO^{t}Bu cubic structure **6.15** was required (Table 6.2). The possible structures of KO^{t}Bu analysed were the dimeric species **6.14**, the monomeric species **6.13** and the free *tert*-butoxide anion **6.12**. The energy profile for the deprotonation of substrates, like **6.1a**, with the various structures of *tert*-butoxide, **6.12 – 6.15**, were calculated to identify the best structure to approximate the activity of the KO^{t}Bu cubic structure **6.15**.

Table 6.2 Comparison of the stability of the possible forms of KO^{t}Bu as well as their energy profile for the deprotonation of 2-acetyl-1-methylpyrrole **6.10**.
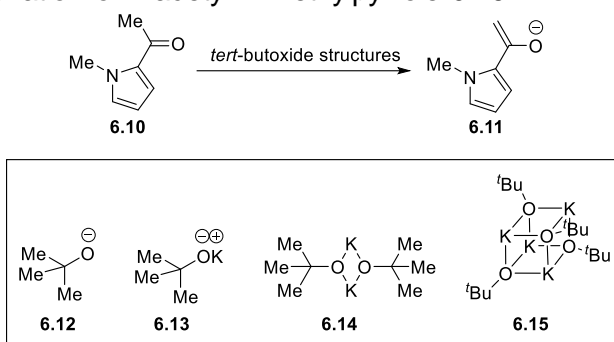
tert-butoxide structure	Relative stability (kcal/mol)	$\Delta G^{\ddagger}$ deprotonation (kcal/mol)	ΔG_{rxn} deprotonation (kcal/mol)
O^{t}Bu anion **6.12**	--	0.39	-12.11
KO^{t}Bu **6.13**	0.00	4.84	-4.06
KO^{t}Bu dimer **6.14**	-30.9	7.84	-3.00
KO^{t}Bu tetramer **6.15**	-54.8	3.94	-14.48

Comparison of the relative stability of the various forms of potassium *tert*-butoxide shows that its most stable form in benzene was the cubic tetramer **6.15**, which is expected because the cubic structure has been identified as the most stable structure, in both the solid and gas phase, in the literature.[154] The energy profile for the deprotonation of 2-acetyl-1-methylpyrrole **6.10** using the various possible forms of *tert*-butoxide were all accessible at room temperature, and all showed that the equilibrium for the deprotonation of **6.10** lies to the right, to the formation of the enolate anion **6.11**. At the start of this project, it was important to determine the most likely species that were present in the reaction mixture, and therefore the

investigation primarily focussed on the relative energies, ΔG_{rxn}, to deduce the possible equilibrium present in the reaction mixture. It was observed that the O^{t}Bu anion **6.12** was the structure that most closely replicated relative energies of the KO^{t}Bu tetramer **6.15**, ΔG_{rxn} = -12.11 *vs*. -14.48 kcal/mol, for this system. Therefore throughout the chapter, the butoxide anion **6.12** will be representative of potassium *tert*-butoxide in the reaction mixture.

Using the *tert*-butoxide anion **6.12**, the equilibria for the deprotonation of both the DKP additive **6.2** and the substrate **6.1a** were calculated to identify the likely reactive species that will be present in the basic reaction mixture (Table 6.3). Under the basic conditions, **6.1a** will exist as its enolate anion **6.6**, and similarly the DKP additive **6.2** will be converted to its enolate anion **6.16** (Table 6.3). The energy profile was determined in both benzene and DMSO as the solvent, and in both solvents the equilibrium favours the formation of the enolate anion. Additionally, the deprotonation of substrate **6.1a** was performed using KO^{t}Bu to provide a comparison of the results of the substrate **6.1a** and the truncated 2-acetyl-1-methylpyrrole **6.10** (Table 6.2). Interestingly, the results for **6.1a** suggest that the O^{t}Bu anion and KO^{t}Bu gave similar results for the equilibrium, ΔG_{rxn}, which is a contrast to the trend observed using truncated 2-acetyl-1-methylpyrrole **6.10**.

Table 6.3 The deprotonation energy profile for DKP **6.2** and substrate **6.1** in both DMSO and benzene ($\Delta G^{\ddagger}$ for the deprotonation is in blue above the reaction arrows, and ΔG_{rxn} is in blue beneath the deprotonated product).

Knowing what reactive species are present in the reaction mixture, the first proposed pathway for the cyclisation of **6.1a** could be modelled. The benzyne formation pathway was modelled using DMSO as the reaction solvent (Scheme 6.2).
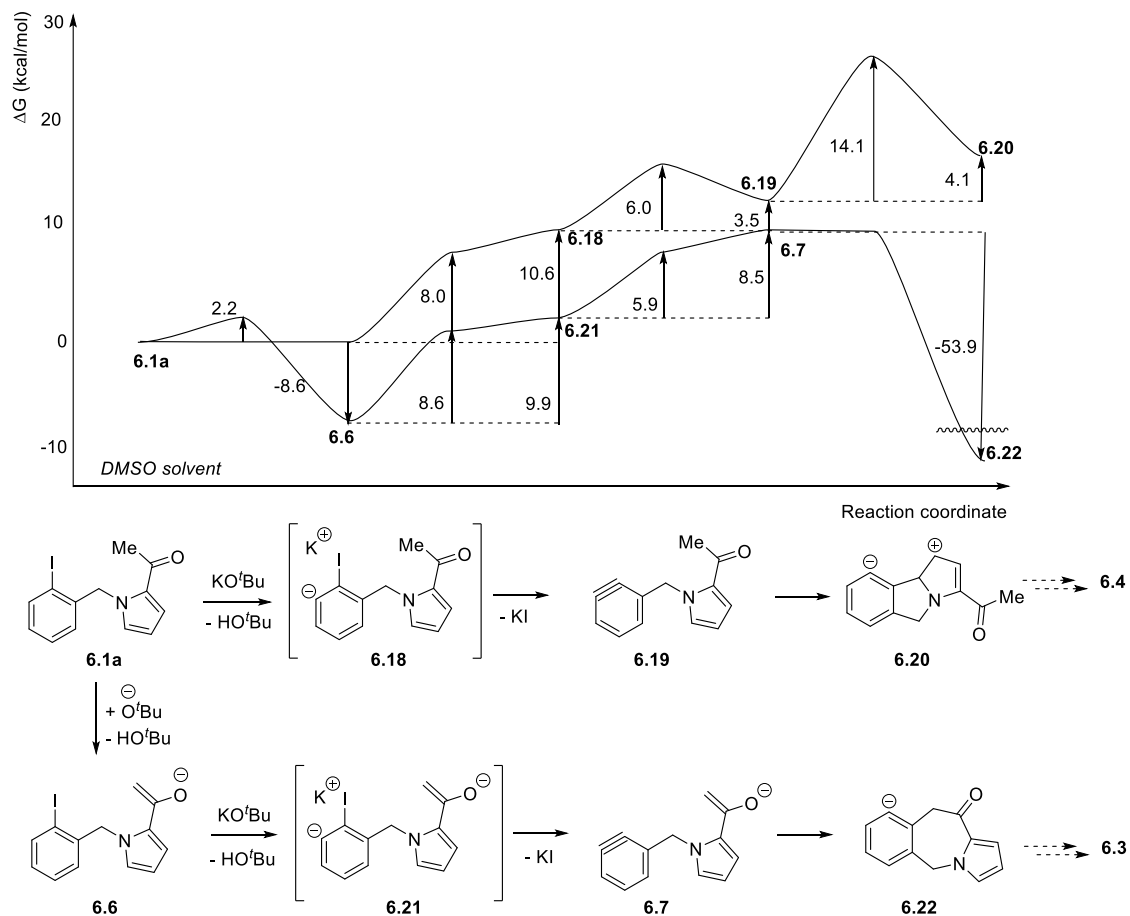
Scheme 6.2 The energy profile for benzyne formation in DMSO from **6.1a** and **6.17**.

The formation of neutral benzyne **6.19** has a relative energy of formation: $\Delta G_{rxn} =$ 14.1 kcal/mol. (It is important to note that in order to model the benzyne formation pathway, the computational optimisation was performed stepwise, finding the local minimum of **6.18**, however it is presumed from the energy profile obtained for the benzyne formation that the reaction does proceed in a concerted pathway). The cyclisation to form **6.20** has an overall $\Delta G^{\ddagger} = 28.2$ kcal/mol and $\Delta G_{rxn} = 18.2$ kcal/mol. This is very unfavourable and the product **6.4** is unlikely to form if the reaction proceeded through the benzyne mechanism (Scheme 6.2). However, it was previously determined that in the basic reaction mixture the substrate **6.1a** will exist

predominantly as an enolate anion **6.6** (Table 6.3), hence the formation of the benzyne species **6.7** was calculated and it was found to be endergonic by $\Delta G_{rxn} =$ 18.4 kcal/mol. The cyclisation of intermediate **6.7** to form **6.22** is barrierless and very exothermic, $\Delta G_{rxn} =$ -53.9 kcal/mol, suggesting that if any benzyne forms, then the cyclisation to form **6.22** (and ultimately the major product **6.3**) will occur. Therefore, it is possible that the cyclisation of **6.1a** to form the major product **6.3** could occur through a benzyne intermediate. To deduce whether the reaction proceeds through benzyne intermediates, the substrate **6.23** was used under these reaction conditions (Scheme 6.3A). This substrate contains a methoxy group *ortho* to the iodine on the haloarene moiety, which blocks any benzyne formation. When **6.23** was treated with KO^{t}Bu and the DKP additive **6.2**, in either DMSO or benzene at 120 °C for 1 h, the products **6.24** and **6.25** formed (Scheme 6.3A-B), albeit with lower product yields than the cyclisation of the analogous substrate **6.1a**.[114] These results suggest that SET is the initiation step in the S$_{RN}$1 reaction of **6.23** (and therefore **6.1a**) and a mechanism can be proposed (Scheme 6.3C).
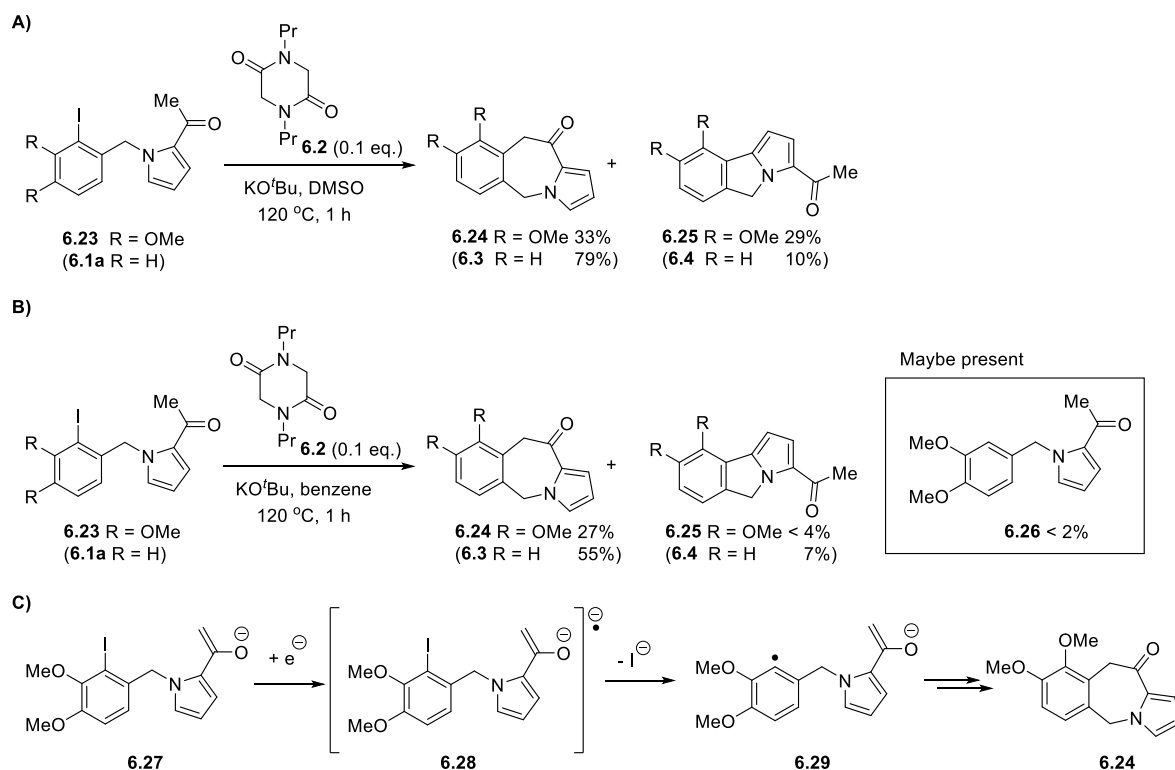
Scheme 6.3A)-B) Comparing the reaction of **6.23** and **6.1a** under the transition metal-free coupling reactions **C)** A mechanism for the cyclisation of **6.27** to form **6.24**.

The substrate **6.23** is in equilibrium with its enolate anion **6.27** in the presence of KO*t*Bu. A SET into the molecule **6.27** will form the radical dianion **6.28**, which will undergo C-I bond cleavage, either in a concerted or step-wise mechanism, to lose an iodide anion and form the aryl radical intermediate **6.29**. This aryl radical **6.29** can cyclise onto the enolate anion through a S$_{RN}$1 cyclisation to ultimately form the cyclised product **6.24**. The lower product yields from cyclisation of substrate **6.23** compared to substrate **6.1a**, in both DMSO and benzene, may be because it is more difficult to donate an electron into the haloarene moiety in **6.23**. The haloarene moiety of **6.23** is more electron-rich due to the presence of the methoxy substituents on the ring, and therefore the electron donation may be more difficult. An alternative proposal is that the low yields observed arise from the difficulty in the cyclisation of the aryl radical **6.29**, due to the methoxy substituents. This explains why low yields of product are seen, yet full conversion of the starting substrate was achieved. Therefore, it is expected that the non-halogenated product, such as **6.26**, would be formed, however attempts to purify the reaction mixture to identify this species were not successful. A final possibility to account for the lower yield from the substrate **6.23**, is that the benzyne pathway, previously described, may contribute to the formation of the major cyclised product, such as **6.3**, as a minor pathway, and hence lower yields of products, such as **6.24**, are achieved when the benzyne pathway is blocked.

Since substrate **6.23** cyclised to form both **6.24** and **6.25** under these reaction conditions (Scheme 6.3A-B), the working hypothesis for the initiation step of these reactions is that a SET occurs to the two substrates, **6.1** and **6.23**. Therefore, it was important to identify whether the reaction occurs through inter- or intramolecular SET. If the reaction occurs through the intermolecular SET, then the possible electron acceptors in the reaction mixture are the neutral substrate **6.1a** and its enolate anion **6.6** (Table 6.4). Indeed analysis of the HOMO and LUMO for these molecules shows that the LUMO of both these species, **6.1a** and **6.6**, resides on the C-I σ* orbital, albeit for **6.1a** the LUMO is delocalised over the acetylpyrrole moiety too. If SET occurs into these two molecules, especially into the enolate anion **6.6**, it will lead to a cleavage of the C-I bond and formation of the aryl radical, analogous to **6.29**

(Scheme 6.3C). The possible electron donors are either the enolate anion of DKP **6.16** (as discussed previously in Section 4.3) or alternatively, because it is known that electron-rich double-bonds can donate an electron, the enolate anion **6.6** of the substrate itself could act as an electron donor.[42,76] Also, when the reaction is performed in DMSO, the dimsyl anion **6.30** should be considered as a possible electron donor.[153] For these three potential electron donor species, the HOMO lies on the electron-rich double-bond, as was to be expected (Table 6.4).

Table 6.4 The HOMO and LUMO of the electron acceptors and electron donors in the reaction mixture, in both benzene and DMSO.
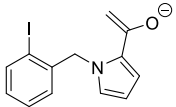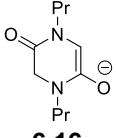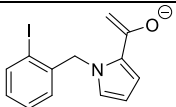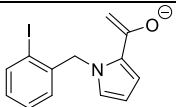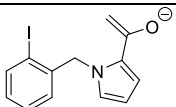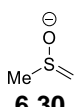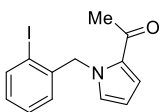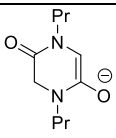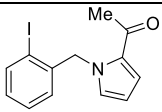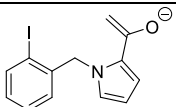
	Electron Acceptor		Electron Donor		
	6.1a	**6.6**	**6.16**	**6.6**	**6.30**[a.]
HOMO/LUMO:	LUMO	LUMO	HOMO	HOMO	HOMO

[a.]*The energy profile for deprotonation by tert-butoxide anion ($\Delta G^{\ddagger} = 2.5$ kcal/mol; $\Delta G_{rxn} = 1.9$ kcal/mol).*

From the calculations of the deprotonation of **6.1a** (Table 6.3) it was determined that within the reaction mixture the enolate anion **6.6** will be the major species present, and therefore it was investigated firstly as a possible electron acceptor (Table 6.5). In benzene, SET to the enolate anion **6.6** may occur from either another molecule of the enolate anion **6.6** or from the enolate anion of DKP **6.16**. SET from **6.16** to **6.6** (Table 6.5, entry 1) has an energy barrier of $\Delta G^{\ddagger} = 34.3$ kcal/mol in benzene, whereas intermolecular SET from another molecule of **6.6** has a much higher barrier

$\Delta G^{\ddagger}$ = 45.8 kcal/mol. This suggests that in benzene the initiation of the $S_{RN}1$ cyclisation of **6.1a** can only occur in the presence of the DKP **6.2** additive and at high temperatures, such as 120 °C. The energy profile for SET to **6.6**, from **6.16** or **6.6**, in DMSO shows a similar trend, $\Delta G^{\ddagger}$ = 22.7 and 33.0 kcal/mol for SET respectively; SET from the enolate anion of DKP **6.16** is more favoured, with a lower activation barrier. The energy profile for SET in DMSO compared to benzene involves lower energy barriers, $\Delta G^{\ddagger}$ = 22.7 and 34.3 kcal/mol for SET from **6.16** to **6.6** respectively. Additionally, the deprotonation and subsequent SET from the dimsyl anion was calculated to be $\Delta G^{\ddagger}$ = 31.4 kcal/mol [ΔG_{rxn} = 1.9 kcal/mol for deprotonation (Table 6.4) and $\Delta G^{\ddagger}$ = 29.5 kcal/mol for SET (Table 6.5)]. These results mean that the enolate additive of DKP **6.16** is a better electron donor than the enolate anion **6.6** or dimsyl anion **6.30**. However, the reactions are performed at temperatures of 120 °C, and therefore all three species could form and donate an electron to the C-I σ* orbital of the haloarene moiety to initiate the $S_{RN}1$ cyclisation.

Table 6.5 The $\Delta G^{\ddagger}$ and ΔG_{rxn} for SET to the neutral substrate **6.1a** or its enolate anion **6.6** from various electron donors, in both benzene and DMSO.

Entry	Electron acceptor	Electron donor	Benzene $\Delta G^{\ddagger}$ / ΔG_{rxn} (kcal/mol)	DMSO $\Delta G^{\ddagger}$ / ΔG_{rxn} (kcal/mol)
1	**6.6**	**6.16**	34.3 / 24.7	22.7 / 10.4
2	**6.6**	**6.6**	45.8 / 42.5	33.0 / 27.8
3	**6.6**	**6.30**	--	29.5 / 20.8
4	**6.1a**	**6.16**	31.9 / 30.7	36.0 / 32.8
5	**6.1a**	**6.6**	69.2 / 48.5	74.1 / 50.2

The computational results also suggest that in DMSO the DKP additive **6.2** is not required to achieve cyclisation at high temperatures, because either the substrate itself or the solvent, DMSO, could form the electron donor and subsequently initiate the reaction. These computational results collectively suggest that by changing the solvent from benzene (which is the more traditional solvent used in the transition metal-free reaction conditions) to DMSO, the reaction should proceed efficiently both in the absence of DKP **6.2** as well as at lower temperatures. In non-polar solvents like benzene, where electron transfer from neutral species to form charged species is not facilitated, a stronger donor, like the enolate anion DKP **6.16**, can play a powerful role in assisting the initiation of the chains. Polar solvents, like DMSO, favour SET reactions in which charged species are formed from neutral starting materials, and so, donor precursors like **6.2** are not needed to initiate the reaction. Considering that the equilibrium for the deprotonation of substrate **6.1a** favours the formation of **6.6**, it can be assumed that the major SET pathway is to the enolate anion **6.6** (Table 6.5, entry 4-5). However, the neutral substrate **6.1a** was still analysed for SET as an electron acceptor. Upon the initial optimisation of the substrate **6.1a**, the radical anion formed after SET to **6.1a** did not lead to spontaneous C-I bond cleavage. Analysis of substrate **6.1a** showed that the LUMO was delocalised over the molecule (previously shown in Table 6.4), therefore suggesting that SET into the LUMO may not lead to spontaneous C-I bond cleavage as was the case with the enolate anion **6.6**. In benzene, although the energy barrier for SET from **6.16** to the neutral substrate **6.1a** was calculated to be more favourable than SET into the enolate anion **6.6** ($\Delta G^{\ddagger}$ = 31.9 kcal/mol *vs*. 34.3 kcal/mol respectively). However, within the basic reaction mixture there will be a small amount of neutral substrate **6.1a** present. Therefore the major reaction pathway in benzene will be the SET into the enolate anion. However, this may explain the lower yields in benzene than in DMSO. In DMSO, the SET to the neutral substrate **6.1a** had a higher barrier than SET into the enolate anion **6.6**, and therefore in DMSO the initiation will be SET into the enolate anion **6.6**, and SET to the neutral species from any of the electron donors in the initiation step will not play a significant role.

From the computational study, there are two predictions that could be made based on the influence the solvent has on the SET initiation step: 1) the cyclisation of **6.1a** will occur in DMSO without the additive **6.2,** however it will not in benzene; and 2) the reaction could be performed in DMSO at room temperature, however in benzene the reaction will only occur at high temperatures. To test these theories several experiments were performed. Blank reactions were performed without the DKP additive **6.2**, to observe how the additive influences the yields of the reaction. A blank reaction in benzene, without the DKP additive **6.2** returned mainly starting material from the reaction (**6.1a**, 73%) with **6.3** formed in low yields (23%). This result gave lower yield of conversion and product formation than when DKP was present (**6.1a**, 0%; **6.3**, 55%) (Scheme 6.4B). However, a blank reaction in DMSO showed the opposite trend, and **6.3** was achieved with higher yields (90%) when the DKP additive **6.2** was omitted from the reaction (Scheme 6.4A). These results gave experimental support to the computational predictions that **6.1a** will cyclise in DMSO without DKP **6.2** (Table 6.4A). However, it was predicted that, in benzene, the additive **6.2** would be needed for cyclisations, yet experimentally this is not true. Although very low conversion of **6.1a** was achieved without DKP additive in benzene, this still shows that cyclisation can happen at high temperatures in benzene. Only the major product **6.3** (23%) formed in benzene, and based on the results gathered so far in this study, it is proposed that the formation of low yields of **6.3** in benzene occurs through benzyne intermediates as a minor pathway.
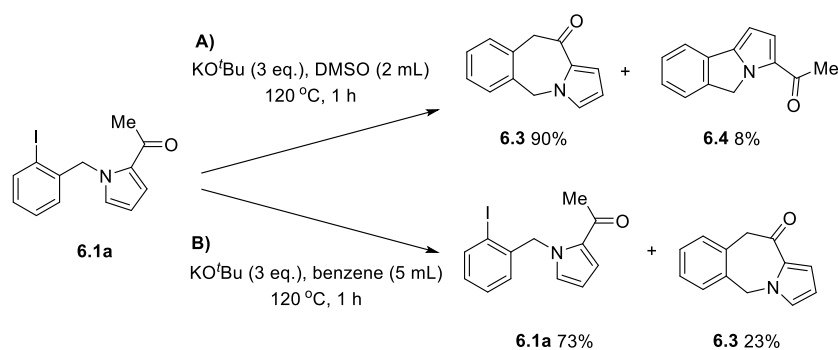
Scheme 6.4 The reactions of substrate **6.1a** without the DKP additive **6.2**.

Next, the prediction that the reaction could occur in DMSO at room temperature, but not in benzene, was investigated. When substrate **6.1a** was exposed to additive **6.2** and KO*t*Bu in benzene at room temperature, no conversion of the starting material was seen, as was predicted from computational studies (Table 6.6, entry 1). When the reaction was performed at room temperature in DMSO, moderate to high yields of cyclised products were isolated both with and without the DKP **6.2** additive respectively (Table 6.6, entries 2 - 3). A reaction that was conducted in the dark provided confirmation that these reactions proceed *via* a thermal SET pathway, with yields matching those carried out in the presence of ambient light and so, even at room temperature, photochemical assistance is not needed for these SRN1 reactions (Table 6.6, entry 4).

Table 6.6 The reaction of **6.1a** at room temperature.
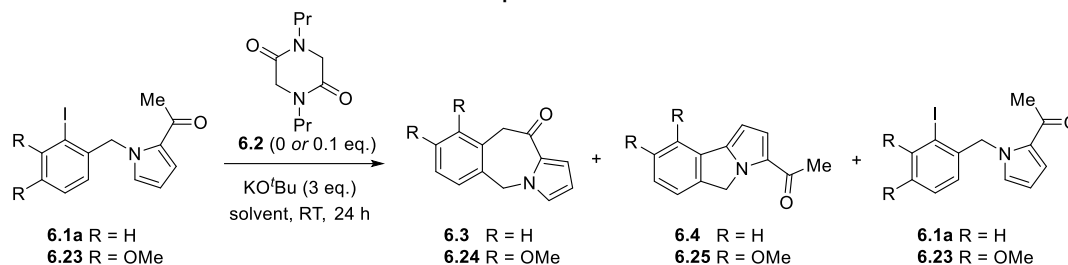
Entry	Substrate	6.2 (eq.)	Solvent (mL)	6.3 / 6.24 (%)	6.4 / 6.25 (%)	6.1a / 6.23 (%)
1	**6.1a**	0.1	benzene (5)	No reaction		
2	**6.1a**	0.1	DMSO (2)	76	10	3
3	**6.1a**	0	DMSO (2)	60	12	19
4[a.]	**6.1a**	0	DMSO (2)	70	10	13
5[b,c.]	**6.23**	0	DMSO (2)	46	17	2

[a.] *Reaction was performed in the dark. Yield calculated using 1,3,5-trimethoxybenzene as the internal standard in* [1]*H-NMR of the crude mixture.*[b.] *Work done by Estelle Dalichampt (placement student).*[c.] *22% of non-halogenated product was observed by* [1]*H-NMR.*

The experimental results agree with the computational results that the reaction can be initiated in DMSO at room temperature using the DKP **6.2**. However, the reaction also worked efficiently at room temperature without the DKP additive **6.2**. To ensure the benzyne pathway was not responsible for the cyclisation, substrate **6.23** was reacted under the same conditions and the cyclised products **6.24** and **6.25** were

observed, which suggests that SET is occurring in these reactions (Table 6.6, entry 5). High conversion of the starting material was observed, however only low yields of **6.24** (46%) and **6.25** (17%) were formed in the reaction. It was observed that, at room temperature, a large amount of the non-halogenated analogue of the starting material (22%) was observed. This agrees with the previous explanation that the methoxy substituents provide a steric hindrance to the aryl halide, to hinder the formation of cyclised products.

Alternatively the formation of the products **6.3** and **6.4** could arise through an intramolecular SET from the enolate anion moiety to the haloarene moiety in substrate **6.1a**. If the enolate anion moiety in **6.6** donated an electron intramolecularly to the LUMO in the haloaryl moiety the diradical **6.9** (Scheme 6.5) would form upon the loss of an iodide anion. The diradical **6.9** would undergo radical coupling in the cyclisation to form product **6.3**. It is expected that intramolecular SET would be easier than intermolecular SET. Time-dependent DFT (TD-DFT) was firstly used to calculate the UV-vis spectrum for substrate **6.1a** to determine the energy required for an electronic excitation from the HOMO to the LUMO (i.e. from the enolate anion moiety to the C-I σ* orbital) (Scheme 6.5). The UV-vis spectrum suggested that the irradiation energy required to induce an electronic transition from the HOMO of **6.6** into its LUMO had a very high value, $\Delta G^{\ddagger}$ = 94.3 kcal/mol, that is too high to be performed under the thermal reaction conditions employed in this study.

Scheme 6.5 TD-DFT calculations of enolate anion 6.6 in DMSO and the predicted UV-vis trace (black) and the HOMO-LUMO transition (vertical red line).
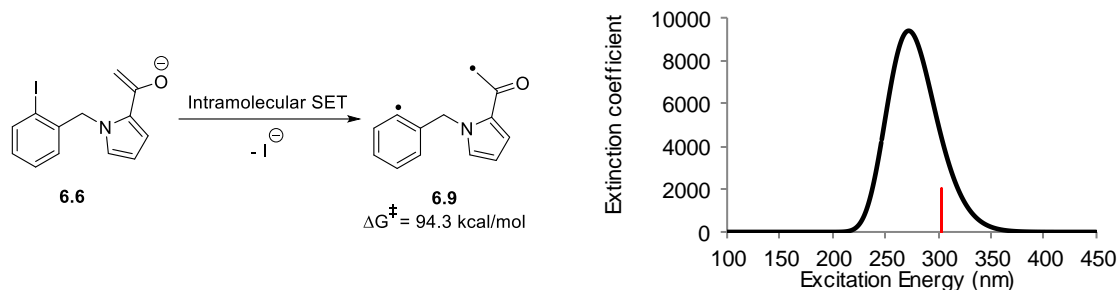
Another method was performed in an attempt to calculate the intramolecular SET process; the Franck-Condon principle was applied to the enolate anion **6.6**. The

Franck-Condon principle states that the electron transfer step is very fast and will occur prior to reorganisation of both the molecule and the solvent. Therefore the energy profile for intramolecular SET were computationally modelled. The first step was the optimisation of the enolate anion **6.6** (prior to SET). With the optimised geometry, a single point energy (SPE) calculation was performed, however the SPE was performed with the charge and multiplicity of the substrate after SET (analogous to **6.31** i.e. an SPE as a triplet anion). This process was repeated for the species after SET, in this example **6.31**. The results calculated using the Franck-Condon method, $\Delta G^{\ddagger} = 66.6$ kcal/mol (DMSO) and 73.3 kcal/mol (benzene), suggest that the intramolecular SET of **6.6** is unlikely to occur in either of the two solvents. These results showed a remarkable difference in the calculated energy profile for the intramolecular SET when compared to the TD-DFT method.
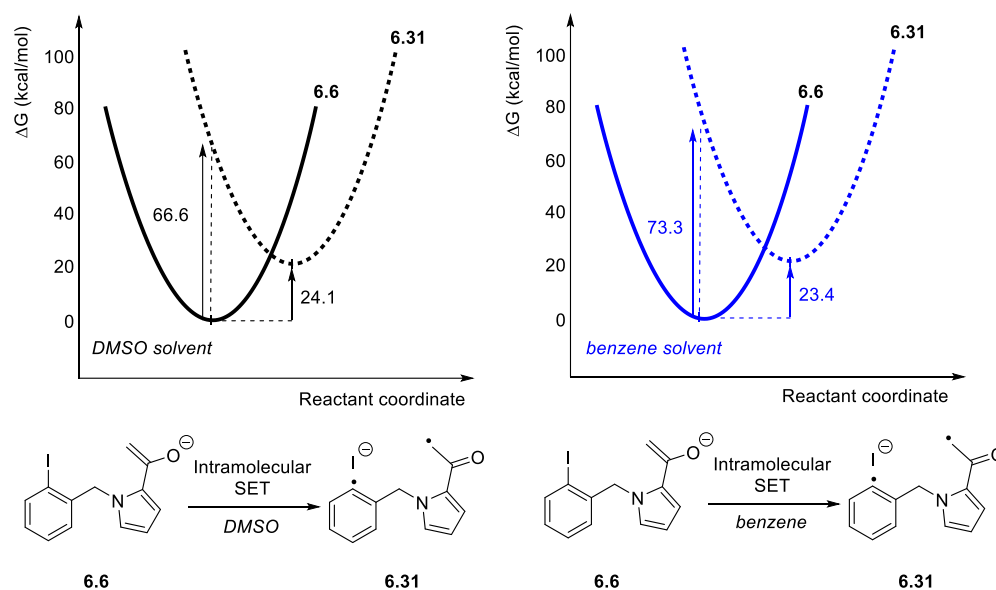
Scheme 6.6 Franck-Condon study of intramolecular SET from **6.6** (black curves are performed using DMSO as the solvent and the blue curves using benzene as the solvent).

From the inconsistent results obtained using either TD-DFT or Franck-Condon method, it suggests that the intramolecular SET for this system cannot be modelled accurately. Since the intramolecular modelling cannot be accurately depicted, then intermolecular SET is the proposed mode of initiation for the rest of the study. It should be noted that future work should be done to attempt to model intramolecular

SET step, and also the intermolecular SET could be modelled using the more accurate method recently developed by Tuttle *et al.* in the attempt to more accurately similar systems.[45]

Through the combination of computational and experimental studies performed on substrate **6.1** it is seen that the cyclisation of substrate **6.1a** occurs through a $S_{RN}1$ mechanism and the mechanism proposed is a revision of a previously proposed mechanism (Scheme 6.7).[85,114] It has been determined that for these cyclisations, the solvent influences the equilibrium for the deprotonation of the substrates, as well as the energetic reaction profile for the SET step. The substrate **6.1a** is predominantly present as the enolate anionic species **6.6** in the presence of KO^{t}Bu. SET to **6.6** from **6.16** (or from another molecule of **6.6**) leads to the formation of the aryl radical **6.8** upon the loss of iodide anion (Scheme 6.7). The radical intermediate **6.8** is capable of either undergoing an $S_{RN}1$ cyclisation of the aryl radical onto the enolate anion, or an aryl-aryl bond formation of the aryl radical onto the pyrrole ring. If the aryl radical **6.8** underwent an intramolecular cyclisation onto its enolate anion *via* an $S_{RN}1$ pathway, the ketyl radical **6.32** would be generated. The $S_{RN}1$ cyclisation of intermediate **6.8**, in both benzene and DMSO, gave comparable Gibbs free energy profiles, with a barrierless cyclisation and exergonic overall relative energies in the formation of **6.32**: ΔG_{rxn} = -42.4 and -41.3 kcal/mol respectively. The aryl-aryl bond formation of the radical **6.8**, whereby the radical attacks the pyrrole ring (which would lead to the formation of **6.4**) instead of the enolate anion, had a greater barrier for cyclisation compared to the barrierless $S_{RN}1$ cyclisation: $\Delta G^{\ddagger}$ = 8.9 kcal/mol and ΔG_{rxn} = -22.3 kcal/mol in DMSO and $\Delta G^{\ddagger}$ = 6.4 kcal/mol in benzene and ΔG_{rxn} = -24.2 kcal/mol. Therefore, in both solvents the cyclisation of **6.8** will proceed *via* the $S_{RN}1$ pathway to form **6.32**. This electron-rich intermediate **6.32** will donate an electron to propagate the cyclisation mechanism, and in doing so the major product **6.3** is formed. Due to the equilibrium for deprotonation of **6.1a** the propagation step is most likely to be a SET to **6.6**, since there is a greater proportion of this species present in the reaction mixture. This was also determined to be the most thermodynamically favoured propagation pathway. However, an electron could be donated to **6.1a** in the propagation step, and this SET has a lower activation barrier

than SET to **6.6**. If the electron is donated to **6.1a** the radical anion **6.33** is formed and aryl radical **6.34** forms on loss of iodide anion. Since there is no enolate anion in **6.34**, the aryl radical will attack the pyrrole ring in the formation of an aryl-aryl bond through the BHAS mechanism to yield **6.4** upon deprotonation and propagation. Therefore, the major pathway leads to product **6.3** and the product **6.4** will form as a minor product, only when propagation occurs to the neutral starting material **6.1a**.
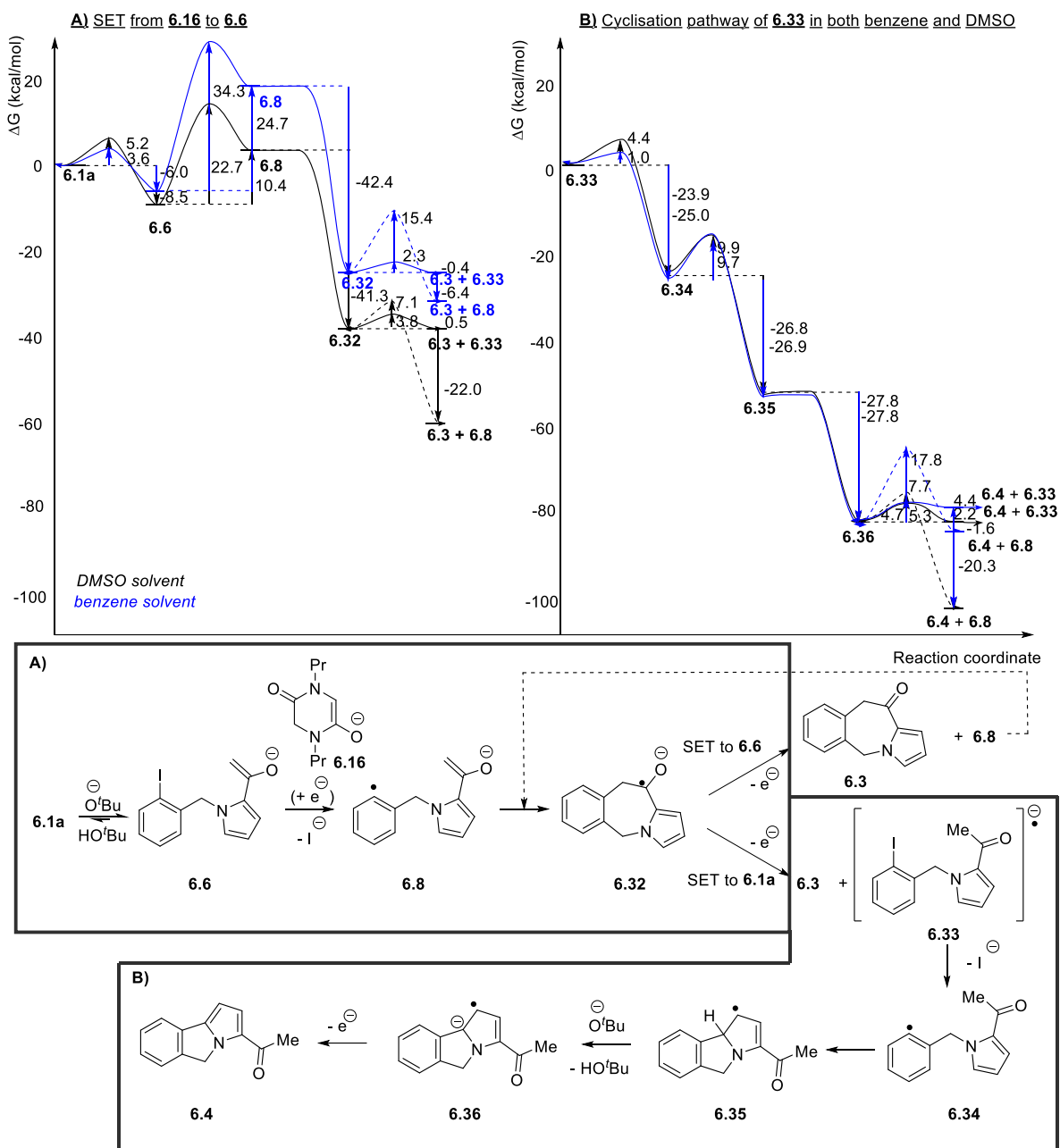
Scheme 6.7 The energy profile for the radical mechanism in the cyclisation of **6.1a**.

6.4 S_{RN}1 cyclisation *vs.* BHAS selectivity

To test the ability of substrates to selectively undergo S_{RN}1 *vs*. BHAS, the substrate **6.37a-b** were synthesised and subjected to the reaction conditions. The products formed were affected by both the solvent and temperature (Table 6.7). Under the thermal activation conditions in benzene, **6.37a** afforded three products in low yields: 1-(phenanthridin-4-yl)ethan-1-one, **6.38** (10%), 1-(phenanthridin-4-yl)ethan-1-ol **6.40** (21%) and the dehalogenated product **6.41** (8%) (Table 6.7, entry 1). This differed markedly from the photoactivated conditions, which afforded solely **6.38** in moderate yields (51%).[85] Surprisingly, when **6.37a** was exposed to the thermal electron transfer conditions in DMSO a completely different product, **6.42**, was isolated in moderate yield (52%) (Table 6.7, entry 2). The product structure was confirmed by X-ray crystallography (Figure 6.1). The formation of **6.42** also occurs in similar yields in the absence of the additive **6.2** (49%) (Table 6.7, entry 3). When **6.37b** was subjected to similar reaction conditions, product **6.42** was isolated in lower yields, showing that changing the halogen to bromine adversely affects the yield (31%) (Table 6.7, entry 4).

Table 6.7 Thermally activated electron transfer reactions of **6.37a-b**.
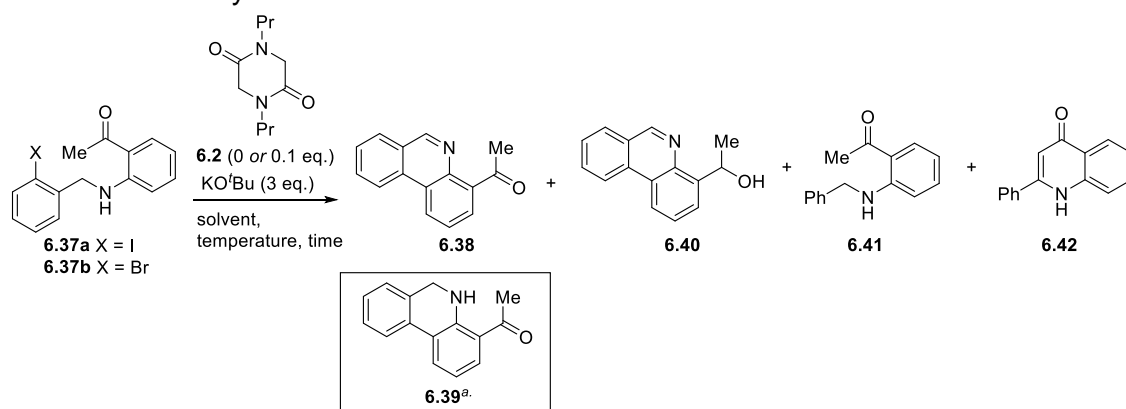
Entry	Substrate	6.2 (eq.)	Solvent (mL)	Temp (°C)	Time (h)	6.38 (%)	6.40 (%)	6.41 (%)	6.42 (%)
1	**6.37a**	0.1	benzene (5)	120	1.5	10[a.]	21	8	0
2	**6.37a**	0.1	DMSO (2)	120	1	0	< 1%	0	52
3	**6.37a**	0	DMSO (2)	120	1	0	0	0	49
4	**6.37b**	0	DMSO (2)	120	16	0	0	0	31

[a.] *The dihydro-analogue* **6.39** *was observed as an inseparable minor component in* **6.38** *but could not be isolated pure (oxidised in air to* **6.38***).*
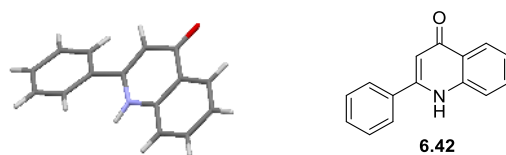
Figure 6.1 The X-ray crystal structure of 2-phenylquinolin-4(1H)-one **6.42** (X-ray crystallographic data in Appendix).
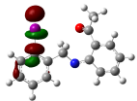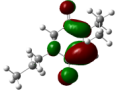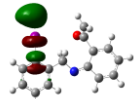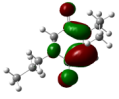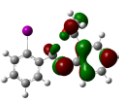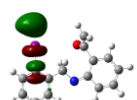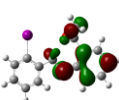
For the deprotonation of substrate **6.37a** by *tert*-butoxide anion, the solvent is playing a key role in differentiating the major species present in the reaction mixture (Scheme 6.8). That is, **6.37a** can potentially form three deprotonated species that may all be present in equilibrium; 1) the enolate anion **6.43**, 2) the *N*-deprotonated species **6.44** and 3) the doubly deprotonated enolate anionic species **6.45**. In benzene, the major species present in the reaction mixture will be the *N*-deprotonated species **6.44**, whereas in DMSO the major species will be doubly deprotonated enolate anionic species **6.45** (Scheme 6.8).
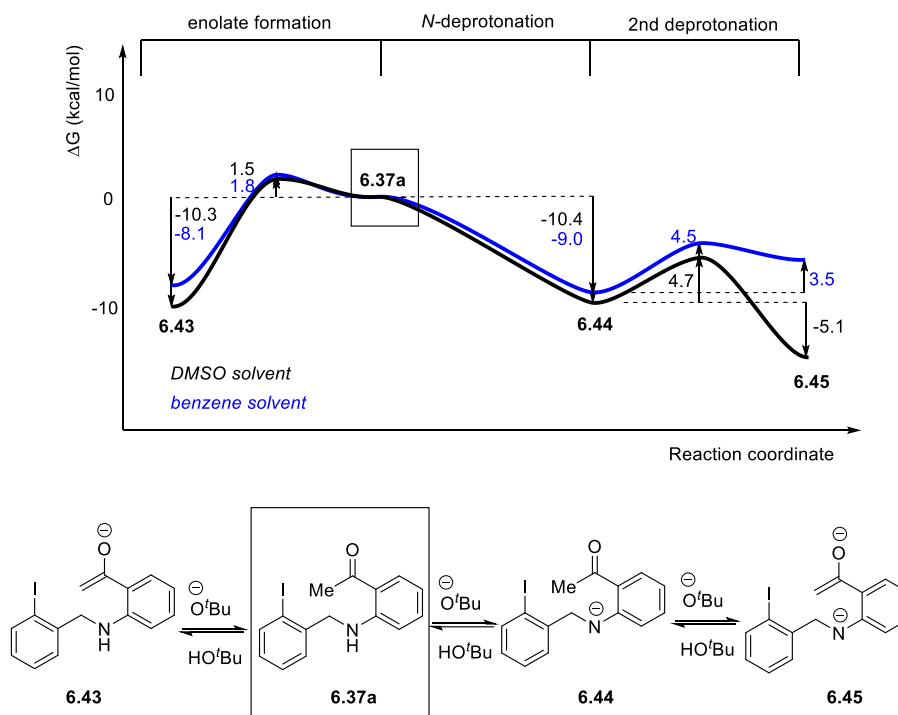
Scheme 6.8 The energy profile for the deprotonation of **6.37a**.

The HOMO and LUMO diagrams of the deprotonated species **6.44** and **6.45** (that will be present in the reactions of **6.37a**) were modelled, and the energy profiles for the SET reactions were determined (Table 6.8). It was observed that the HOMO of the doubly deprotonated species **6.45** (major species in DMSO) resides on the electron rich enolate anion, and based on the results provided so far in this study, it was proposed that **6.45** could itself act as an electron donor. Therefore, the possible electron acceptors present in the reaction could be **6.44** or **6.45**, and the possible electron donors modelled were either the enolate anion of DKP **6.16** or the species **6.45**. The energy profiles for SET follows the same trend as shown for substrate **6.1a**; the SET in benzene has a higher barrier for SET compared to the results in DMSO, and the low barrier for SET in DMSO suggests that the reaction could occur at room temperature. However, interestingly the SET from **6.45** in DMSO was calculated to be easier than SET from the enolate anion of DKP **6.16**, and this suggests that the DKP additive **6.2** is not necessary in the reaction.

Table 6.8 Thermally activated electron transfer reactions of **6.37a-b**.

Electron acceptor (LUMO)	Electron donor (HOMO)	Benzene $\Delta G^{\ddagger}$ / ΔG_{rxn} (kcal/mol)	DMSO $\Delta G^{\ddagger}$ / ΔG_{rxn} (kcal/mol)
6.44	**6.16**	38.7 / 34.3	23.3 / 11.4
6.45	**6.16**	--	22.3 / 13.1
6.44	**6.45**	18.4 / 6.2	20.7 / 10.1
6.45	**6.45**	--	19.8 / 11.8

It was determined that activation of **6.44** by SET, from the enolate anion **6.16** of DKP (or **6.45** in DMSO) forms the radical anion **6.46** upon loss of an iodide anion, and this aryl radical cyclises onto the aromatic system to give **6.48** (Scheme 6.9). Upon deprotonation of **6.48**, **6.49** is produced, which is capable of donating an electron to **6.44** (or **6.45**), to propagate the radical cycle. The pathway for this aryl-aryl bond formation has been calculated in both benzene and DMSO, and it has been determined that both pathways have similar energy profiles for the cyclisation (Scheme 6.9). Upon formation, **6.50** could undergo a hydride elimination to a molecule of *tert*-butanol to form **6.38**, which is driven by a gain in aromatic stabilisation. If **6.38** is already present in the reaction mixture upon the formation of **6.50**, **6.38** and **6.50** will form a complex through π-stacking. Elimination of a hydride anion from **6.50** to **6.38** would yield a new molecule of **6.38** and the alcohol product **6.40** will form upon work-up of intermediate **6.51**. In benzene, the hydride transfer step from **6.50** to **6.38** is endergonic, ΔG_{rxn} = 5.0 kcal/mol, and it has an overall barrier of $\Delta G^{\ddagger}$ = 25.1 kcal/mol. In DMSO, the barrier for the reduction of **6.38** by **6.50** is similar to that in benzene, $\Delta G^{\ddagger}$ = 25.1 kcal/mol and ΔG_{rxn} = -1.0 kcal/mol, so if the reaction is performed at room temperature, the reduction of the ketone in **6.38** is unlikely to occur (Scheme 6.10).[114] Indeed, when substrate **6.37a** was subjected to the reaction conditions at room temperature in DMSO the reduction of product **6.38** (to form **6.40**) was prevented. Although the overall Gibbs free energy profile is similar in both solvents, the relative energies are different. In DMSO, the reduction is exergonic whereas in benzene the reduction is endergonic. Therefore, in benzene, an incomplete conversion of **6.38** to **6.40** may occur, and this was observed previously (Table 6.7, entry 1).

A)

B)

$\Delta G^{\ddagger}$ = 3.9 / *2.9* kcal/mol $\Delta G^{\ddagger}$ = 1.8 / *0.4* kcal/mol $\Delta G^{\ddagger}$ = 4.5 / *3.4* kcal/mol
ΔG_{rxn} = -35.8 / *-36.6* kcal/mol ΔG_{rxn} = -16.8 / *-16.7* kcal/mol ΔG_{rxn} = -29.6 / *-33.3* kcal/mol

$\Delta G_{complexation}$ = 2.5 / *1.2* kcal/mol

$\Delta G^{\ddagger}$ = 25.1 / *25.1* kcal/mol
ΔG_{rxn} = -1.0 / *5.0* kcal/mol
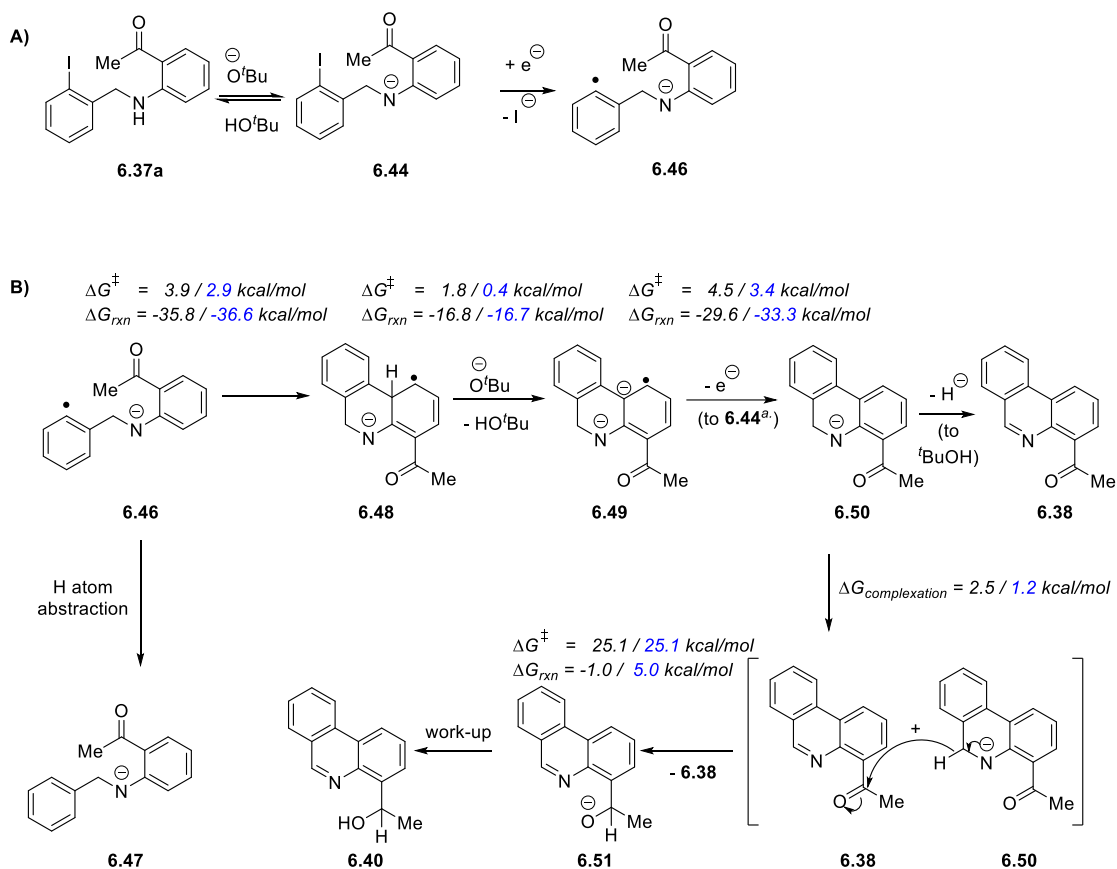
[a.] Propagation to **6.45** was also modelled in DMSO ($\Delta G^{\ddagger}$ = 3.4 kcal/mol and ΔG_{rxn} = -27.9 kcal/mol)

Scheme 6.9 Proposed mechanism and the associated Gibbs free energies for the cyclisation of **6.44**, deprotonated species of substrate **6.37a-b**) in DMSO (*black*) and in benzene (*blue*).
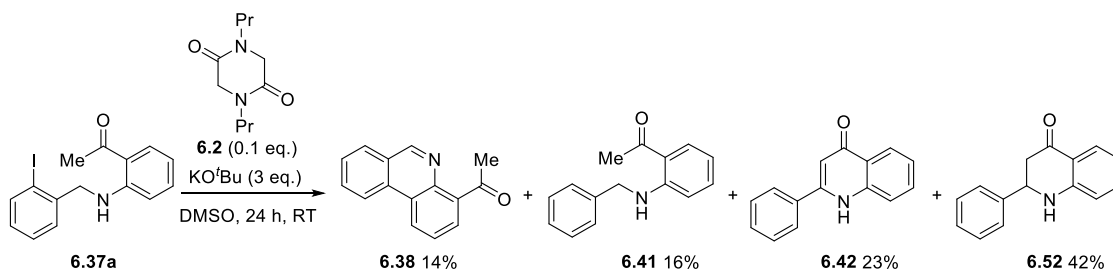
Scheme 6.10 The reaction of **6.37a** at room temperature in DMSO.

The reaction of **6.37a** in DMSO at room temperature generated a mixture of products in low yields, **6.38**, **6.41** and **6.42**, in addition to a new product that formed in moderate yields and was identified as **6.52** (42%). Product **6.52** was only seen at room temperature but its desaturation product, **6.42**, was seen at higher

temperature, 120 °C (as previously shown in Table 6.7, entry 3). The isolation of the product **6.42** at room temperature suggests that **6.52** could be an intermediate in the formation of **6.42**. The major reactive species present in the reaction mixture in DMSO is dianion **6.45**, which was calculated to be capable of donating an electron to **6.44**, with a lower energy barrier than SET from the enolate anion of DKP **6.16**, in the initiation step (Scheme 6.11).
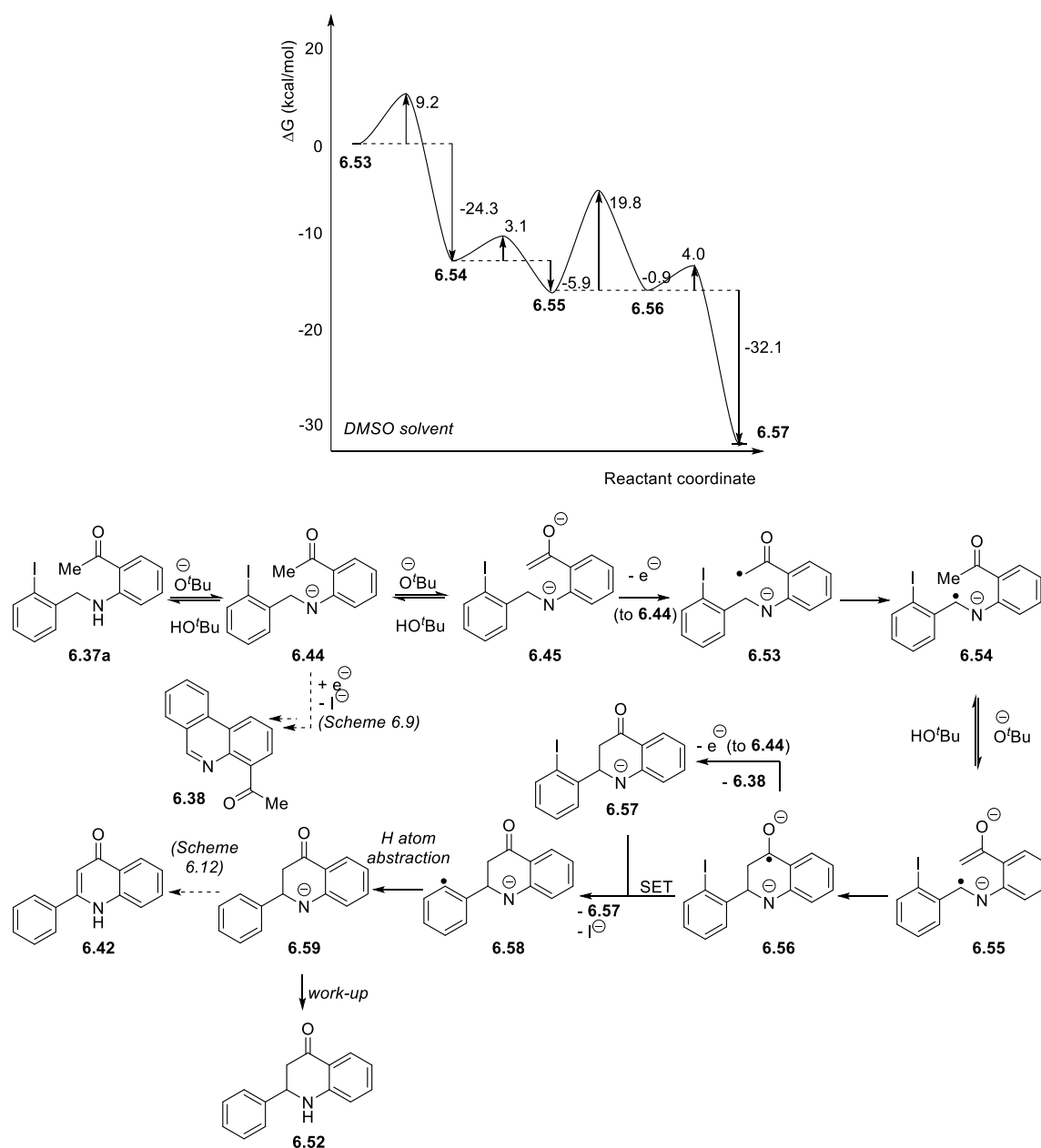
Scheme 6.11 The energy profile to form **6.42** through S$_{RN}$1 cyclisation of **6.53**.

SET from **6.45** gives the intermediate **6.53** which could intramolecularly abstract a hydrogen atom from the benzylic position to yield the more stable radical anionic intermediate **6.54**. The energy change for this hydrogen atom abstraction was exergonic, $\Delta G^{\ddagger}$ = 9.2 kcal/mol and ΔG_{rxn} = - 24.3 kcal/mol. In the basic reaction mixture, an equilibrium will be established between **6.54** and the enolate anion **6.55**. In DMSO, this equilibrium largely favours the enolate anion **6.55**: $\Delta G^{\ddagger}$ = 3.1 kcal/mol and ΔG_{rxn} = - 5.9 kcal/mol. If the enolate anion **6.55** forms, the benzylic radical will undergo an $S_{RN}1$ cyclisation onto the enolate anion to form the cyclised radical dianion **6.56**. This pathway in DMSO has a barrier for cyclisation of $\Delta G^{\ddagger}$ = 19.8 kcal/mol and a relative energy of ΔG_{rxn} = - 0.9 kcal/mol. This means that, in DMSO, the formation of the cyclised product **6.56** is thermodynamically favourable. It was proposed that in DMSO **6.56** could undergo an intramolecular SET in the formation of the intermediate **6.58** but computational studies shows that the intermolecular SET was more energetically favourable. SET from **6.56** (to **6.44**) will yield an anionic intermediate **6.57**. This intermediate can receive an electron (from **6.56**) into the C-I σ^* orbital, to cleave the C-I bond and form an aryl radical intermediate **6.58**. The aryl radical within **6.58** is very reactive and will be quenched in the reaction mixture to form **6.59**.

The intermediate **6.59** could either be protonated in a work-up to form product **6.52**, or it could react further to form **6.42**. Several possible mechanisms to form **6.42** from **6.59** were modelled to determine the most favourable pathway (Scheme 6.12). Computational modelling determined that the formation of **6.42** from **6.59** occurs in two steps (i) a *tert*-butoxide anion will react will **6.59** to form its enolate anion **6.63** and (ii) this enolate anion will undergo a hydride elimination to a molecule of *tert*-butanol, to form **6.42** and hydrogen, and regenerate the *tert*-butoxide anion (Scheme 6.12). Alternatively, this hydride transfer could occur to a molecule of product **6.38** to form **6.40** (as described previously Scheme 6.9). The energy profile for the enolate anion formation and subsequent hydride elimination in the formation of **6.64** from **6.59** is exergonic, ΔG_{rxn} = - 9.7 kcal/mol, with a barrier of $\Delta G^{\ddagger}$ = 21.6 kcal/mol. This energy barrier is the RDS in the reaction pathway, as opposed to the SET step, and it suggests that by lowering the reaction temperature to room temperature this

energetic barrier for the hydride elimination step is harder to overcome. Indeed, when the reaction was performed at room temperature, **6.52** was isolated from the reaction (as previously shown in Scheme 6.10).
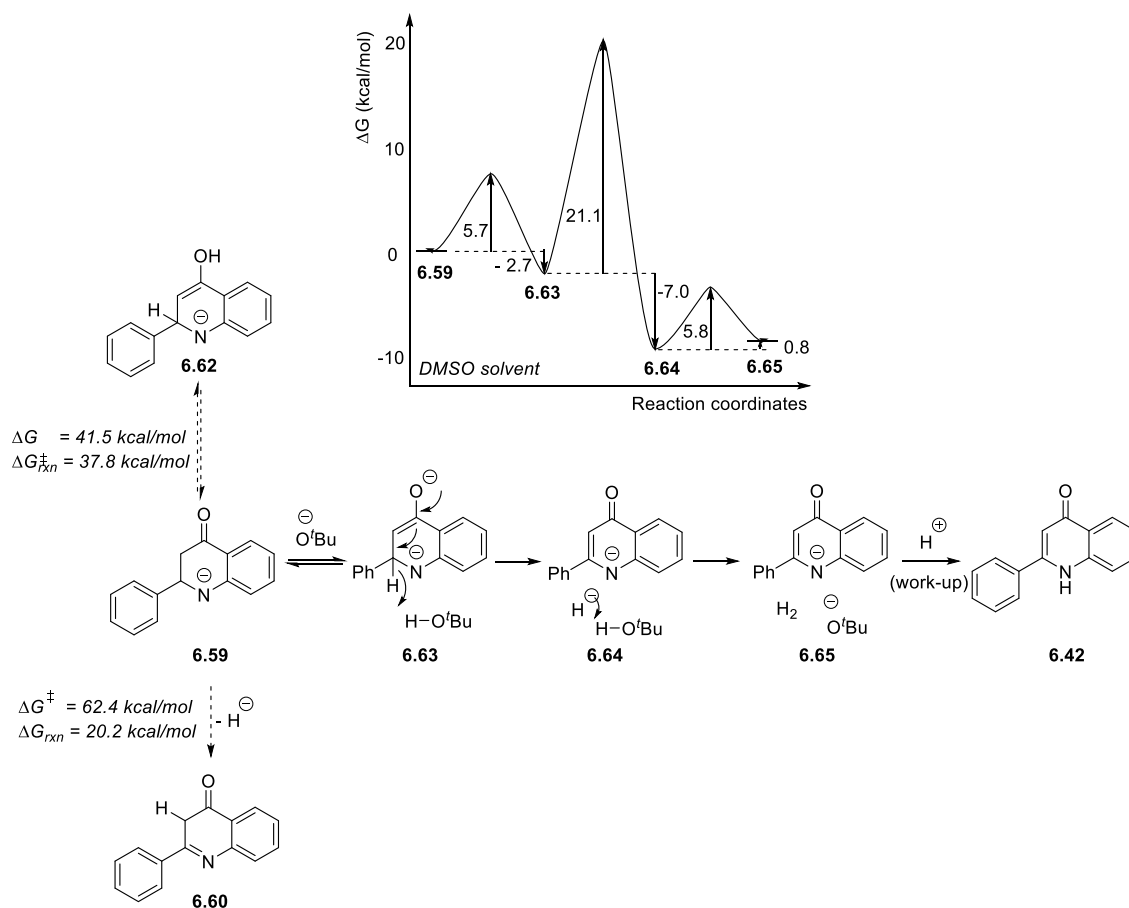
Scheme 6.12 The possible mechanisms to form **6.42** from **6.59**.

Recently, Long *et al.* published an alternative synthesis of analogues of **6.42**, using TEMPO and KO*t*Bu in DMSO, but our route must occur by a different mechanism.[156] The influence of solvent in the cyclisation of **6.37a** is to control which reactive species (**6.44** and **6.45**) is present in the reaction mixture, and because these reactive intermediates react by different pathways, the selectivity of the reaction can be controlled by changing the solvents. In DMSO the reaction will preferentially form **6.42** as the major product, favouring the S$_{RN}$1 cyclisations *via* the doubly deprotonated species **6.45**. However, in benzene, the reaction will selectively favour the BHAS mechanism. In DMSO, because the SET energy barrier can be performed

at room temperature, it has also been shown that the temperature can be altered to dictate product formation: 1) at low temperatures **6.38** will be the major product formed *via* the BHAS mechanism, however increasing that temperature will lead to the formation of **6.40**, 2) by lowering the reaction temperature the intermediate **6.52** was isolated, but increasing the temperature will lead to conversion of **6.52** to give **6.42**.

The formation of **6.42** from intermediate **6.59** (previously shown in Scheme 6.11) is proposed to occur from a hydride elimination to a molecule of *tert*-butanol (Scheme 6.12). Therefore, it was proposed that the formation of **6.59** could also occur through a hydride elimination from the doubly deprotonated species of the substrate **6.37a** to form an imine, analogous to **6.67** (Scheme 6.13A). Therefore, to differentiate whether the reaction was occurring through radical intermediates or an ionic mechanism, the de-halogenated analogue of **6.41** was modelled. The computational energy profile (Scheme 6.13A) shows that the ionic mechanism can occur at high temperatures. The energy profile for the hydride elimination from **6.66** to form **6.68** in DMSO was endergonic, $\Delta G^{\ddagger}$ = 29.0 kcal/mol and ΔG_{rxn} = 23.3 kcal/mol, which would be achievable at the temperatures the reaction is performed at (120 ^{o}C). However, if the reaction was performed at room temperature this ionic pathway to form **6.42** was predicted to be inaccessible. In DMSO at room temperature, only starting material **6.41** was recovered (Scheme 6.13B, condition B), which suggests that at the low temperatures the ionic pathway described is not accessible, as was predicted computationally. A comparison of the results of the reaction of **6.37a** *vs.* **6.41** in DMSO at room temperature shows that the role of the halogen of **6.37a-b** was vital, and without the halogen then the formation of **6.42** does not occur. This suggests that the substrates **6.37a-b** undergoes the SET pathway in DMSO at room temperature. However, if the DMSO reaction mixture is heated, then the ionic pathway could compete in the formation of product **6.42**. The reaction was also performed in benzene at 120 ^{o}C, which showed that the ionic pathway described to form **6.42** through hydride elimination from **6.41** was not possible in benzene (Scheme 6.13C, condition C), and therefore the halogen in the reactions in benzene is vital for the reactivity. The reason the halogen is required for the formation of **6.42**

is because the haloarene moiety of **6.37a**, or its deprotonated forms, is capable of acting as an electron acceptor in the reaction mixture. The doubly deprotonated species of **6.37**, analogous to **6.66**, is capable of donating an electron from the enolate anion moiety into the haloarene C-I σ* orbital, hence this leads to the radical pathways (as previously described Scheme 6.11).
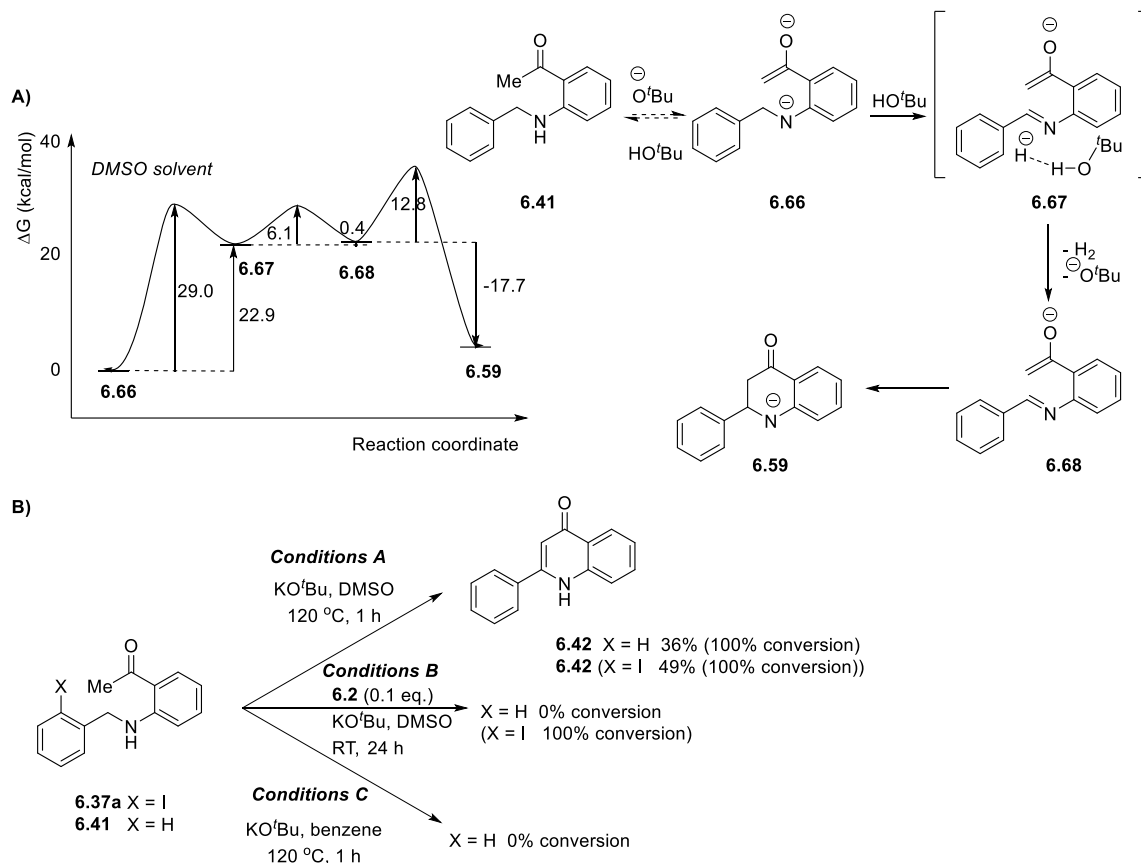
Scheme 6.13A) The proposed ionic mechanism to form intermediate **6.59**. **B)** Experimental evidence of the need for the halogen in the formation of **6.42**.

The aim of the project was to identify whether S_{RN}1 pathways could be selectively achieved in preference to the BHAS mechanism, and it is clear that to achieve S_{RN}1 cyclisations then the enolate anion of the substrates must be present prior to SET. Based on the results presented for substrate **6.37a** it was proposed that if the nitrogen of the tether is protected, in order to prevent the initial nitrogen deprotonation, then deprotonation will selectively form the enolate anion **6.70**, and hence the reaction conditions should favour the S_{RN}1 pathways in preference to the

BHAS mechanism (Scheme 6.14A). Computational analysis was performed to determine the energy profile for deprotonation of **6.69** to form the required enolate anion **6.70** for S_{RN}1 reactivity (Scheme 6.14B-C). The results were that the enolate anion will preferentially exist in the reaction mixture in both DMSO and benzene.
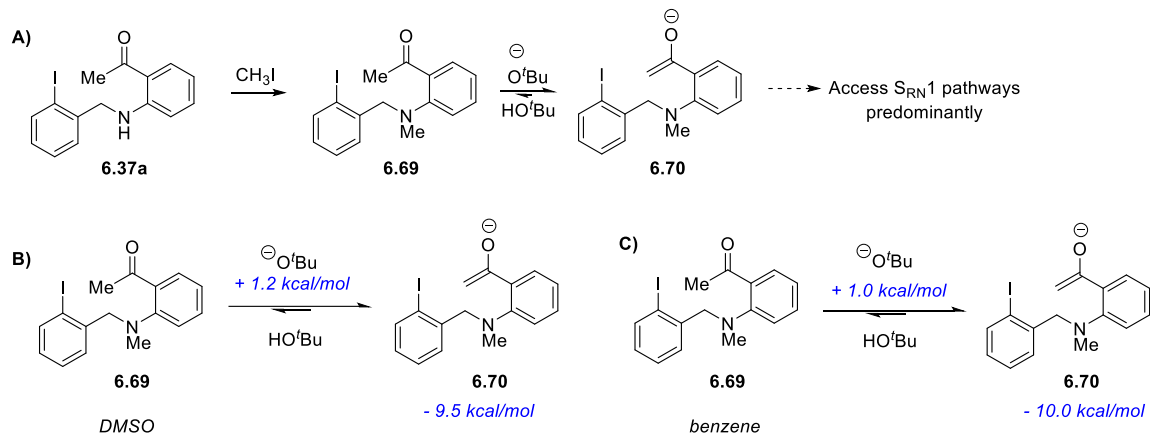
Scheme 6.14A) Proposal to access S_{RN}1 pathways **B)-C)** Energy profile for enolate anion formation **6.70** in both DMSO and benzene ($\Delta G^{\ddagger}$ for the deprotonation is in blue above the reaction arrows, and ΔG_{rxn} is in blue beneath the deprotonated product).

Prior to experimental studies, the energy profile for SET to either **6.69** or **6.70** were modelled (Table 6.9). In both solvents, SET to **6.69** from **6.16** did not achieve C-I cleavage and analysis of the LUMO of **6.69** showed that it resides on the acetyl benzene moiety of **6.69**. Thus SET into **6.69** will form the radical anion **6.71** instead of achieving cleavage of the C-I to form the aryl radical, which is required for S_{RN}1 cyclisations. Due to this result, and the low amounts of **6.69** that will be present in the basic reaction, the energy profile for SET to **6.70** was calculated from the two possible electron donors, the enolate anion of DKP **6.16** or **6.70**. The SET results followed the same trend as was observed for substrate **6.1a**, whereby SET in DMSO has a lower barrier than in benzene, and the barrier is accessible at room temperature in DMSO, but not benzene.

Table 6.9 The energy profile for SET to **6.69** or **6.70**.
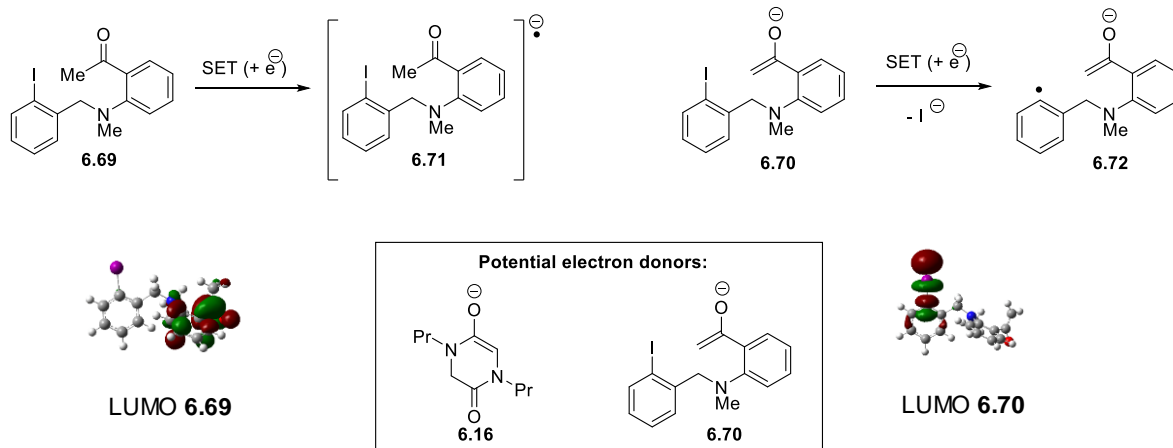
Electron acceptor	Electron donor	Benzene $\Delta G^{\ddagger}$ / ΔG_{rxn} (kcal/mol)	DMSO $\Delta G^{\ddagger}$ / ΔG_{rxn} (kcal/mol)
6.69	**6.16**	27.8 / 27.6	32.3 / 31.1
6.70	**6.16**	31.7 / 23.1	22.3 / 10.8
6.70	**6.70**	43.3 / 40.1	31.0 / 26.5

With the knowledge accumulated thus far, the final substrate tested was substrate **6.69** (Scheme 6.15). When **6.69** was treated with KO*t*Bu and **6.2** in benzene at 120 ᵒC, the two products formed were the tetracycle **6.73** (52%) which was isolated as a novel compound (Figure 6.2), and **6.74**, which was isolated in low yield (9%) (Scheme 6.15, reaction A). When the reaction was performed in DMSO, which was done at room temperature based on SET analysis (Table 6.9), the tetracycle **6.73** was not observed (Scheme 6.15, reaction B). Instead, the products isolated were **6.74**, similar to when the reaction was performed in benzene, **6.75** (which was the only product observed (78%) when the reaction was performed using UV irradiation)[150] and **6.76**.
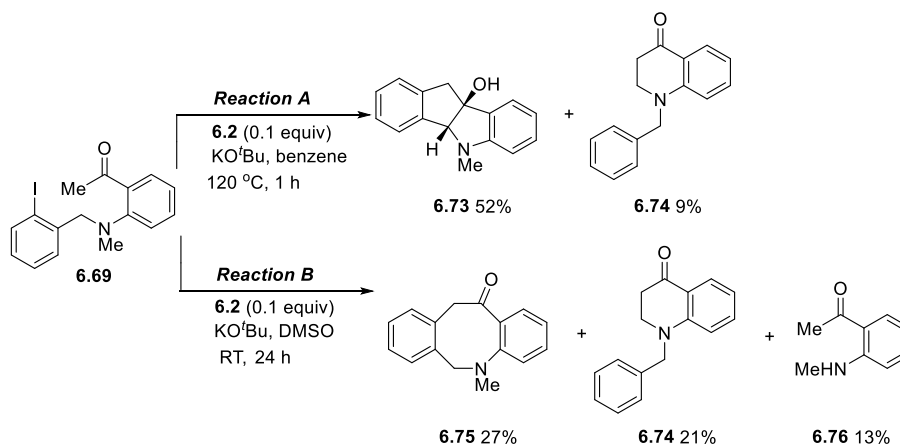
Scheme 6.15 The reaction conditions and products arising from SET to substrate **6.69**.

6.73
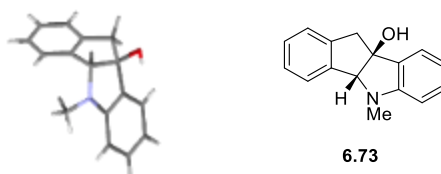
Figure 6.2 The X-ray crystal structure of the (4b*R*,9b*S*)-5-methyl-4b,10-dihydro-indeno[1,2-b]indol-9b(5H)-ol **6.73** (X-ray crystallographic data in the Appendix).

The mechanism proposed in the formation of the products **6.73 – 6.75** involves S$_{RN}$1 steps. Firstly, deprotonation of **6.69**, followed by SET to the enolate anion **6.70** will form the aryl radical intermediate **6.77** that could undergo either an S$_{RN}$1 cyclisation onto its enolate anion to form **6.78**, or it could abstract a hydrogen atom from the methyl group on the nitrogen to form radical **6.81** (Scheme 6.16A). The S$_{RN}$1 cyclisation of **6.77** onto the enolate anion will form the electron-rich intermediate **6.78**, which can donate an electron in a propagation step, to either **6.69** or **6.70**, to form the product **6.75**. The energy profile for this cyclisation is favourable in both solvents (Scheme 6.16B). The product **6.75**, in the presence of a base, could be deprotonated either to form the enolate anion **6.79** or to form the benzylic anion **6.80**. In both solvents the favoured deprotonation is the enolate formation to form **6.79** (Scheme 6.16C); in DMSO the benzylic deprotonation to form **6.80** was endergonic, $\Delta G^{\ddagger}$ = 8.1 kcal/mol and ΔG_{rxn} = 4.9 kcal/mol, however the enolate anion formation to give **6.79** was exergonic, $\Delta G^{\ddagger}$ = 5.0 kcal/mol and ΔG_{rxn} = -1.1 kcal/mol. In benzene,

the deprotonation of the benzylic position to form **6.80** is exergonic, $\Delta G^{\ddagger}$ = 2.2 kcal/mol and ΔG_{rxn} = -2.3 kcal/mol, and has a similar energy profile to the formation of the enolate anion **6.79**, $\Delta G^{\ddagger}$ = 2.2 kcal/mol and ΔG_{rxn} = -3.6 kcal/mol, which demonstrates that in benzene the two species **6.79** and **6.80** will be in equilibrium, and when intermediate **6.80** forms. The benzylic anion can ionically attack the carbonyl group, $\Delta G^{\ddagger}$ = 1.1 kcal/mol and ΔG_{rxn} = - 18.2 kcal/mol, to form **6.73** upon work-up (Scheme 6.16C). Therefore, if the reaction is performed in DMSO, the product **6.75** is formed, but in benzene the product formed will be **6.73**.
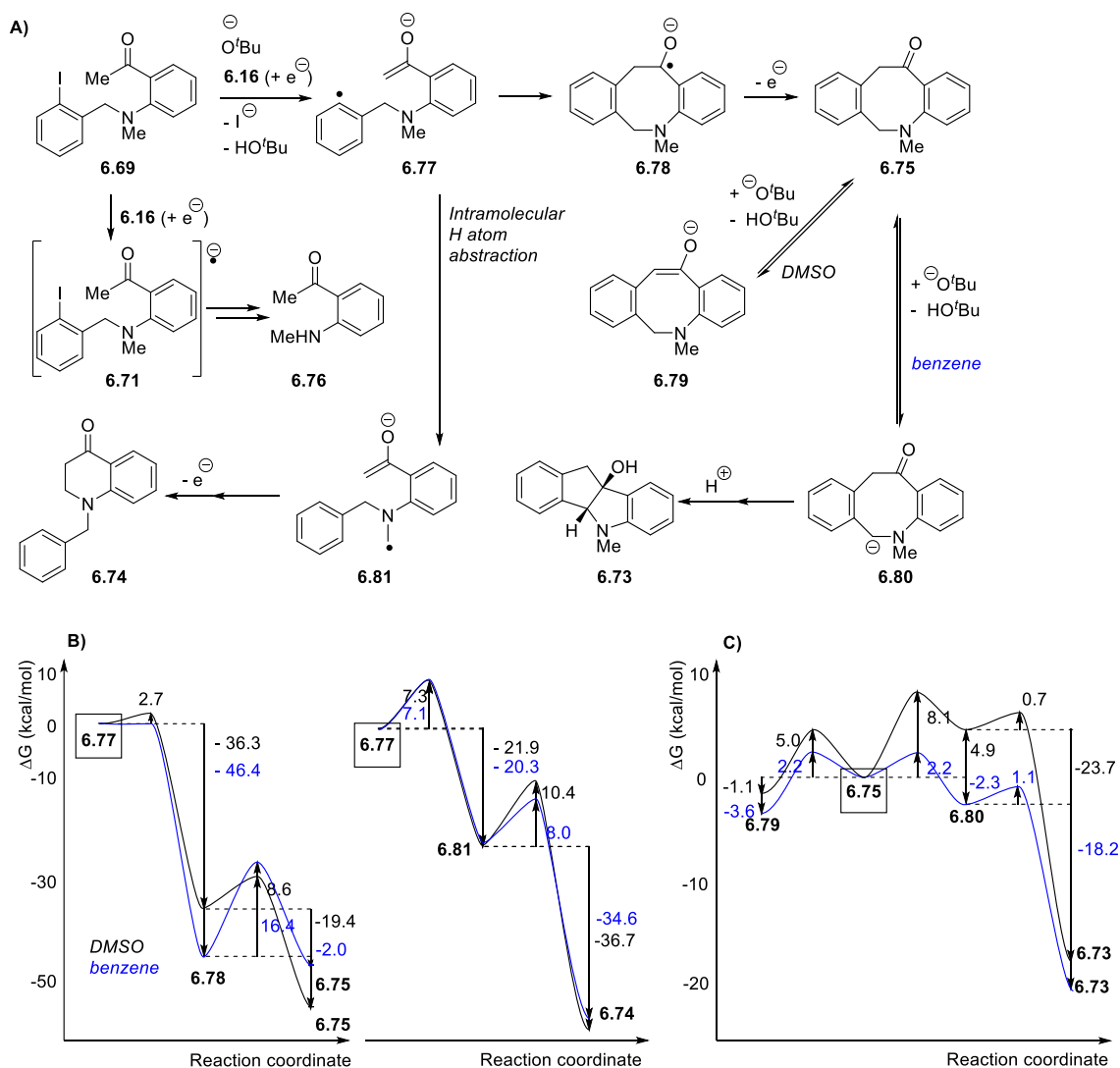
Scheme 6.16A) The proposed mechanisms in the cyclisation of **6.69**. **B)** The computational energy profile for the possible mechanisms of **6.77** and the **C)** deprotonation of **6.75** (benzene solvent – blue line; DMSO – black line).

The reaction in DMSO can occur at room temperature due to the low energetic barrier associated with the SET initiation step for **6.70**, but in benzene it requires high temperatures to achieve SET. The high temperatures employed when benzene is the solvent will establish the thermodynamically more stable product **6.73**, which was experimentally proven when a sample of **6.75** was heated in base in benzene, and the product **6.73** (31%) was formed (Scheme 6.17). It should be noted that this low yield of product **6.73** is likely a concentration effect because the sample was diluted due to the small amount of available material **6.75** (diluted from 0.21 M to 0.042 M). In both solvents the minor pathway from **6.77** is a hydrogen atom abstraction from the methyl protecting group on the nitrogen to form the more stable methyl radical **6.81**, and ultimately **6.74** upon intramolecular $S_{RN}1$ cyclisation of the radical onto the enolate anion and the subsequent propagation step (Scheme 6.16).
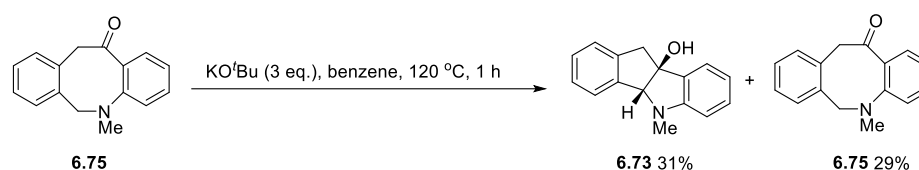
Scheme 6.17 The formation of **6.73** from **6.75**.

An interesting observation during this study is that in the propagation step, SET from **6.78** can occur either to the enolate anion **6.70** or to the neutral species **6.69**. The LUMO for the neutral species **6.69** resides on the acetophenone moiety so if SET occurs to the neutral species the radical anion **6.71** forms, which can undergo C-N fragmentation to form the radical **6.83** and the anionic species **6.84**, which forms **6.76** upon work-up (Scheme 6.18). This pathway will be a minor pathway due to the low population of **6.69** that will be present in the basic reaction mixture. The energy profile for SET into substrate **6.69** from **6.16** in the initiation step of this reaction are too high, $\Delta G^{\ddagger} = 27.8$ kcal/mol and $\Delta G_{rxn} = 27.6$ kcal/mol in benzene, and $\Delta G^{\ddagger} = 32.3$ kcal/mol and $\Delta G_{rxn} = 31.1$ kcal/mol in DMSO (Table 6.9). But, if an electron is donated to **6.69** in the chain propagation step, from the electron-rich intermediate **6.78**, the energy profile for SET is much more accessible, $\Delta G^{\ddagger} = 6.2$ kcal/mol and $\Delta G_{rxn} = 2.6$ kcal/mol in benzene and $\Delta G^{\ddagger} = 6.3$ kcal/mol and $\Delta G_{rxn} = 0.9$ kcal/mol in DMSO (Scheme 6.18). However, in both solvents, the intermediate **6.78** is more

thermodynamically favourable to donate an electron to the enolate anion **6.70**, instead of **6.69** because the SET step would be exergonic, as opposed to endergonic with **6.69** (Scheme 6.18). The isolation of **6.76** in DMSO and not in benzene cannot be explained from these calculations and more work is required to understand this step to allow it to be used for future applications. Similar C-N cleavage reactions have recently been observed using powerful organic electron donors,[122] but this is the first observation of such reactions under KO*t*Bu-facilitated coupling conditions.
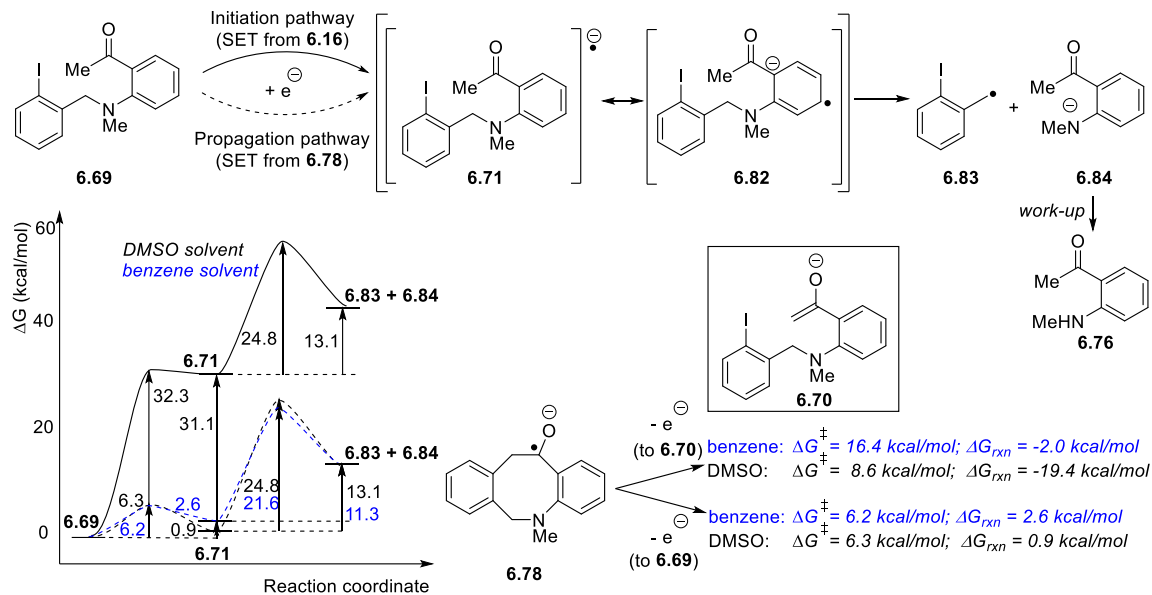
Scheme 6.18 The energy profile for the SET to **6.69** of the initiation *vs.* propagation steps to form **6.76** (the protonated product of **6.84**) (benzene solvent – blue; DMSO – black).

The study presented in this chapter has highlighted the opportunities that the transition metal-free reaction conditions have in expanding their application towards alternative bond transformations that occur through the activation of a C-X bond (X = halogen). Although S$_{RN}$1 reactions are commonly reported using light irradiation, it has been shown that they can efficiently occur in the ground state, and sometimes the products formed are different than the products of photoactivation. Using a combination of computational and experimental studies, the mechanisms for the reactions have been thoroughly investigated to gain a deeper understanding of the pathways involved. This knowledge will hopefully be applicable in the future to identify new bond formations that could be achieved using the ground state transition

metal-free reaction conditions, which until recently have been predominantly used for aryl-aryl bond formations.

6.5 Future work

Within this chapter the transition metal-free reaction conditions have been employed to achieve S$_{RN}$1 cyclisations, in addition to the BHAS cyclisations for which these conditions are best recognised. It has been shown that the product distribution of some of these reactions can be changed by choosing a different solvent (replacing benzene with DMSO), or by changing reaction temperatures. With all this generated mechanistic detail on these possible reaction pathways, it would be interesting to use this knowledge to further expand the utility of these reactions. For example, S$_{RN}$1 cyclisations were targeted by protecting a secondary amine on a tether in substrate **6.69** to favour the enolate anion formation. This knowledge can be used to identify an appropriate protecting group, to replace the methyl protection, so that analogues of the 8-membered cyclised product **6.75** or the fused cyclic system **6.73**, can be made, with alternative functionalities incorporated onto the nitrogen. If there was more time dedicated to this project, it would also be desirable to use experiments to further provide proof of the mechanisms proposed.

A very interesting part of this study was the observation of C-N bond cleavage with these reaction conditions. However, mechanistic studies showed the limitation of C-N bond cleavage is the SET to the neutral species, which is only achievable in the propagation step. However, if a similar electron donor to **6.78** could be generated *in situ* then it would be interesting to investigate the C-N bond cleavages, either as a proof of concept, or in the hope to find stronger electron donors that could potentially be applied to activation of more difficult substrates, such as aryl chlorides.

7.

Studying the Tollens' test

7.1 Introduction

In Chapter 4 it was observed that the enolate anion of the DKP additive was capable of donating electrons to haloarenes under the transition metal-free reaction conditions. Glucose was introduced in Section 1.4.2 when Kumar *et al.*[91] showed that it could even be used as an additive to couple aryl halides to arenes using transition metal-free reaction conditions, albeit in low yields (8%). This suggests that glucose can form an electron donor species under the transition metal-free reaction conditions, similar to DKP (Chapter 4). Therefore, it was interesting to further investigate the role of glucose as an electron donor. One application where glucose is known to be capable of donating an electron is in the reduction of silver(I) cations in the Tollens' test. The Tollens' test is used to qualitatively identify the presence of reducing sugars, such as glucose, or to distinguish between aldehydes and ketones. The Tollens' reagent is a basic reaction mixture containing ammoniacal silver nitrate, which forms the diamminesilver cation, $[Ag(NH_3)_2]^+$, in the presence of ammonia. This silver complex can be reduced by aldehydes and reducing sugars in the basic reaction mixture, and in doing so silver mirror forms, thus giving a positive result for Tollens' test.[157-159]

7.2 Glucose as an additive for transition metal-free aryl-aryl bond formations

Using the knowledge reported for the formation of electron donors *in situ*, from the combination of organic additives and KO*t*Bu, the role of glucose as an electron donor in the transition metal-free reaction conditions was investigated, and analogies were made between glucose and the DKP additive (Chapter 4). In water, glucose **7.1** exists in equilibrium with the ene-diol **7.2** (Scheme 7.1), and this ene-diol contains an electron-rich double-bond that bears resemblance to the electron donor that forms *in situ* from the DKP additive (described in Section 4.3). Therefore, it was proposed that glucose could be used as an additive to couple 4-iodotoluene **7.6** with benzene, in the presence of KO*t*Bu (Table 7.1).
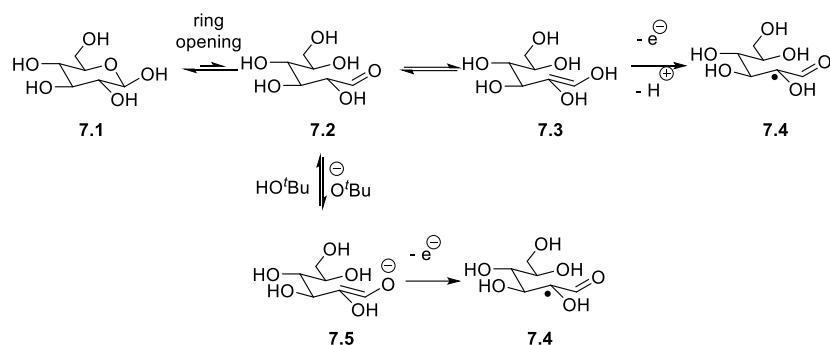
Scheme 7.1 A proposal for the role of glucose **7.1** as an electron donor.

Table 7.1 The coupling of 4-iodotoluene **7.6** with benzene, using a combination of glucose **7.1** and KO^{t}Bu.
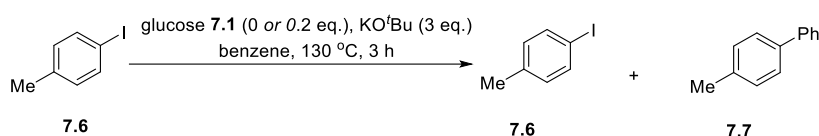
Entry	glucose **7.1** (eq.)	**7.6** (%)	**7.7** (%)
1	0	79	3
2	0.2	52	34

[a.] *Yield calculated using 1,3,5-trimethoxybenzene as the internal standard in ^{1}H-NMR of the crude mixture.*

When 4-iodotoluene **7.6** was reacted in the presence of KO^{t}Bu and glucose **7.1**, at 130 ℃, coupling between 4-iodotoluene and benzene was observed, affording 34% yield of **7.7** (Table 7.1, entry 2). In the absence of glucose, only 3% product **7.7** was observed (Table 7.1, entry 1). This suggests that under these reaction conditions, glucose forms some electron donor species that is capable of donating an electron to 4-iodotoluene **7.6** to initiate the transition metal-free coupling reaction. Based on the knowledge currently within this thesis (Chapter 4) and the literature,[40,42-44] it is proposed that in the presence of KO^{t}Bu, the ring-opened structure of glucose will be deprotonated to form its enolate anion, **7.5**. The electron-rich double-bond within **7.5** could donate an electron to 4-iodotoluene **7.6**, to initiate the transition metal-free aryl-aryl bond formation (Scheme 7.1).

7.3 Tollens' test

7.3.1 Qualitative study

The Tollens' reagent, diamminesilver cation $[Ag(NH_3)_2]^+$, has been historically used to identify the presence of reducing sugars, such as glucose **7.1**, or to differentiate between aldehydes and ketones. Prasad *et al.*[160] proposed that the mechanism for the reduction of the Tollens' reagent by aldehydes involves a hydrate formation from the aldehyde. They proposed that the hydrate **7.9** reduces silver ions to give elemental silver, Ag(0), and ultimately the carboxylic acid **7.12** (Scheme 7.2A). Hughes *et al.*[158] observed that the rate of silver mirror formation is increased in alkali solutions (pH > 10), and they therefore modified the mechanism for the reduction of the Tollens' reagent (Scheme 7.2B). They proposed that the hydrate **7.9** is deprotonated in the basic reaction mixture to form **7.13**, which then interacts with silver ions to form the silver complex **7.14**. Upon the reduction of Ag(I) to elemental silver, the carboxylic acid **7.12** is formed. More recently, the "silver mirror" test was modified into a catalytic method, and the mechanism reported by Li *et al.*[161] contains key features that resemble the two mechanisms previously described (Scheme 7.2C). Firstly, the silver catalyst employed interacts with the aldehyde to form the complex **7.16**, and a hydroxide anion is transferred from the catalyst to the aldehyde to form the complex **7.17**, which resembles the hydrate species **7.9** and **7.14**. An elimination of IPr-Ag-H forms the carboxylic acid **7.12**, and the IPr-Ag-H is oxidised in air to regenerate the active silver catalyst, IPr-Ag-OH. It is not just aldehydes that can reduce silver ions, to form a silver mirror as a positive in the Tollens' test. Ketoses, such as fructose, are also capable of reducing the Tollens' reagent, even though they do not possess an aldehyde moiety (Scheme 7.2D). It is proposed that in the reaction mixture, ketoses and related substrates, **7.19**, could undergo tautomerism to form the ene-diol, such as **7.20**, which can rearrange to form **7.21** and the resulting aldehyde is capable of reducing the Tollens' reagent as previously proposed (Scheme 7.2A-B).[157] At this point, based on the accumulated knowledge of electron donors that can be formed *in situ* from within this thesis and within the literature, it should be noted that the ene-diol **7.20** contains an electron-rich double-bond, and thus may be capable of reducing the Tollens' reagent directly.[163]
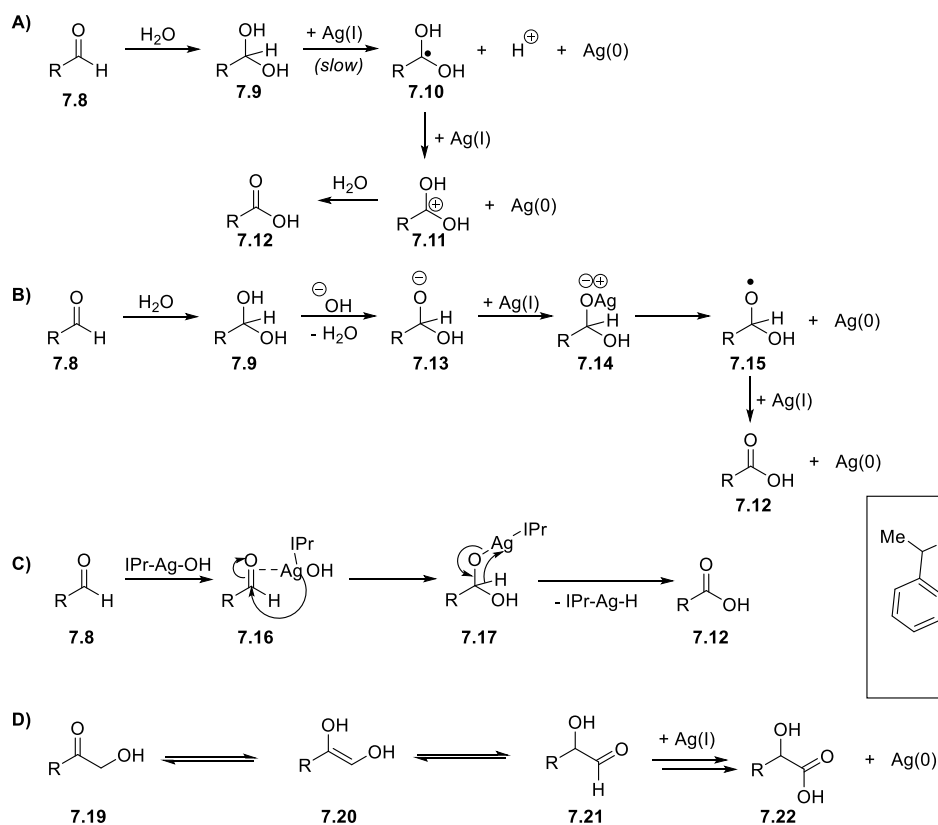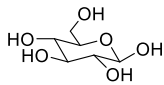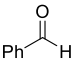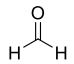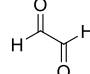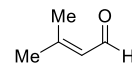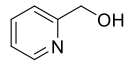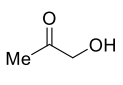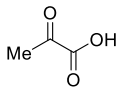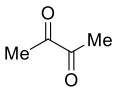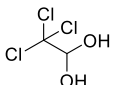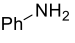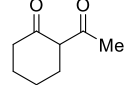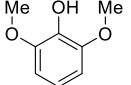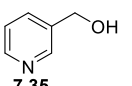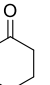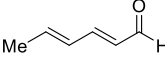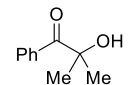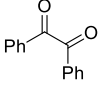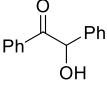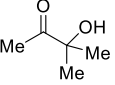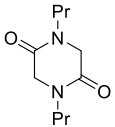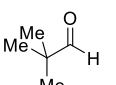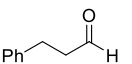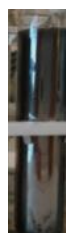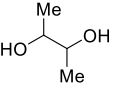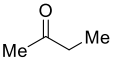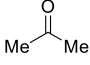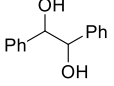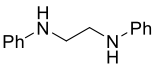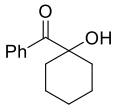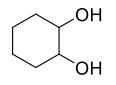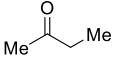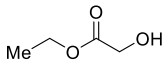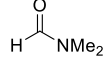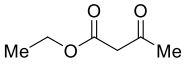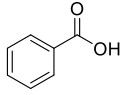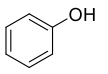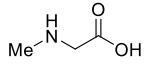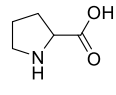
Scheme 7.2 The initial mechanisms proposed for the reduction of Tollens' reagent by aldehydes **7.8** and acetol **7.19**.[158,160-162]

Interestingly, it is reported that other substrates such as phenols,[163] anilines[164] and some ketones, are capable of reducing silver cations in the preparation of silver nanoparticles, therefore it was proposed that these species may also give a positive Tollens' test. To investigate more about what compounds could form electron donors *in situ* that will reduce Tollens' reagent, the initial study undertaken was to expose a broad range of substrates to the Tollens' reagent and report the observed results. The idea was to try and identify common functionalities amongst the substrates tested that may hint to the possible electron donors that will form *in situ* (Scheme 7.3). However, at this point it is important to clarify what constitutes a positive Tollens' test before progressing.

The Tollens' test is often referred to as the "silver mirror" test, because reducing the Tollens' reagent, diamminesilver cation [Ag(NH3)2]+, leads to the formation of elemental silver, Ag(0), which can deposit on the side of the test tube to give a silver

161

reflective surface, i.e. a silver mirror.[159] However, the reduction of Tollens' reagent may not always lead to the formation of a silver mirror. In the preparation of silver nanoparticles, silver ions, such as Tollens' reagent, are reduced to elemental silver in the presence of stabilising additives, such as oleic acid.[165] As Ag(0) forms it agglomerates in solution to form silver aggregates, and the action of oleic acid is to stabilise the silver aggregate to make silver nanoparticles, of varying sizes, instead of a silver mirror (while, without oleic acid, a silver mirror is observed).[165] A positive Tollens' test, which is the reduction of the diamminesilver cation $[Ag(NH_3)_2]^+$ to elemental silver, must therefore take into account both substrates that produce silver mirrors, but also substrates that are capable of forming silver colloidal particles, like nanoparticles. Therefore, within this study, if either a silver mirror or a partial silver mirror was observed, it was recorded as a positive Tollens' test. The partial silver mirror consists of the formation of a small bit of a silver mirror; however, the majority of the silver was in the form of a black precipitate (Scheme 7.3). The black precipitate is colloidal silver metal, which suggests that the silver(0) deposits formed rapidly and agglomerated or the silver(0) aggregates formed from reduction of Tollens' reagent are stabilised by the reducing agent in the reaction mixture. Upon observing the possible molecules that gave positive Tollens' tests, a few proposals can be made as to how the substrates form electron donors in the basic reaction mixture. From the qualitative study (Scheme 7.3) it became clear early on that there are many simple, commercially available, organic molecules that are capable of reducing Tollens' reagent. The results of the study were classified into three categories: (1) the formation of a silver mirror, (2) the formation of a partial mirror and (3) no colour change.

RT	70 °C	
	--	**Silver mirror at room temperature** 7.1, 7.23, 7.24, 7.25, 7.26, 7.27, 7.28, 7.29, 7.30, 7.31
		Partial silver mirror at room temperature; silver mirror at 70 °C 7.32, 7.33, 7.34, 7.35, 7.36, 7.37, 7.38, 7.39, 7.40, 7.41, 7.42, 7.43, 7.44
		No change at room temperature; partial silver mirror at 70 °C 7.45, 7.46, 7.47, 7.48, 7.49, 7.50, 7.51
		No change at room temperature or 70 °C

Scheme 7.3 A qualitative study of the compounds capable of reducing Tollens' reagent.

Aldehydes, such as **7.44**, could form hydrates, **7.52** or **7.53**, in the reaction mixture as proposed in the literature (Scheme 7.4A, and previously shown in Scheme 7.2A-B).[158,160] Alternatively, if the aldehyde can form its enolate anion, such as **7.57**, then this could act as an electron donor, which is analogous to the DKP additive (previously described in Chapter 4). Ketones could also form the enolate anions, or

the hydrate in competition. Interestingly, some of the compounds reported to give positive silver mirrors, such as 2-pyridyl carbinol **7.27** and *N,N'-*dipropyldiketopiperazine **7.42** are compounds that are additives used to promote aryl-aryl bond formation in the transition metal-free reaction conditions. The diamine **7.49** and diols, such as **7.45**, **7.48** and **7.51**, could form structures as reported by Murphy *et al*. (Scheme 7.4B-D). The DKP additive has also been discussed extensively in this thesis to form enolate anion in basic mixtures, which can perform SET. An interesting observation was that all the α-hydroxy ketones tested gave a positive Tollens' test, including tertiary α-hydroxy ketones, such as **7.38**, **7.41** and **7.50** (when heated). This was an important observation since the mechanism proposed in the literature for reduction of Tollens' reagent by α-hydroxy ketones involved the formation of an "ene-diol" species **7.20** (previously shown in Scheme 7.2D),[163] which is not possible for these substrates. Since these tertiary α-hydroxy ketones are capable of reducing Tollens' reagent, it was interesting to gain more mechanistic insight into the reaction pathway because as of yet no mechanism is reported that explains this observation.
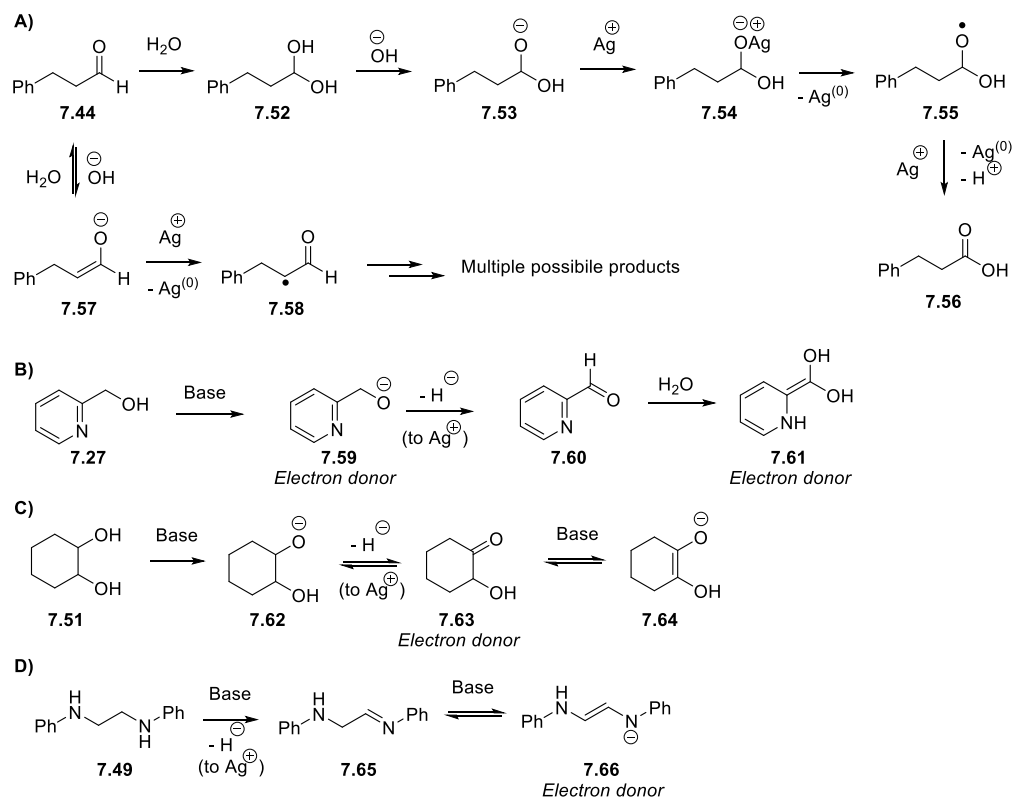
Scheme 7.4 The possible electron donors formed from **A)** aldehydes, **B)** 2-pyridyl carbinol, **C)** diols and **D)** diamines as proposed by Murphy *et al.*[40,42]

7.3.2 Mechanistic investigation into reaction of aldehydes in Tollens' test

It is commonly reported that the products arising from Tollens' test are carboxylic acids resulting from the oxidation of aldehydes.[158,161,166] Therefore, the first substrates to be analysed in this quantitative study were aldehydes (Scheme 7.5).
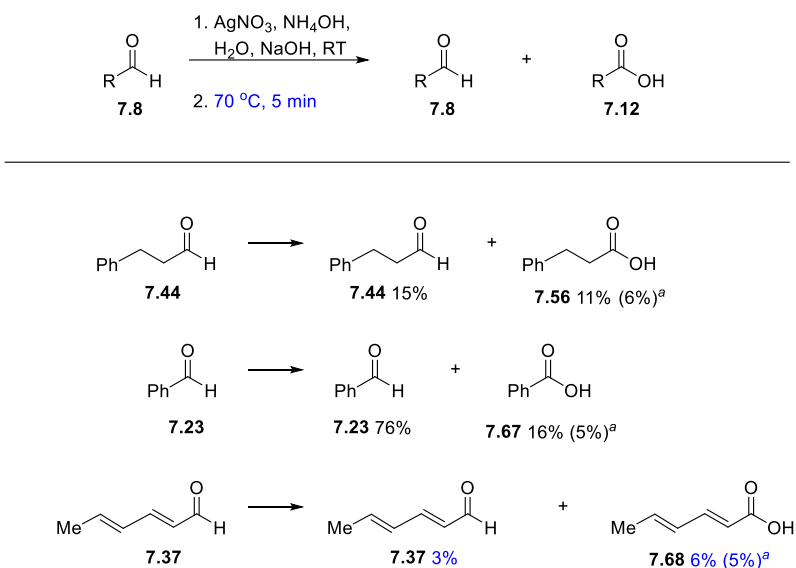
a. Yields determined using 1,3,5-trimethoxybenzene as an internal standard in the ^{1}H-NMR spectrum. Isolated yields are in brackets.

Scheme 7.5 Isolation of carboxylic acids from exposing aldehydes to Tollens' reagent.

When the aldehydes **7.44**, **7.23** and **7.37** were exposed to Tollens' reagent, low yields of their respective acids, **7.56** (11%), **7.67** (16%) and **7.68** (6%) were formed. Although the yields of products are very low, it must be remembered that the Tollens' test is only a qualitative study and high yields of oxidised product are not required for the formation of the silver mirror or particles in the reaction. The mechanism for the oxidation of aldehydes using Tollens' reagent, proposed within the literature, involves the initial formation of a hydrate (as previously shown in Scheme 7.2 and 7.4).[158,160] The hydroxide anion is capable of increasing the rate of the oxidation of aldehydes,[158] and therefore, to confirm the proposed reaction mechanism within the

literature, 3-phenylpropanal **7.44** was exposed to various reaction conditions (Table 7.2).

Table 7.2 The oxidation of 3-phenylpropanal **7.44** with Tollens' reagent.
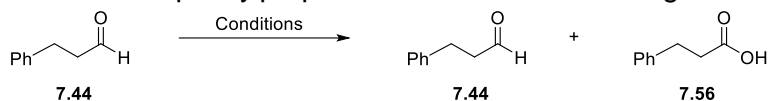
Entry[a.]	AgNO$_3$ (eq.)	Reagents	Temperature (^{o}C)	Silver Mirror?	Recovered **7.44** (%)	Product **7.56** (%)
1.	1	NH$_4$OH, NaOH	25	Yes	15	11 (6)[b.]
2	0	NH$_4$OH, NaOH	25	No	20	2
3	1	NH$_4$OH, NaOH	70	Yes	6	12
4	--	work-up of **7.44**	--	No	92	0

[a.]*Reactions were performed simultaneously using 1.5 mmol substrate.* [b.]*The yield in parentheses is the isolated yield.*

The 3-phenylpropanal **7.44** was exposed to Tollens' reagent at RT, and the oxidation of the aldehyde occurred to yield phenylpropanoic acid **7.56** (11%) (Table 7.2, entry 1). Simultaneously, an analogous reaction was performed in the absence of the AgNO$_3$, and a lower yield of **7.56** (2%) was achieved (Table 7.2, entry 2). When a reaction was performed analogous to entry 1, but with heating (at 70 ^{o}C for 5 minutes), a similar yield of **7.56** (12%) was observed (Table 7.2, entry 3). Finally, the 3-phenylpropanal **7.44** was left in water at room temperature for the same reaction time as entries 1-2, and upon work-up the 3-phenylpropanal **7.44** (92%) was observed as the only product (Table 7.2, entry 4). These results show that the oxidation of 3-phenylpropanal **7.44** by Tollens' reagent occurs as efficiently at room temperature, as it does at 70 ^{o}C. It also shows that, in the absence of the silver in solution, a little formation of **7.56** occurs in the presence of the basic reaction medium; however, in the absence of silver, a neutral solution returned the starting material **7.44**, and no oxidation of the aldehyde was observed. The formation of **7.56** in the absence of silver cations, may occur because in the basic reaction mixture the aldehyde **7.44** could form its hydrate, and atmospheric oxygen could abstract the hydrogen atom to yield the carboxylic acid product. Deducing the possible

166

mechanism or electron donors for these reactions is very complex because the aldehydes could undergo alternative reactions, such as aldol reaction between two molecules of **7.44** to form other species capable of being electron donors in the reaction mixture. Therefore, the study changed to focus on the interesting observations of the α-hydroxy ketones.

7.3.3 Mechanistic insight into reaction of α-hydroxy ketones in Tollens' test

The substrates of interest in this study were the α-hydroxy ketones. Fructose **7.69** is an aldehyde, however it gives a positive Tollens' test. The mechanism proposed for the reduction of Ag(I) by fructose is that fructose **7.69** will ring-open to form the straight-chain isomer **7.70**, which, in the presence of base, will form the ene-diol **7.72**, and ultimately glucose **7.73**, which reduces Tollens' reagent (Scheme 7.6).[157,162]

7.69 **7.70** **7.71** **7.72** **7.73**
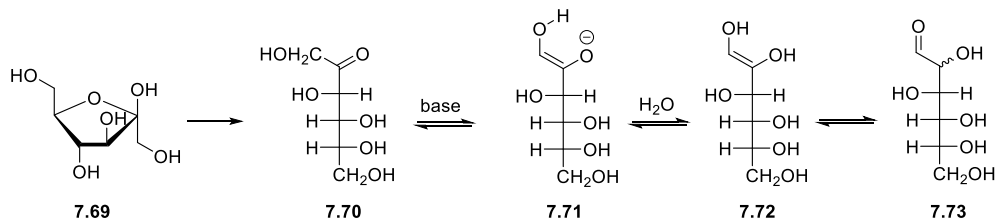
Scheme 7.6 The Lobry de Bruyn-van Ekenstein transformation of fructose to glucose **7.1**.[163]

This mechanism (Scheme 7.6) is used to explain why α-hydroxy ketones produce the positive Tollens test. However, in the qualitative tests previously performed in Section 7.3.1, the tertiary α-hydroxy ketones, such as **7.38**, **7.41** and **7.50**, which are not capable of undergoing the Lobry de Bruyn-van Ekenstein transformation, also gave a positive result for the Tollens' test (Scheme 7.7). Since there are no reports of experimental investigations into the mechanism for the reaction of these α-hydroxy ketones and Tollens' reagent, it would be interesting to investigate the possible products formed in this reaction and hopefully this will give insight into the mechanism involved.
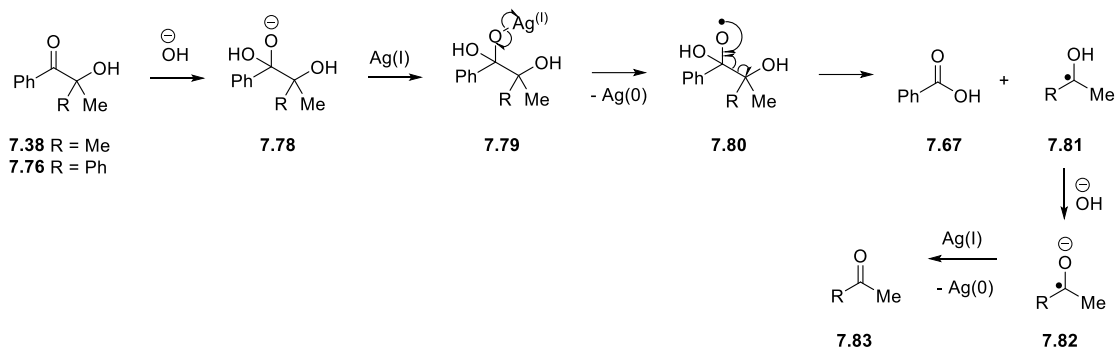
Scheme 7.7 Isolation of products from exposing α-hydroxy ketones or α-diketones to Tollens' reagent.
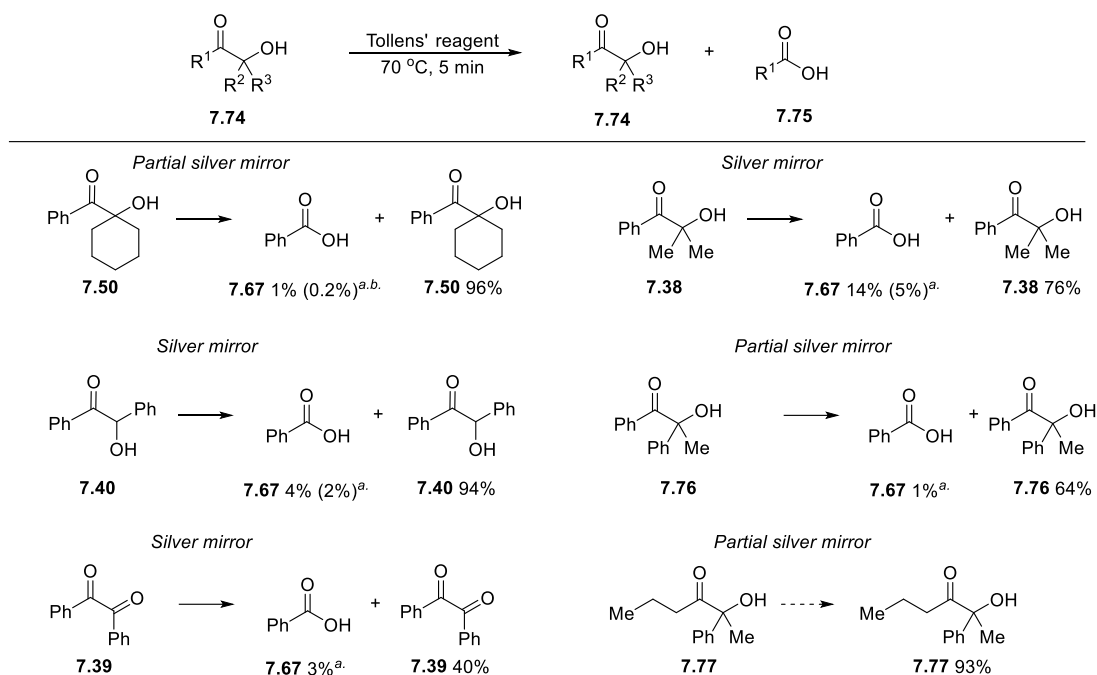
a. Isolated yield in brackets. Otherwise the yields were determined using 1,3,5-trimethoxybenzene as the internal standard in the ¹H-NMR. Partial silver mirror formed. *b.* Conducted on large scale of 7.5 mmol scale. *c.* Inseparable products, detected by reference NMRs.

Benzil **7.39** and several α-hydroxy ketones were exposed to Tollens' reagent, and all of the substrates tested gave a partial silver mirror when heated at 70 °C for 5 min (Scheme 7.7). For the substrates that contain the ketone adjacent to the phenyl group **7.50**, **7.40**, **7.39**, **7.38** and **7.76**, the oxidised product isolated from the reaction was always benzoic acid **7.67**, albeit in low yields. When substrate **7.77** was exposed to Tollens' reagent, no oxidised products were detected. The formation of benzoic acid from **7.50**, **7.40**, **7.39**, **7.38** and **7.76** suggests that Tollens' reagent is capable of performing oxidative C-C bond cleavage on these substrates. The lack of the formation of benzoic acid **7.67**, or any oxidised products, from **7.77** suggests either that the products formed in very low amounts to be undetectable, or that the oxidised products were not isolatable. Due to the lack of evidence, a conclusive decision about the possible mechanism for the reaction of substrate **7.77** could not be

proposed. However, a mechanism has been proposed for the α-cleavage of the other substrates, using **7.38** and **7.76** as representative substrates (Scheme 7.8).


Scheme 7.8 Isolation of products from exposing α-hydroxy ketones to Tollens' reagent.

In the basic reaction mixture of Tollens' reagent, the hydroxide will react with the substrate **7.38** to form **7.78**. This mechanism is similar to that which is proposed for the oxidation of aldehydes by Tollens' reagent (previously shown in Scheme 7.2A-B).[158,160] The intermediate **7.78** donates an electron to Ag(I) in the reaction mixture, to form elemental silver, Ag(0), and the radical intermediate **7.80**. This radical intermediate may undergo C-C cleavage to form benzoic acid **7.67** and the radical intermediate **7.81**. In the basic reaction mixture, deprotonation of **7.81** forms the radical anion **7.82**. The radical anion is electron-rich and could donate an electron to another free silver cation to form the ketone **7.83**. Unfortunately, due to the low yields of the oxidative C-C cleavage none of the ketone products were detected.

Within the literature it is proposed that the concentration of NaOH affects the rate of the oxidation of the aldehyde.[158] When substrate **7.38** was first exposed to Tollens' reagent, diamminesilver cation [Ag(NH₃)₂]⁺, 14% of benzoic acid **7.67** was formed (previously shown in Scheme 7.7). It was therefore interesting to investigate the effect of NaOH on the oxidation of the α-hydroxy ketones and the formation of benzoic acid **7.67** (Scheme 7.9). To prepare Tollens' reagent, AgNO₃ in dissolved in ultrapure water, and to this solution, aqueous NH₄OH is added dropwise until a brown suspension (silver(I) oxide, Ag₂O) is observed. Further addition of aqueous NH₄OH to the solution gives the diamminesilver cation [Ag(NH₃)₂]⁺ as a colourless solution. Then aqueous NaOH is added to the solution, followed by more aqueous

NH₄OH to reform the diamminesilver cation and give Tollens' reagent. This last step is not necessary however, because the active silver complex in Tollens' reagent is the diamminesilver cation, which is formed prior to aqueous NaOH addition, and therefore aqueous NaOH can be omitted from the reaction (Scheme 7.9A).
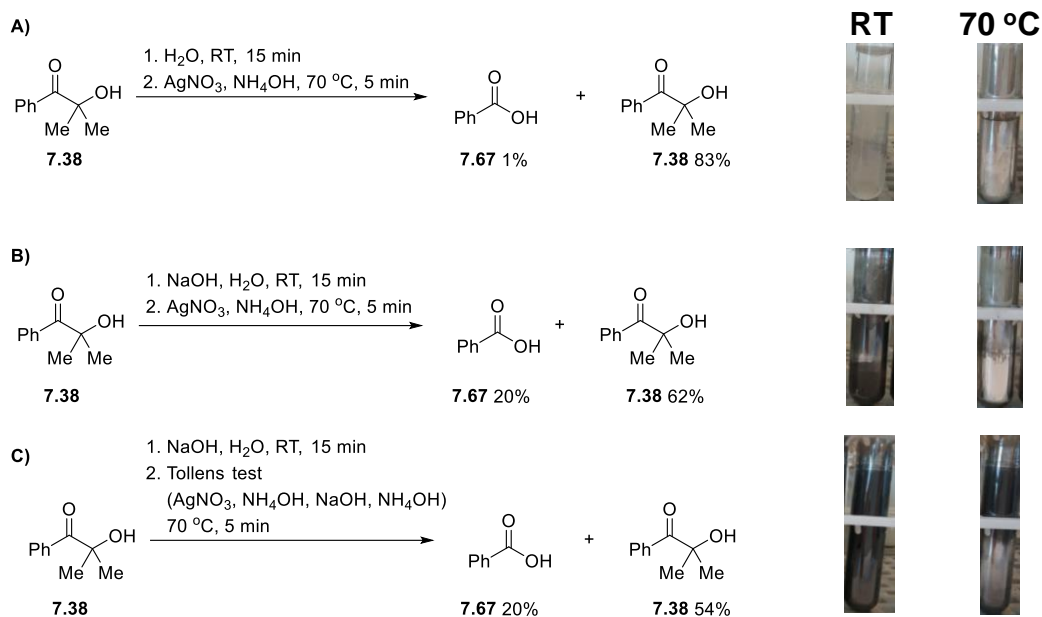

Scheme 7.9 Effect of NaOH on the oxidation of **7.38** by Ag(I).

In the absence of NaOH only 1% of the benzoic acid **7.67** was formed, and the silver mirror was only seen upon heating of the reaction mixture. The yield of benzoic acid formed is significantly higher when NaOH is added to Tollens' reagent (previously shown in Scheme 7.7, 14%). The next reaction performed used the same solution of diamminesilver cation (without NaOH added), however prior to the addition of the substrate to this solution, substrate **7.38** was stirred at RT for 15 min in the presence of NaOH (Scheme 7.9B). The yield of benzoic acid achieved (20%) was higher than seen in both reactions without NaOH (1%), and the reaction with the normal Tollens' reagent (14%). The final test was to expose **7.38** to aqueous NaOH for 15 min before adding the solution to Tollens' reagent (Scheme 7.9C). The yield of benzoic acid in this latter reaction was also 20%. These results suggest that reduction of the diamminesilver cation by substrate **7.38** is facilitated by the presence of NaOH (in Scheme 7.9A, the hydroxide is present in the aqueous NH₄OH solution). The

assumption that the rate of oxidation of the substrate **7.38** is increased by increasing the concentration of hydroxide is supported within the literature.[158]

The mechanism proposed within this study for the reduction of Tollens' reagent by tertiary α-hydroxy ketones (as previously shown in Scheme 7.8) involves the formation of the hydrate of the ketone, by hydroxide attack. The hydrate reduces Ag(I) and the corresponding radical formed undergoes radical C-C bond cleavage to form the carboxylic acid and a radical species of the hydroxyl moiety, which will ultimately form a ketone. However, there was no evidence for the formation of the ketone to support this mechanism. Therefore, a new tertiary α-hydroxy ketone was designed and synthesised, with the aim that, upon oxidative C-C bond cleavage, the products formed will be easily isolated and identified. The substrate **7.86** was synthesised and, when exposed to the Tollens' test, the oxidised product **7.87** was isolated (Scheme 7.10). The formation of product **7.87** supports the mechanism proposed that the oxidative C-C cleavage results in the formation of both the carboxylic acid, by oxidation of the ketone moiety, and the corresponding ketone, by the oxidation of the α-hydroxy functionality.
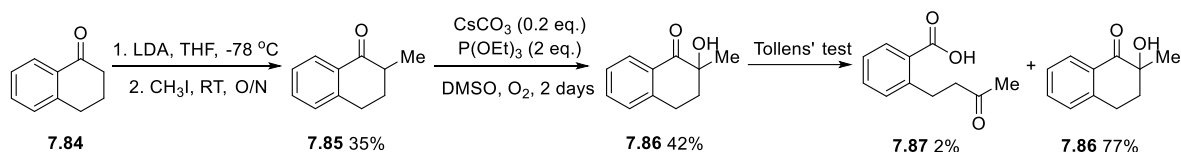

Scheme 7.10 The formation of substrate **7.84** and its product formed in the Tollens' test.

Recently, a homogenous catalyst was reported for the aerobic oxidation of aldehydes to carboxylic acids in water. Many aldehydes were efficiently converted to their respective acids through this more efficient "silver mirror" reaction under the conditions reported.[161] The reaction conditions involve an Ag(I)/bipy catalyst and molecular oxygen, in the absence of hydroxide anions. It is therefore interesting to apply these reaction conditions to investigate whether they are capable of performing oxidative C-C cleavage of α-hydroxy ketones, like in Tollens' reaction (Scheme 7.11).

171
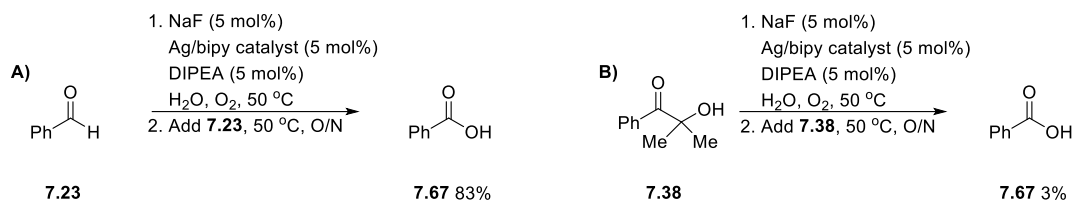
Scheme 7. 11 The reaction of benzaldehyde **7.13** and α-hydroxy ketones **7.38** with Ag/bipy catalyst.[161]

Indeed, when benzaldehyde **7.23** was exposed to these reaction conditions, it was efficiently oxidised to benzoic acid **7.67** (83%). However, when α-hydroxy ketone **7.38** was treated under the same reaction conditions, the C-C cleavage to form **7.67** was very low yielding. This suggests that even in the presence of oxygen overnight, the oxidation of the α-hydroxy ketones is not efficient in these conditions and it is lacking a strong base, NaOH, for higher yields (Tollens' conditions afforded 14% yield of benzoic acid, Scheme 7.7). However, the formation of benzoic acid **7.67** suggests that other mechanisms are possible in the C-C cleavage. One possibility is that the molecular oxygen abstracts the hydrogen from the hydroxyl moiety in **7.38**, which may be favoured if silver is complexed to the carbonyl oxygen, such as **7.88** (Scheme 7.12) and the resulting alkoxyl radical **7.89** would fragment. However, this is just a proposed mechanistic pathway and no evidence has been sought to probe it. The complexity of these mechanisms is shown in the studies by Li *et al.*[161] This study has highlighted the possibility of multiple reaction pathways that form electron donors, which can reduce Tollens' reagent, and these mechanisms are substrate-dependent.
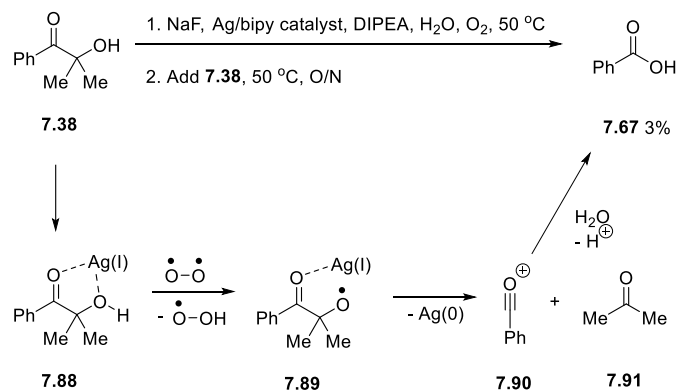
Scheme 7.12 The possible mechanism to achieve C-C bond cleavage of **7.38** in the presence of Ag/bipy and O$_2$.

Therefore, it can be concluded that one of the possible mechanisms for the Tollens' reaction of α-hydroxy ketones that are not capable of forming enolate anions (Scheme 7.8) proceeds similarly to the mechanism reported for the oxidation of aldehydes by Tollens' reagent.[158,160]

7.4 Future work

A broad range of possible substrates have been identified that are capable of donating electrons to Tollens' reagent, and clues to the mechanism have been found. It would be interesting to synthesise a molecule that is analogous to an aldose, such as glucose, to identify what products are generated. Many substrates are capable of reducing silver in these reaction conditions, and this knowledge could be applied to the synthesis of silver nanoparticle, either alone or with the addition of a stabilising agent.

It has been shown that glucose can be used to promote these transition metal-free reaction conditions, and therefore this opens the possibility of using simple sugars to achieve similar transformations, such as the S$_{RN}$1 cyclisations reported in Chapter 6. In the Tollens' test, the SET occurs in water; therefore it would be interesting to investigate whether these substrates, such as sugars, could be used to achieve aqueous transition metal-free coupling reactions. However, much more work is required to achieve this.

8.

Conclusions

The description of the experimental work in this thesis began in Chapter 4 with an investigation into the possible electron donor formed from the combination of *N,N'-*dipropyldiketopiperazine (DKP) and KO*t*Bu. Recent publications proposed that an electron donor is formed *in situ* from the reaction between the base and the organic additive used in the transition metal-free reaction conditions. Continuing the work that Murphy *et al.* have made in the identification of the possible electron donors, Chapter 4 described the design and synthesis of an analogue of the DKP additive **8.1** that contained a tether on the core framework of the DKP, with the sole aim to act as a radical probe (Scheme 8.1). It was proposed that if the enolate anion **8.2** donated an electron then the resulting radical **8.3** could be trapped to provide evidence for the existence of single electron transfer, and the formation and isolation of product **8.4** was observed to this end. The role of DMF **8.5** in transition metal-free reactions to activate aryl halides was also investigated, and more efficient additives, **8.9** and **8.10**, were designed for the transition metal-free coupling reactions (Scheme 8.1).
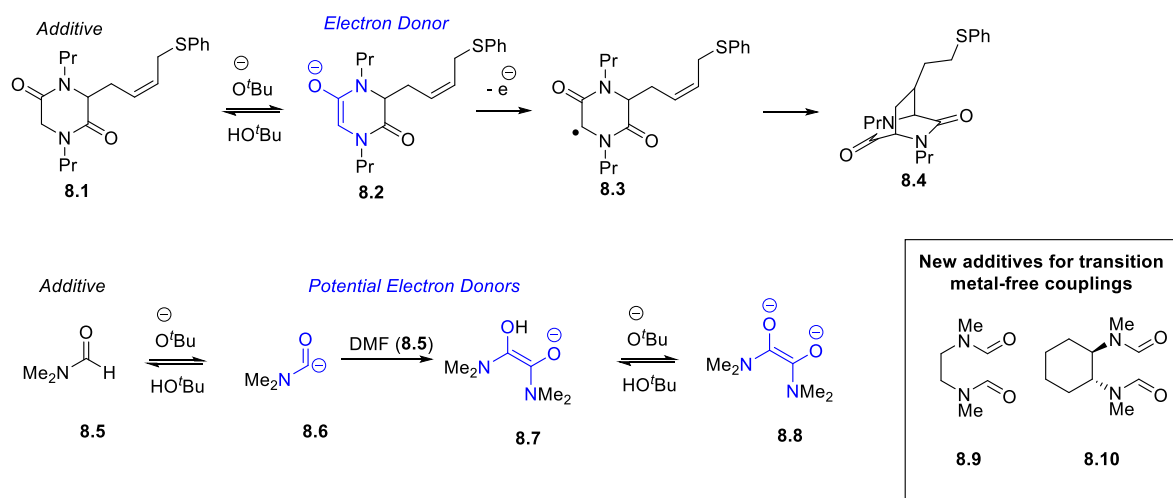
Scheme 8.1 Evidence for SET from the enolate anion of DKP additive **8.1**, and the proposed electron donors formed *in situ* from DMF **8.5**.

Chapter 5 described the efforts made to identify evidence of SET from KO*t*Bu. Unfortunately the initial experiments to trap the possible products of fragmentation of alkoxyl radicals were fruitless. However, these initial studies led to a study

performed using KO*t*Bu and CBr4. It was proposed that KO*t*Bu could donate an electron to a species where the reduction potential was close to the oxidation potential of KO*t*Bu, and therefore CBr4 was chosen as the electron acceptor. The preliminary results showed that KO*t*Bu and CBr4 led to bromination of adamantane, and hence gave initial thoughts that SET from KO*t*Bu was occurring. However, further experiments and computational analysis provided evidence that SET from KO*t*Bu to CBr4 was not possible but that another mechanism was leading to bromination. KO*t*Bu reacts with CBr4 to form the hypobromite, and this undergoes a homolysis to form two reactive radical species capable of initiating the bromination of adamantane (Scheme 8.2).
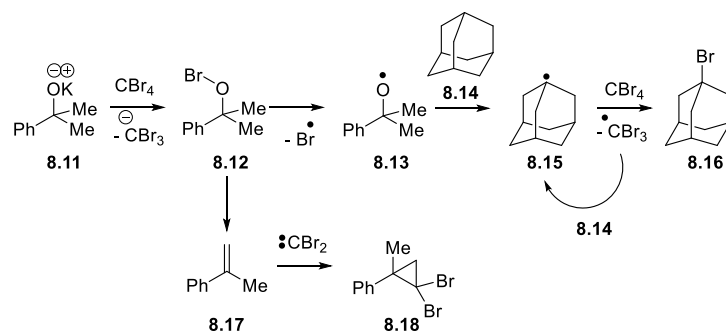
Scheme 8.2 The modified mechanism for the halogenation of adamantane **8.14** from the combination of KO*t*Bu and CBr4, *via* hypobromite intermediates.

The results presented in Chapter 6 expand the reaction scope for these transition metal-free reaction conditions and show that S$_{RN}$1 reactions of substrates such as **8.19** are possible (Scheme 8.3). Through computational analysis and experimental work, the mechanisms for the formation of various, sometimes unexpected, products could be deduced. Computational analysis provided information that drove the experimental work to occur at room temperature in DMSO and also provided a deeper understanding of how solvents were affecting the product distributions observed. Finally, through these detailed studies, a substrate **8.24** was designed that would solely undergo S$_{RN}$1 reaction pathways.
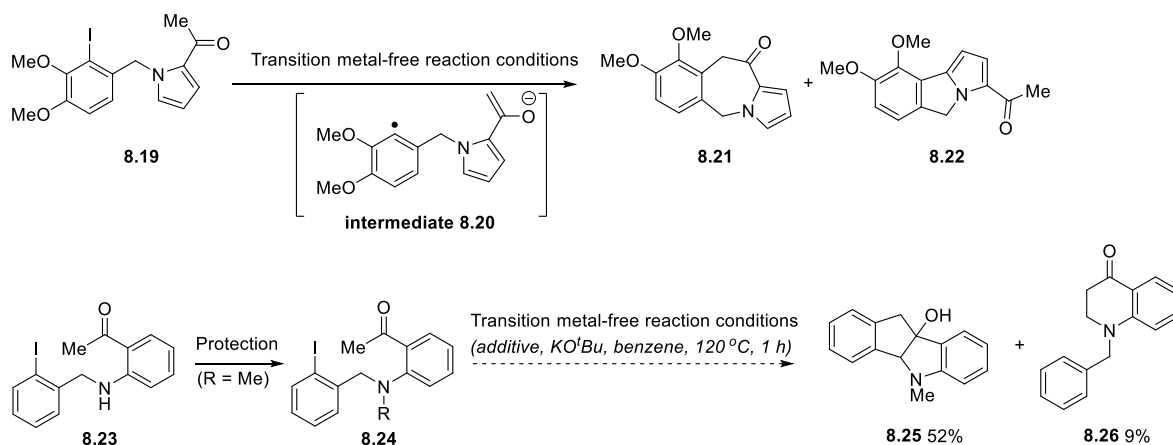
Scheme 8.3 Accessing transition metal-free S$_{RN}$1 cyclisations in the ground-state.

The results presented in Chapter 7 expand on the ability of a base to form possible electron donors. The early studies in Chapter 7 propose that the ene-diol of glucose can act as an electron donor, which led to studies of the Tollens' test.[162] A qualitative study of the Tollens' reactions highlighted the numerous additives that were capable of reducing the Ag(I) in the Tollens' test and, based upon the increased knowledge of electron donors from the literature and within this thesis, several proposals of various possible electron donors were made to explain the observed results from the qualitative study. Of particular interest was the ability of tertiary α-hydroxy ketones to achieve the positive Tollens' test and this led to a more detailed study, and showed that oxidative C-C bond cleavage was occurring in these reactions.

The research performed within this study has highlighted the benefits of using both experimental research and computational studies to develop a deeper understanding of the reaction pathways. The combination of methods led to the discovery of new mechanisms to explain product formation and provided support to mechanisms previously proposed.

9.

Experimental details

9.1 General experimental information

All reagents were bought from commercial suppliers and used without further purification unless stated otherwise. All the reactions were carried out under argon atmosphere. Diethyl ether, tetrahydrofuran, dichloromethane and hexane were dried with a Pure-Solv 400 solvent purification system by Innovative Technology Inc., U.S.A. Organic extracts were, in general, dried over anhydrous sodium sulfate (Na_2SO_4). A Büchi rotary evaporator was used to concentrate the reaction mixtures. Thin layer chromatography (TLC) was performed using aluminium-backed sheets of silica gel and visualised under a UV lamp (254 nm). The plates were developed using phosphomolybdic acid or $KMnO_4$ solution. Column chromatography was performed to purify compounds by using silica gel 60 (200-400 mesh).

The electron transfer reactions were carried out within a glove box (Innovative Technology Inc., U.S.A.) under nitrogen atmosphere, and performed in oven-dried or flame-dried apparatus using anhydrous solvents, which were degassed under reduced pressure, then purged with argon and dried over activated molecular sieves (3 Å), prior to being sealed and transferred to the glovebox. All solvent or samples placed into the glovebox were transferred in through the port, which was evacuated and purged with nitrogen ten times before entry. When the reaction mixtures were prepared, the reaction vessel was removed from the glove box and the rest of the reaction was performed in the fumehood.

Proton (^1H) NMR spectra were recorded at 400, 400 and 500 MHz on Bruker AV3, AV400 and AV500 spectrometers, respectively. Carbon ($^{13}C\{^1H\}$) NMR spectra were recorded using broadband decoupled mode at 101, 101 and 126 MHz on Bruker AV3, AV400 and AV500 spectrometers, respectively. Spectra were recorded in either deuterated chloroform ($CDCl_3$) or deuterated dimethyl sulfoxide (d^6-DMSO), depending on the solubility of the compounds. The chemical shifts are reported in parts per million (ppm) calibrated on the residual non-deuterated solvent signal, and the coupling constants, *J*, are reported in Hertz (Hz). The peak multiplicities are denoted using the following abbreviations: s, singlet; d, doublet; t, triplet; q, quartet;

sx, sextet; m, multiplet; br s, broad singlet; dd, doublet of doublets; dt, doublet of triplets; td, triplet of doublets.

Infra-Red spectra were recorded on an ATR-IR spectrometer.

Melting points were determined on a Gallenkamp Melting point apparatus.

The mass spectra were recorded by either gas-phase chromatography (GCMS) or liquid-phase chromatography (LCMS), using various ionisation techniques, as stated for each compound: atmospheric pressure chemical ionisation (APCI), electron ionisation (EI), electrospray ionisation (ESI). GCMS data were recorded using an Agilent Technologies 7890A GC system coupled to a 5975C inert XL EI/CI MSD detector. Separation was performed using the DB5MS-UI column (30 m x 0.25 mm x 0.25 µm) at a temperature of 320 °C, using helium as the carrier gas. LCMS data were recorded using an Agilent 6130 Dual source mass spectrometer with Agilent 1200, Agilent Poroshell 120 EC-C18 4.6mm x 75mm x 2.7um column.

High-resolution mass spectrometry (HRMS) was performed at the University of Wales, Swansea, in the EPSRC National Mass Spectrometry Centre. Accurate mass was obtained using atmospheric pressure chemical ionisation (APCI), chemical ionisation (CI), electron ionisation (EI), electrospray ionisation (ESI) or nanospray ionisation (NSI) with a LTQ Orbitrap XL mass spectrometer.

9.2 Experimental details for Chapter 4

9.2.1 Synthesis of additive 4.19

Synthesis of 2-chloro-*N*-propylacetamide 9.4.3[167]
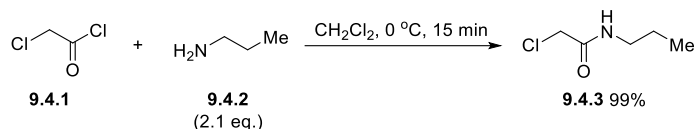
Anhydrous dichloromethane (30 mL) was added to a round-bottomed flask. Under an argon atmosphere, at 0 °C, chloroacetyl chloride **9.4.1** (4 mL, 50 mmol) and propylamine **9.4.2** (8.6 mL, 105 mmol, 2.1 eq.) were simultaneously added dropwise. The reaction mixture was stirred at 0 °C for 15 min and then diluted with diethyl ether (200 mL) and a solid precipitated. The reaction mixture was filtered and the solid was washed with diethyl ether. The filtered solution was concentrated *in vacuo* and diluted with diethyl ether (200 mL) and filtered a second time. The filtered solution was concentrated *in vacuo* to give 2-chloro-*N*-propylacetamide **9.4.3**[167] (6.72 g, 99%) as a pale yellow oil [Found: (HRMS-ESI) 136.0521. $C_5H_{11}ClNO^+$ (M+H)$^+$ requires 136.0524]; v_{max}(film) / cm^{-1} 3292, 3084, 2965, 2936, 2876, 1651, 1539, 1460, 1439, 1258, 1240, 1155; ^{1}H-NMR (500 MHz, CDCl$_3$) δ 0.91 (3 H, t, *J* = 7.2 Hz, C*H*$_3$), 1.50 (2 H, sx, *J* = 7.2 Hz, C*H*$_2$), 3.18 – 3.23 (2 H, m, C*H*$_2$), 4.01 (2 H, s, C*H*$_2$), 6.67 (1 H, br s, N*H*); ^{13}C{^{1}H}-NMR (100 MHz, CDCl$_3$) δ 11.4 (CH$_3$), 22.7 (CH$_2$), 41.6 (CH$_2$), 42.8 (CH$_2$), 165.9 (C).

Synthesis of 1,4-dipropylpiperazine-2,5-dione 4.6[41]
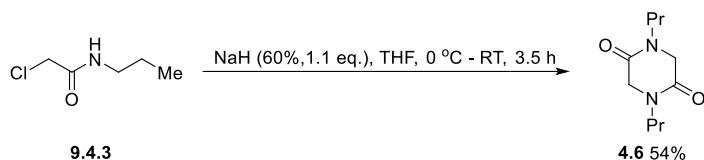
2-Chloro-*N*-propylacetamide **9.4.3** (6.78 g, 50 mmol) and anhydrous tetrahydrofuran (30 mL) were added to a flame-dried round-bottomed flask. At 0 °C, a suspension of sodium hydride (60% in mineral oil, 2.20 g, 55 mmol, 1.1 eq.) in anhydrous tetrahydrofuran (20 mL) was added dropwise *via* cannula and the reaction mixture was stirred at RT for 3.5 h. The reaction mixture was quenched by dropwise addition of water and diluted with diethyl ether (150 mL). The organic phase was dried over Na$_2$SO$_4$, filtered and concentrated *in vacuo*. The crude material was purified by

column chromatography (0 - 100% ethyl acetate in hexane) to give 1,4-dipropylpiperazine-2,5-dione **4.6**[41] (2.66 g, 54%) as pale yellow crystals m.p. 54 – 59 °C (lit:[41] 40 – 42 °C); [Found: (HRMS-ESI) 199.1438. $C_{10}H_{19}N_2O_2^+$ (M+H)$^+$ requires 199.1438]; v_{max}(film) / cm^{-1} 2964, 2932, 2872, 1647, 1483, 1335, 1308, 1277, 1204, 1055; ^{1}H-NMR (500 MHz, CDCl$_3$) δ 0.92 – 0.95 (6 H, m, 2 x C*H$_3$*), 1.59 (4 H, sx, *J* = 7.5 Hz, 2 x C*H$_2$*), 3.37 (4 H, m, 2 x C*H$_2$*), 3.96 (4 H, s, C*H$_2$*); ^{13}C{^{1}H}-NMR (125 MHz, CDCl$_3$) δ 11.2 (2 x CH$_3$), 20.0 (2 x CH$_2$), 47.7 (2 x CH$_2$), 50.0 (2 x CH$_2$), 163.6 (2 x C).

Synthesis of *cis*-4-hydroxybut-2-en-1-yl pivalate 9.4.5[168]

4.38   **9.4.4** (1 eq.)   **9.4.5** 99%
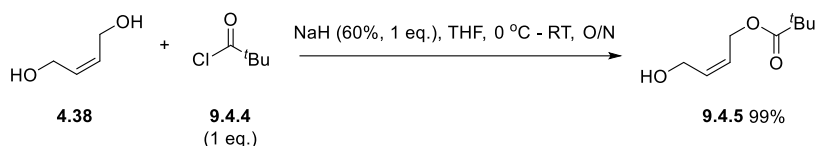
Sodium hydride (60% in mineral oil, 1.1 g, 27.4 mmol, 1.0 eq.) and anhydrous tetrahydrofuran (120 mL) were added to a flame-dried round-bottomed flask. Under an argon atmosphere, at 0 °C, *cis*-2-butene-1,4-diol **4.38** (2.3 mL, 27.4 mmol) was added slowly and the reaction mixture was stirred at 0 °C for 10 min, then at RT for 45 min. Trimethylacetyl chloride **9.4.4** (3.4 mL, 27.4 mmol, 1.0 eq.) was added dropwise *via* syringe pump over a period of 30 min and the reaction mixture was stirred at RT overnight and then quenched with saturated aqueous ammonium chloride solution (100 mL) and extracted with ethyl acetate (3 x 100 mL). The organic phases were combined, washed with brine, dried over Na$_2$SO$_4$, filtered and concentrated *in vacuo*. The crude material was purified by column chromatography (0 – 20% ethyl acetate in hexane) to give *cis*-4-hydroxybut-2-en-1-yl pivalate **9.4.5**[168] (4.70 g, 99%) as a pale yellow oil [Found: (HRMS-ESI) 173.1169. $C_9H_{17}O_3^+$ (M+H)$^+$ requires 173.1172]; v_{max}(film) / cm^{-1} 3412, 2972, 2872, 1726, 1479, 1280, 1146, 1030, 983, 939, 858, 772; ^{1}H-NMR (400 MHz, CDCl$_3$) δ 1.19 (9 H, s, 3 x C*H$_3$*), 4.26 (2 H, d, *J* = 6.4 Hz, C*H$_2$*), 4.67 (2 H, d, *J* = 7.2 Hz, C*H$_2$*), 5.61 (1 H, dt, *J* = 11.2, 7.2 Hz, *cis*-C*H*), 5.85 (1 H, dt, *J* = 11.2, 6.4 Hz, *cis*-C*H*); ^{13}C{^{1}H}-NMR (125 MHz, CDCl$_3$) δ 27.3 (3 x CH$_3$), 38.9 (C), 58.6 (CH$_2$), 60.2 (CH$_2$), 126.0 (CH), 133.3 (CH), 178.9 (C).

Synthesis of *cis*-4-(3,6-dioxo-1,4-dipropylpiperazin-2-yl)but-2-en-1-yl pivalate 4.17
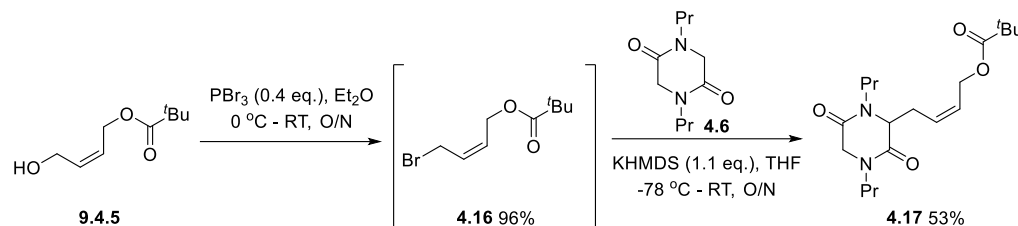

Cis-4-hydroxybut-2-en-1-yl pivalate **9.4.5** (3.05 g, 17.7 mmol) and anhydrous diethyl ether (10 mL) were added to a round-bottomed flask. Under an argon atmosphere, at 0 °C, PBr₃ (0. 7 mL, 7.1 mmol, 0.4 eq.) was added slowly and the reaction mixture was stirred at 0 °C for 45 min, then at RT overnight. The reaction mixture was quenched with water (20 mL) and extracted with diethyl ether (3 x 20 mL). The organic phases were combined, dried over Na₂SO₄, filtered and concentrated *in vacuo* to give *cis*-4-bromobut-2-en-1-yl pivalate **4.16** (4.01 g, 96%) as a colourless oil [Found: (HRMS-APCI) 235.0330. $C_9H_{16}{}^{79}BrO_2{}^+$ (M+H)⁺ requires 235.0334]; v_{max}(film) / cm⁻¹ 2972, 1724, 1479, 1396, 1279, 1140, 1032, 966, 939, 769, 725; ¹H-NMR (400 MHz, CDCl₃) δ 1.21 (9 H, s, 3 x C*H₃*), 4.03 (2 H, d, *J* = 8.4 Hz, C*H₂*), 4.68 (2 H, d, *J* = 6.8 Hz, C*H₂*), 5.68 (1 H, dt, *J* = 10.8, 6.8 Hz, *cis*-C*H*), 5.93 (1 H, dt, *J* = 10.8, 8.4 Hz, *cis*-C*H*); ¹³C{¹H}-NMR (125 MHz, CDCl₃) δ 26.0 (CH₂), 27.3 (3 x CH₃), 38.9 (C), 59.3 (CH₂), 128.6 (CH), 129.8 (CH), 178.4 (C); *m/z* (APCI) 237.0310 [(M+H)⁺, ⁸¹Br, 98%], 235.0330 [(M+H)⁺, ⁷⁹Br, 100].

1,4-Dipropylpiperazine-2,5-dione **4.6** (2.57 g, 13.0 mmol) and anhydrous tetrahydrofuran (110 mL) were added to a flame-dried round-bottomed flask. Under an argon atmosphere, at -10 °C, a solution of KHMDS (2.91 g, 14.5 mmol, 1.1 eq.) in anhydrous tetrahydrofuran (40 mL) was added slowly and the reaction mixture was stirred at -10 °C for 20 min, then at RT for 15 min. At -78 °C, *cis*-4-bromobut-2-en-1-yl pivalate **4.16** (3.67 g, 15.6 mmol, 1.2 eq.) was added slowly and the reaction mixture was stirred at -78 °C for 30 min, then at RT overnight. The reaction mixture was quenched with saturated aqueous ammonium chloride solution (a few drops) and the crude mixture was concentrated *in vacuo*. The crude mixture was diluted with saturated aqueous ammonium chloride solution (50 mL) and extracted with ethyl acetate (3 x 60 mL). The organic phases were combined, washed with brine, dried

over Na_2SO_4, filtered and concentrated *in vacuo*. The crude material was purified by column chromatography (0 - 20% ethyl acetate in hexane) to give *cis-4-(3,6-dioxo-1,4-dipropylpiperazin-2-yl)but-2-en-1-yl pivalate* **4.17** (2.40 g, 53%) as a yellow oil [Found: (HRMS-ESI) 375.2252. $C_{19}H_{32}N_2O_4Na^+$ $(M+Na)^+$ requires 375.2254]; v_{max}(film) / cm^{-1} 2965, 2874, 1724, 1655, 1464, 1329, 1148, 1065, 1032, 953; ^{1}H-NMR (400 MHz, CDCl$_3$); δ 0.91 (6 H, t, *J* = 7.6 Hz, 2 x C*H₃*), 1.18 (9 H, s, 3 x C*H₃*), 1.50 – 1.67 (4 H, m, 2 x C*H₂*), 2.65 (1 H, dt, *J* = 14.8, 7.2 Hz, C*H₂*), 2.77 – 2.84 (2 H, m, 2 x C*H₂*), 3.15 – 3.22 (1 H, m, C*H₂*), 3.47 – 3.52 (1 H, m, C*H₂*), 3.78 (1 H, d, *J* = 17.6 Hz, C*H₂*), 3.89 – 4.09 (3 H, m, C*H₂* and C*H*), 4.56 (2 H, d, *J* = 7.2 Hz, C*H₂*), 5.58 (1 H, dt, *J* = 11.2, 7.6 Hz, *cis*-C*H*), 5.70 (1 H, dt, *J* = 11.2, 6.8 Hz, *cis*-C*H*); ^{13}C{^{1}H}-NMR (125 MHz, CDCl$_3$) δ 11.3 (CH₃), 11.4 (CH₃), 20.1 (CH₂), 20.6 (CH₂), 27.3 (3 x CH₃), 30.4 (CH₂), 38.9 (C), 46.2 (CH₂), 48.0 (CH₂), 50.0 (CH₂), 59.8 (CH₂), 60.1 (CH), 126.8 (CH), 129.3 (CH), 164.2 (C), 165.9 (C), 178.4 (C).
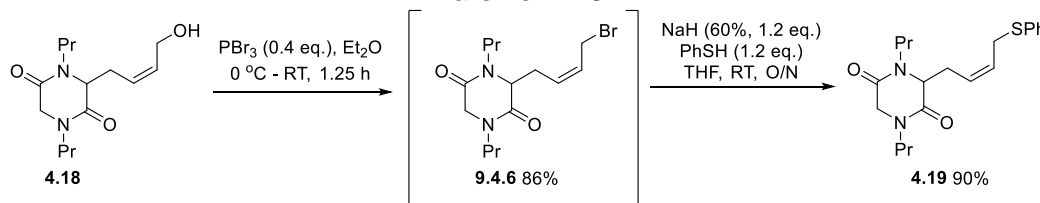
Synthesis of *cis-3-(4-hydroxybut-2-en-1-yl)-1,4-dipropylpiperazine-2,5-dione 4.18*
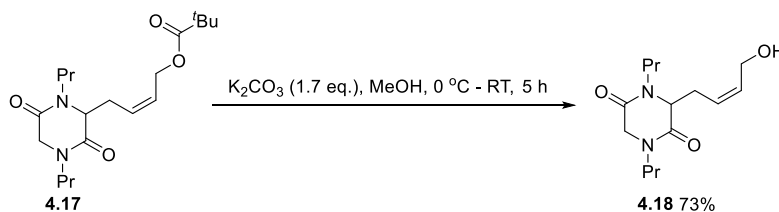
Cis-4-(3,6-dioxo-1,4-dipropylpiperazin-2-yl)but-2-en-1-yl pivalate **4.17** (2.37 g, 6.7 mmol) and methanol (40 mL) were added to a round-bottomed flask. Under an argon atmosphere, at 0 °C, K_2CO_3 (1.11 g, 8.0 mmol, 1.2 eq.) was added and the reaction mixture was stirred at RT for 3 h. The reaction was incomplete by TLC analysis. At 0 °C, K_2CO_3 (463 mg, 3.35 mmol, 0.5 eq.) was added and the reaction mixture was stirred at RT for 2 h. The reaction mixture was quenched with water (a few drops) and the crude mixture was concentrated *in vacuo*. The crude mixture was diluted with water (40 mL) and extracted with dichloromethane (4 x 40 mL). The organic phases were combined, washed with brine, dried over Na_2SO_4, filtered and concentrated *in vacuo*. The crude material was purified by column chromatography (0 - 100% ethyl acetate in hexane) to give *cis-3-(4-hydroxybut-2-en-1-yl)-1,4-dipropylpiperazine-2,5-dione* **4.18** (1.33 g, 73%) as a pale yellow oil [Found: (HRMS-

ESI) 291.1676. $C_{14}H_{24}N_2O_3Na^+$ (M+Na)$^+$ requires 291.1679]; v_{max}(film) / cm^{-1} 3410, 2963, 2932, 2874, 1643, 1468, 1331, 1200, 1032, 718; ^{1}H-NMR (400 MHz, CDCl$_3$) δ 0.89 (6 H, t, J = 7.6 Hz, 2 x CH_3), 1.52 – 1.63 (4 H, m, 2 x CH_2), 2.54 – 2.75 (2 H, m, CH_2 and OH), 2.75 – 2.84 (2 H, m, CH_2), 3.15 – 3.22 (1 H, m, CH_2), 3.40 – 3.47 (1 H, m, CH_2), 3.78 (1 H, d, J = 17.6 Hz, CH_2), 3.87 – 3.94 (1 H, m, CH_2), 4.01 – 4.10 (4 H, m, 3 x CH_2 and the CH), 5.46 (1 H, dt, J = 10.8, 7.6 Hz, *cis*-CH), 5.81 (1 H, dt, J = 10.8, 6.8 Hz, *cis*-CH); ^{13}C{^{1}H}-NMR (125 MHz, CDCl$_3$) δ 11.3 (CH$_3$), 11.3 (CH$_3$), 20.0 (CH$_2$), 20.5 (CH$_2$), 29.9 (CH$_2$), 46.2 (CH$_2$), 48.0 (CH$_2$), 49.9 (CH$_2$), 58.1 (CH$_2$), 60.2 (CH), 124.2 (CH), 134.6 (CH), 164.4 (C), 166.2 (C).

Synthesis of *cis-3-(4-(phenylthio)but-2-en-1-yl)-1,4-dipropylpiperazine-2,5-dione 4.19*
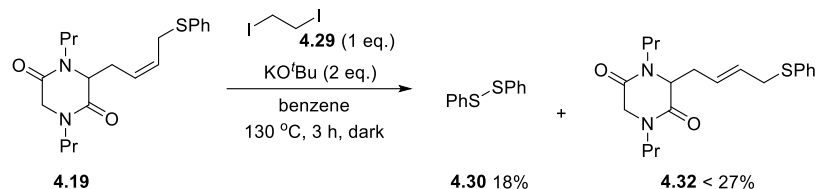

Cis-3-(4-hydroxybut-2-en-1-yl)-1,4-dipropylpiperazine-2,5-dione **4.18** (1.13 g, 4.2 mmol) and anhydrous diethyl ether (2 mL) were added to a round-bottomed flask. Under an argon atmosphere, at 0 °C, PBr$_3$ (0.16 mL, 1.7 mmol, 0.4 eq.) was added slowly and the reaction mixture was stirred at RT for 1 h 15 min. The reaction mixture was quenched with water (10 mL) and extracted with diethyl ether (4 x 10 mL). The organic phases were combined, dried over Na$_2$SO$_4$, filtered and concentrated *in vacuo* to give *cis-3-(4-bromobut-2-en-1-yl)-1,4-dipropylpiperazine-2,5-dione* **9.4.6** (1.20 g, 86%) as a pale yellow oil [Found: (HRMS-ESI) 331.1018. $C_{14}H_{24}^{79}BrN_2O_2^+$ (M+H)$^+$ requires 331.1016]; v_{max}(film) / cm^{-1} 2963, 2932, 2874, 1655, 1466, 1327, 1202, 1155, 1063, 893, 743; ^{1}H-NMR (400 MHz, CDCl$_3$) δ 0.92 (6 H, t, J = 7.6 Hz, 2 x CH_3), 1.54 – 1.66 (4 H, m, 2 x CH_2), 2.63 (1 H, dt, J = 14.4, 7.2 Hz, CH_2), 2.79 – 2.86 (2 H, m, 2 x CH_2), 3.20 – 3.28 (1 H, m, CH_2), 3.41 – 3.49 (1 H, m, CH_2), 3.80 (1 H, d, J = 17.2 Hz, CH_2), 3.85 – 3.98 (3 H, m, 3 x CH_2), 4.02 – 4.08 (2 H, m, CH_2 and CH), 5.55 (1 H, dt, J = 10.8, 7.6 Hz, *cis*-CH), 5.92 (1 H, dt, J = 10.8, 8.4 Hz, *cis*-CH); ^{13}C{^{1}H}-NMR (125 MHz, CDCl$_3$) δ 11.3 (CH$_3$), 11.4 (CH$_3$), 20.1 (CH$_2$), 20.6 (CH$_2$), 25.9 (CH$_2$), 29.7 (CH$_2$), 46.3 (CH$_2$), 48.1 (CH$_2$), 50.0 (CH$_2$), 60.0 (CH), 127.3 (CH),

130.5 (CH), 164.1 (C), 165.7 (C); *m/z* (ESI) 333.0997 [(M+H)$^+$, ^{81}Br, 98%], 331.1018 [(M+H)$^+$, ^{79}Br, 100].

Sodium hydride (60% in mineral oil, 167 mg, 4.2 mmol, 1.2 eq.) and anhydrous tetrahydrofuran (40 mL) were added to a flame-dried round-bottomed flask. Under an argon atmosphere, at 0 °C, thiophenol (0.39 mL, 3.8 mmol, 1.1 eq.) was added slowly and the reaction mixture was stirred at RT for 1 h. A solution of *cis*-3-(4-bromobut-2-en-1-yl)-1,4-dipropylpiperazine-2,5-dione **9.4.6** (1.15 g, 3.5 mmol) in anhydrous tetrahydrofuran (40 mL) was added dropwise and the reaction mixture was stirred at RT overnight. The reaction mixture was quenched with water (a few drops) and the crude mixture was concentrated *in vacuo*. The crude mixture was diluted with water (30 mL) and extracted with ethyl acetate (4 x 30 mL). The organic phases were combined, washed with brine, dried over Na$_2$SO$_4$, filtered and concentrated *in vacuo*. The crude material was purified by column chromatography (0 - 50% ethyl acetate in hexane) to give *cis-3-(4-(phenylthio)but-2-en-1-yl)-1,4-dipropylpiperazine-2,5-dione **4.19*** (1.12 g, 90%) as a pale yellow oil [Found: (HRMS-NSI) 361.1945. C$_{20}$H$_{29}$N$_2$O$_2$S$^+$ (M+H)$^+$ requires 361.1944]; v_{max}(film) / cm^{-1} 2963, 2932, 2872, 2361, 1655, 1468, 1437, 1327, 1271, 1120, 1065, 893, 739; ^{1}H-NMR (400 MHz, CDCl$_3$) δ 0.88 – 0.92 (6 H, m, 2 x C*H$_3$*), 1.52 – 1.60 (4 H, m, 2 x C*H$_2$*), 2.42 (1 H, dt, *J* = 14.4, 8.0 Hz, C*H$_2$*), 2.59 – 2.62 (1 H, m, C*H$_2$*), 2.73 – 2.76 (1 H, m, C*H$_2$*), 3.18 – 3.21 (1 H, m, C*H$_2$*), 3.41 – 3.56 (3 H, m, 3 x C*H$_2$*), 3.75 (1 H, d, *J* = 17.2 Hz, C*H$_2$*), 3.86 – 3.89 (1 H, m, C*H$_2$*), 3.95 (1 H, t, *J* = 4.8 Hz, C*H*), 4.02 (1 H, d, *J* = 17.2 Hz, C*H$_2$*), 5.47 (1 H, dt, *J* = 10.8, 8.4 Hz, *cis*-C*H*), 5.72 (1 H, dt, *J* = 10.8, 8.0 Hz, *cis*-C*H*), 7.23 (1 H, t, *J* = 7.2 Hz, Ar*H*), 7.26 – 7.30 (2 H, m, Ar*H*), 7.35 (2 H, d, *J* = 7.2 Hz, Ar*H*); ^{13}C{^{1}H}-NMR (125 MHz, CDCl$_3$) δ 11.3 (CH$_3$), 11.4 (CH$_3$), 20.1 (CH$_2$), 20.6 (CH$_2$), 29.8 (CH$_2$), 31.5 (CH$_2$), 46.3 (CH$_2$), 48.0 (CH$_2$), 50.0 (CH$_2$), 60.2 (CH), 125.3 (CH), 126.9 (CH), 129.1 (CH), 130.1 (CH), 130.9 (CH), 135.7 (C), 164.2 (C), 165.9 (C); HSQC ^{1}H/^{13}C δ (0.88 – 0.92)/11.3, (0.88 – 0.92)/11.4, (1.52 – 1.60)/20.1, (1.52 – 1.60)/20.6, 2.42/29.8, (2.59 – 2.62)/29.8, (2.73 – 2.76)/46.3, (3.18 – 3.21)/48.0, (3.41 – 3.56)/31.5, (3.41 – 3.56)/31.5, (3.41 – 3.56)/48.0, 3.75/50.0, (3.86 – 3.89)/46.3, 3.95/60.2, 4.02/50.0, 5.47/125.3, 5.72/130.1, 7.23/126.9, (7.26 – 7.30)/129.1, 7.35/130.9.
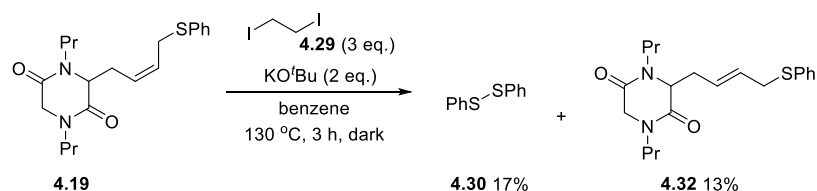
9.2.2 Reduction of diiodoethane using the additive 4.19 (Table 4.1)

Table 4.1, entry 1

Cis-3-(4-(phenylthio)but-2-en-1-yl)-1,4-dipropylpiperazine-2,5-dione **4.19** (72 mg, 0.2 mmol) and 1,2-diiodoethane (56 mg, 0.2 mmol, 1.0 eq.) were added to an oven-dried pressure tube. In the glove box, KO^{t}Bu (45 mg, 0.4 mmol, 2.0 eq.) and anhydrous benzene (2 mL) were added and the reaction mixture was stirred at 130 ºC for 3 h in the dark. The reaction mixture was cooled to RT, quenched with water (6 mL) and extracted with diethyl ether (3 x 10 mL). The organic phases were combined, dried over Na$_2$SO$_4$, filtered and concentrated *in vacuo*. The crude material was purified by column chromatography (0 - 50% ethyl acetate in hexane) to give diphenyl disulfide **4.30**[169] (4 mg, 18%) as white crystals m.p. 54 – 56 ºC (lit:[170] 57 ºC); [Found: (GCMS-EI) C$_{12}$H$_{10}$S$_2$ (M)$^{•+}$ 218.0]; v_{max}(film) / cm^{-1} 1574, 1474, 1437, 1070, 1020, 995, 733; ^{1}H-NMR (400 MHz, CDCl$_3$) δ 7.21 – 7.25 (2 H, m, Ar*H*), 7.28 – 7.33 (4 H, m, Ar*H*), 7.48 – 7.51 (4 H, m, Ar*H*); ^{13}C{^{1}H}-NMR (100 MHz, CDCl$_3$) δ 127.3 (2 x CH), 127.7 (4 x CH), 129.2 (4 x CH), 137.2 (2 x C) and impure (*E*)-3-(4-(phenylthio)but-2-en-1-yl)-1,4-dipropylpiperazine-2,5-dione **4.32** (40.5 mg) as a brown oil. The product (*E*)-3-(4-(phenylthio)but-2-en-1-yl)-1,4-dipropylpiperazine-2,5-dione **4.32** is present with an unidentified product (ratio 1 : 1), giving (*E*)-3-(4-(phenylthio)but-2-en-1-yl)-1,4-dipropylpiperazine-2,5-dione **4.32** (< 27%) based on ^{1}H-NMR (Section 9.2.2 on page 188).
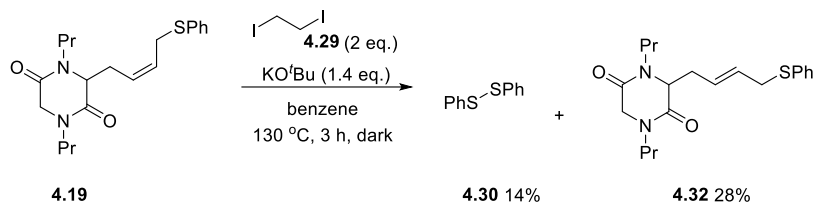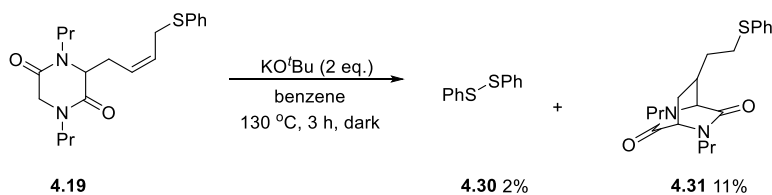
Table 4.1, entry 2

Cis-3-(4-(phenylthio)but-2-en-1-yl)-1,4-dipropylpiperazine-2,5-dione **4.19** (72 mg, 0.2 mmol) and 1,2-diiodoethane (169 mg, 0.6 mmol, 3.0 eq.) were added to an oven-

dried pressure tube. In the glove box, KO^{t}Bu (45 mg, 0.4 mmol, 2.0 eq.) and anhydrous benzene (2 mL) were added and the reaction mixture was stirred at 130 ^{o}C for 3 h in the dark. The reaction mixture was cooled to RT, quenched with water (6 mL) and extracted with diethyl ether (3 x 10 mL). The organic phases were combined, dried over Na$_2$SO$_4$, filtered and concentrated *in vacuo*. The yield of diphenyl disulfide **4.30**[169] (17%) was determined by adding 1,3,5-trimethoxybenzene to the crude mixture as an internal standard for ^{1}H-NMR. The product was identified by the following characteristic signals; ^{1}H-NMR (400 MHz, CDCl$_3$) δ 7.48 – 7.50 (4 H, m) for diphenyl disulfide **4.30**. These signals are consistent with the literature values and reference samples (Section 9.2.2, Table 4.1, entry 1 on page 187). The crude material was purified by column chromatography (0 - 100% ethyl acetate in hexane) to give (*E*)-3-(4-(phenylthio)but-2-en-1-yl)-1,4-dipropylpiperazine-2,5-dione **4.32** (9.6 mg, 13%) as a yellow oil [Found: (HRMS-APCI) 361.1950. C$_{20}$H$_{29}$N$_2$O$_2$S$^+$ (M+H)$^+$ requires 361.1951]; v_{max}(film) / cm^{-1} 2961, 2930, 2872, 1655, 1466, 1437, 1331, 1200, 1059, 970, 739; ^{1}H-NMR (400 MHz, CDCl$_3$) δ 0.89 (6 H, t, *J* = 7.2 Hz, 2 x C*H$_3$*), 1.48 – 1.65 (4 H, m, 2 x C*H$_2$*), 2.54 (1 H, dt, *J* = 13.2, 6.0 Hz, C*H$_2$*), 2.61 – 2.65 (1 H, m, C*H$_2$*), 2.73 – 2.76 (1 H, m, C*H$_2$*), 3.12 – 3.17 (1 H, m, C*H$_2$*), 3.41 – 3.51 (3 H, m, C*H$_2$*), 3.70 (1 H, d, *J* = 17.2 Hz, C*H$_2$*), 3.81 – 3.87 (1 H, m, C*H$_2$*), 3.93 – 4.00 (2 H, m, C*H* and C*H$_2$*), 5.50 (1 H, dt, *J* = 15.2, 7.2 Hz, *trans*-C*H*), 5.67 (1 H, dt, *J* = 15.2, 6.8 Hz, *trans*-C*H*), 7.16 – 7.20 (1 H, m, Ar*H*), 7.25 – 7.36 (4 H, m, Ar*H*); ^{13}C{^{1}H}-NMR (100 MHz, CDCl$_3$) δ 11.3 (CH$_3$), 11.4 (CH$_3$), 20.1 (CH$_2$), 20.6 (CH$_2$), 35.2 (CH$_2$), 36.0 (CH$_2$), 46.3 (CH$_2$), 47.9 (CH$_2$), 50.0 (CH$_2$), 60.5 (CH), 126.1 (CH), 126.4 (CH), 129.1 (2 x CH), 129.6 (2 x CH), 131.2 (CH), 135.9 (C), 164.3 (C), 165.9 (C); HSQC (^{1}H/^{13}C) δ 0.89/11.3, 0.89/11.4, (1.48 – 1.65)/20.1, (1.48 – 1.65)/20.6, 2.54/35.2, (2.61 – 2.65)/36.0, (2.73- 2.76)/46.3, 3.14/47.9, (3.41 – 3.51)/36.0, (3.41 – 3.51)/47.9, 3.70/50.0, 3.83/46.3, (3.93 – 4.00)/50.0, (3.93 – 4.00)/60.5, 5.50/126.1, 5.67/131.2, (7.16 – 7.20)/126.4, (7.25 – 7.36)/129.1, (7.25 – 7.36)/129.6.

Table 4.1, entry 3

4.19   **4.30** 14%   **4.32** 28%

Cis-3-(4-(phenylthio)but-2-en-1-yl)-1,4-dipropylpiperazine-2,5-dione **4.19** (56 mg, 0.15 mmol) and 1,2-diiodoethane (85 mg, 0.3 mmol, 2.0 eq.) were added to an oven-dried pressure tube. In the glove box, KO^{t}Bu (25 mg, 0.2 mmol, 1.4 eq.) and anhydrous benzene (2 mL) were added and the reaction mixture was stirred at 130 ^{o}C for 3 h in the dark. The reaction mixture was cooled to RT, quenched with water (10 mL) and extracted with diethyl ether (3 x 10 mL). The organic phases were combined, dried over Na$_2$SO$_4$, filtered and concentrated *in vacuo*. The yield of diphenyl disulfide **4.30**[169] (14%) was determined by adding 1,3,5-trimethoxybenzene to the crude mixture as an internal standard for ¹H-NMR. The product was identified by the following characteristic signals; ¹H-NMR (400 MHz, CDCl$_3$) δ 7.48 – 7.50 (4 H, m) for diphenyl disulfide **4.30**. These signals are consistent with the literature values and reference samples (Section 9.2.2, Table 4.1, entry 1 on page 187). The crude material was purified by column chromatography (0 - 50% ethyl acetate in hexane) to yield (*E*)-3-(4-(phenylthio)but-2-en-1-yl)-1,4-dipropylpiperazine-2,5-dione **4.32** (20.1 mg, 28%) as a yellow oil (Section 9.2.2 on page 188).

Table 4.1, entry 4

4.19   **4.30** 2%   **4.31** 11%

Cis-3-(4-(phenylthio)but-2-en-1-yl)-1,4-dipropylpiperazine-2,5-dione **4.19** (72 mg, 0.2 mmol) was added to an oven-dried pressure tube. In the glove box, KO^{t}Bu (45 mg, 0.4 mmol, 2.0 eq.) and anhydrous benzene (2 mL) were added and the reaction mixture was stirred at 130 ^{o}C for 3 h in the dark. The reaction mixture was cooled to RT, quenched with water (10 mL) and extracted with diethyl ether (3 x 10 mL). The organic phases were combined, dried over Na$_2$SO$_4$, filtered and concentrated *in*

vacuo. The yields of diphenyl disulfide **4.30**[169] (2%) and 7-(2-(phenylthio)ethyl)-2,5-dipropyl-2,5-diazabicyclo[2.2.2]octane-3,6-dione **4.31** (11%) were determined by adding 1,3,5-trimethoxybenzene to the crude mixture as an internal standard for ^{1}H-NMR. The products were identified by the following characteristic signals; ^{1}H-NMR (400 MHz, CDCl$_3$) δ 7.48 – 7.50 (4 H, m, Ar*H*) for diphenyl disulfide **4.30**; δ 3.87 (1 H, d, *J* = 4.0 Hz, C*H*), 4.01 (1 H, s, C*H*), 7.19 – 7.23 (1 H, m, Ar*H*), 7.28 – 7.36 (4 H, m, Ar*H*) for 7-(2-(phenylthio)ethyl)-2,5-dipropyl-2,5-diazabicyclo[2.2.2]octane-3,6-dione **4.31**. These signals are consistent with the literature values and reference samples (**4.30**: Section 9.2.2, Table 4.1, entry 1 on page 187; **4.31**: Section 9.2.5, Table 4.3, entry 3 on page 196).

9.2.3 Synthesis of *cis*-(4-methoxybut-2-en-1-yl)(phenyl)sulfane **4.41** (Table 4.2)

Synthesis of *cis*-4-methoxybut-2-en-1-ol 4.39[171]
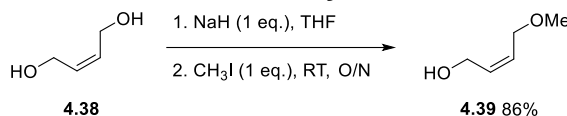
Sodium hydride (60% in mineral oil, 1.0 g, 25 mmol, 1.0 eq.) and anhydrous tetrahydrofuran (20 mL) were added to a flame-dried round-bottomed flask. Under an argon atmosphere, at 0 °C, *cis*-2-butene-1,4-diol **4.38** (6.2 mL, 75 mmol) was added slowly and the reaction mixture was stirred at 0 °C for 15 min, then at RT for 1 h. Methyl iodide (1.6 mL, 25 mmol, 1.0 eq.) was added dropwise and the reaction mixture was stirred at RT overnight and then quenched with saturated aqueous ammonium chloride solution (100 mL) and concentrated *in vacuo*. The crude mixture was diluted with saturated aqueous ammonium chloride solution (20 mL) extracted with ethyl acetate (4 x 20 mL). The organic phases were combined, dried over Na$_2$SO$_4$, filtered and concentrated *in vacuo*. The crude material was purified by column chromatography (0 – 100% ethyl acetate in hexane) to give *cis*-4-methoxybut-2-en-1-ol **4.39**[171] (2.20 g, 86%) as a yellow oil [Found: (GCMS-EI) C$_5$H$_9$O$_2^-$ (M-H)$^-$ 100.7]; v_{max}(film) / cm^{-1} 3364, 2873, 2817, 1450, 1411, 1190, 1084, 1024, 985, 948; ^{1}H-NMR (400 MHz, CDCl$_3$) δ 1.90 (1 H, t, *J* = 6.0 Hz, O*H*), 3.35 (3 H, s, C*H$_3$*), 4.01 (2 H, d, *J* = 6.0 Hz, C*H$_2$*), 4.21 (2 H, t, *J* = 6.0 Hz, C*H$_2$*), 5.70 (1 H, dtt, *J* = 11.2, 6.4, 1.2 Hz, *cis*-C*H*), 5.83 (1 H, dtt, *J* = 11.2, 6.4, 1.2 Hz, *cis*-C*H*);

^{13}C{^{1}H}-NMR (100 MHz, CDCl$_3$) δ 58.3 (CH$_3$), 56.0 (CH$_2$), 68.3 (CH$_2$), 128.5 (CH), 132.4 (CH).

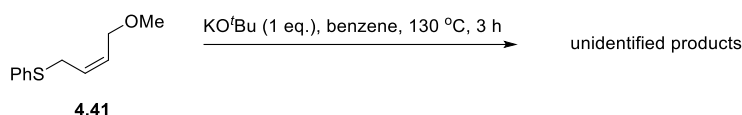### Synthesis of *cis*-(4-methoxybut-2-en-1-yl)(phenyl)sulfane 4.41
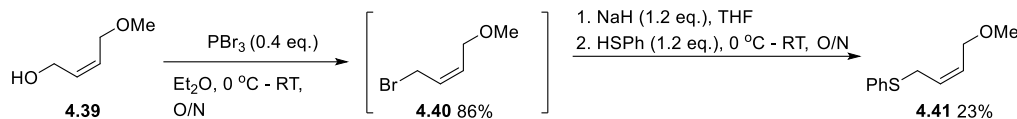
Cis-4-methoxybut-2-en-1-ol **4.39** (2.0 g, 19.6 mmol) and anhydrous diethyl ether (10 mL) were added to a round-bottomed flask. Under an argon atmosphere, at 0 °C, PBr$_3$ (0.73 mL, 7.8 mmol, 0.4 eq.) was added slowly and the reaction mixture was stirred at RT overnight. The reaction mixture was quenched with water (10 mL) and extracted with diethyl ether (4 x 10 mL). The organic phases were combined, dried over Na$_2$SO$_4$, filtered and concentrated *in vacuo* to give *cis-1-bromo-4-methoxybut-2-ene* **4.40** (2.77 g, 86%) as an orange oil [Found: (HRMS-APCI) 162.9756. C$_5$H$_8$BrO$^-$ (M-H)$^-$ requires 162.9759]; v_{max}(film) / cm^{-1} 2923, 2814, 1450, 1207, 1099, 959, 911, 736; ^{1}H-NMR (400 MHz, CDCl$_3$) δ 3.36 (3 H, s, C*H$_3$*), 4.01 (2 H, d, *J* = 8.4 Hz, C*H$_2$*), 4.06 (2 H, d, *J* = 6.4 Hz, C*H$_2$*), 5.70 (1 H, dt, *J* = 10.8, 6.4 Hz, *cis*-C*H*), 5.89 (1 H, dtt, *J* = 10.8, 8.4, 1.6 Hz, *cis*-C*H*); ^{13}C{^{1}H}-NMR (100 MHz, CDCl$_3$) δ 26.5 (CH$_2$), 58.5 (CH$_3$), 67.6 (CH$_2$), 128.5 (CH), 131.3 (CH); *m/z* (APCI) 164.9741 [(M-H)$^-$, ^{81}Br, 100%], 162.9756 [(M-H)$^-$, ^{79}Br, 87].

Sodium hydride (60% in mineral oil, 728 mg, 18.2 mmol, 1.2 eq.) and anhydrous tetrahydrofuran (20 mL) were added to a flame-dried round-bottomed flask. Under an argon atmosphere, at 0 °C, thiophenol (1.87 mL, 18.2 mmol, 1.2 eq.) was added slowly and the reaction mixture was stirred at RT for 1 h. A solution of *cis-1-bromo-4-methoxybut-2-ene* **4.40** (1.15 g, 3.5 mmol) in anhydrous tetrahydrofuran (5 mL) was added dropwise and the reaction mixture was stirred at RT overnight. The reaction mixture was quenched with water (a few drops) and the crude mixture was concentrated *in vacuo*. The crude mixture was diluted with water (30 mL) and extracted with ethyl acetate (4 x 30 mL). The organic phases were combined, washed with brine, dried over Na$_2$SO$_4$, filtered and concentrated *in vacuo*. The crude material was purified by column chromatography (0 - 5% ethyl acetate in hexane) to give *cis-(4-methoxybut-2-en-1-yl)(phenyl)sulfane* **4.41** (682.5 g, 23%) as a pale

yellow oil [Found: (HRMS-APCI) 193.0687. $C_{11}H_{13}OS^-$ (M-H)$^-$ requires 193.0683]; v_{max}(film) / cm^{-1} 2920, 2812, 1582, 1480, 1439, 1192, 1103, 1026, 738, 692; ^{1}H-NMR (400 MHz, CDCl$_3$) δ 3.26 (3 H, s, CH_3), 3.58 (2 H, d, J = 7.2 Hz, CH_2), 3.85 (2 H, d, J = 6.4 Hz, CH_2), 5.60 – 5.74 (2 H, m, 2 x *cis*-CH), 7.19 – 7.23 (1 H, m, ArH), 7.26 – 7.31 (2 H, m, ArH), 7.36 – 7.39 (2 H, m, ArH); ^{13}C{^{1}H}-NMR (100 MHz, CDCl$_3$) δ 31.9 (CH$_2$), 58.2 (CH$_3$), 68.8 (CH$_2$), 126.8 (CH), 128.2 (CH), 129.0 (2 x CH), 129.5 (CH), 130.8 (2 x CH), 135.8 (C).

9.2.4 Reactions of *cis*-(4-methoxybut-2-en-1-yl)(phenyl)sulfane 4.41 (Table 4.2)

Table 4.2, entry 1

Cis-(4-methoxybut-2-en-1-yl)(phenyl)sulfane **4.41** (97 mg, 0.5 mmol) was added to an oven-dried pressure tube. In the glove box, KO^{t}Bu (56 mg, 0.5 mmol, 1.0 eq.) and anhydrous benzene (5 mL) were added and the reaction mixture was stirred at 130 °C for 3 h in the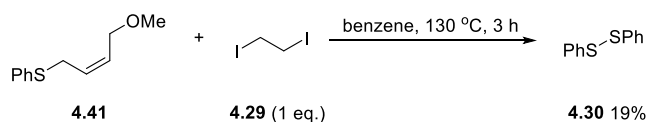 dark. The reaction mixture was cooled to RT, quenched with aqueous hydrochloric acid (1 M, 10 mL) and extracted with dichloromethane (3 x 10 mL). The organic phases were combined, dried over Na$_2$SO$_4$, filtered and concentrated *in vacuo*. Analysis of the ^{1}H-NMR did not identify diphenyl disulfide. (Other products formed in the reaction but could not be identified).

Table 4.2, entry 2
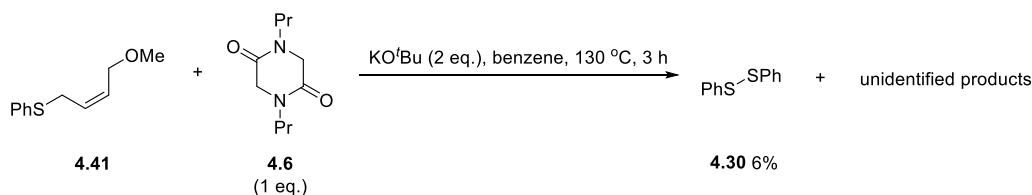
Cis-(4-methoxybut-2-en-1-yl)(phenyl)sulfane **4.41** (97 mg, 0.5 mmol) and 1,4-dipropylpiperazine-2,5-dione **4.6** (99 mg, 0.5 mmol, 1.0 eq.) were added to an oven-dried pressure tube. In the glove box, KO^{t}Bu (112 mg, 1.0 mmol, 2.0 eq.) and anhydrous benzene (5 mL) were added and the reaction mixture was stirred at 130 °C for 3 h in the dark. The reaction mixture was cooled to RT, quenched with

aqueous hydrochloric acid (1 M, 10 mL) and extracted with dichloromethane (3 x 10 mL). The organic phases were combined, dried over Na$_2$SO$_4$, filtered and concentrated *in vacuo*. The yield of diphenyl disulfide **4.30**[169] (6%) was determined by adding 1,3,5-trimethoxybenzene to the crude mixture as an internal standard for ^{1}H-NMR. The product was identified by the following characteristic signals; ^{1}H-NMR (400 MHz, CDCl$_3$) δ 7.48 – 7.50 (4 H, m) for diphenyl disulfide **4.30**. These signals are consistent with the literature values and reference samples (Section 9.2.2, Table 4.1, entry 1 on page 187). (Other products formed in the reaction but could not be identified).

Table 4.2, entry 3

4.41 **4.42** (1 eq.) **4.30** 4%
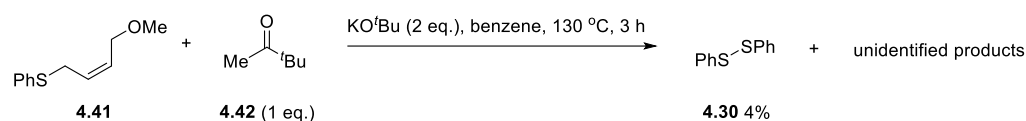
Cis-(4-methoxybut-2-en-1-yl)(phenyl)sulfane **4.41** (97 mg, 0.5 mmol) and pinacolone **4.42** (0.04 mL, 0.5 mmol, 1.0 eq.) were added to an oven-dried pressure tube. In the glove box, KO^{t}Bu (112 mg, 1.0 mmol, 2.0 eq.) and anhydrous benzene (5 mL) were added and the reaction mixture was stirred at 130 °C for 3 h in the dark. The reaction mixture was cooled to RT, quenched with aqueous hydrochloric acid (1 M, 10 mL) and extracted with dichloromethane (3 x 10 mL). The organic phases were combined, dried over Na$_2$SO$_4$, filtered and concentrated *in vacuo*. The yield of diphenyl disulfide **4.30**[169] (4%) was determined by adding 1,3,5-trimethoxybenzene to the crude mixture as an internal standard for ^{1}H-NMR. The product was identified by the following characteristic signals; ^{1}H-NMR (400 MHz, CDCl$_3$) δ 7.48 – 7.50 (4 H, m) for diphenyl disulfide **4.30**. These signals are consistent with the literature values and reference samples (Section 9.2.2, Table 4.1, entry 1 on page 187). (Other products formed in the reaction but could not be identified).

Table 4.2, entry 4

**4.41** **4.29** (1 eq.) **4.30** 19%

Cis-(4-methoxybut-2-en-1-yl)(phenyl)sulfane **4.41** (97 mg, 0.5 mmol) and 1,2-diiodethane (0.07 mL, 0.5 mmol, 1.0 eq.) were added to an oven-dried pressure tube.

In the glove box, anhydrous benzene (5 mL) was added and the reaction mixture was stirred at 130 °C for 3 h in the dark. The reaction mixture was cooled to RT, quenched with aqueous hydrochloric acid (1 M, 10 mL) and extracted with dichloromethane (3 x 10 mL). The organic phases were combined, dried over Na$_2$SO$_4$, filtered and concentrated *in vacuo*. The yield of diphenyl disulfide **4.30**[169] (19%) was determined by adding 1,3,5-trimethoxybenzene to the crude mixture as an internal standard for ^{1}H-NMR. The product was identified by the following characteristic signals; ^{1}H-NMR (400 MHz, CDCl$_3$) δ 7.48 – 7.50 (4 H, m) for diphenyl disulfide **4.30**. These signals are consistent with the literature values and reference samples (Section 9.2.2, Table 4.1, entry 1 on page 187).

9.2.5 Reactions of iodo-*m*-xylene 4.43 with 4.19 (Table 4.3)

Table 4.3, entry 1
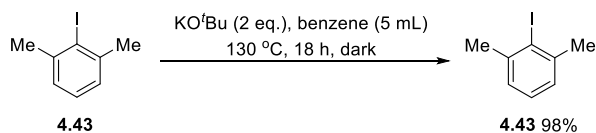
Iodo-*m*-xylene **4.43** (0.07 mL, 0.5 mmol) was added to an oven-dried pressure tube. In the glove box, KO^{t}Bu (112 mg, 1.0 mmol, 2.0 eq.) and anhydrous benzene (5 mL) were added and the reaction was stirred at 130 °C for 18 h in the dark. The reaction mixture was cooled to RT, quenched with water (10 mL) and extracted with diethyl ether (3 x 10 mL). The organic phases were combined, dried over Na$_2$SO$_4$, filtered and concentrated *in vacuo* to give iodo-*m*-xylene **4.43** ^{1}H-NMR (400 MHz, CDCl$_3$) δ 2.48 (6 H, s, 2 x C*H*$_3$), 7.05 (2 H, d, *J* = 8.0 Hz, Ar*H*), 7.13 (1 H, t, *J* = 8.0 Hz, Ar*H*); ^{13}C{^{1}H}-NMR (100 MHz, CDCl$_3$) δ 29.9 (2 x CH$_3$), 108.6 (2 x C), 127.1 (2 x CH), 127.7 (CH), 142.2 (C). The yield of iodo-*m*-xylene **4.43** (98%) was determined by adding 1,3,5-trimethoxybenzene to the crude mixture as an internal standard for ^{1}H-NMR. These signals are consistent a commercial sample.

Table 4.3, entry 2
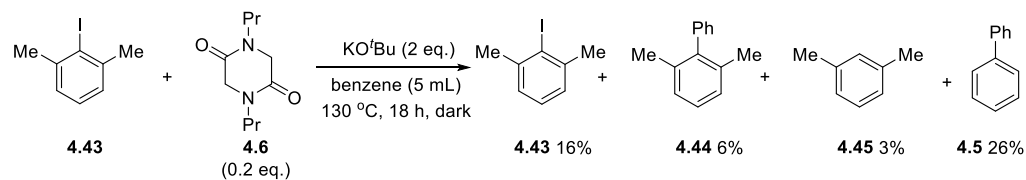
Iodo-*m*-xylene **4.43** (0.07 mL, 0.5 mmol) and 1,4-dipropylpiperazine-2,5-dione **4.6** (194 mg, 0.1 mmol, 0.2 eq.) were added to an oven-dried pressure tube. In the glove box, KO^{t}Bu (112 mg, 1.0 mmol, 2.0 eq.) and anhydrous benzene (5 mL) were added and the reaction was stirred at 130 °C for 18 h in the dark. The reaction mixture was cooled to RT, quenched with water (10 mL) and extracted with diethyl ether (3 x 10 mL). The organic phases were combined, dried over Na$_2$SO$_4$, filtered and concentrated *in vacuo*. The yields of iodo-*m*-xylene **4.43** (16%), 2,6-dimethylbiphenyl **4.44**[172] (6%), xylene **4.45**[173] (3%) and biphenyl **4.5**[174] (26%) were determined by adding 1,3,5-trimethoxybenzene to the crude mixture as an internal standard for ^{1}H-NMR. The products were identified by the following characteristic signals; ^{1}H-NMR (400 MHz, CDCl$_3$) δ 2.48 (6 H, s), 7.05 (2 H, d, *J* = 8.0 Hz), 7.11 (1 H, t, *J* = 8.0 Hz) for iodo-*m*-xylene **4.43**; δ 2.03 (6 H, s), 7.14 − 7.20 (5 H, m), 7.40 − 7.49 (3 H, m) (partly obscured by biphenyl peaks) for 2,6-dimethylbiphenyl **4.44**; δ 2.32 (6 H, s) for xylene **4.45**; δ 7.36 (2 H, t, *J* = 8.0 Hz), 7.45 (4 H, t, *J* = 8.0 Hz), 7.60 (4 H, d, *J* = 8.0 Hz) for biphenyl **4.5**. These signals are consistent with the literature values and reference samples (**4.43**: Section 9.2.2, Table 4.3, entry 1 on page 194).

Table 4.3, entry 3
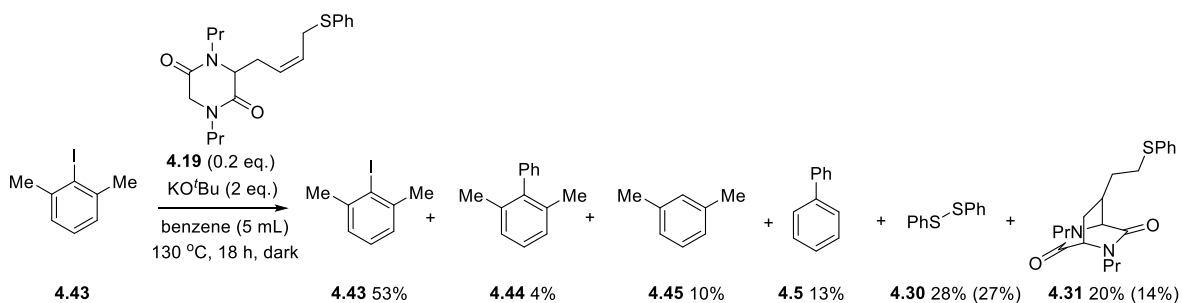
Iodo-*m*-xylene **4.43** (0.07 mL, 0.5 mmol) and *cis*-3-(4-(phenylthio)but-2-en-1-yl)-1,4-dipropylpiperazine-2,5-dione **4.19** (36 mg, 0.1 mmol, 0.2 eq.) were added to an oven-dried pressure tube was added. In the glove box, KO^{t}Bu (112 mg, 1.0 mmol, 2.0 eq.) and anhydrous benzene (5 mL) were added and the reaction was stirred at 130 °C

for 18 h in the dark. The reaction mixture was cooled to RT, quenched with water (10 mL) and extracted with diethyl ether (3 x 10 mL). The organic phases were combined, dried over Na_2SO_4, filtered and concentrated *in vacuo*. The yields of iodo-*m*-xylene **4.43** (53%), 2,6-dimethylbiphenyl **4.44**[172] (4%), xylene **4.45**[173] (10%), biphenyl **4.5**[174] (13%), diphenyl disulfide **4.30** (28%) and 7-(2-(phenylthio)ethyl)-2,5-dipropyl-2,5-diazabicyclo[2.2.2]octane-3,6-dione **4.31** (20%) were determined by adding 1,3,5-trimethoxybenzene to the crude mixture as an internal standard for ^{1}H-NMR. The products were identified by the following characteristic signals; ^{1}H-NMR (400 MHz, $CDCl_3$) δ 2.48 (6 H, s), 7.05 (2 H, d, *J* = 8.0 Hz), 7.11 (1 H, t, *J* = 8.0 Hz) for iodo-*m*-xylene **4.43**; δ 2.03 (6 H, s), 7.14 – 7.20 (5 H, m), 7.40 – 7.49 (3 H, m) (partly obscured by biphenyl peaks) for 2,6-dimethylbiphenyl **4.44**; δ 2.32 (6 H, s) for xylene **4.45**; δ 7.36 (2 H, t, *J* = 8.0 Hz), 7.45 (4 H, t, *J* = 8.0 Hz), 7.60 (4 H, d, *J* = 8.0 Hz) for biphenyl **4.5**;[174] δ 7.21 – 7.26 (2 H, m), 7.48 – 7.50 (4 H, m) for diphenyl disulfide **4.30**; δ 0.84 (3 H, t, *J* = 7.2 Hz), 0.91 (3 H, t, *J* = 7.2 Hz), 1.38 – 1.74 (5 H, m), 1.75 – 1.84 (1 H, m), 1.88 – 1.96 (1 H, m), 2.85 – 2.95 (3 H, m), 3.87 (1 H, d, *J* = 4.0 Hz), 4.01 (1 H, s), 7.19 – 7.23 (1 H, m) for 7-(2-(phenylthio)ethyl)-2,5-dipropyl-2,5-diazabicyclo[2.2.2]octane-3,6-dione **4.31**. These signals are consistent with the literature values and reference samples (**4.30**: Section 9.2.2, Table 4.1, entry 1 on page 187; **4.43**: Section 9.2.5, Table 4.3, entry 1 on page 194). The crude material was purified by column chromatography (0 - 100% ethyl acetate in hexane) to yield both diphenyl disulfide **4.30**[169] (3 mg, 27%) as white crystals and 7-(2-(phenylthio)ethyl)-2,5-dipropyl-2,5-diazabicyclo[2.2.2]octane-3,6-dione **4.31** (4.9 mg, 14%) as a brown oil [Found: (HRMS-EI) 360.1870. $C_{20}H_{28}N_2O_2S$ (M)$^{\bullet+}$ requires 360.1871]; v_{max}(film) / cm^{-1} 2961, 2926, 2872, 1668, 1456, 1429 1290, 1258, 1120, 1070, 1024, 739; ^{1}H-NMR (400 MHz, $CDCl_3$) δ 0.84 (3 H, t, *J* = 7.2 Hz, C*H*$_3$), 0.91 (3 H, t, *J* = 7.2 Hz, C*H*$_3$), 1.38 – 1.46 (1 H, m, C*H*$_2$), 1.47 – 1.63 (4 H, m, C*H*$_2$), 1.64 – 1.72 (1 H, m, C*H*), 1.75 – 1.84 (1 H, m, C*H*$_2$), 1.88 – 1.96 (1 H, m, C*H*$_2$), 1.99 – 2.10 (1 H, m, C*H*$_2$), 2.85 – 2.95 (3 H, m, 2 x C*H*$_2$ and C*H*$_2$), 3.16 – 3.20 (1 H, m, C*H*$_2$), 3.46 – 3.54 (2 H, m, C*H*$_2$), 3.87 (1 H, d, *J* = 4.0 Hz, C*H*), 4.01 (1 H, s, C*H*), 7.19 – 7.23 (1 H, m, Ar*H*), 7.28 – 7.36 (4 H, m, Ar*H*); ^{13}C{^{1}H}-NMR (100 MHz, $CDCl_3$) δ 11.2 (CH_3), 11.4 (CH_3), 21.0 (CH_2), 21.6 (CH_2), 25.2 (CH_2), 27.4 (CH_2), 37.2 (CH_2), 37.7

(CH), 46.4 (CH$_2$), 47.1 (CH$_2$), 59.9 (CH), 62.6 (CH), 126.7 (CH), 129.3 (2 x CH), 129.7 (2 x CH), 135.4 (C), 167.3 (C), 170.4 (C); HSQC (^{1}H/^{13}C) δ 0.84/11.2, 0.91/11.4, (1.38 – 1.46)/27.4, (1.47 – 1.63)/21.0, (1.47 – 1.63)/21.6, (1.64 – 1.72)/37.7, (1.75 – 1.84)/25.2, (1.88 – 1.96)/27.4, (1.99 – 2.10)/25.2, (2.85 – 2.95)/37.2, (2.85 – 2.95)/46.4, (3.16 – 3.20)/47.1, (3.46 – 3.54)/46.4, (3.46 – 3.54)/47.1, 3.87/59.9, 4.01/62.6, (7.19 – 7.23)/126.7, (7.28 – 7.36)/129.3, (7.28 – 7.36)/129.7. (*The yields of **4.30** and **4.31** were determined based on 0.1 mmol of DKP as the limiting reagent*).

Example yield calculation using 1,3,5-trimethoxybenzene as the internal standard ^{1}H-NMR of the crude mixture:

1,3,5-Trimethoxybenzene (16.8 mg, 0.10 mmol) was added to the crude mixture. The integral for the aromatic protons (δ 6.09) is set to 3 units representing 3 protons. For the coupled product, 2,6-dimethylbiphenyl **4.44**, the integral of the dimethyl signal (δ 2.03 has 6 H) was measured and the following calculation gave the yield of coupled product:
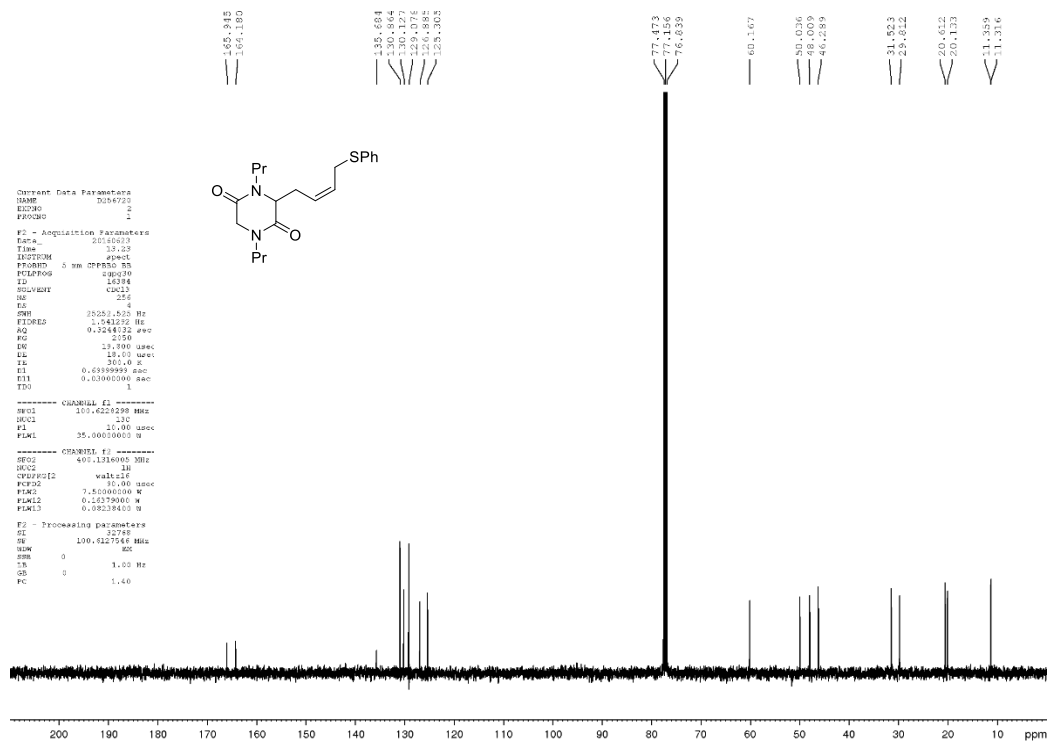
(1.08/6) × 0.1 mmol = 0.018 mmol

(0.018 mmol/0.5 mmol) × 100 = 3.6% = 4%
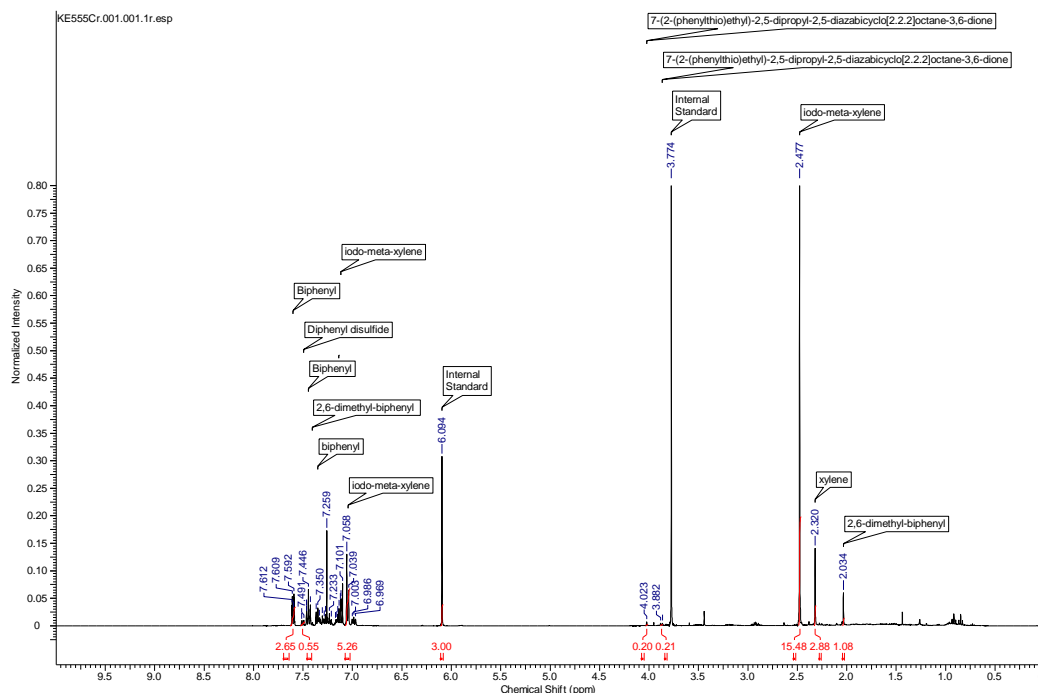
NMR of novel compounds in Chapter 4

<h3 style="text-align:center">^{1}H-NMR and ^{13}C{^{1}H}-NMR 4.16</h3>

^{1}H-NMR and ^{13}C{^{1}H}-NMR 4.17
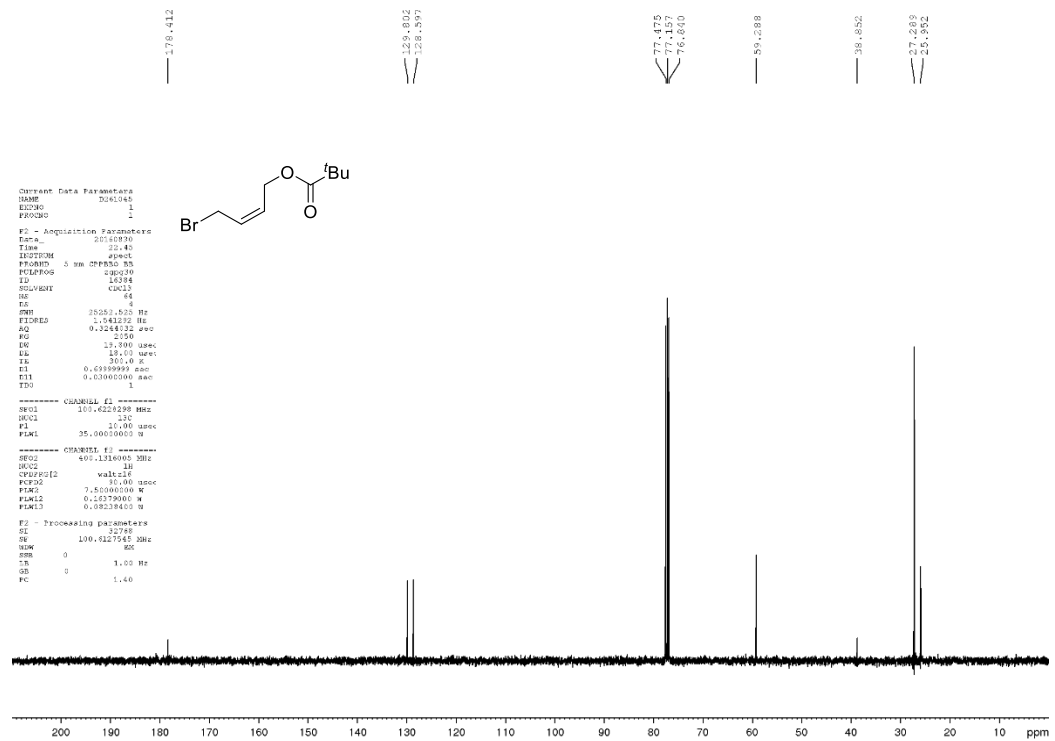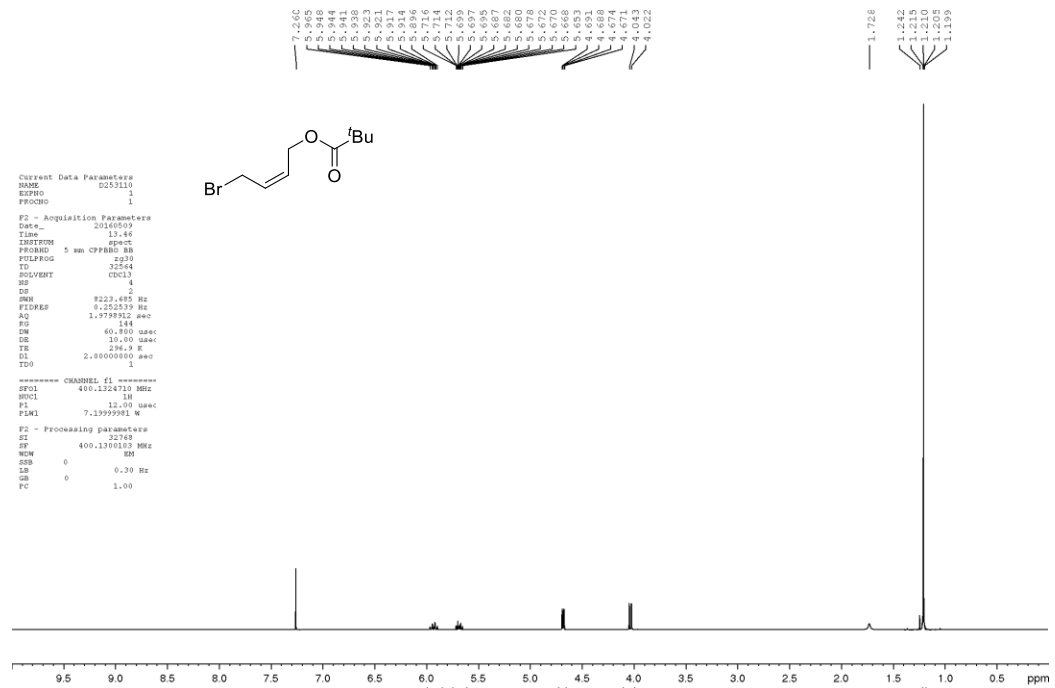
¹H-NMR and ¹³C{¹H}-NMR 4.18

^{1}H-NMR and ^{13}C{^{1}H}-NMR 9.4.6
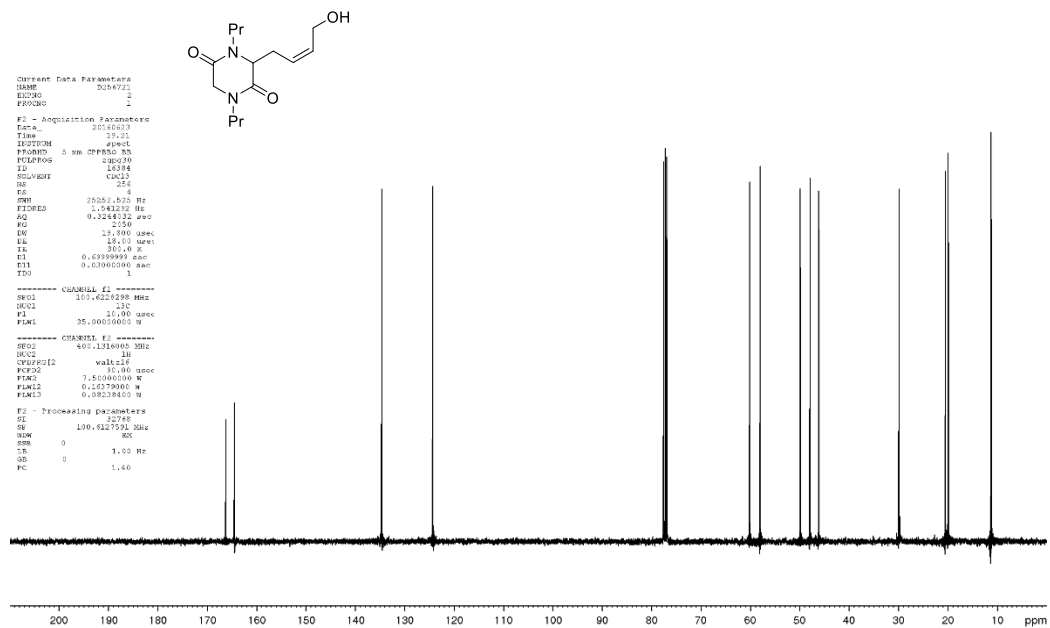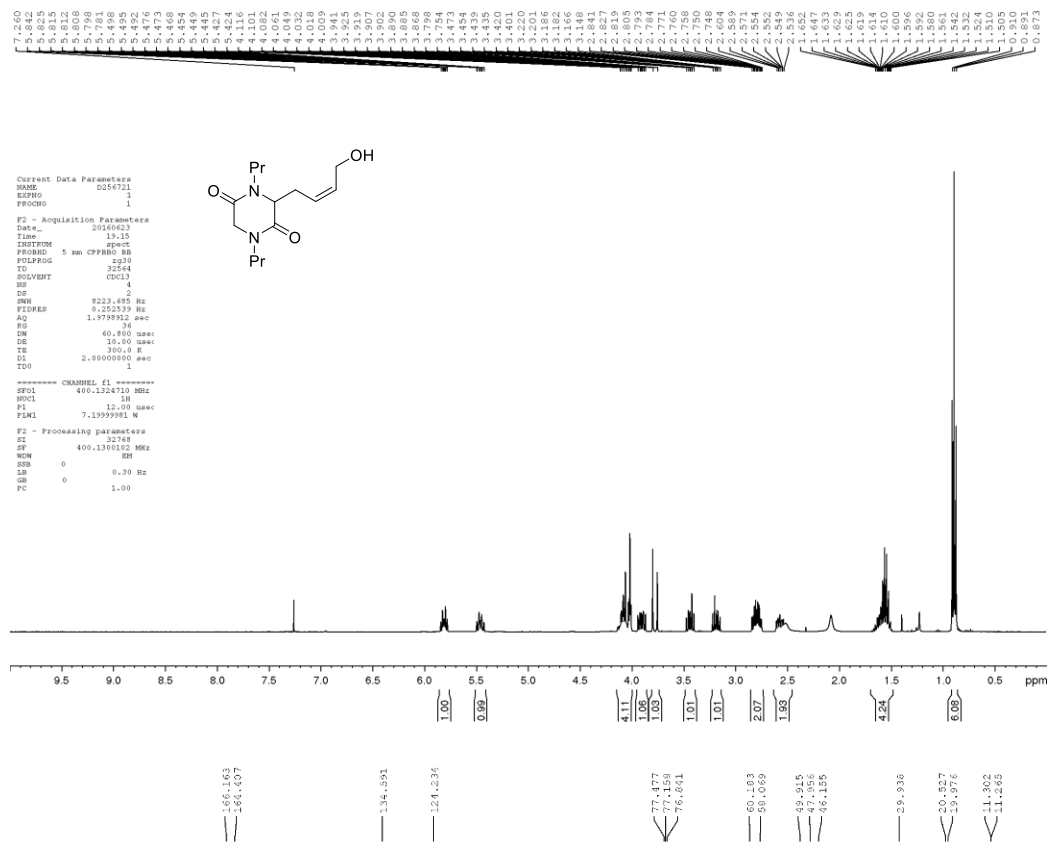
^{1}H-NMR and ^{13}C{^{1}H}-NMR 4.19

HSQC 4.19

HMBC 4.19

^{1}H-NMR and ^{13}C{^{1}H}-NMR 4.32

HSQC 4.32

HMBC 4.32

^{1}H-NMR and ^{13}C{^{1}H}-NMR 4.31

HSQC 4.31

HMBC 4.31

^{1}H-NMR and ^{13}C{^{1}H}-NMR 4.40

¹H-NMR and ¹³C{¹H}-NMR 4.41
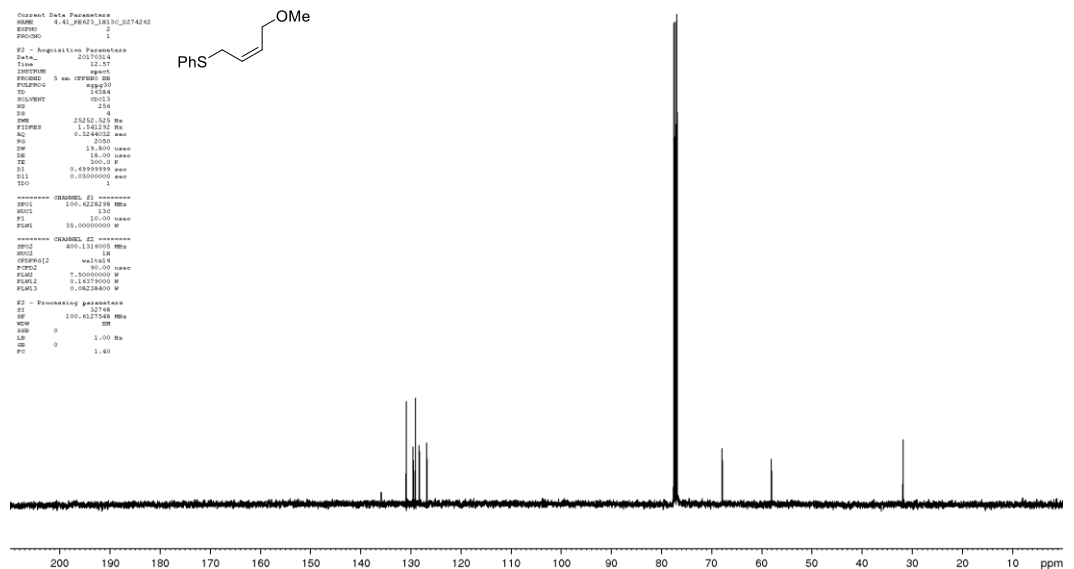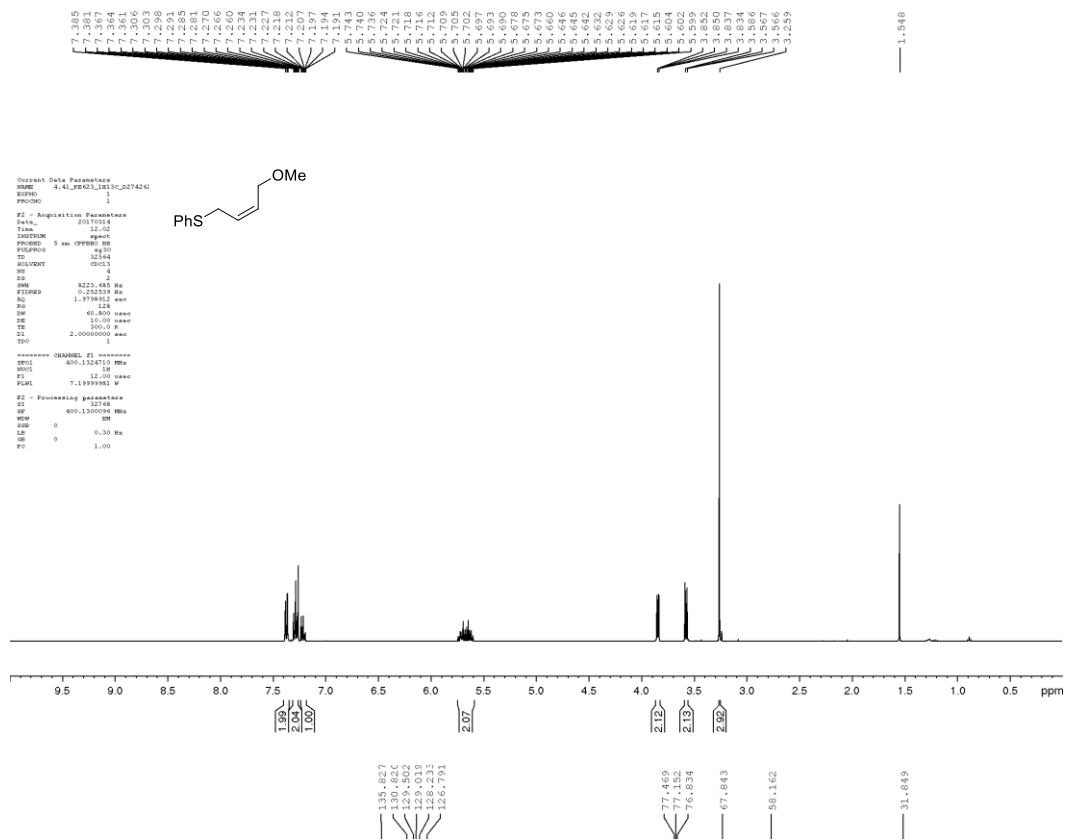
9.3 Experimental details for Chapter 5

9.3.1 Synthesis of a reference sample of 5.9[175]
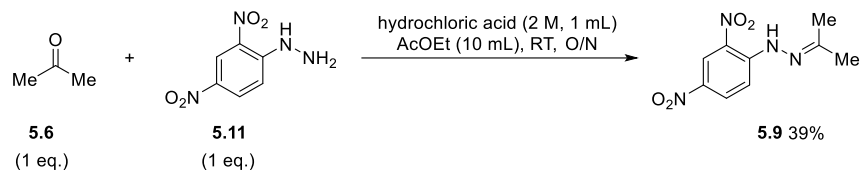
Ethyl acetate (10 mL) and aqueous hydrochloric acid (2 M, 1 mL) were added to a round-bottomed flask, and the reaction mixture was stirred at RT for 5 min. Acetone **5.6** (0.04 mL, 0.5 mmol) and 2,4-dinitrophenylhydrazine **5.11** (99 mg, 0.5 mmol, 1.0 eq.) were added and the reaction mixture was stirred at RT for 24 h. The reaction mixture was washed with brine and the organic phase was dried over Na_2SO_4, filtered and concentrated *in vacuo*. The crude material was purified by column chromatography (10% ethyl acetate in hexane) to give 1-(2,4-dinitrophenyl)-2-(propan-2-ylidene)hydrazine **5.9**[175] (46.7 mg, 39%) as pale orange crystals m.p. 122 - 123 °C (lit:[176] 121 - 122 °C); [Found: (HRMS-NSI) 239.0777. $C_9H_{11}N_4O_4^+$ (M+H)$^+$ requires 239.0775]; v_{max}(film) / cm^{-1} 3310, 3103, 1612, 1589, 1517, 1495, 1422, 1329, 1306, 1277, 1248, 1132, 1099, 1061, 922, 839, 743; ^{1}H-NMR (400 MHz, CDCl$_3$) δ 2.09 (3 H, s, C*H$_3$*), 2.18 (3 H, s, C*H$_3$*), 7.96 (1 H, d, *J* = 9.6 Hz, Ar*H*), 8.30 (1 H, dd, *J* = 9.6, 2.4 Hz, Ar*H*), 9.13 (1 H, d, *J* = 2.4 Hz, Ar*H*), 11.03 (1 H, br s, N*H*); ^{13}C{^{1}H}-NMR (100 MHz, CDCl$_3$) δ 17.2 (CH$_3$), 25.6 (CH$_3$), 116.5 (CH), 123.7 (CH), 129.1 (C), 130.2 (CH), 137.8 (C), 145.3 (C), 155.3 (C).

9.3.2 Detecting acetone in transition metal-free reactions (Table 5.1)

Table 5.1, entry 1
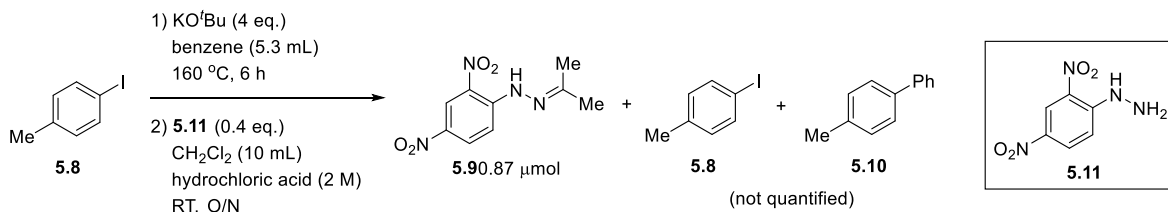
All the equipment used in this experiment was oven-dried. 4-Iodotoluene **5.8** (109 mg, 0.5 mmol) was added to an oven-dried pressure tube. In the glove box, KO^{t}Bu (224 mg, 2 mmol, 4.0 eq.) and anhydrous benzene (5.3 mL) were added. The reaction mixture was stirred at 160 °C for 6 h and then cooled to 0 °C. Aqueous

hydrochloric acid (2 M, 1 mL) and anhydrous dichloromethane (10 mL) were added and the reaction mixture was stirred at RT for 5 min. 2,4-Dinitrophenylhydrazine **5.11** (40 mg, 0.2 mmol, 0.4 eq.) was added and the reaction mixture was stirred at RT overnight. The reaction mixture was phase-separated and the organic phase was dried over Na_2SO_4, filtered and concentrated *in vacuo*. The crude material was purified by column chromatography (0 – 5% ethyl acetate in hexane) to give a crude mixture as a yellow solid. The yield of 1-(2,4-dinitrophenyl)-2-(propan-2-ylidene)hydrazine **5.9** (0.87 µmol) was determined by adding 1,3,5-trimethoxybenzene to the crude mixture as an internal standard for ^{1}H-NMR. The product 1-(2,4-dinitrophenyl)-2-(propan-2-ylidene)hydrazine **5.9** was identified by the following characteristic signals; ^{1}H-NMR (400 MHz, CDCl$_3$) δ 2.09 (3 H, s), 2.18 (3 H, s), 7.96 (1 H, d, *J* = 9.6 Hz), 8.30 (1 H, dd, *J* = 9.6, 2.4 Hz), 9.13 (1 H, d, *J* = 2.4 Hz), 11.03 (1 H, br s). These signals are consistent with the reference sample (Section 9.3.1 on page 210).
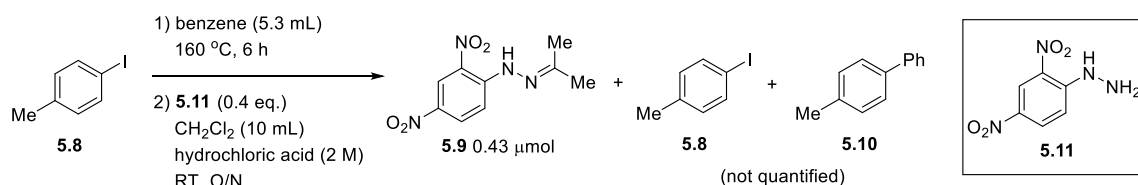
Table 5.1, entry 2

All the equipment used in this experiment was oven-dried. 4-Iodotoluene **5.8** (109 mg, 0.5 mmol) was added to an oven-dried pressure tube. In the glove box, anhydrous benzene (5.3 mL) was added. The reaction mixture was stirred at 160 °C for 6 h. The reaction mixture was cooled to 0 °C. Aqueous hydrochloric acid (2 M, 1 mL) and anhydrous dichloromethane (10 mL) were added and the reaction mixture was stirred at RT for 5 min. 2,4-Dinitrophenylhydrazine **5.11** (40 mg, 0.2 mmol, 0.4 eq.) was added and the reaction mixture was stirred at RT overnight. The reaction mixture was phase-separated and the organic phase was dried over Na_2SO_4, filtered and concentrated *in vacuo*. The crude material was purified by column chromatography (0 – 5% ethyl acetate in hexane) to give a crude mixture as a brown oil. The yield of 1-(2,4-dinitrophenyl)-2-(propan-2-ylidene)hydrazine **5.9** (0.43 µmol) was determined by adding 1,3,5-trimethoxybenzene to the crude mixture as an

internal standard for ^{1}H-NMR. The product 1-(2,4-dinitrophenyl)-2-(propan-2-ylidene)hydrazine **5.9** was identified by the following characteristic signals; ^{1}H-NMR (400 MHz, CDCl₃) δ 2.09 (3 H, s), 2.18 (3 H, s), 7.96 (1 H, d, *J* = 9.6 Hz), 8.30 (1 H, dd, *J* = 9.6, 2.4 Hz), 9.13 (1 H, d, *J* = 2.4 Hz), 11.03 (1 H, br s). These signals are consistent with the reference sample (Section 9.3.1 on page 210).

9.3.3 Reaction of 5.11 in benzene, in an attempt to remove adventitious acetone (Scheme 5.2)
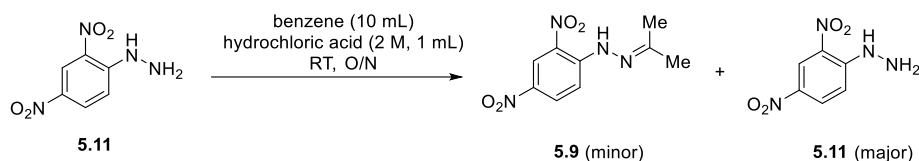
All the equipment used in this experiment was oven-dried. 2,4-Dinitrophenylhydrazine **5.11** (40 mg, 0.2 mmol, 0.4 eq.) was added to an oven-dried pressure tube. In the glove box, anhydrous benzene (5.3 mL) and aqueous hydrochloric acid (2 M, 1 mL) were added and the reaction mixture was stirred at RT overnight. In the glove box, the reaction mixture was quenched by dropwise addition of NaOH (2 M) until pH was neutral. The reaction mixture was phase-separated and the solvent was removed by vacuum in the glove box to give a crude mixture as an orange solid (3 mg). The product 1-(2,4-dinitrophenyl)-2-(propan-2-ylidene)hydrazine **5.9** was identified as a minor component in the crude mixture by the following characteristic signals; ^{1}H-NMR (400 MHz, CDCl₃) δ 2.09 (3 H, s), 2.18 (3 H, s), 7.96 (1 H, d, *J* = 9.6 Hz), 8.30 (1 H, dd, *J* = 9.6, 2.4 Hz), 9.13 (1 H, d, *J* = 2.4 Hz), 11.03 (1 H, br s). These signals are consistent with the reference sample (Section 9.3.1 on page 210).

9.3.4 Synthesis of alkoxide, *potassium 2-phenylpropan-2-olate* **5.12**
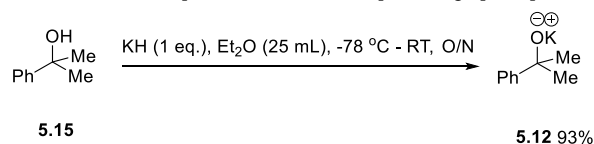
Potassium hydride (586 mg, 15 mmol, 1.0 eq.) was added to a flame-dried three-necked flask, equipped with a vacuum tap. Under an argon atmosphere, at -78 °C, a solution of 2-phenylpropanol **5.15** (2.04 g, 15 mmol) in anhydrous diethyl ether (20

mL) as added and the reaction mixture was stirred at -78 °C for 1 h, then at RT overnight. The solvent was removed on the house vacuum line and the crude material was dried for 1 h to obtain *potassium 2-phenylpropan-2-olate* **5.12** (2.46 g, 14.1 mmol, 93%) as an off-white solid m.p. 128 – 132 °C; [Found: (GCMS-EI) $C_9H_{11}O^-$ (M-K)$^-$ 135.08]; v_{max}(film) / cm^{-1} 3503, 2972, 1663, 1444, 1433, 1236, 1161, 1067, 1029, 955, 881, 861, 764; ^{1}H-NMR (400 MHz, d^6-DMSO) δ 1.41 (6 H, s, 2 x CH_3), 7.15 – 7.19 (1 H, m, ArH), 7.26 – 7.30 (2 H, m, ArH), 7.45 – 7.47 (2 H, m, ArH); ^{13}C{^{1}H}-NMR (100 MHz, d^6-DMSO) δ 31.9 (2 x CH_3), 70.5 (C), 124.4 (2 x CH), 125.8 (CH), 127.7 (2 x CH), 150.5 (C). The product was put under an argon atmosphere, and transported into the glove box immediately.

9.3.5 Synthesis of a reference sample of 5.16[177]
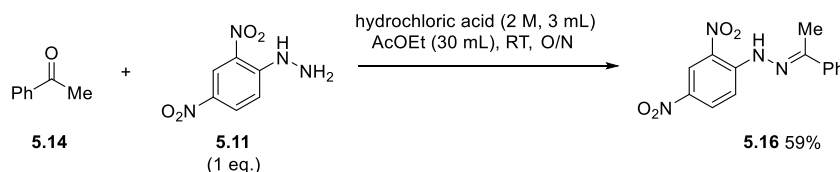
Acetophenone **5.14** (60 mg, 0.5 mmol), ethyl acetate (10 mL) and hydrochloric acid (2 M, 3 mL) were added to a round-bottomed flask and the reaction mixture was stirred at RT for 5 min. 2,4-Dinitrophenylhydrazine **5.11** (99 mg, 0.5 mmol, 1.0 eq.) and ethyl acetate (20 mL) were added and the reaction mixture was stirred at RT for 24 h. The reaction mixture was filtered to yield 1-(2,4-dinitrophenyl)-2-(1-phenylethylidene)hydrazine **5.16**[177] (88.1 mg, 59%) as red crystals m.p. 236 - 238 °C (lit:[178] 238 °C); [Found: (GCMS-CI) $C_{14}H_{11}N_4O_4^-$ (M-H)$^-$ 298.9]; v_{max}(film) / cm^{-1} 3302, 1615, 1583, 1513, 1506, 1492, 1416, 1328, 1311, 1298, 1258, 1219, 1111, 923, 839, 832, 759, 743, 719; ^{1}H-NMR (400 MHz, CDCl$_3$) δ 2.48 (3 H, s, CH_3), 7.46 – 7.47 (3 H, m, ArH), 7.85 – 7.87 (2 H, m, ArH), 8.14 (1 H, d, J = 9.6 Hz, ArH), 8.37 (1 H, dd, J = 9.6, 2.8 Hz, ArH), 9.17 (1 H, d, J = 2.8 Hz, ArH), 11.36 (1 H, br s, NH); ^{13}C{^{1}H}-NMR (100 MHz, CDCl$_3$) δ 13.9 (CH_3), 116.9 (CH), 123.7 (CH), 126.7 (2 x CH), 128.9 (2 x CH), 129.9 (C), 130.3 (CH), 130.3 (CH), 137.4 (C), 138.4 (C), 145.2 (C), 152.5 (C).

9.3.6 Detecting acetophenone in transition metal-free reactions (Table 5.2)

Table 5.2, entry 1
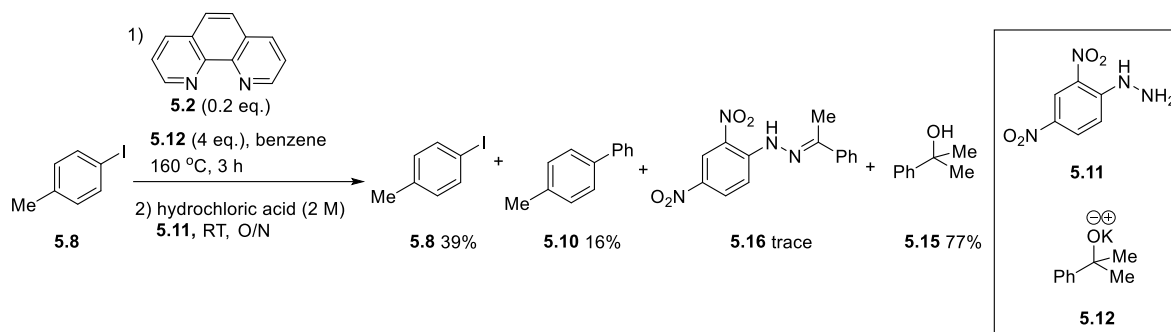
4-Iodotoluene **5.8** (218 mg, 1.0 mmol) and 1,10-phenanthroline **5.2** (36 mg, 0.2 mmol, 0.2 eq.) were added to an oven-dried pressure tube. In the glove box, potassium 2-phenylpropan-2-olate **5.12** (697 mg, 4 mmol, 4.0 eq.) and anhydrous benzene (10 mL) were added. The reaction was stirred at 160 °C for 3 h, and then cooled to RT. Aqueous hydrochloric acid (2 M, 2 mL) and ethyl acetate (10 mL) were added and the reaction mixture was stirred at RT for 5 min. 2,4-Dinitrophenylhydrazine **5.11** (80 mg, 0.4 mmol, 0.4 eq.) was added and the reaction mixture was stirred at RT overnight. The reaction mixture was phase-separated and the organic phase was dried over Na_2SO_4, filtered and concentrated *in vacuo*. The crude material was purified by column chromatography (0 – 20% ethyl acetate in hexane) to give several products: 4-iodotoluene **5.8** (86 mg, 39%) as colourless crystals, 4-methylbiphenyl **5.10** (26.3 mg, 16%) as pale pink crystals m.p. 39 – 41 °C (lit:[179] 41 – 43 °C); [Found: (LCMS-APCI) 168.1. $C_{13}H_{12}$ (M)$^{•+}$ requires 168.1]; v_{max} (film)/cm^{-1} 3055, 3032, 2915, 2859, 1485, 1403, 1377, 1201, 1129, 140, 1006, 823, 752, 736, 689; ^{1}H-NMR (400 MHz, CDCl$_3$) δ 2.40 (3 H, s, C*H*$_3$), 7.24 – 7.26 (2 H, m, Ar*H*), 7.30 – 7.34 (1 H, m, Ar*H*), 7.43 (2 H, d, *J* = 8.0 Hz, Ar*H*), 7.49 (2 H, d, *J* = 8.0 Hz, Ar*H*), 7.57 (2 H, d, *J* = 8.0 Hz, Ar*H*); ^{13}C{^{1}H}-NMR (100 MHz, CDCl$_3$) δ 21.2 (CH$_3$), 127.1 (5 x CH), 128.9 (2 x CH), 129.6 (2 x CH), 137.2 (C), 138.5 (C), 141.3 (C), 2-phenylpropanol **5.15** (189.9 mg, 77%) as an orange solid and a crude mixture containing 1-(2,4-dinitrophenyl)-2-(1-phenylethylidene)hydrazine **5.16** (trace) as an orange oil. The product **5.16** was identified by the following characteristic signals; ^{1}H-NMR (400 MHz, CDCl$_3$) δ 2.48 (3 H, s), 7.46 – 7.47 (3 H, m), 7.85 – 7.87 (2 H, m), 8.14 (1 H, d, *J* = 9.6 Hz), 8.37 (1 H, dd, *J* = 9.6, 2.8 Hz), 9.17 (1 H, d, *J* = 2.8 Hz), 11.36 (1 H, br s)

for 1-(2,4-dinitrophenyl)-2-(1-phenylethylidene)hydrazine **5.16**. These signals are consistent with the reference sample (Section 9.3.5 on page 213).

4-Iodotoluene **5.8** (86 mg, 39%) as colourless crystals ^{1}H-NMR (400 MHz, CDCl$_3$) δ 2.30 (3 H, s, CH_3), 6.92 (2 H, d, J = 8.4 Hz, ArH), 7.57 (2 H, d, J = 8.4 Hz, ArH); ^{13}C{^{1}H}-NMR (100 MHz, CDCl$_3$) δ 21.2 (CH$_3$), 90.3 (C), 131.3 (2 x CH), 137.4 (2 x CH), 137.6 (C). These signals are consistent with a commercial sample used as a reference.

2-Phenylpropanol **5.15**[180] (189.9 mg, 77%) as an orange solid ^{1}H-NMR (400 MHz, CDCl$_3$) δ 1.60 (6 H, s, 2 x CH_3), 1.71 (1 H, br s, OH), 7.23 – 7.27 (1 H, m, ArH), 7.35 (2 H, t, J = 8.0 Hz, ArH), 7.50 (2 H, d, J = 8.0 Hz, ArH). ^{13}C{^{1}H}-NMR (100 MHz, CDCl$_3$) δ 31.9 (2 x CH$_3$), 72.7 (C), 124.5 (2 x CH), 126.8 (CH), 128.4 (2 x CH), 149.1 (C). These signals are consistent with a commercial sample used as a reference.
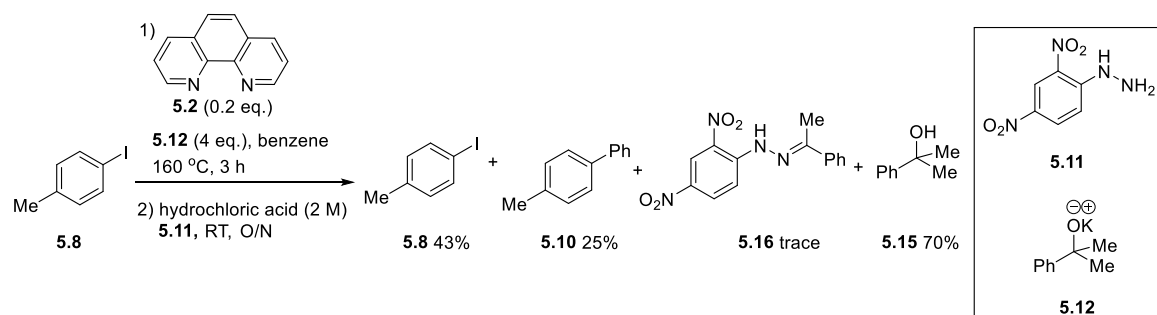
Table 5.2, entry 2

4-Iodotoluene **5.8** (109 mg, 0.5 mmol) and 1,10-phenanthroline **5.2** (18 mg, 0.1 mmol, 0.2 eq.) were added to an oven-dried pressure tube. In the glove box, potassium 2-phenylpropan-2-olate **5.12** (349 mg, 2 mmol, 4.0 eq.) and anhydrous benzene (5 mL) were added. The reaction was stirred at 160 °C for 3 h. The reaction mixture was cooled to RT. Aqueous hydrochloric acid (2 M, 2 mL) and ethyl acetate (10 mL) were added and the reaction mixture was stirred at RT for 5 min. 2,4-Dinitrophenylhydrazine **5.11** (40 mg, 0.2 mmol, 0.4 eq.) was added and the reaction mixture was stirred at RT overnight. The reaction mixture was phase-separated and the organic phase was dried over Na$_2$SO$_4$, filtered and concentrated *in vacuo*. The crude material was purified by column chromatography (0 - 20% ethyl acetate in hexane) to give 4-iodotoluene **5.8** (46 mg, 43%) as pale yellow crystal, 4-methylbiphenyl **5.10** (21 mg, 25%) as pale yellow crystals, 2-phenylpropanol **5.15**

215

(189.9 mg, 70%) as an orange solid and a crude mixture containing 1-(2,4-dinitrophenyl)-2-(1-phenylethylidene)hydrazine **5.16** (trace). The product **5.16** was identified by the following characteristic signals; ^{1}H-NMR (400 MHz, CDCl$_3$) δ 2.48 (3 H, s), 7.46 – 7.47 (3 H, m), 7.85 – 7.87 (2 H, m), 8.14 (1 H, d, *J* = 9.6 Hz), 8.37 (1 H, dd, *J* = 9.6, 2.8 Hz), 9.17 (1 H, d, *J* = 2.8 Hz), 11.36 (1 H, br s) for 1-(2,4-dinitrophenyl)-2-(1-phenylethylidene)hydrazine **5.16**. These signals are consistent with reference samples (**5.8**, **5.10**, **5.15**: Section 9.3.6 on page 214-5, Table 5.2, entry 1; **5.16**: Section 9.3.5 on page 213).

9.3.7 Identifying the source of acetophenone (Scheme 5.4)

<div align="center">

Scheme 5.4A

</div>
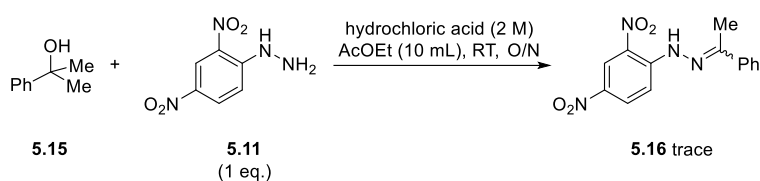
2-Phenylpropanol **5.15** (68 mg, 0.5 mmol), ethyl acetate (10 mL) and aqueous hydrochloric acid (2 M, 1 mL) were added to a round-bottomed flask and the reaction mixture was stirred at RT for 5 min. 2,4-Dinitrophenylhydrazine **5.11** (99 mg, 0.5 mmol, 1.0 eq.) was added and the reaction mixture was stirred at RT for 24 h. The reaction mixture was phase-separated and the organic layer was washed with brine, dried over Na$_2$SO$_4$, filtered and concentrated *in vacuo*. The crude material was purified by column chromatography (5% ethyl acetate in hexane) to give a crude mixture (1.7 mg) as a yellow oil containing 1-(2,4-dinitrophenyl)-2-(1-phenylethylidene)hydrazine **5.16**. The product **5.16** was identified by the following characteristic signals; ^{1}H-NMR (400 MHz, CDCl$_3$) δ 2.48 (3 H, s), 7.46 – 7.47 (3 H, m), 7.85 – 7.87 (2 H, m), 8.14 (1 H, d, *J* = 9.6 Hz), 8.37 (1 H, dd, *J* = 9.6, 2.8 Hz), 9.17 (1 H, d, *J* = 2.8 Hz), 11.36 (1 H, br s) for 1-(2,4-dinitrophenyl)-2-(1-phenylethylidene)hydrazine **5.16**. These signals are consistent with the reference sample (Section 9.3.5 on page 213).

Scheme 5.4B
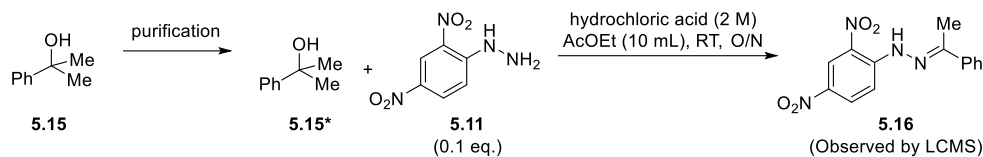
The commercially available 2-phenylpropanol **5.15** was purified by column chromatography (0 - 15% ethyl acetate in hexane) to provide pure 2-phenylpropanol **5.15*** (1.77 g) as a colourless oil. The purified 2-phenylpropanol **5.15*** (272 mg, 2.0 mmol), ethyl acetate (10 mL) and aqueous hydrochloric acid (2 M, 1 mL) were added to an oven-dried round-bottomed flask was added and the reaction mixture was stirred at RT for 5 min. 2,4-Dinitrophenylhydrazine **5.11** (40 mg, 0.2 mmol, 0.1 eq.) was added and the reaction mixture was stirred at RT for 24 h. The reaction mixture was phase-separated and the organic layer was washed with brine, dried over Na_2SO_4, filtered and concentrated *in vacuo*. The crude material was purified by column chromatography (0 - 5% ethyl acetate in hexane) to give a crude mixture (8.9 mg) as a yellow oil. The product 1-(2,4-dinitrophenyl)-2-(1-phenylethylidene)hydrazine **5.16** was not observed by ^{1}H-NMR, but it was observed by LCMS [Found: (LCMS-CI) 299.0, time = 9.006 min. Reference sample **5.16** requires 299.1, time = 9.014 min].

Scheme 5.4C
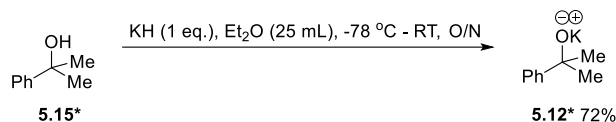
Potassium hydride (401 mg, 10 mmol, 1.0 eq.) was added to a flame-dried three-necked flask, equipped with a vacuum tap. Under an argon atmosphere, at -78 °C, a solution of the purified 2-phenylpropanol **5.15*** (1.36 g, 10 mmol) in anhydrous diethyl ether (15 mL) was added and the reaction mixture was stirred at -78 °C for 1 h, then at RT overnight. The solvent was removed on the house vacuum line and the crude material was dried for 1 h to give potassium 2-phenylpropan-2-olate **5.12*** (1.25 g, 72%) as an off-white solid, which was put under an argon atmosphere and transported into the glove box immediately.

Scheme 5.4D
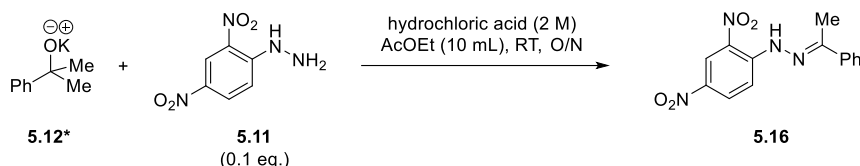
Potassium 2-phenylpropan-2-olate **5.12*** (349 mg, 2.0 mmol), ethyl acetate (10 mL) and aqueous hydrochloric acid (2 M, 1 mL) were added to an oven-dried round-bottomed flask and the reaction mixture was stirred at RT for 5 min. 2,4-Dinitrophenylhydrazine **5.11** (40 mg, 0.2 mmol, 0.1 eq.) was added and the reaction mixture was stirred at RT overnight. The reaction mixture was phase-separated and the organic phase was washed with brine, dried over Na$_2$SO$_4$, filtered and concentrated *in vacuo*. The crude material was purified by column chromatography (2% ethyl acetate in hexane) to give a crude mixture (0.6 mg) as a yellow oil containing 1-(2,4-dinitrophenyl)-2-(1-phenylethylidene)hydrazine **5.16**. The product 1-(2,4-dinitrophenyl)-2-(1-phenylethylidene)hydrazine **5.16** was identified by the following characteristic signals; ^{1}H-NMR (400 MHz, CDCl$_3$) δ 2.48 (3 H, s), 7.46 – 7.47 (3 H, m), 7.85 – 7.87 (2 H, m), 8.14 (1 H, d, *J* = 9.6 Hz), 8.37 (1 H, dd, *J* = 9.6, 2.8 Hz), 9.17 (1 H, d, *J* = 2.8 Hz), 11.38 (1 H, br s). These signals are consistent with the reference sample (Section 9.3.5 on page 213).

9.3.7 Reactions of 4-iodotoluene with different alkoxide bases (Table 5.3)

Table 5.3, entry 1
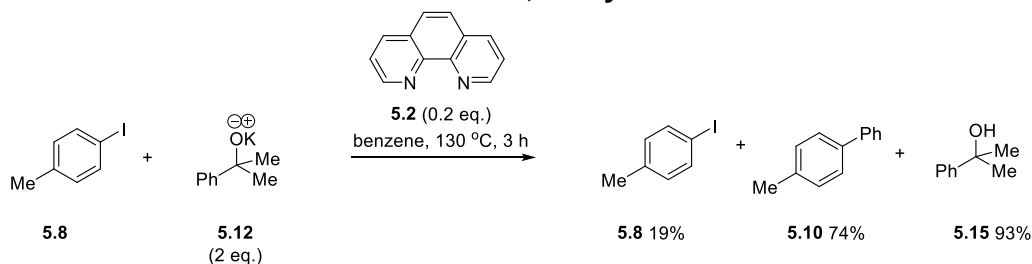
4-Iodotoluene **5.8** (109 mg, 0.5 mmol) and 1,10-phenanthroline **5.2** (18 mg, 0.1 mmol, 0.2 eq.) were added to an oven-dried pressure tube. In the glove box, potassium phenylpropan-2-olate **5.12** (174 mg, 1 mmol, 2.0 eq.) and anhydrous benzene (5 mL) were added and the reaction was stirred at 130 ºC for 3 h. The reaction mixture was cooled to RT and quenched with aqueous hydrochloric acid (1 M, 10 mL) and

extracted with diethyl ether (3 x 10 mL). The organic phases were dried over Na_2SO_4, filtered and concentrated *in vacuo*. The yields of 4-iodotoluene **5.8** (19%), 4-methylbiphenyl **5.10** (74%) and 2-phenylpropanol **5.15** (93%) were determined by adding 1,3,5-trimethoxybenzene to the crude mixture as an internal standard for ^{1}H-NMR. The products were identified by the following characteristic signals; ^{1}H-NMR (400 MHz, $CDCl_3$) δ 2.30 (3 H, s), 6.92 (2 H, d, *J* = 8.4 Hz) for 4-iodotoluene **5.8**; δ 2.40 (3 H, s), 7.43 (2 H, d, *J* = 7.6 Hz) for 4-methylbiphenyl **5.10**; δ 1.60 (6 H, s), 1.71 (1 H, br s), 7.23 – 7.27 (1 H, m), 7.35 (2 H, t, *J* = 8.0 Hz), 7.50 (2 H, d, *J* = 8.0 Hz) for 2-phenylpropanol **5.15**. These signals are consistent with the literature values and reference samples (**5.8**, **5.10**, **5.15**: Section 9.3.6, Table 5.2, entry 1 on page 214-5).

Table 5.3, entry 2

4-Iodotoluene **5.8** (109 mg, 0.5 mmol) and 1,10-phenanthroline **5.2** (18 mg, 0.1 mmol, 0.2 eq.) were added to an oven-dried pressure tube. In the glove box, KO^{t}Bu **5.1** (112 mg, 1 mmol, 2.0 eq.) and anhydrous benzene (5 mL) were added and the reaction was stirred at 130 °C for 3 h. The reaction mixture was cooled to RT and quenched with saturated aqueous hydrochloric acid (1 M, 10 mL) and extracted with diethyl ether (3 x 10 mL). The organic phases were combined, dried over Na_2SO_4, filtered and concentrated *in vacuo*. The yield of 4-methylbiphenyl **5.10** (95%) was determined by adding 1,3,5-trimethoxybenzene to the crude mixture as an internal standard for ^{1}H-NMR. The product was identified by the following characteristic signals; ^{1}H-NMR (400 MHz, $CDCl_3$) δ 2.40 (3 H, s), 7.43 (2 H, d, *J* = 7.6 Hz) for 4-methylbiphenyl **5.10**. These signals are consistent with the literature values and reference samples (Section 9.3.6, Table 5.2, entry 1).

Table 5.3, entry 3

4-Iodotoluene **5.8** (109 mg, 0.5 mmol) and 1,10-phenanthroline **5.2** (18 mg, 0.1 mmol, 0.2 eq.) were added to an oven-dried pressure tube. In the glov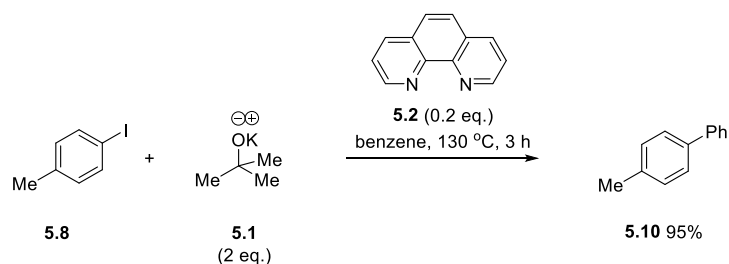e box, potassium phenylpropan-2-olate **5.12** (349 mg, 2 mmol, 4.0 eq.) and anhydrous benzene (5 mL) were added and the reaction was stirred at 160 °C for 3 h. The reaction mixture was cooled to RT and quenched with aqueous hydrochloric acid (1 M, 10 mL) and extracted with diethyl ether (3 x 20 mL). The organic phases were combined and dried over Na_2SO_4, filtered and concentrated *in vacuo*. The crude material was purified by column chromatography (0 - 20% ethyl acetate in petroleum ether) to give 4-methylbiphenyl **5.10** (64.5 mg, 76%) as pink crystals and 2-phenylpropanol **5.15** (205.4 mg, 73%) as a yellow oil. The spectra are consistent with the reference samples (Section 9.3.6, Table 5.2, entry 1 on page 214-5).

Table 5.3, entry 4
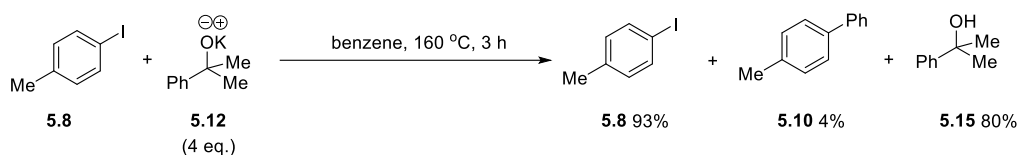
4-Iodotoluene **5.8** (109 mg, 0.5 mmol) was added to an oven-dried pressure tube. In the glove box, potassium phenylpropan-2-olate **5.12** (349 mg, 2 mmol, 4.0 eq.) and anhydrous benzene (5 mL) were added and the reaction was stirred at 160 °C for 3 h. The reaction mixture was cooled to RT, and quenched wi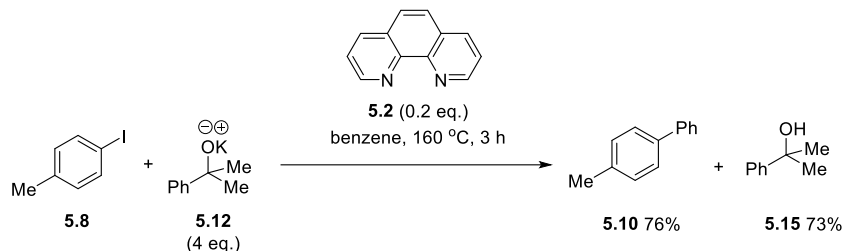th aqueous hydrochloric acid (1 M, 10 mL) and extracted with diethyl ether (3 x 20 mL). The organic phases were combined and dried over Na_2SO_4, filtered and concentrated *in vacuo*. The crude material was purified by column chromatography (0 - 20% ethyl acetate in petroleum ether) to give 2-phenylpropanol **5.15** (217.4 mg, 80%) as a colourless oil and a crude mixture containing 4-methylbiphenyl **5.10** and 4-iodotoluene **5.8** (105.2 mg) as a colourless oil [Based on the integration of signals in the ^{1}H-NMR, the ratio

of **5.10** and **5.8** was calculated to be 1 : 16 respectively. Using this ratio, and the mass of the crude material obtained, yields of products were calculated: **5.10** (4%) and **5.8** (93%)]. The spectra are consistent with the reference samples (Section 9.3.6, Table 5.2, entry 1 on page 214-5).

### 9.3.8 Reaction of iodo-*m*-xylene 5.20 with alkoxide 5.12 (Scheme 5.6)
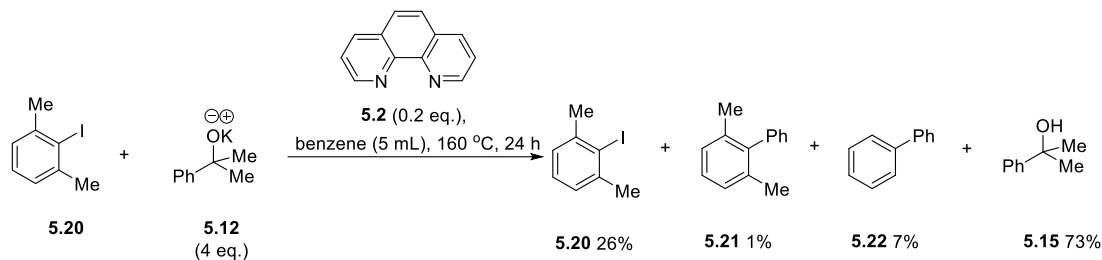
Iodo-*m*-xylene **5.20** (116 mg, 0.5 mmol) and 1,10-phenanthroline **5.2** (18 mg, 0.1 mmol, 0.2 eq.) were added to an oven-dried pressure tube. In the glove box, potassium phenylpropan-2-olate **5.12** (349 mg, 2 mmol, 4.0 eq.) and anhydrous benzene (5 mL) were added and the reaction was stirred at 160 °C for 24 h. The reaction mixture was cooled to RT and quenched with aqueous hydrochloric acid (1 M, 10 mL) and extracted with ethyl acetate (4 x 10 mL). The organic phases were combined, dried over Na₂SO₄, filtered and concentrated *in vacuo*. The crude material was purified by column chromatography (0 - 20% ethyl acetate in petroleum ether) to give 2-phenylpropanol **5.15** (199.3 mg, 73%) as a pale brown oil, iodo-*m*-xylene **5.20** (29.7 mg, 26%) as a colourless oil, and an inseparable mixture of 2,6-dimethylbiphenyl **5.21** and biphenyl **5.22** (4.6 mg) as colourless crystals. The yields of 2,6-dimethylbiphenyl **5.21**[172] (1%), biphenyl **5.22**[174] (7%) were determined by adding 1,3,5-trimethoxybenzene to the crude mixture as an internal standard for ^{1}H-NMR. The products were identified by the following characteristic signals; ^{1}H-NMR (400 MHz, CDCl₃) δ 2.03 (6 H, s), 7.14 – 7.20 (5 H, m), 7.40 – 7.49 (3 H, m) (partly obscured by biphenyl peaks) for 2,6-dimethylbiphenyl **5.21**;[172] δ 7.36 (2 H, d, *J* = 8.0 Hz), 7.45 (4 H, t, *J* = 8.0 Hz), 7.60 (4 H, d, *J* = 8.0 Hz) for biphenyl **5.22**.[174] These signals are consistent with the literature values and reference samples (**5.15** Section 9.3.6, Table 5.2, entry 1 on page 5; **5.20**: Section 9.2.5, Table 4.3, entry 1 on page 194).

9.3.9 Attempted synthesis of alkoxide 5.26 (Scheme 5.7)

Synthesis of trimethyl((1,1a,2,3-tetrahydro-7bH-cyclopropa[a]naphthalen-7b-yl)oxy)silane 9.5.2
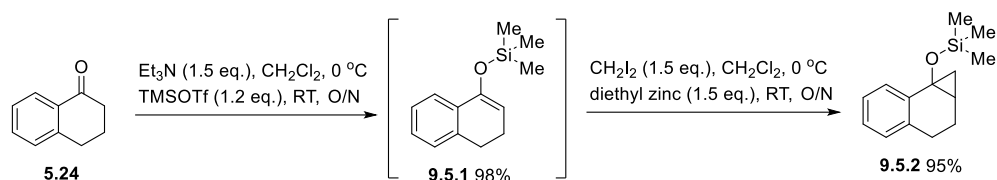
α-Tetralone **5.24** (5.3 mL, 40 mmol) and anhydrous dichloromethane (240 mL) were added to a flame-dried round-bottomed flask. Under an argon atmosphere, at 0 °C, freshly distilled triethylamine (8.4 mL, 60 mmol, 1.5 eq.) was added followed by the dropwise addition of TMSOTf (8.7 mL, 48 mmol, 1.2 eq.) over a period of 15 min. The reaction mixture was stirred at 0 °C for 5 min, then RT overnight. The reaction mixture was quenched with saturated aqueous NaHCO₃ solution (150 mL) and the phases were separated. The aqueous phase was extracted with dichloromethane (2 x 100 mL). The organic phases were combined and washed with water (4 x 100 mL), dried over Na₂SO₄, filtered, and concentrated *in vacuo* to give ((3,4-dihydronaphthalen-1-yl)oxy)trimethylsilane **9.5.1**[181] (8.6 g, 98%) as an orange oil. ^{1}H-NMR (400 MHz, CDCl₃) δ 0.27 (9 H, s, Si(C*H₃*)₃), 2.33 (2 H, td, *J* = 8.0, 4.0 Hz, C*H₂*), 2.77 (2 H, t, *J* = 8.0 Hz, C*H₂*), 5.20 (1 H, t, *J* = 4.0 Hz, C*H*), 7.10 – 7.22 (3 H, m, Ar*H*), 7.42 (1 H, d, *J* = 7.2 Hz, Ar*H*); ^{13}C{^{1}H}-NMR (100 MHz, CDCl₃) δ 0.4 (3 x CH₃), 22.3 (CH₂), 28.3 (CH₂), 105.4 (CH), 122.0 (CH), 126.3 (CH), 127.1 (CH), 127.4 (CH), 133.7 (C), 137.2 (C), 148.2 (C).

((3,4-Dihydronaphthalen-1-yl)oxy)trimethylsilane **9.5.1** (5.0 g, 25 mmol) and anhydrous dichloromethane (250 mL) were added to a flame-dried round-bottomed flask. Under an argon atmosphere, at 0 °C, diiodomethane (3.0 mL, 37.5 mmol, 1.5 eq.) was added followed by the dropwise addition of diethyl zinc (1 M in hexane, 37 mL, 37.5 mmol, 1.5 eq.). The reaction mixture was stirred at RT overnight. The reaction mixture was quenched with a saturated aqueous ammonium chloride solution (100 mL) and the phases were separated. The aqueous phase was extracted with dichloromethane (2 x 100 mL). The organic phases were combined and dried over Na₂SO₄, filtered, and concentrated *in vacuo* to give

trimethyl((1,1a,2,3-tetrahydro-7bH-cyclopropa[a]naphthalen-7b-yl)oxy)silane **9.5.2**[182] (5.54 g, 95%) as an pale yellow oil [Found: (GCMS-EI) $C_{14}H_{20}OSi$ (M)$^{\bullet +}$ 232.1]; v_{max} (film)/cm^{-1} 3018, 2953, 2918, 2854, 1489, 1324, 1251, 1227, 1209, 1104, 1078, 980, 896, 837, 753, 738; ^{1}H-NMR (400 MHz, CDCl$_3$) δ 0.13 (9 H, s, Si(CH_3)$_3$), 1.00 (1 H, t, J = 6.0 Hz, CH_2), 1.16 (1 H, dd, J = 10.0, 6.0 Hz, CH_2), 1.74 – 1.81 (2 H, m, CH and CH_2), 1.99 – 2.04 (1 H, m, CH_2), 2.34 – 2.41 (1 H, m, CH_2), 2.62 (1 H, dd, J = 16.4, 5.2 Hz, CH_2), 7.02 (1 H, d, J = 7.6 Hz, ArH), 7.08 (1 H, t, J = 7.6 Hz, ArH), 7.22 (1 H, t, J = 7.6 Hz, ArH), 7.63 (1 H, d, J = 7.6 Hz, ArH); ^{13}C{^{1}H}-NMR (100 MHz, CDCl$_3$) δ 1.3 (CH$_3$), 16.4 (CH$_2$), 18.5 (CH$_2$), 23.8 (CH), 26.2 (CH$_2$), 56.1 (C), 125.1 (CH), 125.4 (CH), 126.2 (CH), 128.2 (CH), 132.5 (C), 141.2 (C).
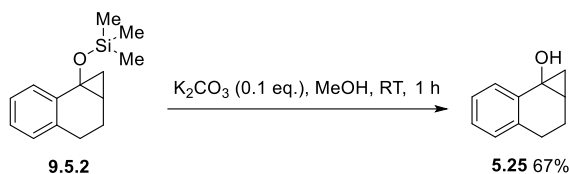
Trimethyl((1,1a,2,3-tetrahydro-7bH-cyclopropa[a]naphthalen-7b-yl)oxy)silane **9.5.2** (5.1 g, 22 mmol) and methanol (60 mL) were added to a flame-dried round-bottomed flask was added. Under an argon atmosphere, K$_2$CO$_3$ (304 mg, 2.2 mmol, 0.1 eq.) was added and the reaction mixture was stirred at RT for 1 h. The reaction mixture was quenched with saturated aqueous ammonium chloride solution (few drops) and concentrated *in vacuo*. The crude mixture was diluted with saturated aqueous ammonium chloride solution (40 mL) and extracted with ethyl acetate (3 x 50 mL). The organic phases were combined and dried over Na$_2$SO$_4$, filtered, and concentrated *in vacuo*. The crude material was purified by column chromatography (2 - 10% ethyl acetate in hexane) to give 1,1a,2,3-tetrahydro-7bH-cyclopropa[a]naphthalen-7b-ol **5.25**[183-184] (2.35 g, 67%) as a white solid m.p. 99 - 102 °C (lit:[185] 100 - 104 °C); [Found: (GCMS-EI) $C_{11}H_{12}O$ (M)$^{\bullet +}$ 160.1]; v_{max}(film) / cm^{-1} 3254, 3011, 2920, 2854, 1681, 1601, 1488, 1447, 1272, 1222, 1205, 1063, 1021, 924, 753, 738 ; ^{1}H-NMR (400 MHz, CDCl$_3$) δ 1.08 (1 H, t, J = 8.0 Hz, CH_2), 1.24 (1 H, dd, J = 8.0, 4.0 Hz, CH_2), 1.72 – 1.81 (2 H, m, CH and CH_2), 1.97 – 2.03 (1 H, m, CH_2), 2.33 – 2.42 (2 H, m, CH_2 and OH), 2.63 (1 H, dd, J = 14.0, 8.0 Hz, CH_2), 7.06 (1 H, d, J = 8.0 Hz, ArH), 7.13 (1 H, t, J = 8.0 Hz, ArH), 7.25 – 7.29 (1 H, m, ArH), 7.72 (1 H, d, J = 8.0 Hz, ArH); ^{13}C{^{1}H}-NMR (100 MHz, CDCl$_3$) δ 16.6 (CH$_2$), 18.5

(CH2), 24.7 (CH), 26.2 (CH2), 54.8 (C), 124.2 (CH), 125.7 (CH), 126.5 (CH), 128.3 (CH), 133.0 (C), 140.7 (C).

5.25   **5.26** 0%   **5.30** 73%
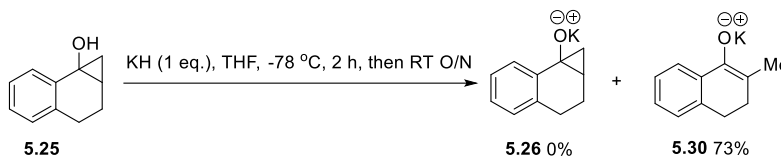
Potassium hydride (551 mg, 13.7 mmol, 1.0 eq.) was added to a flame-dried three-necked flask, equipped with a vacuum tap. Under an argon atmosphere, at -78 °C, a solution of 1,1a,2,3-tetrahydro-7bH-cyclopropa[a]naphthalen-7b-ol **5.25** (2.2 g, 13.7 mmol) in anhydrous tetrahydrofuran (17 mL) was added and the reaction mixture was stirred at -78 °C for 1 h, then at RT overnight. The solvent was removed on the house vacuum line and the crude material was dried for 3 h to obtain *potassium 2-methyl-3,4-dihydronaphthalen-1-olate* **5.30** (1.97 g, 73%) as a pale brown solid m.p. 197 °C; [Found: (GCMS-APCI) 160.1 $C_{11}H_{12}O$ (M)$^{\bullet+}$ (under the MS analysis **5.30** is protonated to **5.29**)]; v_{max} (film)/cm^{-1} 3057, 2916, 2869, 1681, 1582, 1558, 1393, 1374, 1292, 1212, 1086, 970, 771, 738; ^{1}H-NMR (400 MHz, d^{6}-DMSO) δ 1.67 (3 H, s, C*H3*), 2.13 (2 H, t, *J* = 7.6 Hz, C*H2*), 2.56 (2 H, t, *J* = 7.6 Hz, C*H2*), 6.76 – 6.82 (2 H, m, Ar*H*), 6.94 (1 H, t, *J* = 7.2 Hz, Ar*H*), 7.53 (1 H, d, *J* = 7.2 Hz, Ar*H*); ^{13}C{^{1}H}-NMR (100 MHz, d^{6}-DMSO) δ 18.6 (CH3), 29.8 (CH2), 30.8 (CH2), 90.0 (C), 122.1 (CH), 122.7 (CH), 124.8 (2 x CH), 136.7 (C), 142.4 (C), 155.1 (C). The product was put under an argon atmosphere, and transported into the glove box immediately.

5.30   **5.29** 100%
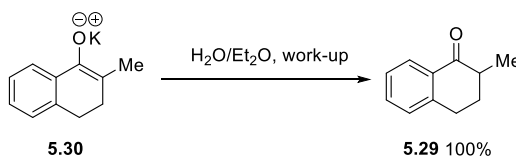
Potassium 2-methyl-3,4-dihydronaphthalen-1-olate **5.30** (10 mg, 0.05 mmol) and water (2 mL) and diethyl ether (2 mL) were added to a round-bottomed flask and the reaction mixture was stirred at RT for 1 min. The reaction mixture was phase-separated and the organic phase was dried over Na2SO4, filtered, and concentrated *in vacuo* to give 2-methyl-3,4-dihydronaphthalen-1(2H)-one **5.29**[186] (8 mg, 100%) as a yellow oil [Found: (GCMS-EI) $C_{11}H_{12}O$ (M)$^{\bullet+}$ 160.1]; v_{max} (film)/cm^{-1} 2960, 2930, 2859, 1679, 1601, 1465, 1269, 1225, 969, 738; ^{1}H-NMR (400 MHz, CDCl3) δ 1.27

(3 H, d, J = 8.0 Hz, C*H*$_3$), 1.83 – 1.94 (1 H, m, C*H*$_2$), 2.17 – 2.23 (1 H, m, C*H*$_2$), 2.55 – 2.64 (1 H, m, C*H*$_2$), 2.94 – 3.07 (2 H, m, C*H*$_2$ and C*H*), 7.23 (1 H, d, J = 8.0 Hz, Ar*H*), 7.29 (1 H, t, J = 8.0 Hz, Ar*H*), 7.45 (1 H, t, J = 8.0 Hz, Ar*H*), 8.03 (1 H, d, J = 8.0 Hz, Ar*H*); ^{13}C{^{1}H}-NMR (100 MHz, CDCl$_3$) δ 15.6 (CH$_3$), 29.0 (CH$_2$), 31.5 (CH$_2$), 42.8 (CH), 126.7 (CH), 127.5 (CH), 128.8 (CH), 132.5 (C), 133.2 (CH), 144.3 (C), 200.9 (C).

9.3.10 Reactions of potassium 2-phenylpropan-2-olate 5.12 at 160 °C (Table 5.4)

Table 5.4, entry 1
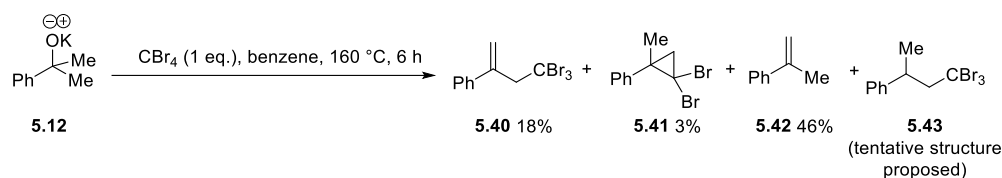
Potassium 2-phenylpropan-2-olate **5.12** (87 mg, 0.5 mmol) and CBr$_4$ (166 mg, 0.5 mmol, 1.0 eq.) were added to an oven-dried pressure tube. In the glove box, anhydrous benzene (1.33 mL) was added and the reaction was stirred at 160 °C for 6 h. The reaction mixture was cooled to RT and quenched with aqueous hydrochloric acid (1 M, 5 mL) and extracted with diethyl ether (4 x 10 mL). The organic phases were combined, dried over Na$_2$SO$_4$, filtered and concentrated *in vacuo*. The yield of (4,4,4-tribromobut-1-en-2-yl)benzene **5.40** (18%), (2,2-dibromo-1-methylcyclopropyl)benzene **5.41** (3%) and methylstyrene **5.42** (46%) were determined by adding 1,3,5-trimethoxybenzene to the crude mixture as an internal standard for ^{1}H-NMR. The products were identified by the following characteristic signals; ^{1}H-NMR (400 MHz, CDCl$_3$) δ 4.26 (2 H, s), 5.58 (1 H, s), 5.68 (1 H, s) for (4,4,4-tribromobut-1-en-2-yl)benzene **5.40**; δ 1.72 (3 H, s), 1.78 (1 H, d, J = 7.6 Hz) for (2,2-dibromo-1-methylcyclopropyl)benzene **5.41**; δ 2.17 (3 H, s), 5.09 (1 H, s), 5.37 (1 H, s) for methylstyrene **5.42**.[187] The crude material was purified by column chromatography (100% hexane) to give an inseparable mixture of (4,4,4-tribromobut-1-en-2-yl)benzene **5.40**, (2,2-dibromo-1-methylcyclopropyl)benzene **5.41** and *(4,4,4-tribromobutan-2-yl)benzene* **5.43** (54 mg) as a yellow oil. (The purification of compound **5.40** is performed by derivatisation, shown in Section

9.3.11 on page 227. A pure sample of **5.41** is prepared as a reference in Section 9.3.11 on page 229. The structure of **5.43** is a tentatively proposed based on ^{1}H-NMR, Section 9.3.11 on page 227).

Methylstyrene **5.42**[187] ^{1}H-NMR (400 MHz, CDCl$_3$) δ 2.16 (3 H, m, C*H*$_3$), 5.09 (1 H, m, alkene-C*H*), 5.37 (1 H, m, alkene-C*H*), 7.29 – 7.25 (1 H, m, Ar*H*), 7.29 – 7.25 (1 H, m, Ar*H*), 7.49 – 7.46 (2 H, m, Ar*H*); ^{13}C{^{1}H}-NMR (100 MHz, CDCl$_3$) δ 21.9 (CH$_3$), 112.53 (CH$_2$), 125.6 (2 x CH), 127.5 (CH), 128.3 (2 x CH), 141.4 (C), 143.4 (C). (A commercial sample was recorded and is reported here to use as a reference)

Table 5.4, entry 2

Potassium 2-phenylpropan-2-olate **5.12** (87 mg, 0.5 mmol) were added to an oven-dried pressure tube. In the glove box, anhydrous benzene (1.33 mL) was added and the reaction was stirred at 160 °C for 6 h. The reaction mixture was cooled to RT and quenched with aqueous hydrochloric acid (1 M, 5 mL) and extracted with diethyl ether (4 x 10 mL). The organic phases were combined, dried over Na$_2$SO$_4$, filtered and concentrated *in vacuo*. The yield of 2-phenylpropanol **5.15** (76%) and methylstyrene **5.42** (< 0.5%) were determined by adding 1,3,5-trimethoxybenzene to the crude mixture as an internal standard for ^{1}H-NMR. The products were identified by the following characteristic signals; ^{1}H-NMR (400 MHz, CDCl$_3$) δ 1.60 (6 H, s) for 2-phenylpropanol **5.15**; δ 2.17 (3 H, s), 5.09 (1 H, s), 5.37 (1 H, s) for methylstyrene **5.42**. These signals are consistent with the literature values and reference samples (**5.15**: Section 9.3.6, Table 5.2, entry 1 on page 215; **5.42**: Section 9.3.10, Table 5.4, entry 1 on page 226).

9.3.11 Synthesis and characterisation of (4,4,4-tribromobut-1-en-2-yl)benzene 5.40 and (2,2-dibromo-1-methylcyclopropyl)benzene 5.41

Synthesis and characterisation of (4,4,4-tribromobut-1-en-2-yl)benzene 5.40
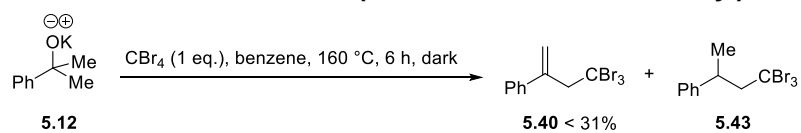
226

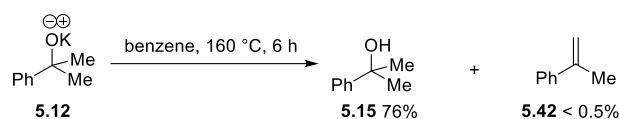In the glove box, potassium 2-phenylpropan-2-olate **5.12** (87 mg, 0.5 mmol) and CBr$_4$ (166 mg, 0.5 mmol, 1.0 eq.) were added to an oven-dried pressure tube, followed by anhydrous benzene (1.33 mL). This was repeated exactly in two other pressure tubes. The three reaction mixtures were stirred at 160 °C for 6 h. After the mixtures had cooled, aqueous hydrochloric acid (1 M, 5 mL) was added and the mixtures was diluted with diethyl ether (5 mL). All three reaction mixtures were combined and the phases were separated. The aqueous phase was extracted using diethyl ether (3 x 30 mL) and organic phases were combined, dried over Na$_2$SO$_4$, filtered, and concentrated *in vacuo*. The crude material was purified by column chromatography (100% hexane) to give impure (4,4,4-tribromobut-1-en-2-yl)benzene **5.40**[188-189] (169.7 mg, < 31%) as a yellow oil [Found: (GCMS-EI) C$_{10}$H$_9$Br$_3$ (M)$^{\bullet+}$ 365.8]; ^{1}H-NMR (400 MHz, CDCl$_3$) δ 4.26 (2 H, s, C*H*$_2$), 5.58 (1 H, s, C*H*), 5.68 (1 H, s, C*H*), 7.29 – 7.31 (1 H, m, Ar*H*), 7.33 – 7.37 (2 H, m, Ar*H*), 7.41 – 7.43 (2 H, m, Ar*H*); ^{13}C{^{1}H}-NMR (100 MHz, CDCl$_3$) δ 39.5 (C), 62.9 (CH$_2$), 122.5 (CH$_2$), 127.2 (2 x CH), 127.9 (CH), 128.5 (2 x CH), 141.2 (C), 144.2 (C); *m/z* (EI) 371.8 (M+6, ^{81}Br^{81}Br^{81}Br, 31%), 369.8 (M+4, ^{79}Br^{81}Br^{81}Br, 97), 367.8 (M+2, ^{79}Br^{79}Br^{81}Br, 100), 365.8 (M, ^{79}Br^{79}Br^{79}Br, 33); containing *(4,4,4-tribromobutan-2-yl)benzene **5.43*** [tentative structure proposed based on ^{1}H-NMR (400 MHz, CDCl$_3$) δ 1.19 (3 H, d, *J* = 8.0 Hz, C*H*$_3$), 3.17 – 3.25 (1 H, m, C*H*), 3.35 (1 H, dd, *J* = 12.0, 4.0 Hz, C*H*$_2$), 3.55 (1 H, 1 H, dd, *J* = 12.0, 4.0 Hz, C*H*$_2$); ^{13}C{^{1}H}-NMR (100 MHz, CDCl$_3$) δ 24.2, 40.2, 41.6, 66.7, 126.7, 127.6, 128.8, 146.2)].
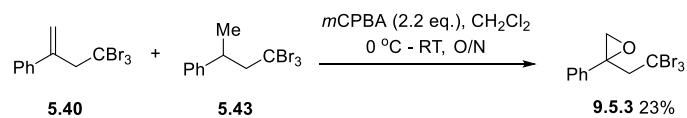
The impure (4,4,4-tribromobut-1-en-2-yl)benzene **5.40** (77 mg, 0.21 mmol) was diluted in dichloromethane (1 mL). This solution was added to a solution of *m*CPBA (113 mg, 0.46 mmol, 70%, 2.2 eq.) in dichloromethane (1 mL) at 0 °C. The reaction mixture was stirred at RT overnight. The mixtures was diluted with dichloromethane (5 mL) and washed with saturated aqueous sodium sulfite (5 mL) and aqueous sodium hydroxide (10% by weight, 3 x 5 mL). The organic phases were combined, dried over Na$_2$SO$_4$, filtered, and concentrated *in vacuo*. The crude material was purified by column chromatography (50% dichloromethane in hexane) to give *2-*

phenyl-2-(2,2,2-tribromoethyl)oxirane **9.5.3** (33.9 mg, 23%) as a colourless oil [Found: (HRMS-APCI) 381.8204. $C_{10}H_9Br_3$ (M)$^{\bullet+}$ requires 381.8202]; v_{max} (thin film)/cm^{-1} 3057, 3026, 2916, 1448, 1214, 1024, 991, 863, 764, 734, 699, 673; ^{1}H-NMR (400 MHz, CDCl$_3$) δ 3.04 (1 H, dd, J = 4.8, 0.8 Hz), 3.31 (1 H, d, J = 4.8 Hz, CH_2), 3.68 (1 H, d, J = 15.6 Hz, CH_2), 3.87 (1 H, dd, J = 15.6, 0.8 Hz, CH_2), 7.32 – 7.39 (3 H, m, ArH), 7.50 – 7.53 (2 H, m, ArH); ^{13}C{^{1}H}-NMR (100 MHz, CDCl$_3$) δ 33.2 (C), 54.1 (CH$_2$), 60.6 (C), 64.3 (CH$_2$), 128.1 (2 x CH), 128.4 (2 x CH), 128.7 (CH), 137.7 (C); *m/z* (APCI) 387.8147 [(M)$^{\bullet+}$, ^{81}Br^{81}Br^{81}Br, 35%], 385.8163 [(M)$^{\bullet+}$, ^{79}Br^{81}Br^{81}Br, 100], 383.8183 [(M)$^{\bullet+}$, ^{79}Br^{79}Br^{81}Br, 100], 381.8202 [(M)$^{\bullet+}$, ^{79}Br^{79}Br^{79}Br, 32], 302.9016 [[(M)$^{\bullet+}$ - ^{79}Br] and impure (4,4,4-tribromobut-1-en-2-yl)benzene **5.40** (169.7 mg, < 31%) as a yellow oil containing (2,2-dibromo-1-methylcyclopropyl)benzene **5.41** and *(4,4,4-tribromobutan-2-yl)benzene* **5.43**. The crude material was purified again by column chromatography (0 - 50% dichloromethane in hexane) to an impure mixture of *2-phenyl-2-(2,2,2-tribromoethyl)oxirane* **9.5.3** and *(4,4,4-tribromobutan-2-yl)benzene* **5.43**. (13.2 mg) as a colourless oil. (The ^{1}H-NMR and ^{13}C{^{1}H}-NMR are shown below to support the tentatively proposed structure of **5.43**).

^{1}H-NMR and ^{13}C{^{1}H}-NMR 5.40, containing the proposed impurity 5.43
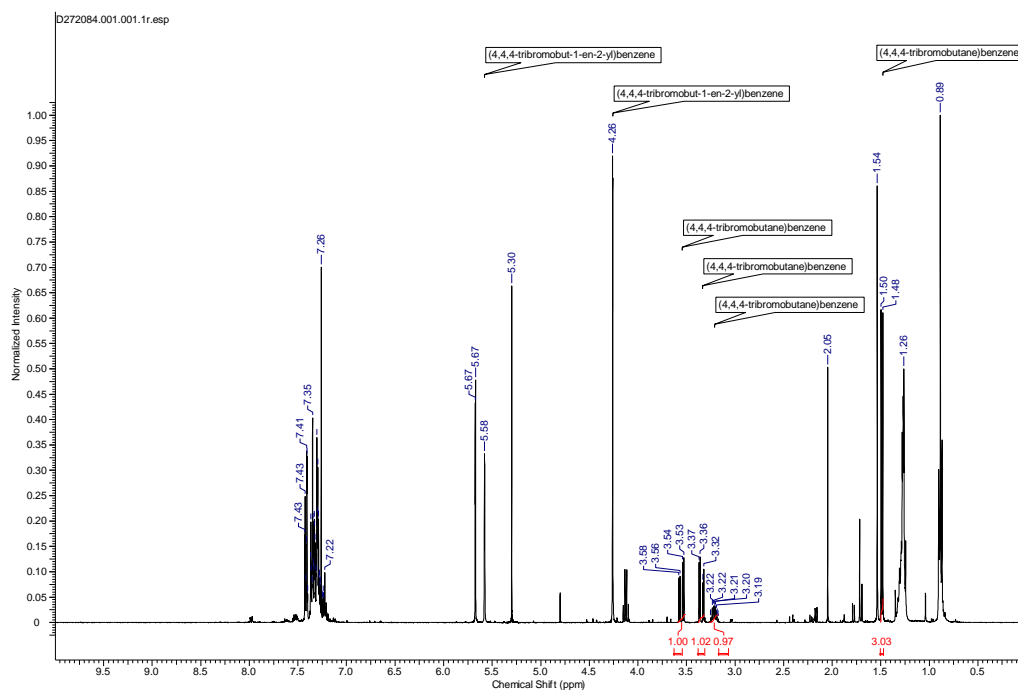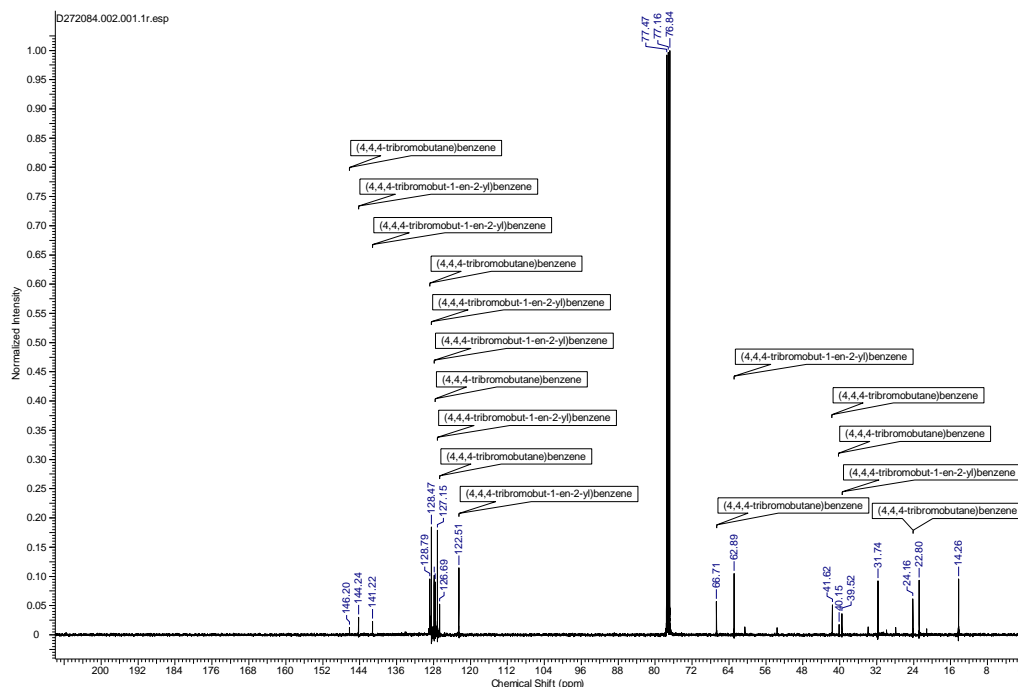
Synthesis and characterisation of (2,2-dibromo-1-methylcyclopropyl)benzene 5.41
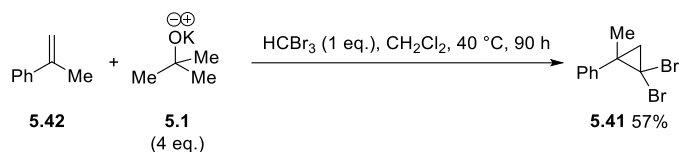
KO^{t}Bu **5.1** (224 mg, 2 mmol, 4.0 eq.), HCBr$_3$ (0.04 mL, 0.5 mmol, 1.0 eq.) and methylstyrene **5.42** (0.07 mL, 0.5 mmol) were added to an oven-dried pressure tube. Dichloromethane (3.13 mL) was added and the reaction mixture was stirred at 40 °C for 90 h. The reaction mixture was cooled to RT and quenched with aqueous hydrochloric acid (1 M, 5 mL) and extracted with diethyl ether (4 x 10 mL). The organic phases were combined, dried over Na$_2$SO$_4$, filtered and concentrated *in vacuo*. The crude material was purified by column chromatography (100% hexane) to give (2,2-dibromo-1-methylcyclopropyl)benzene **5.41**[190] (82.4 mg, 57%) as a colourless oil [Found: (GCMS-CI) C$_{10}$H$_{11}$Br$_2^+$ (M+H)$^+$ 288.7]; v_{max} (film)/cm^{-1} 1496, 1445, 1426, 1060, 1019, 763, 691; ^{1}H-NMR (400 MHz, CDCl$_3$) δ 1.72 (3 H, s, C*H$_3$*), 1.78 (1 H, d, *J* = 7.6 Hz, C*H$_2$*), 2.17 (1 H, d, *J* = 7.6 Hz, C*H$_2$*), 7.29 – 7.38 (5 H, m, Ar*H*); ^{13}C{^{1}H}-NMR (100 MHz, CDCl$_3$) δ 27.9 (CH$_3$), 33.8 (CH$_2$), 35.9 (C), 36.9 (C),

127.4 (CH), 128.5 (2 x CH), 128.6 (2 x CH), 142.5 (C); *m/z* (CI) 292.6 [(M+H)$^+$, ^{81}Br^{81}Br, 61%), 290.6 [(M+H)$^+$, ^{79}Br^{81}Br, 100), 288.7 [(M+H)$^+$, ^{79}Br^{79}Br, 70)].

9.3.12 Reaction of KO*t*Bu with CBr$_4$ and methylstyrene 5.42 at 160 °C (Scheme 5.9B)
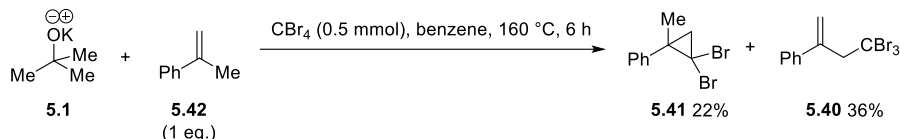
KO*t*Bu **5.1** (56 mg, 0.5 mmol), CBr$_4$ (166 mg, 0.5 mmol, 1.0 eq.) and methylstyrene **5.42** (0.07 mL, 0.5 mmol, 1.0 eq.) were added to an oven-dried pressure tube. In the glove box, anhydrous benzene (1.33 mL) was added and the reaction mixture was stirred at 160 °C for 6 h. The reaction mixture was cooled to RT and quenched with aqueous hydrochloric acid (1 M, 5 mL) and extracted with diethyl ether (4 x 10 mL). The organic phases were combined, dried over Na$_2$SO$_4$, filtered and concentrated *in vacuo*. The yield of (4,4,4-tribromobut-1-en-2-yl)benzene **5.40** (36%) and (2,2-dibromo-1-methylcyclopropyl)benzene **5.41** (22%) were determined by adding 1,3,5-trimethoxybenzene to the crude mixture as an internal standard for ^{1}H-NMR. The products were identified by the following characteristic signals; ^{1}H-NMR (400 MHz, CDCl$_3$) δ 4.26 (2 H, s), 5.58 (1 H, s), 5.68 (1 H, s) for (4,4,4-tribromobut-1-en-2-yl)benzene **5.40**; δ 1.72 (3 H, s), 1.78 (1 H, d, *J* = 7.6 Hz) for (2,2-dibromo-1-methylcyclopropyl)benzene **5.41**. These signals are consistent with the literature values and reference samples (Section 9.3.11 on pages 227 and 229).

9.3.13 Reaction of KO*t*Bu with HCBr$_3$ and methylstyrene 5.42 at 160 °C (Scheme 5.9C)

KO*t*Bu (56 mg, 0.5 mmol), HCBr$_3$ (0.04 mL, 0.5 mmol, 1.0 eq.) and methylstyrene **5.42** (0.07 mL, 0.5 mmol, 1.0 eq.) were added to an oven-dried pressure tube. In the glove box, anhydrous benzene (1.33 mL) was added and the reaction mixture was stirred at 160 °C for 6 h. The reaction mixture was cooled to RT and quenched with aqueous hydrochloric acid (1 M, 5 mL) and extracted with diethyl ether (4 x 10 mL).

The organic phases were combined, dried over Na_2SO_4, filtered and concentrated *in vacuo*. The yield of (2,2-dibromo-1-methylcyclopropyl)benzene **5.41** (55%) and methylstyrene **5.42** (6%) were determined by adding 1,3,5-trimethoxybenzene to the crude mixture as an internal standard for ^{1}H-NMR. The products were identified by the following characteristic signals; ^{1}H-NMR (400 MHz, CDCl₃) δ 1.72 (3 H, s), 1.78 (1 H, d, *J* = 7.6 Hz) for (2,2-dibromo-1-methylcyclopropyl)benzene **5.41**; δ 2.17 (3 H, s), 5.09 (1 H, s), 5.37 (1 H, s) for methylstyrene **5.42**. These signals are consistent with the literature values and reference samples (**5.41**: Section 9.3.11 on page 229; **5.42**: Section 9.3.10, Table 5.4, entry 1 on page 226).

9.3.14 Reactions of CBr₄ and adamantane 5.50 (Scheme 5.11A)

Reaction at 160 °C

Adamantane **5.50** (68 mg, 0.5 mmol) and CBr₄ (166 mg, 0.5 mmol, 1.0 eq.) were added to an oven-dried pressure tube. In the glove box, anhydrous benzene (1.33 mL) was added and the reaction mixture was stirred at 160 °C for 6 h in the dark. The reaction mixture was cooled to RT and quenched with aqueous hydrochloric acid (1 M, 5 mL) and extracted with diethyl ether (4 x 10 mL). The organic phases were combined, dried over Na_2SO_4, filtered and concentrated *in vacuo*. The yield of adamantane **5.50** (16%), 1-bromoadamantane **5.51** (41%), 2-bromoadamantane **5.52** (6%) and 1,3-dibromoadamantane **5.53** (8%) were determined by adding 1,3,5-trimethoxybenzene to the crude mixture as an internal standard for ^{1}H-NMR. The products were identified by the following characteristic signals; ^{1}H-NMR (400 MHz, CDCl₃) δ 1.74 – 1.76 (12 H, m), 1.88 (4 H, br s) for adamantane **5.50**; δ 1.72 (6 H, m), 2.10 (3 H, br s), 2.36 (6 H, m) for 1-bromoadamantane **5.51**;[191] δ 1.97 – 2.00 (2 H, m), 2.15 (2 H, br s), 2.33 (2 H, br s), 4.68 (1 H, br s) for 2-bromoadamantane **5.52**;[192] δ 1.70 (2 H, m), 2.25 – 2.30 (10 H, m), 2.87 (2 H, br s) for 1,3-dibromoadamantane **5.53**;[191] ^{13}C{^{1}H}-NMR (100 MHz, CDCl₃) δ 28.5, 37.9 adamantane **5.50**; δ 32.8, 35.7, 49.5 for 1-bromoadamantane **5.51**;[191] δ 27.0, 27.7, 31.8, 36.5, 38.9, 64.1 for 2-bromoadamantane **5.52**;[192] δ 33.7, 35.2, 47.2, 59.2, 62.3

for 1,3-dibromoadamantane **5.53**;[191] (GCMS-EI) 8.27 min = m/z 136.1 [(M)$^{\bullet+}$] for adamantane **5.50**; 10.7 min = m/z 216.0 [(M)$^{\bullet+}$, ^{81}Br, 90%], m/z 214.0 [(M)$^{\bullet+}$, ^{79}Br, 100), m/z 135.1 [(M)$^{\bullet+}$- ^{79}Br] for 1-bromoadamantane **5.51**; 11.0 min = m/z 216.0 [(M)$^{\bullet+}$, ^{81}Br, 90%], m/z 214.0 [(M)$^{\bullet+}$, ^{79}Br, 100], m/z 135.1 [(M)$^{\bullet+}$- ^{79}Br] for 2-bromoadamantane **5.52**; 12.3 min = m/z 295.1 [(M)$^{\bullet+}$, ^{81}Br^{81}Br, 39%], m/z 292.9 [(M)$^{\bullet+}$, ^{81}Br^{79}Br, 100], m/z 290.9 [(M)$^{\bullet+}$, ^{79}Br^{79}Br, 53] for 1,3-dibromoadamantane **5.53**. These signals are consistent with literature and reference values (Section 9.3.14, Scheme 5.12 on page 234). Analysis of the crude material showed that the products were inseparable, hence the analysis of the product mixture was performed using experimental ^{1}H-NMR and ^{13}C{^{1}H}-NMR values reported within the literature as a reference.

1-Bromoadamantane **5.51**[191] ^{1}H-NMR (200 MHz, CDCl$_3$) δ 1.72 (6 H, m, C*H$_2$*), 2.09 (3 H, m, C*H*), 2.38 (6 H, m, C*H$_2$*); ^{13}C{^{1}H}-NMR (50 MHz, CDCl$_3$) δ 35.6, 36.7, 49.4.

2-Bromoadamantane **5.52**[192] ^{1}H-NMR (500 MHz, CDCl$_3$) δ 1.61 – 1.64 (2 H, m, C*H$_2$*), 1.77 (2 H, br s, C*H*), 1.85 – 1.88 (4 H, m, C*H$_2$*), 1.96 – 1.99 (2 H, m, C*H$_2$*), 2.15 (2 H, br s, C*H*), 2.33 – 2.36 (2 H, m, C*H$_2$*), 4.68 (1 H, s, C*H*); ^{13}C{^{1}H}-NMR (125 MHz, CDCl$_3$) δ 27.1, 27.7, 31.9, 36.6, 38.1, 38.9, 64.2.

1,3-Dibromoadamantane **5.53**[191] ^{1}H-NMR (200 MHz, CDCl$_3$) δ 1.70 (2 H, m, C*H$_2$*), 2.26 (10 H, m, C*H$_2$*), 2.87 (2 H, m, C*H*); ^{13}C{^{1}H}-NMR (50 MHz, CDCl$_3$) δ 33.6, 35.1, 47.0, 59.0, 62.3.

The compounds 5.50, 5.51, 5.52 and 5.53 are inseparable: ¹H-NMR
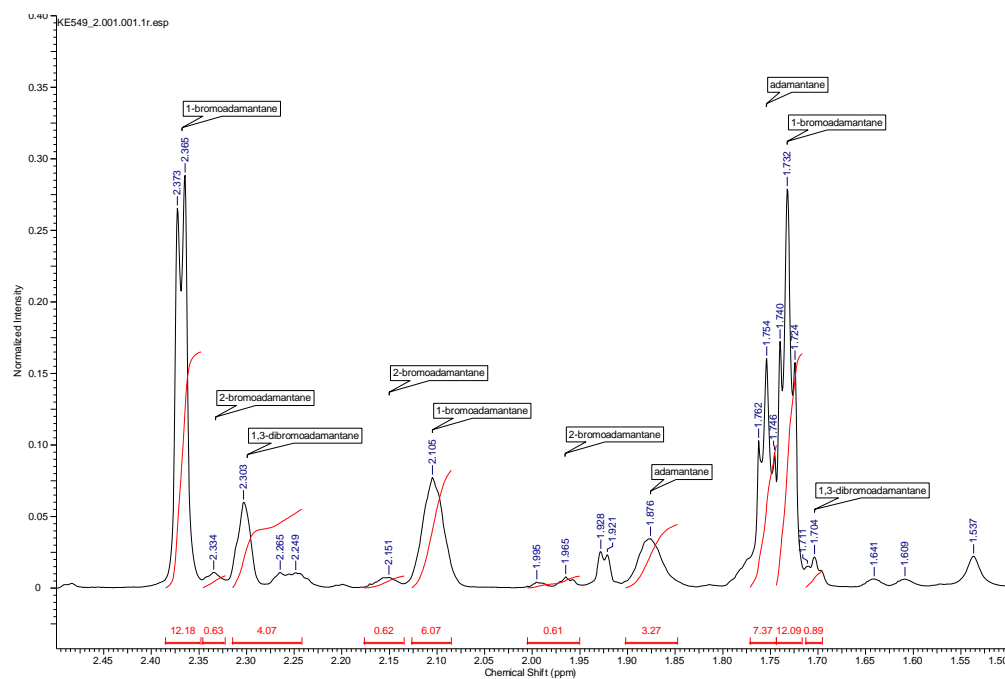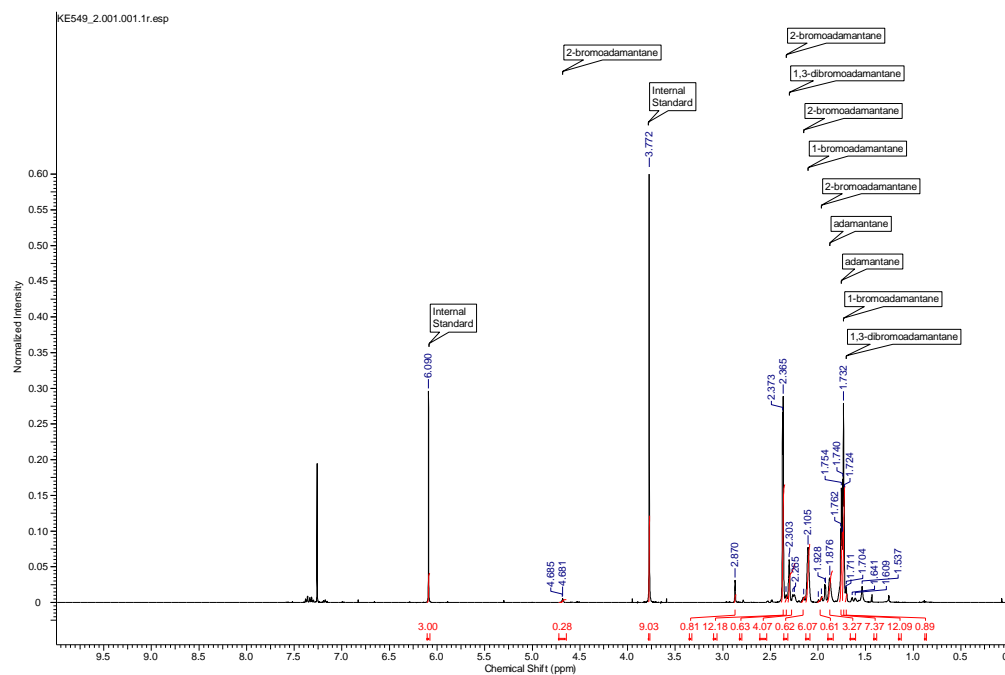
Reaction at 40 °C (Scheme 5.12)
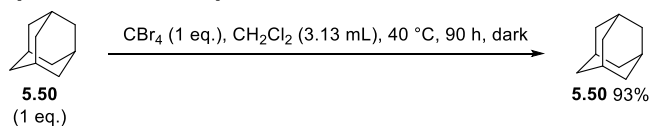
5.50
(1 eq.)

CBr₄ (1 eq.), CH₂Cl₂ (3.13 mL), 40 °C, 90 h, dark

5.50 93%

Adamantane **5.50** (68 mg, 0.5 mmol), CBr₄ (166 mg, 0.5 mmol, 1.0 eq.) and dichloromethane (3.13 mL) were added to an oven-dried pressure tube and the

reaction mixture was stirred at 40 °C for 90 h in the dark. The reaction mixture was cooled to RT and quenched with aqueous hydrochloric acid (1 M, 5 mL) and extracted with diethyl ether (4 x 10 mL). The organic phases were combined, dried over Na_2SO_4, filtered and concentrated *in vacuo*. ^{1}H-NMR (400 MHz, CDCl$_3$) δ 1.76 – 1.75 (12 H, m, CH_2), 1.88 (4 H, br s, CH); ^{13}C{^{1}H}-NMR (100 MHz, CDCl$_3$) δ 28.5 (6 x CH$_2$), 37.9 (4 x CH). The yield of adamantane **5.50**[193] (93%) was determined by adding 1,3,5-trimethoxybenzene to the crude mixture as an internal standard for ^{1}H-NMR. These signals are consistent with the literature values and reference samples.

9.3.15 Reactions of 5.12 in dichloromethane (Table 5.5)

Table 5.5, entry 1

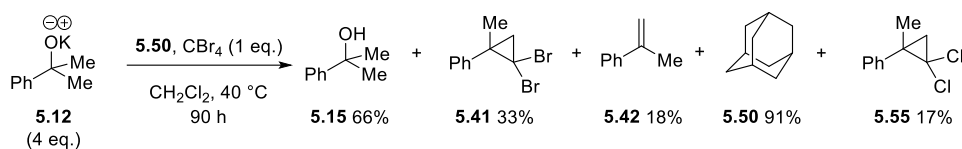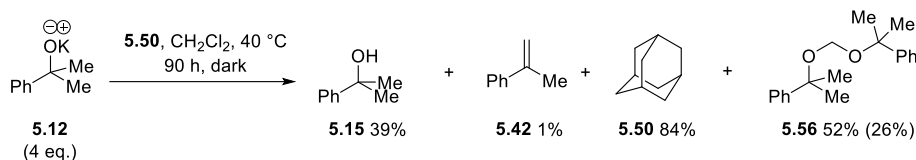Potassium 2-phenylpropan-2-olate **5.12** (349 mg, 2 mmol, 4.0 eq.), adamantane **5.50** (68 mg, 0.5 mmol), CBr$_4$ (166 mg, 0.5 mmol, 1.0 eq.) and dichloromethane (3.13 mL) were added to an oven-dried pressure tube and the reaction mixture was stirred at 40 °C for 90 h. The reaction mixture was cooled to RT and quenched with aqueous hydrochloric acid (1 M, 5 mL) and extracted with diethyl ether (4 x 10 mL). The organic phases were combined, dried over Na$_2$SO$_4$, filtered and concentrated *in vacuo*. The yield of 2-phenylpropanol **5.15** (66%), (2,2-dibromo-1-methylcyclopropyl)benzene **5.41** (33%), methylstyrene **5.42** (18%), adamantane **5.50** (91%) and (2,2-dichloro-1-methylcyclopropyl)benzene **5.55** (17%) were determined by adding 1,3,5-trimethoxybenzene to the crude mixture as an internal standard for ^{1}H-NMR. The products were identified by the following characteristic signals; ^{1}H-NMR (400 MHz, CDCl$_3$) δ 1.60 (6 H, s) for 2-phenylpropanol **5.15**; δ 1.72 (3 H, s), 1.78 (1 H, d, J = 7.6 Hz), 2.17 (1 H, d, J = 7.6 Hz) for (2,2-dibromo-1-methylcyclopropyl)benzene **5.41**; δ 2.16 (3 H, s), 5.09 (1 H, s), 5.37 (1 H, s) for methylstyrene **5.42**; δ 1.75 – 1.77 (12 H, m), 1.88 (4 H, br s) for adamantane **5.50**; δ 1.68 (3 H, s), 1.96 (1 H, d, J = 7.2 Hz) for (2,2-dichloro-1-methylcyclopropyl)benzene **5.55**. These signals are consistent with the literature values and reference samples (**5.15**: Section 9.3.6, Table 5.2, entry 1 on page 215; **5.41**: Section 9.3.11 on page

229; **5.42**: Section 9.3.10, Table 5.4, entry 1 on page 226; **5.50**: Section 9.3.14, Scheme 5.12 on page 234). (The compounds **5.41** and **5.55** were inseparable so a pure sample of **5.55** is prepared as a reference in Section 9.3.16 on pages 236-237).

Table 5.5, entry 2

Potassium 2-phenylpropan-2-olate **5.12** (349 mg, 2 mmol, 4.0 eq.), adamantane **5.50** (68 mg, 0.5 mmol) and dichloromethane (3.13 mL) were added to an oven-dried pressure tube and the reaction mixture was stirred at 40 °C for 90 h in the dark. The reaction mixture was cooled to RT and quenched with aqueous hydrochloric acid (1 M, 5 mL) and extracted with diethyl ether (4 x 10 mL). The organic phases were combined, dried over Na_2SO_4, filtered and concentrated *in vacuo*. The yield of 2-phenylpropanol **5.15** (39%), methylstyrene **5.42** (1%), adamantane **5.50** (84%) and bis((2-phenylpropan-2-yl)oxy)methane **5.56** (52%) were determined by adding 1,3,5-trimethoxybenzene to the crude mixture as an internal standard for ^{1}H-NMR. The products were identified by the following characteristic signals; ^{1}H-NMR (400 MHz, CDCl$_3$) δ 1.60 (6 H, s) for 2-phenylpropanol **5.15**; δ 2.16 (3 H, s), 5.09 (1 H, s), 5.37 (1 H, s) for methylstyrene **5.42**; δ 1.75 – 1.77 (12 H, m), 1.88 (4 H, br s) for adamantane **5.50**; δ 4.51 (2 H, s), 7.20 – 7.24 (2 H, m) for bis((2-phenylpropan-2-yl)oxy)methane **5.56**. These signals are consistent with the literature values and reference samples (**5.15**: Section 9.3.6, Table 5.2, entry 1 on page 215; **5.42**: Section 9.3.10, Table 5.4, entry 1 on page 226; **5.50**: Section 9.3.14, Scheme 5.12 on page 234). This crude material was purified by column chromatography (0 - 5% ethyl acetate in hexane) to give bis((2-phenylpropan-2-yl)oxy)methane **5.56** (44.7 mg, 26%) as a colourless oil [Found: (HRMS-ESI) 302.2118. $C_{19}H_{28}O_2N$ (M+NH$_4$)$^+$ requires 302.2115]; v_{max}(film) / cm^{-1} 2978, 2934, 1493, 1447, 1381, 1364, 1258, 1153, 1072, 1018, 991, 818, 762; ^{1}H-NMR (400 MHz, CDCl$_3$) δ 1.59 (12 H, s, 4 x C*H*$_3$), 4.50 (2 H, s, C*H*$_2$), 7.20 – 7.23 (2 H, m, Ar*H*), 7.27 – 7.31 (4 H, m, Ar*H*), 7.38 – 7.40 (4 H, m, Ar*H*); ^{13}C{^{1}H}-NMR (100 MHz, CDCl$_3$) δ 29.5 (4 x CH$_3$), 77.7 (2 x C), 86.8 (CH$_2$), 125.9 (4 x CH), 126.9 (2 x CH), 128.2 (4 x CH), 146.9 (2 x C).

Table 5.5, entry 3
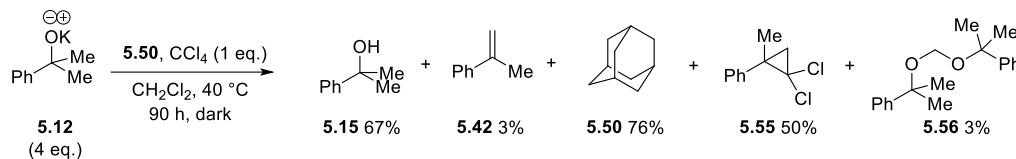
Potassium 2-phenylpropan-2-olate **5.12** (349 mg, 2 mmol, 4.0 eq.), adamantane **5.50** (68 mg, 0.5 mmol), CCl_4 (0.05 mL, 0.5 mmol, 1.0 eq.) and dichloromethane (3.13 mL) were added to an oven-dried pressure tube and the reaction mixture was stirred at 40 °C for 90 h in the dark. The reaction mixture was cooled to RT and quenched with aqueous hydrochloric acid (1 M, 5 mL) and extracted with diethyl ether (4 x 10 mL). The organic phases were combined, dried over Na_2SO_4, filtered and concentrated *in vacuo*. The yield of 2-phenylpropanol **5.15** (67%), methylstyrene **5.42** (3%), adamantane **5.50** (76%), (2,2-dichloro-1-methylcyclopropyl)benzene **5.55** (50%) and bis((2-phenylpropan-2-yl)oxy)methane **5.56** (3%) were determined by adding 1,3,5-trimethoxybenzene to the crude mixture as an internal standard for ^{1}H-NMR. The products were identified by the following characteristic signals; ^{1}H-NMR (400 MHz, $CDCl_3$) δ 1.60 (6 H, s) for 2-phenylpropanol **5.15**; δ 2.17 (3 H, s), 5.10 (1 H, s), 5.38 (1 H, s) for methylstyrene **5.42**; δ 1.76 – 1.78 (12 H, m), 1.89 (4 H, br s) for adamantane **5.50**; δ 1.68 (3 H, s), 1.97 (1 H, d, *J* = 7.2 Hz) for (2,2-dichloro-1-methylcyclopropyl)benzene **5.55**; δ 4.51 (2 H, s), 7.20 – 7.24 (2 H, m) for bis((2-phenylpropan-2-yl)oxy)methane **5.56**. These signals are consistent with the literature values and reference samples (**5.15**: Section 9.3.6, Table 5.2, entry 1 on page 215; **5.42**: Section 9.3.10, Table 5.4, entry 1 on page 226; **5.50**: Section 9.3.14, Scheme 5.12 on page 234; **5.55**: Section 9.3.16 on page 237; **5.56**: Section 9.3.15, Table 5.5, entry 2 on page 235).

### 9.3.16 Synthesis of *(2,2-dichloro-1-methylcyclopropyl)benzene* **5.55**
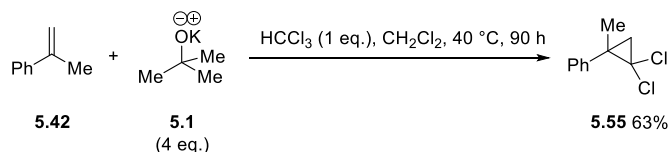
KO^{t}Bu **5.1** (224 mg, 2 mmol, 4.0 eq.), $HCCl_3$ (0.04 mL, 0.5 mmol, 1.0 eq.) and methylstyrene **5.42** (0.07 mL, 0.5 mmol) were added to an oven-dried pressure tube
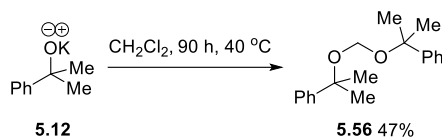
was added. Dichloromethane (3.13 mL) was added and the reaction mixture was stirred at 40 °C for 90 h. The reaction mixture was cooled to RT and quenched with aqueous hydrochloric acid (1 M, 5 mL) and extracted with diethyl ether (4 x 10 mL). The organic phases were combined, dried over Na_2SO_4, filtered and concentrated *in vacuo*. The crude material was purified by column chromatography (100% hexane) to give (2,2-dichloro-1-methylcyclopropyl)benzene **5.55**[190] (63.7 mg, 63%) as a colourless oil [Found: (HRMS-EI) 200.0157. $C_{10}H_{10}Cl_2$ (M) $^{\bullet+}$ requires 200.0160]; v_{max}(film) / cm^{-1} 1497, 1446, 1425, 1075, 1033, 1026, 936, 868, 772, 754, 697, 595; ^{1}H-NMR (400 MHz, CDCl$_3$) δ 1.60 (1 H, d, J = 7.2 Hz, CH_2), 1.68 (3 H, s, CH_3), 1.96 (1 H, d, J = 7.2 Hz, CH_2), 7.27 – 7.38 (5 H, m, ArH); ^{13}C{^{1}H}-NMR (100 MHz, CDCl$_3$) δ 25.7 (CH$_3$), 32.0 (CH$_2$), 36.6 (C), 66.0 (C), 127.4 (CH), 128.6 (2 x CH), 128.7 (2 x CH), 141.4 (C); *m/z* (CI) 203.9 [(M)$^{\bullet+}$, ^{37}Cl^{37}Cl, 12%], 201.9 [(M)$^{\bullet+}$, ^{35}Cl^{37}Cl, 70], 199.9 [(M)$^{\bullet+}$, ^{35}Cl^{35}Cl, 100].

9.3.17 Reaction of phenylmethanol 5.63 with KO^{t}Bu in dichloromethane (Scheme 5.14B)
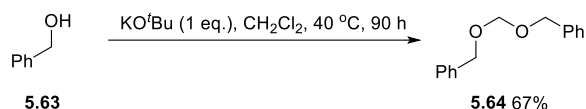
KO^{t}Bu (224 mg, 2 mmol, 1.0 eq.), phenylmethanol **5.63** (0.21 mL, 2 mmol) and dichloromethane (3.13 mL) were added to an oven-dried pressure tube and the reaction mixture was stirred at 40 °C for 90 h. The reaction mixture was cooled to RT and quenched with aqueous hydrochloric acid (1 M, 5 mL) and extracted with diethyl ether (4 x 10 mL). The organic phases were combined, dried over Na_2SO_4, filtered and concentrated *in vacuo*. This crude material was purified by column chromatography (5% ethyl acetate in hexane) to give bis(benzyloxy)methane **5.64**[138] (153.3 mg, 67%) as a colourless oil [Found: (GCMS-EI) $C_{15}H_{16}O_2$ (M) $^{\bullet+}$ 228.0]; v_{max}(film) / cm^{-1} 3030, 2936, 2882, 1497, 1452, 1377, 1165, 1103, 1040, 1024, 959, 733; ^{1}H-NMR (400 MHz, CDCl$_3$) δ 4.66 (4 H, s, 2 x CH_2), 4.86 (2 H, s, CH_2), 7.38 – 7.28 (10 H, m, ArH); ^{13}C{^{1}H}-NMR (100 MHz, CDCl$_3$) δ 69.7 (2 x CH$_2$), 94.1 (CH$_2$), 127.9 (CH), 128.1 (2 x CH), 128.6 (2 x CH), 138.0 (C).

9.3.18 Reaction of potassium 2-phenylpropan-2-olate 5.12 in dichloromethane (Scheme 5.14C)

Potassium 2-phenylpropan-2-olate **5.12** (349 mg, 2 mmol) and dichloromethane (3.13 mL) were added to an oven-dried pressure tube and the reaction mixture was stirred at 40 °C for 90 h. The reaction mixture was cooled to RT and quenched with aqueous hydrochloric acid (1 M, 5 mL) and extracted with diethyl ether (4 x 10 mL). The organic phases were combined, dried over Na_2SO_4, filtered and concentrated *in vacuo*. This crude material was purified by column chromatography (1% ethyl acetate in hexane) to give bis((2-phenylpropan-2-yl)oxy)methane **5.56** (134 mg, 47%) as a colourless oil [Found: (HRMS-ESI) 302.2118. $C_{19}H_{28}O_2N$ $(M+NH_4)^+$ requires 302.2115]; v_{max}(film) / cm^{-1} 2978, 2934, 1493, 1447, 1381, 1364, 1258, 1153, 1072, 1018, 991, 818, 762; ^{1}H-NMR (400 MHz, CDCl$_3$) δ 1.59 (12 H, s, 4 x CH_3), 4.50 (2 H, s, CH_2), 7.20 – 7.23 (2 H, m, ArH), 7.27 – 7.31 (4 H, m, ArH), 7.38 – 7.40 (4 H, m, ArH); ^{13}C{^{1}H}-NMR (100 MHz, CDCl$_3$) δ 29.5 (4 x CH$_3$), 77.7 (2 x C), 86.8 (CH$_2$), 125.9 (4 x CH), 126.9 (2 x CH), 128.2 (4 x CH), 146.9 (2 x C).

9.3.19 The reaction of KO^{t}Bu with CBr$_4$ and adamantane (Scheme 5.15)

Scheme 5.15A
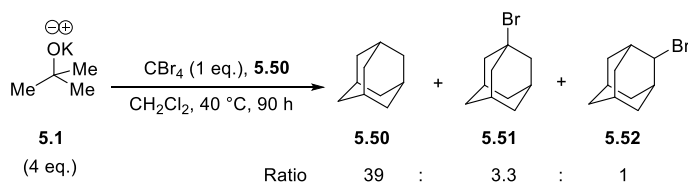
KO^{t}Bu **5.1** (224 mg, 2 mmol, 4.0 eq.), CBr$_4$ (166 mg, 0.5 mmol, 1.0 eq.), adamantane **5.50** (68 mg, 0.5 mmol) and dichloromethane (3.13 mL) were added to an oven-dried pressure tube and the reaction mixture was stirred at 40 °C for 90 h in the dark. The reaction mixture was cooled to RT and quenched with aqueous hydrochloric acid (1 M, 5 mL) and extracted with diethyl ether (4 x 10 mL). The organic phases were combined, dried over Na_2SO_4, filtered and concentrated *in vacuo*. The ratio of adamantane **5.50** : 1-bromoadamantane **5.51** : 2-bromoadamantane **5.52** was

determined to be 39 : 3.3 : 1 respectively from the ^{1}H-NMR spectrum of the crude mixture. The products were identified by the following characteristic signals; ^{1}H-NMR (400 MHz, CDCl$_3$) δ 1.74 – 1.76 (12 H, m, CH_2 x 6), 1.88 (4 H, br s, CH x 4) for adamantane **5.50**; δ 1.73 (6 H, m, CH_2 x 3), 2.10 (3 H, br s, CH x 3), 2.36 (6 H, m, CH_2 x 3) for 1-bromoadamantane **5.51**;[191] δ 1.96 – 2.00 (2 H, m, CH_2), 2.15 (2 H, br s, CH x 2), 2.33 (2 H, br s, CH x 2), 4.68 (1 H, br s, CH) for 2-bromoadamantane **5.52**.[192] These signals are consistent with the literature values and reference samples (Section 9.3.14 on page 232).
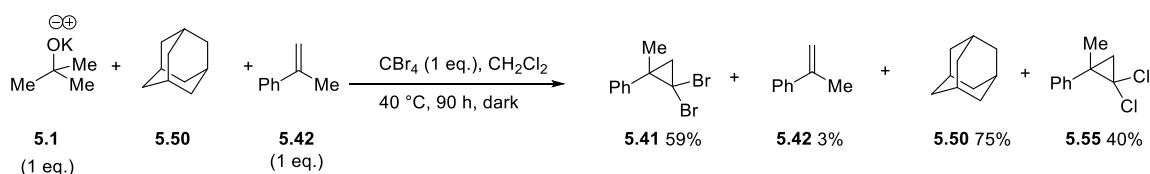
Scheme 5.15B

KO^{t}Bu **5.1** (224 mg, 2 mmol, 4.0 eq.), CBr$_4$ (166 mg, 0.5 mmol, 1.0 eq.), adamantane **5.50** (68 mg, 0.5 mmol), methylstyrene **5.42** (0.07 mL, 0.5 mmol, 1.0 eq.) and dichloromethane (3.13 mL) were added to an oven-dried pressure tube and the reaction mixture was stirred at 40 °C for 90 h in the dark. The reaction mixture was cooled to RT and quenched with aqueous hydrochloric acid (1 M, 5 mL) and extracted with diethyl ether (4 x 10 mL). The organic phases were combined, dried over Na$_2$SO$_4$, filtered and concentrated *in vacuo*. The yield of (2,2-dibromo-1-methylcyclopropyl)benzene **5.41** (59%), methylstyrene **5.42** (3%), adamantane **5.50** (75%) and (2,2-dichloro-1-methylcyclopropyl)benzene **5.55** (40%) were determined by adding 1,3,5-trimethoxybenzene to the crude mixture as an internal standard for ^{1}H-NMR. The products were identified by the following characteristic signals; ^{1}H-NMR (400 MHz, CDCl$_3$) δ 1.72 (3 H, s), 1.78 (1 H, d, J = 7.6 Hz) for (2,2-dibromo-1-methylcyclopropyl)benzene **5.41**; δ 5.09 (1 H, s), 5.37 (1 H, s) for methylstyrene **5.42**; δ 1.75 – 1.78 (12 H, m), 1.88 (4 H, br s) for adamantane **5.50**; δ 1.60 (1 H, d, J = 7.2 Hz), 1.69 (3 H, s), 1.97 (1 H, d, J = 7.2 Hz) for (2,2-dichloro-1-methylcyclopropyl)benzene **5.55**. These signals are consistent with the literature values and reference samples (**5.41**: Section 9.3.11 on page 229; **5.42**: Section 9.3.10, Table 5.4, entry 1 on page 226; **5.50**: Section 9.3.14, Scheme 5.12 on page 234; **5.55**: Section 9.3.16 on page 237).

9.3.20 Reaction of adamantane with alkoxides in CCl₄ (Scheme 5.16)

Scheme 5.16A
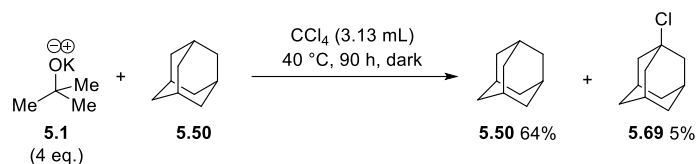
KO^{t}Bu **5.1** (224 mg, 2 mmol, 4.0 eq.), adamantane **5.50** (68 mg, 0.5 mmol) and CCl₄ (3.13 mL) were added to an oven-dried pressure tube and the reaction mixture was stirred at 40 °C for 90 h in the dark. The reaction mixture was cooled to RT and quenched with aqueous hydrochloric acid (1 M, 5 mL) and extracted with diethyl ether (4 x 10 mL). The organic phases were combined, dried over Na₂SO₄, filtered and concentrated *in vacuo*. The yield of adamantane **5.50** (64%) and 1-chloroadamantane **5.69** (5%) were determined by adding 1,3,5-trimethoxybenzene to the crude mixture as an internal standard for ^{1}H-NMR. The products were identified by the following characteristic signals; ^{1}H-NMR (400 MHz, CDCl₃) δ 1.75 – 1.78 (12 H, m), 1.88 (4 H, br s) for adamantane **5.50**; δ 1.68 – 1.69 (6 H, s), 2.14 (9 H, s) for 1-chloroadamantane **5.69**.[194] These signals are consistent with the literature values and reference samples (**5.50**: Section 9.3.14 on page 234; **5.69**: Section 9.3.24 on page 245).

Scheme 5.16B
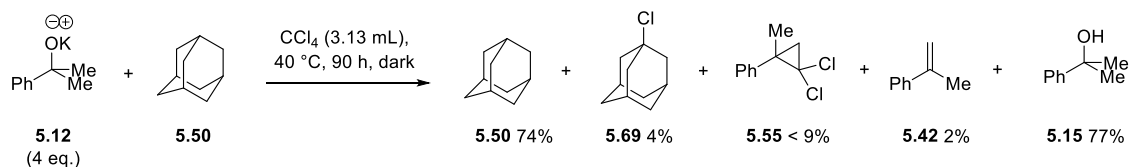
Potassium 2-phenylpropan-2-olate **5.12** (349 mg, 2 mmol, 4.0 eq.), adamantane **5.50** (68 mg, 0.5 mmol) and CCl₄ (3.13 mL) were added to an oven-dried pressure tube and the reaction mixture was stirred at 40 °C for 90 h in the dark. The reaction mixture was cooled to RT and quenched with aqueous hydrochloric acid (1 M, 5 mL) and extracted with diethyl ether (4 x 10 mL). The organic phases were combined, dried over Na₂SO₄, filtered and concentrated *in vacuo*. The yields of adamantane **5.50** (74%), 1-chloroadamantane **5.69** (4%) and (2,2-dichloro-1-methylcyclopropyl)benzene **5.55** (< 9% peaks overlapping with **5.69**) methylstyrene **5.42** (2%), 2-phenylpropanol **5.15** (77%) were determined by adding 1,3,5-

240

trimethoxybenzene to the crude mixture as an internal standard for ^{1}H-NMR. The products were identified by the following characteristic signals; ^{1}H-NMR (400 MHz, CDCl$_3$) δ 1.75 – 1.78 (12 H, m), 1.88 (4 H, br s) for adamantane **5.50**; δ 1.68 (3 H, s), 1.97 (1 H, d, *J* = 7.2 Hz) for (2,2-dichloro-1-methylcyclopropyl)benzene **5.55**; δ 2.16 (3 H, s), 5.09 (1 H, s), 5.37 (1 H, s) for methylstyrene **5.42**; δ 1.60 (6 H, s) for 2-phenylpropanol **5.15**; δ 1.68 – 1.69 (6 H, s), 2.14 (9 H, s) for 1-chloroadamantane **5.69**.[194] These signals are consistent with the literature values and reference samples (**5.50**: Sec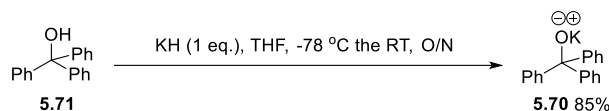tion 9.3.14, Scheme 5.12 on page 234; **5.55**: Section 9.3.16 on page 237; **5.42**: Section 9.3.10, Table 5.4, entry 1 on page 226; **5.15**: Section 9.3.6, Table 5.2, entry 1 on page 215; **5.69**: Section 9.3.24 on page 245).

9.3.21 Synthesis of potassium triphenylmethanolate 5.70

Potassium hydride (802 mg, 20 mmol, 1.0 eq.) was added to a flame-dried three-necked flask, equipped with a vacuum tap. Under an argon atmosphere, at -78 °C, a solution of triphenylmethanol **5.71** (5.21 g, 20 mmol) in anhydrous tetrahydrofuran (25 mL) was added and the reaction mixture was stirred at -78 °C for 1 h, then at RT overnight. The solvent was removed on the house vacuum line and the crude material was dried for 1 h to give *potassium triphenylmethanolate* **5.70** (5.07 g, 17 mmol, 85%) as an off-white solid m.p. 238 °C (dec.); [Found: (GCMS-EI) C$_{19}$H$_{16}$O (M)$^{\bullet+}$ 260.1 (under the MS analysis **5.70** is protonated to **5.71**)]; v_{max}(film) / cm^{-1} 3057, 3022, 1595, 1487, 1443, 1414, 1329, 1155, 1053, 1009, 891, 756; ^{1}H-NMR (400 MHz, d^6-DMSO) δ 6.93 – 6.98 (3 H, m, Ar*H*), 7.04 – 7.08 (6 H, m, Ar*H*), 7.34 – 7.37 (6 H, m, Ar*H*); ^{13}C{^{1}H}-NMR (100 MHz, d^6-DMSO) δ 84.7 (C), 123.6 (3 x CH), 126.0 (6 x CH), 128.2 (6 x CH), 157.6 (3 x C). The product was put under an argon atmosphere, and transported into the glove box immediately.

9.3.22 Reaction of potassium triphenylmethanolate 5.70 (Table 5.6)

Table 5.6, entry 1
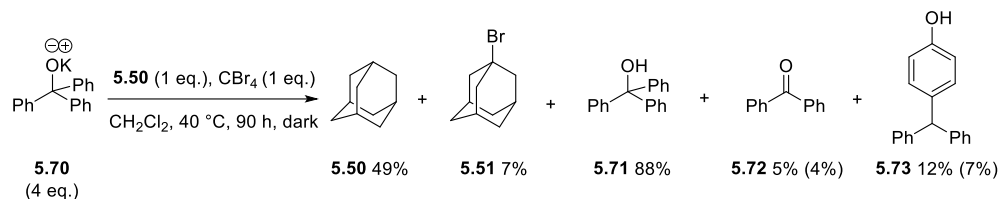
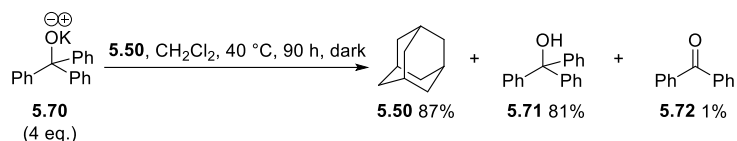Potassium triphenylmethanolate **5.70** (597 mg, 2 mmol, 4.0 eq.), CBr$_4$ (166 mg, 0.5 mmol, 1.0 eq.), adamantane **5.50** (68 mg, 0.5 mmol) and dichloromethane (3.13 mL) were added to an oven-dried pressure tube and the reaction mixture was stirred at 40 °C for 90 h in the dark. The reaction mixture was cooled to RT and quenched with aqueous hydrochloric acid (1 M, 5 mL) and extracted with diethyl ether (4 x 10 mL). The organic phases were combined, dried over Na$_2$SO$_4$, filtered and concentrated *in vacuo*. The yield of adamantane **5.50** (49%) 1-bromoadamantane **5.51** (7%) triphenylmethanol **5.71** (88%), benzophenone **5.72** (5%) and 4-benzhydrylphenol **5.73** (12%) were determined by adding 1,3,5-trimethoxybenzene to the crude mixture as an internal standard for ^{1}H-NMR. The products were identified by the following characteristic signals; ^{1}H-NMR (400 MHz, CDCl$_3$) δ 1.75 – 1.78 (12 H, m), 1.88 (4 H, br s) for adamantane **5.50**; δ 1.74 (6 H, m), 2.12 (3 H, br s), 2.38 (6 H, m) for 1-bromoadamantane **5.51**;[191] δ 7.27 – 7.34 (15 H, m) for triphenylmethanol **5.71**; δ 7.49 (4 H, d, *J* = 8.0 Hz), 7.60 (2 H, d, *J* = 8.0 Hz), 7.82 (4 H, d, *J* = 8.0 Hz) for benzophenone **5.72**;[195] δ 5.49 (1 H, s), 6.73 – 6.77 (2 H, m), 6.97 – 7.00 (2 H, m) for 4-benzhydrylphenol **5.73**.[196] These signals are consistent with the literature values and reference samples (**5.50**: Section 9.3.14, Scheme 5.12 on page 234; **5.51**: Section 9.3.14, Scheme 5.11A on page 232). This crude material was purified by column chromatography (0 - 10% ethyl acetate in hexane) to give both benzophenone **5.72**[195] (7 mg, 4%) as a yellow oil [Found: (GCMS-EI) C$_{13}$H$_{10}$O (M)$^{\bullet+}$ 182.0]; v_{max}(film) / cm^{-1} 3057, 1655, 1597, 1445, 1275, 1175, 939, 918, 808 762; ^{1}H-NMR (400 MHz, CDCl$_3$) δ 7.49 (4 H, t, *J* = 8.0 Hz, Ar*H*), 7.60 (2 H, t, *J* = 8.0 Hz, Ar*H*), 7.82 (4 H, d, *J* = 8.0 Hz, Ar*H*); ^{13}C{^{1}H}-NMR (100 MHz, CDCl$_3$) δ 128.2 (4 x CH), 130.2 (4 x CH), 132.6 (2 x CH), 137.5 (2 x C), 196.7 (C) and 4-benzhydrylphenol **5.73**[196] (18.9 mg, 7%) as a yellow oil [Found: (GCMS-EI) C$_{19}$H$_{16}$O (M)$^{\bullet+}$ 260.1];

v_{max}(film) / cm^{-1} 3366, 2361, 2336, 1595, 1508, 1491, 1449, 1238, 1173, 1103, 1030, 816, 800, 750, 735; ^{1}H-NMR (400 MHz, CDCl$_3$) δ 4.82 (1 H, br s, O*H*), 5.49 (1 H, s, C*H*), 6.73 – 6.77 (2 H, m, Ar*H*), 6.97 – 7.00 (2 H, m, Ar*H*), 7.11 – 7.13 (4 H, m, Ar*H*), 7.19 – 7.32 (6 H, m, Ar*H*); ^{13}C{^{1}H}-NMR (100 MHz, CDCl$_3$) δ 56.1 (CH), 115.3 (2 x CH), 126.4 (2 x CH), 128.4 (4 x CH), 129.5 (4 x CH), 130.7 (2 x CH), 136.4 (C), 144.3 (2 x C), 154.1 (C).

Triphenylmethanol **5.71** ^{1}H-NMR (400 MHz, CDCl$_3$) δ 2.79 (1 H, s, O*H*), 7.26 – 7.34 (15 H, m, Ar*H*), 7.57 (2 H, d, *J* = 8.4 Hz, Ar*H*); ^{13}C{^{1}H}-NMR (100 MHz, CDCl$_3$) δ 82.2 (C), 127.4 (9 x CH), 128.1 (6 x CH), 147.0 (3 x C). These signals are consistent with a commercial sample used as a reference.

Table 5.6, entry 2

Potassium triphenylmethanolate **5.70** (597 mg, 2 mmol, 4.0 eq.), adamantane **5.50** (68 mg, 0.5 mmol) and dichloromethane (3.13 mL) were added to an oven-dried pressure tube was added and the reaction mixture was stirred at 40 °C for 90 h in the dark. The reaction mixture was cooled to RT and quenched with aqueous hydrochloric acid (1 M, 5 mL) and extracted with diethyl ether (4 x 10 mL). The organic phases were combined, dried over Na$_2$SO$_4$, filtered and concentrated *in vacuo*. The yield of adamantane **5.50** (87%), triphenylmethanol **5.71** (81%) and benzophenone **5.72** (1%) were determined by adding 1,3,5-trimethoxybenzene to the crude mixture as an internal standard for ^{1}H-NMR. The products were identified by the following characteristic signals; ^{1}H-NMR (400 MHz, CDCl$_3$) δ 1.75 – 1.78 (12 H, m), 1.88 (4 H, br s) for adamantane **5.50**; δ 7.27 – 7.34 (15 H, m) for triphenylmethanol **5.71**, δ 7.49 (4 H, d, *J* = 8.0 Hz, Ar*H*), 7.60 (2 H, d, *J* = 8.0 Hz, Ar*H*), 7.82 (4 H, d, *J* = 8.0 Hz, Ar*H*) for benzophenone **5.72**; ^{13}C{^{1}H}-NMR (100 MHz, CDCl$_3$) δ 28.3, 37.7 for adamantane **5.50**; δ 82.2, 127.4, 128.0, 147.0 triphenylmethanol **5.71**.[196] These signals are consistent with the literature values and reference samples (**5.71** and **5.72**: Section 9.3.22, Table 5.6, entry 1 on pages 242-243; **5.50**: Section 9.3.14, Scheme 5.12 on page 234).

9.3.23 Formation of *tert*-butyl hypochlorite 5.83 (Scheme 5.18)
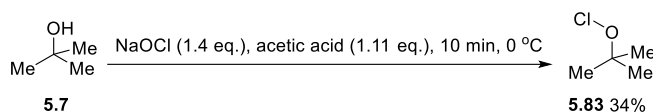
Throughout the experiment, all the equipment was covered in aluminium foil and the reaction mixture was always kept in the dark. A solution of NaOCl (0.6 M, 200 mL, 1.4 eq.) was added to a round-bottomed flask and the reaction mixture was stirred at 0 °C for 10 min. A mixture of *tert*-butanol **5.7** (8 mL, 84 mmol) and acetic acid (5.3 mL, 92 mmol, 1.11 eq.) was added, in one batch under vigorous stirring, and the reaction mixture was stirred at 0 °C for 10 min. The reaction mixture phase-separated. The top yellow phase was separated from the reaction mixture, washed with saturated aqueous $NaHCO_3$ solution (50 mL) and water (50 mL), dried over Na_2SO_4 to give *tert*-butyl hypochlorite **5.83**[197-198] (0.82 mL, d = 1.128 g mL^{-1}, 34%) as a yellow oil ^{1}H-NMR (400 MHz, CDCl$_3$) δ 1.32 (9 H, s, 3 x C*H$_3$*); ^{13}C{^{1}H}-NMR (100 MHz, CDCl$_3$) δ 26.9 (3 x CH$_3$), 84.0 (C). These signals are consistent with the literature values. The hypochlorite **5.83** was used immediately.

9.3.24 Reactions of *tert*-butyl hypochlorite 5.83 or KO^{t}Bu with adamantane 5.50 (Table 5.7)

Table 5.7, entry 1
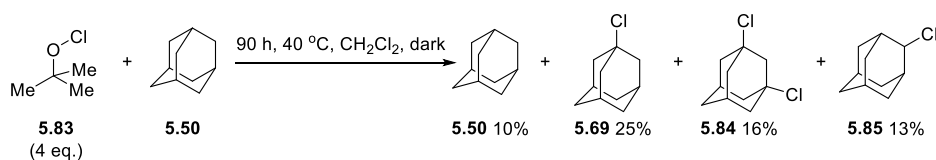
Tert-butyl hypochlorite **5.83** (0.19 mL, freshly prepared, 2 mmol, 4.0 eq.), adamantane **5.50** (68 mg, 0.5 mmol) and dichloromethane (3.13 mL) were added to an oven-dried pressure tube and the reaction mixture was stirred at 40 °C for 90 h in the dark. The reaction mixture was cooled to RT and quenched with aqueous hydrochloric acid (1 M, 5 mL) and extracted with dichloromethane (4 x 10 mL). The organic phases were combined, dried over Na_2SO_4, filtered and concentrated *in vacuo*. The yield of adamantane **5.50** (10%), 1-chloroadamantane **5.69** (25%), 1,3-dichloroadamantane **5.84** (16%) and 2-chloroadamantane **5.85** (13%) were determined by adding 1,3,5-trimethoxybenzene to the crude mixture as an internal standard for ^{1}H-NMR. The products were identified by the following characteristic

signals; ^{1}H-NMR (400 MHz, CDCl$_3$) δ 1.75 – 1.78 (12 H, m), 1.88 (4 H, br s) for adamantane **5.50**; δ 1.68 (6 H, s), 2.14 (9 H, s) for 1-chloroadamantane **5.69**;[194] δ 2.06 (8 H, d, *J* = 4 Hz), 2.47 (2 H, s) for 1,3-chloroadamantane **5.84**;[199] δ 4.40 (1 H, s) 2-chloroadamantane **5.85**;[192] ^{13}C{^{1}H}-NMR (100 MHz, CDCl$_3$) δ 28.5, 37.9 for adamantane **5.50**; δ 31.9, 35.7, 47.9 for 1-chloroadamantane **5.69**;[194] δ 33.5, 33.8, 45.9, 56.6, 66.9 for 1,3-dichloroadamantane **5.84**;[199] δ 26.9, 27.5, 31.1, 35.9, 37.8, 38.3, 68.4 2-chloroadamantane **5.85**. Analysis of the crude material showed that the products were inseparable, hence the analysis of the product mixture was performed using experimental ^{1}H-NMR and ^{13}C{^{1}H}-NMR values reported within the literature as a reference.

1-Chloroadamantane **5.69**[194] ^{1}H-NMR (400 MHz, CDCl$_3$) δ 1.68 – 1.69 (6 H, m, 6 x C*H*$_2$), 2.14 (9 H, s, 3 x C*H* and 3 x C*H*$_2$); ^{13}C{^{1}H}-NMR (100 MHz, CDCl$_3$) δ 31.9, 35.7, 47.9, 69.1.

1,3-Dichloroadamantane **5.84**[199-200] ^{1}H-NMR (400 MHz, CDCl$_3$) δ 1.63 (2 H, br s, C*H*$_2$), 2.06 (8 H, d, 4 x C*H*$_2$), 2.30 (2 H, br s, 2 x C*H*), 2.46 (2 H, s, C*H*$_2$); ^{13}C{^{1}H}-NMR (100 MHz, CDCl$_3$) δ 33.4 (CH$_2$), 33.7, (2 x CH), 45.7 (4 x CH$_2$), 56.5 (CH$_2$), 66.7 (2 x C).

2-Chloroadamantane **5.85**[192] ^{1}H-NMR (500 MHz, CDCl$_3$) δ 1.56 – 1.59 (2 H, m, C*H*$_2$), 1.76 – 1.87 (6 H, m, 2 x C*H* and 2 x C*H*$_2$), 1.93 – 1.96 (2 H, m, C*H*$_2$), 2.08 (2 H, br s, 2 x C*H*), 2.26 – 2.29 (2 H, m, C*H*$_2$), 4.40 (1 H, s, C*H*); ^{13}C{^{1}H}-NMR (125 MHz, CDCl$_3$) δ 27.0, 27.6, 31.2, 36.0, 37.9, 38.3, 68.5.

Representative ^{1}H-NMR
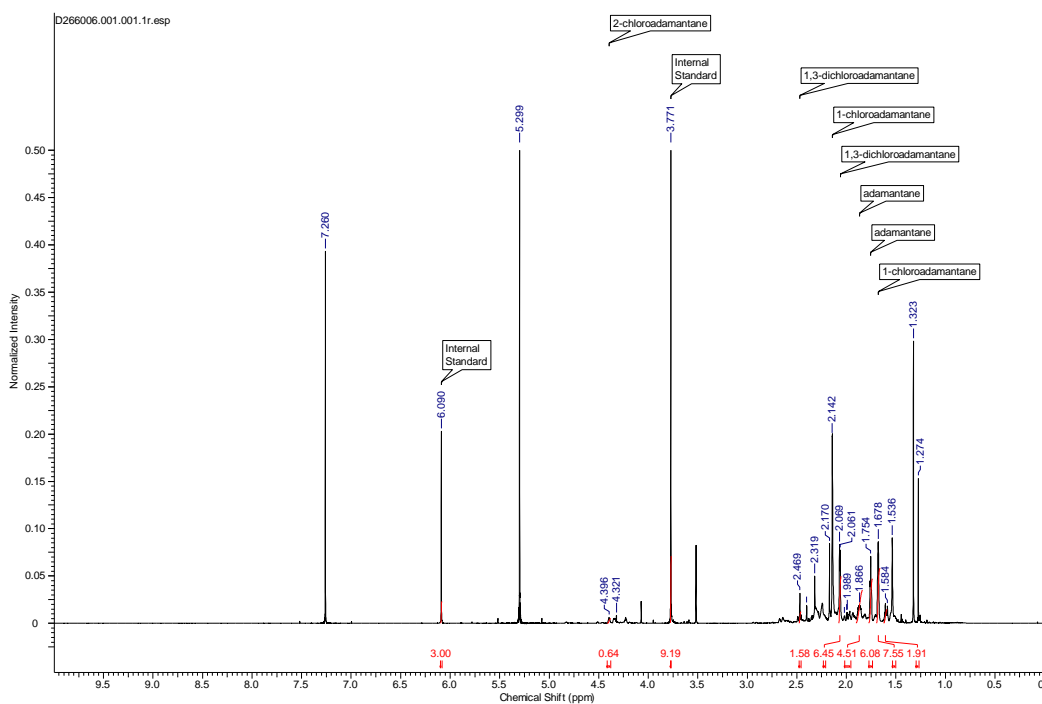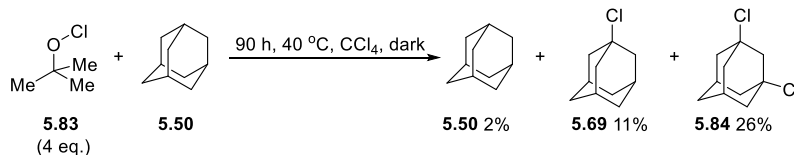
D266006.001.001.1r.esp

Table 5.7, entry 2

5.83
(4 eq.) **5.50** **5.50** 2% **5.69** 11% **5.84** 26%

Tert-butyl hypochlorite **5.83** (0.19 mL, freshly prepared, 2 mmol, 4.0 eq.), adamantane **5.50** (68 mg, 0.5 mmol) and CCl_4 (3.13 mL) were added to an oven-dried pressure tube and the reaction mixture was stirred at 40 °C for 90 h in the dark. The reaction mixture was cooled to RT and quenched with aqueous hydrochloric acid (1 M, 5 mL) and extracted with dichloromethane (4 x 10 mL). The organic phases were combined, dried over Na_2SO_4, filtered and concentrated *in vacuo*. The yield of adamantane **5.50** (2%), 1-chloroadamantane **5.69** (11%) and 1,3-dichloroadamantane **5.84** (26%) were determined by adding 1,3,5-trimethoxybenzene to the crude mixture as an internal standard for ^{1}H-NMR. The products were identified by the following characteristic signals; ^{1}H-NMR (400 MHz, CDCl$_3$) δ 1.75 – 1.78 (12 H, m), 1.88 (4 H, br s) for adamantane **5.50**; δ 1.68 (6 H, s), 2.14 (9 H, s) for 1-chloroadamantane **5.69**;[194] δ 2.06 (8 H, d, *J* = 4.0 Hz), 2.47 (2 H, s) for 1,3-chloroadamantane **5.84**.[199] These signals are consistent with the

literature values and reference samples (**5.50**: Section 9.3.14, Scheme 5.12 on page 234; **5.69** and **5.84**: Section 9.3.24, Table 5.7, entry 1 on page 245).

Table 5.7, entry 3
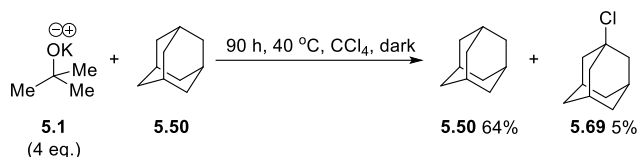
KO^{t}Bu **5.1** (224 mg, 2 mmol, 4.0 eq.), adamantane **5.50** (68 mg, 0.5 mmol) and CCl$_4$ (3.13 mL) were added to an oven-dried pressure tube and the reaction mixture was stirred at 40 °C for 90 h in the dark. The reaction mixture was cooled to RT and quenched with aqueous hydrochloric acid (1 M, 5 mL) and extracted with dichloromethane (4 x 10 mL). The organic phases were combined, dried over Na$_2$SO$_4$, filtered and concentrated *in vacuo*. The yield of adamantane **5.50** (64%) and 1-chloroadamantane **5.69**[194] (5%) were determined by adding 1,3,5-trimethoxybenzene to the crude mixture as an internal standard for ^{1}H-NMR. The products were identified by the following characteristic signals; ^{1}H-NMR (400 MHz, CDCl$_3$) δ 1.75 – 1.78 (12 H, m), 1.88 (4 H, br s) for adamantane **5.50**; δ 1.68 (6 H, s), 2.14 (9 H, s) for 1-chloroadamantane **5.69**.[194] These signals are consistent with the literature values and reference samples (**5.50**: Section 9.3.14, Scheme 5.12 on page 234; **5.69**: Section 9.3.24, Table 5.7, entry 1 on page 245).

9.3.25 Synthesis of *tert*-butyl hypobromite 5.86
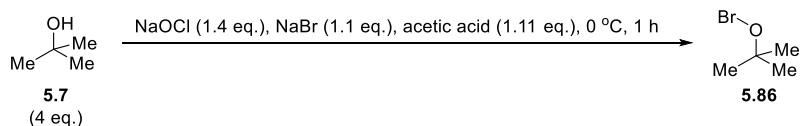
Throughout the experiment all the equipment was covered in aluminium foil and the reaction mixture was always kept in the dark. A solution of NaOCl (0.6 M, 200 mL, 1.4 eq.) was added to a round-bottomed flask and the reaction mixture was stirred at 0 °C for 10 min. NaBr (9.26 g, 90 mmol, 1.1 eq.) was added and the reaction mixture was stirred at 0 °C for 2 min. A mixture of *tert*-butanol **5.7** (8 mL, 84 mmol) and acetic acid (5.3 mL, 92 mmol, 1.11 eq.) was added in one batch under vigorous stirring and the reaction mixture was stirred at 0 °C for 1 h. The reaction mixture was extracted with dichloromethane (10 mL), washed with water (100 mL), dried over

Na$_2$SO$_4$ to give *tert*-butyl hypobromite **5.86**[163,201] as a dark red solution in dichloromethane ^{1}H-NMR (400 MHz, CDCl$_3$) δ 1.27 (9 H, s, 3 x C*H$_3$*); ^{13}C{^{1}H}-NMR (100 MHz, CDCl$_3$) δ 27.5 (3 x CH$_3$), 82.9 (C). The hypobromite **5.86** was used immediately.

To quantify the amount of *tert*-butyl hypobromite **5.86** formed, 0.2 mL of the *tert*-butyl hypobromite/dichloromethane solution was transferred to a small vial and a solution of 1,2-dibromoethane (internal standard) in dichloromethane (1 mL, 0.5 M, 0.5 mmol) was added. The concentration was determined from ^{1}H-NMR: In 0.2 mL of the *tert*-butyl hypobromite / dichloromethane solution, there is 0.052 mmol of *tert*-butyl hypobromite **5.86**. The compound was used immediately in reactions. To ensure the *tert*-butyl hypobromite **5.86** had not decomposed prior to being used in the reactions, the *tert*-butyl hypobromite / dichloromethane solution was analysed in the same way immediately after being used, to determine the amount of *tert*-butyl hypobromite **5.86** present in the *tert*-butyl hypobromite/dichloromethane solution: the amount was determined from ^{1}H-NMR: In 0.2 mL of the *tert*-butyl hypobromite/dichloromethane solution, there was 0.052 mmol of *tert*-butyl hypobromite **5.86**.

9.3.26 Reactions of *tert*-butyl hypobromite 5.86 (Scheme 5.19A)
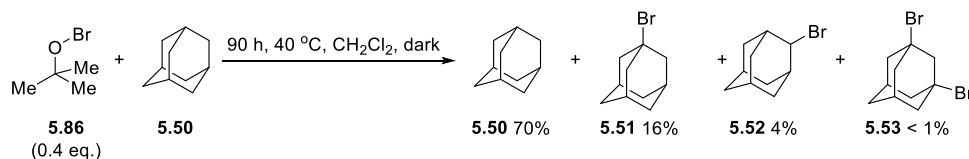
Tert-butyl hypobromite **5.86** (0.87 mL, freshly prepared and used immediately, 0.22 mmol, 0.4 eq.), adamantane **5.50** (68 mg, 0.5 mmol) and dichloromethane (3.13 mL) were added to an oven-dried pressure tube and the reaction mixture was stirred at 40 °C for 90 h in the dark. The reaction mixture was cooled to RT and quenched with aqueous hydrochloric acid (1 M, 5 mL) and extracted with dichloromethane (4 x 10 mL). The organic phases were combined, dried over Na$_2$SO$_4$, filtered and concentrated *in vacuo*. The yield of adamantane **5.50** (70%), 1-bromoadamantane **5.51** (16%), 2-bromoadamantane **5.52** (4%) and 1,3-bromoadamantane **5.53** (< 1%) were determined by adding 1,3,5-trimethoxybenzene to the crude mixture as an internal standard for ^{1}H-NMR. The products were identified by the following

characteristic signals; ^{1}H-NMR (400 MHz, CDCl₃) δ 1.74 – 1.76 (12 H, m), 1.88 (4 H, br s) for adamantane **5.50**; δ 1.72 (6 H, m), 2.10 (3 H, br s), 2.36 (6 H, m) for 1-bromoadamantane **5.51**;[191] δ 1.97 – 2.00 (2 H, m), 2.15 (2 H, br s), 2.33 (2 H, br s), 4.68 (1 H, br s) for 2-bromoadamantane **5.52**;[192] δ 1.70 (2 H, m), 2.25 – 2.30 (10 H, m), 2.87 (2 H, br s) for 1,3-dibromoadamantane **5.53**.[191] These signals are consistent with the literature values and reference samples (**5.50**: Section 9.3.14, Scheme 5.12 on page 234; **5.51**-**5.53**: Section 9.3.14, Section 5.11A on page 232).

9.3.27 Reactions of KO*t*Bu with adamantane and CBr₄ (Scheme 5.19B)
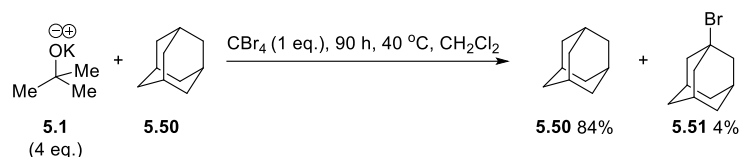
KO*t*Bu **5.1** (224 mg, 2 mmol, 4.0 eq.), adamantane **5.50** (68 mg, 0.5 mmol), CBr₄ (166 mg, 0.5 mmol, 1.0 eq.) and dichloromethane (3.13 mL) were added to an oven-dried pressure tube and the reaction mixture was stirred at 40 °C for 90 h in the dark. The reaction mixture was cooled to RT and quenched with aqueous hydrochloric acid (1 M, 5 mL) and extracted with dichloromethane (4 x 10 mL). The organic phases were combined and dried over Na₂SO₄, filtered and concentrated *in vacuo*. The yield of adamantane **5.50** (84%) and 1-bromoadamantane **5.51** (4%) were determined by adding 1,3,5-trimethoxybenzene to the crude mixture as an internal standard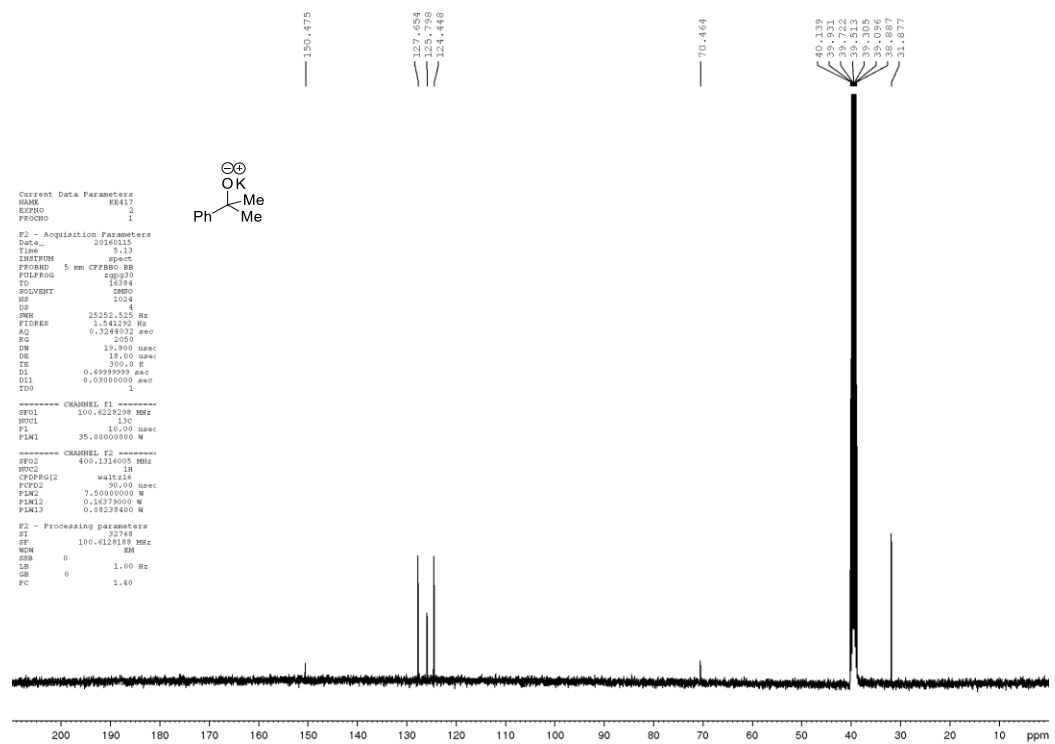 for ^{1}H-NMR. The products were identified by the following characteristic signals; ^{1}H-NMR (400 MHz, CDCl₃) δ 1.74 – 1.76 (12 H, m), 1.88 (4 H, br s) for adamantane **5.50**; δ 1.72 (6 H, m), 2.10 (3 H, br s), 2.36 (6 H, m) for 1-bromoadamantane **5.51**.[191] These signals are consistent with the literature values and reference samples (**5.50**: Section 9.3.14, Scheme 5.12 on page 234; **5.51**: Section 9.3.14, Section 5.11A on page 232).

NMR of novel compounds in Chapter 5

^{1}H-NMR and ^{13}C{^{1}H}-NMR 5.12
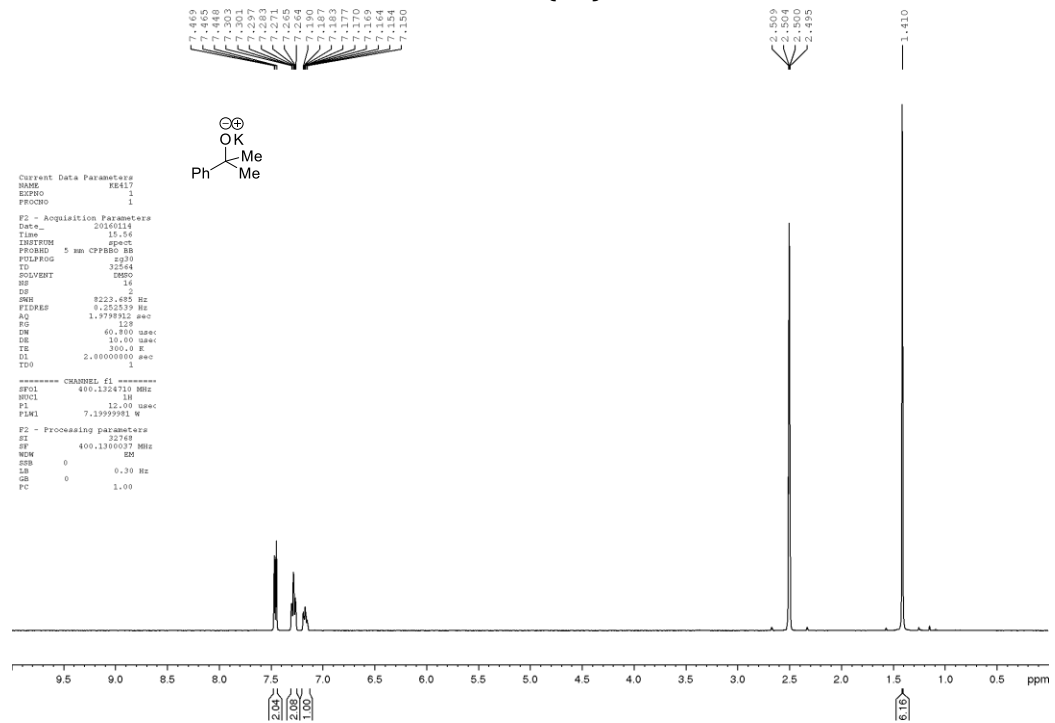
^{1}H-NMR and ^{13}C{^{1}H}-NMR 5.30
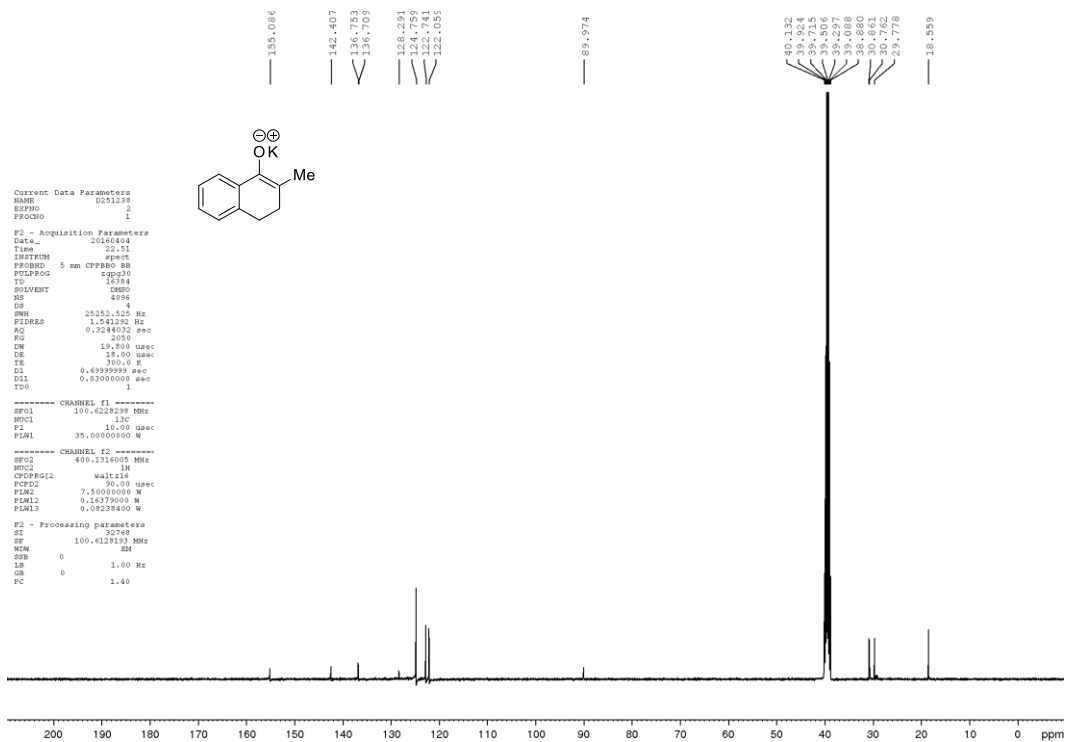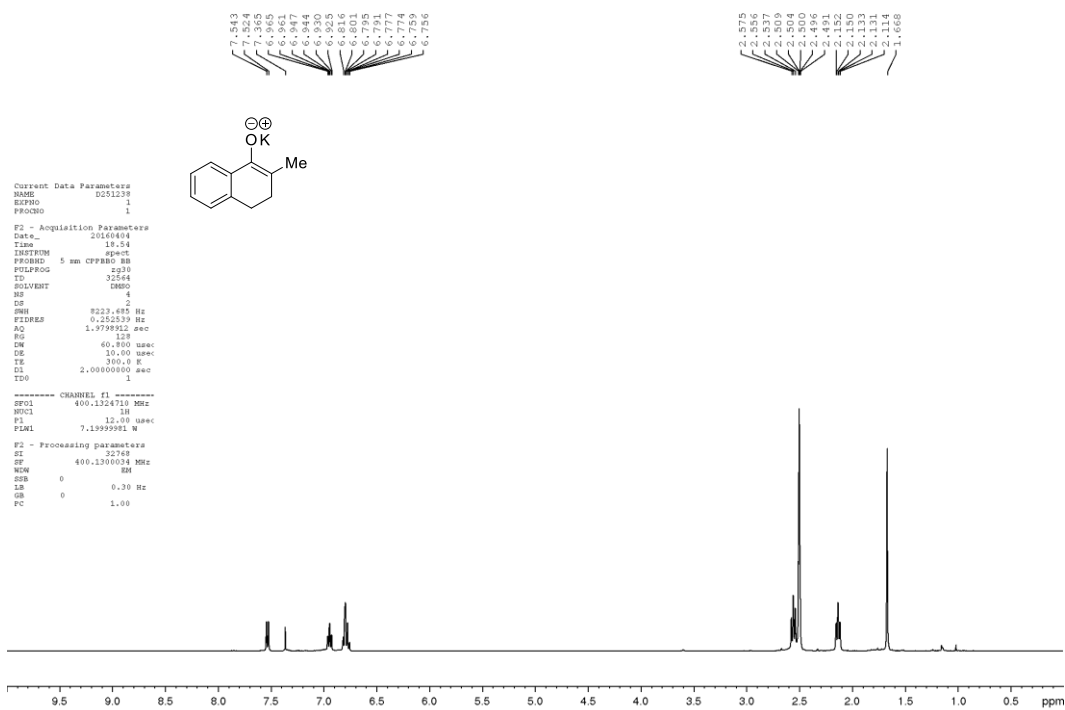
^{1}H-NMR and ^{13}C{^{1}H}-NMR 9.5.3

7.529 7.524 7.519 7.513 7.510 7.508 7.505 7.386 7.379 7.364 7.360 7.350 7.345 7.337 7.341 7.325 7.323 7.260

3.886 3.884 3.847 3.845 3.699 3.660 3.321 3.308 3.045 3.043 3.033 3.031

1.547 1.255 0.897 0.881 0.864

Ph—CBr$_3$ (epoxide with O)

(contains impurity δ 0.88 and 1.26 ppm)

Current Data Parameters
NAME   D272142
EXPNO   1
PROCNO   1

F2 - Acquisition Parameters
Date_   20170215
Time   17.00
INSTRUM   spect
PROBHD   5 mm CPPBBO BB
PULPROG   zg30
TD   32564
SOLVENT   CDCl3
NS   4
DS   2
SWH   8223.685 Hz
FIDRES   0.252539 Hz
AQ   1.9798912 sec
RG   144
DW   60.800 usec
DE   10.00 usec
TE   300.0 K
D1   2.00000000 sec
TD0   1

======== CHANNEL f1 ========
SFO1   400.1324710 MHz
NUC1   1H
P1   12.00 usec
PLW1   7.19999981 W

F2 - Processing parameters
SI   32768
SF   400.1300097 MHz
WDW   EM
SSB   0
LB   0.30 Hz
GB   0
PC   1.00

0.08 0.10   1.92 2.97   1.00 1.02 0.98 1.00

137.705   128.658 128.437 128.106   77.471 77.154 76.836   64.251 64.214 60.637   54.076   33.243 29.843

Ph—CBr$_3$ (epoxide with O)

(contains impurity δ 29.8 ppm)

Current Data Parameters
NAME   D272142
EXPNO   2
PROCNO   1

F2 - Acquisition Parameters
Date_   20170215
Time   21.59
INSTRUM   spect
PROBHD   5 mm CPPBBO BB
PULPROG   zgpg30
TD   16384
SOLVENT   CDCl3
NS   2048
DS   4
SWH   25252.525 Hz
FIDRES   1.541292 Hz
AQ   0.3244032 sec
RG   2050
DW   19.800 usec
DE   18.00 usec
TE   300.0 K
D1   0.69999999 sec
D11   0.03000000 sec
TD0   1

======== CHANNEL f1 ========
SFO1   100.6228298 MHz
NUC1   13C
P1   10.00 usec
PLW1   35.00000000 W

======== CHANNEL f2 ========
SFO2   400.1316005 MHz
NUC2   1H
CPDPRG[2   waltz16
PCPD2   90.00 usec
PLW2   7.50000000 W
PLW12   0.16379000 W
PLW13   0.08238400 W

F2 - Processing parameters
SI   32768
SF   100.6127546 MHz
WDW   EM
SSB   0
LB   1.00 Hz
GB   0
PC   1.40

^{1}H-NMR and ^{13}C{^{1}H}-NMR 5.55

¹H-NMR and ¹³C{¹H}-NMR 5.56
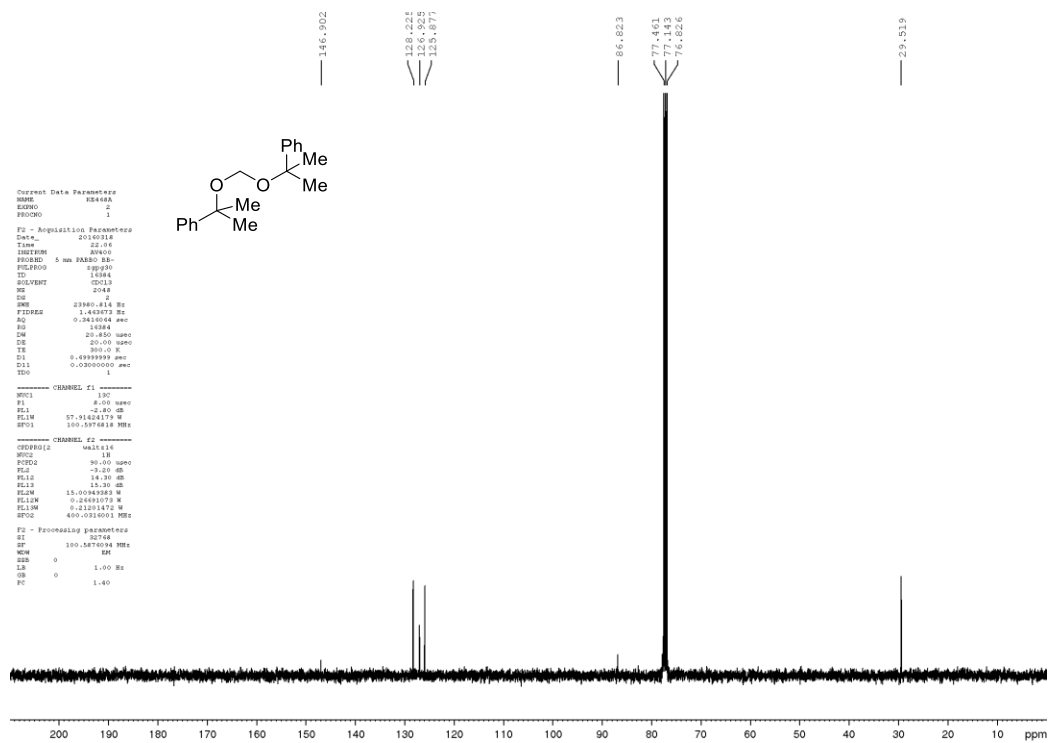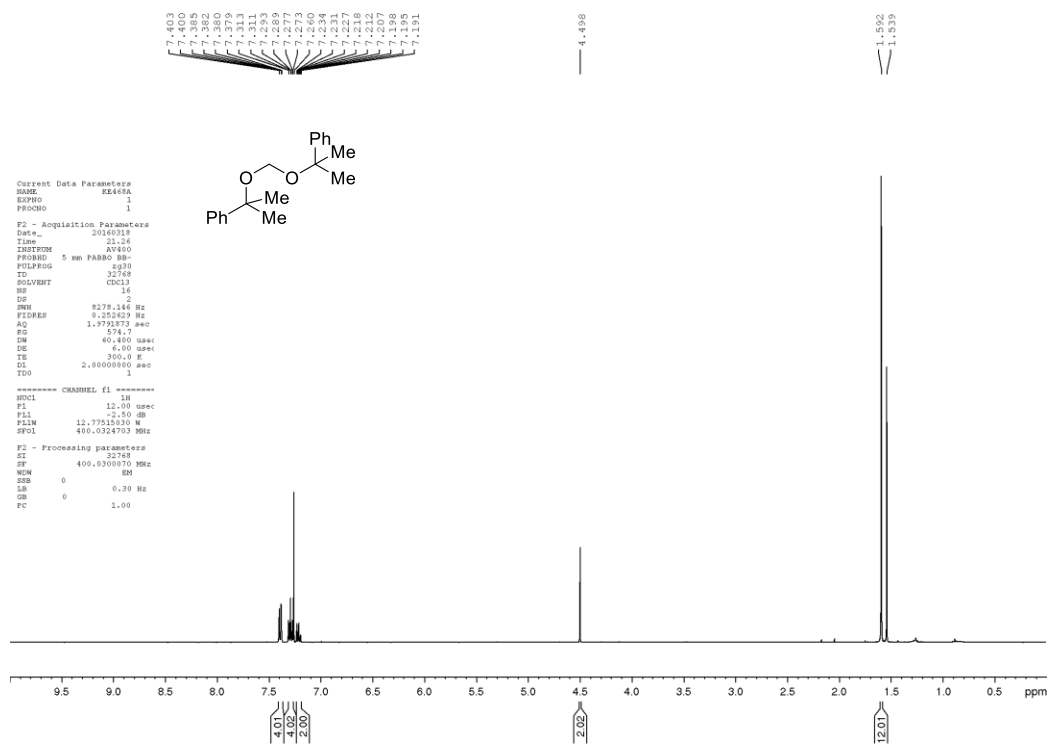
^{1}H-NMR and ^{13}C{^{1}H}-NMR 5.70

7.368 7.365 7.360 7.348 7.345 7.340 7.077 7.073 7.059 7.056 7.044 7.040 7.036 6.975 6.972 6.969 6.959 6.954 6.949 6.940 6.936 6.933

2.509 2.504 2.500 2.495 2.491

Current Data Parameters
NAME   D275927
EXPNO   1
PROCNO   1

F2 - Acquisition Parameters
Date_   20170404
Time   16.49
INSTRUM   aspect
PROBHD   5 mm CPPBBO BB
PULPROG   zg30
TD   32564
SOLVENT   DMSO
NS   4
DS   2
SWH   8223.685 Hz
FIDRES   0.252539 Hz
AQ   1.9798912 sec
RG   57
DW   60.800 usec
DE   10.00 usec
TE   308.0 K
D1   2.00000000 sec
TD0   1

======== CHANNEL f1 ========
SFO1   400.1324710 MHz
NUC1   1H
P1   12.00 usec
PLW1   7.19999981 W

F2 - Processing parameters
SI   32768
SF   400.1300835 MHz
WDW   EM
SSB   0
LB   0.30 Hz
GB   0
PC   1.00

9.5 9.0 8.5 8.0 7.5 7.0 6.5 6.0 5.5 5.0 4.5 4.0 3.5 3.0 2.5 2.0 1.5 1.0 0.5 ppm

6.06   6.04 3.00

157.625

128.216 126.049 123.593

84.666

39.933 39.724 39.516 39.307 39.099

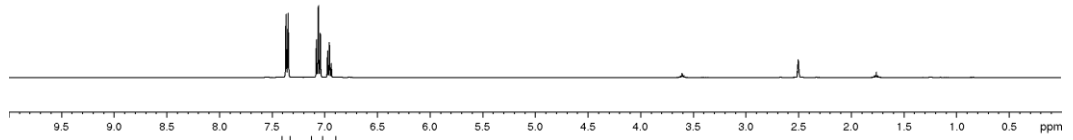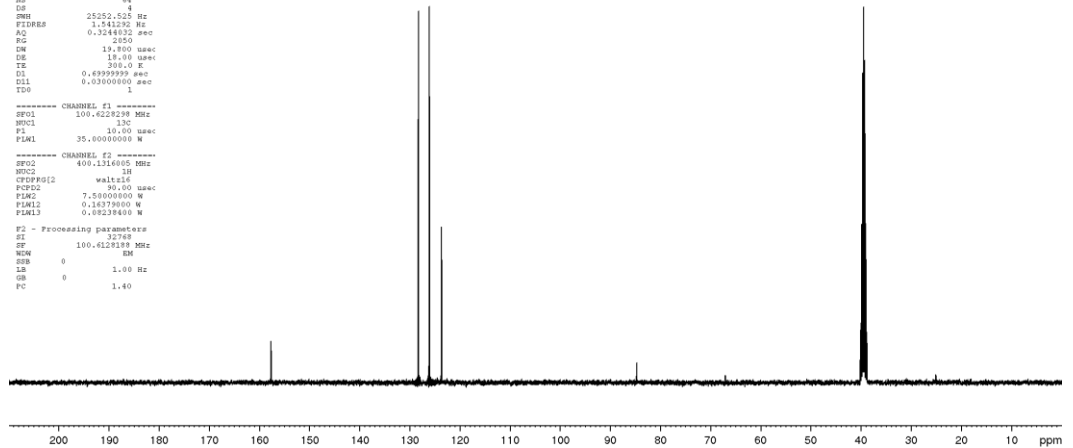Current Data Parameters
NAME   D275927
EXPNO   2
PROCNO   1

F2 - Acquisition Parameters
Date_   20170404
Time   16.52
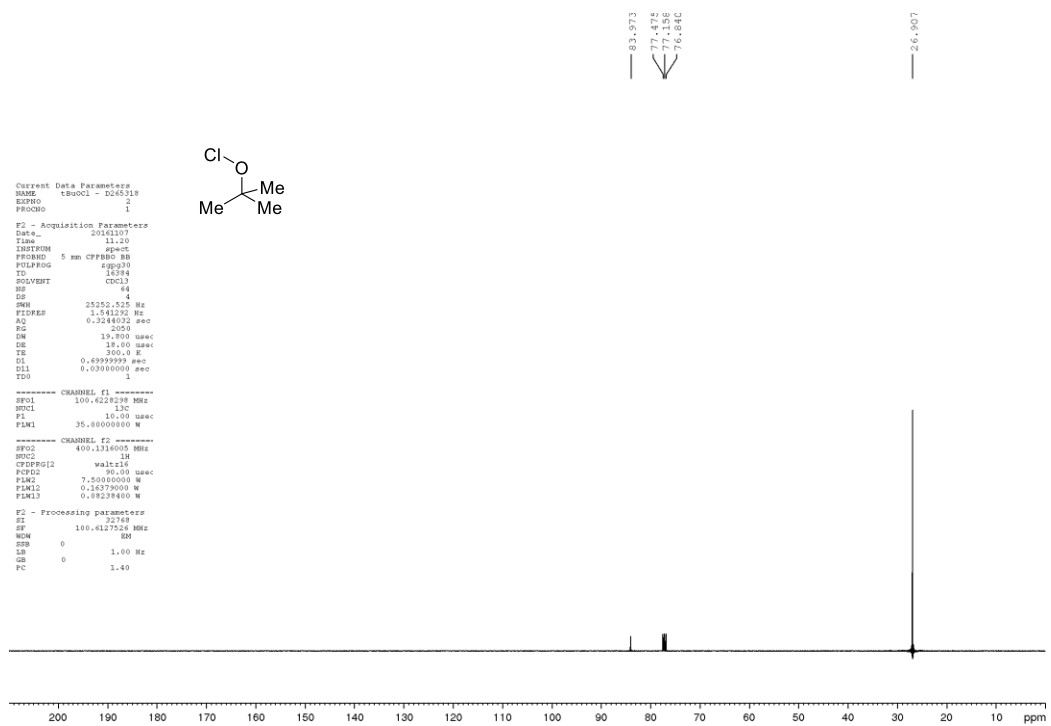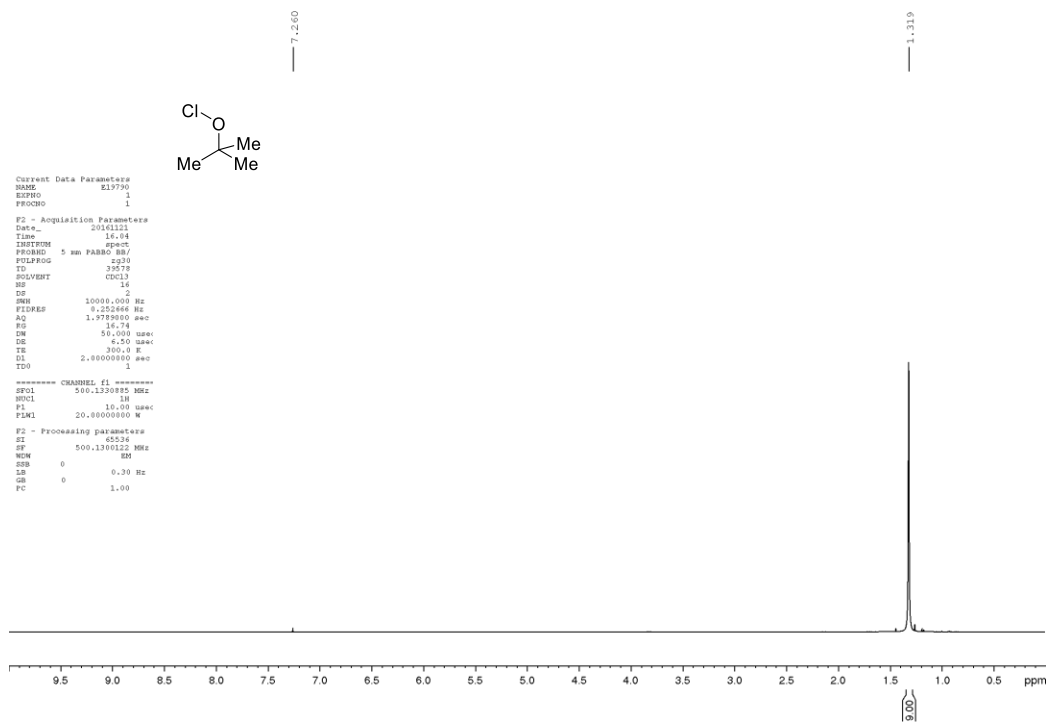INSTRUM   aspect
PROBHD   5 mm CPPBBO BB
PULPROG   zgpg30
TD   16384
SOLVENT   DMSO
NS   64
DS   4
SWH   25252.525 Hz
FIDRES   1.541292 Hz
AQ   0.3244032 sec
RG   2050
DW   19.800 usec
DE   18.00 usec
TE   300.0 K
D1   0.69999999 sec
D11   0.03000000 sec
TD0   1

======== CHANNEL f1 ========
SFO1   100.6228298 MHz
NUC1   13C
P1   10.00 usec
PLW1   35.00000000 W

======== CHANNEL f2 ========
SFO2   400.1316005 MHz
NUC2   1H
CPDPRG[2   waltz16
PCPD2   90.00 usec
PLW2   7.50000000 W
PLW12   0.16379000 W
PLW13   0.08238400 W

F2 - Processing parameters
SI   32768
SF   100.6128188 MHz
WDW   EM
SSB   0
LB   1.00 Hz
GB   0
PC   1.40

200 190 180 170 160 150 140 130 120 110 100 90 80 70 60 50 40 30 20 10 ppm

¹H-NMR and ¹³C{¹H}-NMR 5.83

7.260
1.319

Cl—O
Me—Me
Me

Current Data Parameters
NAME   E19790
EXPNO   1
PROCNO   1

F2 - Acquisition Parameters
Date_   20161121
Time   16.04
INSTRUM   spect
PROBHD   5 mm PABBO BB/
PULPROG   zg30
TD   39578
SOLVENT   CDCl3
NS   16
DS   2
SWH   10000.000 Hz
FIDRES   0.252666 Hz
AQ   1.9789000 sec
RG   16.74
DW   50.000 usec
DE   6.50 usec
TE   300.0 K
D1   2.00000000 sec
TD0   1

======= CHANNEL f1 ========
SFO1   500.1330885 MHz
NUC1   1H
P1   10.00 usec
PLW1   20.00000000 W

F2 - Processing parameters
SI   65536
SF   500.1300122 MHz
WDW   EM
SSB   0
LB   0.30 Hz
GB   0
PC   1.00

9.5 9.0 8.5 8.0 7.5 7.0 6.5 6.0 5.5 5.0 4.5 4.0 3.5 3.0 2.5 2.0 1.5 1.0 0.5 ppm

9.00

83.973
77.475
77.156
76.840
26.907

Cl—O
Me—Me
Me

Current Data Parameters
NAME   tBuOCl - D265318
EXPNO   2
PROCNO   1

F2 - Acquisition Parameters
Date_   20161107
Time   11.20
INSTRUM   spect
PROBHD   5 mm CPPBBO BB
PULPROG   zgpg30
TD   16384
SOLVENT   CDCl3
NS   64
DS   4
SWH   25252.525 Hz
FIDRES   1.541292 Hz
AQ   0.3244032 sec
RG   2050
DW   19.800 usec
DE   18.00 usec
TE   300.0 K
D1   0.69999999 sec
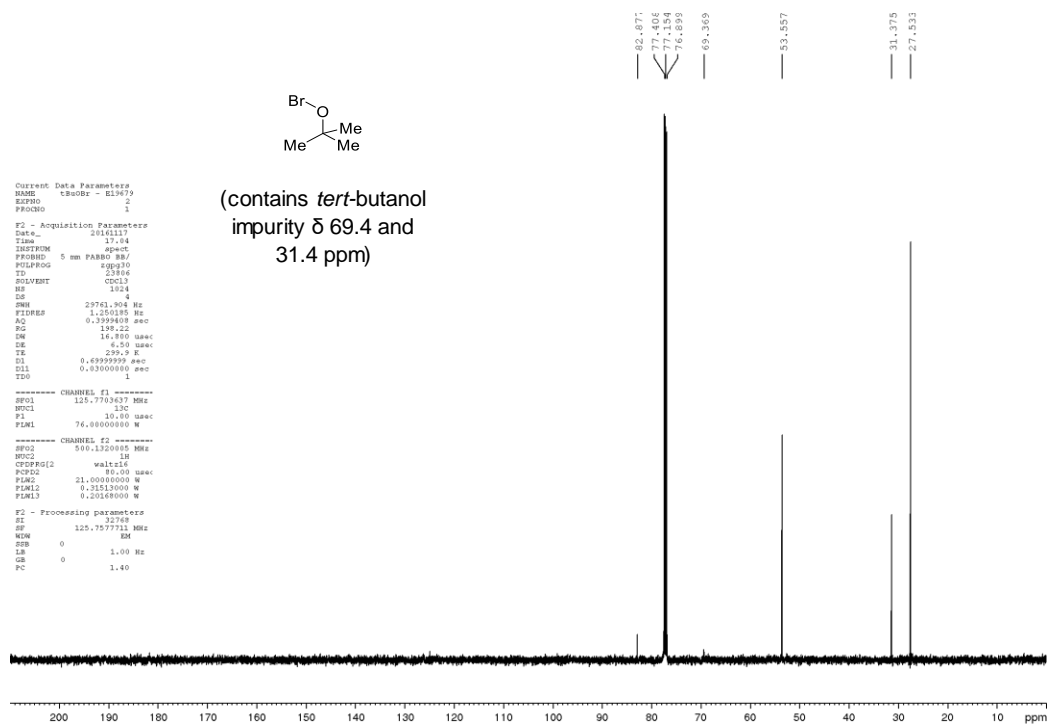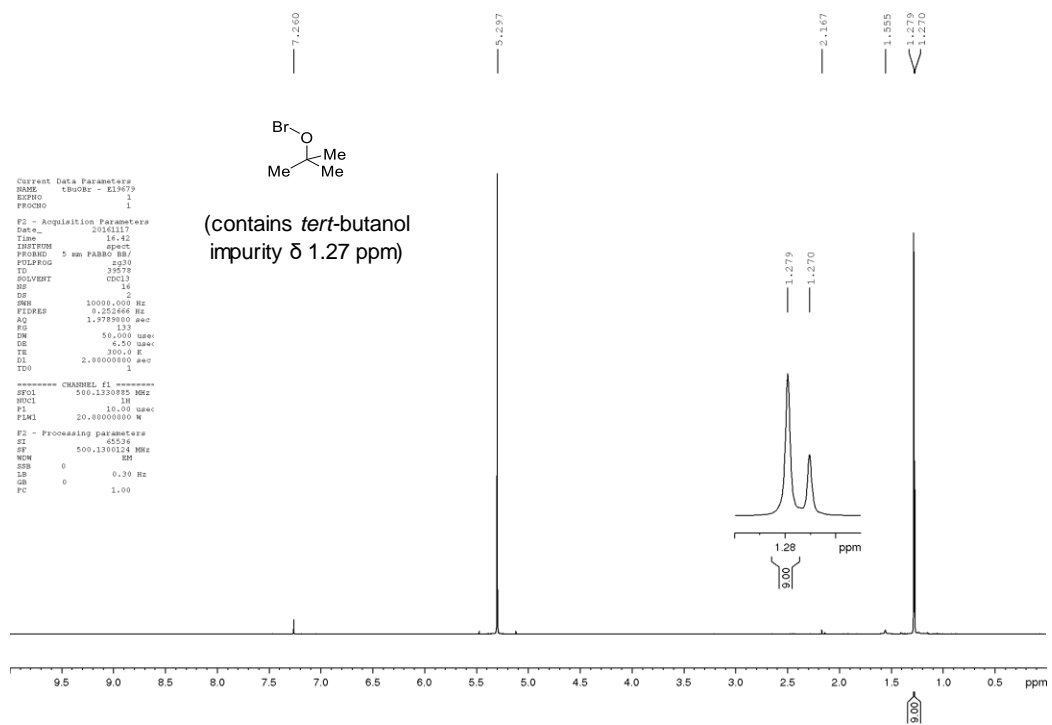D11   0.03000000 sec
TD0   1

======= CHANNEL f1 ========
SFO1   100.6228298 MHz
NUC1   13C
P1   10.00 usec
PLW1   35.00000000 W

======= CHANNEL f2 ========
SFO2   400.1316005 MHz
NUC2   1H
CPDPRG[2   waltz16
PCPD2   90.00 usec
PLW2   7.50000000 W
PLW12   0.16379000 W
PLW13   0.08238400 W

F2 - Processing parameters
SI   32768
SF   100.6127526 MHz
WDW   EM
SSB   0
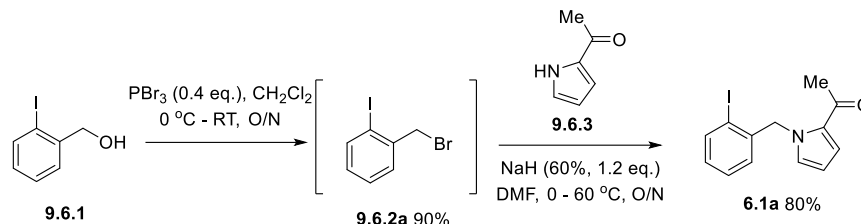LB   1.00 Hz
GB   0
PC   1.40

200 190 180 170 160 150 140 130 120 110 100 90 80 70 60 50 40 30 20 10 ppm

256

^{1}H-NMR and ^{13}C{^{1}H}-NMR 5.86

(contains *tert*-butanol
impurity δ 1.27 ppm)

(contains *tert*-butanol
impurity δ 69.4 and
31.4 ppm)

257

9.4 Experimental details for Chapter 6

9.4.1 Synthesis of 1-(1-(2-halobenzyl)-1H-pyrrol-2-yl)ethan-1-one 6.1a-c

### Synthesis of 1-(1-(2-iodobenzyl)-1H-pyrrol-2-yl)ethan-1-one, 6.1a[85]

(2-Iodophenyl)methanol **9.6.1** (8.2 g, 35 mmol) and anhydrous dichloromethane (60 mL) were added to an oven-dried round-bottomed flask. At 0 °C, PBr$_3$ (1.32 mL, 14 mmol, 0.4 eq.) was added slowly and the reaction mixture was stirred at 0 °C for 30 min, then at RT overnight. The reaction mixture was quenched with water (20 mL) and extracted with dichloromethane (3 x 20 mL). The organic phases were combined, washed with water then brine, dried over Na$_2$SO$_4$, filtered and concentrated *in vacuo* to give 1-(bromomethyl)-2-iodobenzene **9.6.2a**[202] (9.37 g, 90%) as white crystals m.p. 62 – 64 °C (lit.[203]: 56 – 60 °C); [Found: (GCMS-EI) C$_7$H$_6$^{79}BrI (M)$^{\bullet+}$ 295.9]; ^{1}H-NMR (400 MHz, CDCl$_3$) δ 4.61 (2 H, s, C*H$_2$*), 6.99 (1 H, t, *J* = 8.0 Hz, Ar*H*), 7.35 (1 H, t, *J* = 8.0 Hz, Ar*H*), 7.49 (1 H, d, *J* = 8.0 Hz, Ar*H*), 7.87 (1 H, d, *J* = 8.0 Hz, Ar*H*); ^{13}C{^{1}H}-NMR (100 MHz, CDCl$_3$) δ 38.9 (CH$_2$), 100.2 (C), 129.0 (CH), 130.2 (CH), 130.6 (CH), 140.2 (CH), 140.3 (C).

Sodium hydride (60% in mineral oil, 720 mg, 18 mmol, 1.2 eq.) and anhydrous dimethylformamide (5 mL) were added to an oven-dried three-necked flask, equipped with condenser. At 0 °C, a solution of 1-(1H-pyrrol-2-yl)ethan-1-one **9.6.3** (1.64 g, 15 mmol) in anhydrous dimethylformamide (10 mL) was added slowly and the reaction mixture was stirred at 0 °C for 5 min, then at RT for 1 h. A solution of 1-(bromomethyl)-2-iodobenzene **9.6.2a** (5.12 g, 17.25 mmol, 1.15 eq.) in anhydrous dimethylformamide (10 mL) was added dropwise and the reaction mixture was stirred at 60 °C overnight. The reaction mixture was cooled to RT, quenched dropwise with water (80 mL) and extracted with ethyl acetate (3 x 50 mL). The organic phases were combined, washed with water then brine, dried over Na$_2$SO$_4$, filtered and concentrated *in vacuo*. The crude material was purified by column

chromatography (0 - 10% diethyl ether in petroleum ether) to give 1-(1-(2-iodobenzyl)-1H-pyrrol-2-yl)ethan-1-one **6.1a**[150] (3.90 g, 80%) as off-white crystals m.p. 99 – 100 °C (lit.[85,150]: 100.3 – 101.5 °C); [Found: (HRMS-ESI) 326.0034. $C_{13}H_{13}INO^+$ (M+H)$^+$ requires 326.0042]; v_{max}(film) / cm^{-1} 3109, 2359, 2342, 1634, 1533, 1468, 1433, 1397, 1331, 1252, 1094, 1011, 947, 752, 743, 720; ^{1}H-NMR (400 MHz, CDCl$_3$) δ 2.43 (3 H, s, CH_3), 5.57 (2 H, s, CH_2), 6.22 – 6.24 (1 H, m, ArH), 6.47 (1 H, d, J = 8.0 Hz, ArH), 6.84 – 6.85 (1 H, m, ArH), 6.92 – 6.96 (1 H, m, ArH), 7.05 (1 H, dd, J = 4.0, 1.6 Hz, ArH), 7.21 (1 H, t, J = 8.0 Hz, ArH), 7.84 (1 H, d, J = 8.0 Hz, ArH); ^{13}C{^{1}H}-NMR (100 MHz, CDCl$_3$) δ 27.3 (CH$_3$), 57.9 (CH$_2$), 97.6 (C), 109.0 (CH), 120.4 (CH), 127.3 (CH), 128.7 (CH), 129.1 (CH), 130.5 (CH), 130.7 (C), 139.5 (CH), 140.9 (C), 188.5 (C).

### Synthesis of 1-(1-(2-bromobenzyl)-1H-pyrrol-2-yl)ethan-1-one, 6.1b[85]
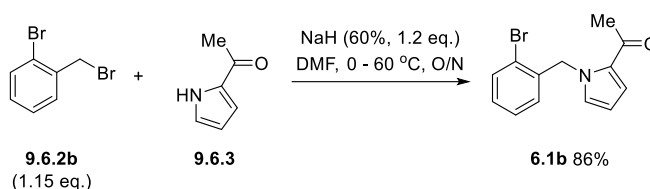
Sodium hydride (60% in mineral oil, 240 mg, 6 mmol, 1.2 eq.) and anhydrous dimethylformamide (5 mL) were added to an oven-dried three-necked flask, equipped with condenser. At 0 °C, a solution of 1-(1H-pyrrol-2-yl)ethan-1-one **9.6.3** (546 mg, 5 mmol) in anhydrous dimethylformamide (5 mL) was added slowly and the reaction mixture was stirred at 0 °C for 5 min, then at RT for 1 h. A solution of 1-(bromomethyl)-2-bromobenzene **9.6.2b** (1.44 g, 5.75 mmol, 1.15 eq.) in anhydrous dimethylformamide (5 mL) was added dropwise and the reaction mixture was stirred at 60 °C overnight. The reaction mixture was cooled to RT, quenched dropwise with water (60 mL) and extracted with ethyl acetate (3 x 40 mL). The organic phases were combined, washed with water then brine, dried over Na$_2$SO$_4$, filtered and concentrated *in vacuo*. The crude material was purified by column chromatography (0 - 5% diethyl ether in petroleum ether) to give 1-(1-(2-bromobenzyl)-1H-pyrrol-2-yl)ethan-1-one **6.1b**[150] (1.20 g, 86%) as pale-yellow crystals m.p. 90 – 91 °C (lit.[150]: 80 – 81 °C); [Found: (HRMS-ESI) 278.0176. $C_{13}H_{13}^{79}BrNO^+$ (M+H)$^+$ requires 278.0175]; v_{max}(film) / cm^{-1} 1651, 1528, 1470, 1439, 1422, 1398, 1356, 1325, 1244,

1086, 1024, 943, 758, 741, 677; ^{1}H-NMR (400 MHz, CDCl$_3$) δ 2.43 (3 H, s, C*H*$_3$), 5.65 (2 H, s, C*H*$_2$), 6.22 – 6.24 (1 H, m, Ar*H*), 6.52 – 6.54 (1 H, m, Ar*H*), 6.88 – 6.89 (1 H, m, Ar*H*), 7.04 – 7.06 (1 H, m, Ar*H*), 7.09 – 7.13 (1 H, m, Ar*H*), 7.15 – 7.19 (1 H, m, Ar*H*), 7.56 (1 H, dd, *J* = 7.6, 1.2 Hz, Ar*H*); ^{13}C{^{1}H}-NMR (125 MHz, CDCl$_3$) δ 27.4 (CH$_3$), 53.0 (CH$_2$), 108.9 (CH), 120.4 (CH), 122.5 (C), 127.9 (2 x CH), 128.9 (CH), 130.6 (CH), 130.7 (C), 132.8 (CH), 138.0 (C), 188.5 (C); *m/z* (ESI) 280.0153 ([M+H]$^+$, ^{81}Br, 100%], 278.0176 [(M+H)$^+$, ^{79}Br, 100].

Synthesis of 1-(1-(2-chlorobenzyl)-1H-pyrrol-2-yl)ethan-1-one, 6.1c[85]
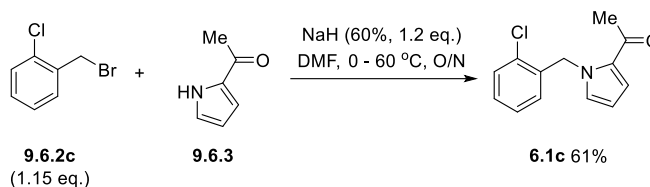
Sodium hydride (60% in mineral oil, 240 mg, 6 mmol, 1.2 eq.) and anhydrous dimethylformamide (5 mL) were added to an oven-dried three-necked flask, equipped with condenser. At 0 °C, a solution of 1-(1H-pyrrol-2-yl)ethan-1-one **9.6.3** (546 mg, 5 mmol) in anhydrous dimethylformamide (5 mL) was added slowly and the reaction mixture was stirred at 0 °C for 10 min, then at RT for 1 h. A solution of 1-(bromomethyl)-2-chorobenzene **9.6.2c** (0.75 mL, 5.75 mmol, 1.15 eq.) in anhydrous dimethylformamide (5 mL) was added dropwise and the reaction mixture was stirred at 60 °C overnight. The reaction mixture was cooled to RT, quenched dropwise with water (40 mL) and extracted with ethyl acetate (3 x 30 mL). The organic phases were combined, washed with water then brine, dried over Na$_2$SO$_4$, filtered and concentrated *in vacuo*. The crude material was purified by column chromatography (0 - 2% ethyl acetate in petroleum ether) to give 1-(1-(2-chlorobenzyl)-1H-pyrrol-2-yl)ethan-1-one **6.1c**[150] (717 mg, 61%) as pale yellow crystals m.p. 77 – 80 °C (lit.[150]: 69 – 70 °C); [Found: (GC-CI) C$_{13}$H$_{13}$^{35}ClNO$^+$ (M+H)$^+$ 234.1]; v_{max}(film) / cm^{-1} 2980, 1647, 1468, 1397, 1331, 1244, 1086, 1038, 945, 745, 694, 633, 615; ^{1}H-NMR (400 MHz, CDCl$_3$) δ 2.43 (3 H, s, C*H*$_3$), 5.68 (2 H, s, C*H*$_2$), 6.22 (1 H, d, *J* = 4.0 Hz, Ar*H*), 6.61 (1 H, d, *J* = 7.6 Hz, Ar*H*), 6.89 – 6.90 (1 H, m, Ar*H*), 7.04 – 7.05 (1 H, m, Ar*H*), 7.11 – 7.21 (2 H, m, Ar*H*), 7.37 (1 H, dd, *J* = 8.0, 1.2 Hz, Ar*H*); ^{13}C{^{1}H}-NMR (125 MHz, CDCl$_3$) δ 27.4 (CH$_3$), 50.5 (CH$_2$), 108.9 (CH),

120.5 (CH), 127.2 (CH), 127.8 (CH), 128.7 (CH), 129.5 (CH), 130.6 (C), 130.7 (CH), 132.6 (C), 136.4 (C), 188.5 (C); *m/z* (ESI) 236.1 [(M+H)$^+$, ^{37}Cl, 32%], 234.1 [(M+H)$^+$, ^{35}Cl, 100].

9.4.2 Synthesis of 1,4-dipropylpiperazine-2,5-dione 6.2

Synthesis of 2-chloro-*N*-propylacetamide 9.6.6[167]
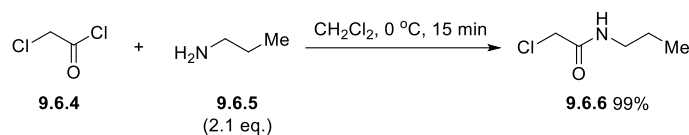
Anhydrous dichloromethane (30 mL) was added to a round-bottomed flask was added. Under an argon atmosphere, at 0 °C, chloroacetyl chloride **9.6.4** (4 mL, 50 mmol) and propylamine **9.6.5** (8.6 mL, 105 mmol, 2.1 eq.) were simultaneously added dropwise. The reaction mixture was stirred at 0 °C for 15 min and then diluted with diethyl ether (200 mL) and a solid precipitated. The reaction mixture was filtered and the solid was washed with diethyl ether. The filtered solution was concentrated *in vacuo* and diluted with diethyl ether (200 mL) and filtered a second time. The filtered solution was concentrated *in vacuo* to give 2-chloro-*N*-propylacetamide **9.6.6**[167] (6.72 g, 99%) as a pale yellow oil [Found: (HRMS-ESI) 136.0521. C$_5$H$_{11}$ClNO$^+$ (M+H)$^+$ requires 136.0524]; v_{max}(film) / cm^{-1} 3292, 3084, 2965, 2936, 2876, 1651, 1539, 1460, 1439, 1258, 1240, 1155; ^{1}H-NMR (500 MHz, CDCl$_3$) δ 0.91 (3 H, t, *J* = 7.5 Hz, C*H$_3$*), 1.48 – 1.54 (2 H, m, C*H$_2$*), 3.24 (2 H, q, *J* = 6.5 Hz, C*H$_2$*), 4.01 (2 H, s, C*H$_2$*), 6.67 (1 H, br s, N*H*); ^{13}C{^{1}H}-NMR (100 MHz, CDCl$_3$) δ 11.4 (CH$_3$), 22.7 (CH$_2$), 41.6 (CH$_2$), 42.8 (CH$_2$), 165.9 (C).

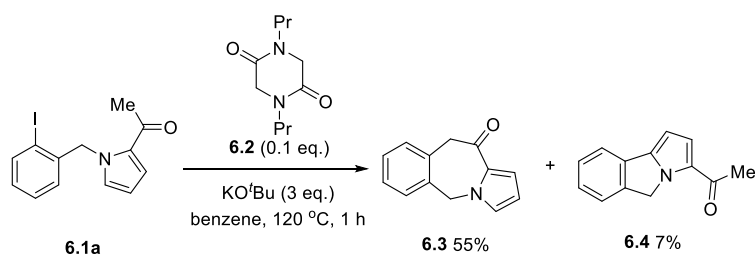### Synthesis of 4-dipropylpiperazine-2,5-dione 6.2[41]
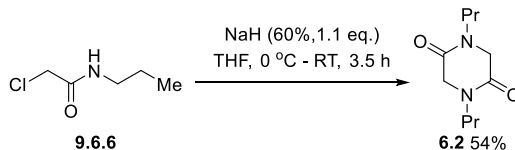
2-Chloro-*N*-propylacetamide **9.6.6** (6.78 g, 50 mmol) and anhydrous tetrahydrofuran (30 mL) were added to a flame-dried round-bottomed flask. At 0 °C, a suspension of sodium hydride (60% in mineral oil, 2.20 g, 55 mmol, 1.1 eq.) in anhydrous tetrahydrofuran (20 mL) was added dropwise *via* cannula and the reaction mixture was stirred at RT for 3.5 h. The reaction mixture was quenched by dropwise addition of water and diluted with diethyl ether (150 mL) and the organic phase was dried

over Na_2SO_4, filtered and concentrated *in vacuo*. The crude material was purified by column chromatography (0 - 100% ethyl acetate in hexane) to give 1,4-dipropylpiperazine-2,5-dione **6.2**[41] (2.66 g, 54%) as pale yellow crystals m.p. 54 – 59 °C (lit:[41] 40 – 42 °C); [Found: (HRMS-ESI) 199.1438. $C_{10}H_{19}N_2O_2^+$ (M+H)$^+$ requires 199.1438]; v_{max}(film) / cm^{-1} 2964, 2932, 2872, 1647, 1483, 1335, 1308, 1277, 1204, 1055; ^{1}H-NMR (500 MHz, CDCl$_3$) δ 0.92 – 0.95 (6 H, m, 2 x C*H$_3$*), 1.59 (4 H, sx, *J* = 7.5 Hz, 2 x C*H$_2$*), 3.37 (4 H, m, 2 x C*H$_2$*), 3.96 (4 H, s, C*H$_2$*); ^{13}C{^{1}H}-NMR (125 MHz, CDCl$_3$) δ 11.2 (2 x CH$_3$), 20.0 (2 x CH$_2$), 47.7 (2 x CH$_2$), 50.0 (2 x CH$_2$), 163.6 (2 x C).

9.4.3 Electron transfer reactions on 1-(1-(2-halobenzyl)-1H-pyrrol-2-yl)ethan-1-one (Table 6.1)

Table 6.1, entry 1

1-(1-(2-Iodobenzyl)-1H-pyrrol-2-yl)ethan-1-one **6.1a** (163 mg, 0.5 mmol) and 1,4-dipropylpiperazine-2,5-dione **6.2** (10 mg, 0.05 mmol, 0.1 eq.) were added to an oven-dried pressure tube. In the glove box, KO^{t}Bu (168 mg, 1.5 mmol, 3.0 eq.) and anhydrous benzene (5 mL) were added and the reaction mixture was stirred at 120 °C for 1 h. The reaction mixture was quenched with water (20 mL) and extracted with diethyl ether (3 x 20 mL). The organic phases were combined, washed with brine, dried over Na_2SO_4, filtered and concentrated *in vacuo*. The crude material was purified by column chromatography (10 - 20% ethyl acetate in petroleum ether) to give both 5,10-dihydro-11H-benzo[e]pyrrolo[1,2-a]azepin-11-one **6.3**[150,204] (54 mg, 55%) as a pale green solid m.p. 176 – 177 °C (lit.[204]: 174 – 176 °C); [Found: (HRMS-ESI) 198.0911. $C_{13}H_{12}NO^+$ (M+H)$^+$ requires 198.0913]; v_{max}(film) / cm^{-1} 2963, 2359, 2342, 1636, 1520, 1489, 1466, 1398, 1337, 739, 677; ^{1}H-NMR (400 MHz, CDCl$_3$) δ 4.09 (2 H, s, C*H$_2$*), 5.26 (2 H, s, C*H$_2$*), 6.15 – 6.17 (1 H, m, Ar*H*), 6.94 – 6.95 (1 H, m, Ar*H*), 7.10 – 7.12 (1 H, m, Ar*H*), 7.25 – 7.35 (4 H, m, Ar*H*); ^{13}C{^{1}H}-NMR (125
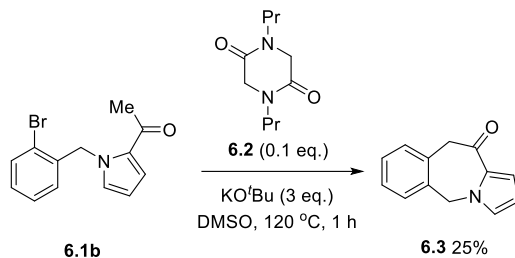
MHz, CDCl$_3$) δ 49.1 (CH$_2$), 53.7 (CH$_2$), 109.2 (CH), 118.6 (CH), 127.5 (CH), 127.9 (CH), 128.3 (CH), 129.3 (CH), 129.9 (CH), 132.4 (C), 134.3 (C), 135.2 (C), 184.4 (C), and 1-(5H-pyrrolo[2,1-a]isoindol-3-yl)ethan-1-one **6.4**[150] (7.2 mg, 7%) as a yellow solid m.p. 128 – 129 °C; [Found: (HRMS-ESI) 198.0913. C$_{13}$H$_{12}$NO$^+$ (M+H)$^+$ requires 198.0913]; v_{max}(film) / cm^{-1} 2922, 2359, 2342, 1626, 1614, 1476, 1439, 1395, 1306, 1262, 1192, 1138, 1098, 1067, 1026, 1017, 963, 924, 747, 718, 696, 655; ^{1}H-NMR (400 MHz, CDCl$_3$) δ 2.48 (3 H, s, C*H*$_3$), 5.22 (2 H, s, C*H*$_2$), 6.41 (1 H, d, J = 4.0 Hz, Ar*H*), 7.07 (1 H, d, J = 4.0 Hz, Ar*H*), 7.30 – 7.34 (1 H, m, Ar*H*), 7.38 – 7.42 (1 H, m, Ar*H*), 7.49 – 7.51 (1 H, m, Ar*H*), 7.63 (1 H, d, J = 7.6 Hz, Ar*H*); ^{13}C{^{1}H}-NMR (100 MHz, CDCl$_3$) δ 26.0 (CH$_3$), 53.2 (CH$_2$), 100.2 (CH), 120.2 (CH), 121.7 (CH), 123.5 (CH), 127.1 (CH), 128.1 (CH), 129.2 (C), 131.9 (C), 142.1 (C), 144.8 (C), 187.4 (C).

Table 6.1, entry 2

1-(1-(2-Iodobenzyl)-1H-pyrrol-2-yl)ethan-1-one **6.1a** (163 mg, 0.5 mmol) and 1,4-dipropylpiperazine-2,5-dione **6.2** (10 mg, 0.05 mmol, 0.1 eq.) were added to an oven-dried pressure tube. In the glove box, KO^{t}Bu (168 mg, 1.5 mmol, 3.0 eq.) and anhydrous DMSO (2 mL) were added and the reaction mixture was stirred at 120 °C for 1 h. The reaction mixture was quenched with saturated aqueous ammonium chloride solution (20 mL) and extracted with dichloromethane (3 x 20 mL). The organic phases were combined, washed with brine, dried over Na$_2$SO$_4$, filtered and concentrated *in vacuo*. The crude material was purified by column chromatography (5 - 25% ethyl acetate in hexane) to give 5,10-dihydro-11H-benzo[e]pyrrolo[1,2-a]azepin-11-one **6.3** (77.8 mg, 79%) as a pale-brown solid and 1-(5H-pyrrolo[2,1-a]isoindol-3-yl)ethan-1-one **6.4** (9.6 mg, 10%) as pale brown crystals. The spectra are consistent with the reference samples (Section 9.4.3, Table 6.1, entry 1 on pages 262-263).

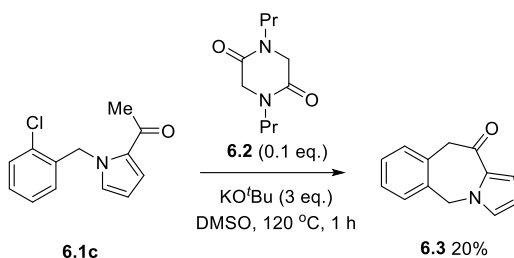**Table 6.1, entry 3**

6.1b

6.3 25%

1-(1-(2-Bromobenzyl)-1H-pyrrol-2-yl)ethan-1-one **6.1b** (139 mg, 0.5 mmol) and 1,4-dipropylpiperazine-2,5-dione **6.2** (10 mg, 0.05 mmol, 0.1 eq.) were added to an oven-dried pressure tube. In the glove box, KO^{t}Bu (168 mg, 1.5 mmol, 3.0 eq.) and anhydrous DMSO (2 mL) were added and the reaction mixture was stirred at 120 °C for 1 h. The reaction mixture was quenched with saturated aqueous ammonium chloride solution (20 mL) and extracted with dichloromethane (3 x 20 mL). The organic phases were combined, washed with brine, dried over Na$_2$SO$_4$, filtered and concentrated *in vacuo*. The crude material was purified by column chromatography (2 - 25% ethyl acetate in hexane) to give 5,10-dihydro-11H-benzo[e]pyrrolo[1,2-a]azepin-11-one **6.3** (24.2 mg, 25%) as dark green crystals. The spectra are consistent with the reference samples (Section 9.4.3, Table 6.1, entry 1 on page 262).

Table 6.1, entry 4
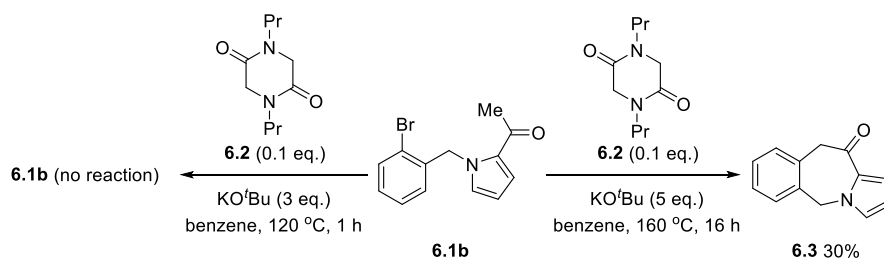
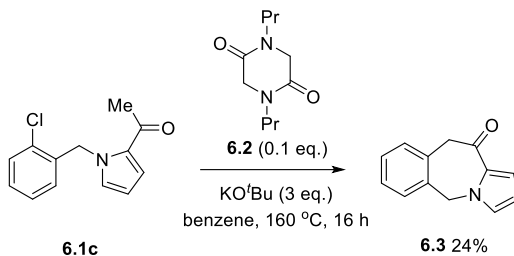**6.1b** (no reaction)

6.1b

6.3 30%

1-(1-(2-Bromobenzyl)-1H-pyrrol-2-yl)ethan-1-one **6.1b** (139 mg, 0.5 mmol) and 1,4-dipropylpiperazine-2,5-dione **6.2** (10 mg, 0.05 mmol, 0.1 eq.) were added to an oven-dried pressure tube. In the glove box, KO^{t}Bu (168 mg, 1.5 mmol, 3.0 eq.) and anhydrous benzene (5 mL) were added and the reaction mixture was stirred at 120 °C for 1 h. The reaction mixture was quenched with water (20 mL) and extracted with diethyl ether (3 x 20 mL). The organic phases were combined, washed with brine,

dried over Na₂SO₄, filtered and concentrated *in vacuo*. Only the starting material **6.1b** was observed in the crude mixture by ¹H-NMR and TLC.

1-(1-(2-Bromobenzyl)-1H-pyrrol-2-yl)ethan-1-one **6.1b** (139 mg, 0.5 mmol) and 1,4-dipropylpiperazine-2,5-dione **6.2** (10 mg, 0.05 mmol, 0.1 eq.) were added to an oven-dried pressure tube. In the glove box, KO^{t}Bu (281 mg, 2.5 mmol, 5 eq.) and anhydrous benzene (5 mL) were added and the reaction mixture was stirred at 160 °C for 16 h. The reaction mixture was quenched with water (20 mL) and extracted with diethyl ether (3 x 20 mL). The organic phases were combined, washed with brine, dried over Na₂SO₄, filtered and concentrated *in vacuo*. The crude material was purified by column chromatography (10 - 20% ethyl acetate in petroleum ether) to give 5,10-dihydro-11H-benzo[e]pyrrolo[1,2-a]azepin-11-one **6.3** (29.3 mg, 30%) as a brown solid. The spectra are consistent with the reference samples (Section 9.4.3, Table 6.1, entry 1 on page 262).

Table 6.1, entry 5

1-(1-(2-Chlorobenzyl)-1H-pyrrol-2-yl)ethan-1-one **6.1c** (117 mg, 0.5 mmol) and 1,4-dipropylpiperazine-2,5-dione **6.2** (10 mg, 0.05 mmol, 0.1 eq.) were added to an oven-dried pressure tube. In the glove box, KO^{t}Bu (168 mg, 1.5 mmol, 3.0 eq.) and anhydrous DMSO (2 mL) were added and the reaction mixture was stirred at 120 °C for 1 h. The reaction mixture was quenched with saturated aqueous ammonium chloride solution (20 mL) and extracted with dichloromethane (3 x 20 mL). The organic phases were combined, washed with brine, dried over Na₂SO₄, filtered and concentrated *in vacuo*. The crude material was purified by column chromatography (2 - 40% ethyl acetate in hexane) to give 5,10-dihydro-11H-benzo[e]pyrrolo[1,2-a]azepin-11-one **6.3** (19.8 mg, 20%) as a brown solid. The spectra are consistent with the reference samples (Section 9.4.3, Table 6.1, entry 1 on page 262).

Table 6.1, entry 6

6.1c

6.3 24%

1-(1-(2-Chlorobenzyl)-1H-pyrrol-2-yl)ethan-1-one **6.1c** (117 mg, 0.5 mmol) and 1,4-dipropylpiperazine-2,5-dione **6.2** (10 mg, 0.05 mmol, 0.1 eq.) were added to an oven-dried pressure tube. In the glove box, KO^{t}Bu (168 mg, 1.5 mmol, 3.0 eq.) and anhydrous benzene (2 mL) were added and the reaction mixture was stirred at 160 ^{o}C for 16 h. The reaction mixture was quenched with water (20 mL) and extracted with diethyl ether (3 x 20 mL). The organic phases were combined, washed with brine, dried over Na_2SO_4, filtered and concentrated *in vacuo*. The crude material was purified by column chromatography (5 - 100% ethyl acetate in petroleum ether) to give 5,10-dihydro-11H-benzo[e]pyrrolo[1,2-a]azepin-11-one **6.3** (23.5 mg, 24%) as a brown solid. The spectra are consistent with the reference samples (Section 9.4.3, Table 6.1, entry 1 on page 262).

9.4.4 Synthesis of *1-(1-(2-iodo-3,4-dimethoxybenzyl)-1H-pyrrol-2-yl)ethan-1-one*, 6.23

9.6.7

9.6.8 90%

6.23 62%
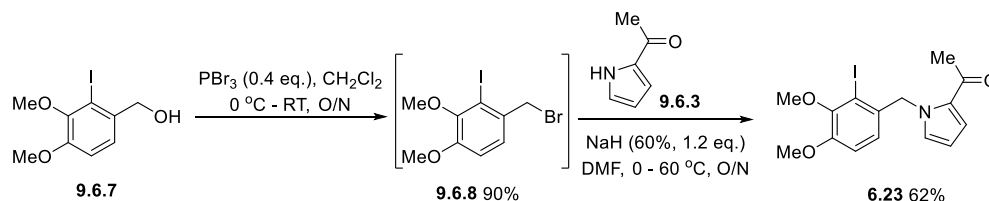
(2-Iodo-3,4-dimethoxyphenyl)methanol **9.6.7** (2.94 g, 10 mmol) and anhydrous dichloromethane (20 mL) were added to an oven-dried round-bottomed flask. At 0 ^{o}C, PBr$_3$ (0.4 mL, 4 mmol, 0.4 eq.) was added slowly and the reaction mixture was stirred at 0 ^{o}C for 30 min, then at RT overnight. The reaction mixture was quenched with water (20 mL) and extracted with dichloromethane (3 x 15 mL). The organic phases were combined, washed with water then brine, dried over Na_2SO_4, filtered and concentrated *in vacuo* to give *1-(bromomethyl)-2-iodo-3,4-dimethoxybenzene* **9.6.8** (3.57 g, 90%) as off-white crystals [Found: (HRMS-NSI) 373.9249.

$C_9H_{14}{}^{79}BrINO_2$ (M+NH$_4$)$^+$ requires 373.9247]; ^{1}H-NMR (400 MHz, CDCl$_3$) δ 3.84 (3 H, s, CH_3), 3.87 (3 H, s, CH_3), 4.66 (2 H, s, CH_2), 6.86 (1 H, d, J = 8.0 Hz, ArH), 7.23 (1 H, d, J = 8.0 Hz, ArH); ^{13}C{^{1}H}-NMR (100 MHz, CDCl$_3$) δ 39.8 (CH$_2$), 56.2 (CH$_3$), 60.4 (CH$_3$), 99.4 (C), 112.5 (CH), 126.3 (CH), 133.2 (C), 149.6 (C), 152.6 (C), *m/z* (NSI) 375.9228 [(M+NH$_4$)$^+$, ^{81}Br, 98%], 373.9249 [(M+NH$_4$)$^+$, ^{79}Br, 100].

Sodium hydride (60% in mineral oil, 352 mg, 8.81 mmol, 1.2 eq.) and anhydrous dimethylformamide (5 mL) were added to an oven-dried round-bottomed flask, equipped with condenser. At 0 °C, a solution of 1-(1H-pyrrol-2-yl)ethan-1-one **9.6.3** (800 mg, 7.34 mmol) in anhydrous dimethylformamide (5 mL) was added slowly and the reaction mixture was stirred at 0 °C for 5 min, then at RT for 1 h. A solution of 1-(bromomethyl)-2-iodo-3,4-dimethoxybenzene **9.6.8** (3.01 g, 8.44 mmol, 1.15 eq.) in anhydrous dimethylformamide (10 mL) was added dropwise and the reaction mixture was stirred at 60 °C overnight. The reaction mixture was cooled to RT, quenched dropwise with water (40 mL) and extracted with ethyl acetate (3 x 30 mL). The organic phases were combined, washed with water then brine, dried over Na$_2$SO$_4$, filtered and concentrated *in vacuo*. The crude material was purified by column chromatography (0 - 20% ethyl acetate in petroleum ether) to give *1-(1-(2-iodo-3,4-dimethoxybenzyl)-1H-pyrrol-2-yl)ethan-1-one* **6.23** (1.75 g, 62%) as off-white crystals m.p. 89 – 90 °C; [Found: (HRMS-ESI) 386.0250. $C_{15}H_{17}INO_3{}^+$ (M+H)$^+$ requires 386.0248]; v_{max}(film) / cm^{-1} 1641, 1479, 1460, 1397, 1290, 1265, 1225, 1144, 1086, 1022, 947, 743, 631; ^{1}H-NMR (400 MHz, CDCl$_3$) δ 2.44 (3 H, s, CH_3), 3.82 (3 H, s, CH_3), 3.85 (3 H, s, CH_3), 5.54 (2 H, s, CH_2), 6.20 – 6.21 (1 H, m, ArH), 6.28 (1 H, d, J = 8.4 Hz, ArH), 6.76 (1 H, d, J = 8.4 Hz, ArH), 6.82 – 6.83 (1 H, m, ArH), 7.04 – 7.05 (1 H, m, ArH); ^{13}C{^{1}H}-NMR (100 MHz, CDCl$_3$) δ 27.4 (CH$_3$), 56.2 (CH$_3$), 57.6 (CH$_3$), 60.4 (CH$_2$), 96.8 (C), 108.8 (CH), 112.7 (CH), 120.4 (CH), 123.2 (CH), 130.3 (C), 130.7 (C), 133.7 (CH), 149.0 (C), 151.8 (C), 188.5 (C).

9.4.5 Electron transfer reactions on *1-(1-(2-iodo-3,4-dimethoxybenzyl)-1H-pyrrol-2-yl)ethan-1-one*, 6.23 (Scheme 6.3)
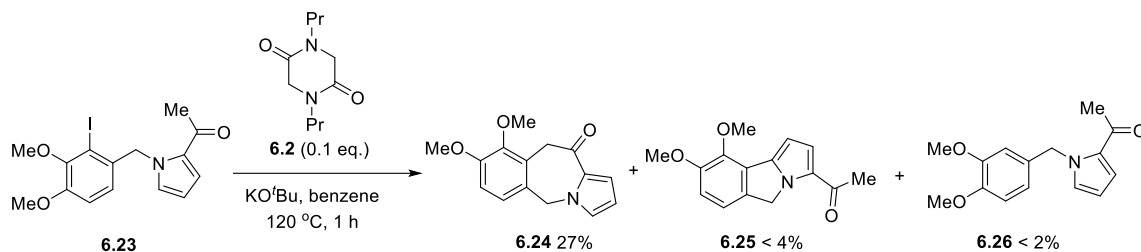
Scheme 6.3A
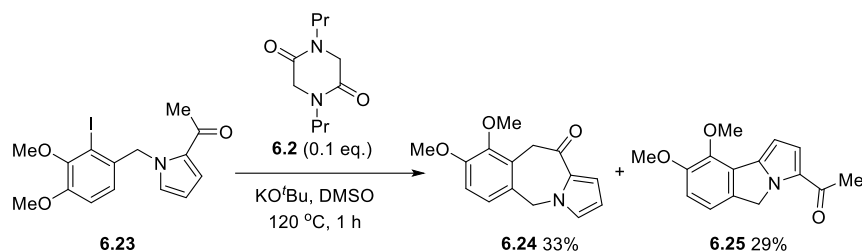
1-(1-(2-Iodo-3,4-dimethoxybenzyl)-1H-pyrrol-2-yl)ethan-1-one **6.23** (193 mg, 0.5 mmol) and 1,4-dipropylpiperazine-2,5-dione **6.2** (10 mg, 0.05 mmol, 0.1 eq.) were added to an oven-dried pressure tube. In the glove box, KO^tBu (168 mg, 1.5 mmol, 3.0 eq.) and anhydrous DMSO (2 mL) were added and the reaction mixture was stirred at 120 °C for 1 h. The reaction mixture was quenched with water (20 mL) and extracted with diethyl ether (3 x 20 mL). The organic phases were combined, washed with water then brine, dried over Na_2SO_4, filtered and concentrated *in vacuo*. The crude material was purified by column chromatography (10 - 30% ethyl acetate in petroleum ether) to give both 8,9-dimethoxy-5,10-dihydro-11H-benzo[e]pyrrolo[1,2-a]azepin-11-one **6.24** (42.9 mg, 33%) as yellow crystals m.p. 184 – 187 °C; [Found: (HRMS-ESI) 258.1124. $C_{15}H_{16}NO_3^+$ (M+H)$^+$ requires 258.1125]; v_{max}(film) / cm^{-1} 2924, 1638, 1491, 1398, 1341, 1279, 1267, 1076, 976, 812, 747, 689; ^{1}H-NMR (400 MHz, CDCl₃) δ 3.81 (3 H, s, C*H₃*), 3.85 (3 H, s, C*H₃*), 4.15 (2 H, s, C*H₂*), 5.19 (2 H, s, C*H₂*), 6.14 – 6.16 (1 H, m, Ar*H*), 6.75 (1 H, d, *J* = 8.4 Hz, Ar*H*), 6.92 – 6.93 (1 H, m, Ar*H*), 7.05 (1 H, d, *J* = 8.4 Hz, Ar*H*), 7.09 – 7.11 (1 H, m, Ar*H*); ^{13}C{^{1}H}-NMR (100 MHz, CDCl₃) δ 41.1 (CH₂), 53.5 (CH₂), 56.0 (CH₃), 61.8 (CH₃), 109.0 (CH), 110.5 (CH), 118.4 (CH), 123.8 (CH), 127.6 (CH), 128.5 (C), 128.7 (C), 132.7 (C), 147.5 (C), 153.5 (C), 184.5 (C), and 1-(8,9-dimethoxy-5H-pyrrolo[2,1-a]isoindol-3-yl)ethan-1-one **6.25** (37.3 mg, 29%) as green crystals m.p. 136 – 144 °C; [Found: (HRMS-ESI) 258.1126. $C_{15}H_{16}NO_3^+$ (M+H)$^+$ requires 258.1125]; v_{max}(film) / cm^{-1} 2938, 1636, 1495, 1397, 1252, 1223, 1921, 1105, 1057, 1042, 1022, 934, 806, 774, 750, 694, 625; ^{1}H-NMR (400 MHz, CDCl₃) δ 2.47 (3 H, s, C*H₃*), 3.91 (3 H, s, C*H₃*), 3.99 (3 H, s, C*H₃*), 5.16 (2 H, s, C*H₂*), 6.50 (1 H, d, *J* = 4.0 Hz, Ar*H*), 6.87 (1 H, d, *J* = 8.0 Hz,
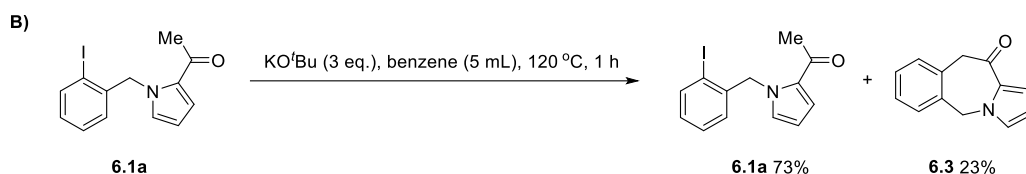
Ar*H*), 7.07 (1 H, d, *J* = 4.0 Hz, Ar*H*), 7.14 (1 H, d, *J* = 8.0 Hz, Ar*H*); $^{13}C\{^1H\}$-NMR (100 MHz, CDCl$_3$) δ 26.0 (CH$_3$), 52.8 (CH$_2$), 56.5 (CH$_3$), 60.8 (CH$_3$), 102.6 (CH), 112.0 (CH), 118.8 (CH), 121.7 (CH), 126.2 (C), 129.2 (C), 135.3 (C), 142.6 (C), 143.2 (C), 152.6 (C), 187.4 (C).

Scheme 6.3B

1-(1-(2-Iodo-3,4-dimethoxybenzyl)-1H-pyrrol-2-yl)ethan-1-one **6.23** (193 mg, 0.5 mmol) and 1,4-dipropylpiperazine-2,5-dione **6.2** (10 mg, 0.05 mmol, 0.1 eq.) were added to an oven-dried pressure tube. In the glove box, KO*t*Bu (168 mg, 1.5 mmol, 3.0 eq.) and anhydrous benzene (3 mL) were added and the reaction mixture was stirred at 120 °C for 1 h. The reaction mixture was quenched with water (20 mL) and extracted with diethyl ether (3 x 20 mL). The organic phases were combined, washed with water then brine, dried over Na$_2$SO$_4$, filtered and concentrated *in vacuo*. The crude material was purified by column chromatography (5 - 50% ethyl acetate in petroleum ether) to give 8,9-dimethoxy-5,10-dihydro-11H-benzo[e]pyrrolo[1,2-a]azepin-11-one **6.24** (34.5 mg, 27%) as pale brown crystals and impure 1-(8,9-dimethoxy-5H-pyrrolo[2,1-a]isoindol-3-yl)ethan-1-one **6.25** (8.1 mg) as green crystals. The spectra are consistent with the reference samples (Section 9.4.5, Scheme 6.3A on page 268). The proposed impurity in **6.25** is 1-(1-(3,4-dimethoxybenzyl)-1H-pyrrol-2-yl)ethan-1-one **6.26** (ratio 2 : 1 respectively), giving 1-(8,9-dimethoxy-5H-pyrrolo[2,1-a]isoindol-3-yl)ethan-1-one **6.25** (< 4%) and 1-(1-(3,4-dimethoxybenzyl)-1H-pyrrol-2-yl)ethan-1-one **6.26** (< 2%) [tentative structure proposed based on ^{1}H-NMR (400 MHz, CDCl$_3$) δ 2.43 (3 H, s, C*H$_3$*), 3.82 (3 H, s, C*H$_3$*), 3.84 (3 H, s, C*H$_3$*), 5.50 (2 H, s, C*H$_2$*), 6.16 – 6.18 (1 H, m, Ar*H*), 6.68 – 6.70 (1 H, m, Ar*H*), 6.73 (1 H, d, *J* = 2 Hz, Ar*H*), 6.78 (1 H, d, *J* = 8.4 Hz, Ar*H*), 6.88 (1 H, s, Ar*H*), 6.99 – 7.01 (1 H, m, Ar*H*)].

.

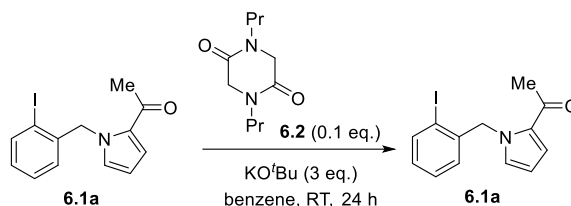### 9.4.6 Reactions 1-(1-(2-iodobenzyl)-1H-pyrrol-2-yl)ethan-1-one, 6.1a without additive (Scheme 6.4)
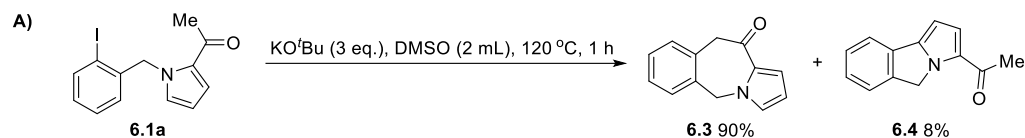
1-(1-(2-Iodobenzyl)-1H-pyrrol-2-yl)ethan-1-one **6.1a** (163 mg, 0.5 mmol) were added to an oven-dried pressure tube. In the glove box, KO^{t}Bu (168 mg, 1.5 mmol, 3.0 eq.) and anhydrous DMSO (2 mL) were added and the reaction mixture was stirred at 120 °C for 1 h. The reaction mixture was quenched with water (20 mL) and extracted with diethyl ether (3 x 20 mL). The organic phases were combined, washed with brine, dried over Na$_2$SO$_4$, filtered and concentrated *in vacuo*. The crude material was purified by column chromatography (5 - 20% ethyl acetate in petroleum ether) to give 5,10-dihydro-11H-benzo[e]pyrrolo[1,2-a]azepin-11-one **6.3** (88.6 mg, 90%) as pale brown crystals and 1-(5H-pyrrolo[2,1-a]isoindol-3-yl)ethan-1-one **6.4** (7.6 mg, 8%) as brown crystals. The spectra are consistent with the reference samples (Section 9.4.3, Table 6.1, entry 1 on pages 262-3).

1-(1-(2-Iodobenzyl)-1H-pyrrol-2-yl)ethan-1-one **6.1a** (163 mg, 0.5 mmol) was added to an oven-dried pressure tube. In the glove box, KO^{t}Bu (168 mg, 1.5 mmol, 3.0 eq.) and anhydrous benzene (5 mL) were added and the reaction mixture was stirred at 120 °C for 1 h. The reaction mixture was quenched with saturated aqueous ammonium chloride solution (20 mL) and extracted with dichloromethane (3 x 20 mL). The organic phases were combined, washed with brine, dried over Na$_2$SO$_4$, filtered and concentrated *in vacuo*. The crude mixture was purified by column chromatography (5 - 20% ethyl acetate in hexane) to give 5,10-dihydro-11H-benzo[e]pyrrolo[1,2-a]azepin-11-one **6.3** (22.9 mg, 23%) as pale yellow crystals and the starting material **6.1a** (118.9 mg, 73%) as yellow crystals. The spectra are consistent with the reference samples (**6.1a**: Section 9.4.1 on page 259 ; **6.3**: Section 9.4.3, Table 6.1, entry 1 on page 262).
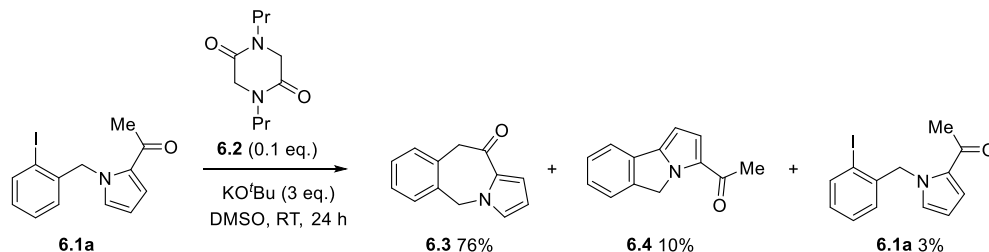
9.4.7 Reactions 1-(1-(2-iodobenzyl)-1H-pyrrol-2-yl)ethan-1-one, 6.1a at room temperature (Table 6.6)
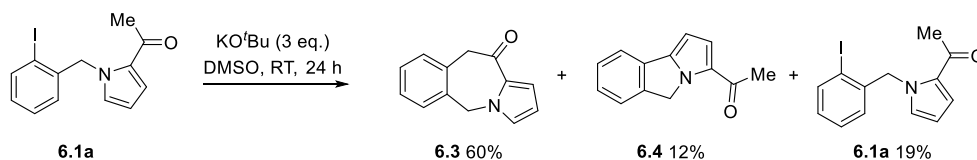
Table 6.6, entry 1

1-(1-(2-Iodobenzyl)-1H-pyrrol-2-yl)ethan-1-one **6.1a** (163 mg, 0.5 mmol) and 1,4-dipropylpiperazine-2,5-dione **6.2** (10 mg, 0.05 mmol, 0.1 eq.) were added to an oven-dried pressure tube. In the glove box, KO^{t}Bu (168 mg, 1.5 mmol, 3.0 eq.) and anhydrous benzene (5 mL) were added and the reaction mixture was stirred at RT for 24 h. The reaction mixture was quenched with saturated aqueous ammonium chloride solution (20 mL) and extracted with dichloromethane (3 x 20 mL). The organic phases were combined, washed with brine, dried over Na$_2$SO$_4$, filtered and concentrated *in vacuo*. Only the starting material **6.1a** was observed in the crude mixture by ^{1}H-NMR and TLC.

Table 6.6, entry 2

1-(1-(2-Iodobenzyl)-1H-pyrrol-2-yl)ethan-1-one **6.1a** (163 mg, 0.5 mmol) and 1,4-dipropylpiperazine-2,5-dione **6.2** (10 mg, 0.05 mmol, 0.1 eq.) were added to an oven-dried pressure tube. In the glove box, KO^{t}Bu (168 mg, 1.5 mmol, 3.0 eq.) and anhydrous DMSO (2 mL) were added and the reaction mixture was stirred at RT for 24 h. The reaction mixture was quenched with saturated aqueous ammonium chloride solution (20 mL) and extracted with dichloromethane (3 x 20 mL). The organic phases were combined, washed with brine, dried over Na$_2$SO$_4$, filtered and concentrated *in vacuo*. The crude material was purified by column chromatography (5 - 25% ethyl acetate in hexane) to give 5,10-dihydro-11H-benzo[e]pyrrolo[1,2-

a]azepin-11-one **6.3** (74.9 mg, 76%) as off-white crystals, 1-(5H-pyrrolo[2,1-a]isoindol-3-yl)ethan-1-one **6.4** (9.5 mg, 10%) as off-white crystals and the starting material **6.1a** (4.7 mg, 3%) as a pale brown solid. The spectra are consistent with the reference samples (**6.1a**: Section 9.4.1 on page 259; **6.3** and **6.4**: Section 9.4.3, Table 6.1, entry 1 on pages 262-263).

Table 6.6, entry 3

1-(1-(2-Iodobenzyl)-1H-pyrrol-2-yl)ethan-1-one **6.1a** (163 mg, 0.5 mmol) was added to an oven-dried pressure tube. In the glove box, KO^{t}Bu (168 mg, 1.5 mmol, 3.0 eq.) and anhydrous DMSO (2 mL) were added and the reaction mixture was stirred at RT for 24 h. The reaction mixture was quenched with saturated aqueous ammonium chloride solution (20 mL) and extracted with dichloromethane (3 x 20 mL). The organic phases were combined, washed with brine, dried over Na$_2$SO$_4$, filtered and concentrated *in vacuo*. The crude material was purified by column chromatography (5 - 25% ethyl acetate in hexane) to give 5,10-dihydro-11H-benzo[e]pyrrolo[1,2-a]azepin-11-one **6.3** (58.8 mg, 60%) as off-white crystals, 1-(5H-pyrrolo[2,1-a]isoindol-3-yl)ethan-1-one **6.4** (12.1 mg, 12%) as off-white crystals and the starting material **6.1a** (30.9 mg, 19%) as pale brown crystals. The spectra are consistent with the reference samples (**6.1a**: Section 9.4.1 on page 259; **6.3** and **6.4**: Section 9.4.3, Table 6.1, entry 1 on pages 262-263).

Table 6.6, entry 4
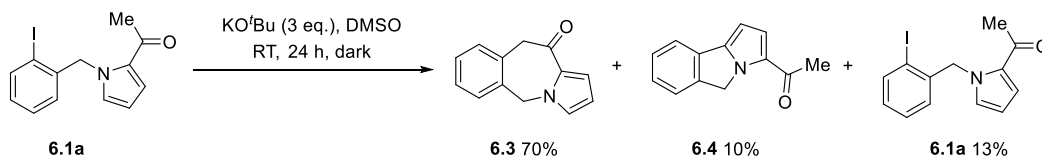
1-(1-(2-Iodobenzyl)-1H-pyrrol-2-yl)ethan-1-one **6.1a** (163 mg, 0.5 mmol) was added to an oven-dried pressure tube. In the glove box, KO^{t}Bu (168 mg, 1.5 mmol, 3.0 eq.) and anhydrous DMSO (2 mL) were added and the reaction mixture was stirred at

RT for 24 h in the dark. The reaction mixture was quenched with saturated aqueous ammonium chloride solution (20 mL) and extracted with dichloromethane (3 x 20 mL). The organic phases were combined, washed with brine, dried over Na_2SO_4, filtered and concentrated *in vacuo*. The yields of 5,10-dihydro-11H-benzo[e]pyrrolo[1,2-a]azepin-11-one **6.3** (70%), 1-(5H-pyrrolo[2,1-a]isoindol-3-yl)ethan-1-one **6.4** (10%) and starting material **6.1a** (13%) were determined by adding 1,3,5-trimethoxybenzene to the crude mixture as an internal standard for ^{1}H-NMR. The products were identified by the following characteristic signals; ^{1}H-NMR (400 MHz, CDCl$_3$) δ 2.43 (3 H, s), 5.57 (2 H, s), 6.22 – 6.24 (1 H, m) for 1-(1-(2-iodobenzyl)-1H-pyrrol-2-yl)ethan-1-one **6.1a**; δ 4.09 (2 H, s), 5.26 (2 H, s), 6.15 – 6.17 (1 H, m), 6.94 – 6.95 (1 H, m), 7.10 – 7.12 (1 H, m) for 5,10-dihydro-11H-benzo[e]pyrrolo[1,2-a]azepin-11-one **6.3**; δ 2.48 (3 H, s), 5.22 (2 H, s), 6.41 (1 H, d, *J* = 4.0 Hz) for 1-(5H-pyrrolo[2,1-a]isoindol-3-yl)ethan-1-one **6.4**. These signals are consistent with the literature values and reference samples (**6.1a**: Section 9.4.1 on page 259; **6.3** and **6.4**: Section 9.4.3, Table 6.1, entry 1 on pages 262-263).

### 9.4.8 Synthesis of 1-(2-((2-halobenzyl)amino)phenyl)ethan-1-one

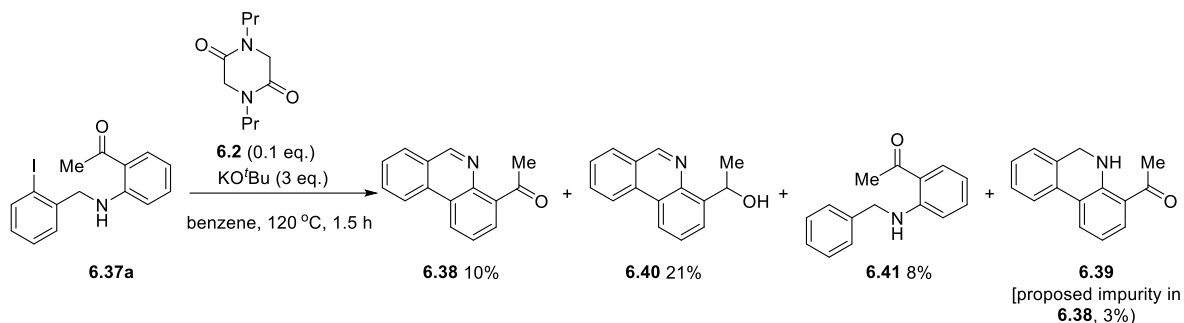**1-(2-((2-iodobenzyl)amino)phenyl)ethan-1-one 6.37a** [85]
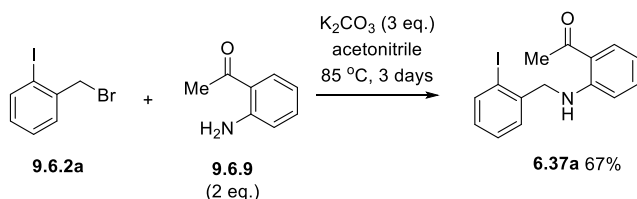
1-(Bromomethyl)-2-iodobenzene **9.6.2a** (1.48 g, 5 mmol)**,** 1-(2-aminophenyl)ethan-1-one **9.6.6** (1.22 mL, 10 mmol, 2.0 eq.), K$_2$CO$_3$ (2.07 g, 15 mmol, 3.0 eq.) and acetonitrile (5 mL) were added to an oven-dried pressure tube and the reaction mixture was stirred at 85 °C for 3 days. The reaction mixture was cooled to RT, diluted with water (20 mL) and extracted with dichloromethane (3 x 20 mL). The organic phases were combined, washed with brine, dried over Na$_2$SO$_4$, filtered and concentrated *in vacuo*. The crude material was purified by column chromatography (5% ethyl acetate in petroleum ether) to give 1-(2-((2-iodobenzyl)amino)phenyl)ethan-1-one **6.37a**[85] (1.18 g, 67%) as a yellow solid m.p.

137 – 138 °C (lit.[85]: 128.3 – 129.3 °C); [Found: (HRMS-ESI) 352.0188. $C_{15}H_{15}INO^+$ $(M+H)^+$ requires 352.0193]; v_{max}(film) / cm^{-1} 3296, 2359, 2342, 1626, 1570, 1516, 1435, 1418, 1356, 1331, 1248, 1229, 1173, 1150, 1013, 955, 743, 667; ^{1}H-NMR (400 MHz, CDCl$_3$) δ 2.62 (3 H, s, C*H*$_3$), 4.43 (2 H, d, *J* = 6.0 Hz, C*H*$_2$), 6.53 (1 H, d, *J* = 8.4 Hz, Ar*H*), 6.63 (1 H, m, Ar*H*), 6.96 (1 H, m, Ar*H*), 7.27 – 7.32 (3 H, m, Ar*H*), 7.79 (1 H, dd, *J* = 8.0, 1.6 Hz, Ar*H*), 7.86 (1 H, d, *J* = 7.6 Hz, Ar*H*), 9.39 (1 H, br s, N*H*); ^{13}C{^{1}H}-NMR (100 MHz, CDCl$_3$) δ 28.1 (CH$_3$), 52.1 (CH$_2$), 98.4 (C), 112.4 (CH), 114.9 (CH), 118.2 (C), 128.2 (CH), 128.6 (CH), 129.0 (CH), 132.9 (CH), 135.2 (CH), 139.6 (CH), 140.3 (C), 150.7 (C), 201.2 (C).

1-(2-((2-Bromobenzyl)amino)phenyl)ethan-1-one **6.37b**
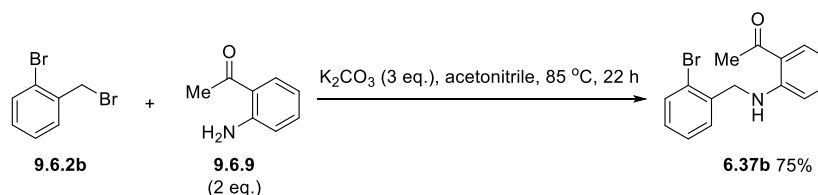
1-(Bromomethyl)-2-bromobenzene **9.6.2b** (1.25 g, 5 mmol), 1-(2-aminophenyl)ethan-1-one **9.6.6** (1.22 mL, 10 mmol, 2.0 eq.), K$_2$CO$_3$ (2.07 g, 15 mmol, 3.0 eq.) and acetonitrile (10 mL) were added to an oven-dried three-necked flask, equipped with condenser and the reaction mixture was stirred at 85 °C for 22 h. The reaction mixture was cooled to RT, quenched dropwise with water (30 mL) and extracted with ethyl acetate (3 x 30 mL). The organic phases were combined, washed with water then brine, dried over Na$_2$SO$_4$, filtered and concentrated *in vacuo*. The crude material was purified by column chromatography (2 - 4% diethyl ether in petroleum ether) to give *1-(2-((2-bromobenzyl)amino)phenyl)ethan-1-one* **6.37b** (1.14 g, 75%) as yellow crystals m.p. 141 – 143 °C; [Found: (HRMS-ESI) 304.0328. $C_{15}H_{15}^{79}BrNO^+$ $(M+H)^+$ requires 304.0332]; v_{max}(film) / cm^{-1} 3291, 2924, 2359, 1634, 1572, 1516, 1437, 1418, 1356, 1250, 1229, 1152, 1024, 955, 745, 677; ^{1}H-NMR (400 MHz, CDCl$_3$) δ 2.63 (3 H, s, C*H*$_3$), 4.53 (2 H, s, C*H*$_2$), 6.56 – 6.58 (1 H, m, Ar*H*), 6.61 – 6.66 (1 H, m, Ar*H*), 7.10 – 7.15 (1 H, m, Ar*H*), 7.23 (1 H, td, *J* = 7.6, 1.2 Hz, Ar*H*), 7.28 – 7.33 (2 H, m, Ar*H*), 7.57 (1 H, dd, *J* = 8.0, 1.2 Hz, Ar*H*), 7.79 (1 H, dd, *J* = 8.0, 1.6 Hz, Ar*H*), 9.39 (1 H, br s, N*H*); ^{13}C{^{1}H}-NMR (100 MHz, CDCl$_3$) δ 28.1 (CH$_3$), 47.1 (CH$_2$), 112.4 (CH), 114.9 (CH), 118.2 (C), 123.2 (C), 127.7 (CH), 128.6

(CH), 128.8 (CH), 132.9 (CH), 132.9 (CH), 135.2 (CH), 137.5 (C), 150.7 (C), 201.2 (C); *m/z* (ESI) 306.0304 [(M+H)$^+$, ^{81}Br, 96%], 304.0328 [(M+H)$^+$, ^{79}Br, 100].

9.4.9 Reactions of 1-(2-((2-halobenzyl)amino)phenyl)ethan-1-one (Table 6.7 & Scheme 6.10)
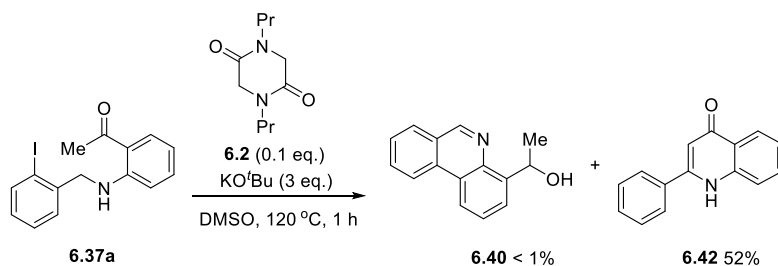
Table 6.7, entry 1

1-(2-((2-Iodobenzyl)amino)phenyl)ethan-1-one **6.37a** (176 mg, 0.5 mmol) and 1,4-dipropylpiperazine-2,5-dione **6.2** (10 mg, 0.05 mmol, 0.1 eq.) were added to an oven-dried pressure tube. In the glove box, KO^{t}Bu (168 mg, 1.5 mmol, 3.0 eq.) and anhydrous benzene (5 mL) were added and the reaction mixture was stirred at 120 °C for 1.5 h. The reaction mixture was quenched with saturated aqueous ammonium chloride solution (20 mL) and extracted with dichloromethane (3 x 20 mL). The organic phases were combined, washed with brine, dried over Na$_2$SO$_4$, filtered and concentrated *in vacuo*. The crude mixture was purified by column chromatography (5 - 100% ethyl acetate in petroleum ether, then 0 - 2% methanol in ethyl acetate) to give several products: impure 1-(phenanthridin-4-yl)ethan-1-one **6.38** (30.8 mg) and *1-(phenanthridin-4-yl)ethanol **6.40*** (22.9 mg, 21%) as an orange oil (HRMS-ESI) 246.0888. C$_{15}$H$_{13}$NONa$^+$ (M+Na)$^+$ requires 246.0889]; ν$_{max}$(film) / cm^{-1} 3320, 2967, 2922, 1614, 1587, 1516, 1445, 1261, 1231, 1159, 1098, 1069, 1053, 1007, 889, 752; ^{1}H-NMR (400 MHz, CDCl$_3$) δ 1.77 (3 H, d, *J* = 6.8 Hz, C*H$_3$*), 5.51 (1 H, q, *J* = 6.8 Hz, C*H*), 7.62 – 7.67 (2 H, m, Ar*H*), 7.72 – 7.76 (1 H, m, Ar*H*), 7.87 – 7.92 (1 H, m, Ar*H*), 8.09 (1 H, d, *J* = 7.6 Hz, Ar*H*), 8.51 (1 H, dd, *J* = 7.2, 2.4 Hz, Ar*H*), 8.64 (1 H, d, *J* = 8.4 Hz, Ar*H*), 9.26 (1 H, s, Ar*H*); ^{13}C{^{1}H}-NMR (100 MHz, CDCl$_3$) δ 24.8 (CH$_3$), 70.8 (CH), 121.5 (CH), 122.3 (CH), 124.7 (C), 126.1 (C), 126.1 (CH), 127.1 (CH), 127.8 (CH), 129.1 (CH), 131.4 (CH), 133.1 (C), 142.5 (C), 142.8 (C), 151.7 (CH); 1-(2-(benzylamino)phenyl)ethan-1-one **6.41** (9.4 mg, 8%) as a yellow solid m.p. 83 – 85

°C (lit.[205]: 79 – 81 °C); [Found: (HRMS-ESI) 226.1227. $C_{15}H_{16}NO^+$ (M+H)$^+$ requires 226.1226]; v_{max}(film) / cm^{-1} 3323, 1638, 1566, 1514, 1493, 1418, 1362, 1244, 1225, 1165, 1024, 953, 747, 729, 706, 692, 667; ^{1}H-NMR (400 MHz, CDCl$_3$) δ 2.61 (3 H, s, C*H$_3$*), 4.47 (2 H, d, *J* = 5.6 Hz, C*H$_2$*), 6.59 – 6.63 (1 H, m, Ar*H*), 6.65 (1 H, d, *J* = 8.0 Hz, Ar*H*), 7.24 – 7.36 (5 H, m, Ar*H*), 7.77 (1 H, dd, *J* = 8.0, 1.6 Hz, Ar*H*), 9.31 (1 H, br s, N*H*); ^{13}C{^{1}H}-NMR (100 MHz, CDCl$_3$) δ 28.1 (CH$_3$), 46.8 (CH$_2$), 112.3 (CH), 114.5 (CH), 117.9 (C), 127.1 (2 x CH), 127.3 (CH), 128.8 (2 x CH), 132.8 (CH), 135.2 (CH), 138.8 (C), 151.0 (C), 201.1 (C). The impure mixture of **6.38** was purified again by column chromatography (10 - 100% dichloromethane in hexane) to give both 1-(phenanthridin-4-yl)ethan-1-one **6.38**[85] (7.4 mg, 7%) as yellow crystals m.p. 91 – 94 °C (lit.[85]: 93.7 – 95.5 °C); [Found: (GC-Cl) $C_{15}H_{12}NO^+$ (M+H)$^+$ 222.2]; v_{max}(film) / cm^{-1} 2922, 2359, 2342, 1684, 1580, 1346, 1275, 1184, 1165, 1111, 889, 768, 747, 731, 720, 637; ^{1}H-NMR (400 MHz, CDCl$_3$) δ 2.95 (3 H, s, C*H$_3$*), 7.69 – 7.78 (2 H, m, Ar*H*), 7.86 – 7.92 (2 H, m, Ar*H*), 8.08 (1 H, d, *J* = 8.0 Hz, Ar*H*), 8.62 (1 H, d, *J* = 8.0 Hz, Ar*H*), 8.69 (1 H, d, *J* = 8.0 Hz, Ar*H*), 9.32 (1 H, s, Ar*H*); ^{13}C{^{1}H}-NMR (100 MHz, CDCl$_3$) δ 33.0 (CH$_3$), 122.2 (CH), 124.3 (C), 125.2 (CH), 126.3 (C), 126.8 (CH), 127.8 (CH), 128.1 (CH), 129.0 (CH), 131.5 (CH), 132.4 (C), 141.1 (C), 141.9 (C), 153.6 (CH), 205.2 (C), and impure 1-(phenanthridin-4-yl)ethan-1-one **6.38** (6.2 mg). The proposed impurity in **6.38** is *1-(5,6-dihydrophenanthridin-4-yl)ethan-1-one* **6.39** (ratio 1 : 1), giving 1-(phenanthridin-4-yl)ethan-1-one **6.38** (3%) and *1-(5,6-dihydrophenanthridin-4-yl)ethan-1-one* **6.39** (3%) [tentative structure proposed based on [Found: (GC-Cl) $C_{15}H_{14}NO^+$ (M+H)$^+$ 224.1]; ^{1}H-NMR (400 MHz, CDCl$_3$) δ 2.60 (3 H, s, C*H$_3$*), 4.59 (2 H, s, C*H$_2$*), 6.68 (1 H, t, *J* = 8.0 Hz, ArH), 7.10 (1 H, d, *J* = 7.2 Hz, Ar*H*), 7.22 – 7.32 (2 H, m, Ar*H*), 7.66 – 7.68 (2 H, m, Ar*H*), 7.82 (1 H, d, *J* = 7.6 Hz, Ar*H*), 9.00 (1 H, br s, *NH*).

Table 6.7, entry 2

1-(2-((2-Iodobenzyl)amino)phenyl)ethan-1-one **6.37a** (176 mg, 0.5 mmol) and 1,4-dipropylpiperazine-2,5-dione **6.2** (10 mg, 0.05 mmol, 0.1 eq.) were added to an oven-dried pressure tube. In the glove box, KO*t*Bu (168 mg, 1.5 mmol, 3.0 eq.) and anhydrous DMSO (2 mL) were added and the reaction mixture was stirred at 120 °C for 1 h. The reaction mixture was quenched with saturated aqueous ammonium chloride solution (20 mL) and extracted with dichloromethane (3 x 20 mL). The organic phases were combined, washed with brine, dried over Na$_2$SO$_4$, filtered and concentrated *in vacuo*. The crude mixture was purified by column chromatography (1 - 100% ethyl acetate in hexane, then 0 - 2% methanol in ethyl acetate) to give impure *1-(phenanthridin-4-yl)ethanol* **6.40** (2.7 mg, < 1% by analysis of ^{1}H-NMR) as an orange oil and 2-phenylquinolin-4(1H)-one **6.42**[206] (57.1 mg, 52%) as pale-yellow solid m.p. 252 – 255 °C (lit.[207]: 251 – 253 °C); [Found: (HRMS-ESI) 222.0915. C$_{15}$H$_{12}$NO$^+$ (M+H)$^+$ requires 222.0913]; v_{max}(film) / cm^{-1} 2955, 2922, 2853, 1632, 1580, 1543, 1497, 1470, 1449, 1431, 1356, 1254, 1138, 839, 790, 754, 689, 662; ^{1}H-NMR (400 MHz, d^6-DMSO) δ 6.33 (1 H, s, C*H*), 7.32 – 7.36 (1 H, m, Ar*H*), 7.58 – 7.60 (3 H, m, Ar*H*), 7.65 – 7.69 (1 H, m, Ar*H*), 7.76 (1 H, d, *J* = 8.0 Hz, Ar*H*), 7.83 – 7.84 (2 H, m, Ar*H*), 8.10 (1 H, dd, *J* = 8.0, 1.2 Hz, Ar*H*), 11.68 (1 H, br s, N*H*); ^{13}C{^{1}H}-NMR (100 MHz, d^6-DMSO) δ 107.3 (CH), 118.7 (CH), 123.2 (CH), 124.7 (CH), 124.9 (C), 127.4 (2 x CH), 128.9 (2 x CH), 130.4 (CH), 131.7 (CH), 134.2 (C), 140.5 (C), 150.0 (C), 176.9 (C); HSQC (^{1}H/^{13}C) δ 6.33/107.3, (7.32 – 7.36)/123.2, (7.58 – 7.60)/130.4, (7.58 – 7.60)/128.9, (7.65 – 7.69)/131.7, 7.76/118.7, (7.83 – 7.84)/127.4, 8.10/124.7; **6.42** was recrystallised (acetone) to give crystals for X-ray analysis (X-ray crystallographic data in Appendix).
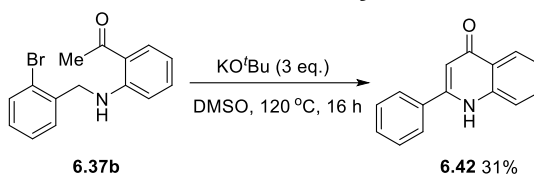
Table 6.7, entry 3
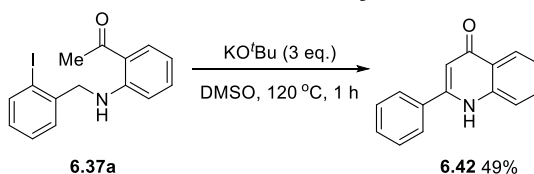
1-(2-((2-Iodobenzyl)amino)phenyl)ethan-1-one **6.37a** (176 mg, 0.5 mmol) was added to an oven-dried pressure tube. In the glove box, KO*t*Bu (168 mg, 1.5 mmol, 3.0 eq.) and anhydrous DMSO (2 mL) were added and the reaction mixture was stirred at 120 °C for 1 h. The reaction mixture was quenched with water (20 mL) and
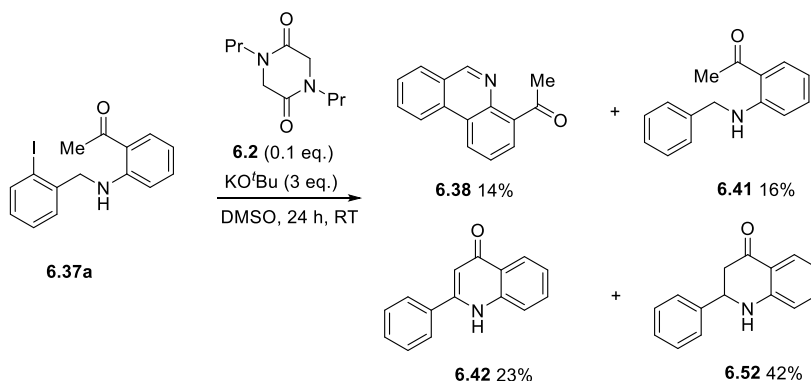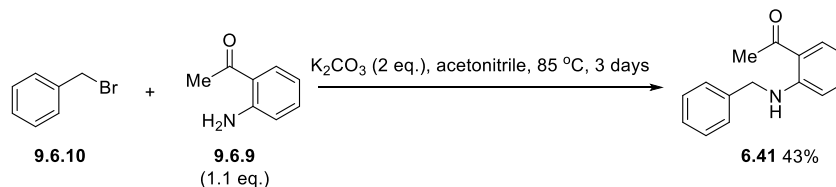
extracted with ethyl acetate (3 x 20 mL). The organic phases were combined, washed with brine, dried over Na₂SO₄, filtered and concentrated *in vacuo*. The crude mixture was purified by column chromatography (5 – 100% ethyl acetate in petroleum ether) to give 2-phenylquinolin-4(1H)-one **6.42** (54.7 mg, 49%) as off-white crystals. The spectra are consistent with the reference samples (Section 9.4.9, Table 6.7, entry 2 on page 277). (Trace amounts of other products were identified by thin layer chromatography although these weren't isolated).

Table 6.7, entry 4

6.37b   **6.42** 31%

1-(2-((2-Bromobenzyl)amino)phenyl)ethan-1-one **6.38b** (152 mg, 0.5 mmol) was added to an oven-dried pressure tube. In the glove box, KO^tBu (168 mg, 1.5 mmol, 3.0 eq.) and anhydrous DMSO (2 mL) were added and the reaction mixture was stirred at 120 °C for 16 h. The reaction mixture was quenched with water (20 mL) and extracted with ethyl acetate (3 x 20 mL). The organic phases were combined, washed with brine, dried over Na₂SO₄, filtered and concentrated *in vacuo*. The crude mixture was purified by column chromatography (5 – 100% ethyl acetate in petroleum ether) to give 2-phenylquinolin-4(1H)-one **6.42** (33.8 mg, 31%) as a pale brown solid. The spectra are consistent with the reference samples (Section 9.4.9, Table 6.7, entry 2 on page 277). (Trace amounts of other products were identified by thin layer chromatography although these weren't isolated).

Scheme 6.10

6.37a

6.38 14%   **6.41** 16%

6.42 23%   **6.52** 42%

1-(2-((2-Iodobenzyl)amino)phenyl)ethan-1-one **6.37a** (176 mg, 0.5 mmol) and 1,4-dipropylpiperazine-2,5-dione **6.2** (10 mg, 0.05 mmol, 0.1 eq.) were added to an oven-dried pressure tube. In the glove box, KO^{t}Bu (168 mg, 1.5 mmol, 3.0 eq.) and anhydrous DMSO (2 mL) were added and the reaction mixture was stirred at RT for 24 h. The reaction mixture was quenched with saturated aqueous ammonium chloride solution (20 mL) and extracted with dichloromethane (3 x 20 mL). The organic phases were combined, washed with brine, dried over Na$_2$SO$_4$, filtered and concentrated *in vacuo*. The crude mixture was purified by column chromatography (2 - 100% dichloromethane in hexane then 0 - 2% methanol in ethyl acetate) to give 1-(phenanthridin-4-yl)ethan-1-one **6.38** (15 mg, 14%) as yellow crystals, 1-(2-(benzylamino)phenyl)ethan-1-one **6.41** (17.5 mg, 16%) as yellow crystals, 2-phenylquinolin-4(1H)-one **6.42** (25.6 mg, 23%) as pale yellow solid and 2-phenyl-2,3-dihydroquinolin-4(1H)-one **6.52**[208] (46.4 mg, 42%) as yellow crystals m.p. 144 – 146 ºC (lit.[208]: 148 – 149 ºC); [Found: (GC-CI) C$_{15}$H$_{14}$NO$^+$ (M+H)$^+$ 223.9.]; v$_{max}$(film) / cm^{-1} 3331, 1653, 1603, 1479, 1330, 1302, 1153, 764, 698; ^{1}H-NMR (400 MHz, CDCl$_3$) δ 2.77 – 2.95 (2 H, m, C*H*$_2$), 4.49 (1 H, br s, N*H*), 4.76 (1 H, dd, *J* = 13.6, 4.0 Hz, C*H*Ph), 6.71 (1 H, d, *J* = 8.4 Hz, Ar*H*), 6.78 – 6.82 (1 H, m, Ar*H*), 7.32 – 7.48 (6 H, m, Ar*H*), 7.88 (1 H, dd, *J* = 8.0, 1.6 Hz, Ar*H)*; ^{13}C{^{1}H}-NMR (100 MHz, CDCl$_3$) δ 46.6 (CH), 58.7 (CH$_2$), 116.1 (CH), 118.6 (CH), 119.2 (C), 126.8 (2 x CH), 127.8 (CH), 128.6 (CH), 129.2 (2 x CH), 135.6 (CH), 141.2 (C), 151.7 (C), 193.4 (C). The spectra are consistent with the reference samples (**6.38**, **6.40** and **6.41**: Section 9.4.9, Table 6.7, entry 1 on pages 275-276; **6.42**: Section 9.4.9, Table 6.7, entry 2 on page 277).

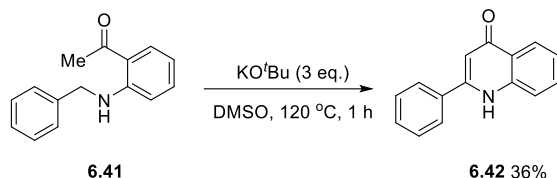### 9.4.10 Synthesis of 1-(2-(benzylamino)phenyl)ethan-1-one, 6.41[84]

(Bromomethyl)benzene **9.6.10** (855 mg, 5 mmol), 1-(2-(aminomethyl)phenyl)ethan-1-one **9.6.6** (0.73 mL, 6 mmol, 1.1 eq.), K$_2$CO$_3$ (1.38 g, 10 mmol, 2.0 eq.) and acetonitrile (5 mL) were added to an oven-dried pressure tube. The reaction mixture

was stirred at 85 °C for 3 days. The reaction mixture was cooled to RT, diluted with water (20 mL) and extracted with dichloromethane (3 x 20 mL). The organic phases were combined, washed with brine, dried over Na$_2$SO$_4$, filtered and concentrated *in vacuo*. The crude material was purified by column chromatography (20 – 40% toluene in hexane) to give 1-(2-(benzylamino)phenyl)ethan-1-one **6.41**[205] (482 mg, 43%) as yellow crystals m.p. 83 – 85 °C (lit.[205]: 79 – 81 °C); [Found: (HRMS-ESI) 226.1227. C$_{15}$H$_{16}$NO$^+$ (M+H)$^+$ requires 226.1226]; v_{max}(film) / cm^{-1} 3323, 1638, 1566, 1514, 1493, 1418, 1362, 1244, 1225, 1165, 1024, 953, 747, 729, 706, 692, 667; ^{1}H-NMR (400 MHz, CDCl$_3$) δ 2.61 (3 H, s, C*H$_3$*), 4.47 (2 H, d, *J* = 5.6 Hz, C*H$_2$*), 6.59 – 6.63 (1 H, m, Ar*H*), 6.65 (1 H, d, *J* = 8.0 Hz, Ar*H*), 7.24 – 7.36 (6 H, m, Ar*H*), 7.77 (1 H, dd, *J* = 8.0, 1.6 Hz, Ar*H*), 9.31 (1 H, br s, N*H*); ^{13}C{^{1}H}-NMR (100 MHz, CDCl$_3$) δ 28.1 (CH$_3$), 46.8 (CH$_2$), 112.3 (CH), 114.5 (CH), 117.9 (C), 127.1 (2 x CH), 127.3 (CH), 128.8 (2 x CH), 132.8 (CH), 135.2 (CH), 138.8 (C), 151.0 (C), 201.1 (C).

9.4.11 Reactions of 1-(2-(benzylamino)phenyl)ethan-1-one, 6.38c (Scheme 6.13B)

Conditions A (For comparison with the reaction of **6.37a** refer to Table 6.7, entry 3, Section 9.4.9)

1-(2-(Benzylamino)phenyl)ethan-1-one **6.41** (99.6 mg, 0.5 mmol) was added to an oven-dried pressure tube. In the glove box, KO^{t}Bu (168 mg, 1.5 mmol, 3.0 eq.) and anhydrous DMSO (2 mL) were added and the reaction mixture was stirred at 120 °C for 1 h. The reaction mixture was quenched with saturated aqueous ammonium chloride solution (15 mL) and extracted with dichloromethane (4 x 20 mL). The organic phases were combined, washed with brine, dried over Na$_2$SO$_4$, filtered and concentrated *in vacuo*. The crude mixture was purified by column chromatography (2 - 100% ethyl acetate in hexane) to give 2-phenyl-2,3-dihydroquinolin-4(1H)-one **6.42** (39.7 mg, 36%) as a pale brown solid. The spectra are consistent with the reference samples (Section 9.4.9, Table 6.7, entry 2 on page 277).

Conditions B (For comparison with the reaction of **6.37a** refer to Section 9.49, Scheme 6.10)


6.41
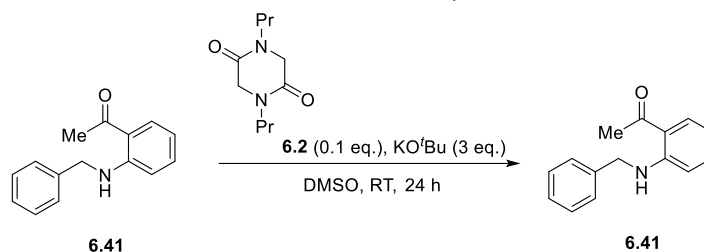
1-(2-(Benzylamino)phenyl)ethan-1-one **6.41** (99.6 mg, 0.5 mmol) and 1,4-dipropylpiperazine-2,5-dione **6.2** (10 mg, 0.05 mmol, 0.1 eq.) were added to an oven-dried pressure tube. In the glove box, KO^{t}Bu (168 mg, 1.5 mmol, 3.0 eq.) and anhydrous DMSO (2 mL) were added and the reaction mixture was stirred at RT for 24 h. The reaction mixture was quenched with saturated aqueous ammonium chloride solution (15 mL) and extracted with dichloromethane (4 x 20 mL). The organic phases were combined, washed with brine, dried over Na$_2$SO$_4$, filtered and concentrated *in vacuo*. Only the starting material **6.41** was observed in the crude mixture by ^{1}H-NMR and TLC.

Conditions C
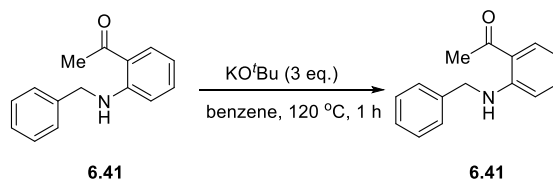
6.41

1-(2-(Benzylamino)phenyl)ethan-1-one **6.41** (99.6 mg, 0.5 mmol) was added to an oven-dried pressure tube. In the glove box, KO^{t}Bu (168 mg, 1.5 mmol, 3.0 eq.) and anhydrous benzene (5 mL) were added and the reaction mixture was stirred at 120 °C for 1 h. The reaction mixture was quenched with saturated aqueous ammonium chloride solution (15 mL) and extracted with dichloromethane (4 x 20 mL). The organic phases were combined, washed with brine, dried over Na$_2$SO$_4$, filtered and concentrated *in vacuo*. Only the starting material **6.41** was observed in the crude mixture by ^{1}H-NMR and TLC.

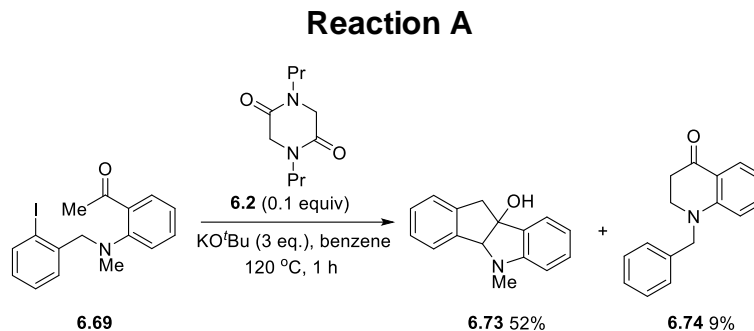## 9.4.12 Synthesis of 1-(2-((2-iodobenzyl)(methyl)amino)phenyl)ethan-1-one, 6.69
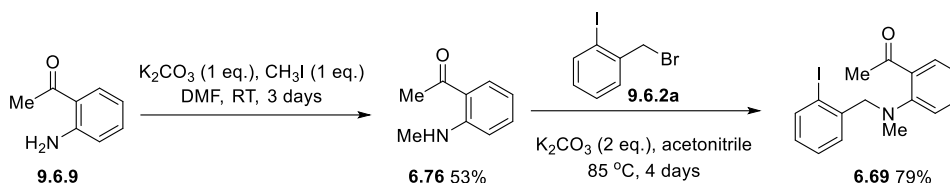
K$_2$CO$_3$ (3.46 g, 25 mmol, 1.0 eq.) and anhydrous dimethylformamide (15 mL) were added to an oven-dried round-bottomed flask. Under an argon atmosphere, 1-(2-aminophenyl)ethan-1-one **9.6.9** (3.04 mL, 25 mmol) was added and the reaction mixture was stirred at RT for 15 min. A solution of methyl iodide (1.56 mL, 25 mmol, 1.0 eq.) in anhydrous dimethylformamide, was added dropwise to the reaction mixture. The reaction mixture was stirred at RT for 3 days. The reaction mixture was diluted with water (60 mL) and extracted with ethyl acetate (3 x 40 mL). The organic phases were combined, washed with water, then brine, dried over Na$_2$SO$_4$, filtered and concentrated *in vacuo*. The crude material was purified by column chromatography (3 – 5% ethyl acetate in petroleum ether) to give 1-(2-(methylamino)phenyl)ethan-1-one **6.76**[209] (1.98 g, 53%) as yellow crystals m.p. 45 – 47 °C (lit.[209]: 37 – 39 °C); [Found: (HRMS-ESI) 150.0910. C$_9$H$_{12}$NO$^+$ (M+H)$^+$ requires 150.0913]; v_{max}(film) / cm^{-1} 3321, 1632, 1562, 1516, 1410, 1234, 1165, 951, 743, 652, 613; ^{1}H-NMR (400 MHz, CDCl$_3$) δ 2.57 (3 H, s, C*H$_3$*), 2.91 (3 H, d, *J* = 4.8 Hz, C*H$_3$*), 6.57 – 6.61 (1 H, m, Ar*H*), 6.68 (1 H, d, *J* = 8.4 Hz, Ar*H*), 7.36 – 7.40 (1 H, m, Ar*H*), 7.73 – 7.75 (1 H, m, Ar*H*), 8.78 (1 H, br s, N*H*); ^{13}C{^{1}H}-NMR (100 MHz, CDCl$_3$) δ 27.9 (CH$_3$), 29.3 (CH$_3$), 111.3 (CH), 113.9 (CH), 117.6 (C), 132.7 (CH), 135.1 (CH), 152.0 (C), 200.8 (C).

1-(Bromomethyl)-2-iodobenzene **9.6.2a** (1.48 g, 5 mmol), 1-(2-(methylamino)phenyl)ethan-1-one **6.76** (895 mg, 6 mmol, 1.1 eq.), K$_2$CO$_3$ (1.38 g, 10 mmol, 2.0 eq.) and acetonitrile (5 mL) were added to an oven-dried pressure tube and the reaction mixture was stirred at 85 °C for 4 days. The reaction mixture was cooled to RT, diluted with water (20 mL) and extracted with dichloromethane (3 x 15 mL). The organic phases were combined, dried over Na$_2$SO$_4$, filtered and concentrated *in vacuo*. The crude material was purified by column chromatography (5% ethyl acetate in petroleum ether) to give 1-(2-((2-

iodobenzyl)(methyl)amino)phenyl)ethan-1-one **6.69**[85] (1.45 g, 79%) as orange crystals m.p. 66 – 68 °C; [Found: (GCMS-ESI) $C_{16}H_{17}INO^+$ (M+H)$^+$ 366.1]; v_{max}(film) / cm^{-1} 1668, 1503, 1221, 1211, 1119, 1015, 953, 750; ^{1}H-NMR (400 MHz, CDCl$_3$) δ 2.63 (3 H, s, C*H*$_3$), 2.78 (3 H, s, C*H*$_3$), 4.31 (2 H, s, C*H*$_2$), 6.95 – 6.99 (2 H, m, Ar*H*), 7.02 (1 H, d, *J* = 8.4 Hz, Ar*H*), 7.25 – 7.32 (2 H, m, Ar*H*), 7.33 – 7.38 (1 H, m, Ar*H*), 7.46 (1 H, d, *J* = 7.6 Hz, Ar*H*), 7.85 (1 H, d, *J* = 8.0 Hz, Ar*H*); ^{13}C{^{1}H}-NMR (100 MHz, CDCl$_3$) δ 29.7 (CH$_3$), 42.8 (CH$_3$), 64.4 (CH$_2$), 99.6 (C), 118.9 (CH), 120.8 (CH), 128.4 (CH), 129.1 (CH), 129.4 (CH), 129.6 (CH), 131.9 (CH), 132.9 (C), 139.5 (C), 139.8 (CH), 151.0 (C), 203.3 (C).

9.4.13 Reactions of 1-(2-((2-iodobenzyl)(methyl)amino)phenyl)ethan-1-one (Scheme 6.15)
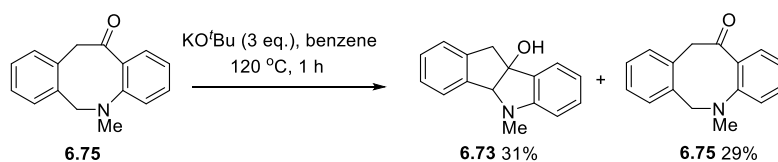
Reaction A

1-(2-((2-Iodobenzyl)(methyl)amino)phenyl)ethan-1-one **6.69** (183 mg, 0.5 mmol) and 1,4-dipropylpiperazine-2,5-dione **6.2** (10 mg, 0.05 mmol, 0.1 eq.) were added to an oven-dried pressure tube. In the glove box, KO^{t}Bu (168 mg, 1.5 mmol, 3.0 eq.) and anhydrous benzene (5 mL) were added and the reaction mixture was stirred at 120 °C for 1 h. The reaction mixture was quenched with saturated aqueous ammonium chloride solution (15 mL) and extracted with dichloromethane (3 x 20 mL). The organic phases were combined, washed with brine, dried over Na$_2$SO$_4$, filtered and concentrated *in vacuo*. The crude mixture was purified by column chromatography (25 - 100% dichloromethane in hexane) to give both *5-methyl-4,10-dihydroindeno[1,2]indol-9(5H)-ol* **6.73** (61.6 mg, 52%) as a yellow solid m.p. 102 – 106 °C; [Found: (HRMS-NSI) 238.1222. $C_{16}H_{16}NO^+$ (M+H)$^+$ requires 238.1226]; v_{max}(film) / cm^{-1} 3304, 1668, 1609, 1489, 1373, 1314, 1263, 1219, 1123, 1057, 1040, 982, 745, 727, 654, 631; ^{1}H-NMR (400 MHz, CDCl$_3$) δ 2.18 (1 H, br s, O*H*), 3.08 (3 H, s, C*H*$_3$), 3.48 – 3.49 (2 H, m, C*H*$_2$), 4.74 (1 H, s, C*H*), 6.47 (1 H, d, *J* = 8.0 Hz,

Ar*H*), 6.74 (1 H, td, *J* = 7.6, 0.8 Hz, Ar*H*), 7.17 – 7.28 (4 H, m, Ar*H*), 7.37 (1 H, dd, *J* = 7.2, 0.8 Hz, Ar*H*), 7.44 – 7.46 (1 H, m, Ar*H*); $^{13}C\{^1H\}$-NMR (100 MHz, CDCl$_3$) δ 33.8 (CH$_3$), 46.1 (CH$_2$), 82.8 (CH), 88.3 (C), 107.4 (CH), 117.8 (CH), 123.4 (CH), 125.4 (CH), 125.5 (CH), 127.1 (CH), 128.6 (CH), 130.1 (CH), 132.6 (C), 140.6 (C), 142.8 (C), 151.2 (C); **6.73** was recrystallised (dichloromethane/hexane) to give crystals for X-ray analysis (X-ray crystallographic data in Appendix), and 1-benzyl-2,3-dihydroquinolin-4(1H)-one **6.74**[210] (11.3 mg, 9%) as yellow crystals m.p. 114 – 117 °C (lit.[210]: 111 – 114 °C); [Found: (GC-CI) C$_{16}$H$_{16}$NO$^+$ (M+H)$^+$ 238.2]; ν$_{max}$(film) / cm^{-1} 2918, 2907, 1661, 1603, 1497, 1449, 1346, 1289, 1229, 1198, 1180, 1121, 999, 856, 752, 731, 698; ^1H-NMR (400 MHz, CDCl$_3$) δ 2.74 – 2.78 (2 H, m, C*H*$_2$), 3.58 – 3.62 (2 H, m, C*H*$_2$), 4.57 (2 H, s, C*H*$_2$), 6.69 – 6.75 (2 H, m, Ar*H*), 7.29 – 7.37 (6 H, m, Ar*H*), 7.93 (1 H, dd, *J* = 7.6, 1.6 Hz, Ar*H*); $^{13}C\{^1H\}$-NMR (100 MHz, CDCl$_3$) δ 38.2 (CH$_2$), 49.6 (CH$_2$), 55.4 (CH$_2$), 113.6 (CH), 117.1 (CH), 119.9 (C), 126.9 (2 x CH), 127.6 (CH), 128.4 (CH), 129.0 (2 x CH), 135.6 (CH), 137.4 (C), 151.9 (C), 193.7 (C).

Reaction B

1-(2-((2-Iodobenzyl)(methyl)amino)phenyl)ethan-1-one **6.69** (183 mg, 0.5 mmol) and 1,4-dipropylpiperazine-2,5-dione **6.2** (10 mg, 0.05 mmol, 0.1 eq.) were added to an oven-dried pressure tube. In the glove box, KO^{t}Bu (168 mg, 1.5 mmol, 3.0 eq.) and anhydrous DMSO (2 mL) were added and the reaction mixture was stirred at RT for 24 h. The reaction mixture was quenched with saturated aqueous ammonium chloride solution (15 mL) and extracted with dichloromethane (4 x 20 mL). The organic phases were combined, washed with brine, dried over Na$_2$SO$_4$, filtered and concentrated *in vacuo*. The crude mixture was purified by column chromatography (2 - 25% ethyl acetate in hexane) to give several products: 5-methyl-6,11-dihydrodibenzo[b,f]azocin-12(5H)-one **6.75**[85] (32.4 mg, 27%) as yellow solid m.p. 102 – 106 °C (lit.[85]: 108 – 109 °C); [Found: (GC-CI) C$_{16}$H$_{16}$NO$^+$ (M+H)$^+$ 238.1]; ν$_{max}$(film) / cm^{-1} 1661, 1591, 1487, 1350, 1285, 1163, 1088, 1009, 756, 735, 623; ^{1}H-

NMR (400 MHz, CDCl$_3$) δ 3.01 (3 H, s, CH_3), 4.08 (2 H, s, CH_2), 4.22 (2 H, s, CH_2), 6.91 (1 H, td, *J* = 7.6, 0.8 Hz, Ar*H*), 7.05 (1 H, d, *J* = 8.4 Hz, Ar*H*), 7.11 (1 H, d, *J* = 7.6 Hz, Ar*H*), 7.21 – 7.29 (3 H, m, Ar*H*), 7.40 – 7.45 (1 H, m, Ar*H*), 7.61 (1 H, dd, *J* = 7.6, 1.6 Hz, Ar*H*); ^{13}C{^{1}H}-NMR (100 MHz, CDCl$_3$) δ 37.8 (CH$_3$), 48.1 (CH$_2$), 64.4 (CH$_2$), 115.2 (CH), 119.0 (CH), 127.2 (CH), 128.4 (CH), 128.8 (CH), 129.5 (CH), 130.9 (CH), 131.2 (C), 132.7 (CH), 135.3 (C), 135.8 (C) 153.0 (C), 210.9 (C); 1-benzyl-2,3-dihydroquinolin-4(1H)-one **6.74** (25.2 mg, 21%) as yellow crystals and 1-(2-(methylamino)phenyl)ethan-1-one **6.76** (9.5 mg, 13%) as a yellow oil [Found: (HRMS-ESI) 150.0910. C$_9$H$_{12}$NO$^+$ (M+H)$^+$ requires 150.0913]; v_{max}(film) / cm^{-1} 3321, 1632, 1562, 1516, 1410, 1234, 1165, 951, 743, 652, 613; ^{1}H-NMR (400 MHz, CDCl$_3$) δ 2.57 (3 H, s, CH_3), 2.91 (3 H, d, *J* = 4.8 Hz, CH_3), 6.57 – 6.61 (1 H, m, Ar*H*), 6.68 (1 H, d, *J* = 8.4 Hz, Ar*H*), 7.36 – 7.40 (1 H, m, Ar*H*), 7.73 – 7.75 (1 H, m, Ar*H*), 8.78 (1 H, br s, N*H*); ^{13}C{^{1}H}-NMR (100 MHz, CDCl$_3$) δ 27.9 (CH$_3$), 29.3 (CH$_3$), 111.3 (CH), 113.9 (CH), 117.6 (C), 132.7 (CH), 135.1 (CH), 152.0 (C), 200.8 (C). The spectra are consistent with the reference samples (Section 9.4.13, Scheme 6.15, Reaction A on page 284).

### 9.4.14 Formation of 6.73 from 6.75 (Scheme 6.17)

5-Methyl-6,11-dihydrodibenzo[b,f]azocin-12(5H)-one **6.75** (10 mg, 0.042 mmol) was added to an oven-dried pressure tube. In the glove box, KO^{t}Bu (14 mg, 0.126 mmol, 3.0 eq.) and anhydrous benzene (1 mL) were added and the reaction mixture was stirred at 120 °C for 1 h. The reaction mixture was quenched with water (2 mL) and extracted with ethyl acetate (3 x 2 mL). The organic phases were combined, washed with brine, dried over Na$_2$SO$_4$, filtered and concentrated *in vacuo*. The yields of *5-methyl-4,10-dihydroindeno[1,2]indol-9(5H)-ol* **6.73** (31%) and starting material **6.75** (29%) were determined by adding 1,3,5-trimethoxybenzene to the crude mixture as an internal standard for ^{1}H-NMR. The products were identified by the following characteristic signals; ^{1}H-NMR (400 MHz, CDCl$_3$) δ 3.08 (3 H, s, CH_3), 3.50 (2 H, d, *J* = 2.4 Hz, CH_2), 4.74 (1 H, s, C*H*) for *5-methyl-4,10-dihydroindeno[1,2]indol-9(5H)-*

ol, **6.73**; δ 3.01 (3 H, s, CH_3), 4.08 (2 H, s, CH_2), 4.22 (2 H, s, CH_2), for 5-methyl-6,11-dihydrodibenzo[b,f]azocin-12(5H)-one **6.75**. These signals are consistent with the literature values and reference samples (Section 9.4.13, Scheme 6.15 on pages 283-285).

NMR of novel compounds in Chapter 6

^{1}H-NMR and ^{13}C{^{1}H}-NMR 9.6.8

^{1}H-NMR and ^{13}C{^{1}H}-NMR 6.23
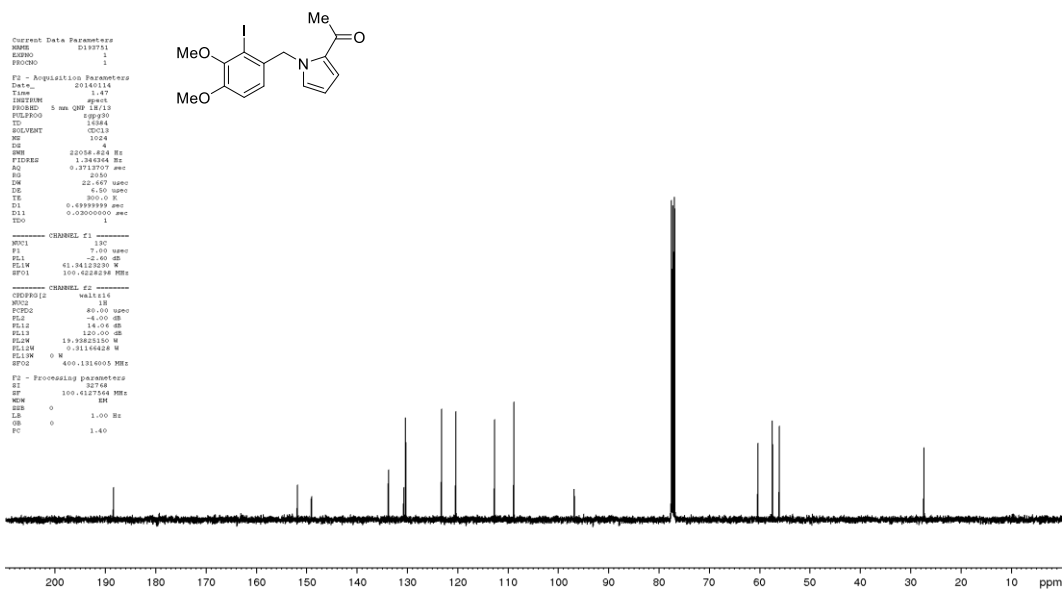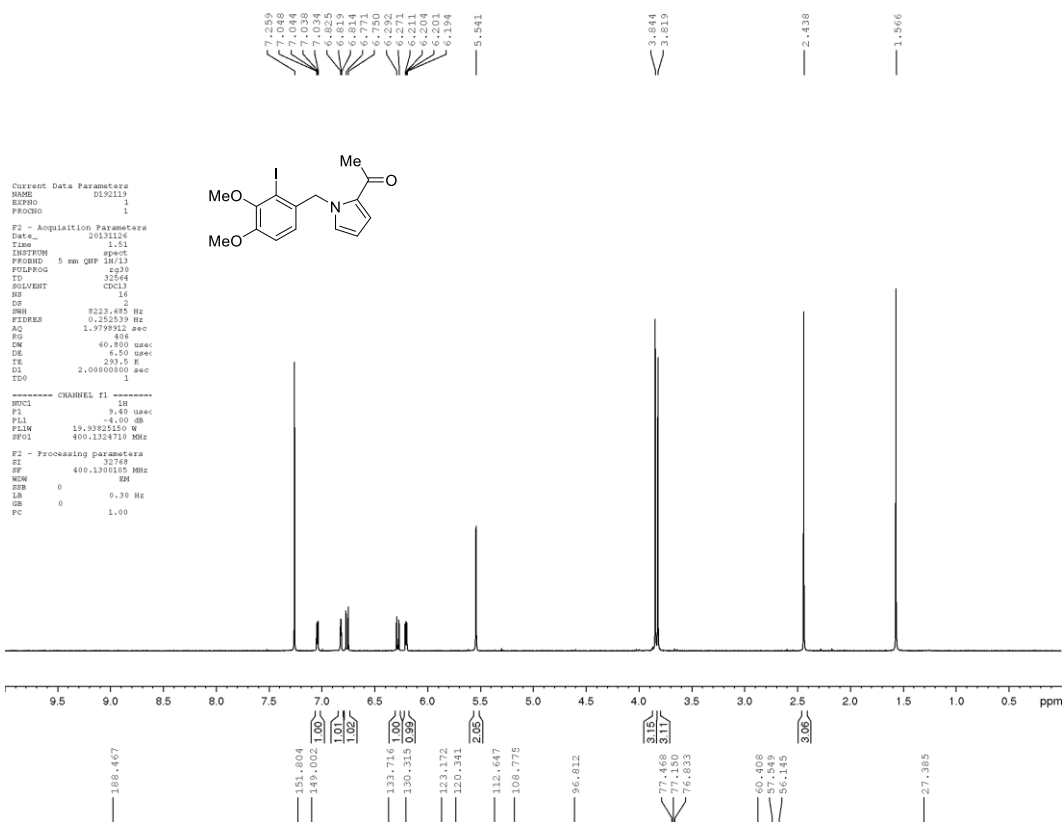
^{1}H-NMR and ^{13}C{^{1}H}-NMR 6.24
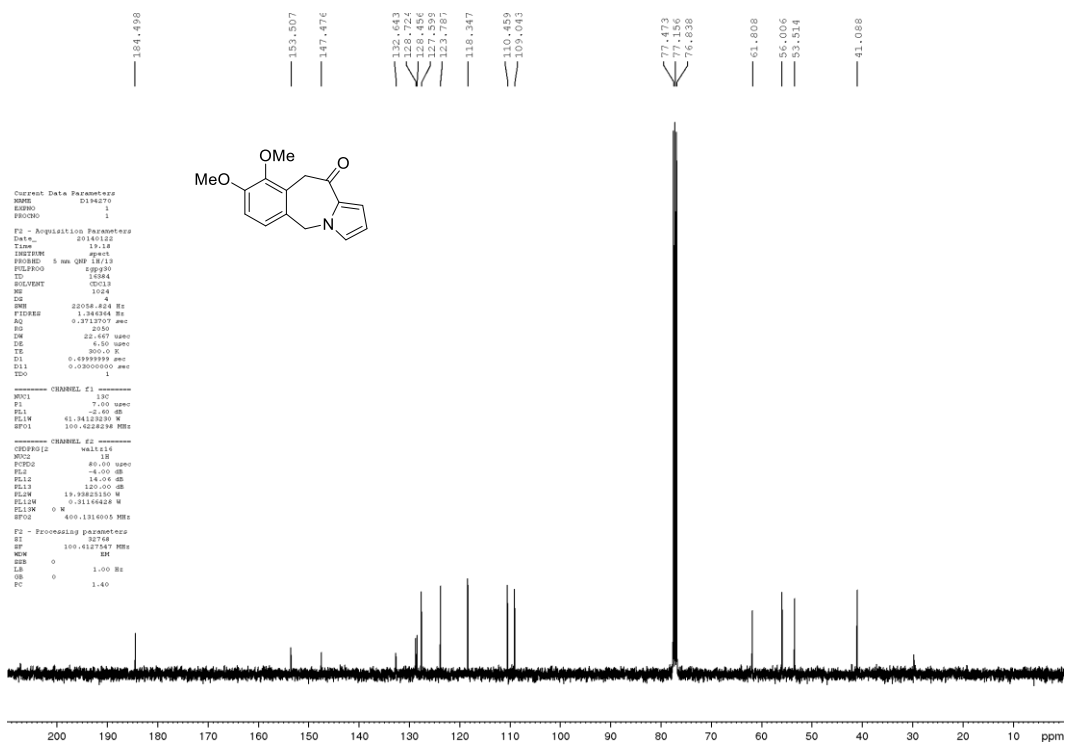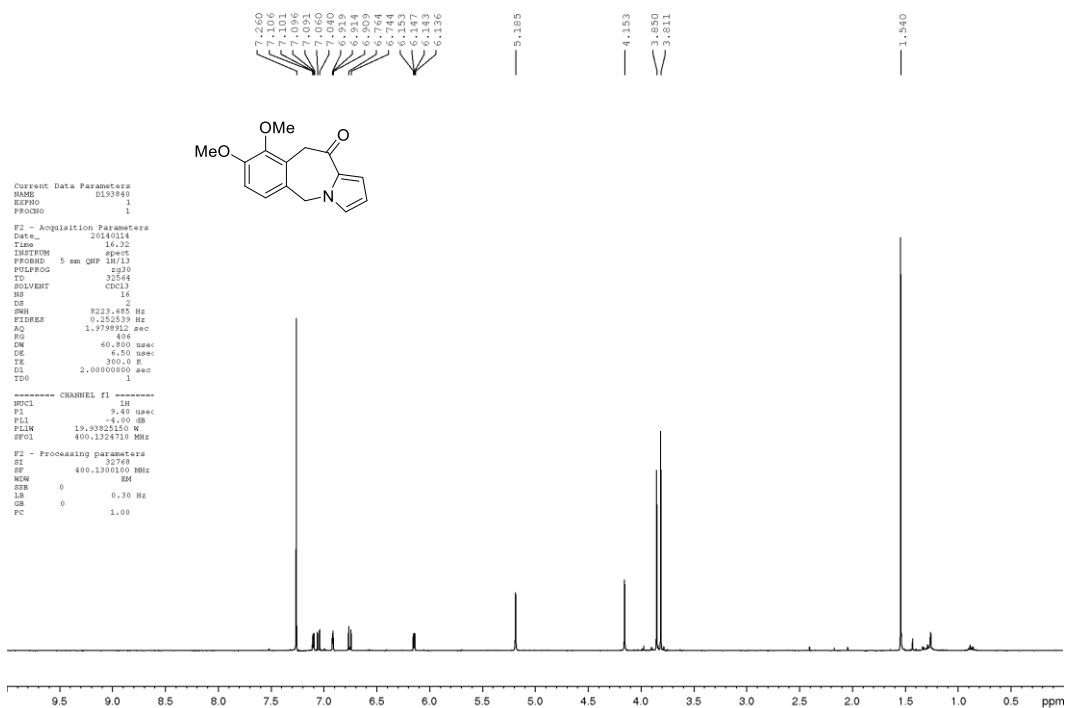
^{1}H-NMR and ^{13}C{^{1}H}-NMR 6.25
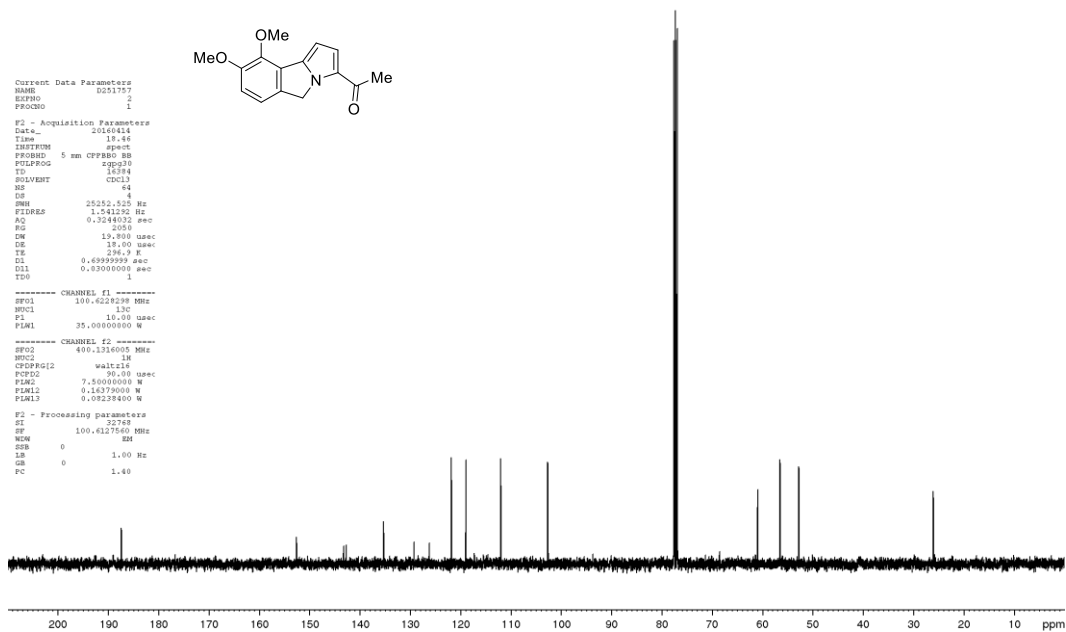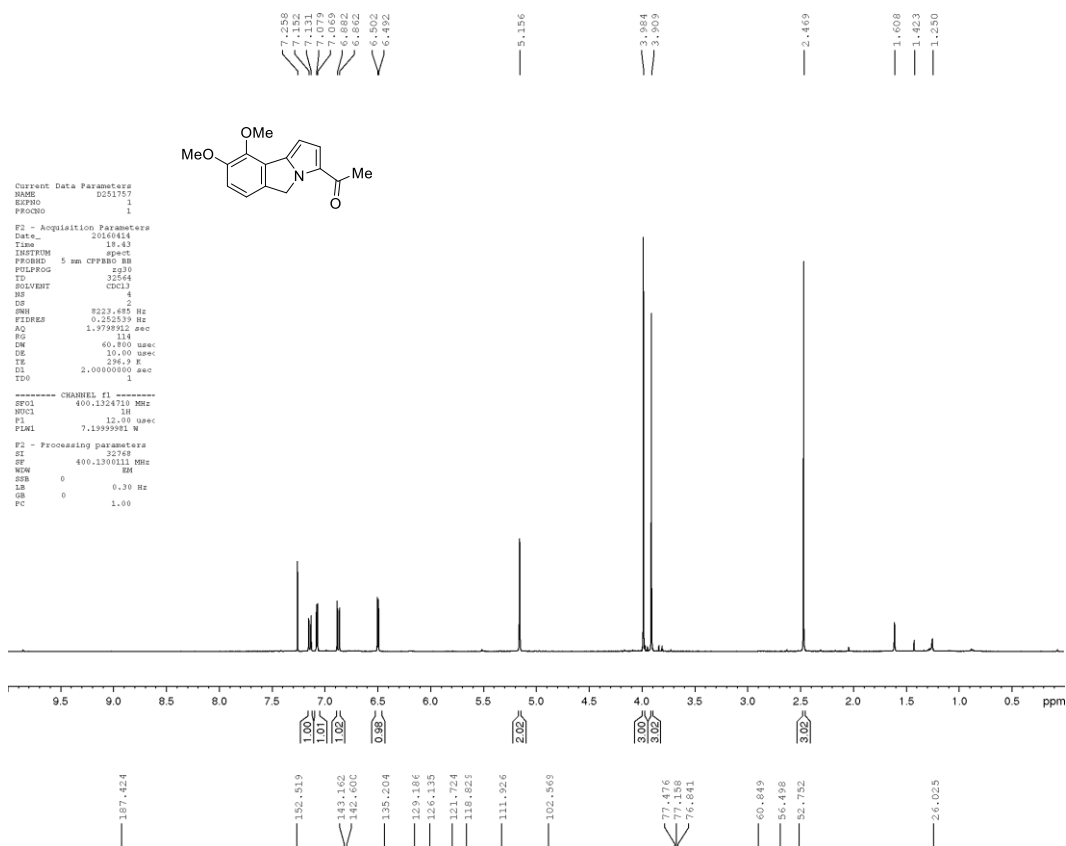
^{1}H-NMR and ^{13}C{^{1}H}-NMR 6.37b
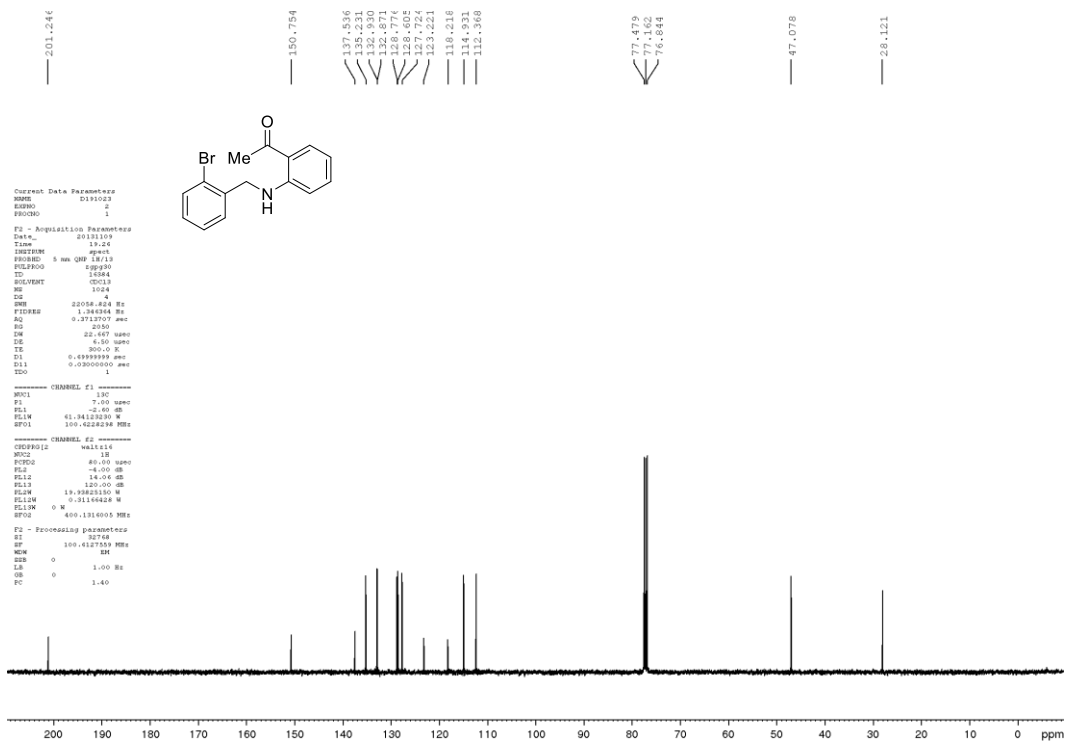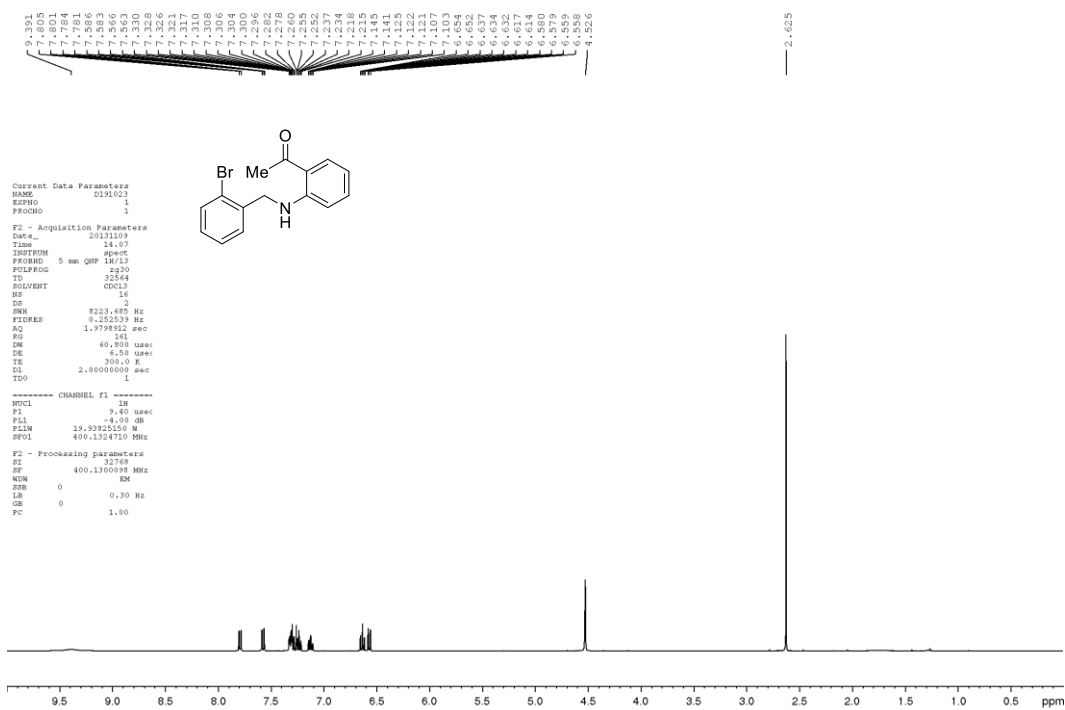
^{1}H-NMR and ^{13}C{^{1}H}-NMR 6.40

^{1}H-NMR and ^{13}C{^{1}H}-NMR 6.73
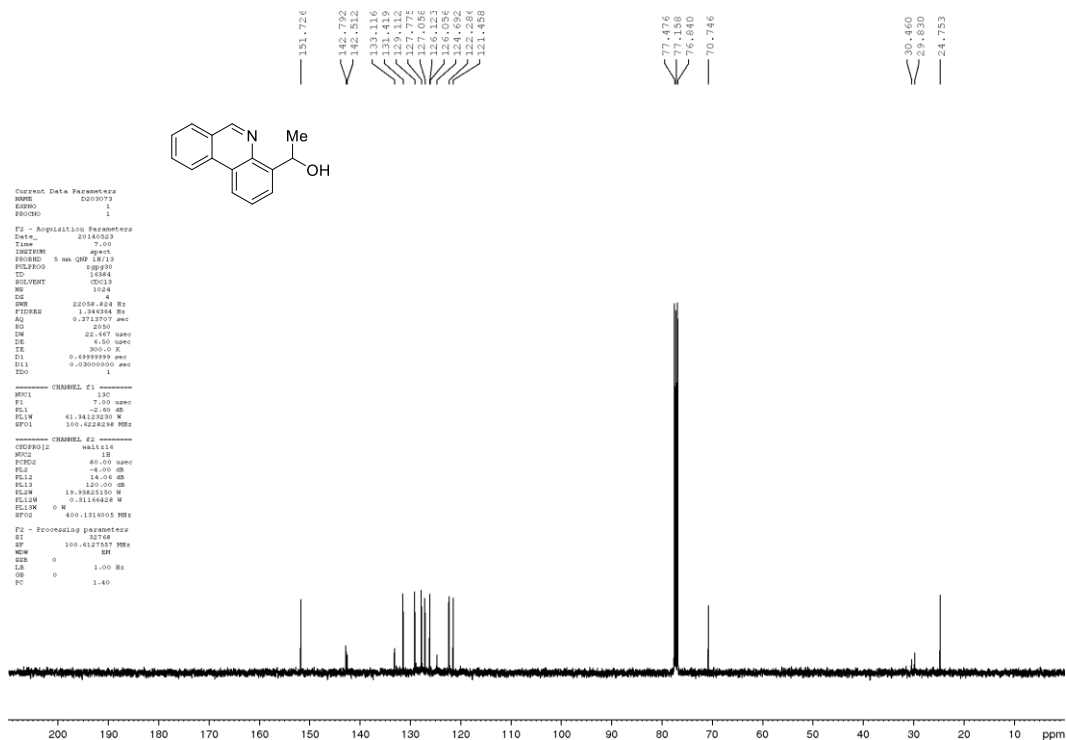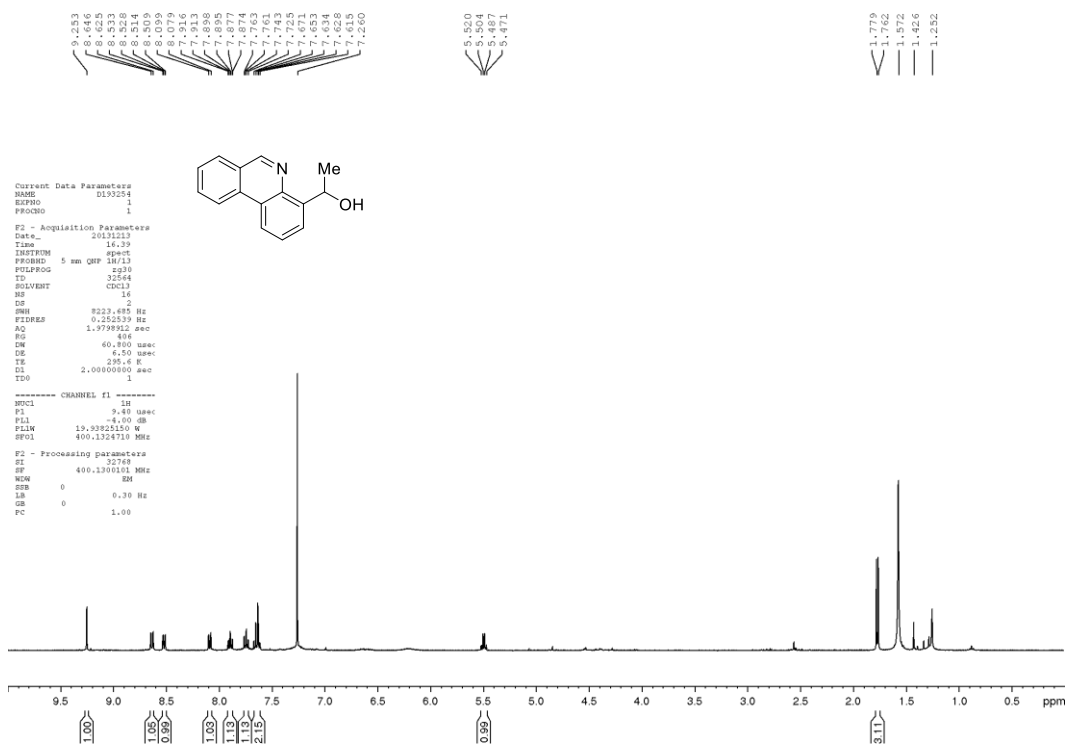
9.5 Experimental details for Chapter 7

9.5.1 Electron transfer reactions using glucose as the additive (Table 7.1)

Table 7.1, entry 1

7.6   **7.6** 79%   **7.7** 3%
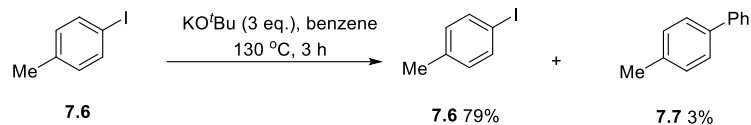
4-Iodotoluene **7.6** (109 mg, 0.5 mmol) was added an oven-dried pressure tube. In the glove box, KO^{t}Bu (168 mg, 1.5 mmol, 3.0 eq.) and anhydrous benzene (5 mL) were added and the reaction mixture was stirred at 130 °C for 3 h. The reaction mixture was cooled to RT, quenched with aqueous hydrochloric acid (1 M, 10 mL) and extracted with ethyl acetate (3 x 10 mL). The organic phases were combined, dried over Na$_2$SO$_4$, filtered and concentrated *in vacuo*. The yields of 4-iodotoluene **7.6** (79%) and 4-methylbiphenyl **7.7** (3%) were determined by adding 1,3,5-trimethoxybenzene to the crude mixture as an internal standard for ^{1}H-NMR. The products were identified by the following characteristic signals; ^{1}H-NMR (400 MHz, CDCl$_3$) δ 2.30 (3 H, s), 6.92 (2 H, d, *J* = 8.4 Hz) for 4-iodotoluene **7.6**; δ 2.40 (3 H, s), 7.43 (2 H, t, *J* = 7.6 Hz) for 4-methylbiphenyl **7.7**. These signals are consistent with the literature values and reference samples (Section 9.3.6, Table 5.2, entry 1 on pages 214-215).

Table 7.1, entry 2

7.6   **7.6** 52%   **7.7** 34%
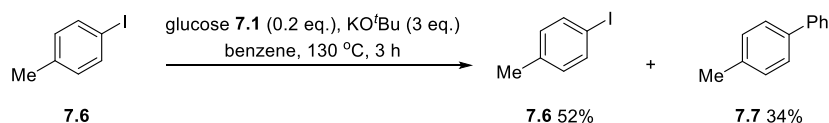
4-Iodotoluene **7.6** (109 mg, 0.5 mmol) and glucose **7.1** (18 mg, 0.1 mmol, 0.2 eq.) were added to an oven-dried pressure tube. In the glove box, KO^{t}Bu (168 mg, 1.5 mmol, 3.0 eq.) and anhydrous benzene (5 mL) were added and the reaction mixture was stirred at 130 °C for 3 h. The reaction mixture was cooled to RT, quenched with aqueous hydrochloric acid (1 M, 10 mL) and extracted with ethyl acetate (3 x 10 mL). The organic phases were combined, dried over Na$_2$SO$_4$, filtered and concentrated *in vacuo*. The yields of 4-iodotoluene **7.6** (52%) and 4-methylbiphenyl **7.7** (34%) were determined by adding 1,3,5-trimethoxybenzene to the crude mixture as an internal standard for ^{1}H-NMR. The products were identified by the following

characteristic signals; ^{1}H-NMR (400 MHz, CDCl$_3$) δ 2.30 (3 H, s), 6.92 (2 H, d, J = 8.4 Hz) for 4-iodotoluene **7.6**; δ 2.40 (3 H, s), 7.43 (2 H, t, J = 7.6 Hz) for 4-methylbiphenyl **7.7**. These signals are consistent with the literature values and reference samples (Section 9.3.6, Table 5.2, entry 1 on pages 214-215).

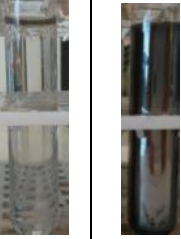### 9.5.2 Preparation of Tollens' reagent

AgNO$_3$ (250 mg, 1.5 mmol) and water (2.5 mL) were added to a test tube. Aqueous NH$_4$OH (28% NH$_3$) was added dropwise until the reaction mixture became a brown suspension, followed by further dropwise addition of aqueous NH$_4$OH (28% NH$_3$) until the reaction mixture became a colourless solution. Aqueous NaOH (2 M) was added dropwise until the reaction mixture became a black suspension. Aqueous NH$_4$OH (28% NH$_3$) was added dropwise until the reaction mixture became a colourless solution of Tollens' reagent, which was used immediately.

9.5.3 Qualitative testing of the reduction of Tollens' reagent (Scheme 7.3)

The general procedure for the Tollens' test was applied to various substrates and the observations are reported in Table 9.5.1. No work-up procedure was performed.

Table 9.5.1 The compounds used in the qualitative Tollens' test (Scheme 7.3)

Compound	Observation at 25 °C	Observation at 70 °C	Compound	Observation at 25 °C	Observation at 70 °C
None	No change	No change	**7.37**	Partial Mirror	Silver Mirror
7.1	Silver Mirror	Silver Mirror	**7.38**	Partial Mirror	Silver Mirror
7.23	Silver Mirror	Silver Mirror	**7.39**	Partial Mirror	Silver Mirror
7.24	Silver Mirror	Silver Mirror	**7.40**	Partial Mirror	Silver Mirror
7.25	Silver Mirror	Silver Mirror	**7.41**	Partial Mirror	Silver Mirror
7.26	Silver Mirror	Silver Mirror	**7.42**	Partial Mirror	Silver Mirror
7.27	Silver Mirror	Silver Mirror	**7.43**	Partial Mirror	Silver Mirror
7.28	Silver Mirror	Silver Mirror	**7.44**	Partial Mirror	Silver Mirror
7.29	Silver Mirror	Silver Mirror	**7.45**	No change	Partial Mirror
7.30	Silver Mirror	Silver Mirror	**7.46**	No change	Partial Mirror
7.31	Silver Mirror	Silver Mirror	**7.47**	No change	Partial Mirror
7.32	Partial Mirror	Silver Mirror	**7.48**	No change	Partial Mirror
7.33	Partial Mirror	Silver Mirror	**7.49**	No change	Partial Mirror
7.34	Partial Mirror	Silver Mirror	**7.50**	No change	Partial Mirror
7.35	Partial Mirror	Silver Mirror	**7.51**	No change	Partial Mirror
7.36	Partial Mirror	Silver Mirror			

RT	70 °C	
	--	**Silver mirror at room temperature**
		Partial silver mirror at room temperature; silver mirror at 70 °C
		No change at room temperature; partial silver mirror at 70 °C

9.5.4 General procedure for the Tollens' test

For every substrate subjected to the Tollens' test, a blank reaction (with no substrate) and a reference reaction (using glucose as the substrate) were performed simultaneously. The Tollens' reagent for all three reactions (blank, glucose and substrate) were prepared identically and simultaneously.

<u>Blank reaction:</u>

Water (2 mL) was added to the test tube containing Tollens' reagent. Observations were reported at RT. The reaction mixture was heated to 70 °C for 5 min using a water bath, and once the reaction had cooled to RT, observations were reported.

<u>Glucose/substrate reaction:</u>

A solution or suspension of the substrate (1.5 mmol, 1.0 eq.) in water (2 mL) was added to the test tube containing Tollens' reagent. Observations were reported at RT. The reaction mixture was heated to 70 °C for 5 min using a water bath, and once the reaction had cooled to RT, observations were reported.

<u>Work-up procedure:</u>

Upon completion, the reaction mixture was extracted with ethyl acetate (3 x 5 mL). The organic phases were combined, dried over Na$_2$SO$_4$, filtered and concentrated *in vacuo* to give the "Basic Fraction". The aqueous phase was acidified with dropwise addition of aqueous hydrochloric acid (2 M). The aqueous phase was extracted with ethyl acetate (3 x 5 mL) and the organic phases were combined, dried over Na$_2$SO$_4$, filtered and concentrated *in vacuo* to give the "Acidic Fraction".

9.5.5 Tollens' test on various aldehydes (Scheme 7.5)

Tollens' test on 3-phenylpropanal 7.44
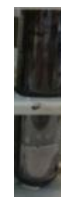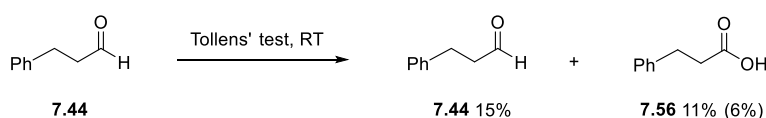
The general procedure for the Tollens' test was applied to 3-phenylpropanal **7.44** (201 mg, 1.5 mmol). At RT a partial mirror was observed. The reaction was not heated to 70 °C. The work-up procedure was performed.

<u>The Basic Fraction</u>: The yield of 3-phenylpropanal **7.44**[211] (15%) was determined by adding 1,3,5-trimethoxybenzene to the crude mixture as an internal standard for ^{1}H-NMR. ^{1}H-NMR (400 MHz, CDCl$_3$) δ 2.79 (2 H, t, *J* = 8.0 Hz, C*H*$_2$), 2.97 (2 H, t, *J* = 8.0 Hz, C*H*$_2$), 7.19 – 7.23 (3 H, m, Ar*H*), 7.30 (2 H, t, *J* = 8.0 Hz, Ar*H*), 9.83 (1 H, t, *J* = 1.6 Hz, C*H*O); ^{13}C{^{1}H}-NMR (100 MHz, CDCl$_3$) δ 28.3 (CH$_2$), 45.4 (CH$_2$), 126.5 (CH), 128.4 (2 x CH), 128.8 (2 x CH), 140.5 (C), 201.7 (C). These signals are consistent with a commercial sample. (Many unidentified products were present in the fraction).

<u>The Acidic Fraction</u>: The yield of 3-phenylpropanoic acid **7.56**[212] (11%) was determined by adding 1,3,5-trimethoxybenzene to the crude mixture as an internal

standard for ^{1}H-NMR. The product was identified by the following characteristic signals; ^{1}H-NMR (400 MHz, CDCl$_3$) δ 2.70 (2 H, t, J = 8.0 Hz), 2.98 (2 H, t, J = 8.0 Hz) for 3-phenylpropanoic acid **7.56**. The crude material was purified by column chromatography (50 - 100% dichloromethane in hexane) to give 3-phenylpropanoic acid **7.56**[212] (12.6 mg, 6%) as colourless crystals m.p. 44 - 45 °C (lit.[212]: 44 - 45 °C); [Found: (GCMS-EI) C$_9$H$_{10}$O$_2$ (M)$^{•+}$ 149.9]; v$_{max}$ (film)/cm^{-1} 3028, 2931, 2622, 1694, 1408, 1302, 1220, 931, 757, 703; ^{1}H-NMR (400 MHz, CDCl$_3$) δ 2.70 (2 H, t, J = 8.0 Hz, CH_2), 2.97 (2 H, t, J = 8.0 Hz, CH_2), 7.21 – 7.24 (3 H, m, ArH), 7.29 – 7.32 (2 H, m, ArH), 10.00 (1 H, br s, COOH); ^{13}C{^{1}H}-NMR (100 MHz, CDCl$_3$) δ 30.7 (CH$_2$), 35.7 (CH$_2$), 126.5 (CH), 128.4 (2 x CH), 128.7 (2 x CH), 140.3 (C), 179.1 (C).
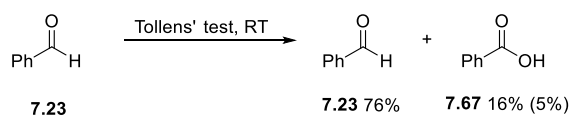
Tollens' test on benzaldehyde 7.23

The general procedure for the Tollens' test was applied to benzaldehyde **7.23** (159 mg, 1.5 mmol). At RT a partial mirror was observed. The reaction was not heated to 70 °C. The work-up procedure was performed.

The Basic Fraction: The yield of benzaldehyde **7.23**[213] (76%) was determined by adding 1,3,5-trimethoxybenzene to the crude mixture as an internal standard for ^{1}H-NMR. ^{1}H-NMR (400 MHz, CDCl$_3$) δ 7.54 (2 H, t, J = 8.0 Hz, ArH), 7.64 (1 H, t, J = 8.0 Hz, ArH), 7.89 (2 H, d, J = 8.0 Hz, ArH), 10.03 (1 H, br s, CHO); ^{13}C{^{1}H}-NMR (100 MHz, CDCl$_3$) δ 129.2 (2 x CH), 129.9 (2 x CH), 134.6 (CH), 136.6 (C), 192.5 (C). These signals are consistent with a commercial sample.

The Acidic Fraction: The yield of benzoic acid **7.67**[214] (16%) was determined by adding 1,3,5-trimethoxybenzene to the crude mixture as an internal standard for ^{1}H-NMR. The product was identified by the following characteristic signals; ^{1}H-NMR (400 MHz, CDCl$_3$) δ 7.49 (2 H, t, J = 8.0 Hz), 7.62 (1 H, t, J = 8.0 Hz), 8.13 (2 H, d, J = 8.0 Hz) for benzoic acid **7.67**. The crude material was purified by column chromatography (50 - 100% dichloromethane in hexane) to give benzoic acid **7.67** (10 mg, 5%) as a white crystals m.p. 119 - 120 °C (lit.[215]: 118 – 120.4 °C); [Found:

(GCMS-EI) $C_7H_6O_2$ (M)$^{\bullet+}$ 122.0]; ν_{max} (film)/cm^{-1} 3068, 2825, 2661, 2551, 1679, 1601, 1582, 1464, 1419, 1324, 1290, 1181, 933, 807, 706, 669; ^{1}H-NMR (400 MHz, CDCl$_3$) δ 7.49 (2 H, t, *J* = 8.0 Hz, Ar*H*), 7.62 (1 H, t, *J* = 8.0 Hz, Ar*H*), 8.13 (2 H, dd, *J* = 7.6, 1.2 Hz, Ar*H*); ^{13}C{^{1}H}-NMR (100 MHz, CDCl$_3$) δ 128.6 (CH), 129.4 (C), 130.4 (CH), 134.0 (CH), 172.3 (C).

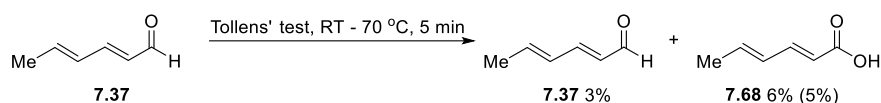## Tollens' test on (2E,4E)-hexa-2,4-dienal 7.37[216]

The general procedure for the Tollens' test was applied to (2E,4E)-hexa-2,4-dienal **7.37** (144 mg, 1.5 mmol). At RT a partial mirror was observed. After heating at 70 °C a silver mirror was observed. The work-up procedure was performed.

The Basic Fraction: The yield of (2E,4E)-hexa-2,4-dienal **7.37**[217] (3%) was determined by adding 1,3,5-trimethoxybenzene to the crude mixture as an internal standard for ^{1}H-NMR. ^{1}H-NMR (400 MHz, CDCl$_3$) δ 1.90 (3 H, d, *J* = 4.0 Hz, C*H$_3$*), 6.06 (1 H, dd, *J* = 16.0, 8.0 Hz, C*H*), 6.25 – 6.37 (2 H, m, 2 x C*H*), 7.07 (1 H, dd, *J* = 16.0, 8.0 Hz, C*H*), 9.53 (1 H, d, *J* = 8.0 Hz, C*H*O); ^{13}C{^{1}H}-NMR (100 MHz, CDCl$_3$) δ 19.0 (CH$_3$), 130.0 (CH), 130.3 (CH), 142.0 (CH), 152.8 (CH), 190.1 (C). These signals are consistent with a commercial sample.

The Acidic Fraction: The yield of (2E,4E)-hexa-2,4-dienoic acid **7.68**[216] (6%) was determined by adding 1,3,5-trimethoxybenzene to the crude mixture as an internal standard for ^{1}H-NMR. The product was identified by the following characteristic signals; ^{1}H-NMR (400 MHz, CDCl$_3$) δ 1.78 (3 H, d, *J* = 5.2 Hz), 5.77 (1 H, d, *J* = 16.0 Hz), 6.16 – 6.26 (2 H, m), 7.33 (1 H, dd, *J* = 16.0, 8.0 Hz) for (2*E*,4*E*)-hexa-2,4-dienoic acid **7.68**.[216] The crude material was purified by column chromatography (50 - 100% dichloromethane in hexane) to give (2*E*,4*E*)-hexa-2,4-dienoic acid **7.68** (8.7 mg, 5%) as a white crystals m.p. 130 – 132 °C (lit.[218]: 133 – 136 °C); [Found: (GCMS-EI) $C_6H_8O_2$ (M)$^{\bullet+}$ 112.0.]; ν_{max} (film)/cm^{-1} 2918, 1676, 1635, 1610, 1414, 1376, 1326, 1262, 1203, 1153, 995, 947, 916, 872, 804; ^{1}H-NMR (400 MHz, CDCl$_3$) δ 1.88 (3 H, d, *J* = 5.2 Hz, C*H$_3$*), 5.77 (1 H, d, *J* = 16.0 Hz, C*H*), 6.16 – 6.26 (2 H, m, 2 x

C*H*), 7.33 (1 H, dd, *J* = 16.0, 8.0 Hz, C*H*); ^{13}C{^{1}H}-NMR (100 MHz, CDCl$_3$) δ 18.9 (CH$_3$), 118.3 (CH), 129.9 (CH), 140.9 (CH), 147.5 (CH), 172.8 (C).

9.5.6 Tollens' test on 3-phenylpropanol under several conditions (Table 7.2)

Table 7.2, entry 1

The general procedure for the Tollens' test was applied to 3-phenylpropanal **7.44** (201 mg, 1.5 mmol). At RT a partial mirror was observed. The reaction was not heated to 70 °C. The work-up procedure was performed.
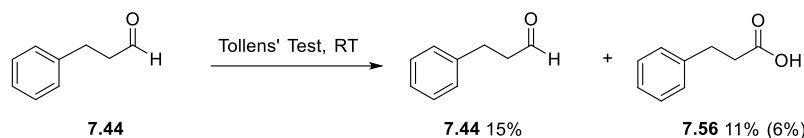
The Basic Fraction: The yield of 3-phenylpropanal **7.44**[211] (15%) was determined by adding 1,3,5-trimethoxybenzene to the crude mixture as an internal standard for ^{1}H-NMR. The product was identified by the following characteristic signals; ^{1}H-NMR (400 MHz, CDCl$_3$) δ 2.79 (2 H, t, *J* = 7.6 Hz), 2.97 (2 H, t, *J* = 7.6 Hz), 7.18 – 7.30 (5 H, m), 9.83 (1 H, br s) for 3-phenylpropanal **7.44**. These signals are consistent with the literature values and reference sample (Section 9.5.5 on page 298). (Many unidentified products were present in the fraction).

The Acidic Fraction: The yield of 3-phenylpropanoic acid **7.56**[212] (11%) was determined by adding 1,3,5-trimethoxybenzene to the crude mixture as an internal standard for ^{1}H-NMR. The product was identified by the following characteristic signals; ^{1}H-NMR (400 MHz, CDCl$_3$) δ 2.70 (2 H, t, *J* = 8.0 Hz), 2.98 (2 H, t, *J* = 8.0 Hz) for 3-phenylpropanoic acid **7.56**. These signals are consistent with the literature values and reference samples (reported in Section 9.5.5 on page 298). The crude material was purified by column chromatography (50 - 100% dichloromethane in hexane) to give 3-phenylpropanoic acid **7.56**[212] (12.6 mg, 6%) as colourless crystals.

Table 7.2, entry 2
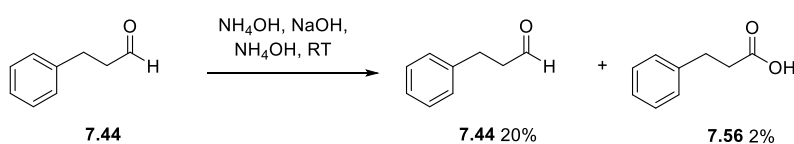
Water (2.5 mL) was added to a test tube. Aqueous NH$_4$OH (28% NH$_3$) was added dropwise until the reaction mixture became a brown suspension, followed by further

dropwise addition of aqueous NH$_4$OH (28% NH$_3$) until the reaction mixture became a colourless solution. Aqueous NaOH (2 M) was added dropwise until the reaction mixture became a black suspension, followed by further dropwise addition of aqueous NH$_4$OH (28% NH$_3$) until the reaction mixture became a colourless solution. The solution was used immediately. A suspension of 3-phenylpropanal **7.44** (201 mg, 1.5 mmol, 1.0 eq.) in water (2 mL) was added to the test tube. At RT a cloudy white suspension was observed. After heating at 70 °C a cloudy white suspension was observed. The work-up procedure was performed.

The Basic Fraction: The yield of 3-phenylpropanal **7.44**[211] (20%) was determined by adding 1,3,5-trimethoxybenzene to the crude mixture as an internal standard for ^{1}H-NMR. The product was identified by the following characteristic signals; ^{1}H-NMR (400 MHz, CDCl$_3$) δ 2.79 (2 H, t, *J* = 7.6 Hz), 2.97 (2 H, t, *J* = 7.6 Hz), 7.18 – 7.30 (5 H, m), 9.83 (1 H, br s) for 3-phenylpropanal **7.44**. These signals are consistent with the literature values and reference sample (Section 9.5.5 on page 298). (Many unidentified products were present in the fraction).

The Acidic Fraction: The yield of 3-phenylpropanoic acid **7.56**[212] (2%) was determined by adding 1,3,5-trimethoxybenzene to the crude mixture as an internal standard for ^{1}H-NMR. The product was identified by the following characteristic signals; ^{1}H-NMR (400 MHz, CDCl$_3$) δ 2.70 (2 H, t, *J* = 8.0 Hz), 2.98 (2 H, t, *J* = 8.0 Hz) for 3-phenylpropanoic acid **7.56**. These signals are consistent with the literature values and reference sample (Section 9.5.5 on page 298).
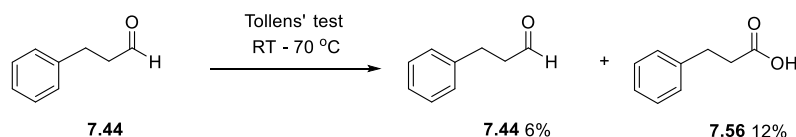
Table 7.2, entry 3

The general procedure for the Tollens' test was applied to 3-phenylpropanal **7.44** (201 mg, 1.5 mmol). At RT a partial mirror was observed. After heating at 70 °C a silver mirror was observed. The work-up procedure was performed.

The Basic Fraction: The yield of 3-phenylpropanal **7.44**[211] (6%) was determined by adding 1,3,5-trimethoxybenzene to the crude mixture as an internal standard for ^{1}H-NMR. The product was identified by the following characteristic signals; ^{1}H-NMR

(400 MHz, CDCl$_3$) δ 2.79 (2 H, t, J = 7.6 Hz), 2.97 (2 H, t, J = 7.6 Hz), 7.18 – 7.30 (5 H, m), 9.83 (1 H, br s) for 3-phenylpropanal **7.44**. These signals are consistent with the literature values and reference sample (Section 9.5.5 on page 298). (Many unidentified products were present in the fraction).

The Acidic Fraction: The yield of 3-phenylpropanoic acid **7.56**[212] (12%) was determined by adding 1,3,5-trimethoxybenzene to the crude mixture as an internal standard for ^{1}H-NMR. The product was identified by the following characteristic signals; ^{1}H-NMR (400 MHz, CDCl$_3$) δ 2.70 (2 H, t, J = 8.0 Hz), 2.98 (2 H, t, J = 8.0 Hz) for 3-phenylpropanoic acid **7.56**. These signals are consistent with the literature values and reference sample (Section 9.5.5 on page 298).

Table 7.2, entry 4

7.44   **7.44** 92%
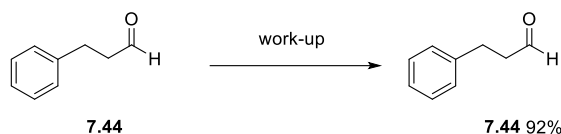
Water (2.5 mL) was added to a test tube, followed by the addition of a suspension of 3-phenylpropanal **7.44** (201 mg, 1.5 mmol) in water (2 mL). At RT a colourless solution was observed. The work-up procedure was performed.

The Basic Fraction: The yield of 3-phenylpropanal **7.44**[211] (92%) was determined by adding 1,3,5-trimethoxybenzene to the crude mixture as an internal standard for ^{1}H-NMR. The product was identified by the following characteristic signals; ^{1}H-NMR (400 MHz, CDCl$_3$) δ 2.79 (2 H, t, J = 7.6 Hz), 2.97 (2 H, t, J = 7.6 Hz), 7.18 – 7.30 (5 H, m), 9.83 (1 H, br s) for 3-phenylpropanal **7.44**. These signals are consistent with the literature values and reference samples (Section 9.5.5 on page 298). (Many unidentified products were present in the fraction).

The Acidic Fraction: No 3-phenylpropanoic acid **7.56** was observed.

9.5.7 Synthesis of tertiary α-hydroxy ketones

The compounds **7.50**, **7.40**, **7.39** and **7.38** were supplied commercially.

<div align="center">

Synthesis of 7.76[219-220]
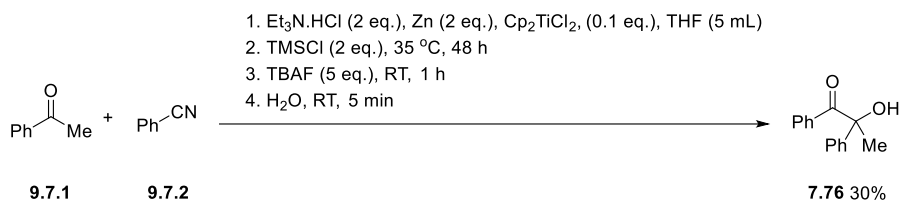
</div>

Et₃N.HCl (1.37 g, 10 mmol, 2.0 eq.), zinc powder (654 mg, 10 mmol, 2.0 eq.) and Cp₂TiCl₂ (125 mg, 0.5 mmol, 0.1 eq.) were added to an oven-dried pressure tube. In the glovebox, anhydrous, degassed tetrahydrofuran (5 mL) was added. The reaction mixture was stirred at RT for 1 min (the colour of the reaction mixture changed from a red to green). A suba-seal was placed on the pressure tube and it was removed from the glove box. Under an argon atmosphere, benzonitrile **9.7.2** (2.6 mL, 25 mmol, 5.0 eq.) was added (the colour of the reaction mixture changed from green to purple). Acetophenone **9.7.1** (0.6 mL, 5 mmol) was added, followed by the dropwise addition of TMSCl (1.3 mL, 10 mmol, 2.0 eq.). The reaction mixture was stirred at 35 °C for 48 h. The reaction mixture was cooled to RT. TBAF (1 M in tetrahydrofuran, 5 mL) was added, and the reaction mixture was stirred at RT for 1 h. Water (5 mL) was added, and the reaction mixture was stirred at RT for 5 min. The reaction mixture was extracted with dichloromethane (4 x 80 mL). The organic phases were combined, washed with brine, dried over Na₂SO₄, filtered and concentrated *in vacuo*. The crude material was purified by column chromatography (40 - 70% dichloromethane in hexane) to give 2-hydroxy-1,2-diphenylpropan-1-one **7.76**[220] (335 mg, 30%) as yellow crystals m.p. 59 - 61 °C (lit.[221]: 60 – 62 °C); [Found: (GCMS-EI) $C_{15}H_{14}O_2$ (M) $^{\bullet +}$ 226.1]; v_{max} (film)/cm⁻¹ 3433, 3061, 2994, 2923, 1666, 1595, 1446, 1227, 1741, 1151, 1075, 987, 755, 697, 684; ¹H-NMR (400 MHz, CDCl₃) δ 1.90 (3 H, s, C*H₃*), 4.72 (1 H, br s, O*H*), 7.28 – 7.35 (3 H, m, Ar*H*), 7.39 (2 H, t, *J* = 8.0 Hz, Ar*H*), 7.43 – 7.47 (3 H, m, Ar*H*), 7.68 (2 H, d, *J* = 8.0 Ar*H*); ¹³C{¹H}-NMR (100 MHz, CDCl₃) δ 26.2 (CH₃), 79.2 (C), 126.1 (2 x CH), 128.3 (CH), 128.4 (2 x CH), 129.1 (2 x CH), 130.3 (2 x CH), 133.1 (CH), 133.6 (C), 142.6 (C), 202.1 (C).

Synthesis of 7.77[219]
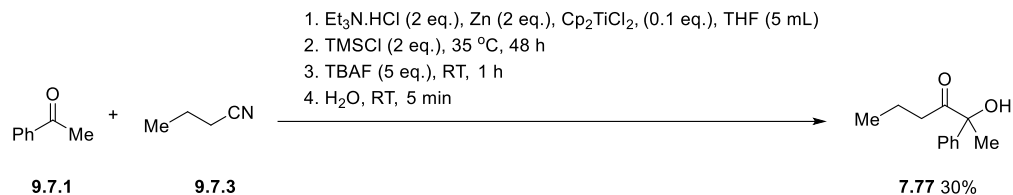
1. Et$_3$N.HCl (2 eq.), Zn (2 eq.), Cp$_2$TiCl$_2$, (0.1 eq.), THF (5 mL)
2. TMSCl (2 eq.), 35 °C, 48 h
3. TBAF (5 eq.), RT, 1 h
4. H$_2$O, RT, 5 min

9.7.1   **9.7.3**   **7.77** 30%
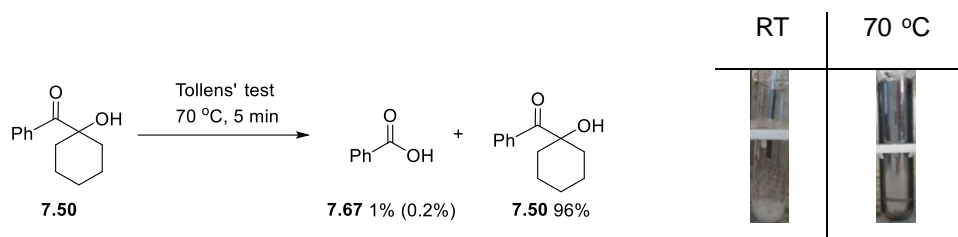
Et$_3$N.HCl (1.37 g, 10 mmol, 2.0 eq.), zinc powder (654 mg, 10 mmol, 2.0 eq.) and Cp$_2$TiCl$_2$ (125 mg, 0.5 mmol, 0.1 eq.) were added to an oven-dried pressure tube. In the glovebox, anhydrous, degassed tetrahydrofuran (5 mL) was added. The reaction mixture was stirred at RT for 1 min (the colour of the reaction mixture changed from a red to green). A suba-seal was placed on the pressure tube and it was removed from the glove box. Under an argon atmosphere, butyronitrile **9.7.3** (2.18 mL, 25 mmol, 5.0 eq.) was added (the colour of the reaction mixture changed from green to blue). Acetophenone **9.7.1** (0.6 mL, 5 mmol, 1.0 eq.) was added, followed by the dropwise addition of TMSCl (1.3 mL, 10 mmol, 2.0 eq.). The reaction mixture was stirred at 35 °C for 48 h. The reaction mixture was cooled to RT. TBAF (1 M in tetrahydrofuran, 5 mL) was added, and the reaction mixture was stirred at RT for 1 h. Water (5 mL) was added, and the reaction mixture was stirred at RT for 5 min. The reaction mixture was extracted with dichloromethane (4 x 80 mL). The organic phases were combined, washed with brine, dried over Na$_2$SO$_4$, filtered and concentrated *in vacuo*. The crude material was purified by column chromatography (40 - 100% dichloromethane in hexane) to give 2-hydroxy-2-phenylhexan-3-one **7.77**[219] (289 mg, 30%) as a yellow oil [Found: (GCMS-EI) C$_{12}$H$_{17}$O$_2$$^+$ (M+H)$^+$ 193.0]; v$_{max}$ (film)/cm^{-1} 3463, 2931, 2960, 1703, 1447, 1354, 1129, 1026, 760, 701; ^{1}H-NMR (400 MHz, CDCl$_3$) δ 0.75 (3 H, t, J = 8.0 Hz, CH_3), 1.42 – 1.59 (2 H, m, CH_2), 1.77 (3 H, s, CH_3), 2.24 – 2.32 (1 H, m, CH_2), 2.38 – 2.46 (1 H, m, CH_2), 4.62 (1 H, br s, OH), 7.27 – 7.32 (1 H, m, ArH), 7.39 (2 H, t, J = 8.0 Hz, ArH), 7.43 (2 H, d, J = 8.0 Hz, ArH); ^{13}C{^{1}H}-NMR (100 MHz, CDCl$_3$) δ 13.6 (CH$_3$), 17.5 (CH$_2$), 24.1 (CH$_3$), 37.6 (CH$_2$), 79.8 (C), 126.2 (2 x CH), 128.1 (CH), 128.7 (2 x CH), 141.6 (C), 212.0 (C).

9.5.8 Reactions of α-hydroxy ketones and α-diketones (Schemes 7.7 and 7.9)

Tollens' test on (1-hydroxycyclohexyl)(phenyl)methanone 7.50

The general procedure for the Tollens' test was applied to (1-hydroxycyclohexyl)(phenyl)methanone **7.50** (306 mg, 1.5 mmol). At RT a white suspension was observed. After heating at 70 °C a partial mirror was observed. This was repeated four times. The five reaction mixtures were combined and the work-up procedure was performed.

The Basic Fraction: The yield of (1-hydroxycyclohexyl)(phenyl)methanone **7.50**[220] (96%) was determined by adding 1,3,5-trimethoxybenzene to the crude mixture as an internal standard for ^{1}H-NMR. ^{1}H-NMR (400 MHz, CDCl$_3$) δ 1.30 – 1.41 (1 H, m, CH_2), 1.64 – 1.83 (7 H, m CH_2), 2.01 – 2.08 (2 H, m, CH_2), 7.44 (2 H, t, J = 8.0 Hz, ArH), 7.54 (1 H, t, J = 8.0 Hz, ArH), 8.00 (2 H, d, J = 8.0 Hz, ArH); ^{13}C{^{1}H}-NMR (100 MHz, CDCl$_3$) δ 21.6 (2 x CH$_2$), 25.5 (CH$_2$), 35.5 (2 x CH$_2$), 78.8 (C), 128.4 (2 x CH), 129.6 (2 x CH), 132.5 (CH), 135.3 (C), 205.7 (C). These signals are consistent with a commercial sample.

The Acidic Fraction: The yield of benzoic acid **7.67**[214] (1%) was determined by adding 1,3,5-trimethoxybenzene to the crude mixture as an internal standard for ^{1}H-NMR. The product was identified by the following characteristic signals; ^{1}H-NMR (400 MHz, CDCl$_3$) δ 7.49 (2 H, t, J = 8.0 Hz), 7.62 (1 H, t, J = 8.0 Hz), 8.13 (2 H, d, J = 8.0 Hz) for benzoic acid **7.67**. These signals are consistent with the literature values and reference samples (Section 9.5.5 on page 299). The crude material was purified by column chromatography (50 - 100% dichloromethane in hexane) to give benzoic acid **7.67**[214] (2.7 mg, 0.2%) as a white crystals.

Tollens' test on 2-hydroxy-1,2-diphenylethan-1-one 7.40

The general procedure for the Tollens' test was applied to 2-hydroxy-1,2-diphenylethan-1-one **7.40** (318 mg, 1.5 mmol). At RT a grey suspension was observed. After heating at 70 °C a partial mirror was observed. The work-up procedure was performed.

The Basic Fraction: The yield of 2-hydroxy-1,2-diphenylethan-1-one **7.40**[222] (94%) was determined by adding 1,3,5-trimethoxybenzene to the crude mixture as an internal standard for ^{1}H-NMR. ^{1}H-NMR (400 MHz, CDCl$_3$) δ 4.54 (1 H, d, J = 8.0 Hz, CH), 5.95 (1 H, d, J = 8.0 Hz, OH), 7.25 – 7.35 (5 H, m, ArH), 7.40 (2 H, t, J = 8.0 Hz, ArH), 7.52 (1 H, t, J = 8.0 Hz, ArH), 7.92 (2 H, d, J = 8.0 Hz, ArH); ^{13}C{^{1}H}-NMR (100 MHz, CDCl$_3$) δ 76.4 (CH), 127.9 (2 x CH), 128.7 (CH), 128.8 (2 x CH), 129.3 (4 x CH), 133.7 (C), 134.1 (CH), 139.2 (C), 199.1 (C). These signals are consistent with a commercial sample.
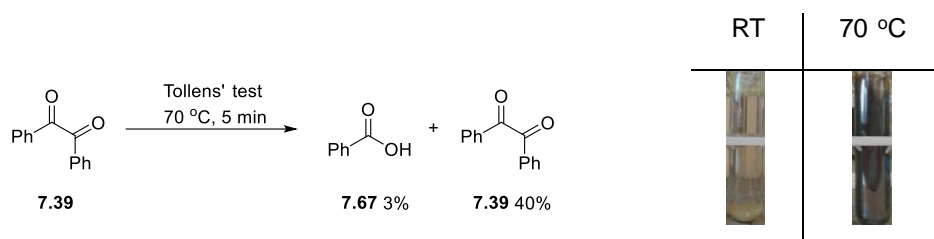
The Acidic Fraction: The yield of benzoic acid **7.67**[214] (4%) was determined by adding 1,3,5-trimethoxybenzene to the crude mixture as an internal standard for ^{1}H-NMR. The product was identified by the following characteristic signals; ^{1}H-NMR (400 MHz, CDCl$_3$) δ 7.49 (2 H, t, J = 8.0 Hz), 7.62 (1 H, t, J = 8.0 Hz), 8.13 (2 H, d, J = 8.0 Hz) for benzoic acid **7.67**. These signals are consistent with the literature values and reference samples (Section 9.5.5 on page 299). The crude material was purified by column chromatography (0 - 100% dichloromethane in hexane) to give benzoic acid **7.67**[214] (4.4 mg, 2%) as a white crystals.

Tollens' test on benzil 7.39

The general procedure for the Tollens' test was applied to benzil **7.39** (315 mg, 1.5 mmol). At RT a grey/yellow suspension was observed. After heating at 70 °C a partial mirror was observed. The work-up procedure was performed.

<u>The Basic Fraction</u>: The yield of benzil **7.39**[223] (40%) was determined by adding 1,3,5-trimethoxybenzene to the crude mixture as an internal standard for ^{1}H-NMR. ^{1}H-NMR (400 MHz, CDCl$_3$) δ 7.52 (4 H, t, J = 8.0 Hz, ArH), 7.66 (2 H, t, J = 8.0 Hz, ArH), 7.98 (4 H, d, J = 8.0 Hz, ArH); ^{13}C{^{1}H}-NMR (100 MHz, CDCl$_3$) δ 129.2 (4 x CH), 130.1 (4 x CH), 133.2 (2 x C), 135.0 (2 x CH), 194.7 (2 x C). These signals are consistent with a commercial sample.
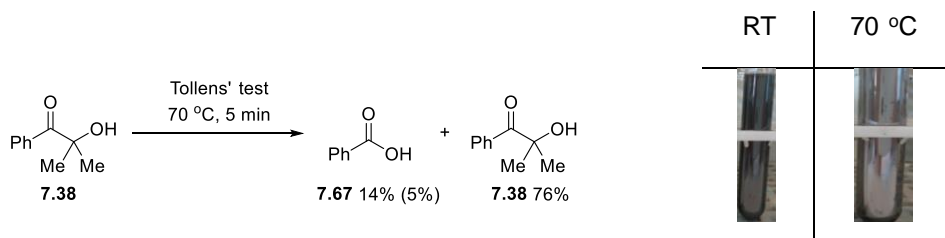
<u>The Acidic Fraction</u>: The yield of benzoic acid **7.67**[214] (3%) was determined by adding 1,3,5-trimethoxybenzene to the crude mixture as an internal standard for ^{1}H-NMR. The product was identified by the following characteristic signals; ^{1}H-NMR (400 MHz, CDCl$_3$) δ 7.49 (2 H, t, J = 8.0 Hz), 7.62 (1 H, t, J = 8.0 Hz), 8.13 (2 H, d, J = 8.0 Hz) for benzoic acid **7.67**. These signals are consistent with the literature values and reference sample (Section 9.5.5 on page 299).

Tollens' test on 2-hydroxy-2-methyl-1-phenylpropan-1-one 7.38

The general procedure for the Tollens' test was applied to 2-hydroxy-2-methyl-1-phenylpropan-1-one **7.38** (204 mg, 1.25 mmol). At RT a partial mirror was observed. After heating at 70 °C a partial mirror was observed. The work-up procedure was performed.

The Basic Fraction: The yield of 2-hydroxy-2-methyl-1-phenylpropan-1-one **7.38**[220] (76%) was determined by adding 1,3,5-trimethoxybenzene to the crude mixture as an internal standard for ^{1}H-NMR. ^{1}H-NMR (400 MHz, CDCl$_3$) δ 1.64 (6 H, s, 2 x C*H$_3$*), 4.06 (1 H, br s, O*H*), 7.47 (2 H, t, *J* = 8.0 Hz, Ar*H*), 7.57 (1 H, t, *J* = 8.0 Hz, Ar*H*), 8.00 (2 H, d, *J* = 8.0 Hz, Ar*H*); ^{13}C{^{1}H}-NMR (100 MHz, CDCl$_3$) δ 28.6 (2 x CH$_3$), 76.4 (C), 128.6 (2 x CH), 129.8 (2 x CH), 133.1 (CH), 133.9 (C), 204.9 (C). These signals are consistent with a commercial sample.

The Acidic Fraction: The yield of benzoic acid **7.67**[214] (14%) was determined by adding 1,3,5-trimethoxybenzene to the crude mixture as an internal standard for ^{1}H-NMR. The product was identified by the following characteristic signals; ^{1}H-NMR (400 MHz, CDCl$_3$) δ 7.49 (2 H, t, *J* = 8.0 Hz), 7.62 (1 H, t, *J* = 8.0 Hz), 8.13 (2 H, d, *J* = 8.0 Hz) for benzoic acid **7.67**. These signals are consistent with the literature values and ref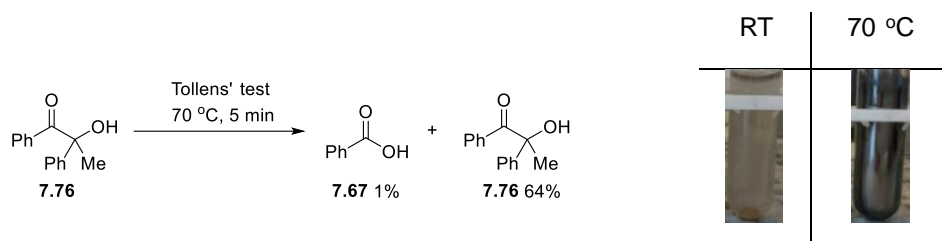erence samples (Section 9.5.5 on page 299). The crude material was purified by column chromatography (0 - 100% dichloromethane in hexane) to give benzoic acid **7.67**[214] (7.7 mg, 5%) as white crystals.

Tollens' test on 2-hydroxy-2-methyl-1-phenylpropan-1-one 7.76

The general procedure for the Tollens' test was applied to 2-hydroxy-2-methyl-1-phenylpropan-1-one **7.76** (226 mg, 1.0 mmol). At RT a grey/brown solution was observed. After heating at 70 °C a partial mirror was observed. The work-up procedure was performed.

The Basic Fraction: The yield of 2-hydroxy-2-methyl-1-phenylpropan-1-one **7.76**[220] (64%) was determined by adding 1,3,5-trimethoxybenzene to the crude mixture as an internal standard for ^{1}H-NMR. The product was identified by the following characteristic signals; ^{1}H-NMR (400 MHz, CDCl$_3$) δ 1.90 (3 H, s), 4.72 (1 H, br s), 7.28 – 7.35 (3 H, m), 7.39 (2 H, t, *J* = 8.0 Hz), 7.43 – 7.47 (3 H, m), 7.68 (2 H, d, *J* = 8.0, 4.0 Hz) for 2-hydroxy-2-methyl-1-phenylpropan-1-one **7.76**. These signals are

consistent with the literature values and reference sample (Section 9.5.7 on pages 303-304).

<u>The Acidic Fraction</u>: The yield of benzoic acid **7.67**[214] (1%) was determined by adding 1,3,5-trimethoxybenzene to the crude mixture as an internal standard for ^{1}H-NMR. The product was identified by the following characteristic signals; ^{1}H-NMR (400 MHz, CDCl$_3$) δ 7.49 (2 H, t, *J* = 8.0 Hz), 7.62 (1 H, t, *J* = 8.0 Hz), 8.13 (2 H, d, *J* = 8.0 Hz) for benzoic acid **7.67**. These signals are consistent with the literature values and reference sample (Section 9.5.5 on page 299).

Tollens' test on 2-hydroxy-2-phenylhexan-3-one 7.77
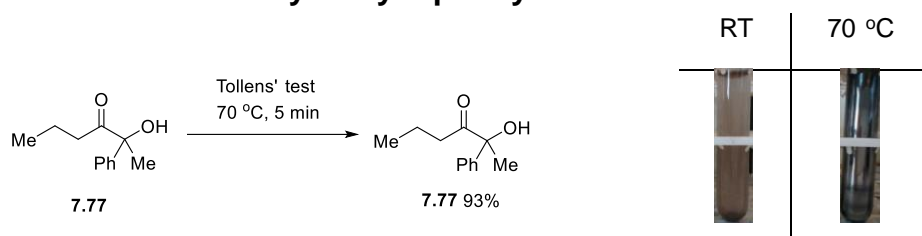

The general procedure for the Tollens' test was applied to 2-hydroxy-2-phenylhexan-3-one **7.77** (192 mg, 1.0 mmol). At RT a brown emulsion was observed. After heating at 70 °C a partial mirror was observed. The work-up procedure was performed.

<u>The Basic Fraction</u>: The yield of 2-hydroxy-2-phenylhexan-3-one **7.77**[219] (93%) was determined by adding 1,3,5-trimethoxybenzene to the crude mixture as an internal standard for ^{1}H-NMR. The product was identified by the following characteristic signals; ^{1}H-NMR (400 MHz, CDCl$_3$) δ 0.75 (3 H, t, *J* = 8.0 Hz), 1.42 – 1.59 (2 H, m), 1.77 (3 H, s), 2.24 – 2.33 (1 H, m), 2.38 – 2.45 (1 H, m), 4.62 (1 H, br s), 7.27 – 7.31 (1 H, m), 7.39 (2 H, t, *J* = 8.0 Hz), 7.43 (2 H, d, *J* = 8.0 Hz) for 2-hydroxy-2-phenylhexan-3-one **7.77**. These signals are consistent with the literature values and reference samples (Section 9.5.7 on pages 304-305).

<u>The Acidic Fraction</u>: No oxidised products were observed.

9.5.9 Effect of NaOH on the oxidation of 7.38 in the Tollens' test (Scheme 7.9)

Scheme 7.9A

2-Hydroxy-2-methyl-1-phenylpropan-1-one **7.38** (246 mg, 1.5 mmol) and water (2 mL) were added to a test tube, and the reaction mixture was stirred at RT for 15 min. $AgNO_3$ (250 mg, 1.5 mmol) and water (2.5 mL) were added to a second test tube, and aqueous NH_4OH (28% NH_3) was added dropwise until the reaction mixture became a brown suspension, followed by further dropwise addition of aqueous NH_4OH (28% NH_3) until the reaction mixture became a colourless solution. The solution was used immediately. The reaction mixture from the first test tube was added to this solution. At RT a cloudy emulsion was observed. After heating at 70 °C a silver mirror was observed. The work-up procedure was performed.

The Basic Fraction: The yield of 2-hydroxy-2-methyl-1-phenylpropan-1-one **7.38**[220] (83%) was determined by adding 1,3,5-trimethoxybenzene to the crude mixture as an internal standard for ^{1}H-NMR. The product was identified by the following characteristic signals; ^{1}H-NMR (400 MHz, $CDCl_3$) δ 1.64 (6 H, s), 3.77 (1 H, br s), 7.47 (2 H, t, J = 8.0 Hz), 7.57 (1 H, t, J = 8.0 Hz), 8.02 (2 H, d, J = 8.0 Hz) for 2-hydroxy-2-methyl-1-phenylpropan-1-one **7.38**. These signals are consistent with the literature values and reference sample (Section 9.5.8 on page 308).

The Acidic Fraction: The yield of benzoic acid **7.67**[214] (1%) was determined by adding 1,3,5-trimethoxybenzene to the crude mixture as an internal standard for ^{1}H-NMR. The product was identified by the following characteristic signals; ^{1}H-NMR (400 MHz, $CDCl_3$) δ 7.49 (2 H, t, J = 7.6 Hz), 7.62 (1 H, t, J = 15.6 Hz), 8.13 (2 H, dd, J = 7.6, 1.2 Hz) for benzoic acid **7.67**. These signals are consistent with the literature values and reference sample (Section 9.5.5 on page 299).

Scheme 7.9B

2-Hydroxy-2-methyl-1-phenylpropan-1-one **7.38** (246 mg, 1.5 mmol), NaOH (60 mg, 1.5 mmol) and water (2 mL) were added to a test tube, and the reaction mixture was stirred at RT for 15 min. AgNO$_3$ (250 mg, 1.5 mmol) and water (2.5 mL) were added to a second test tube, and aqueous NH$_4$OH (28% NH$_3$) was added dropwise until the reaction mixture became a brown suspension, followed by further dropwise addition of aqueous NH$_4$OH (28% NH$_3$) until the reaction mixture became a colourless solution. The solution was used immediately. The reaction mixture from the first test tube was added to this solution. At RT a partial mirror was observed. After heating at 70 °C a silver mirror was observed. The work-up procedure was performed.

The Basic Fraction: The yield of 2-hydroxy-2-methyl-1-phenylpropan-1-one **7.38**[220] (62%) was determined by adding 1,3,5-trimethoxybenzene to the crude mixture as an internal standard for ^{1}H-NMR. The product was identified by the following characteristic signals; ^{1}H-NMR (400 MHz, CDCl$_3$) δ 1.64 (6 H, s), 3.77 (1 H, br s), 7.47 (2 H, t, $J = 8.0$ Hz), 7.57 (1 H, t, $J = 8.0$ Hz), 8.02 (2 H, d, $J = 8.0$ Hz) for 2-hydroxy-2-methyl-1-phenylpropan-1-one **7.38**. These signals are consistent with the literature values and reference sample (Section 9.5.8 on page 308).

The Acidic Fraction: The yield of benzoic acid **7.67**[214] (20%) was determined by adding 1,3,5-trimethoxybenzene to the crude mixture as an internal standard for ^{1}H-NMR. The product was identified by the following characteristic signals; ^{1}H-NMR (400 MHz, CDCl$_3$) δ 7.49 (2 H, t, $J = 7.6$ Hz), 7.62 (1 H, t, $J = 15.6$ Hz), 8.13 (2 H, d, $J = 7.6$ Hz) for benzoic acid **7.67**. These signals are consistent with the literature values and reference sample (Section 9.5.5 on page 299).
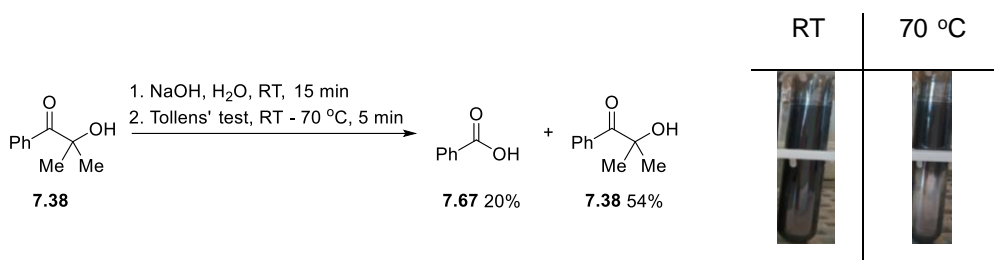
Scheme 7.9C

2-Hydroxy-2-methyl-1-phenylpropan-1-one **7.38** (246 mg, 1.5 mmol), NaOH (60 mg, 1.5 mmol) and water (2 mL) were added to a test tube. The reaction mixture was stirred at RT for 15 min. The Tollens' reagent was prepared in a second test tube and used immediately. The reaction mixture from the first test tube was added to this solution. At RT a partial mirror was observed. After heating at 70 °C a partial mirror was observed. The work-up procedure was performed.

The Basic Fraction: The yield of 2-hydroxy-2-methyl-1-phenylpropan-1-one **7.38**[220] (54%) was determined by adding 1,3,5-trimethoxybenzene to the crude mixture as an internal standard for ^{1}H-NMR. The product was identified by the following characteristic signals; ^{1}H-NMR (400 MHz, CDCl$_3$) δ 1.64 (6 H, s), 3.77 (1 H, br s), 7.47 (2 H, t, J = 8.0 Hz), 7.57 (1 H, t, J = 8.0 Hz), 8.02 (2 H, d, J = 8.0 Hz) for 2-hydroxy-2-methyl-1-phenylpropan-1-one **7.38**. These signals are consistent with the literature values and reference sample (Section 9.5.8 on page 308).

The Acidic Fraction: The yield of benzoic acid **7.67**[214] (20%) was determined by adding 1,3,5-trimethoxybenzene to the crude mixture as an internal standard for ^{1}H-NMR. The product was identified by the following characteristic signals; ^{1}H-NMR (400 MHz, CDCl$_3$) δ 7.49 (2 H, t, J = 7.6 Hz), 7.62 (1 H, t, J = 15.6 Hz), 8.13 (2 H, dd, J = 7.6, 1.2 Hz) for benzoic acid **7.67**. These signals are consistent with the literature values and reference sample (Section 9.5.5 on page 299).
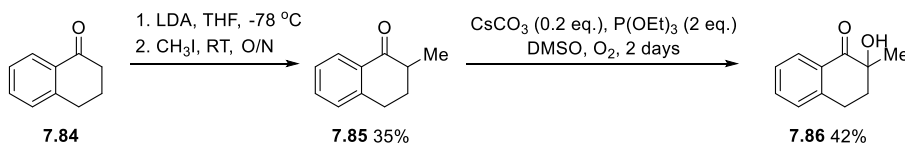
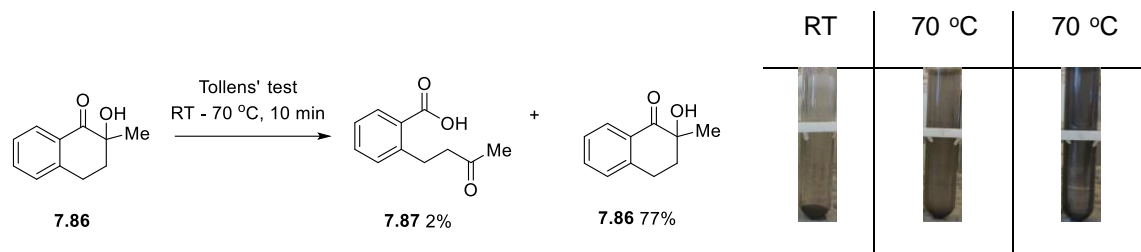### 9.5.10 Synthesis and reaction of substrate 7.86

Anhydrous tetrahydrofuran (50 mL) was added to a flame-dried round-bottomed flask. Under an argon atmosphere, at -78 °C, LDA (1.8 M, 9.2 mL, 16.5 mmol, 1.1

eq.) was added, and the reaction mixture was stirred at -78 °C for 15 min. α-Tetralone **7.84** (2 mL, 15 mmol) was added and the reaction mixture was stirred at -78 °C for 20 min. Methyl iodide (1.0 mL, 16.5 mmol, 1.1 eq.) was added and the reaction mixture was stirred at RT overnight. The reaction mixture was quenched with saturated aqueous ammonium chloride solution (50 mL) and extracted with diethyl ether (3 x 50 mL). The organic phases were combined and dried over Na_2SO_4, filtered and concentrated *in vacuo*. The crude material was purified by column chromatography (0 - 2% ethyl acetate in hexane) to give 2-methyl-3,4-dihydronaphthalen-1(2H)-one **7.85**[224-225] (846 mg, 35%) as pale yellow oil [Found: (GCMS-EI) $C_{11}H_{12}O$ (M)$^{\bullet+}$ 160.2]; v_{max} (film)/cm^{-1} 2960, 2930, 2859, 1679, 1601, 1465, 1269, 1225, 969, 738; ^{1}H-NMR (400 MHz, $CDCl_3$) δ 1.27 (3 H, d, *J* = 8.0 Hz, C*H₃*), 1.83 – 1.94 (1 H, m, C*H₂*), 2.17 – 2.23 (1 H, m, C*H₂*), 2.55 – 2.64 (1 H, m, C*H₂*), 2.94 – 3.07 (2 H, m, C*H₂* and C*H*), 7.23 (1 H, d, *J* = 8.0 Hz, Ar*H*), 7.29 (1 H, t, *J* = 8.0 Hz, Ar*H*), 7.45 (1 H, t, *J* = 8.0 Hz, Ar*H*), 8.03 (1 H, d, *J* = 8.0 Hz, Ar*H*); ^{13}C{^{1}H}-NMR (100 MHz, $CDCl_3$) δ 15.6 (CH_3), 29.0 (CH_2), 31.5 (CH_2), 42.8 (CH), 126.7 (CH), 127.5 (CH), 128.8 (CH), 132.5 (C), 133.2 (CH), 144.3 (C), 200.9 (C).

Cs_2CO_3 (345 mg, 1 mmol, 0.2 eq.), triethylphosphite (1.82 mL, 10.6 mmol, 2.0 eq.), 2-methyl-3,4-dihydronaphthalen-1(2H)-one **7.85** (846 mg, 5.3 mmol) and DMSO (20 mL) were added to a flame-dried round-bottomed flask, equipped with a vacuum tap. Oxygen was bubbled through the reaction mixture for 10 min, and under an oxygen atmosphere, the reaction was stirred at RT for 2 days. The reaction mixture was diluted with ethyl acetate (50 mL) and washed with water (5 x 50 mL). The organic phase was dried over Na_2SO_4, filtered and concentrated *in vacuo*. The crude material was purified by column chromatography (0 - 50% ethyl acetate in hexane) to give 2-hydroxy-2-methyl-3,4-dihydronaphthalen-1(2H)-one **7.86**[220] (396 mg, 42%) as a colourless oil [Found: (GCMS-EI) $C_{11}H_{11}O_2^-$ (M-H)$^-$ 175.0]; v_{max} (film)/cm^{-1} 3469, 2970, 2931, 2862, 1681, 1601, 1456, 1370, 1289, 1222, 1155, 1097, 972, 907, 740; ^{1}H-NMR (400 MHz, $CDCl_3$) δ 1.40 (3 H, s, C*H₃*), 2.18 – 2.30 (2 H, m, C*H₂*), 3.00 – 3.15 (2 H, m, C*H₂*), 3.83 (1 H, br s, O*H*), 7.25 – 7.27 (1 H, m, Ar*H*), 7.35 (1 H, t, *J* = 8.0 Hz, Ar*H*), 7.53 (1 H, t, *J* = 8.0 Hz, Ar*H*), 8.04 (1 H, d, *J* = 8.0 Hz, Ar*H*); ^{13}C{^{1}H}-

NMR (100 MHz, CDCl$_3$) δ 24.0 (CH$_3$), 26.9 (CH$_2$), 36.0 (CH$_2$), 73.7 (C), 127.0 (CH), 128.2 (CH), 129.1 (CH), 130.1 (C), 134.2 (CH), 143.6 (C), 201.9 (C).

Tollens' test of 2-hydroxy-2-methyl-3,4-dihydronaphthalen-1(2H)-one 7.86 (Scheme 7.10)

The general procedure for the Tollens' test was applied 2-hydroxy-2-methyl-3,4-dihydronaphthalen-1(2H)-one **7.86** (264 mg, 1.5 mmol). At RT a grey precipitate was observed. After heating at 70 °C a grey suspension was observed. After heating at 70 °C, a second time, a partial mirror was observed. The work-up procedure was performed.

The Basic Fraction: The yield of 2-hydroxy-2-methyl-3,4-dihydronaphthalen-1(2H)-one **7.86** (77%) was determined by adding 1,3,5-trimethoxybenzene to the crude mixture as an internal standard for ^{1}H-NMR. The product was identified by the following characteristic signals; ^{1}H-NMR (400 MHz, CDCl$_3$) δ 1.40 (3 H, s), 2.18 – 2.30 (2 H, m), 3.00 – 3.15 (2 H, m), 3.84 (1 H, br s), 7.25 – 7.27 (1 H, m), 7.35 (1 H, t, *J* = 8.0 Hz), 7.53 (1 H, t, *J* = 8.0 Hz), 8.04 (1 H, d, *J* = 8.0 Hz) for 2-hydroxy-2-methyl-3,4-dihydronaphthalen-1(2H)-one **7.86**. These signals are consistent with the literature values and reference sample (Section 9.5.10 on pages 313-314).

The Acidic Fraction: The crude material was purified by column chromatography (50 - 100% dichloromethane in hexane) to give 2-(3-oxobutyl)benzoic acid **7.87** (6.5 mg, 2%) as a white crystals m.p. 106 – 107 °C (lit.[226]: 105 °C); [Found: (HRMS-NSI) 191.0717. C$_{11}$H$_{11}$O$_3^-$ (M-H)$^-$ requires 191.0714]; v$_{max}$ (film)/cm^{-1} 2916, 2847, 2641, 2516, 1688, 1575, 1489, 1408, 1305, 1262, 1162, 930, 755, 705, 664; ^{1}H-NMR (400 MHz, CDCl$_3$) δ 2.16 (3 H, s, C*H$_3$*), 2.83 (2 H, t, *J* = 7.6 Hz, C*H$_2$*), 3.26 (2 H, t, *J* = 7.6 Hz, C*H$_2$*), 7.29 – 7.33 (2 H, m, Ar*H*), 7.48 (1 H, t, *J* = 7.6 Hz, Ar*H*), 8.04 (1 H, d, *J* = 8.0, Ar*H*); ^{13}C{^{1}H}-NMR (100 MHz, CDCl$_3$) δ 29.0 (CH$_2$), 30.0 (CH$_3$), 45.4 (CH$_2$),

126.7 (CH), 128.3 (C), 131.5 (CH), 132.0 (CH), 133.3 (CH), 144.0 (C), 171.7 (C), 208.6 (C).

9.5.11 Reactions using Ag/bipy and molecular oxygenation with 7.23 and 7.38

Preparation of the Ag/bipy catalyst[161]

$$AgPF_6 \xrightarrow{\text{2,2'-bipyridine (1 eq.), } CH_2Cl_2, \text{ RT, O/N}} AgPF_6/bipy$$
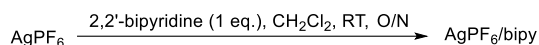
Anhydrous dichloromethane (200 mL) was added to a flame-dried three-necked flask and the reaction mixture was stirred for 3 h with a steady stream of argon bubbling through. $AgPF_6$ (379 mg, 1.5 mmol) and 2,2'-bipyridine (234 mg, 1.5 mmol, 1.0 eq.) were added to a flame-dried three-necked flask, equipped with two vacuum taps. The flask was evacuated and filled with argon 5 times, and anhydrous degassed dichloromethane (45 mL) was added. Under an argon atmosphere, the reaction mixture was stirred at RT for 15 h. The solvent was removed on the house vacuum line and the crude material was dried for 3 h. The crude material was put under an argon atmosphere, and transported into the glove box immediately.

Reaction of the Ag/bipy catalyst and O_2 with benzaldehyde 7.23[161]
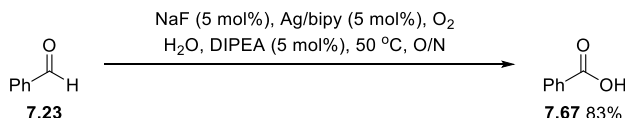
NaF (1.05 mg, 0.025 mmol, 0.05 eq.) was added to an oven-dried pressure tube. In the glove box, Ag/bipy catalyst (6.6 mg, 0.025 mmol, 0.05 eq.) was added. The pressure tube was gently flushed with oxygen for 1 min. A suba-seal was placed on the pressure tube. Water (5 mL) and diisopropylamine (4.5 µL, 0.025 mmol, 0.05 eq.) were added, and the reaction mixture was stirred at 50 °C for 5 min. Benzaldehyde **7.23** (0.05 mL, 0.5 mmol) was added and the reaction was stirred at 50 °C overnight. The reaction mixture was cooled and basified to pH 11 with aqueous NaOH (0.1 M). The reaction mixture was washed with dichloromethane (3 x 15 mL), and the aqueous phase was acidified to pH 2 with aqueous hydrochloric acid solution (0.1 M). The aqueous phase was extracted with diethyl ether (3 x 15 mL). The organic phases were combined, dried over Na_2SO_4, filtered and concentrated *in vacuo*. The yield of benzoic acid **7.67**[214] (83%) was determined by adding 1,3,5-

trimethoxybenzene to the crude mixture as an internal standard for ^{1}H-NMR. The product was identified by the following characteristic signals; ^{1}H-NMR (400 MHz, CDCl$_3$) δ 7.49 (2 H, t, *J* = 7.6 Hz, Ar*H*), 7.62 (1 H, t, *J* = 7.6 Hz, Ar*H*), 8.13 (2 H, d, *J* = 7.6 Hz, Ar*H*) for benzoic acid **7.67**. These signals are consistent with the literature values and reference sample (Section 9.5.5 on page 299).

Reaction of the Ag/bipy catalyst and O₂ with 2-hydroxy-2-methyl-1-phenylpropan-1-one 7.38
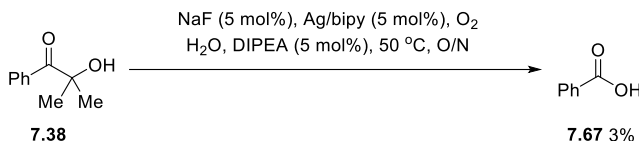
NaF (1.05 mg, 0.025 mmol, 0.05 eq.) was added to an oven-dried pressure tube. In the glove box, Ag/bipy catalyst (6.6 mg, 0.025 mmol, 0.05 eq.) was added. The pressure tube was gently flushed with oxygen for 1 min. A suba-seal was placed on the pressure tube. Water (5 mL) and diisopropylamine (4.5 µL, 0.025 mmol, 0.05 eq.) were added, and the reaction mixture was stirred at 50 °C for 5 min. 2-Hydroxy-2-methyl-1-phenylpropan-1-one **7.38** (82 mg, 0.5 mmol) was added, and the reaction was stirred at 50 °C overnight. The reaction mixture was cooled and basified to pH 11 with aqueous NaOH (0.1 M). The reaction mixture was washed with dichloromethane (3 x 15 mL), and the aqueous phase was acidified to pH 2 with aqueous hydrochloric acid solution (0.1 M). The aqueous phase was extracted with diethyl ether (3 x 15 mL). The organic phases were combined, dried over Na$_2$SO$_4$, filtered and concentrated *in vacuo*. The yield of benzoic acid **7.67**[214] (3%) was determined by adding 1,3,5-trimethoxybenzene to the crude mixture as an internal standard for ^{1}H-NMR. The product was identified by the following characteristic signals; ^{1}H-NMR (400 MHz, CDCl$_3$) δ 7.49 (2 H, t, *J* = 7.6 Hz, Ar*H*), 7.62 (1 H, t, *J* = 7.6 Hz, Ar*H*), 8.13 (2 H, dd, *J* = 7.6, 1.2 Hz, Ar*H*) for benzoic acid **7.67**. These signals are consistent with the literature values and reference sample (Section 9.5.5 on page 299).

9.6 XYZ coordinates of species from computational studies

The XYZ data files for all the species reported throughout the computational discussion are to be found in the Appendix.

References

1. D. Alberico, M. E. Scott, M. Lautens, *Chem. Rev.*, 2007, **107**, 174-238.
2. J. H. Docherty, J. Peng, A. P. Dominey, S. P. Thomas, *Nat. Chem.*, 2017, DOI: 10.1038/nchem.2697.
3. F. Ullmann, J. Bielecki, *Ber. Dtsch Chem. Ges.*, 1901, **34**, 2174-2185.
4. M. Zembayashi, K. Tamao, J.-i. Yoshida, M. Kumada, *Tetrahedron Lett.*, 1977, **18**, 4089-4091.
5. T. T. Tsou, J. K. Kochi, *J. Am. Chem. Soc.*, 1979, **101**, 7547-7560.
6. A. Sekiya, N. Ishikawa, *J. Organomet. Chem.*, 1976, **118**, 349-354.
7. A. Minato, K. Tamao, T. Hayashi, K. Suzuki, M. Kumada, *Tetrahedron Lett.*, 1981, **22**, 5319-5322.
8. J. E. Milne, S. L. Buchwald, *J. Am. Chem. Soc.*, 2004, **126**, 13028-13032.
9. J. K. Stille, *Angew. Chem. Int. Ed.*, 1986, **25**, 508-524.
10. N. Miyaura, T. Yanagi, A. Suzuki, *Synth. Commun.*, 1981, **11**, 513-519.
11. C. C. C. Johansson Seechurn, M. O. Kitching, T. J. Colacot, V. Snieckus, *Angew. Chem. Int. Ed.*, 2012, **51**, 5062-5085.
12. S. Oi, Y. Ogino, S. Fukita, Y. Inoue, *Org. Lett.*, 2002, **4**, 1783-1785.
13. S. Oi, S. Fukita, N. Hirata, N. Watanuki, S. Miyano, Y. Inoue, *Org. Lett.*, 2001, **3**, 2579-2581.
14. F. Kakiuchi, S. Kan, K. Igi, N. Chatani, S. Murai, *J. Am. Chem. Soc.*, 2003, **125**, 1698-1699.
15. R. B. Bedford, M. E. Limmert, *J. Org. Chem.*, 2003, **68**, 8669-8682.
16. S. Oi, S. Fukita, Y. Inoue, *Chem. Commun.*, 1998, 2439-2440.
17. S. Oi, S.-i. Watanabe, S. Fukita, Y. Inoue, *Tetrahedron Lett.*, 2003, **44**, 8665-8668.
18. K.-i. Fujita, M. Nonogawa, R. Yamaguchi, *Chem. Commun.*, 2004, 1926-1927.
19. T. Satoh, Y. Kawamura, M. Miura, M. Nomura, *Angew. Chem. Int. Ed.*, 1997, **36**, 1740-1742.
20. Y. Kametani, T. Satoh, M. Miura, M. Nomura, *Tetrahedron Lett.*, 2000, **41**, 2655-2658.
21. M. Lafrance, K. Fagnou, *J. Am. Chem. Soc.*, 2006, **128**, 16496-16497.
22. M. Tobisu, T. Shimasaki, N. Chatani, *Angew. Chem. Int. Ed.*, 2008, **47**, 4866-4869.
23. S. K. Gurung, S. Thapa, A. Kafle, D. A. Dickie, R. Giri, *Org. Lett.*, 2014, **16**, 1264-1267.
24. N. E. Leadbeater, M. Marco, *Org. Lett.*, 2002, **4**, 2973-2976.
25. N. E. Leadbeater, M. Marco, *Angew. Chem. Int. Ed.*, 2003, **42**, 1407-1409.
26. N. E. Leadbeater, M. Marco, *J. Org. Chem.*, 2003, **68**, 5660-5667.
27. A. H. M. de Vries, J. M. C. A. Mulders, J. H. M. Mommers, H. J. W. Henderickx, J. G. de Vries, *Org. Lett.*, 2003, **5**, 3285-3288.
28. R. K. Arvela, N. E. Leadbeater, M. S. Sangi, V. A. Williams, P. Granados, R. D. Singer, *J. Org. Chem.*, 2005, **70**, 161-168.
29. G. B. Bajracharya, O. Daugulis, *Org. Lett.*, 2008, **10**, 4625-4628.
30. T. Truong, O. Daugulis, *J. Am. Chem. Soc.*, 2011, **133**, 4243-4245.
31. T. Truong, O. Daugulis, *Org. Lett.*, 2012, **14**, 5964-5967.
32. S. Yanagisawa, K. Ueda, T. Taniguchi, K. Itami, *Org. Lett.*, 2008, **10**, 4673-4676.
33. W. Liu, H. Cao, H. Zhang, H. Zhang, K. H. Chung, C. He, H. Wang, F. Y. Kwong, A. Lei, *J. Am. Chem. Soc.*, 2010, **132**, 16737-16740.
34. C.-L. Sun, H. Li, D.-G. Yu, M. Yu, X. Zhou, X.-Y. Lu, K. Huang, S.-F. Zheng, B.-J. Li, Z.-J. Shi, *Nat. Chem.*, 2010, **2**, 1044-1049.
35. E. Shirakawa, K.-i. Itoh, T. Higashino, T. Hayashi, *J. Am. Chem. Soc.*, 2010, **132**, 15537-15539.
36. E. C. Ashby, A. B. Goel, R. N. DePriest, *J. Org. Chem.*, 1981, **46**, 2429-2431.
37. E. C. Ashby, J. N. Argyropoulos, *J. Org. Chem.*, 1986, **51**, 3593-3597.
38. A. Studer, D. P. Curran, *Angew. Chem. Int. Ed.*, 2011, **50**, 5018-5022.
39. L. Pause, M. Robert, J.-M. Savéant, *J. Am. Chem. Soc.*, 1999, **121**, 7158-7159.
40. J. P. Barham, G. Coulthard, R. G. Kane, N. Delgado, M. P. John, J. A. Murphy, *Angew. Chem. Int. Ed.*, 2016, **55**, 4492-4496.
41. E. Doni, S. Zhou, J. A. Murphy, *Molecules*, 2015, **20**, 1755 - 1774.
42. S. Zhou, E. Doni, G. M. Anderson, R. G. Kane, S. W. MacDougall, V. M. Ironmonger, T. Tuttle, J. A. Murphy, *J. Am. Chem. Soc.*, 2014, **136**, 17818-17826.
43. J. P. Barham, G. Coulthard, K. J. Emery, E. Doni, F. Cumine, G. Nocera, M. P. John, L. E. A. Berlouis, T. McGuire, T. Tuttle, J. A. Murphy, *J. Am. Chem. Soc.*, 2016, **138**, 7402-7410.

44. S. Zhou, G. M. Anderson, B. Mondal, E. Doni, V. Ironmonger, M. Kranz, T. Tuttle, J. A. Murphy, *Chem. Sci.*, 2014, **5**, 476-482.
45. G. M. Anderson, I. Cameron, J. A. Murphy, T. Tuttle, *RSC Adv.*, 2016, **6**, 11335-11343.
46. Y. Qiu, Y. Liu, K. Yang, W. Hong, Z. Li, Z. Wang, Z. Yao, S. Jiang, *Org. Lett.*, 2011, **13**, 3556-3559.
47. H. Liu, B. Yin, Z. Gao, Y. Li, H. Jiang, *Chem. Commun.*, 2012, **48**, 2033-2035.
48. G. Pratsch, T. Wallaschkowski, M. R. Heinrich, *Chem. Eur. J*, 2012, **18**, 11555-11559.
49. J. Hofmann, T. Clark, M. R. Heinrich, *J. Org. Chem.*, 2016, **81**, 9785-9791.
50. W.-C. Chen, Y.-C. Hsu, W.-C. Shih, C.-Y. Lee, W.-H. Chuang, Y.-F. Tsai, P. P.-Y. Chen, T.-G. Ong, *Chem. Commun.*, 2012, **48**, 6702-6704.
51. H. Zhao, J. Shen, J. Guo, R. Ye, H. Zeng, *Chem. Commun.*, 2013, **49**, 2323-2325.
52. K. Tanimoro, M. Ueno, K. Takeda, M. Kirihata, S. Tanimori, *J. Org. Chem.*, 2012, **77**, 7844-7849.
53. W. Liu, F. Tian, X. Wang, H. Yu, Y. Bi, *Chem. Commun.*, 2013, **49**, 2983-2985.
54. Y. Wu, P. Y. Choy, F. Y. Kwong, *Org. Biomol. Chem.*, 2014, **12**, 6820-6823.
55. O. Vakuliuk, B. Koszarna, D. T. Gryko, *Adv. Synth. Catal.*, 2011, **353**, 925-930.
56. C.-L. Sun, Y.-F. Gu, W.-P. Huang, Z.-J. Shi, *Chem. Commun.*, 2011, **47**, 9813-9815.
57. D. S. Roman, Y. Takahashi, A. B. Charette, *Org. Lett.*, 2011, **13**, 3242-3245.
58. N. Stevens, N. O'Connor, H. Vishwasrao, D. Samaroo, E. R. Kandel, D. L. Akins, C. M. Drain, N. J. Turro, *J. Am. Chem. Soc.*, 2008, **130**, 7182-7183.
59. E. U. Sharif, G. A. O'Doherty, *Eur. J. Org. Chem.*, 2012, **2012**, 2095-2108.
60. Y. Wu, S. M. Wong, F. Mao, T. L. Chan, F. Y. Kwong, *Org. Lett.*, 2012, **14**, 5306-5309.
61. B. S. Bhakuni, A. Kumar, S. J. Balkrishna, J. A. Sheikh, S. Konar, S. Kumar, *Org. Lett.*, 2012, **14**, 2838-2841.
62. S. De, S. Ghosh, S. Bhunia, J. A. Sheikh, A. Bisai, *Org. Lett.*, 2012, **14**, 4466-4469.
63. K.-S. Masters, S. Bräse, *Angew. Chem. Int. Ed.*, 2013, **52**, 866-869.
64. M. E. Budén, J. F. Guastavino, R. A. Rossi, *Org. Lett.*, 2013, **15**, 1174-1177.
65. X. Zheng, L. Yang, W. Du, A. Ding, H. Guo, *Chem. Asian J.*, 2014, **9**, 439-442.
66. G. Deng, K. Ueda, S. Yanagisawa, K. Itami, C.-J. Li, *Chem. Eur. J.*, 2009, **15**, 333-337.
67. C.-L. Sun, Y.-F. Gu, B. Wang, Z.-J. Shi, *Chem. Eur. J.*, 2011, **17**, 10844-10847.
68. M. Rueping, M. Leiendecker, A. Das, T. Poisson, L. Bui, *Chem. Commun.*, 2011, **47**, 10629-10631.
69. J. F. Guastavino, M. E. Budén, R. A. Rossi, *J. Org. Chem.*, 2014, **79**, 9104-9111.
70. H. Zhang, R. Shi, A. Ding, L. Lu, B. Chen, A. Lei, *Angew. Chem. Int. Ed.*, 2012, **51**, 12542-12545.
71. T. Kawamoto, A. Sato, I. Ryu, *Chem. Eur. J.*, 2015, **21**, 14764-14767.
72. J. F. Bunnett, J. K. Kim, *J. Am. Chem. Soc.*, 1970, **92**, 7464-7466.
73. J. F. Bunnett, J. K. Kim, *J. Am. Chem. Soc.*, 1970, **92**, 7463-7464.
74. R. A. Rossi, J. F. Bunnett, *J. Am. Chem. Soc.*, 1972, **94**, 683-684.
75. R. G. Scamehorn, J. F. Bunnett, *J. Org. Chem.*, 1977, **42**, 1449-1457.
76. R. A. Rossi, J. F. Bunnett, *J. Org. Chem.*, 1973, **38**, 3020-3025.
77. J. F. Bunnett, J. E. Sundberg, *J. Org. Chem.*, 1976, **41**, 1702-1706.
78. J. F. Bunnett, X. Creary, *J. Org. Chem.*, 1974, **39**, 3173-3174.
79. J. F. Bunnett, X. Creary, *J. Org. Chem.*, 1974, **39**, 3612-3614.
80. J. E. Swartz, J. F. Bunnett, *J. Org. Chem.*, 1979, **44**, 340-346.
81. R. A. Rossi, R. H. De Rossi, A. F. Lopez, *J. Org. Chem.*, 1976, **41**, 3371-3373.
82. R. G. Scamehorn, J. M. Hardacre, J. M. Lukanich, L. R. Sharpe, *J. Org. Chem.*, 1984, **49**, 4881-4883.
83. M. Pichette Drapeau, I. Fabre, L. Grimaud, I. Ciofini, T. Ollevier, M. Taillefer, *Angew. Chem. Int. Ed.*, 2015, **54**, 10587–10591.
84. W.-t. Wei, X.-j. Dong, S.-z. Nie, Y.-y. Chen, X.-j. Zhang, M. Yan, *Org. Lett.*, 2013, **15**, 6018-6021.
85. J. F. Guastavino, R. A. Rossi, *J. Org. Chem.*, 2012, **77**, 460-472.
86. M. Newcomb, M. T. Burchill, *J. Am. Chem. Soc.*, 1984, **106**, 2450-2451.
87. J. Cuthbertson, V. J. Gray, J. D. Wilden, *Chem. Commun.*, 2014, **50**, 2575-2578.
88. H. Yi, A. Jutand, A. Lei, *Chem. Commun.*, 2015, **51**, 545-548.

89. M. Patil, *J. Org. Chem.*, 2016, **81**, 632-639.
90. B. Pieber, D. Cantillo, C. O. Kappe, *Chem. Eur. J.*, 2012, **18**, 5047-5055.
91. S. Sharma, M. Kumar, V. Kumar, N. Kumar, *Tetrahedron Lett.*, 2013, **54**, 4868-4871.
92. F. Wudl, G. M. Smith, E. J. Hufnagel, *J. Chem. Soc. D*, 1970, 1453-1454.
93. C. Burkholder, W. R. Dolbier, M. Médebielle, *J. Org. Chem.*, 1998, **63**, 5385-5394.
94. J. A. Murphy, T. A. Khan, S. Zhou, D. W. Thomson, M. Mahesh, *Angew. Chem. Int. Ed.*, 2005, **44**, 1356-1360.
95. P. Hohenberg, W. Kohn, *Phys. Rev.*, 1964, **136**, B864-B871.
96. F. Jensen, *Introduction to Computational Chemistry*. John Wiley & Sons, 2006.
97. C. J. Cramer, *Essentials of Computational Chemistry: Theories and Models*. Wiley-Blackwell, 2005.
98. M. C. H. Wolfram Koch, *A Chemist's Guide to Density Functional Theory*. John Wiley & Sons, 2001.
99. Y. Zhao, D. G. Truhlar, *Theor. Chem. Acc.*, 2008, **120**, 215-241.
100. R. F. S. W. J. Hehre, J. A. Pople, *J. Chem. Phys.*, 1969, **51**, 2657-2664.
101. R. A. Marcus, *J. Chem. Phys.*, 1965, **43**, 679-701.
102. S. F. Nelsen, S. C. Blackstock, Y. Kim, *J. Am. Chem. Soc.*, 1987, **109**, 677-682.
103. Y. Zhao, D. G. Truhlar, *Acc. Chem. Res.*, 2008, **41**, 157-167.
104. Y. Zhao, D. G. Truhlar, *J. Chem. Phys.*, 2006, **125**, 194101.
105. R. Krishnan, J. S. Binkley, R. Seeger, J. A. Pople, *J. Chem. Phys.*, 1980, **72**, 650-654.
106. M. J. Frisch, J. A. Pople, J. S. Binkley, *J. Chem. Phys.*, 1984, **80**, 3265-3269.
107. A. D. McLean, G. S. Chandler, *J. Chem. Phys.*, 1980, **72**, 5639-5648.
108. J.-P. Blaudeau, M. P. McGrath, L. A. Curtiss, L. Radom, *J. Chem. Phys.*, 1997, **107**, 5016-5021.
109. T. Clark, J. Chandrasekhar, G. W. Spitznagel, P. V. R. Schleyer, *J. Comput. Chem.*, 1983, **4**, 294-301.
110. A. Bergner, M. Dolg, W. Küchle, H. Stoll, H. Preuß, *Mol. Phys.*, 1993, **80**, 1431-1441.
111. M. Cossi, N. Rega, G. Scalmani, V. Barone, *J. Comput. Chem.*, 2003, **24**, 669-681.
112. V. Barone, M. Cossi, *J. Phys. Chem. A*, 1998, **102**, 1995-2001.
113. M. J. Frisch, G. W. Trucks, H. B. Schlegel, G. E. Scuseria, M. A. Robb, J. R. Cheeseman, G. Scalmani, V. Barone, B. Mennucci, G. A. Petersson, H. Nakatsuji, M. Caricato, X. Li, H. P. Hratchian, A. F. Izmaylov, J. Bloino, G. Zheng, J. L. Sonnenberg, M. Hada, M. Ehara, K. Toyota, R. Fukuda, J. Hasegawa, M. Ishida, T. Nakajima, Y. Honda, O. Kitao, H. Nakai, T. Vreven, J. A. Montgomery Jr., J. E. Peralta, F. Ogliaro, M. J. Bearpark, J. Heyd, E. N. Brothers, K. N. Kudin, V. N. Staroverov, R. Kobayashi, J. Normand, K. Raghavachari, A. P. Rendell, J. C. Burant, S. S. Iyengar, J. Tomasi, M. Cossi, N. Rega, N. J. Millam, M. Klene, J. E. Knox, J. B. Cross, V. Bakken, C. Adamo, J. Jaramillo, R. Gomperts, R. E. Stratmann, O. Yazyev, A. J. Austin, R. Cammi, C. Pomelli, J. W. Ochterski, R. L. Martin, K. Morokuma, V. G. Zakrzewski, G. A. Voth, P. Salvador, J. J. Dannenberg, S. Dapprich, A. D. Daniels, Ö. Farkas, J. B. Foresman, J. V. Ortiz, J. Cioslowski, D. J. Fox *Gaussian 09*, Gaussian, Inc.: Wallingford, CT, USA, 2009.
114. K. J. Emery, T. Tuttle, A. R. Kennedy, J. A. Murphy, *Tetrahedron*, 2016, **72**, 7875-7887.
115. T. Amatov, R. Pohl, I. Císařová, U. Jahn, *Angew. Chem. Int. Ed.*, 2015, **54**, 12153-12157.
116. M. Mahesh, J. A. Murphy, F. LeStrat, H. P. Wessel, *Beilstein J. Org. Chem.*, 2009, **5**, 1.
117. K. Griesbaum, *Angew. Chem. Int. Ed.*, 1970, **9**, 273-287.
118. E. C. Kooyman, *Pure Appl. Chem.*, 1967, **15**, 81 - 88.
119. H.-L. D. W Ho, *Laser Spectroscopy and Photochemistry on Metal Surfaces, Part 2*. World Scientific Publishing and Imperial College Press, 1995.
120. D. R. Carbery, T. J. Donohoe, *Chem. Commun.*, 2004, 722-723.
121. D. J. Procter, R. A. Flowers, T. Skrydstrup, In *Organic Synthesis using Samarium Diiodide: A Practical Guide*, Royal Society of Chemistry, 2009, pp 5-19.
122. S. O'Sullivan, E. Doni, T. Tuttle, J. A. Murphy, *Angew. Chem. Int. Ed.*, 2014, **53**, 474-478.
123. F. Dénès, M. Pichowicz, G. Povie, P. Renaud, *Chem. Rev.*, 2014, **114**, 2587-2693.
124. N. S. Nudelman, G. E. García Liñares, *J. Org. Chem.*, 2000, **65**, 1629-1635.
125. P. Gray, A. Williams, *Chem. Rev.*, 1959, **59**, 239-328.
126. A. Ledwith, P. J. Russell, L. H. Sutcliffe, *J. Chem. Soc., Perkin Trans. 2*, 1973, 630-633.

127. C. Walling, P. Wagner, *J. Am. Chem. Soc.*, 1963, **85**, 2333-2334.
128. D. V. Avila, C. E. Brown, K. U. Ingold, J. Lusztyk, *J. Am. Chem. Soc.*, 1993, **115**, 466-470.
129. G. A. Swan, *J. Chem. Soc.*, 1948, 1408-1412.
130. T. R. Lea, R. Robinson, *J. Chem. Soc.*, 1926, **129**, 2351-2355.
131. A. I. Savchenko, *Russ. J. Org. Chem.*, 2001, **37**, 1182-1183.
132. P. R. Schreiner, O. Lauenstein, I. V. Kolomitsyn, S. Nadi, A. A. Fokin, *Angew. Chem. Int. Ed.*, 1998, **37**, 1895-1897.
133. E. Murayama, A. Kohda, T. Sato, *J. Chem. Soc., Perkin Trans. 1*, 1980, 947-949.
134. J. Tang, S. Zhao, Y. Wei, Z. Quan, C. Huo, *Org. Biomol. Chem.*, 2017, **15**, 1565-1569.
135. Y. Shiota, N. Kihara, T. Kamachi, K. Yoshizawa, *J. Org. Chem.*, 2003, **68**, 3958-3965.
136. G. W. Smith, H. D. Williams, *J. Org. Chem.*, 1961, **26**, 2207-2212.
137. Y. Nishina, B. Ohtani, K. Kikushima, *Beilstein J. Org. Chem.*, 2013, **9**, 1663-1667.
138. R. Cacciapaglia, S. Di Stefano, L. Mandolini, *J. Am. Chem. Soc.*, 2005, **127**, 13666-13671.
139. A. Cornélis, P. Laszlo, *Synthesis*, 1982, **1982**, 162-163.
140. E. V. Dehmlow, J. Schmidt, *Tetrahedron Lett.*, 1976, **17**, 95-96.
141. R. Montoro, T. Wirth, *Synthesis*, 2005, **2005**, 1473-1478.
142. M. Salamone, M. Bietti, A. Calcagni, G. Gente, *Org. Lett.*, 2009, **11**, 2453-2456.
143. G. A. DiLabio, K. U. Ingold, S. Lin, G. Litwinienko, O. Mozenson, P. Mulder, T. T. Tidwell, *Angew. Chem. Int. Ed.*, 2010, **49**, 5982-5985.
144. G. Bucher, *Angew. Chem. Int. Ed.*, 2010, **49**, 6934-6935.
145. M. Smeu, G. A. DiLabio, *J. Org. Chem.*, 2007, **72**, 4520-4523.
146. J. Li, X. Zhang, H. Shen, Q. Liu, J. Pan, W. Hu, Y. Xiong, C. Chen, *Adv. Synth. Catal.*, 2015, **357**, 3115-3120.
147. J. M. Altimari, J. P. Delaney, L. Servinis, J. S. Squire, M. T. Thornton, S. K. Khosa, B. M. Long, M. D. Johnstone, C. L. Fleming, F. M. Pfeffer, S. M. Hickey, M. P. Wride, T. D. Ashton, B. L. Fox, N. Byrne, L. C. Henderson, *Tetrahedron Lett.*, 2012, **53**, 2035-2039.
148. C. E. McKenna, L. A. Khawli, *J. Org. Chem.*, 1986, **51**, 5467-5471.
149. R. A. Rossi, A. B. Pierini, A. B. Peñéñory, *Chem. Rev.*, 2003, **103**, 71-168.
150. J. F. Guastavino, R. A. Rossi, *J. Org. Chem.*, 2011, **77**, 460-472.
151. R. A. Alonso, R. A. Rossi, *J. Org. Chem.*, 1980, **45**, 4760-4763.
152. M. Pichette Drapeau, I. Fabre, L. Grimaud, I. Ciofini, T. Ollevier, M. Taillefer, *Angew. Chem. Int. Ed.*, 2015, **54**, 10587-10591.
153. M.-X. Zhang, X.-H. Hu, Y.-H. Xu, T.-P. Loh, *Asian J. Org. Chem.*, 2015, **4**, 1047-1049.
154. E. Ostreng, H. H. Sonsteby, S. Oien, O. Nilsen, H. Fjellvag, *Dalton Trans.*, 2014, **43**, 16666-16672.
155. M. H. Chisholm, S. R. Drake, A. A. Naiini, W. E. Streib, *Polyhedron*, 1991, **10**, 337-345.
156. W. Hu, J.-P. Lin, L.-R. Song, Y.-Q. Long, *Org. Lett.*, 2015, **17**, 1268-1271.
157. C. Pettegrew, Z. Dong, M. Z. Muhi, S. Pease, M. A. Mottaleb, M. R. Islam, *ISRN Nanotechnology*, 2014, **2014**, 8.
158. W. E. Benet, G. S. Lewis, L. Z. Yang, P. D. E. Hughes, *J. Chem. Res.*, 2011, **35**, 675-677.
159. B. Tollens, *Ber. Dtsch. Chem. Ges.*, 1882, **15**, 1635-1639.
160. T. R. S. Prasad, B.; Rao, T. Navneeth, *Curr. Sci.*, 1982, **51**, 749-751.
161. M. Liu, H. Wang, H. Zeng, C.-J. Li, *Sci. Adv.*, 2015, **1**, DOI: 10.1126/sciadv.1500020.
162. Z. Wang, In *Comprehensive Organic Name Reactions and Reagents*, John Wiley & Sons, Inc., 2010, pp 1763-1766.
163. J. A. Jacob, H. S. Mahal, N. Biswas, T. Mukherjee, S. Kapoor, *Langmuir*, 2008, **24**, 528-533.
164. Z. Khan, J. I. Hussain, A. A. Hashmi, S. A. Al-Thabaiti, *Arabian J. Chem.*, doi.org/10.1016/j.arabjc.2013.05.001.
165. X. Wang, Z. Zhao, D. Ou, B. Tu, D. Cui, X. Wei, M. Cheng, *IET Micro Nano Lett.*, 2016, **11**, 454-456.
166. P. R. S. Murray, *Principles of Organic Chemistry: A Modern and Comprehensive Text for Schools and Colleges*. Heinemann Educational Books, 1977.
167. M.-Y. Chang, S.-T. Chen, N.-C. Chang, *Tetrahedron*, 2002, **58**, 3623-3628.
168. A. Hamasaki, S. Maruta, A. Nakamura, M. Tokunaga, *Adv. Synth. Catal.*, 2012, **354**, 2129-2134.

169. M. A. Zolfigol, A. Khazaei, A. R. Moosavi-Zare, A. Zare, H. G. Kruger, Z. Asgari, V. Khakyzadeh, M. Kazem-Rostami, *J. Org. Chem.*, 2012, **77**, 3640-3645.
170. A. Habibi, M. H. Baghersad, M. Bilabary, Y. Valizadeh, *Tetrahedron Lett.*, 2016, **57**, 559-562.
171. E. Tayama, S. Otoyama, W. Isaka, *Chem. Commun.*, 2008, 4216-4218.
172. J. Yu, J. Liu, G. Shi, C. Shao, Y. Zhang, *Angew. Chem. Int. Ed.*, 2015, **54**, 4079-4082.
173. T. Krüger, K. Vorndran, T. Linker, *Chem. Eur. J.*, 2009, **15**, 12082-12091.
174. V. K. R. Kumar, S. Krishnakumar, K. R. Gopidas, *Eur. J. Org. Chem.*, 2012, **2012**, 3447-3458.
175. J. Chen, W. Wu, A. J. McNeil, *Chem. Commun.*, 2012, **48**, 7310-7312.
176. D. N. Kuznetsov, A. G. Ruchkina, K. I. Kobrakov, *Chem. Heterocycl. Compd.*, 2011, **47**, 441.
177. C. Zhu, A. Yoshimura, Y. Wei, V. N. Nemykin, V. V. Zhdankin, *Tetrahedron Lett.*, 2012, **53**, 1438-1444.
178. L. De Luca, G. Giacomelli, S. Masala, A. Porcheddu, *J. Org. Chem.*, 2003, **68**, 4999-5001.
179. R.-J. Tang, Q. He, L. Yang, *Chem. Commun.*, 2015, **51**, 5925-5928.
180. M. Hatano, O. Ito, S. Suzuki, K. Ishihara, *J. Org. Chem.*, 2010, **75**, 5008-5016.
181. S. Pramanik, P. Ghorai, *Org. Lett.*, 2014, **16**, 2104-2107.
182. D. Cheng, D. Huang, Y. Shi, *Org. Biomol. Chem.*, 2013, **11**, 5588-5591.
183. S. Ren, C. Feng, T.-P. Loh, *Org. Biomol. Chem.*, 2015, **13**, 5105-5109.
184. J. C. Lorenz, J. Long, Z. Yang, S. Xue, Y. Xie, Y. Shi, *J. Org. Chem.*, 2004, **69**, 327-334.
185. G. M. Rubottom, M. I. Lopez, *J. Org. Chem.*, 1973, **38**, 2097-2099.
186. O. S. Shneider, E. Pisarevsky, P. Fristrup, A. M. Szpilman, *Org. Lett.*, 2015, **17**, 282-285.
187. C. B. Tripathi, S. Mukherjee, *Angew. Chem. Int. Ed.*, 2013, **52**, 8450-8453.
188. C.-J. Wallentin, J. D. Nguyen, P. Finkbeiner, C. R. J. Stephenson, *J. Am. Chem. Soc.*, 2012, **134**, 8875-8884.
189. C. Dai, J. M. R. Narayanam, C. R. J. Stephenson, *Nat. Chem.*, 2011, **3**, 140-145.
190. H. Clavier, K. L. Jeune, I. d. Riggi, A. Tenaglia, G. Buono, *Org. Lett.*, 2011, **13**, 308-311.
191. S. E. Denmark, B. R. Henke, *J. Am. Chem. Soc.*, 1991, **113**, 2177-2194.
192. Y. Liu, Y. Xu, S. H. Jung, J. Chae, *Synlett*, 2012, **23**, 2692-2698.
193. A. Dewanji, C. Mück-Lichtenfeld, A. Studer, *Angew. Chem. Int. Ed.*, 2016, **55**, 6749-6752.
194. L. Candish, E. A. Standley, A. Gómez-Suárez, S. Mukherjee, F. Glorius, *Chem. Eur. J.*, 2016, **22**, 9971-9974.
195. T. Das, A. Chakraborty, A. Sarkar, *Tetrahedron Lett.*, 2014, **55**, 7198-7202.
196. Y. Sato, T. Aoyama, T. Takido, M. Kodomari, *Tetrahedron*, 2012, **68**, 7077-7081.
197. G. Bentzinger, W. De Souza, C. Mullié, P. Agnamey, A. Dassonville-Klimpt, P. Sonnet, *Tetrahedron: Asymmetry*, 2016, **27**, 1-11.
198. F. Kleinbeck, G. J. Fettes, L. D. Fader, E. M. Carreira, *Chem. Eur. J.*, 2012, **18**, 3598-3610.
199. J. Y. Becker, S. Yatziv, *J. Org. Chem.*, 1988, **53**, 1744-1748.
200. R. I. Khusnutdinov, N. A. Shchadneva, A. R. Bayguzina, T. M. Oshnyakova, Y. Y. Mayakova, U. M. Dzhemilev, *Russ. J. Org. Chem.*, 2013, **49**, 1557-1566.
201. C. Walling, J. A. McGuinness, *J. Am. Chem. Soc.*, 1969, **91**, 2053-2058.
202. R. Olivera, R. SanMartin, E. Domínguez, X. Solans, M. K. Urtiaga, M. I. Arriortua, *J. Org. Chem.*, 2000, **65**, 6398-6411.
203. K. P. Landge, K. S. Jang, S. Y. Lee, D. Y. Chi, *J. Org. Chem.*, 2012, **77**, 5705-5713.
204. G. Stefancich, M. Artico, S. Massa, S. Vomero, *J. Heterocyclic Chem.*, 1979, **16**, 1443-1447.
205. A. Baeyer, *Ber. Dtsch. Chem. Ges.*, 1884, **17**, 970-973.
206. A. Romek, T. Opatz, *Eur. J. Org. Chem.*, 2010, **2010**, 5841-5849.
207. D. Ding, X. Li, X. Wang, Y. Du, J. Shen, *Tetrahedron Lett.*, 2006, **47**, 6997-6999.
208. M. Castaing, S. L. Wason, B. Estepa, J. F. Hooper, M. C. Willis, *Angew. Chem. Int. Ed.*, 2013, **52**, 13280-13283.
209. M. Martjuga, S. Belyakov, E. Liepinsh, E. Suna, *J. Org. Chem.*, 2011, **76**, 2635-2647.
210. R. A. Bunce, T. Nago, *J. Heterocycl. Chem.*, 2009, **46**, 623-628.
211. A. D. Chowdhury, R. Ray, G. K. Lahiri, *Chem. Commun.*, 2012, **48**, 5497-5499.
212. K. Takagi, H. Fukuda, S. Shuto, A. Otaka, M. Arisawa, *Adv. Synth. Catal.*, 2015, **357**, 2119-2124.
213. B. Yi, Y. Yin, Z. Yi, W. Zhou, H. Liu, N. Tan, H. Yang, *Tetrahedron Lett.*, 2016, **57**, 2320-2323.
214. M. Liu, C.-J. Li, *Angew. Chem. Int. Ed.*, 2016, **55**, 10806-10810.
215. A. Mart, M. S. Shashidhar, *Tetrahedron*, 2012, **68**, 9769-9776.

216. L. Crombie, W. M. L. Crombie, *J. Chem. Soc., Perkin Trans. 1*, 1994, 1267-1274.
217. G. V. Kryshtal, G. M. Zhdankina, N. V. Ignat'ev, M. Schulte, S. G. Zlotin, *Tetrahedron*, 2011, **67**, 173-178.
218. B. Narasimhan, V. Judge, R. Narang, R. Ohlan, S. Ohlan, *Bioorg. Med. Chem. Lett.*, 2007, **17**, 5836-5845.
219. M. Feurer, G. Frey, H.-T. Luu, D. Kratzert, J. Streuff, *Chem. Commun.*, 2014, **50**, 5370-5372.
220. Y.-F. Liang, N. Jiao, *Angew. Chem. Int. Ed.*, 2014, **53**, 548-552.
221. J. N. Moorthy, N. Singhal, K. Senapati, *Org. Biomol. Chem.*, 2007, **5**, 767-771.
222. P. Muthupandi, S. K. Alamsetti, G. Sekar, *Chem. Commun.*, 2009, 3288-3290.
223. W. Dai, Y. Lv, L. Wang, S. Shang, B. Chen, G. Li, S. Gao, *Chem. Commun.*, 2015, **51**, 11268-11271.
224. T. Mahapatra, N. Jana, S. Nanda, *Tetrahedron: Asymmetry*, 2008, **19**, 1224-1232.
225. Y. Li, D. Xue, W. Lu, C. Wang, Z.-T. Liu, J. Xiao, *Org. Lett.*, 2014, **16**, 66-69.
226. W. Hückel, R. Cramer, S. Läufer, *Justus Liebigs Ann. Chem.*, 1960, **630**, 89-104.